Fort Peck EIS

Alternative Effects on Pallid Sturgeon;

Model Documentation and Study Report

Prepared by

J. Craig Fischenich

Sara A. Reynolds

Philip Halteman

for

Missouri River Recovery Program

U.S. Army Corps of Engineers

Omaha District

July 23 2021

Contents

Figures and Tables

Figures

Tables

Preface

This model study was conducted for the USACE Omaha District under Contract W9128F19P0021 – Adaptive Management Support for the Missouri River Recovery Program. The USACE technical monitor was Mike Delvaux and the project manager was Tiffany Vanosdall.

The work was performed under direction of ESSA Technologies Ltd. Carol Murray was the Program Manager overseeing the work for ESSA.

The authors thank Robert B. Jacobson, Susannah Irwin, Kimberly Chojnacki, Pat Braaten, and Aaron DeLonay from the Columbia Environmental Research Center, USGS and Mike Colven from Mississippi State University for their contributions to the development of this report. We also thank the various technical experts who contributed to this study via technical support and input to relevant portions of the parent study; they include Graham Long (Compass Resource Management), Pat Braaten, Aaron Delonay, Robb Jacobson, Steve Krentz, Rob Holm (USFWS), Wayne Nelson-Stastny (USFWS), Ryan Larsen and Clayton Ridenour (USACE), Zach Shattuck (MTFWP), Todd Slack (ERDC), and Kirk Steffensen (NEGPC). A technical review of the model was provided by Pat Braaten and an editorial review of the report by Carol Murray.

Unit Conversion Factors

Multiply	By	To Obtain
acres	4,046.873	square meters
acre-feet	1,233.5	cubic meters
cubic feet	0.02831685	cubic meters
degrees Fahrenheit	(F-32)/1.8	degrees Celsius
feet	0.3048	meters
hectares	1.0 E+04	square meters
inches	0.0254	meters
miles (U.S. statute)	1,609.347	meters
miles per hour	0.44704	meters per second
square feet	0.09290304	square meters
square inches	6.4516 E-04	square meters
square miles	2.589998 E+06	square meters
square yards	0.8361274	square meters

1 Background

1.1 Missouri River Recovery Program

The Missouri River Recovery Program (MRRP) is a U.S. Army Corps of Engineers (USACE) program for implementing actions on the mainstem Missouri River that will avoid a finding of jeopardy for the piping plover, the interior least tern, and the pallid sturgeon. The current action, described in the U.S. Army Corps of Engineers' October 2017 Biological Assessment (BA), includes a Science and Adaptive Management Plan (SAMP; Fischenich et al. 2016) to guide the assessment of action effectiveness and identification of new actions, if warranted. Actions under the MRRP allow the Corps to operate for all authorized purposes while complying with all applicable laws, regulations, and treaty and trust responsibilities.

The geographic scope for the MRRP encompasses the mainstem portions of the Missouri River from the Fort Peck Reservoir, Mont., to St. Louis, Mo. It also includes the Bank Stabilization and Navigation Project Mitigation Project (BSNP) applies to the portion of the river from Sioux City, Iowa, to St. Louis, Mo. The fundamental objective and two sub-objectives for pallid sturgeon as described in the SAMP are shown in Figure 1-1.

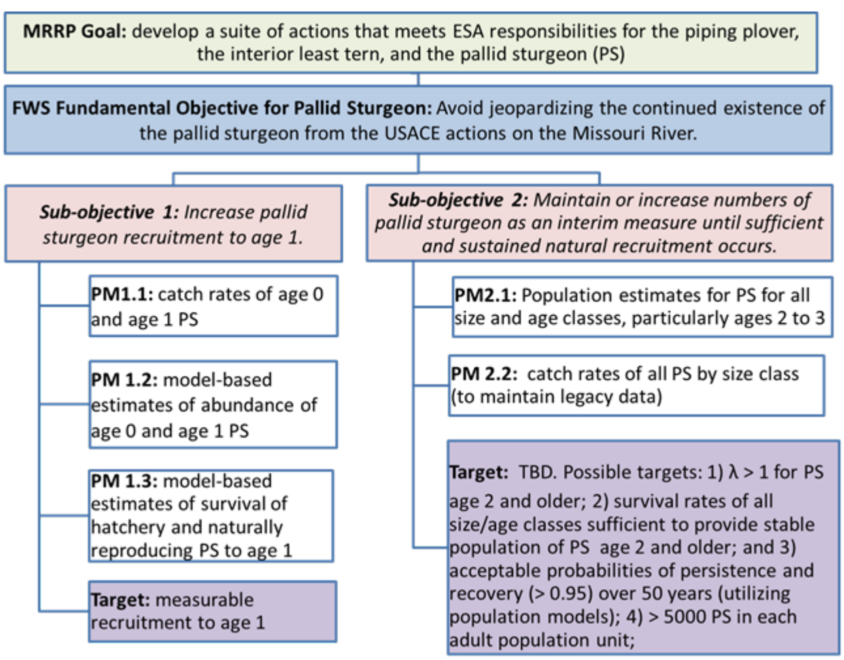

Figure 1-1. Pallid sturgeon objectives, sub-objectives, and associated performance measures from the MRRP SAMP (Fischenich et al. 2016).

There has been only one confirmed year (2011) of spawning in the Upper Missouri River (UMR) below Fort Peck Dam and above the Yellowstone confluence (Jacobson et al. 2015), and no documented recruitment to age-1 of natural origin pallid sturgeon on the same reach extended downstream into Lake Sakakawea (Figure 1-2). Flow alteration, low water temperature, and the limited length of free-flowing river below Fort Peck dam are hypothesized to limit the likelihood that any naturally produced age-0 pallid sturgeon are retained in lotic habitat (Jacobson et al. 2015, Jacobson et al. 2016). Instead, free embryos (if produced) drift into the headwaters of Lake Sakakawea, which is presumed fatal due to anoxic conditions at the bed (Guy et al. 2015).

Hypotheses H3 and H5 in the SAMP postulate that management operations at Fort Peck Dam that decrease flows and increase water temperatures will potentially increase retention in lotic habitat upriver of Lake Sakakawea (Fischenich et al. 2018). Furthermore, Fort Peck management operations in early spring may increase spawning success (SAMP UMR hypothesis H2; Fischenich et al. 2018). USACE has proposed alternative flows out of Fort Peck Dam to promote spawning and increase drift retention; however, which flow scenarios will likely to have the greatest positive effect on the pallid sturgeon population residing in the UMR below Fort Peck Dam and on the Yellowstone River are unknown. Using models to project the possible effects of alternative flow scenarios on the pallid sturgeon population is an effective method for comparing alternatives and informing the management decision-making process for Fort Peck Dam.

1.2 Fort Peck Adaptive Management Framework

In its 2017 Amendment to the Missouri River Recovery Management Plan (MRRMP) BA, the USACE committed “to review previous information and information generated since the Effects Analysis to formulate test flow releases from Fort Peck Dam and an adaptive management (AM) framework for their implementation.” Working with the US Fish and Wildlife Service (USFWS) and the Missouri River Recovery Implementation Committee (MRRIC), the USACE reviewed existing science and data to determine an appropriate approach for meeting its requirements under the USFWS 2018 Biological Opinion pertaining to operations of Fort Peck Dam and their effects on pallid sturgeon on the upper Missouri River.

The *Fort Peck Adaptive Management Framework for Upper Missouri River Pallid Sturgeon* (Fort Peck Framework; dated 12 December 2018), affirms that limited distance between Fort Peck Dam and the presumed anoxic zone in the headwaters of the Lake Sakakawea pool, along with alterations of the natural hydrograph, water temperatures, and turbidity are the factors most likely restricting recruitment of pallid sturgeon on the upper Missouri River (UMR). These factors are represented on the location map in Figure 1-2.

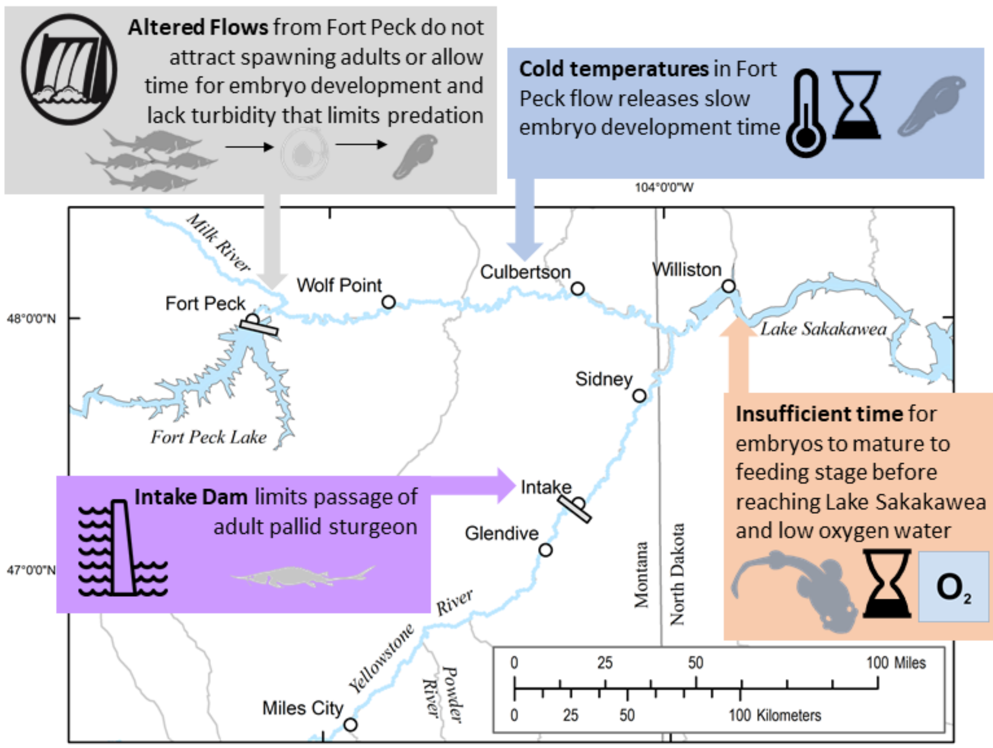

Figure 1-2. Location map showing key factors affecting pallid sturgeon recruitment on the upper Missouri River and its tributaries.

The framework presents two proposed hydrographs that could serve as a basis for Level 2* studies to assess whether flow management at Fort Peck could improve recruitment potential. The framework identifies a systematic series of Level 1 and Level 2 scientific investigations and experiments that would address critical uncertainties and, if implemented under adaptive management, ultimately lead to the implementation of activities needed to meet objectives. It also conceptually describes how criteria and mechanisms gained from studies and experimentation could guide decisions about what implementation activities (if any) are warranted, and how they should be structured.

* Level 1 through Level 4 activities in this report are in reference to the Pallid Sturgeon Framework described in Section 4.2.1.1 and Table 39 of the SAMP.

1.3 Fort Peck EIS

Recognizing the potential need for management of flows from Fort Peck Dam to address pallid sturgeon objectives for the upper river, the USACE determined that it would investigate alternatives to improve pallid sturgeon recruitment potential on the UMR and increase the upper basin pallid sturgeon population relative to its status without intervention. The National Environmental Policy Act (NEPA) requires federal agencies to evaluate and consider a range of alternatives that address the purpose of, and need for action.

Alternatives were informed by the current state of pallid sturgeon science as described in the MRRP SAMP (Fischenich et al. 2018), the 2018 BiOp (USFWS 2018), and by the Fort Peck Framework (USACE 2018b). Input received through the scoping process and from MRRIC engagements also shaped the alternatives. These documents have affirmed that the USACE's System Operations have altered 1) water temperatures, 2) flow regime, and 3) sediment regime and turbidity such that they may limit recruitment of pallid sturgeon to age-1 on the UMR. The most effective management actions to address these issues would likely result from modifying System operations to better replicate historical flow and temperature attributes on the UMR during spawning periods.

1.4 Alternative description

Two action alternatives, each consisting of three variations, were developed to meet the pallid sturgeon recruitment and population objectives. The alternatives are based upon the two conceptual hydrographs presented in the Fort Peck Framework and described below. These hydrographs were refined to address technical issues and respond to concerns with the initial hydrographs identified during scoping. The action alternatives and the No Action Alternative are described in section 1.3.2. Advection/dispersion (A/D) modeling occurred in three "rounds" of analysis, with the modeling assumptions in each round updated to reflect new information from ongoing Level 1 science under the MRRP and input from expert elicitation. Population modeling was conducted using A/D model results from the second and third rounds of analysis; some population modeling using Round 3 retention outputs is still underway. The hydrology associated with Round 1 differed slightly from Rounds 2 and 3, but the alternatives remained the same. The draft EIS (USACE 2020) provides a detailed comparison of alternative parameters.

1.4.1 Fort Peck Framework conceptual hydrographs

In compliance with the 2018 BiOP, the MRRP Technical Team formulated two flow regimes (conceptual hydrographs) in the Fort Peck Framework (USACE 2018b) to illustrate how hydrograph development might proceed when formulating alternatives for evaluation. The hydrographs were based on the best available science as described in the SAMP, augmented with new information collected since the SAMP was prepared.

The general approach was to link biological functions with components of the annual hydrograph and hypothesize how they might drive flow-release strategies. The functions anticipated for the hydrograph relate to reproductive ecology of the pallid sturgeon and include: 1) attractant flow to motivate pallid sturgeon movement as far upstream as possible to maximize drift (larval dispersal) distance, 2) flows that will retain the fish in the upstream reaches, 3) an additional flow pulse to aggregate fish and create a spawning cue, and 4) and low flows on the receding limb of the hydrograph to minimize velocities, and therefore, to maximize drift time. Figure 1 shows the reproductive functions relative to the historical regulated and unregulated flows at Fort Peck Dam.

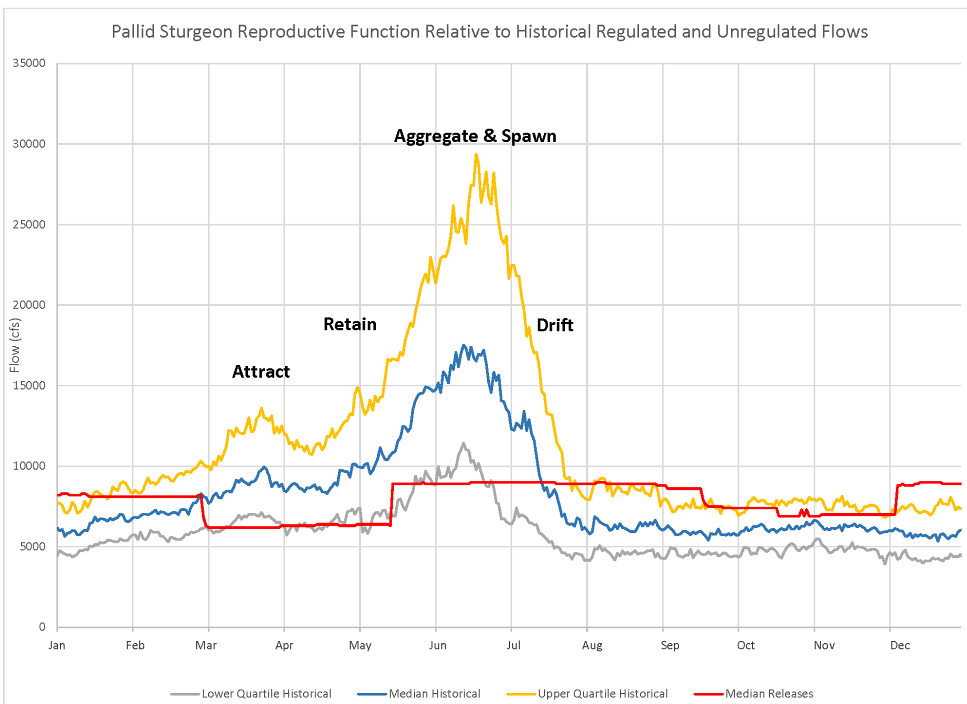

Figure 1-3. Pallid sturgeon reproductive functions relative to historical regulated and unregulated flows at Fort Peck Dam.

A fundamental assumption of the conceptual hydrograph design process was that the unregulated flow regime could be used to fill in gaps and detail where current understanding of biological needs was insufficient to parameterize the hydrograph based on hypothesized functions. While the hydrographs focused on the response of pallid sturgeon to flow, correlated temperature and turbidity conditions were implicit in their formulation. Temperature, in particular, was identified as a spawning trigger and a critical component of early larval development. The Fort Peck Framework describes the basis for the development of each hydrograph and the resultant criteria and conditions.

1.4.2 Alternative hydrographs evaluated under the DEIS

The alternative hydrographs are presented in detail in the Draft EIS (DEIS; USACE 2021). The following descriptions represent the alternatives at the time of evaluation for pallid sturgeon drift and settling.

No Action Alternative: The impacts of No Action Alternative serve as the baseline of comparison for the impacts of the other alternatives. It assumes that no test flow release for pallid sturgeon would occur from Fort Peck Dam. Operations at Fort Peck were assumed to closely follow the Master Manual with no deviations for a pallid sturgeon test flow. When modeling the No Action alternative, local inflows were adjusted by the difference between the historic and present level depletions to ensure the period-of-record datasets are homogenous and reflect current water use. All modeled flood targets were as outlined in the 2018 Master Manual and reservoir storages were based on current reservoir surveys. All four navigation target locations were used when setting navigation releases and the model balances system storage by March 1. It was assumed that other activities and actions for pallid sturgeon in the Upper Basin would be implemented as described in the MRRMP-EIS and 2018 BiOp and the Yellowstone Intake Bypass EIS. These actions include fish bypass construction at Yellowstone Intake, continued propagation and stocking of pallid sturgeon in the Upper Basin, and continued pallid sturgeon science and monitoring activities in the Upper Basin.

Attributes Common to All of the Action Alternatives: There are several differences from the conceptual hydrographs that are common to both of the action alternatives:

- Target flows for increases and decreases in flow releases were established in the model at Wolf Point rather than for releases from Fort Peck Dam. Establishing targets at Wolf Point, the nearest gage downstream of the dam, rather than measuring releases from Fort Peck Dam, takes into account flows from the Milk River and is intended to give a better estimate of the magnitude of releases needed from Fort Peck Dam in order to achieve downstream objectives.

- During the drifting portion of the flow regime, target flows were set to a minimum of 8,000 cfs until September 1. In comparison, the Fort Peck AM Framework conceptual hydrograph 1 included lower flows to a minimum of 4,200 cfs until September 1 and conceptual hydrograph 2 included a return to normal rebalancing operations, which would emphasize refilling Fort Peck Reservoir after the test flow release resulting in low flows below the dam. Changing to a flow of 8,000 cfs was done to reduce the risk of impacting irrigation intakes with lower flows. Additionally, flows that are too low have a chance of concentrating the flow in the main channel which could have the undesired effect of speeding larval drift.
- Under the conceptual hydrographs, the test flows would have been initiated any time the minimum Fort Peck Reservoir elevation was above 2225.0 feet. Limitations during flow regimes are consistent across both action alternatives and include:
    - A forecasted Fort Peck to Garrison runoff less than the upper quartile range
    - Minimum forecasted Fort Peck Lake pool elevation of 2227.0 feet
    - Flow limit at Wolf Point and Culbertson of 35,000 cfs
    - Maximum forecasted Garrison Lake pool elevation of 1850.0 feet
    - Minimum forecasted Williston levee freeboard (distance from the base flood elevation (1% annual chance flood elevation) to top of the levee) of 6.4 feet (based on a water surface elevation of 1853.5 feet)
    - Maximum forecasted Williston stage of 22.0 feet (the National Weather Service flood stage at Williston).

Alternative 1: System operations under this alternative are based on those described under the No Action Alternative except that it includes a flow release regime from Fort Peck Dam to benefit pallid sturgeon.

The Attraction Flow Regime begin on April 16 and the peak flow would be twice as large as the spring release from Fort Peck Dam in the given year. For example, the typical early spring release from Fort Peck Dam is approximately 8,000 cfs; therefore the Attraction Flow Regime peak flow would be 16,000 cfs as measured at the Wolf Point gage. Beginning on April 16, spring release flows is increased by 1,700 cfs per day until the peak flow is reached at the Wolf Point gage. The peak flow is held for 3 days and then decreases by 1,300 cfs per day until the Retention Flow is reached. The Retention Flow is 1.5 times the Fort Peck Dam early spring release as measured at the Wolf Point gage, 12,000 cfs using the example.

The Retention Flow is held until May 28 when the Spawning Cue Flow Regime is initiated.

The Spawning Cue Flow Regime under Alternative 1 begins on May 28 and is be 3.5 times the Fort Peck Dam spring flow release in the given year. Assuming 8,000 cfs as the typical spring flow, this equates to approximately 28,000 cfs at the peak as measured at the Wolf Point gage. Beginning on May 28, the release is increased by 1,100 cfs per day until the peak flow is reached as measured at the Wolf Point gage. The peak is held for 3 days and then decreases by 1,000 cfs per day for 12 days then decreased by 3,000 cfs per day until the Drifting Flow Regime of 8,000 cfs is reached. The 8,000 cfs Drifting Flow Regime is held until September 1 when releases to balance storage resume.

Variation 1A: This test flow is a variation of Alternative 1. The parameters for 1A are the same as described for Alternative 1 except that the Attraction Flow is initiated on April 9, rather than April 16, and the Spawning Cue Flow Regime is initiated on May 21, rather than May 28. The April 9 initiation date is closer to the timing of the initial pulse shown on the unregulated hydrograph. Moving the initiation date earlier in April is intended to analyze the differences in forecasted impacts that may result from altering the start of the test releases. In Alternative 1, the later initiation date of April 16 is designed to enhance the contrast between Missouri River and Yellowstone River discharges by moving the start date approximately two weeks later than the initial pulse shown on the unregulated hydrograph..

Variation 1B: This test flow is another variation of Alternative 1. The parameters for 1B are the same as described for Alternative 1 except that the Attraction Flow is initiated on April 23 and the Spawning Cue Flow is initiated on June 4. Similar to the concept described in Variation 1A, the later initiation date is intended to provide contrast explore any differences in forecasted impacts from a later flow initiation date.

Alternative 2: The parameters for Alternative 2 are the same as described for Alternative 1 except that the Attraction Flow Regime peak is 14,000 cfs (the maximum powerhouse capacity) rather than twice the average Fort Peck spring flow in the given year. The maximum amount of flow that can be run through the generators is 14,000 cfs. Any additional flow is run through the spillway and does not generate hydroelectricity. Additionally, releases as measured at Wolf Point gage are held at 14,000 cfs until the Spawning Cue release is initiated. The rationale for keeping the releases high through this period – foregoing the inter-pulse saddle – is the hypothesis that persistent high flows are needed to hold migrated, reproductive adult pallids upstream near the dam.

Variation 2A: This test flow is a variation of Alternative 2. The parameters for Alternative 2A are the same as described for Alternative 2 except that the Attraction Flow is initiated on April 9, rather than April 16, and the Spawning Cue flow would be initiated on May 21, rather than May 28. The difference in timing follows the same reasoning as described for Alternative 1A.

Variation 2B: This test flow is a variation of Alternative 2. The parameters for Alternative 2B are the same as described for Alternative 2 except that the Attraction Flow is initiated on April 23, rather than April 16, and the Spawning Cue flow is initiated on June 4, rather than May 21. The difference in timing follows the same reasoning as described for Alternative 1B.

1.5 Objectives

The fundamental and sub-objectives for pallid sturgeon (see Figure 1-1) provide the preferred basis for evaluation of the effects of alternatives on pallid sturgeon. Quantifying each alternative's effect on recruitment to age 1 and on population size of the UMR demographic unit of pallid sturgeon (upper Missouri and Yellowstone Rivers) would permit comparison of effects of each alternative to the no action alternative using those metrics.

While the ability to quantify those attributes remains limited and subject to moderate uncertainty, recent advances in scientific understanding derived from Level 1 and 2 research efforts under the MRRP have led to the development of modeling capabilities suitable for alternative comparisons. These models can quantify the frequency with which test flows might be implemented, the probability that any drifting free embryos produced might settle in lotic habitats on the UMR, and the effects of associated recruitment on pallid sturgeon population size. As the models are refined and validated using monitoring results and data from ongoing and planned research, their use for guiding future management decisions (e.g. experimental designs, near real-time operations, assessing performance of test flows, etc.) will be enhanced.

2 Modeling Approach

2.1 Existing Conceptual Models

Conceptual Ecological Models (CEMs) are recommended for all USACE ecosystem restoration projects due to their utility to increase understanding, identify potential alternatives, and facilitate team dialog (Fischenich 2008, USACE 2011). Conceptual models also inform the development of quantitative ecological models (Swannack et al. 2012).

Population-level CEMs developed during the MRRP Effects Analysis (EA) used the Wildhaber et al (2007) model as a basis for describing pallid sturgeon life cycle transitions and the effects of System operations on recruitment to the next life stage (Jacobson et al. 2015).

Best available science developed during the EA and presented in the SAMP was reviewed and updated to reflect new knowledge since the EA by the MRRP Technical Team in the Fort Peck Framework. Four effects pathway diagrams (a form of CEM) were prepared to help organize discussions of currently hypothesized links between system operations and impacts to pallid sturgeon. A diagram was developed for each hydrograph component: A) attraction and holding (in the Missouri River); B) spawning; C) drift; D) post-drift.

The effects pathway diagrams, the CEMs from the EA presented in the SAMP, and the supporting documentation for each provided a foundation for the development of alternatives for Fort Peck and the associated adaptive management framework that would guide their implementation, evaluation, and (if needed) adjustment over time.

2.2 Conceptualization underpinning the Drift and Settling Model

Despite documented spawning in the Yellowstone River and recent evidence of spawning in the UMR (DeLonay et al. 2016b), there has been no detectable survival from spawning through the first year of life of wild pallid sturgeon over the past several decades (Braaten et al. 2012, Braaten et al. 2015). The lack of observed pallid sturgeon recruitment in the UMR has been tied to several factors, most notably 1) inadequate dispersal distance due to fragmentation as a result of the construction of the water management system and its ongoing operation, 2) altered water temperatures, 3) altered flow regime, and 4) altered sediment/turbidity regime (Jacobson et al. 2016; Fischenich et al. 2018; USFWS 2018).

The larval drift hypothesis (LDH) asserts that "there is insufficient length of free-flowing riverine habitat available between spawning and settling locations in fragmented river reaches for pallid sturgeon free embryos to complete ontogenetic development, transition to benthic-oriented larvae, and survive" (Braaten et al. 2016). Anoxic reservoir sediments in the headwaters of Lake Sakakawea have been associated with larval mortality based on observations in Fort Peck Lake (Bramblett and Scholl 2015; Guy et al. 2015). Reservoir conditions may also contribute to mortality through enhanced predation on larval sturgeons and limited opportunities for juvenile foraging (DeLonay et al. 2016a) or due to a lack of currents for orientation (Mrnak et al. 2020). It is hypothesized by extension that drifting larval fish that enter the Lake Sakakawea headwaters perish. The DSM estimates the proportion of drifting free embryos that settle upriver of the headwater zone and are available to contribute to population growth, which is assessed using a demographic population model.

In the present analysis, management actions to address these issues include modifying the operational hydrograph at Fort Peck Dam to better replicate aspects of the historical hydrograph linked to adult pallid sturgeon attraction, aggregation and spawning. Spillway releases are used to increase water temperatures in the UMR during the attraction period and through spawning, hatch, and downstream dispersal in order to increase developmental rates and, correspondingly, the proportion of exogenously-feeding larvae that remain upstream of anoxic zones in the Lake Sakakawea pool where mortality is assumed.

The generic form of the proposed action is conceptualized in Figure 2-1, with an emphasis on the physical processes and the ecological responses associated with the pallid sturgeon objectives. The focus of the DSM is the assessment of the combined effects of flow and temperature alterations on the proportion of pallid sturgeon embryos remaining upstream of the Lake Sakakawea anoxic zone at settling and first feeding. This then becomes a key variable in the Pallid Sturgeon Demographic Population Model (DPM) (p_{ret} in the population model), which quantifies the effects of these actions on the long-term population growth rate (λ in the population model) and expected time to quasiextinction.

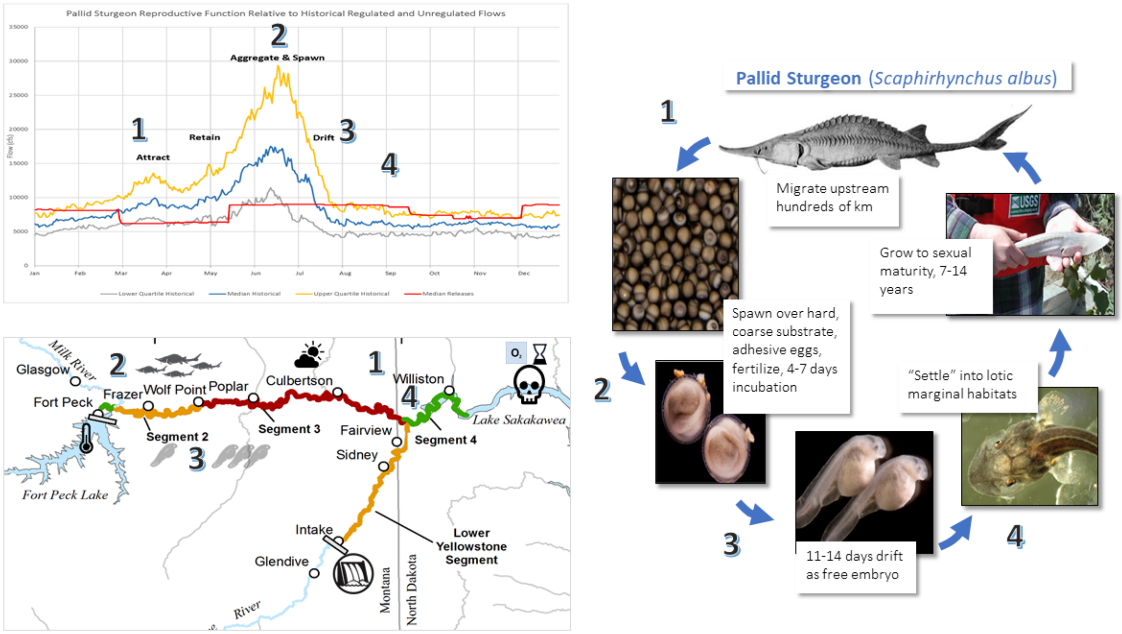

Figure 2-1. Conceptual model of the effects of Fort Peck management actions on pallid sturgeon used to guide numerical model development.

A March-April attraction flow (1) draws adult pallid sturgeon well upstream on the Missouri River - preferably near the Milk River or spillway confluence - and retains the fish while they condition for the spawn. Spawning (2) is triggered by a second hydrograph rise in May-June that is accompanied by warmer water releases over the Fort Peck spillway (and potentially from Milk River inflows). The Fort Peck Framework describes the assumptions underpinning this component of the action, which involves a doubling of the normal flow using historical rates of change in flow magnitude for the rising and falling limbs of the release. Components 1 and 2 are not directly addressed by the DSM, but are included in the spawning submodel and can be more fully parameterized in the population model.

The DSM is focused on post-hatch larval drift and development (3) to settling (4) stages of the pallid sturgeon life cycle. Drift refers to the dispersal (movement of young fish away from a spawning site), mainly by hydraulic processes. Free embryos drift passively and develop physiologically until they are capable of rheotactic orientation (Mrnak et al. 2020), after which they are presumed to exhibit some benthic orientation, drift more slowly, and develop exogenous feeding capability, at which point they settle and begin benthic feeding. The drift and development process is temperature-dependent and lasts a week or two. The distribution of a cohort at the time of settling is, therefore, dependent upon the time and location of spawning, (velocity driven) dispersion, and (temperature driven) development rate.

2.3 Conceptualization underpinning the Demographic Population Model

The conceptual underpinning of the DPM builds upon that of the DSM, described in the previous section. While the DSM focuses on the post-hatch larval drift and development to settling stages of the pallid sturgeon life cycle (3 and 4 in Figure 2-1), the DPM focuses on the full pallid sturgeon life cycle, from egg to spawning adult, combining the effects of management actions on spawning and recruitment to exogenously feeding (1-4 in Figure 2-1).

The DPM uses the CEM presented in Jacobson et al. (2015) as its conceptual basis, eliminates the stocking components and incorporates the various stages into age classes. In the DPM, for example, age-15 females include females from the juvenile and pre-spawning, spawning, post-spawning, and recrudescent adult CEM stages by proportioning this age-class into immature, reproductively-ready, and mature but not reproductively-ready to spawn females. A conceptual model of the age-structured DPM is depicted in Figure 4-1.

2.4 Model Structure for the Fort Peck DEIS

Figure 2-2 represents the modeling framework applied to the Fort Peck DEIS to generate measures of benefit and impact for each alternative. Hydrologic Engineering Center (HEC) Reservoir System Simulation (HEC-ResSim) and River Analysis System (HEC-RAS) models were used to assess the hydrologic and hydraulic effects of alternatives and serve as a basis for all other modeling. These are described in detail in the EIS appendices (USACE 2021).

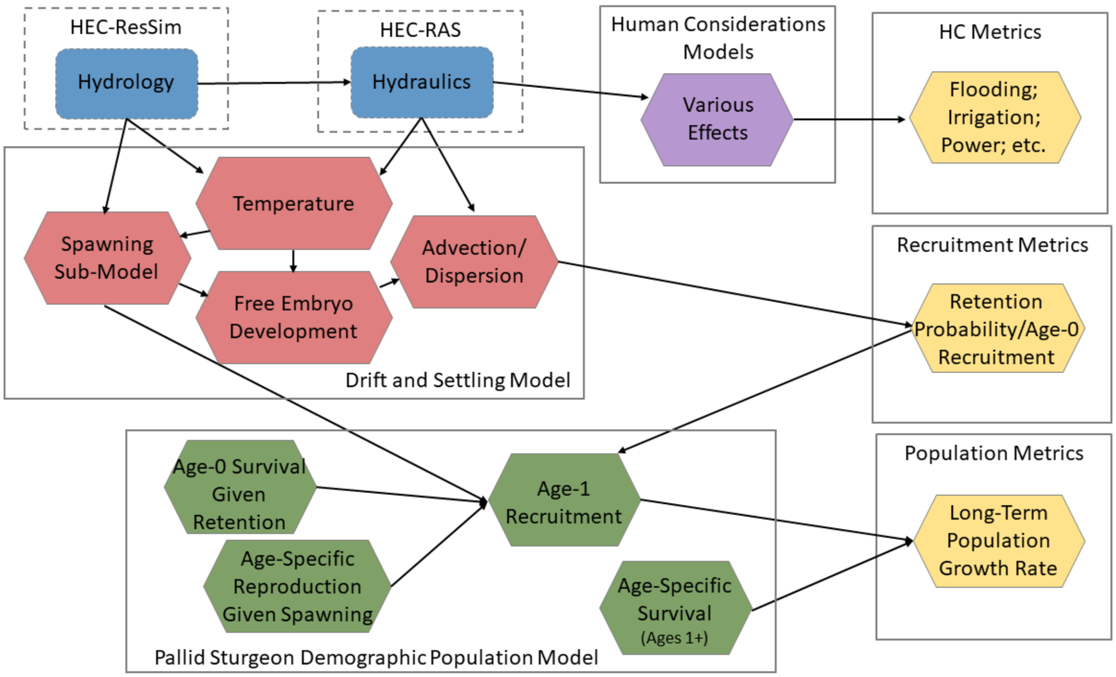

Figure 2-2. Graphical representation of the modeling for the Fort Peck DEIS.

Human Considerations (HC) impacts models provided a measure of the consequences of alternatives to the following categories of stakeholder interests: agriculture; commercial sand and gravel dredging; environmental conservation / fish and wildlife; flood risk management; irrigation; hydropower; local government; navigation; recreation; Tribal and cultural; water quality and water supply; thermal power; and wastewater. These models are described in the DEIS (USACE 2021).

Benefits to pallid sturgeon were assessed using two connected models:

a. an integrated advection/dispersion and temperature model to estimate the fraction of embryos that would develop to the exogenously feeding stage and be “retained” (by settling) in the riverine portion of the UMR (Fischenich 2019); and

b. population modeling to assess expected long-term population growth rates given the predicted retention, age-0 survival given retention, age-specific reproduction given spawning, and age-specific survival for age-1+ pallid sturgeon (Reynolds and Colvin 2019).

The Drift and Settling Model (DSM) couples an assessment of larval dispersion and temperature-dependent development to determine the proportion of larvae likely to remain upriver of the Lake Sakakawea headwaters, which are presumed to be lethal to pallid sturgeon larvae due to anoxic conditions at the bed (Bramblett and Scholl 2015; Guy et al. 2015). The primary model output, retention probability, serves as both a useful benefit metric for the EIS and as a critical input to the DPM, which assesses the effects of alternatives on the long-term population trends for the Upper River pallid sturgeon demographic unit. The DSM is described in detail in Chapter 3.

A key difference from earlier A/D modeling (Fischenich et al. 2014; Erwin et al. 2018) is that the DSM couples one-dimensional A/D computations with hourly water temperatures throughout the system calculated using an energy budget based on prevailing weather conditions (air temperature, humidity, cloudiness, pressure, solar radiation and wind speed), water temperatures for the reservoir and tributaries, and release operations. A spawning submodel (see section 2.5) is applied to determine the likelihood of spawning in a given year based on flow and temperature conditions. A settling submodel is used to determine the distribution of pallid sturgeon larvae at the onset of settling and exogenous feeding. Settling is assumed to occur once thermal exposure thresholds are met using one of two free embryo development models (Braaten 2011; Chojnacki and DeLonay 2019). A relation for onset of rheotaxis (upstream orientation) by Mrnek et al. (2020) was also applied using the same thermal calculations and used as a check on the settling model (i.e., rheotactic development occurs shortly prior to settling).

The DPM (Reynolds and Colvin 2019; Chapter 4) is an age-structured model used to assess the effects to population dynamics of alternative management actions at Fort Peck Dam. It is a pre-breeding Leslie matrix model constructed and analyzed in R (R Development Core Team 2010), in which age-specific fertility values are a function of the probability of free-embryo retention and the proportion of reproductively-ready females spawning in the Missouri River. These vary by management alternative and annual conditions. The DPM has two primary population metric outputs: (1) long-term population growth rate given alternative and annual conditions and (2) expected time to quasiextinction given environmental variability. The model is described in detail in Chapter 4.

In addition to providing a metrics for comparing Fort Peck flow alternatives, the DSM and DPM can be used for sensitivity analyses that inform actions and conditions that improve population growth rates. The DPM can further be used to explore the regions of parameter space (spawning, retention, age-0 survival space) for which population growth is expected, a first step in understanding pallid sturgeon population viability as related to management actions.

2.5 Attraction and Spawning Assumptions

The proposed management actions at Fort Peck Dam evaluated in this EIS are intended to attract reproductive pallid sturgeon as far upstream on the UMR as possible, encourage spawning under suitable flow conditions, and promote physiological development of drifting free embryos to the settling stage prior to drifting into the Lake Sakakawea headwaters (through reduced flows and increased water temperatures). The knowledge required to model the alternatives has been significantly advanced recently for the post-hatch components of the process, as described in Chapter 3. Assumptions regarding attraction and spawning remain more uncertain.

A spawning submodel is utilized to determine whether a spawning event is assumed in each year of the simulation period for each alternative, as well as the date in the time series that spawning and hatch are expected. Spawning is treated as a binary condition in the DSM (i.e., spawning is assumed to occur and drift is analyzed for that year, or no spawning and zero retention/recruitment is assumed). Spawning is further parameterized in the DPM in order to quantify the magnitude of the spawning (i.e., the proportion of gravid females likely to spawn in the UMR near Fort Peck Dam).

The precise factors necessary for spawning remain a source of uncertainty for the Fort Peck EIS. A conceptual model of spawning would incorporate several environmental variables, including temperature, flow, photoperiod, etc., as well as biological factors such as maturity and time since last spawn. Confirmed spawning in the UMR above the Yellowstone confluence has occurred only once (Jacobson et al. 2015), so empirical evidence is drawn mainly from the Yellowstone River. Spawning generally occurs there early in the hydrograph recession from mid June to the first week in July. An apparent water temperature threshold for pallid sturgeon spawning of 16°C has also been identified (DeLonay et al. 2016a).

The temperature at which a female spawns is conditioned by the temperatures experienced in the weeks or months previous to spawning that cause the progression of egg maturation during migration and ovulation at the spawning site. Thus, a thermal stimulus is required and female fish must be able to identify a location with warming water for her oocytes to mature to the point where she can respond to the attentions of males, ovulate, and spawn (A. DeLonay personal communication, October, 2019).

Temperature of releases from Fort Peck Dam reflect the deep-water intake in the reservoir pool, so discharges remain relatively cold throughout most of the year. Temperatures are typically below 14°C in late spring/early summer when spawning would otherwise occur (USACE 2009). Surface temperatures (upper five feet) in Fort Peck Lake warm rapidly during this period; typically from about 16°C to more than 20°C (Figure 2-3). Consequently, proposed management actions for the Fort Peck DEIS involve spillway releases of Fort Peck surface waters to augment flows passing through the powerhouse, increasing flow magnitude and temperatures in order to attract and condition fish for spawning.

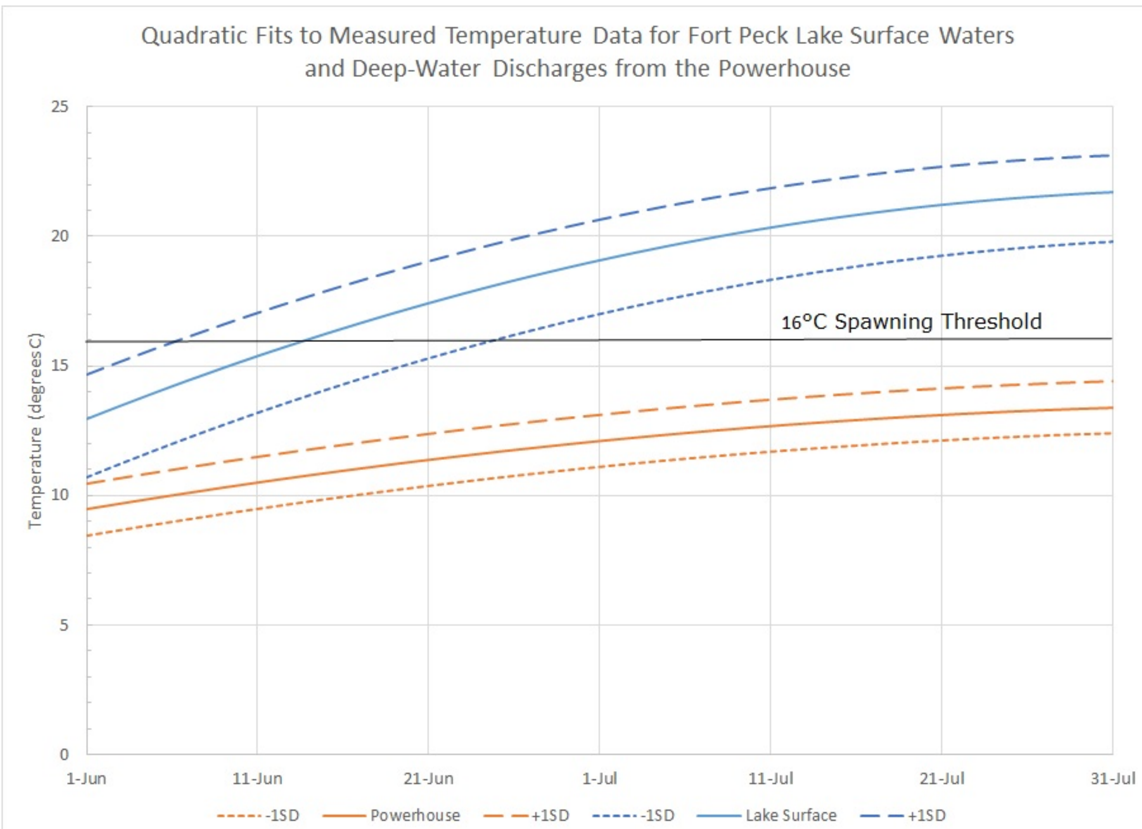

Figure 2-3. June/July Fort Peck Lake surface and powerhouse release temperatures based on a best fit of historical measurements.

The spawning submodel applies a rule set requiring the following conditions be met for spawning: a 16°C temperature threshold occurring in conjunction with a flow peak in excess of 20,000 cfs in June or July and spillway flows sufficient to maintain a warm-water seam downstream of the spillway confluence. This roughly translates to a flow in excess of 17,500 cfs after June 15 in a year with "normal" temperatures. These criteria are applied to each year in the period of record (POR) for each alternative to screen for years to analyze for drift and settling. Hydrographs are taken directly from the ResSim models for each alternative, while water temperatures are calculated using relations derived from quadratic fits to measured water temperatures organized by Julian calendar day for the lake surface (spillway flows) and UMR immediately below the powerhouse. Relations developed for median and ± one standard deviation (SD) were used to represent "normal" conditions as well as warm and cool periods, respectively. Quadratic regression analyses of the data for lake surface waters yielded the fallowing relations:

$T = -0.00195d^2 + 0.865 - 76$	cool conditions	2-1
$T = -0.00195d^2 + 0.86d - 73$	normal conditions	2-2
$T = -0.00195d^2 + 0.855d - 70.5$	warm conditions	2-3

Where

T = water temperature in degrees Celsius
d = day of the Julian calendar year

Note that the above relations are applicable only to dates in the March to November period as both lake surface and UMR temperatures tend to zero the remainder of the year. Observed temperatures from just downstream of the Fort Peck Powerhouse yield the following approximations:

$T = -0.00075d^2 + 0.34 - 26$	cool conditions	2-4
$T = -0.00075d^2 + 0.34 - 25$	normal conditions	2-5
$T = -0.00075d^2 + 0.34d - 24$	warm conditions	2-6

Mixing processes at the confluence of the spillway apron and the river can have significant practical implications for water temperatures and spawning. Cold hypolimnetic releases from the powerhouse travel 7.8 miles before the confluence with warmer spilled flows, which tend to hug the south bank of the river for several miles (Figure 2-4). The Milk River enters on the north bank of the river about 1.2 miles further downstream and warm inputs from the Milk River can maintain warmer temps on the north bank of the river for several miles.

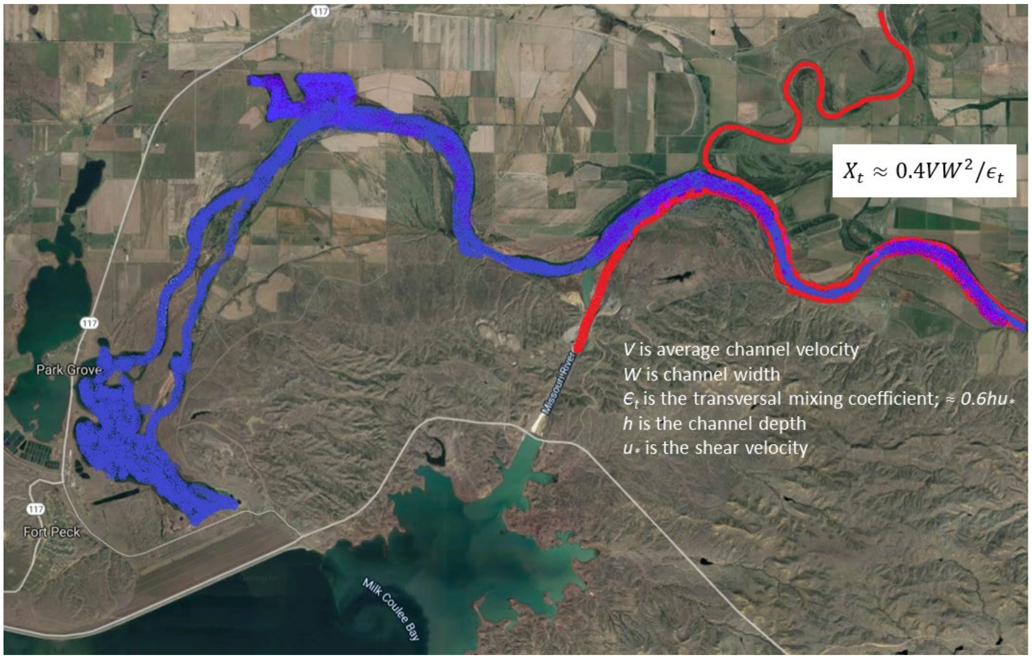

Figure 2-4. Depiction of transversal mixing of relatively warm flows from the spillway (south side of channel) and Milk River (north side of channel) with cold water from the powerhouse.

Theory suggests that the distance required for complete downstream mixing at river confluences increases as the square of post junction width (Rodriguez Benitez, et al. 2015), which partly explains why big rivers can take so long to mix. While field observations suggest that mixing is not due strictly to turbulent diffusive processes and certain hydrodynamic, weather, and water quality conditions also affect mixing rate, mixing distance can be approximated by (Julien 2002):

$$X_t \approx 0.4VW^2/\epsilon_t \qquad 2\text{-}7$$

Where

V is average channel velocity

W is channel width

ϵ_t is the transversal mixing coefficient; ≈ $0.6hu_*$

h is the channel depth

u_* is the shear velocity

Because transversal mixing is low, pallid sturgeon can utilize the seam of warm water below the spillway (or the Milk River) confluence for conditioning and spawning, even when powerhouse releases and cross-channel average temperatures downstream of the mixing zone are below thresholds. The spawning model for preliminary analyses utilized a flow threshold of 20,000 cfs as a criterion to ensure adequate warm water for spawning. The model was refined for subsequent analyses and the 16 °C criterion could be met by either mixed flows or spillway flows in isolation, provided the spillway flows are at least 20 percent of the total flow (required to maintain an unmixed warmwater seam for spawning).

The spawning model was also used to establish a date for onset of drift, which occurs immediately after hatch for pallid sturgeon (Jacobson et al. 2016). If the temperature criteria were met during the rising limb of the hydrograph or within three days post peak, spawning was assumed to occur three days after the initiation of recession (the mean time to spawning observed on the Yellowstone River; R. Jacobson, personal communication, September, 2019). If the criteria were met three or more days after recession onset, spawning was assumed to occur that same day. Figure 2-5 is a schematic of the spawning criteria.

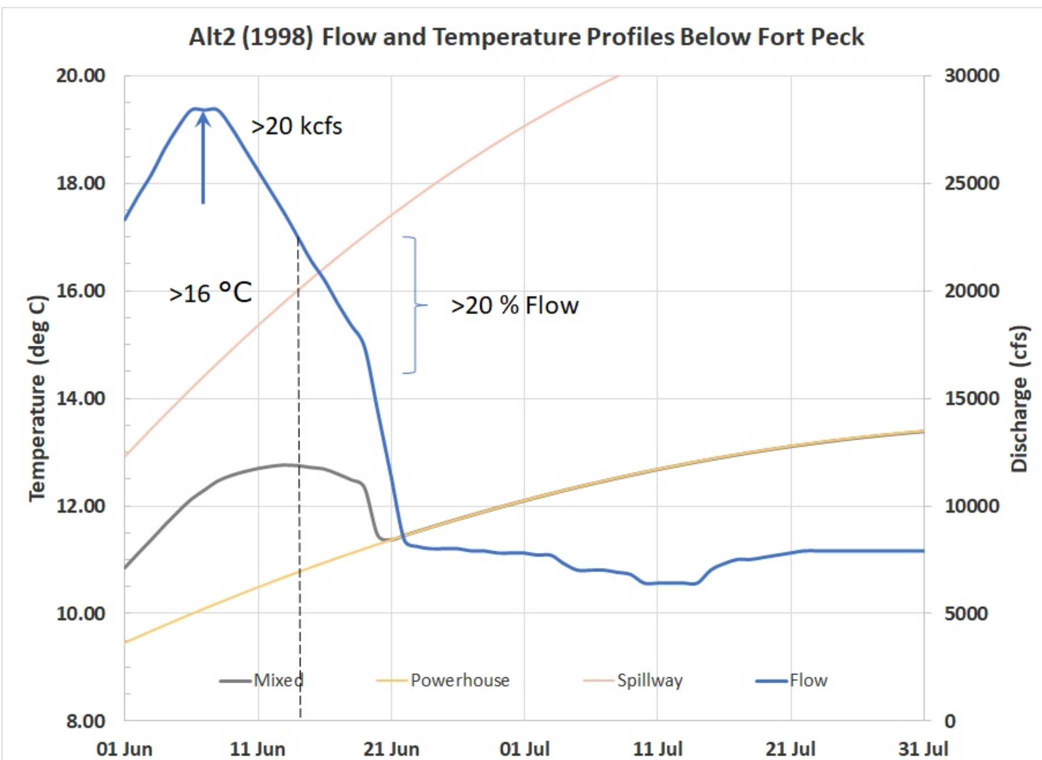

Figure 2-5. Depiction of spawning assumptions applied to an example hydrograph and temperature series.

The embryo life stage from fertilization to hatch is usually about 5–8 days, depending on temperature (DeLonay 2016). Given the DSM thermal limit for spawning (16 ˚C) is on the low end of the temperature spectrum, 7 days was used as the development time from spawning to assumed hatch in the modeling.

Although there is strong evidence of synchronicity in pallid sturgeon spawning, variability among individual spawners and in time to hatch is likely significant.

Given the uncertainty regarding the above criteria and natural variation in spawning and time to hatch, assumptions regarding hatch date could be a significant factor in calculated retention. Accordingly, further sensitivity analyses to test assumptions and study (research and monitoring) regarding spawning, hatch, and drift onset is recommended. The USACE initiated an expert elicitation process to inform analyses for the EIS and advance understanding needed for experimental design and monitoring strategies under adaptive management. This is described in Chapter 6.

The spawning model was also used to establish the proportion of females spawning below Fort Peck dam, a highly uncertain value. As a first approach, it was assumed that half of all reproductively-ready female pallid sturgeon spawn below Fort Peck dam, provided spawning conditions were met. This 0.5 spawning proportion represents a scenario in which spawning conditions on the UMR and the Yellowstone River are equal and no atresia occurs. If the discharge and water temperature criteria were not met, then the UMR spawning proportion was estimated as 0, assuming all reproductively-ready (i.e., gravid) females either spawn in the Yellowstone River or become atretic after not finding suitable spawning conditions.

It is unlikely that the proportion of reproductively-ready females that spawn below Fort Peck is constant across flow alternatives and years; moreover, spawning proportion could be a significant factor in comparing flow alternatives. As such, further studies and modeling analyses are recommended to assess spawning proportion as a function of temperature and flow, and to assess the implications of this factor on alternative performance. Improving the current formulation of the spawning model with respect to spawning proportion is one objective of the ongoing expert elicitation mentioned in the previous paragraph and described in Chapter 6.

3 Drift and Settling Model

Figure 2-2 shows the DSM in relation to the other models used in the Fort Peck DEIS. Retention probability (p_{ret}) is the primary DSM output and refers to the proportion of drifting free embryos that settle in free-flowing reaches of the UMR upstream of the Lake Sakakawea headwaters. It is both a measure of benefit (for relative comparisons of alternatives) and a critical input variable for the DPM. In order to determine the retention probability, the DSM employs several submodels. These are shown in Figure 3-1 and discussed in the following sections.

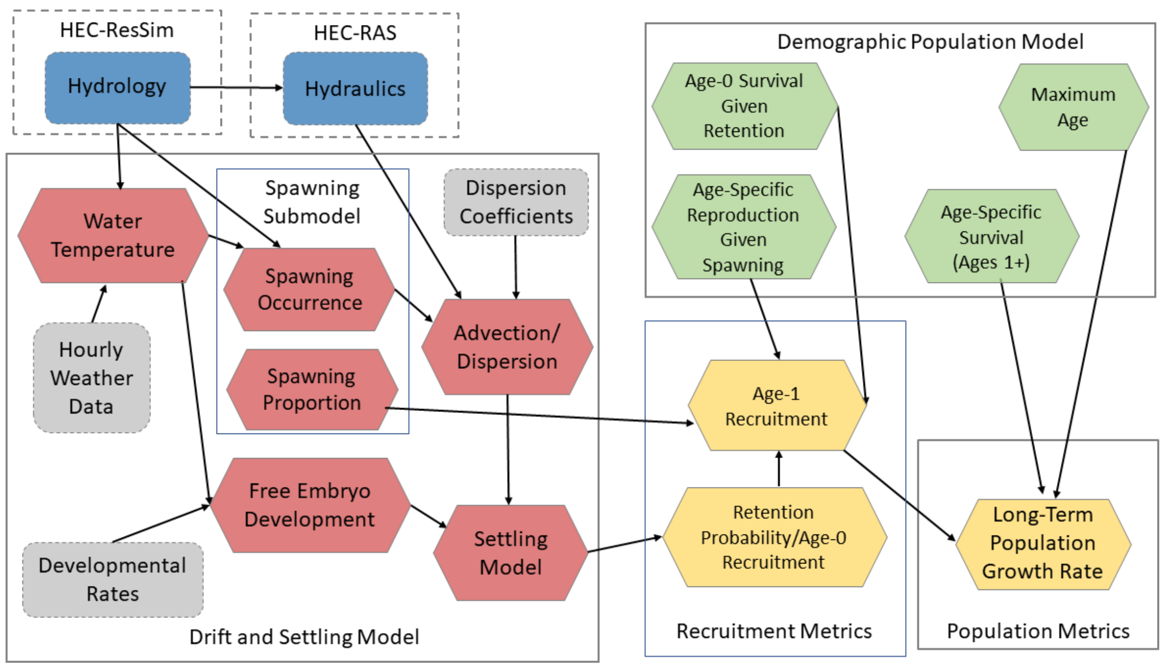

Figure 3-1. Schematic of the Drift and Settling Model and its relationship to other models used for the Fort Peck DEIS.

The spawning submodel is used to determine whether a spawning event is assumed to occur for each year of the simulation period for each alternative, as well as when spawning would be expected. Spawning is treated as a binary condition in the DSM (i.e. spawning is assumed to occur and drift is analyzed for that year, or no spawning and zero retention/recruitment is assumed). Spawning is further parameterized in the DPM in order to quantify the magnitude of the spawning by specifying the proportion of gravid females spawning on the UMR.

Spawning and hatch assumptions remain important in the DSM analyses because decisions about whether spawning occurs materially affects performance of an alternative and model results are highly sensitive to temperature (water and air) and flow conditions, both of which vary temporally within the sphere of assumptions about spawning and hatch. This is covered further in section 3.5.1, which covers sensitivity analyses.

The temperature submodel predicts the water temperatures released from Fort Peck and for the UMR tributaries; these are calculated using Excel-based models based on historical measurements and utilized as boundary conditions in HEC-RAS. The water quality module in HEC-RAS is used to calculate time-variant water temperatures throughout the model domain, which includes the UMR from Fort Peck Dam to Garrison Dam, inclusive of the lower segments of tributaries.

Dispersal is simulated using a 1-D advection/dispersion (AD) model for drifting free embryos. This is also accomplished using the water quality module in HEC-RAS, parameterized with data from field measurements of dispersion. Although more sophisticated models have been used to simulate dispersal (see Erwin et al. 2018), HEC-RAS is currently well-integrated and extensively used in Missouri River Basin to route flow and evaluate effects of management actions and has been used previously for modeling pallid sturgeon AD (Fischenich 2014).

A settling submodel is used to determine the distribution of pallid sturgeon larvae at the onset of exogenous feeding. Larvae settling within the anoxic zone of Lake Sakakawea are assigned a survival probability of zero, while those retained upstream of this zone are given a higher probability. The settling submodels (there are four optional models described in section 3.4) integrate HEC-RAS outputs of the distribution of drifting free embryos and temperatures over time to track their cumulative thermal exposure. Settling is assumed to occur once exposure thresholds are met using one of two free embryo development models (Braaten 2011; Chojnacki and DeLonay 2019). In addition, thermal exposure is used to assess onset of rheotaxis using a relation from Mrnak et al (2020); this provides a check on settling calculations.

Primary outputs from the model are the retention probabilities in each year of the analysis period for each alternative. The Fort Peck DEIS analysis spans the period of record (POR) used for other study purposes, which is 1930 to 2012. Years without spawning are given a zero retention probability. In addition to the primary outputs, the DSM has been used for sensitivity analyses to develop response functions for environmental conditions, operational alternatives, etc.

3.1 Spawning Submodel Outputs

The primary output from the spawning model is a matrix showing the years in which spawning is assumed to occur for each alternative and the date of presumed spawning or hatch. Intermediate products include plots of the discharge and temperatures in the reach of the Missouri River from Fort Peck Dam to the point of full mixing – approximately 20 or 30 miles downstream of the confluence of the spillway flows with the mainstem river. Figure 3-2 is a matrix showing the dates in the POR for which the spawning criteria are met for each alternative. Years not listed in the table failed the spawning criteria for all alternatives.

Year	Hatch Date From Spawning Submodel							Temp Class
	Alt 1	Alt 1a	Alt 1b	Alt 2	Alt 2a	Alt 2b	No Action	
1930			24-Jun			24-Jun		Normal
1949			24-Jun			23-Jun		High
1966			*			3-Jul		Low
1975	16-Jul	16-Jul	16-Jul	16-Jul	16-Jul	16-Jul	16-Jul	Normal
1976	*		*	*		*	*	Normal
1980	21-Jun		26-Jun	21-Jun		25-Jun		Normal
1983	22-Jun		28-Jun	22-Jun		25-Jun		Normal
1985	22-Jun		28-Jun	22-Jun		25-Jun		Normal
1986	*		*	16-Jun		*		High
1987	17-Jun	*	25-Jun	17-Jun	15-Jun	25-Jun		High
1994			22-Jun			*		Normal
1997	5-Jul	5-Jul	12-Jul	5-Jul	12-Jul	5-Jul	5-Jul	High
2000	21-Jun		23-Jun	*		21-Jun		Normal
2011	3-Jul	3-Jul	3-Jul	3-Jul	3-Jul	3-Jul	3-Jul	Low
2012	21-Jun		*	*		*		Normal

Figure 3-2. Spawning submodel results showing years in which spawning is assumed to occur for each alternative and the presumed hatch date (spawning is 7 days earlier). Light orange cells with asterisk indicate criteria nearly met and may represent low probability of spawning. Temperature class for each year is shown on the right.

An example of the assessment that occurs for each year/alternative is shown for 1985 and Alternative 2 inFigure 3-3. June 1-15 temperatures at Glasgow, MT were classified as "normal" (see section 2.6), so the normal temperature curve for spill temperatures is applied. The 16 °C threshold is not met for mixed flows, but the spillway flows reach this threshold while flows are more than 20 percent of the total, so spawning is assumed to occur. Because the threshold is met on the recession of the hydrograph, the spawning date is set on the date the threshold is met (June 15) and the hatch date is set seven days later (22 June).

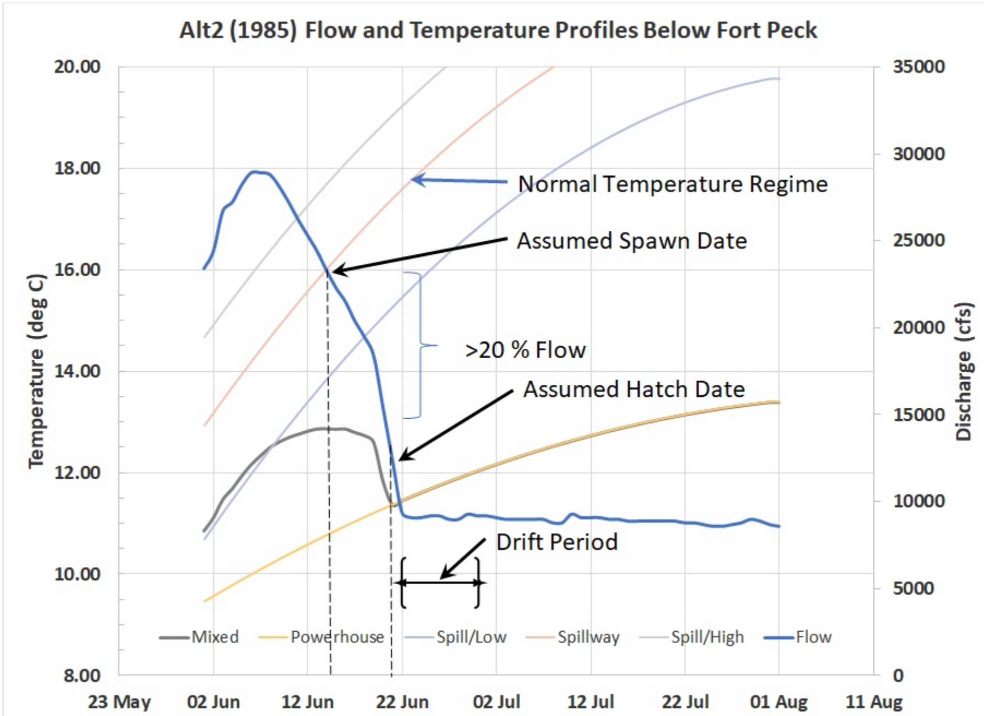

Figure 3-3. Example output plot from spawning submodel showing calculated temperatures (1985 had "normal" temperatures) and flows with a consequent determination that spawning would likely occur with hatch on 21 June.

In Figure 3-4, a hydrograph is executed for Alternative 2b in 1994. The 16 °C threshold is not met for the lake surface/spillway flows until after flows drop to 8,000 cfs. To meet power demands, the entire flow is from cold powerhouse releases. Spawning is assumed not to occur and AD modeling not performed.

The DSM does not provide a direct measure of recruitment to age 1 or population demographics. Rather, it provides a critical input to the UMR DPM, which does provide estimates for these metrics. Specifically, the DSM assesses the likelihood of spawning on the UMR and estimates the proportion of drifting pallid sturgeon larvae that remain upstream of the Lake Sakakawea pool when they reach settling stage, based on temperature-dependent models of larval development.

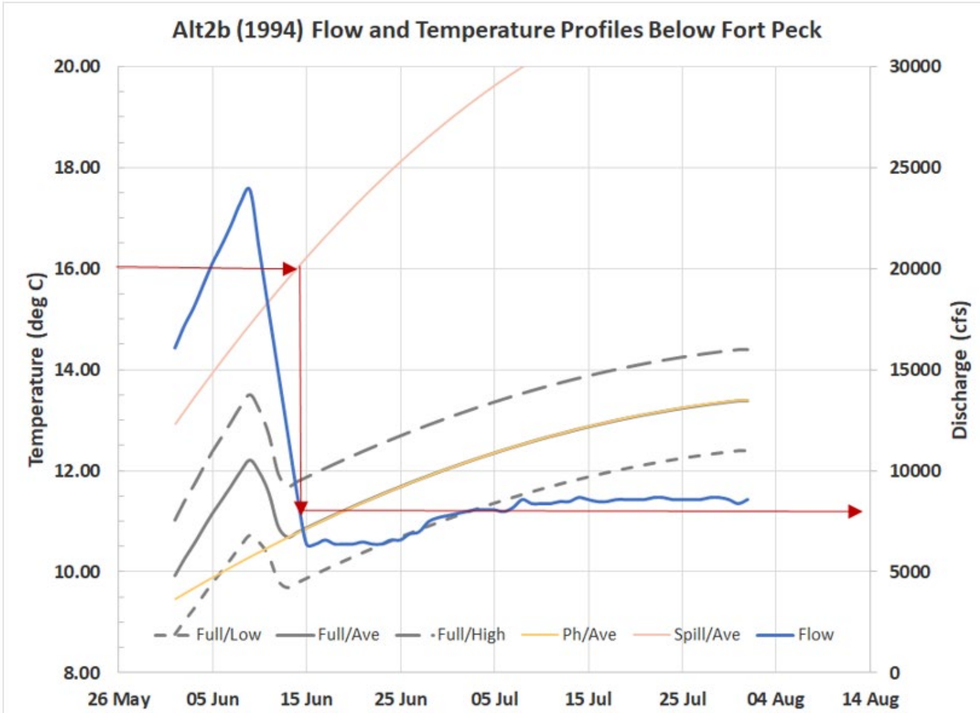

Figure 3-4. Example of an alternative/year when spawning criteria are not met.

3.2 Advection and Dispersion Modeling

Free embryo dispersal in the DSM is simulated with a one-dimensional AD model. This is accomplished using the water quality module in HEC-RAS, parameterized with data from field measurements of dispersion (Erwin et al. 2018). The water quality module permits the modeling of an arbitrary constituent using the QUICKEST-ULTIMATE explicit numerical scheme (Leonard, 1991) to solve the 1-D AD equation:

$$V^{n+1}\varphi^{n+1} = V^{n}\varphi^{n} + \Delta t\left[Q_{up}\varphi^{*}_{up} - Q_{dn}\varphi^{*}_{up} + \Gamma_{dn}A_{dn}\frac{\partial\varphi^{*}}{\partial x_{dn}} - \Gamma_{up}A_{up}\frac{\partial\varphi^{*}}{\partial x_{up}}\right] + \Delta t\frac{\partial\varphi}{\partial t}SS \quad 3\text{-}1$$

Where

φ^{n+1} = concentration at present time step (kg m-3)

φ^{n} = concentration at previous time step (kg m-3)

φ^{*}_{up} = concentration at upstream face (kg m-3)

$\frac{\partial\varphi^{*}}{\partial x_{up}}$ = derivative at upstream face (kg m-4)

Γ_{up} = upstream face dispersion coefficient ($m^2\ s^{-1}$)

V^{n+1} = volume of the water quality cell at next time step (m^3)

V^n = volume of the water quality cell at current time step (m^3)

Q_{up} = upstream face flow ($m^3\ s^{-1}$)

A_{up} = cross sectional upstream face area (m^2)

$\frac{\partial \varphi}{\partial t} SS$ = cell energy budget terms ($C\ m^{-3}s^{-1}$)

Subscripts up and dn refer to the upstream or downstream face, respectively, of water quality cells established at cross sections in the HEC-RAS models. Calculations of AD are based on hydraulic conditions at the faces and are applied at the midpoint of each cell (Figure 3-5). Cell size and differences in hydraulic conditions across cell faces influence computational time and model stability. The model allows setting a minimum cell size, so multiple cells may be combined.

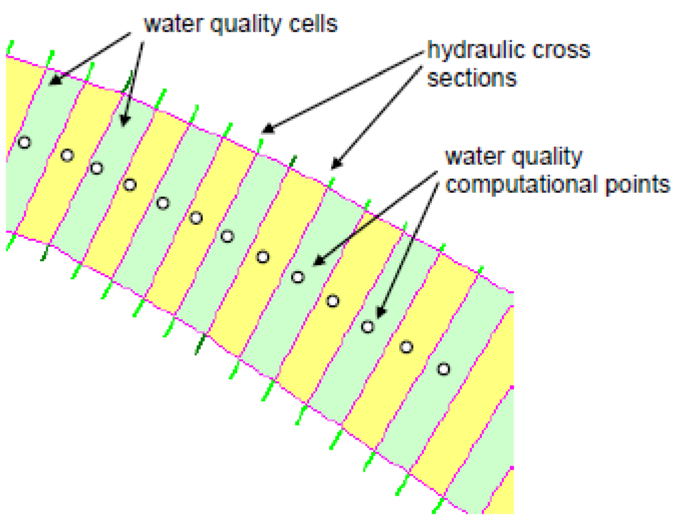

Figure 3-5. Schematic of water quality cells established within RAS models for calculating advection and dispersion.

Working, calibrated HEC-RAS models are needed to run the water quality model. The HEC-RAS models used in these analyses were developed by the USACE as part of ongoing adaptive management of the Missouri River, and were updated for the Fort Peck DEIS assessment using hydrology for each alternative from the ResSim models. Preliminary analyses used models calibrated to 2018 flows; subsequent analyses used models updated with bathymetric data collected in 2018 and 2019, calibrated to 2019 water surface elevations. The ResSim and HEC-RAS models are described in the DEIS documentation (USACE 2021).

The water quality module allows the user to specify a mass injection along a specified cross section within the HEC-RAS model using a previously run hydraulic solution. For the Fort Peck DEIS, the midpoint between the spillway apron and the Milk River confluence was used (RM 1762). The parameter capturing the magnitude of shear dispersion in the model is the longitudinal dispersion coefficient, Γ. Solution of the AD model requires a longitudinal dispersion coefficient, Γ that may either be specified by the user or computed based upon calculated velocity variations in the hydraulic model. In the latter case, the user may also specify upper and/or lower limits. For these analyses, values of Γ were calculated using the Fischer et al. (1979) relation in HEC-RAS

The A/D component of the water quality model simulates free embryos as passively drifting particles of neutral buoyancy. Improved understanding of drift, a complex, three-dimensional process, has been achieved with multidimensional particle tracking models and high-resolution data from laboratory studies that capture complex interactions between hydraulics and rapidly developing fish morphology and behavior (Schludermann et al. 2012, Glas et al. 2017). While more sophisticated numerical models that couple hydrodynamics and behavioral aspects of dispersal may be feasible, they are not needed for many decisions and the required high-resolution inputs, data-intensive parameterization, and computationally expensive attributes of more robust models can preclude their use.

In the current application, the model is sufficiently accurate for a relative comparison of alternatives; precise quantification of retention is not needed and higher-resolution models are unlikely to provide results that would alter the relative performance of alternatives. Moreover, the same modeling strategy has been successfully applied to this and other reaches of the Missouri River. Fischenich (2014) applied the same modeling approach to assess drift in the UMR and the results were substantiated by a dye trace study and monitoring of released free embryos and glass beads in a 2016 experiment (Erwin et al. 2018). The approach was also applied in the Erwin et al. analysis (2018) to data collected from a 2007 drift experiment near Wolf Point, MT. These field studies show that the DSM very closely matches the measured dispersion, but does tend to overestimate advection rates for drifting free embryos by about 5 to 10 percent. This observation is addressed further in section 3.4.3, which describes a rate adjustment applied in the settling submodel.

3.2.1 Model Parameterization and Calibration

Two Hydrologic Engineering Center (HEC) models underpin the DSM. USACE used the Reservoir System Simulation (HEC-ResSim) and River Analysis System

(HEC-RAS) models to assess effects of the alternatives. Outputs from HEC-ResSim provide the hydrology used in the DSM, while HEC-RAS is used for the hydraulic computations and water quality simulations. Parameterization and calibration of the ResSim models and the hydraulic component of HEC-RAS are addressed in the DEIS (USACE 2021). Application of the HEC-RAS water quality module to AD is discussed in this section and its application to temperature modeling is discussed in section 2.6.

Solution of the AD model requires a longitudinal dispersion coefficient, Γ that may either be specified by the user or computed based upon calculated velocity variations in the hydraulic model. In the latter case, the user may also specify upper and/or lower limits. For these analyses, values of Γ were calculated using the Fischer et al. (1979) relation in HEC-RAS but were constrained based on measurements and values calculated from dye trace studies and a controlled drift experiment involving the release and tracking of free embryos in the study reach (Erwin et al. 2018).

Dispersion coefficients for each water quality cell are calculated using Fischer's (1979) equation:

$$\boldsymbol{\Gamma = m * 0.011 \frac{u^2 w^2}{y\sqrt{gdS}}} \qquad 3\text{-}2$$

where

m = user assigned multiplier (unitless)

u = velocity at the face of the cell (m/s)

w = average channel width (m)

y = average channel depth (m)

u^* = shear velocity = $\sqrt{gdS}$ (m/s)

As used in the one-dimensional AD modeling approach, Γ represents the complex, three-dimensional transport processes that spread passive particles along the transport pathway; accurate estimation of Γ is therefore critical for accurate results. While HEC-RAS employs the theoretical approach proposed by Fischer et al. (1979), it permits specification of Γ values determined by other means. Approaches for estimating Γ: (1) experimental measurement (e.g. tracer studies), (2) empirical relations, and (3) application of theoretical equations like Fischer's (Carr and Rehmann 2007, Launay et al. 2015).

The multiplier in Equation 10 is used to address the fact that Fischer's equation is known to generate results up to four times that indicated by field data (USACE HEC 2016). A multiplier of 0.6 was applied to the present studies based on ADCP data, 2-D modeling, and dye tests for segments of the river within the project reach (Erwin and Jacobson 2014; USGS ADCP-derived coefficients [506 – 6047 ft2/s]; ERDC dye studies/2-D modeling [355, 408, 515 ft^2/s]). In addition to the multiplier, upper and lower limits were placed on the longitudinal dispersion coefficients based on the results of a comprehensive dye trace study in the reach and monitoring of drift for free embryos and glass beads released in the study reach in 2016. Limits for longitudinal dispersion coefficient were set at 100/500 ft^2/s for the smaller tributaries, and 1,500/3,000 ft^2/s for the Missouri and Yellowstone Rivers.

Requirements for modeling an arbitrary constituent include a time series of constituent concentration at all boundaries and initial condition values for each reach. These are all set to zero for the DSM simulations because simulation time windows are set to begin 7 days prior to hatch (to allow full stabilization of temperatures, which are calculated concurrently). Hatch is simulated by introducing a mass injection of the constituent at the presumed hatch location and time. We inject 1,000,000 grams at RM 1762 at time 0000 on the hatch date and assume 1 gram represents 1 free embryo.

Because computational time is determined by the shortest cell length, setting a minimum length can make a substantial difference in run times. We set the minimum cell length at 600 ft. Hydraulic simulations typically begin 7 days prior to hatch and end 14 days after hatch, with a computation interval of 5 minutes. A computation-level output file is generated from the unsteady hydraulic computations. Computation windows for AD analyses are the same as for the hydraulic simulations. Hydrodynamic continuity error resolution is set to mass conservation (at the cost of irregular concentrations). The upper limit on the computational time step is set to 15 minutes (actual time steps are determined by the model based on continuity) and outputs for velocity and advection mass of the constituent are generated on a three-hour interval and saved in a DSS file.

3.2.2 Model Outputs

AD model outputs are written to an output file (*.wqxx) that contains velocities and the mass and concentration of the arbitrary constituent for all water quality cells at the specified time interval. The output is also written to a DSS file. HEC-RAS has the ability to generate time series plots and animations that display model results and observed data at specified locations. These are useful for assessing mass or concentration over time at a location on the Missouri River and provide the shape of the AD curve (Figure 3-6).

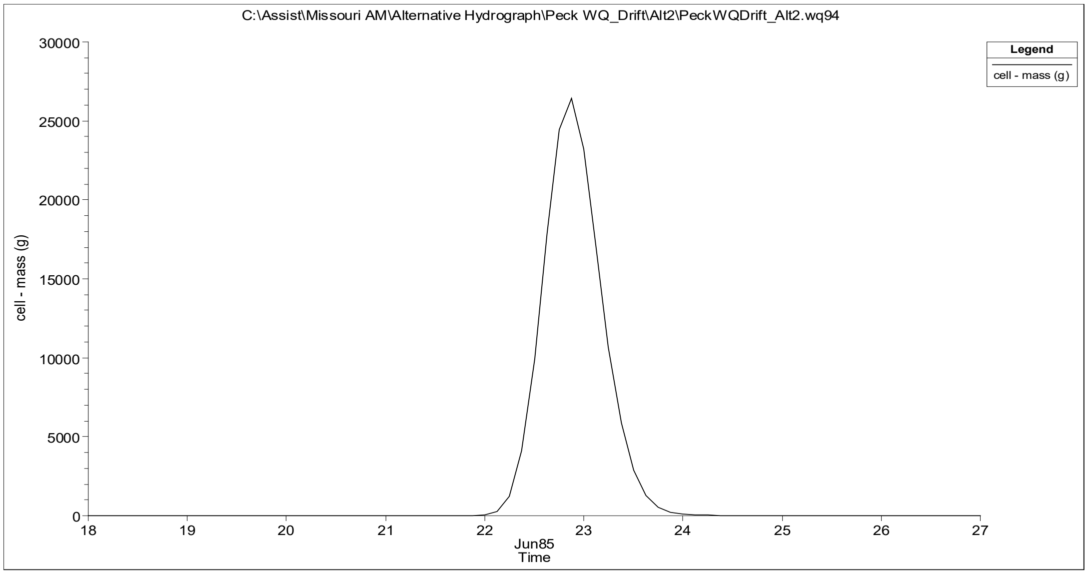

Figure 3-6. Example time-series plot showing cell mass at RM1550 for Alt 2 in 1985.

Spatial plots of any output variable can be generated (e.g. Figure 3-7). In addition to profile plots for particular simulation times, profile plots of daily mean, maximum, and minimum are also available. Schematic plots that display results in the form of a color-coded map can be generated (see Figure 3-8) and animated for presentation purposes.

Tabular outputs of time-series or spatial data may be generated from the *.wqxx file or DSS. The DSM uses tables of constituent mass at each water quality cell on a three-hour time step for retention calculations. These are generated in HEC-RAS and used as input to the Excel-based settling model (see section 3.4). Table 3-1 is an example of the AD output used for this purpose.

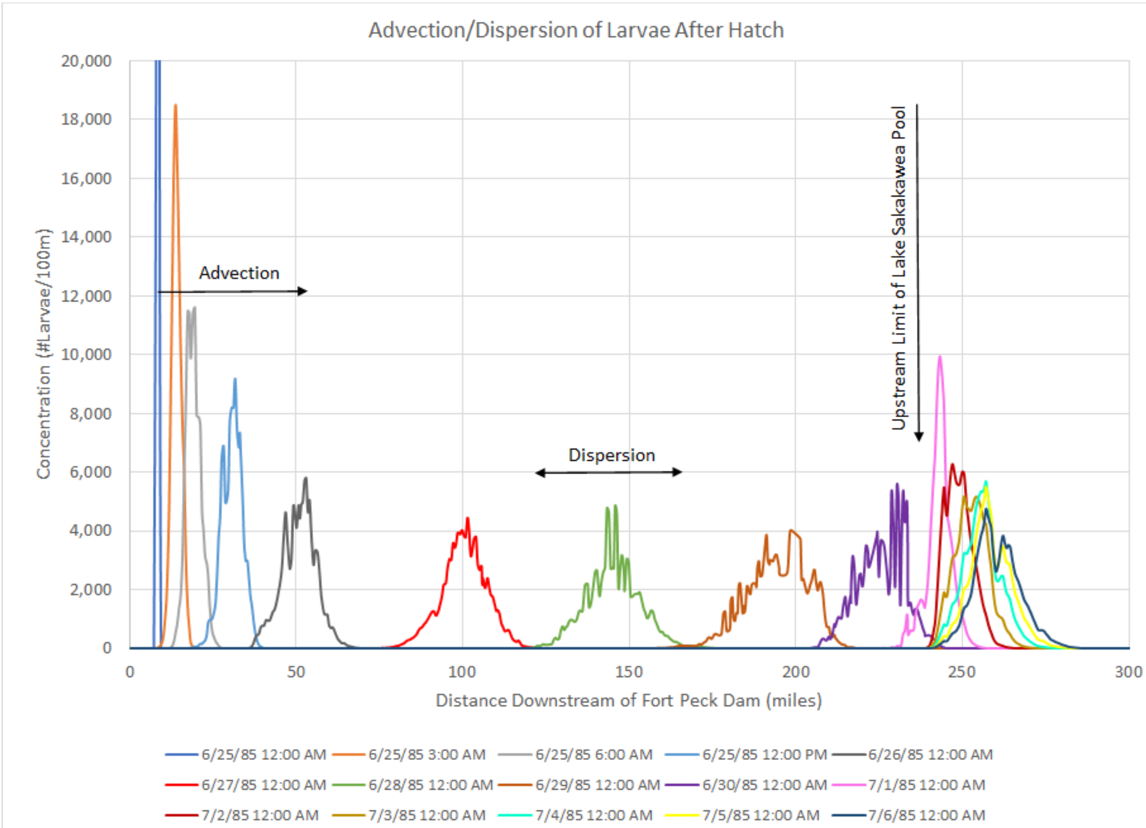

Figure 3-7. Example plot showing spatial distribution of simulated PS larvae, temperature, and velocity at three hour timesteps for alternative 2b in 1985.

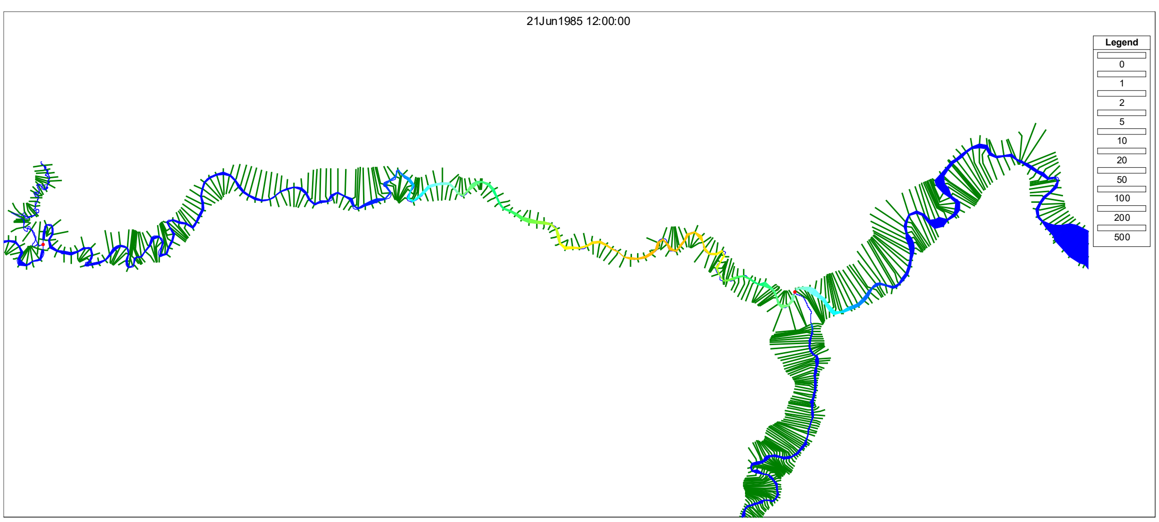

Figure 3-8. Spatial plot showing distribution of pallid sturgeon larvae at noon on 22 June 1985 for Alternative 2 based on AD modeling.

Table 3-1. Example tabular output from an AD model simulation of Alt 2/1985 showing the number of free embryos in each cell for a 10-mile reach over a 24-hour period.

River Mile	WQ Cell Length (m)	Cell Mass (g), or # Free Embryos for Indicated Date/Time in 1985								
		18-Jun 12:00	18-Jun 15:00	18-Jun 18:00	18-Jun 21:00	19-Jun 0:00	19-Jun 3:00	19-Jun 6:00	19-Jun 9:00	19-Jun 12:00
1732.58	771.43	631	38518	75761	24706	2979	250	45	28	25
1732.09	756.22	312	30844	83770	36384	5693	561	74	34	28
1731.63	860.75	152	25594	98990	57120	11286	1284	147	47	35
1731.05	866.85	51	15057	79802	57592	13376	1674	183	45	31
1730.51	809.36	16	7997	55527	48346	12847	1749	190	39	24
1730.02	845.65	7	5678	53226	57479	17880	2696	297	50	27
1729.51	842.39	2	3480	42098	53479	18523	2981	333	51	24
1729.02	998.39	1	2158	34614	52837	20741	3613	415	57	24
1728.37	796.41	0	1167	24518	44441	19601	3678	436	56	21
1727.87	885.44	0	763	20348	42553	20609	4098	498	61	20
1727.33	653.29	0	356	11717	27824	14653	3073	383	46	14
1726.88	891.50	0	344	14039	37960	21697	4798	615	72	20
1726.31	745.62	0	198	10333	32365	20363	4793	635	73	18
1725.8	801.99	0	140	9171	32758	22426	5572	760	86	20
1725.22	810.47	0	95	8044	33667	25645	6845	974	110	23
1724.67	860.48	0	66	7413	36640	31177	8962	1333	151	28
1724.14	870.90	0	39	6025	36073	34989	11009	1733	197	33
1723.6	857.67	0	22	4862	35608	39711	13797	2319	269	41
1723.06	885.09	0	12	4092	38475	51556	20576	3817	463	64

3.3 Temperature Modeling

Rate of development for drifting free embryos is temperature dependent, so temperature modeling is necessary to determine when the larvae are sufficiently mature to begin exogenous benthic feeding. The DSM temperature submodel uses the water quality module in HEC-RAS to calculate time-variant water temperatures in the UMR. The DSM also includes the tools to determine water temperatures released from Fort Peck and initial temperatures for the UMR tributaries; these are calculated external to HEC-RAS using Excel-based models fitted to measured data and are utilized as boundary conditions in the HEC-RAS model.

Water temperature simulation in HEC-RAS employs a full energy budget approach. Model input requirements include a full hydrodynamic solution from a HEC - RAS unsteady flow model, water temperatures at hydrodynamic boundaries, and detailed meteorological data. Output from the water temperature model includes results of intermediate calculations such as computation of individual energy budget terms, as well as computed water temperatures.

The HEC-RAS water temperature model solves the one-dimensional equation for thermal energy with additional terms to account for lateral inflow, solar radiation, and heat exchange with the atmosphere and streambed. Lateral inflow represents additional water entering the model domain as surface inflow, overland flow, interflow, and groundwater discharge. The heat transport equation is:

$$\frac{\partial}{\partial t}(\boldsymbol{VT_w}) = -\frac{\partial}{\partial x}(\boldsymbol{QT_w})\Delta \boldsymbol{x} + \frac{\partial}{\partial x}\left(\boldsymbol{A\Gamma}\frac{\partial T_w}{\partial x}\right)\Delta \boldsymbol{x} + \boldsymbol{S_L} + \boldsymbol{S} \qquad \text{3-3}$$

where

V is the volume of the computational cell (m^3),

Tw is water temperature (°C), t is time (s),

Q is flow rate ($m^3\ s^{-1}$),

A is channel cross-sectional area (m^2),

x is distance along channel (m),

Δx is distance between cross-sections (m),

Γ is dispersion coefficient ($m^2\ s^{-1}$),

S_L is a source/sink term representing the time rate of inflow heat exchange (°C $m^3\ s^{-1}$),

S is source/sink term representing the time rate of change of local external heat exchange (°C $m^3\ s^{-1}$).

Sources of heat exchange at the water surface, including short-wave solar radiation, long-wave atmospheric radiation, and conduction of heat from the atmosphere to the water, are included in S. The primary heat exchange sinks are long-wave radiation emitted by the water, evaporation, and conduction from the water to the atmosphere. Heat exchange at the sediment-water interface is via conduction. Units of heat flux (W m^{-2}) are used to describe heat exchange at interfaces. The sign convention is positive (+) for heat entering the water column, and negative (-) for heat leaving the water.

Net heat flux (q_{net}) for the water column is:

$$q_{net} = q_{sw} + q_{atm} - q_b \pm q_h \pm q_l \pm q_{sed} \qquad \text{3-4}$$

where

q_{sw} is short wave radiation (W m^{-2}),
q_{atm} is atmospheric long-wave radiation flux (W m^{-2}),
q_b is back long-wave radiation flux (W m^{-2}),
q_h is sensible heat flux (W m^{-2}), q_l is latent heat flux (W m^{-2}),
q_{sed} is sediment-water heat flux (W m^{-2}).

Equations for each of the above terms and a discussion of their application is given in USACE HEC (2016). Implementation of the temperature model is concurrent with the AD modeling described in section 3.2 and has the same requirements except that the parameterization of the model boundary conditions and initial conditions is more demanding.

3.3.1 Model Parameterization and Calibration

3.3.1.1 Meteorological Data

At least one full meteorological data set is needed to model water temperature. The model supports data sets for multiple meteorological stations and each water quality cell is assigned to the nearest data set (unless set to a specific set). For the Fort Peck DEIS, the nearest weather station with the requisite data is Glasgow, MT. This station was used after a review of partial data sets from other nearby stations demonstrated relatively little regional variability in weather during the period of interest.

Required meteorological data includes a time series of air temperature, humidity, cloudiness, and wind speed with a sampling frequency of at least once per three hours. Atmospheric pressure and solar radiation are also required and, while a measured time series is preferred, values for these variables can be calculated from site location and elevation.

In addition to time series data, each meteorological data set includes physical information including latitude, longitude, and site elevation. Water temperature model calibration parameters are stored with meteorological data sets. Calibration parameters include the dust coefficient (used only if a synthetic solar radiation time series is applied) and wind function parameters (used to control the magnitude of sensible and latent heat).

Climate data for the Fort Peck DEIS was assembled from a variety of sources. Meteorological data for 1960 to 1990 from Glasgow, MT and Minot, ND were obtained from EPA's Environmental Modeling Community of Practice website (https://www.epa.gov/ceam/meteorological-data). Average, high and low temperatures for 1980 to 2010 at Glasgow were obtained from the High Plains Regional Climate Center (http://climod.unl.edu/).

NOAA's National Center for Environmental Information site (https://gis.ncdc.noaa.gov/maps/ncei/cdo/hourly) was used to obtain data from 1 Jan, 1990 to 27 Jul, 2019. NOAA's data included all necessary fields except cloud cover and solar radiation, which were obtained from the National Solar Radiation Data Base (NSRDB) archives.

Collectively, the above data sources contributed to an hourly data set spanning 1960 to 2019 for atmospheric pressure, air temperature, relative humidity, dew point, solar radiation, wind speed, and cloudiness at Glasgow, MT as well as incomplete comparison data sets from Montana (Wolf Point, Landusky, and Sydney) and North Dakota (Williston and Minot). These data were imported into a DSS file for reference by HEC-RAS.

For years prior to 1960, reliable meteorological data were limited to daily means for temperature, wind, humidity, and pressure. Because the models require hourly data that are hard to reconstruct from these averages, representative data from other years were used to synthesize hourly series. Years were classified according to their June temperatures; those in the upper quartile were placed in the "High" category, those in the lower quartile the "Low" category, and those from 25 to 75 percent exceedance were classified as "Normal." Hourly meteorological data for model runs simulating 1930, 1949, and 1953 were randomly selected from years with the same classification in the 1960 to 2019 data series.

3.3.1.2 Surface Water Temperatures

A temperature time series must be specified at all locations where flow enters the system (boundary condition) including: upstream boundaries of the main channel and its tributaries and lateral inflows. Only limited data are available for tributary or mainstem Missouri River water temperatures, so it is not possible to furnish the model with measured values. Rather, the necessary boundary conditions must be specified with synthesized data, regression or other relationships, or addressed through other means.

Late spring to early summer surface water temperatures in the region exhibit several characteristics (Figure 3-9). Temperatures on the UMR are lower than the tributaries or the lake surface. They display a rising trend (peak is around 1 August) and are subject to weather patterns that cause rapid increases or decreases on a day to week timescale. Not fully evident in the figure because of sampling frequency is a strong diurnal fluctuation on the order of 2 °C.

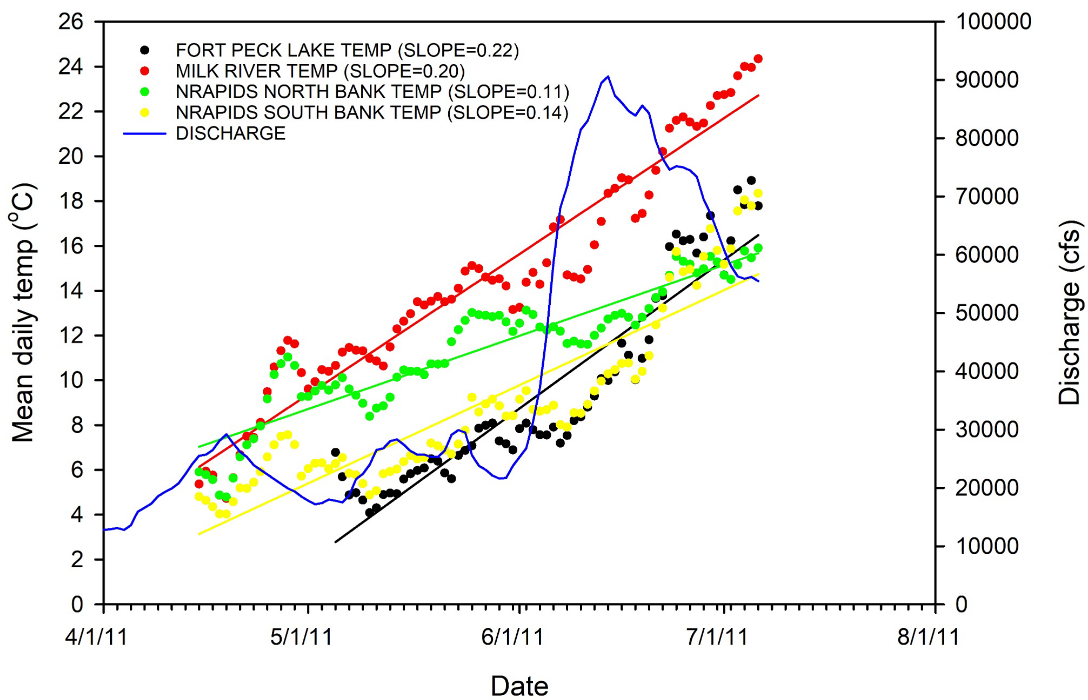

Figure 3-9. Temperature measurements on the UMR, Milk River, and Fort Peck Lake that show important characteristics and trends.

The water quality module in HEC-RAS does a good job of capturing the heat fluxes that accompany diurnal and weather trends. Because modeled tributary lengths are several miles, the water quality module can resolve a steady, average estimate at the upstream boundary and generate an accurate diurnal variation and weather condition adjustment by the time the tributary flows enter the mainstem Missouri River. Therefore, a mean daily temperature based on the date and prevailing weather is sufficient for tributary boundary conditions.

Measured data from the period of record were obtained from several sources for each tributary and analyzed using quadratic regression to obtain a parabola that best fits the data. This required transforming the data such that the dates were based on Julian calendar day of the year. The applicable general relation is:

$$T = ad^2+bd+c \qquad \textbf{3-5}$$

where

T = water temperature in degrees Celsius

d = day of the year

a, b, c are coefficients to the quadratic equation

Figure 3-10 shows observed temperature data for the Poplar River and associated regression fits using Equation 3-5. Data were drawn from the National Water Information System water-quality database for station 06181000 and included 350 measurements between 1975 and 2013. Dates were transformed to Julian calendar day (x-axis). A quadratic regression of all the data (green dashed line) provides a poor fit in the dates of interest, which are calendar days 152-212 (June and July) due to the zero-degree days from mid-November through mid-March.

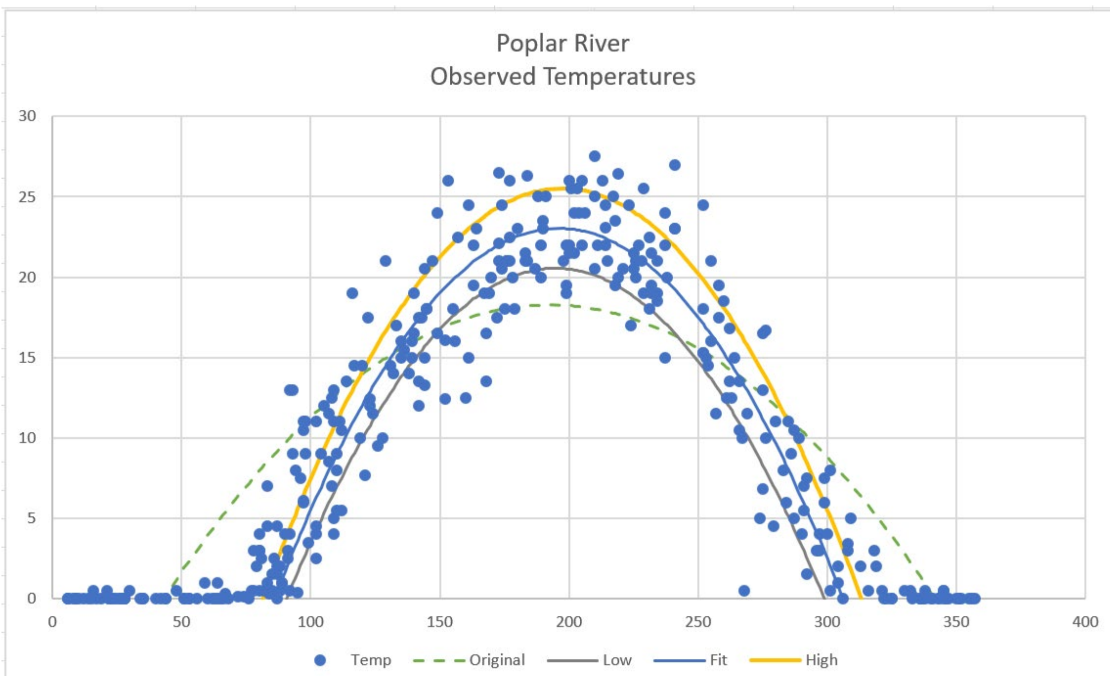

Figure 3-10. Example quadratic regression fit to data for the Poplar River.

Regression on the data from Julian day 80 through 310 provides a good representation of expected mean daily water temperatures for the June and July period analyzed for the Fort Peck DEIS. Quadratic regressions representing ±1 SD were also developed to use for sensitivity analyses, to represent diurnal variations, and to have relations applicable to varying weather conditions (i.e., cooler or warmer than normal conditions). Resulting relations for the Poplar River are:

$T = -0.0019d^2 + 0.74d - 51.5$	- 1SD	3-6
$T = -0.0019d^2 + 0.745d - 50$	Median	3-7
$T = -0.0019d^2 + 0.75d - 48.5$	+ 1SD	3-8

Quadratic regression analyses were applied to measured data for other tributaries, for four locations on the UMR, and at the upstream study boundary for flows through the powerhouse and over the spillway. Table 3-2 provides a Summary of coefficients to Equation 3-5 derived from quadratic regression and used to predict mean daily temperatures for tributaries and points on the UMR.

Table 3-2. Summary of coefficients to Equation 3-5 derived from quadratic regression and used to predict mean temperatures for tributaries and points on the Missouri River.

	Cool Conditions (-1SD)			Normal Conditions (median)			Warm Conditions (+1SD)		
	a	b	c	a	b	c	a	b	c
Powerhouse	-0.00075	0.340	-26.0	-0.00075	0.340	-25.0	-0.00075	0.340	-24
Spillway Flows	-0.00195	0.865	-76.0	-0.00195	0.860	-73.0	-0.00195	0.855	-71
Milk River	-0.00190	0.775	-58.0	-0.00190	0.780	-56.5	-0.00190	0.780	-54
Poplar River	-0.00190	0.740	-51.5	-0.00190	0.745	-50.0	-0.00190	0.750	-49
Yellowstone R.	-0.00140	0.555	-36.0	-0.00140	0.560	-34.0	-0.00140	0.555	-31
Below Fort Peck	-0.00080	0.340	-25.0	-0.00080	0.340	-21.0	-0.00080	0.340	-18
Wolf Point, MT	-0.00110	0.445	-27.0	-0.00105	0.425	-22.0	-0.00100	0.410	-18
Culbertson, MT	-0.00110	0.445	-29.0	-0.00105	0.425	-24.0	-0.00100	0.410	-20
Williston, ND	-0.00150	0.620	-47.0	-0.00150	0.625	-44.0	-0.00150	0.625	-41

Boundary and initial condition temperatures for powerhouse, spillway and tributary flows as well as lateral inflows specified to balance depletions in HEC-RAS are established in the DSM using Equation 3-5 and lookup tables with the coefficients in Table 3-2. Initial conditions for each reach of the Missouri River use the nearest of the last four relations in the table. These relations are also used to assess model performance; model outputs are compared to predicted values at the specified locations. Observed temperatures at these locations were used to assist with calibration.

Only one upstream boundary exists in the HEC-RAS model, and spillway flows are not modeled as a tributary. Therefore, a single time series of temperatures is used to reflect the combined powerhouse and spillway flows, despite the lack of mixing as described in section 2.5. Observed temperatures from 1999 through 2015 for the surface waters of Fort Peck Lake (upper 5 ft) were used to estimate temperatures for water spilled from Fort Peck Reservoir. Data were obtained at the STORET station COEOMAHA_WQX-FTPLK1772A, located just upstream of the Fort Peck Dam. Observed temperatures from 2011 through 2013 immediately below the Fort Peck Powerhouse were used to establish coefficients for powerhouse flow temperatures.

An Excel spreadsheet tool with lookup tables for the relations (Table 3-2) and for POR flows for each alternative generated from the ResSim models was developed to generate spillway temperatures used in the spawning submodel and mixed spillway/powerhouse temperatures for use in the temperature model. The tool includes multiple rule sets for operations that apportion the total flow from ResSim between the spillway and powerhouse. It has dropdowns for each simulation year and alternative that, when selected, automatically update the temperature series for each operational ruleset and generates plots like shown in Figure 3-11. The user can copy the table values for the appropriate operations and paste them into the “table” selection of the HEC-RAS water quality dataset for the upstream boundary condition, or import the tables into a DSS file called by HEC-RAS.

Historical air temperatures at Glasgow, MT during the first 15 days of June in each year were evaluated to classify years as “Low”, “Normal”, or “High” temperature. The DSM includes a lookup table of these classifications to determine which of coefficient sets to apply in each year. Air temperature has often been used as an independent variable in regression analysis of stream temperature because it can be viewed as a surrogate for the net heat exchange (Webb et al., 2003). Linear and non-linear regression relationships between air and stream temperatures have been developed and successfully applied by previous researchers (Van Vliet et al., 2012; Rabi et al., 2015). For the DSM, years with a June 1-15 mean temperature in the lower quartile were classified cool, the upper quartile was considered warm, and the median regression was used to represent the inner two quartiles, which were designated “normal”.

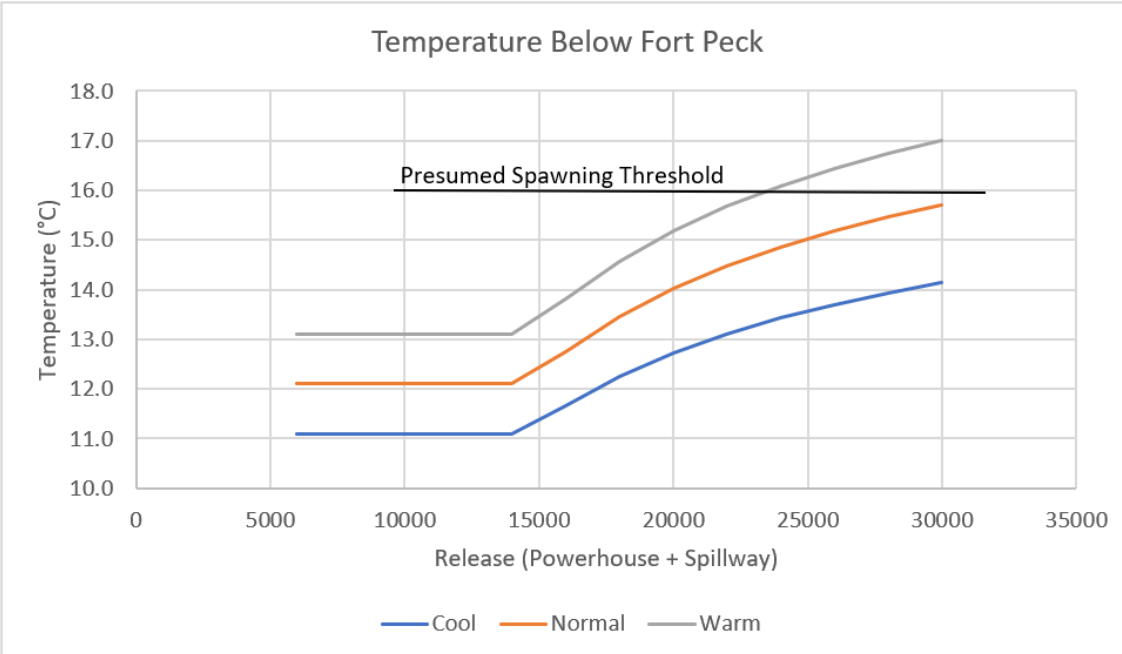

Figure 3-11. Example of the effect of adding warm spillway flows to releases from Fort Peck Dam. Data shown is for July 1 (effects vary by date due to seasonal warming in Fort Peck Lake. “Cool” “Normal” and “Warm” refer to year class described above.

3.3.2 Temperature Submodel Outputs

Outputs from the Fort Peck operations tool described above include tables and plots of mean daily flows and water temperatures for the spillway, powerhouse, and mixed flow in the Missouri River used to assess spawning (see section 2.5). Outputs are generated for multiple operations rule sets dictating the contribution of spillway flows to total flow. Temperature outputs from the tool include those for cool, normal and warm years.

Outputs from the temperature calculations in the HEC-RAS Water Quality Module are similar to those described in section 3.2.2 for the AD model. Time-series plots of temperatures at a location (see Figure 3-12) and spatial plots of temperatures at a time in the simulation window (Figure 3-13) are useful for assessing model performance. In addition to state variable concentrations, which are always available as model output, water quality sources and sinks and other incremental computations are also available as optional model output. Most of these additional output variables are component parts of the difference equation for advection and diffusion (3-3).

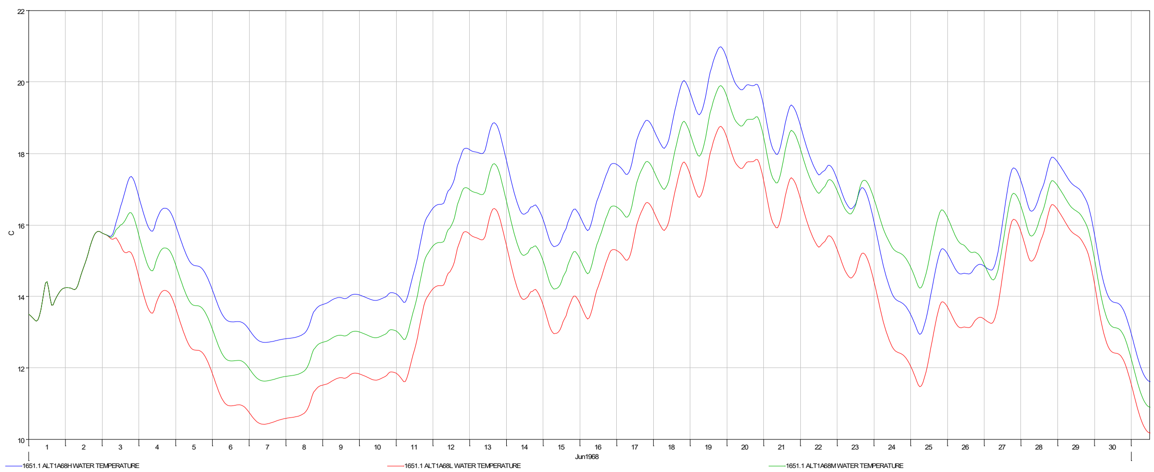

Figure 3-12. Example time-series plot of daily minimum, median, and maximum temperature at a location in the model domain.

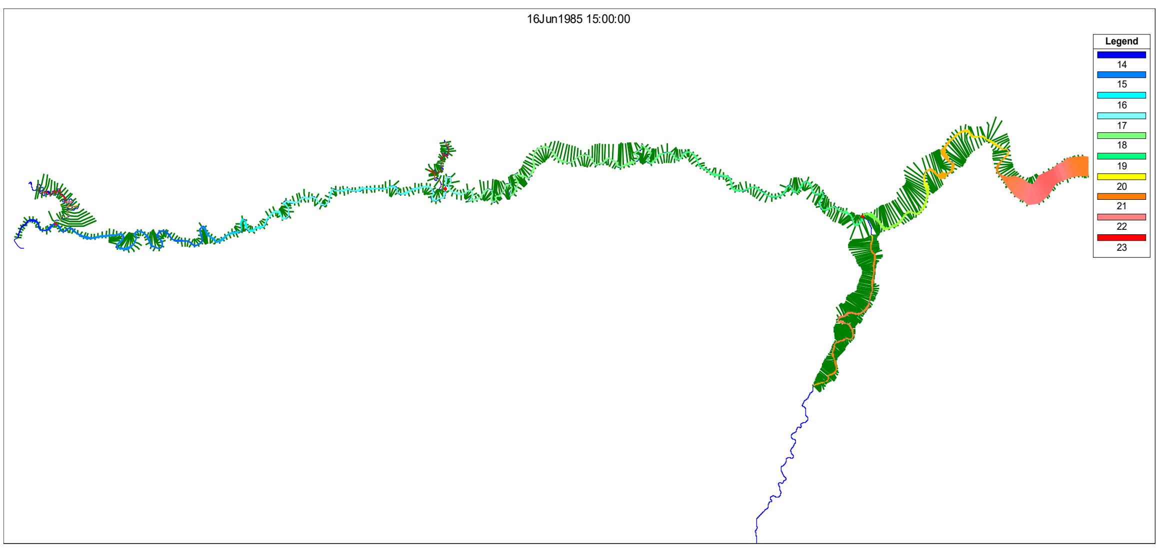

Figure 3-13. Example spatial plot of temperatures (°C) at a time step of a 1985 simulation.

The primary output of the water quality submodel for the DSM is a table of temperatures, velocities, and mass (a substitute for larvae quantity) for each water quality cell at each timestep (see Table 3-3). A table is generated for each alternative/year combination, generally at a 3-hour timestep for 21 days, with velocity, water temperature, advection mass and cell mass output for each of the 573 computation cells. These are used as input to the settling submodel, which determines larval development and their distribution at settling stage.

Table 3-3. Example of output from the temperature model showing a time series of velocity, temperature, and tracer mass*.

		18-Jun 6:00			18-Jun 9:00			18-Jun 12:00			18-Jun 15:00			18-Jun 18:00		
River Mile	WQ Cell Length (m)	Veloc-ity (m/s)	Water Temp. (°C)	Cell Mass (g)	Veloc-ity (m/s)	Water Temp. (°C)	Cell Mass (g)	Veloc-ity (m/s)	Water Temp. (°C)	Cell Mass (g)	Veloc-ity (m/s)	Water Temp. (°C)	Cell Mass (g)	Veloc-ity (m/s)	Water Temp. (°C)	Cell Mass (g)
1747.59	838.2	1.15	13.61	2642.34	1.15	14.21	53858.83	1.15	15.03	11105.70	1.15	15.88	412.38	1.15	16.44	22.97
1747.17	822.6	1.13	13.63	1619.87	1.13	14.25	56058.07	1.14	15.05	14209.14	1.14	15.90	578.58	1.14	16.49	27.12
1746.68	805.7	1.01	13.63	864.61	1.01	14.25	50721.20	1.01	15.04	15484.62	1.01	15.89	680.26	1.01	16.51	28.26
1746.16	622.8	1.28	13.64	425.99	1.28	14.23	44918.05	1.28	15.02	18136.26	1.27	15.86	948.17	1.27	16.52	34.46
1745.76	947.2	0.72	13.65	334.00	0.72	14.22	77655.96	0.72	14.99	44182.74	0.71	15.83	2800.89	0.71	16.53	93.25
1745.17	912.2	0.72	13.66	86.21	0.71	14.22	52592.97	0.71	14.97	40794.53	0.71	15.81	3006.65	0.71	16.54	96.74
1744.6	924.2	1.16	13.69	21.89	1.16	14.24	36145.77	1.16	14.98	37542.05	1.16	15.80	3203.01	1.16	16.55	103.12
1744.05	759.1	1.06	13.71	5.50	1.06	14.25	25090.56	1.06	14.97	33562.02	1.06	15.79	3246.92	1.06	16.56	106.49
1743.54	763.6	1.18	13.73	1.45	1.19	14.25	21907.21	1.19	14.97	38242.91	1.19	15.78	4269.66	1.19	16.56	146.16
1743.07	752.9	0.99	13.76	0.25	0.99	14.26	21190.57	0.99	14.97	52295.02	0.99	15.77	7218.24	0.99	16.56	273.68
1742.6	777.4	0.74	13.79	0.06	0.74	14.26	18460.43	0.74	14.96	67870.71	0.74	15.74	11979.53	0.74	16.55	522.51
1742.13	734.7	0.70	13.82	0.01	0.70	14.25	12031.45	0.70	14.94	64860.27	0.69	15.72	14553.46	0.69	16.53	739.36
1741.66	889.9	0.77	13.87	0.00	0.77	14.26	10016.62	0.76	14.93	88611.30	0.76	15.69	27453.53	0.76	16.50	1727.53
1741.1	849.3	0.55	13.92	0.00	0.55	14.26	5400.50	0.55	14.92	75184.42	0.55	15.67	29541.29	0.55	16.48	2132.31
1740.55	883.1	0.96	13.94	0.00	0.96	14.25	2428.74	0.96	14.91	49418.63	0.96	15.64	23230.74	0.96	16.45	1844.92
1739.77	893.7	1.21	13.97	0.00	1.21	14.25	1524.33	1.20	14.89	46607.07	1.20	15.62	27146.56	1.20	16.42	2453.19
1739.25	869.3	0.97	14.03	0.00	0.96	14.26	1049.58	0.96	14.88	53944.08	0.96	15.59	42108.80	0.96	16.39	4624.76
1738.69	852.8	0.67	14.08	0.00	0.67	14.27	537.96	0.67	14.88	46942.23	0.67	15.58	47829.10	0.67	16.37	6205.20
1738.17	923.1	0.91	14.14	0.00	0.91	14.29	259.07	0.90	14.87	41355.61	0.90	15.55	58182.68	0.90	16.33	9449.33
1737.64	914.8	0.68	14.20	0.00	0.68	14.33	112.75	0.68	14.87	36503.64	0.68	15.53	73573.79	0.68	16.30	15286.50

* Shown is a 12-hour series from a simulation of Alt 2 in 1985 at a 3-hour timestep for 20 cells. The full simulation sequence was 21 days and there are 573 model cells.

3.4 Settling Submodel

The settling submodel is used to determine the distribution of pallid sturgeon larvae at the onset of settling and exogenous feeding. Larvae that settle in the anoxic zone of Lake Sakakawea are assigned a low survival probability (presently zero) in the DPM, while those that settle upstream in this zone are given a higher survival probability. The settling submodel integrates the drifting free embryo distribution with temperature over time and tracks thermal exposure at each time step, as well at the cumulative thermal exposure (CTE) over time. Settling is assumed to occur once exposure thresholds are met using one of two free embryo development models described below.

The proportion of drifting free embryos that settle upriver of the anoxic zone (also referred to as percent retained) can serve as a direct benefit metric in the Fort Peck DEIS and indirectly as a critical variable in the Demographic Population Model. The process for estimating this proportion requires:

1. determining cumulative drift distance (AD submodel) and temperature exposure (temperature submodel) during ontogenetic development,
2. calculating the CTE for the population of drifting larvae,
3. establishing the relationship between water temperature and development of pallid sturgeon larva to estimate when free embryos transition from endogenous to exogenous feeding larvae,
4. identifying the location of the anoxic zone, and
5. using the above information to establish larval distribution when they transition from drifting free embryos and settle to benthic habitats.

Calculation of CTE (in °C) for the general case is accomplished using outputs from the AD/temperature model runs (e.g. Table 3-3) with the following:

$$\boldsymbol{CTE_n} = \sum_{t=0}^{n}\left(\sum_{i=1}^{m}(\boldsymbol{T} * \boldsymbol{P_i})\,/\boldsymbol{P}\right) * \Delta\boldsymbol{t} \qquad 3\text{-}9$$

where

T = temperature (°C)

P = embryo population size

t = time (days)

i = WQ cell number

m = the total number of cells in the modeled reach

n = the number of time steps since hatch

The distribution of the drifting free embryos, which are represented in the AD submodel by mass of an arbitrary constituent (1gm = 1 free embryo), is evaluated at each time step by the settling submodel to determine the proportion that remain in cells upstream of the anoxic zone. The proportion of the total mass upstream of the anoxic zone at the settling threshold is interpolated using the value for days post hatch (DPH) at settling determined from the CTE threshold described above. For example, if 1,000,000 grams of constituent are simulated and 5000 grams are upstream of the anoxic zone when the settling threshold is reached, the proportion retained is 5,000/1,000,000 = 0.005 (or 0.5%).

Location of the Lake Sakakawea anoxic zone is ill-defined, but areas of high benthic BOD correspond with the regions where velocities slow and significant amounts of organic material accumulate on the bed. Location of the zone would logically vary with pool elevation and related backwater conditions. Channel slope of the UMR downstream from the Yellowstone River confluence is about 1 foot per mile and the range of historical pool levels suggests significant variation in the location of the transition to a low velocity zone (Figure 3-14).

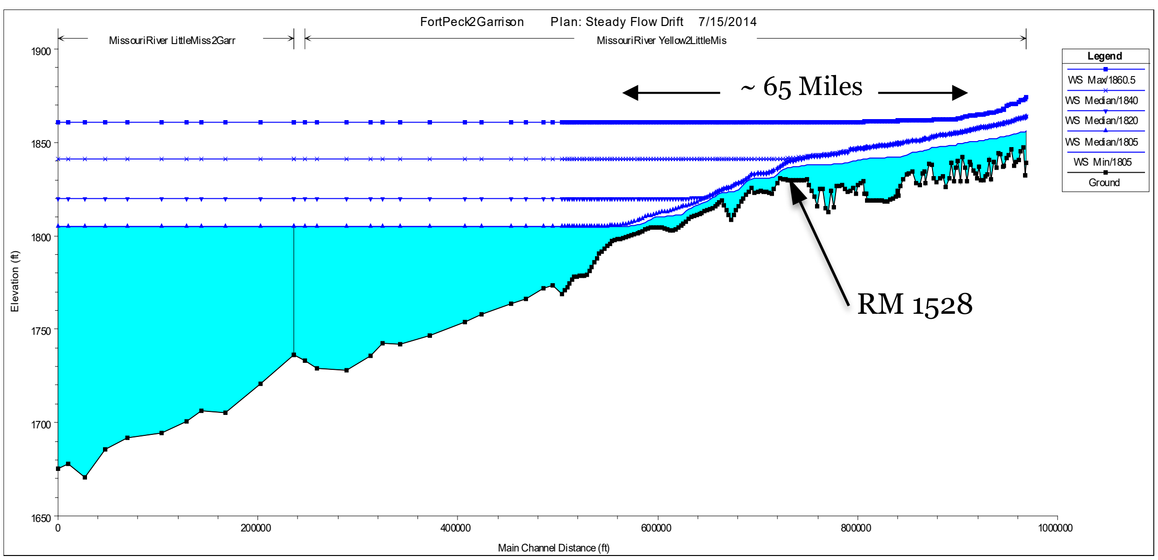

Figure 3-14. Range of pool levels on Lake Sakakawea showing up to 65 miles of potentially free-flowing river exists between the historical high and low pool levels.

Figure 3-14 is somewhat misleading because the pool elevation range includes conditions while the reservoir was filling as well as the flood-of-record pool in 2011. Omitting these outliers, pool fluctuation is about 20 feet around a post-closure June mean of 1834 ft msl, mainly due to climate cycles. River mile (RM) 1528 was identified as a reasonable approximation of the associated transition zone, and was used for all alternative/year combinations. Considering advection rates are on the order of 2 miles per hour, and that the local channel geometry and slope change considerably at about RM 1528, errors associated with using this location will be very small.

3.4.1 Braaten Development Model

The developmental model used exclusively in the DSM for preliminary analyses (Round 1) and for subsequent analyses is referred to herein as the Braaten et al. (2012) model. Using observations of growth rates from laboratory studies, researchers determined that free embryos transition to exogenous feeding at a length of about 18–19 mm with about 200 cumulative thermal units (CTUs) of exposure (Snyder 2002; Kynard et al. 2007; Braaten et al. 2008). CTUs are the sum of mean daily water temperature (in °C) for each day of life after hatching and are equivalent to CTEs in Equation 3-9.

Application of the Braaten developmental model in the DSM requires the calculation of incremental thermal exposure at each time step and their summation over time. This is accomplished in an Excel spreadsheet model that applies Equation 3-9 to output from the AD and temperature submodels (e.g., Table 3-3). Incremental thermal units (ITUs) of exposure at each timestep are added to the total from the previous timestep to obtain the cumulative exposure in CTUs at each time. The timestep in days post hatch (DPH) at which the 200 CTU threshold is crossed is interpolated from the output.

Table 3-4 shows a subset of the thermal exposure and retention outputs from the settling submodel using the Braaten criterion (200 CTUs) for three years in the POR for Alt. 2. Using 2012 as an example, the settling threshold is reached at 7.89 DPH. The proportion of larvae upstream of the anoxic zone (~RM 1528) at settling is 0.0053, or 0.53 percent.

Figure 3-15 shows a plot of cumulative thermal exposure and percent retained upstream of the anoxic zone for all test flow years associated with Alt 1b in preliminary analyses. These plots provide examples of the application of sensitivity analyses using the DSM. In this instance, temperatures reflecting cool, normal, and warm conditions were analyzed to assess system responsiveness to variable weather patterns. Similar sensitivity analyses were conducted during preliminary analyses to test model response, inform alternative development, and develop useful response functions.

Table 3-4. Example of computed series for thermal exposure and percent retained

Drift Post Hatch (days)	2012			2011			1998		
	ITU	CTU	% Ret	ITU	CTU	% Ret	ITU	CTU	% Ret
7.25	4.06	179.0	2.19%	3.64	187.7	0.63%	3.11	135.6	2.76%
7.375	4.09	183.1	1.54%	3.66	191.4	0.46%	3.13	138.7	1.99%
7.5	4.12	187.2	1.12%	3.68	195.1	0.34%	3.16	141.9	1.47%
7.625	4.15	191.3	0.85%	3.69	198.8	0.25%	3.15	145.0	1.12%
7.75	4.15	195.5	0.66%	3.70	202.5	0.19%	3.12	148.2	0.87%
7.875	4.14	199.6	0.54%	3.70	206.2	0.14%	3.09	151.2	0.69%
8	4.13	203.8	0.44%	3.70	209.9	0.11%	3.05	154.3	0.56%
8.125	4.13	207.9	0.37%	3.70	213.6	0.08%	3.01	157.3	0.46%
8.25	4.15	212.0	0.31%	3.71	217.3	0.06%	2.98	160.3	0.39%
8.375	4.18	216.2	0.27%	3.72	221.0	0.05%	2.95	163.2	0.33%
8.5	4.22	220.4	0.23%	3.74	224.7	0.04%	2.93	166.2	0.28%
8.625	4.23	224.7	0.20%	3.75	228.5	0.03%	2.91	169.1	0.24%
8.75	4.21	228.9	0.18%	3.76	232.2	0.02%	2.88	172.0	0.21%
8.875	4.20	233.1	0.16%	3.76	236.0	0.02%	2.86	174.8	0.18%
9	4.18	237.3	0.14%	3.76	239.7	0.01%	2.83	177.6	0.16%
9.125	4.16	241.4	0.12%	3.76	243.5	0.01%	2.81	180.5	0.14%
9.25	4.16	245.6	0.11%	3.76	247.3	0.01%	2.80	183.3	0.12%
9.375	4.17	249.7	0.10%	3.77	251.0	0.01%	2.80	186.1	0.11%
9.5	4.19	253.9	0.09%	3.78	254.8	0.00%	2.81	188.9	0.09%
9.625	4.20	258.1	0.08%	3.79	258.6	0.00%	2.82	191.7	0.08%
9.75	4.19	262.3	0.07%	3.79	262.4	0.00%	2.81	194.5	0.07%
9.875	4.17	266.5	0.06%	3.79	266.2	0.00%	2.79	197.3	0.07%
10	4.16	270.7	0.06%	3.79	270.0	0.00%	2.78	200.1	0.06%
10.125	4.15	274.8	0.05%	3.79	273.7	0.00%	2.76	202.8	0.05%
10.25	4.16	279.0	0.05%	3.81	277.6	0.00%	2.76	205.6	0.05%

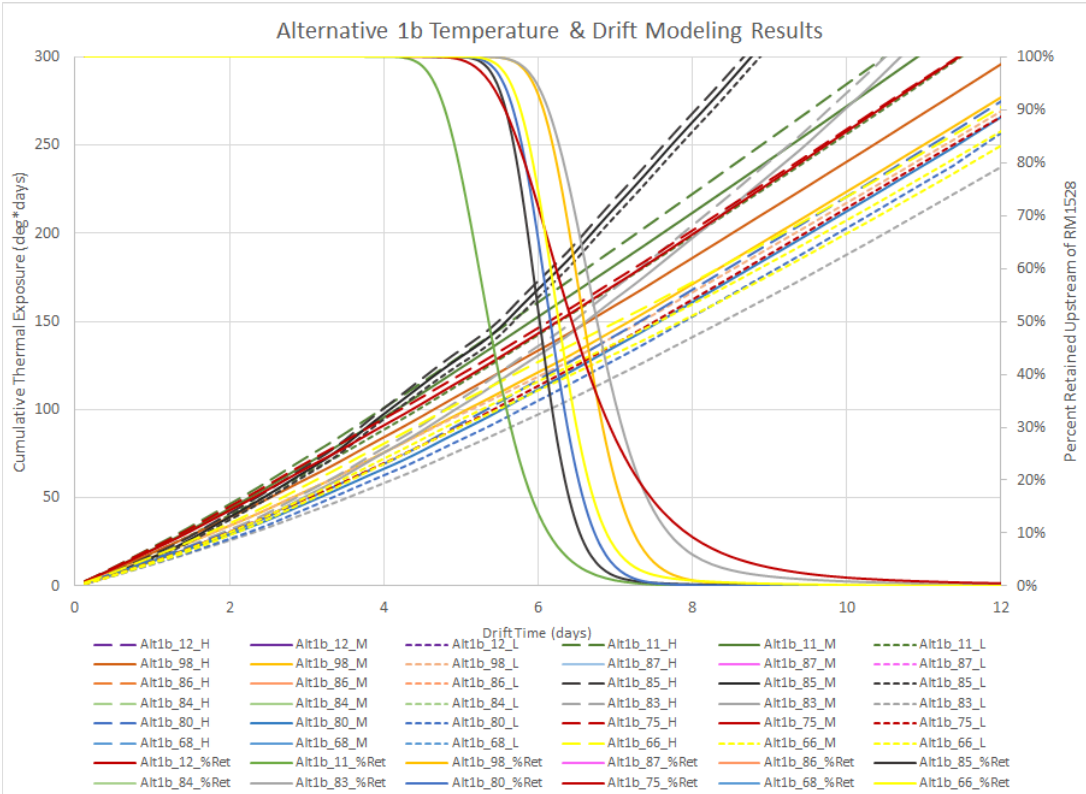

Figure 3-15. Plot of cumulative thermal exposure and percent retained upstream of the anoxic zone for all test flow years associated with Alt 1b in preliminary analyses.

Figure 3-16 is an example of settling model output showing the intersection of calculated thermal exposure with a 200 CTU threshold to determine DPH and corresponding retention rates for cool, normal, and high temperatures. Graphical assessment of response curve intersections with exposure thresholds using DPH as a pivot provide a useful way to assess and convey results.

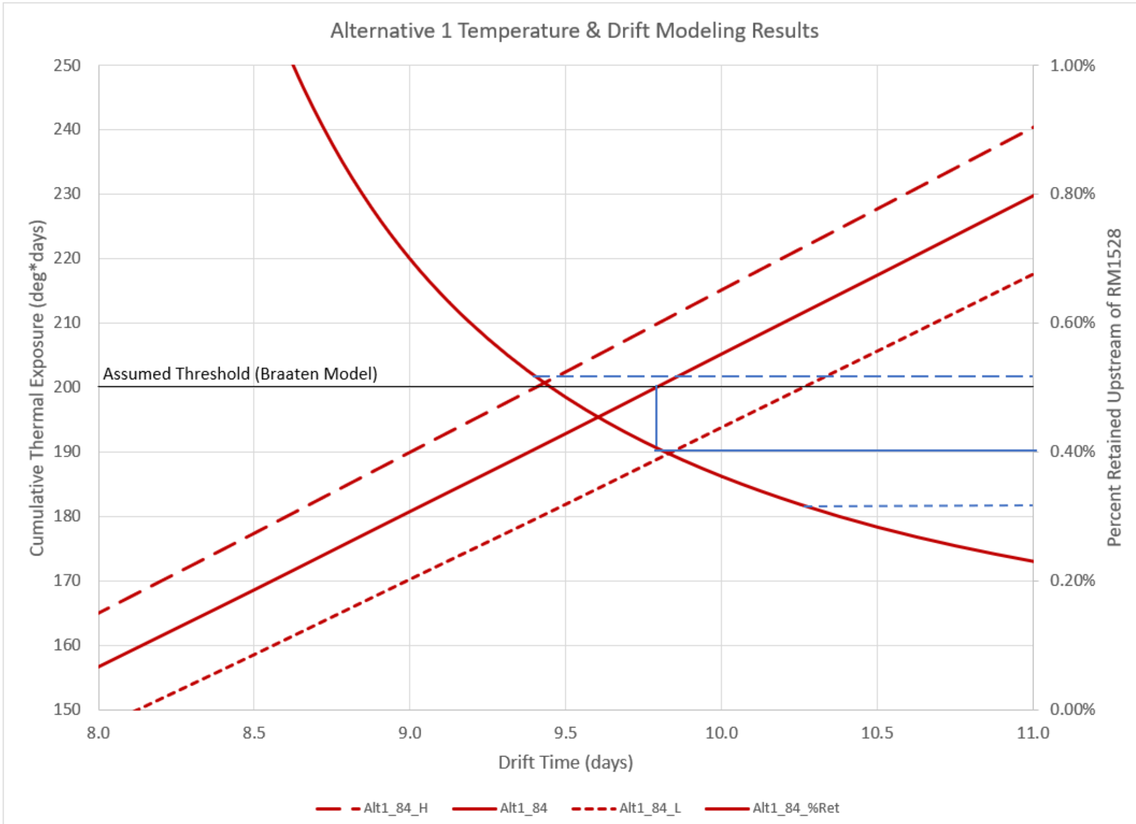

Figure 3-16. Graphical example of settling model output showing the intersection of calculated thermal exposure with a 200 CTU threshold to determine time of drift post hatch (DPH) for cool, normal, and high temperatures, then determining corresponding retention rates by intersection with a cumulative percent retained curve.

3.4.2 Stage Onset Developmental Model

A new developmental model (Chojnacki, Dodson, and DeLonay 2021) was added to the DSM as an alternative to the Braaten et al. model for the second and third round of analyses. The stage onset model (referred to as the "New" model in output tables) is based on a recently completed developmental series exposing pallid sturgeon free embryos to a range of temperatures from hatch through yolk plug expulsion (the approximate onset of exogenous feeding).

Table 3-5 shows mean and range (in parentheses) of onset of developmental stages 37-45 of pallid sturgeon free embryos from the time of hatch (stage 36), in CTUs and DPH at 5 nominal temperatures from 14-26 degrees Celsius. Cumulative thermal units (degree-days) are the proportional sum of water temperatures (in degrees Celsius) accumulated from the time of hatching. The new model is appealing because it recognizes the roles of both time and temperature in developmental rate and allows for more refined analyses of the percent retention. The stage onset model will provide utility for experimental designs, monitoring strategies, and informing management decisions in near real time.

Implementation of the stage onset model in the DSM requires adjustment to the approach using Equation 3-9. Because both the development rate and the threshold is temperature dependent (and temperatures are changing in the model domain), it is necessary to track incremental progress toward settling by means other than just CTU. The approach adopted was to assess progress toward settling in relative terms (i.e., as a percentage of needed thermal exposure for full development) at each time step and tracking cumulative exposure over the range of time steps.

Calculations for the stage onset model build from a fit of the data provided by Chojnacki, Dodson, and DeLonay (2019; Figure 3-17). Settling is assumed to occur when cumulative thermal exposure is 100% of the required magnitude. Incremental thermal exposure at each timestep is calculated in the same way as for the right-hand side of Equation 3-9, except this value is divided at each cell for each time step by the total needed, which is temperature dependent (Equation 3-10). When CTE (in %) equals 100, the number of time steps defines the time of settling.

$$\boldsymbol{CTE_n} = \sum_{t=0}^{n}\left(\sum_{i=1}^{m}\frac{(T * P_i)}{P * 1923 * T^{-0.74}}\right) * \Delta t \qquad \text{3-10}$$

where

T = temperature (°C)

P = embryo population size

t = time (DPH)

i = WQ cell number

m = the total number of cells in the modeled reach

n = the number of time steps since hatch

The new stage-development relations were developed from experiments in which the temperature variation was minimal (SD averaged 0.36 °C). This raises questions about the direct application to conditions involving diurnal variations of ± 1 °C, weather patterns that change temperatures by ± 2 °C, and a general warming trend of ~ 1 °C/week.

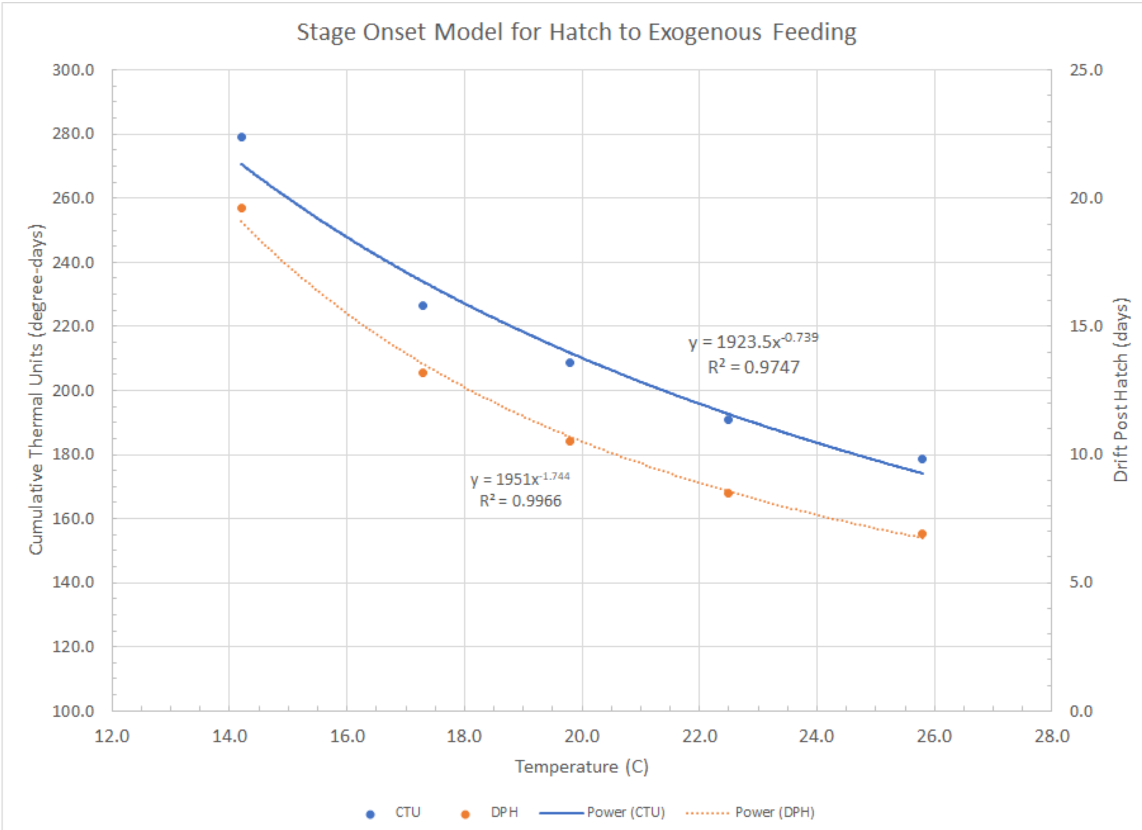

Figure 3-17. Data fit for Stage Onset (AKA “New”) Model.

Table 3-5. Provisional data from the Stage Onset developmental model (Chojnacki and DeLonay 2019, in press).

Development Stage	14 degrees Celsius		17 degrees Celsius		20 degrees Celsius		23 degrees Celsius		26 degrees Celsius	
	CTU	DPH	CTU	DPH	CTU	DPH	CTU	DPH	CTU	DPH
Stage 36	- -	- -	- -	- -	- -	- -	- -	- -	- -	- -
Stage 37	NA	NA	8.7 (3.1- 14.2)	0.5 (0.2- 0.8)	6.5 (3.3- 9.7)	0.3 (0.2- 0.5)	9.5 (4.2- 14.8)	0.4 (0.2- 0.7)	10.6 (4.6- 16.7)	0.4 (0.2- 0.6)
Stage 38	33.3 (27.8- 38.9)	2.3 (2- 2.7)	37.4 (33.8- 41)	2.2 (2- 2.3)	26.4 (23- 29.6)	1.3 (1.2- 1.5)	23.6 (18.6- 29.9)	1 (0.8- 1.3)	34.4 (29.6- 39.1)	1.3 (1.2- 1.5)
Stage 39	53.2 (53.1- 53.3)	3.8 (3.7- 3.8)	43.2 (42.3- 44.1)	2.5 (2.5- 2.5)	37.5 (36.3- 39.7)	1.9 (1.8- 2)	31 (25.8- 33.7)	1.4 (1.2- 1.5)	40.8 (38.3- 43.4)	1.6 (1.5- 1.7)
Stage 40	64.9 (62.9- 66.8)	4.6 (4.4- 4.8)	48.9 (48.1- 49.8)	2.8 (2.8- 2.8)	42.8 (39.4- 49.3)	2.2 (2- 2.5)	41 (33.5- 48.4)	1.8 (1.5- 2.2)	47.3 (46.9- 47.7)	1.8 (1.8- 1.9)
Stage 41	72.1 (71.4- 72.8)	5.1 (5- 5.2)	58.8 (52.5- 65)	3.4 (3- 3.8)	50.7 (42.8- 66.2)	2.6 (2.2- 3.3)	52.2 (48.2- 59.7)	2.3 (2.2- 2.7)	60.1 (56- 64.3)	2.3 (2.2- 2.5)
Stage 42	136.4 (134.7- 138.1)	9.6 (9.2- 10)	107.8 (107.2- 108.3)	6.3 (6.2- 6.3)	89.3 (79.5- 98.9)	4.5 (4- 5)	83.4 (78.4- 89.5)	3.7 (3.5- 4)	88.3 (86.1- 90.6)	3.4 (3.3- 3.5)
Stage 43	181.8 (176.3- 187.3)	12.8 (12- 13.5)	140.5 (137.2- 143.9)	8.2 (7.8- 8.5)	120.3 (109.3- 132.5)	6.1 (5.5- 6.7)	105.7 (93.2- 115.9)	4.7 (4.2- 5.2)	107.5 (107.2- 107.8)	4.2 (4.2- 4.2)
Stage 44	200.9 (196.1- 205.8)	14.1 (13.4- 14.8)	162 (152- 172.1)	9.4 (8.7- 10.2)	141.3 (132.5- 152.4)	7.1 (6.7- 7.7)	119.6 (104.5- 134.7)	5.3 (4.7- 6)	122.8 (120.4- 125.2)	4.7 (4.7- 4.8)
Stage 45 (onset)	279.1 (269.6- 288.6)	19.6 (18.3- 20.8)	226.4 (216.2- 236.7)	13.2 (12.3- 14)	208.6 (205.1- 215.3)	10.5 (10.3- 10.8)	190.7 (179.2- 198.4)	8.5 (8- 8.8)	178.8 (171.9- 185.6)	6.9 (6.7- 7.2)

[CTU, cumulative thermal units; DPH, days post hatch; N, number of family crosses observed at each developmental stage and temperature combination; - -, no data]

3.4.3 TableRate Adjustment to Models

The 1-D modeling treatment of free embryos as passive and neutrally buoyant contrasts with what is known of pallid sturgeon free embryos. Specifically, free embryos are not neutrally buoyant and exhibit passive drift only initially after hatch. It is also known (from Braaten et al. 2010, 2012) that free embryos primarily drift in the lower portions of the water column and that ad the larvae become more mature, they exhibit more benthic affinity. Consequently, the downstream drift (advection) of free embryos slows gradually with increasing distance (or time) and the 1-D A/D models tend to overpredict advection rates.

To adjust for this phenomena, both the Braaten and Stage-Onset Models have been modified to include an adjustment factor that increases residence time in each water quality cell by 10 percent. This has the same effect as decreasing the advection rate so that it is approximately 90 percent of the calculated value. This matches well with observations from Braaten (2012) and the 2016 and 2019 drift experiments on the Missouri River below Fort Peck dam. Rather than replace the previously described models, the "0.9 Adjusted" models are included as variants of those models.

3.4.4 Assessment of Rheotaxis

Mrnak et al. (2020) evaluated the effects of water velocity and temperature on the swimming activity, energy use, settling behavior, and mortality of pallid sturgeon larvae. They used direct observation to quantify the time (dph) for larvae to make a behavioral transition from negative to positive rheotaxis (orientation into current) at 18.7, 20.4, and 23.3 ^{O}C. Equating this transition with a shift from drifting to settling, the MRRP Independent Science Advisory Panel (ISAP) recommended that the USACE apply the following relation to the Fort Peck EIS as an additional settling model:

$$Ro = 24.3-0.85(T) \qquad 3\text{-}11$$

where

Ro is the onset of rheotactic behavior (in DPH), and

T is the average water temperature in ^{o}C

The application of Equation 3-11 to the UMR requires a mechanism for integrating temperatures that vary in space and time with a distributed population of larvae that are also changing position over time. The approach used is similar to that for the Braaten development model described in section 3.4.1, using the following:

$$\boldsymbol{T_t} = \sum_{\boldsymbol{t=0}}^{\boldsymbol{n}} \left(\sum_{\boldsymbol{i=1}}^{\boldsymbol{m}} (\boldsymbol{T_i} * \boldsymbol{P_i}) / \boldsymbol{P} \right) / \boldsymbol{n} \qquad \text{3-12}$$

where

T_n = average temperature (°C) at time t

P = embryo population size

t = time (DPH)

Δt = time step (days)

i = WQ cell number

m = the total number of cells in the modeled reach

n = the number of time steps since hatch

Onset of rheotaxis occurs when the temperature from Equation 3-12 yields a value for R_o using Equation 3-11 that equals n * Δt. The utility of this relation for predicting settling of pallid sturgeon larvae on the UMR is challenged for some of the same reasons described for the stage onset development model in section 3.4.2; the relation is based on constant temperatures and velocities, both of which differ in magnitude from conditions encountered on the UMR. While rheotaxis is certainly a prerequisite for larval settling, it may not be sufficient. Additional physiological development may be necessary before settled larvae are capable of exogenous feeding, for example. Results from the application of the Mrnak et al. (2020) relation bear this out; rheotaxis onset generally occurs much more quickly than predicted settling using the other relations and, if correct, suggests that the UMR should not be recruitment-limited for the reasons currently hypothesized. This is discussed further in Chapter 5.

3.4.5 Model Outputs

Primary outputs from the settling submodel are the various plots and tables shown in the previous section (e.g., Figure 3-15 and Table 3-4). Additionally, the submodel generates a few products that can be regarded as overarching DSM outputs. Table 3-6 is an example summary output table from the preliminary analyses showing retention probabilities for each alternative over the POR and the probabilities for conditions representing ±1SD in temperature for the boundary conditions. Years without spawning are given a zero retention probability.

Years marked with an asterisk in the table are partial hydrograph runs that may result in spawning if the temperatures for that year happen to be in the upper quartile. A different approach was utilized in the second and third rounds of analyses; rather than use the temperature relations for sensitivity, measured air temperatures at Glasgow, MT for that year were used to classify the year as cool, normal, or warm and the associated set of relations are used to compute retention. Results from later rounds of analysis for the EIS are presented and discussed in Chapter 5.

Table 3-6. Example summary output table showing retention probabilities for each alternative over the POR and the probabilities for conditions representing ±1SD in temperature.

	1947	1949	1966	1968	1975	1980	1983	1984	1985	1986	1987	1998	2011	2012
					5.21%								0.07%	
NA					**3.42%**								**0.03%**	
					1.88%								0.01%	
				0.06%	15.48%	0.12%	1.38%	0.53%	0.12%			0.11%	0.34%	1.66%
Alt 1			*	**0.05%**	**11.28%**	**0.10%**	**1.07%**	**0.42%**	**0.10%**	*	*	**0.07%**	**0.13%**	**1.01%**
				0.04%	7.12%	0.05%	0.70%	0.32%	0.09%			0.05%	0.05%	0.82%
				1.03%	7.80%				0.02%				0.52%	
Alt 1a			*	**0.97%**	**5.21%**	*	*	*	**0.02%**	*	*	*	**0.05%**	*
				0.97%	3.58%				0.02%				0.02%	
			0.49%		10.48%	0.06%	9.04%		11.60%			0.40%	0.58%	
Alt 1b	*	*	0.36%	*	9.16%	0.04%	5.96%	*	7.25%		*	0.20%	0.31%	*
			0.29%		2.45%	0.02%	1.05%		4.53%			0.15%	0.10%	
			0.34%	0.05%	12.33%	0.08%	0.27%	0.62%	0.09%	10.54%	10.08%	0.09%	0.63%	0.85%
Alt 2			**0.29%**	**0.05%**	**9.53%**	**0.06%**	**0.21%**	**0.48%**	**0.07%**	**7.47%**	**8.75%**	**0.07%**	**0.25%**	**0.54%**
			0.23%	0.04%	5.82%	0.04%	0.15%	0.38%	0.06%	4.64%	7.78%	0.04%	0.11%	0.44%
			1.27%	0.34%	17.35%	0.48%	3.83%	4.36%	0.20%		34.93%	1.23%	0.83%	0.51%
Alt 2a			**1.05%**	**0.27%**	**15.34%**	**0.35%**	**2.66%**	**3.67%**	**0.18%**	*	**28.82%**	**0.91%**	**0.34%**	**0.35%**
			0.88%	0.24%	12.02%	0.22%	2.66%	2.36%	0.13%		24.00%	0.69%	0.11%	0.25%
	2.30%	83.58%	3.14%		36.74%	2.54%	6.10%		0.75%		55.01%	28.22%	0.68%	
Alt 2b	**2.30%**	**68.93%**	**2.61%**	*	**32.65%**	**1.62%**	**4.86%**	*	**0.56%**		**52.35%**	**20.52%**	**0.28%**	*
	0.28%	52.03%	1.91%		25.65%	0.71%	3.93%		0.49%		49.84%	14.65%	0.28%	

Values like those in Table 3-6 (or Chapter 5) are used as inputs for the DPM, which is used to population demographics for each alternative. The calculated values of retention can also be used as a direct metric of benefit for alternative comparison in the DEIS since recruitment to age 1 is a stated objective. While quantification of actual recruitment would require an estimation of spawning magnitude, adjustments to retention values to account for mortality during drift, etc., these are roughly independent of the alternative. Therefore, the estimates of retention are valid for making relative comparisons among alternatives and against the “no action” alternative.

The DSM can generate other summary outputs for retention to assist with alternative comparisons. Figure 3-18 is an example summary plot from the preliminary analyses that shows cumulative retention for each alternative across a series of spawning years (blue columns). Average rate of retention per spawning event can also be generated as a metric (orange line). The example provided by Figure 3-18 suggests that Alternative 2b outperforms the other alternatives, and that all alternatives outperform the “no action” option.

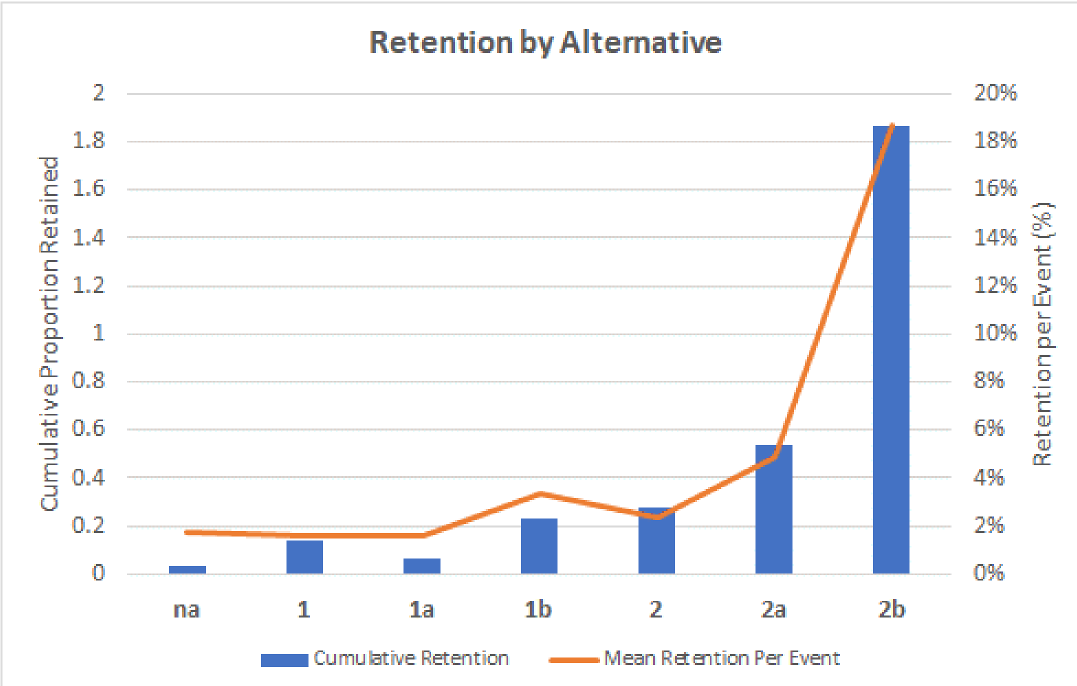

Figure 3-18. Example summary plot from preliminary analyses showing the cumulative retention across all spawning years for each alternative and an average rate of retention per spawning event.

3.5 Model Performance

A number of sensitivity analyses were conducted to assess general model performance and the response to varying model parameters and variables. Additionally, a limited model validation was performed using preliminary data from the 2019 Drift Study. Results demonstrate that the model behavior conforms to expectations and that the models provide reasonable predictions of measured conditions.

3.5.1 Sensitivity Analyses

Previous studies have shown that the A/D models are only moderately sensitive to the dispersion coefficient (Fischenich 2014; Erwin et al. 2018). Figure 3-19 shows approximately 125 miles from the leading to trailing edge (+/- 1SD) of drifting free embryos after 4 days of drift. Bounding lines in the figure show the effect of varying dispersion coefficients between upper and lower calculated limits. Dispersion coefficients used for all analyses described in this report were maintained at values determined from the 2016 drift experiment on the same reach of the Missouri River. These values provided reasonable results for the model validation using 2019 conditions (discussed below).

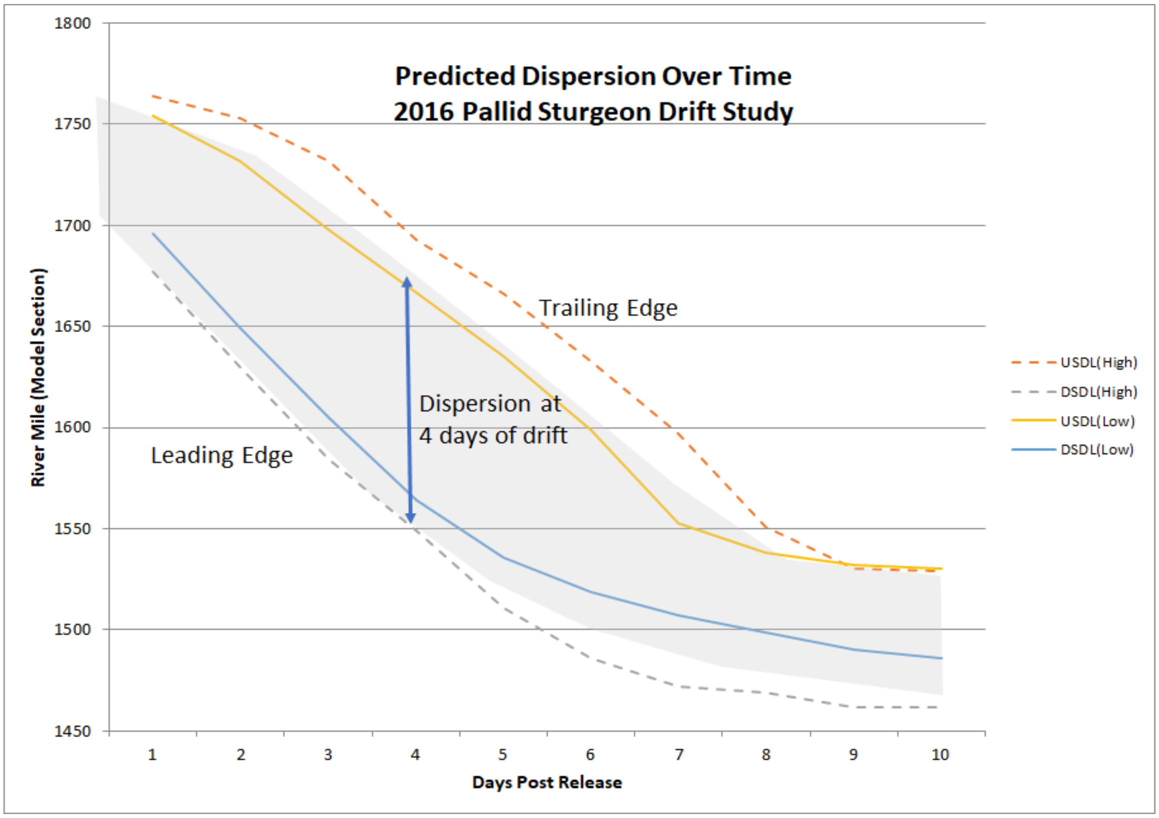

Figure 3-19. Predicted dispersion from models applied to 2016 drift experiment.

Preliminary analyses were conducted using HEC-RAS models with the same geometry as used for the 2016 drift experiment. Model results for subsequent analyses were obtained with the same HEC-RAS models as used for other analyses supporting the draft Fort Peck EIS (USACE 2021). These models incorporate updated geometry and were calibrated to 2014 and 2018 measured water surface profiles obtained at discharges within the range of the alternatives. Although varying model geometry and resistance coefficients likely affect results – particularly at lower discharges – the sensitivity of outputs to these parameters was not evaluated in the present study.

The effects of varying in discharge are primarily manifest in advection and dispersion rates, as was demonstrated in previous studies for this reach (Fischenich, 2014). Figure 3-20 shows the effect of varying discharge on advection rate for the peak of simulated embryo movement. Point scatter in the figure reflects variable rate of downstream movement due to local geometry, resistance, channel slope, etc. Although the relationship is not linear, the effect within the range of interest can be approximated by an increase of about 0.75 miles/day for every 1 kcfs increase in flow magnitude (Table 3-7).

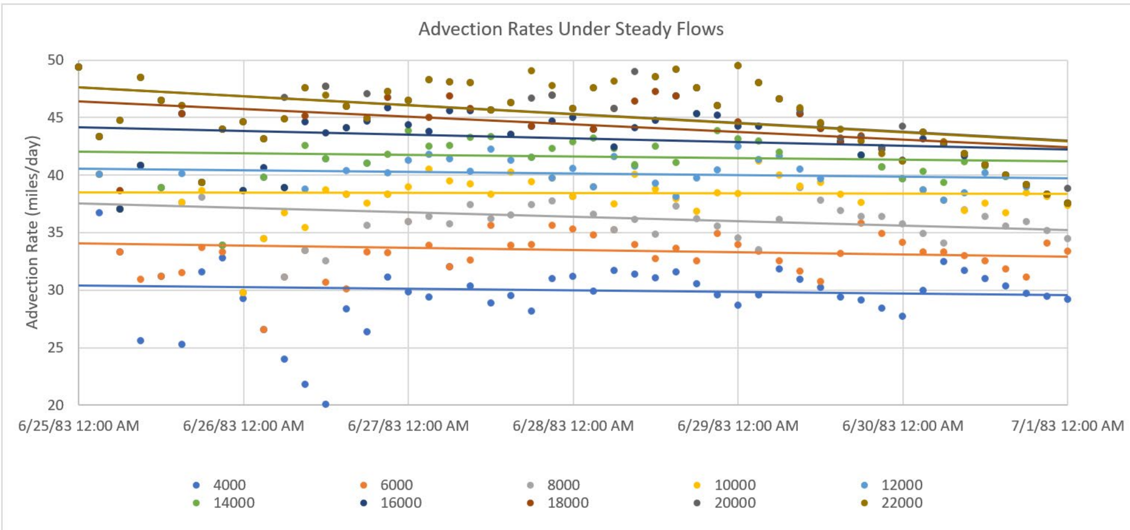

Figure 3-20. Advection rate as a function of discharge.

Table 3-7. Mean advection rate for steady flows.

Flow (kcfs)	Advection (miles/day)
4	29.7
6	33.4
8	36.1
10	37.9
12	39.4
14	40.7
16	42.1
18	43.2
20	43.9
22	43.9

Model results – primarily retention probability – are significantly affected by weather conditions. Figure 3-21 shows model sensitivity to variation in a) air temperature (-2 to +2 ^{o}C), b) solar radiation (+/- 20%), and c) cloud cover (+/- 25% of sky area). Of these parameters, sensitivity is greatest for air temperature, when scaled as a percentage change in the underlying variable, followed by solar radiation and then cloud cover. Wind speed (not shown) is also a highly sensitive variable; its affects are on the same order as solar radiation.

Assumptions regarding the presumed hatch date were a significant source of uncertainty for the dispersal and population modeling. They are also a potentially significant source of variability in outcome because they implicitly incorporate varying flow, water temperature, and weather conditions over the range of assumed dates (Figure 3-22). Figure 3-23 provides additional perspective on sensitivity, relating retention to flow magnitude over three temperature regimes.

3.5.2 Validation using conditions and preliminary data from the 2019 Drift Study

A limited model validation was performed using data from the 2019 drift experiment, which involved the release of 772,000 1-day post-hatch (1-dph) embryos and 201,000 5-dph embryos at RM 1700, just downstream from Wolf Point, MT in the Upper Missouri River, and monitoring their drift down to RM 1550 upstream from Williston, ND in Lake Sakakawea. Multi-dimensional hydrodynamic models were constructed with high-resolution topography for the zone of the 2019 drift experiment, and are being tested with biological field data from the drift study as well as being informed by laboratory flume studies. While the data are still being analyzed and the genetic analyses are incomplete, preliminary results from the study and the multi-dimensional modeling provide a useful basis for validating components of the DSM as applied to the Fort Peck EIS.

Application of the drift and settling model to the 2019 conditions required acquisition of hourly meteorological data through July, 2019. These were obtained for the Glasgow, MT NWS station from NOAA's National Center for Environmental Information site (https://gis.ncdc.noaa.gov/maps/ncei/cdo/hourly). The National Solar Radiation Data Base (NSRDB) provided sky cover and solar radiation data. Flow releases from Fort Peck Dam were provided by the MRWMD, while tributary inflows were obtained from the USGS online data portal (https://waterdata.usgs.gov/nwis/rt). USGS field crews made discharge measurements at locations on the Missouri River leading up to and throughout the experiment (Call et al. 2021); these were used to help allocate ungaged flows in the models.

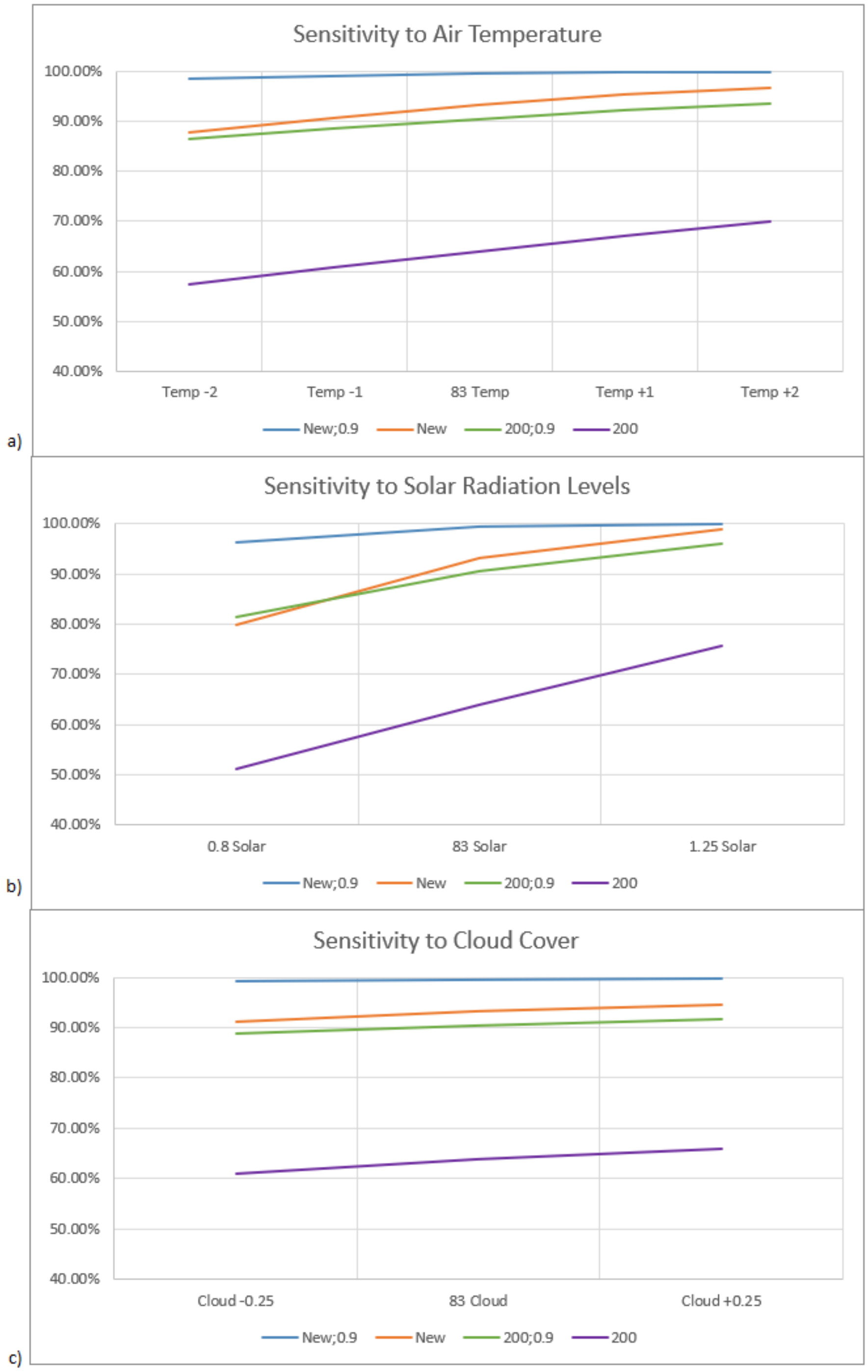

Figure 3-21. Retention as a function of model selection and a) air temperature, b) solar radiation levels, and c) cloud cover.

Figure 3-22. Retention as a function of hatch date across three temperature regimes using four models.

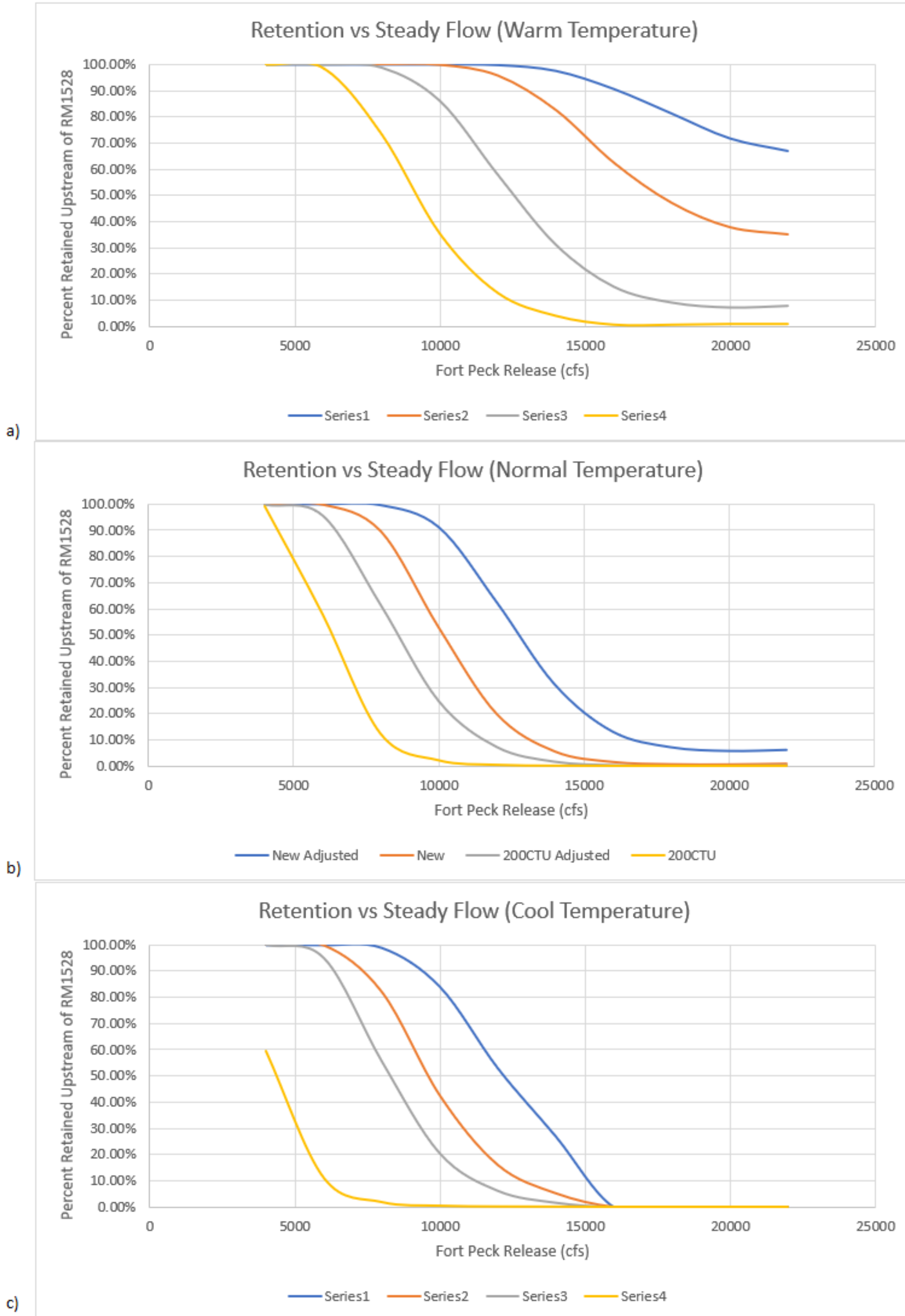

Figure 3-23. Retention as a function of flow magnitude for three temperature regimes using four models.

The validation exercise was made using the same models, calibrations, and other assumptions as were employed for the DEIS analyses. Retention calculations for 5dph larvae assumed they were released at 50% of the development trajectory from hatch to settling. The models and analyses should be regarded as preliminary, as they have not been subjected to independent technical review. Notably, the field measurements were preliminary at the time of comparison and the locations of USGS temperature and velocity measurements at specific points along the channel were compared to the nearest model cell, typically ~500 m long.

Despite the above caveats, results from the modeling compared favorably with measurements from the field experiment. Calculated mean channel velocities from the model were within 0.09 m/s, on average (range -0.04 to 0.87;Figure 3-24). Temperatures calculated by the model were, on average, 0.25 °C higher than measurements until a cold front drove measured temperatures lower. Overall, the models predicted temperatures 0.85 °C higher than measurements, on average (range -0.11 to 1.89;Figure 3-25). The USGS measurements were made by moving boat at specific points along the channel, whereas calculated velocities are mean cross-section values and temperatures were for each model cell.

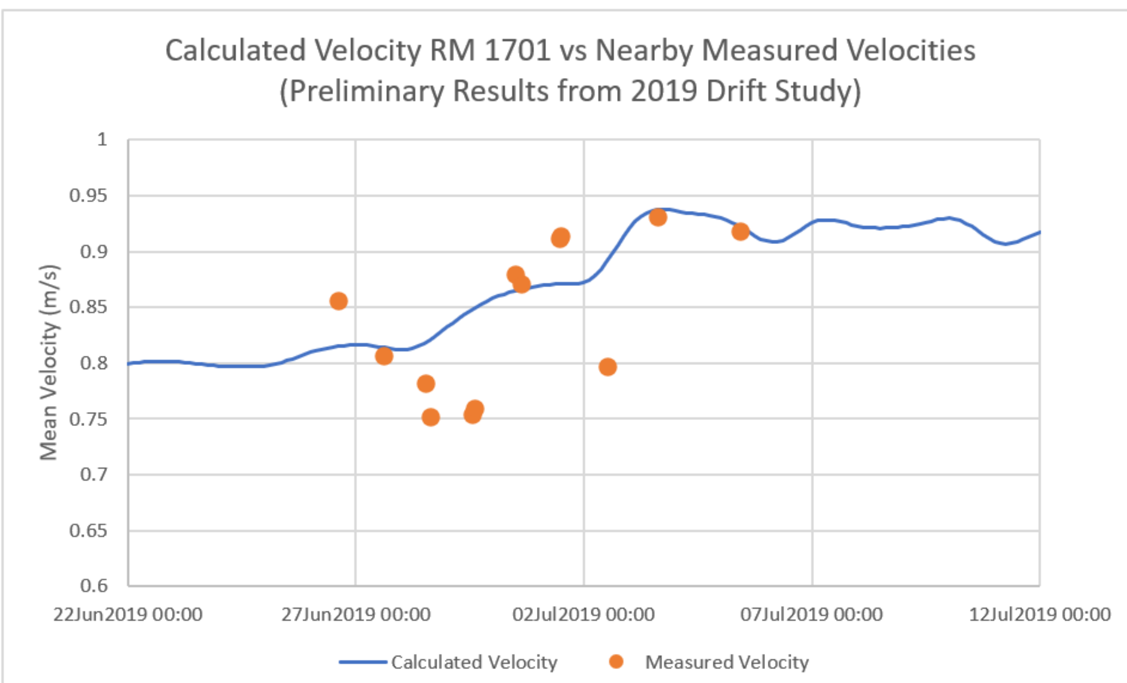

Figure 3-24. Plot of calculated mean channel velocity over time for the model cell at RM 1701 and point velocity measurements in the cell taken during the drift study (Call et al. 2021).

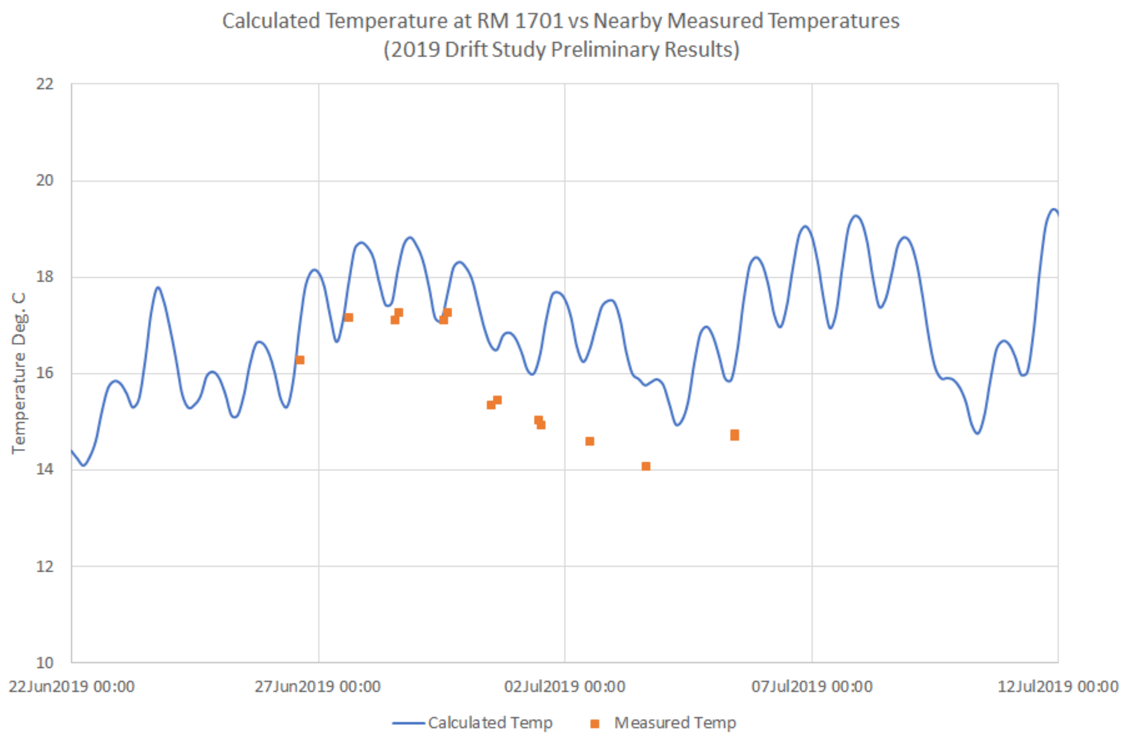

Figure 3-25. Plot of calculated temperatures for the model cell at RM1701 over time and temperature measurements taken during the 2019 drift study (Call et al. 2021).

Figure 3-26 shows the modeled and measured dispersion of larvae over time at the five USGS sampling sites on the Missouri River downstream of Wolf Point, MT used in the 2019 drift study (Braaten and Holley 2021). Results align well for the two furthest upstream sites. Calculated peak advection is about 6 hours early for the next two transects, and about 3 hours early for the furthest downstream. Results shown are for the New Stage-Development series adjusted to account for observed advection rates (adjustment results in about a 10% reduction of modeled advection rate). The model results align well with the trailing leg of measurements for the transects more than 25 miles downstream of the release site.

Calculated retention for embryos released in the drift study are shown in Table 3-8. Percentages reflect the proportion of the full sample remaining upstream of RM 1528 when the threshold condition is met. The four models described in section X were used, and include both rate-adjusted and unadjusted versions of the two development models. Note that these results would differ from the alternatives in the DEIS due to 1) a release site about 60 miles further downstream for the drift study, 2) use of 1- and 5-day old larvae at release, and 3) unique flow and weather conditions for the drift study.

Table 3-8. Modeled retention rates for larvae released during the 2019 drift study.

Larvae Age	Calculated % Retained 2019 Drift			
	New;0.9	New	200; 0.9	200
1dph	10.47%	5.53%	10.53%	5.32%
5dph	99.29%	95.27%	99.89%	99.88%

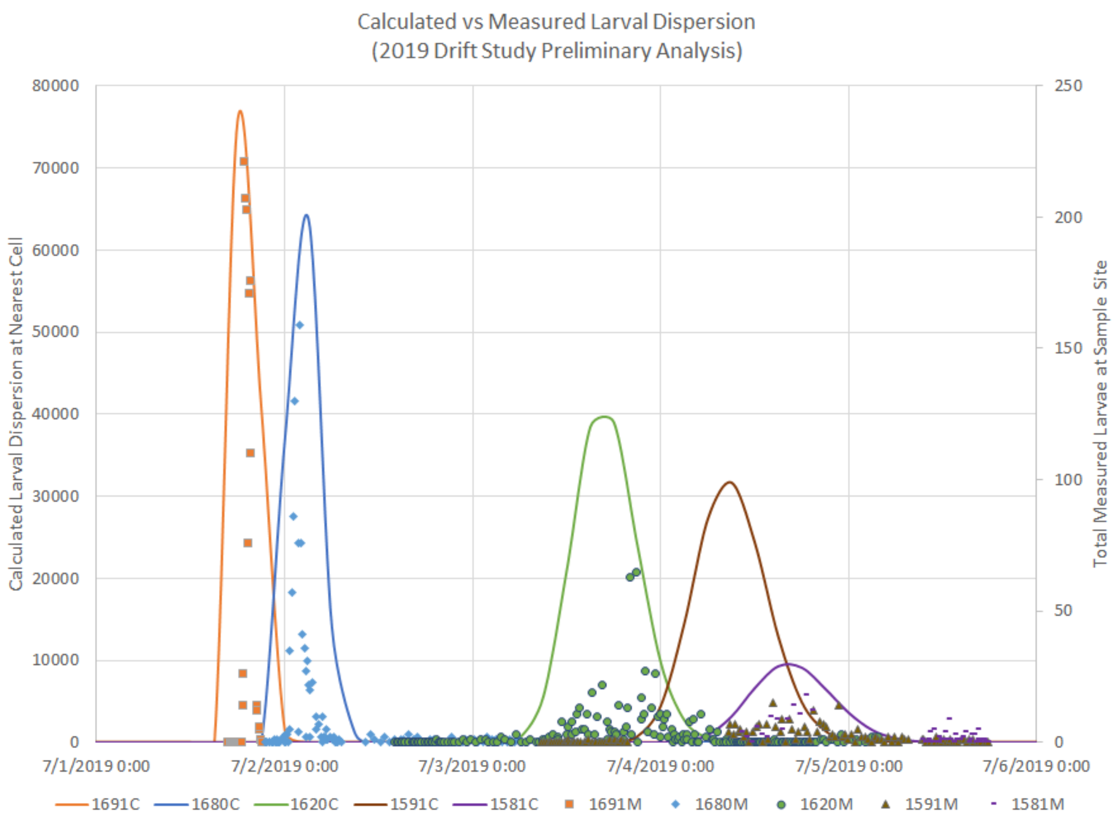

Figure 3-26. Calculated and measured distributions of larvae at five USGS sampling transects downstream of the release point near Wolf Point, MT for the 2019 drift study (measured values from Braaten and Holley 2021).

On balance, the velocity, temperature, and advection/dispersion results from the models align well with preliminary measured values from the 2019 drift study. Together with previous validation exercises (e.g. from the 2016 drift experiment) and comparisons of the HEC-RAS models to measured hydraulic conditions (USACE 2020) and temperatures (Zhang and Johnson 2017), we feel the DSM has been adequately validated for application to the Fort Peck EIS.

Notwithstanding the above statement, it is important to recognize that considerable uncertainty remains regarding biological and physical factors influencing spawning, hatch, dispersal, and recruitment of pallid sturgeon in the reach of the

Missouri River below Fort Peck Dam. The best application of the DSM at present is, therefore, in the relative comparison of alternatives and for sensitivity analyses to inform decision making. Reliance on model results as absolute predictors of outcomes is discouraged, although it is expected that additional data collected in conjunction with test flow releases (if any) would lead to model improvements and/or reduced uncertainty.

3.6 Discussion

The DSM is a purpose-built tool for evaluating proposed management actions at Fort Peck Dam on the UMR to evaluate the effects of those actions on retention (and by extension recruitment) of early life stage pallid sturgeon. Components of the toolset were initially developed in conjunction with the MRRP-MP Effects Analysis and subsequent EIS and were applied to AD modeling on the upper Missouri and lower Yellowstone Rivers for those purposes (Fischenich 2016). To our knowledge, that was the first time the water quality module in HEC-RAS had been used to simulate drifting embryos for any species or system.

By design, the DSM utilizes the models and modeling framework first described in Fischenich et al. (2014) and developed by the USACE Omaha and Kansas City Districts and contractors to support management decisions for the MRRP while servicing other ongoing planning, engineering, and operations needs for the Missouri River Reservoir System, BSNP, and a host of related concerns. This includes HEC ResSim and HEC-RAS models of nearly the entire system. These models have been subjected to comprehensive internal, external peer, and independent external peer review since 2014, but they have also been nearly continuously updated and improved over that timeframe.

While the ResSim and HEC-RAS models used as the backbone of the DSM do not require planning model certification, the relatively novel application of those tools to quantifying larval pallid sturgeon dispersal and development merits a careful review by individuals qualified to do so. Several pre- and post-processing tools are used to facilitate the analyses. Some address limitations in the HEC model suite; others are employed to ease the management of large data sets.

Model documentation for the DSM was compiled in November, 2019 and submitted to the USACE for model certification. The documentation focuses mainly on what the individual models do and the supporting science. Explicit descriptions of how the models were applied are limited, but may be important to an independent review and certainly important to their use in generating information for the DEIS.

Relatedly, no user manual or documentation beyond the model certification documentation and this report has been prepared to describe the DSM. Near-term application of the DSM is focused on the DEIS. Because of the emphasis on the DEIS, relatively little effort has been extended to data management, user interfaces, and the like. The Technical Team has provided the modeling support to the USACE for the EIS. Future applications of the model by the USACE in support of management decisions would benefit from appropriate documentation, users manuals, and training. Broader certification (e.g., Regional Application) may also become necessary if the model, or an improved version thereof, is to be more widely-used or reapplied periodically in support of the MRRP.

The Fort Peck Framework noted that *"The models used in the Fort Peck EIS to evaluate relative performance in terms of pallid sturgeon reproductive success will necessarily be indirect and simplified. We expect the effects models to improve continuously through application of adaptive management, however. Ongoing research that is focused on improving effects models, and the accumulation of information through monitoring of the results of flow releases, will improve realism and utility of the models. These improvements will assure that future decisions are substantially better informed"* (USACE 2018).

The MRRP has compiled a population model for the UMR (Reynolds and Colvin 2019), undertaken a second field experiment involving the release and tracking of pallid sturgeon free embryos in the UMR, compiled data to generate a new developmental series for pallid sturgeon, updated the HEC-RAS and ResSim models for the study reach, integrated temperature with AD modeling strategies, conducted expert elicitation workshops to improve model parameterization and guide experimental designs for test flows at Fort Peck Dam, and conducted scientific investigations under the MRRP Integrated Science Program that have provided critical knowledge related to UMR pallid sturgeon recruitment.

Understanding of pallid sturgeon biology and population ecology is rapidly evolving, as is the capacity of the MRRP to evaluate the implications of that new information, but significant uncertainties remain. Appendix A of the Fort Peck Framework outlines the relevant issues. Because the MRRP is being implemented under an AM framework, there is an ongoing need to develop and improve information and tools that can be applied to future decisions. Accordingly, the models reported on herein will be improved and applied to numerous AM needs, including the experimental design for flow tests, development of a monitoring and assessment plan, and ultimately the support of near-real-time decision making during the execution of flow tests.

4 Pallid Sturgeon UMR Demographic Population Model Description

4.1 Overview

The Pallid Sturgeon UMR Demographic Population Model (DPM) focuses on pallid sturgeon population dynamics and long-term population outcomes in response to changes in spawning and retention rates with alternative flows from Fort Peck Dam. The model is intended to be used for comparing the relative benefit of Fort Peck alternatives, as measured by long-term population growth rate and expected time to quasiextinction for the pallid sturgeon population residing in the UMR below Fort Peck Dam. While similar approaches could be used to model other pallid sturgeon populations, the UMR DPM was specifically constructed and parameterized to model the pallid sturgeon population residing in the UMR from Fort Peck Dam downstream to Lake Sakakawea, including the Yellowstone River downstream of Intake Dam (Figure 1-2), with the assumption that spawning on the Yellowstone River does not lead to age-1 recruitment due to drift of free-embryos into the anoxic zone above Lake Sakakawea (Bramblett and Scholl 2015; Guy et al. 2015). The model computes annual population changes and is mainly used to analyze projected long-term population dynamics. A stochastic version of the model that accounts for annual environmental variability can also be used to examine population projections in terms of time to quasiextinction.

The Pallid Sturgeon UMR DPM is an age-structured model that accounts for the transitions illustrated in Figure 4-1. The model was restricted to females, assuming that sperm from male pallid sturgeon is not a limiting factor for annual spawning (Caswell 2001). It is a pre-breeding Leslie matrix model constructed and analyzed in R (R Development Core Team 2010), a free, open-source software environment. Leslie matrix models have been extensively used in ecology and are a type of population projection matrix model (Caswell 2001); moreover, age-structured models have been used to model Lower Missouri River pallid sturgeon populations (e.g., Steffensen et al., 2013a; Wildhaber et al., 2017). A Leslie matrix model was chosen for its ability to incorporate observed differences in survival, maturity, and fecundity among UMR pallid sturgeon age classes, while being quick and easy to analyze in terms of relative projected population outcomes. In general, Leslie matrix models assume that the demography of the species under study is dependent on age (more so than stage or size) and that there is no individual variation within an age class.

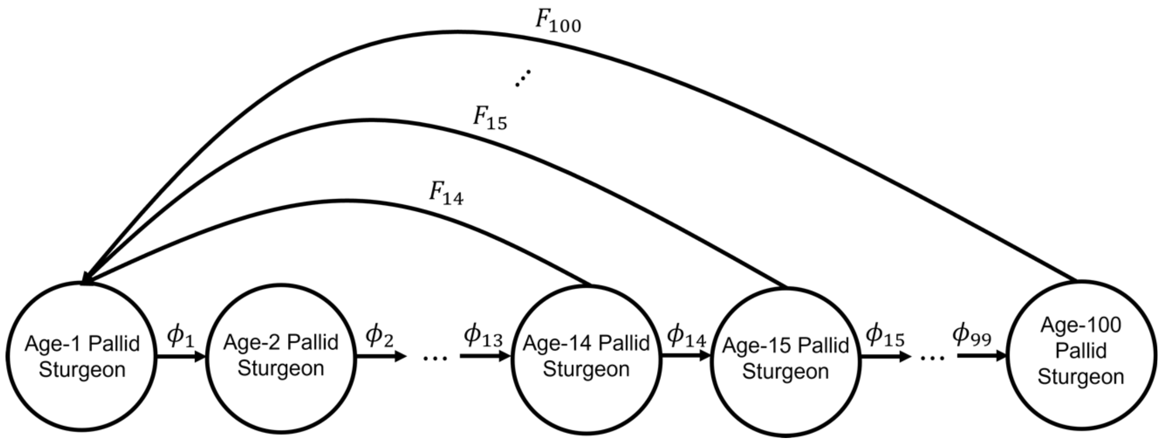

Figure 4-1. A conceptual diagram of the annual transitions of the pallid sturgeon demographic model. Pallid sturgeon annual survival ($\boldsymbol{\phi_i}$) and female fertility values ($\boldsymbol{F_i}$) are age-dependent. Only age-14 and older female pallid sturgeon contribute to reproduction with a maximum age, or age of female senescence, of 100 years old.

The Pallid Sturgeon UMR DPM depends on age-specific fertility values, age-specific survival values, and the maximum age (age of senescence) of female pallid sturgeon. Age-specific fertilities are broken down into underlying components for the purpose of parameterization (Figure 4-2). In addition to internal parameters related to survival, maturation, spawning period, and age-0 survival given retention (Figure 4-2, lower level green boxes), the model also includes two externally computed model inputs that vary by management alterative and year: 1) the probability of free-embryo retention upriver of the Lake Sakakawea anoxic zone, and 2) the proportion of reproductively-ready females spawning in the UMR (Figure 4-2, red boxes). Internal parameters are fixed at baseline values representative of UMR pallid sturgeon, while external model inputs vary across the Fort Peck test flow alternatives analyzed.

The main output of the DPM is the long-term population growth rate (Figure 4-2, yellow box). Additional outputs include the stable age-structure, sensitivity values, long-term population growth-decline boundaries, and the expected time to quasiextinction under environmental variability.

The following section provides details of the model structure. Parameter values are described in section 4.3, with baseline values listed in Table 4-1. Variable inputs are described in section 4.4. Model outputs are described in section 4.5.

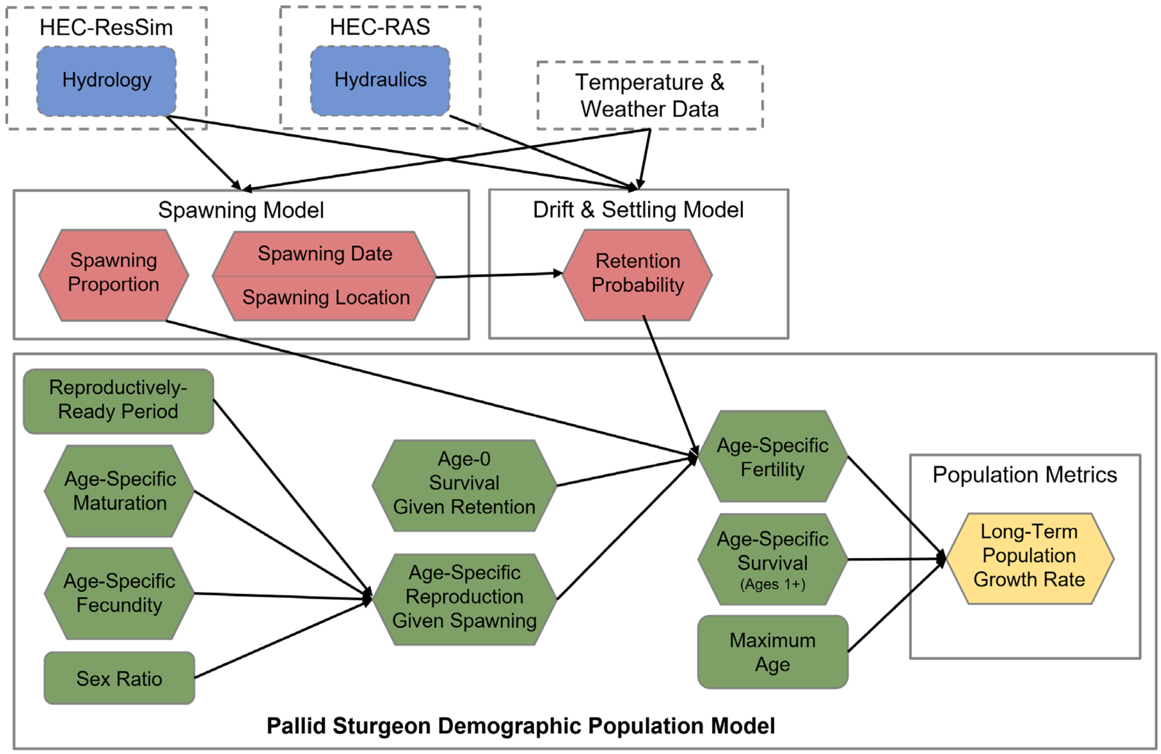

Figure 4-2. Graphical representation of the population modeling for pallid sturgeon as part of the Fort Peck DEIS.

4.2 Model Structure

The Pallid Sturgeon UMR DPM is an age-structured model of female pallid sturgeon accounting for the transitions illustrated in Figure 4-1. Mathematically, this model is a pre-breeding Leslie matrix model that projects annual pallid sturgeon population abundance given an initial population:

$$N_{t+1} = \mathbf{A}_t N_t, \qquad \text{4-1}$$

with

$$\mathbf{A}_t = \begin{pmatrix} F_{1,t} & F_{2,t} & F_{3,t} & \cdots & F_{a_{max-1},t} & F_{a_{max},t} \\ \phi_1 & 0 & 0 & \cdots & 0 & 0 \\ 0 & \phi_2 & 0 & \cdots & 0 & 0 \\ 0 & 0 & \phi_3 & \ddots & 0 & 0 \\ \vdots & \vdots & \vdots & \ddots & \vdots & \vdots \\ 0 & 0 & 0 & \cdots & \phi_{a_{max-1}} & 0 \end{pmatrix}, \qquad \text{4-2}$$

where

> N_t is a vector of female pallid sturgeon population sizes by age-class in year t,
>
> $\mathbf{A}_t$ is the prebreeding Leslie projection matrix in year t,
>
> $F_{i,t}$ is the expected fertility value of an age-i female in year t,
>
> ϕ_i is the probability that a female survives from age-i to age-$i+1$, and
>
> a_{max} is the maximum age of a reproducing female pallid sturgeon.

Each age-specific fertility value ($F_{i,t}$), or the expected number of female age-1 recruits per age-i female in year t, is a function of several underlying components (Figure 4-2) that either contribute to determining the number of females, female age-specific reproduction (the expected number of eggs released per age-i female), or age-0 survival (the probability of surviving from egg to age-1):

$$F_{i,t} = r \cdot R_{i,t} \cdot \phi_{0,t}, \qquad \text{4-3}$$

where

> $F_{i,t}$ is the fertility value of an age-i female, i.e., the expected number of age-1 female recruits per age-i female, in year t,
>
> r is the probability a fertilized egg is female, or the sex ratio,
>
> $R_{i,t}$ is the expected number of eggs released per age-i female in year t, and
>
> $\phi_{0,t}$ is the probability of surviving from egg to age-1 in year t.

Inclusion of the sex ratio (r), written in terms of the probability a pallid sturgeon is female, ensures that we are only counting recruited females. By utilizing a female-specific model, we've assumed that sperm from male pallid sturgeon is not a limiting factor for annual spawning.

Female age-specific reproduction ($R_{i,t}$) is defined by several components required to account for successful spawning and release of eggs in the UMR below Fort Peck Dam. For a female to spawn below Fort Peck Dam at a given age, she must be reproductively ready. The probability of being mature (m_i) and the distribution of time periods between reproductive readiness (p_τ) determine the proportion of age-i females that are reproductively ready to spawn (ψ_i). Not all reproductively ready females in the UMR will spawn below Fort Peck Dam (e.g., in the past several decades, nearly all have spawned in the Yellowstone River). Therefore, the proportion of reproductively ready females that spawns in the Missouri River (γ_t) contributes to the age-specific reproduction. Lastly, age-specific reproduction must account for age-specific fecundity given spawning (E_i). We assume the number of eggs released by a spawning female is related to her length, an attribute that changes with aging due to growth. Therefore, female fecundity also varies with female age.

Age-0 survival depends on what occurs during free-embryo drift. In particular, the model distinguishes between free-embryos that drift into Lake Sakakawea and those that settle out of the drift while still in the free-flowing Missouri River:

$$\phi_{0,t} = \phi_{0,MR} \cdot p_{ret,t} + \phi_{0,LS} \cdot (1 - p_{ret,t}), \qquad \text{4-4}$$

where

$\phi_{0,t}$ is the probability of surviving from egg to age-1 in year t,

$\phi_{0,MR}$ is the probability of surviving from egg to age-1 given retention in the free-flowing Missouri River,

$\phi_{0,LS}$ is the probability of surviving from egg to age-1 given free-embryo drift into Lake Sakakawea, and

$p_{ret,t}$ is the retention probability, i.e., the probability a free-embryo settles out of the drift while in the free-flowing Missouri River, in year t.

Combining all the underlying components of age-specific reproduction and age-0 survival, the age- and year-specific fertilities are defined as

$$F_{i,t} = r \cdot \psi_i(m_i, p_\tau) \cdot \gamma_t \cdot E_i \cdot (\phi_{0,MR} \cdot p_{ret,t} + \phi_{0,LS} \cdot (1 - p_{ret,t})), \qquad \text{4-5}$$

where

r is the sex ratio (fraction of the population that is female),

ψ_i represents the proportion of age-i females that are reproductively ready to spawn and is a function of m_i and p_τ,

m_i is the probability a female fish matures between age $i-1$ and age i,

p_τ is the probability that, for a female, the period between being reproductively ready is τ years,

γ_t is the fraction of reproductively-ready females that spawn in the Missouri River below Fort Peck Dam, or simply, spawning proportion, in year t,

E_i is the expected number of eggs released per spawning age-i female, and

$\phi_{0,MR}$, $\phi_{0,LS}$, and $p_{ret,t}$ are as described in equation 4-4.

The majority of the components (a_{max}, ϕ_i, m_i, p_τ, E_i, $\phi_{0,MR}$, and $\phi_{0,LS}$) that define the Leslie matrix model are parameters, quantities that are fixed to biologically reasonably values for pallid sturgeon residing in the UMR below Fort Peck Dam. The two remaining components—the probability of free-embryo retention ($p_{ret,t}$) and the proportion of reproductively-ready females spawning in the Missouri River (γ_t)—are externally computed model inputs (calculated by the DSM and spawning submodel, respectively) that vary by the flow alternative and year (t) under consideration.

4.3 Model Parameters

Long-term population growth rates are computed for various inputs to the Leslie matrix model (Equations 4-1, 4-2, and 4-5) with parameters a_{max}, ϕ_i, m_i, p_τ, E_i, $\phi_{0,MR}$, and $\phi_{0,LS}$ fixed to or computed from the baseline values given in Table 4-1. A description of the methods used to parameterize the model follows. Whenever possible pallid sturgeon data from the UMR below Fort Peck Dam was used.

Table 4-1. Pallid Sturgeon UMR Demographic Population Model baseline parameter values.

Parameter	Description	Baseline Value	Source and explanation
a_{max}	maximum age of a female pallid sturgeon (years)	100	Braaten et al. (2015) Hamel et al. (2020)
ϕ_1	probability of surviving from age-1 to age-2	0.64	Rotella (2017)
ϕ_2	probability of surviving from age-2 to age-3	0.69	Rotella (2017)

Parameter	Description	Baseline Value	Source and explanation
ϕ_3	probability of surviving from age-3 to age-4	0.72	Rotella (2017)
ϕ_4	probability of surviving from age-4 to age-5	0.76	Rotella (2017)
ϕ_5	probability of surviving from age-5 to age-6	0.79	Rotella (2017)
ϕ_6	probability of surviving from age-6 to age-7	0.82	Rotella (2017)
ϕ_7	probability of surviving from age-7 to age-8	0.84	Rotella (2017)
ϕ_8	probability of surviving from age-8 to age-9	0.86	Rotella (2017)
ϕ_9	probability of surviving from age-9 to age-10	0.88	Rotella (2017)
ϕ_{10}	probability of surviving from age-10 to age-11	0.895	extrapolation
ϕ_{11}	probability of surviving from age-11 to age-12	0.91	extrapolation
ϕ_{12}	probability of surviving from age-12 to age-13	0.92	extrapolation
ϕ_{13}	probability of surviving from age-13 to age-14	0.93	extrapolation
ϕ_{14}	probability of surviving from age-14 to age-15	0.935	extrapolation
ϕ_{15+}	annual survival probability for age-15+ fish	0.94	Klungle and Baxter (2005) and Jaeger et al. (2009)
r	probability a pallid sturgeon is female	0.5	equal sex ratio
a_h	age at which half the female population is mature	19	Molly Webb, USFWS, personal communication
k	related to the variance in maturation age	0.77	$3 \cdot \text{standard deviation} \approx 7$ years
a_m	minimum age at maturation	14	George et al. (2012), Steffensen et al. (2013b) with UMR fish maturing later; Molly Webb, USFWS, personal comm.
a_M	maximum age at which a fish will mature	27	Keenlyne and Jenkins (1993); Molly Webb, USFWS, personal comm.

Parameter	Description	Baseline Value	Source and explanation
p_1, p_{6+}	probability the period of time between female reproductive readiness is 1 year or greater than 5 years	0	DeLonay et al. (2016a)
p_2	probability the period of time between female reproductive readiness is 2 years	0.38	DeLonay et al. (2016a) and Fuller et al. (2008).
p_3	probability the period of time between female reproductive readiness is 3 years	0.37	DeLonay et al. (2016a) and Fuller et al. (2008).
p_4	probability the period of time between female reproductive readiness is 4 years	0.17	DeLonay et al. (2016a) and Fuller et al. (2008). Assumes 4 years is twice as likely as 5 years
p_5	probability the period of time between female reproductive readiness is 5 years	0.08	DeLonay et al. (2016a) and Fuller et al. (2008). Assumes 4 years is twice as likely as 5 years
E_1 - E_7	number of eggs released by females ages 1-7	0	minimum maturation age is 8
E_{14}	average number of eggs released by age-8 females	28,030	see in-text fecundity simulation details
N	eggs released by females ages 15-99	N	number of eggs increases approximately linearly at first and then with diminishing returns under simulation results
E_{100}	average number of eggs released by age-100 females	168,820	see in-text fecundity simulation details
$\phi_{0,MR}$	probability of surviving from egg to age-1 given retention in the free-flowing Missouri River	0.000075	Pine and others (2001) Gulf Sturgeon age-0 survival less than or equal to 0.0004
$\phi_{0,LS}$	Probability of surviving from egg to age-1 given free-embryo drift into Lake Sakakawea	0	Guy et al. 2015 Bramblett and Scholl 2015

4.3.1 Maximum Age (a_{max})

Braaten et al. (2015) estimated the ages of 11 deceased natural-origin pallid sturgeon from the UMR. They determined longevity to be at least 50 years, with all individual estimates varying from 37-59 years old. The baseline maximum age of a female pallid sturgeon was set at 100 years old, a value reasonably greater than the oldest aged fish by Braaten et al. (2015) and the maximum UMR pallid sturgeon age determined by Hamel et al. (2020).

4.3.2 Age-Specific Survivals (ϕ_i)

Age-specific survivals were estimated for pallid sturgeon ages 1 through 9 years old using cohort abundance estimates in Rotella (2017). Survival estimates for this analysis were limited to fingerlings released in research priority management area 2 (RPMA 2) within the Missouri River (i.e., the Missouri River below Fort Peck Dam to the headwaters of Lake Sakakawea) without fin curl or iridovirus. Fingerlings released into the river at about 3 months old were used to estimate age-specific survival with the expectation that 9 months of acclimation to river conditions would allow for a better estimate of natural age-1 to age-2 survival than yearlings released closer to age-1. Data tables provided in Rotella (2017) contained information for each cohort of fingerlings released into the Missouri River. The provided information included the estimated number of fish at the start and end of several consecutive intervals after release. Interval periods were not equal in length; however, start and end dates were provided in the tables. Therefore, for each healthy cohort of fingerlings released, we calculated daily survivals from the data provided in the tables as

$$\text{Interval Daily Survial} = \left(\frac{N \text{ at Interval End}}{N \text{ at Interval Start}} \right)^{1/\text{Days in Intervals}}, \quad \text{4-6}$$

We then used cohort-specific interval daily survivals to compute cohort-specific survivals from age-class to age-class, assuming all fish were born on June 1st. The weighted average of cohort-specific annual survivals was used as an estimate for the age-specific annual survivals:

$$\phi_i = \frac{\sum_{c \in C} \phi_{i,c} N_{i,c}}{\sum_{c \in C} N_{i,c}}, \quad \text{4-7}$$

where

ϕ_i is the age-i survival probability for ages $i = 1, 2, \ldots, 9$,

$\phi_{i,c}$ is the probability that a fish in cohort c survives from age-i to age-$i+1$,

$N_{i,c}$ is the expected number of age i fish in cohort c on June 1st, and

C is the set of all healthy cohorts (no iridovirus or fin curl) released into the Missouri River within RPMA 2 as fingerlings.

Adult annual survival (ϕ_{adult}) was computed from RPMA 2 wild adult population estimates in 2004 and 2008 (Klungle and Baxter 2005, Jaeger et al. 2009) as

$$\phi_{adult} = \left(\frac{125}{158}\right)^{1/4} \approx 0.94\,, \tag{4-8}$$

and set as the survival probability of all females age-15 and older. Survival probabilities for age-10 to age-14 pallid sturgeon were extrapolated to fall between the probabilities calculated for younger and older fish (Figure 4-3, Table 4-1).

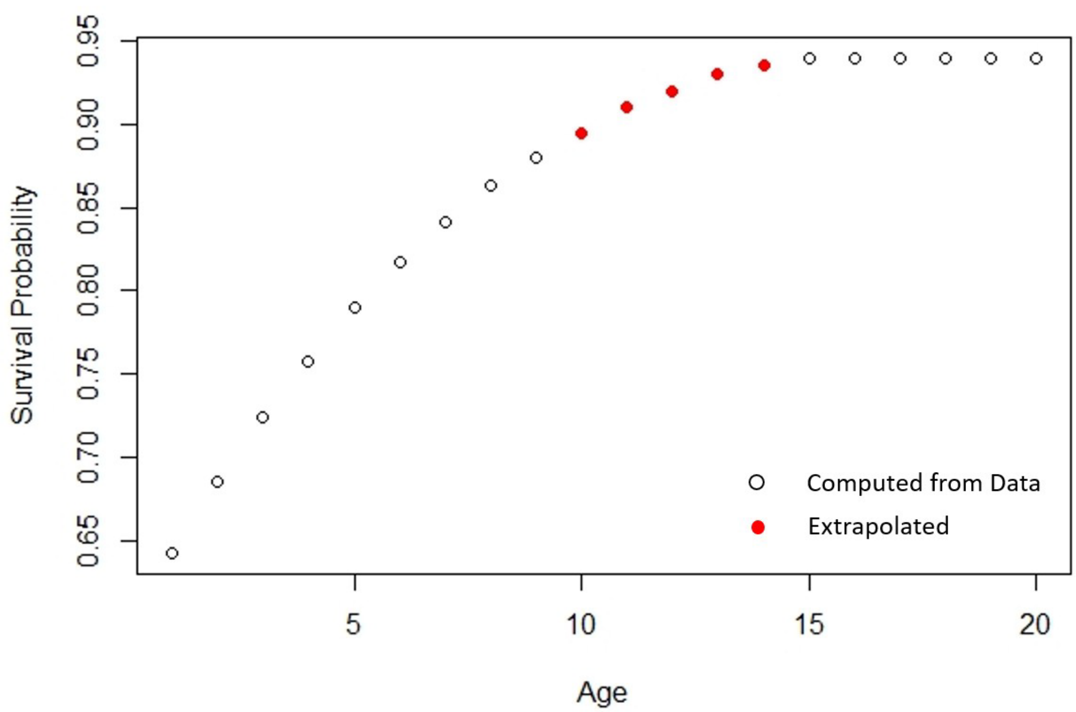

Figure 4-3. Baseline age-specific survival probabilities (ϕ_i). Values were computed from Rotella (2017) for ages 1-9 and from Klungle and Baxter (2005) and Jaeger et al. (2009) for ages 15+. Vales for ages 10-14 were extrapolated based on survivals of younger and older fish.

4.3.3 Sex Ratio (r)

The probability a fertilized egg is female (r) was set to 0.5, assuming an equal sex ratio. While the current wild adult population is expected to have fewer females than males (Jaeger et al. 2009), this is likely a result of selective harvesting (e.g., for caviar) prior to pallid sturgeon being federally listed as endangered in 1991 and not because fewer fertilized eggs were females than males.

4.3.4 Probability of Being Reproductively Ready ($\psi_i(m_i, p_\tau)$)

The proportion of age-i females that are reproductively ready to spawn is a function of maturation and spawning period:

$$\psi_i = \begin{cases} m_i, & i = 1,\ldots,a_m, \\ m_i + \sum_{j=a_m}^{i-1} \psi_j p_{i-j}, & i = a_m + 1,\ldots,a_{max} \end{cases}, \qquad \text{4-9}$$

with

$$\sum_{i=1}^{a_{max}} m_i = 1 \quad \text{and} \quad \sum_{\tau=1}^{\infty} p_\tau = 1, \qquad \text{4-10}$$

where

ψ_i is the proportion of age-i females that are reproductively ready to spawn,

m_i is the probability a female fish matures between age $i-1$ and age i,

p_τ is the probability that the period between being reproductively ready is τ years,

a_m is the minimum age at which a female matures, and

a_{max} is the maximum age of a reproductive female fish.

4.3.4.1 *Age-specific Maturation Probability* (m_i)

The maturation age of female pallid sturgeon is uncertain and is a subject of further informational need (DeLonay et al. 2016a). Age of maturation could also vary by region of the river, with observations from the UMR suggesting that female pallid sturgeon mature later than those in the Lower Missouri and Mississippi Rivers (M. Webb, USFWS, pers. comm.). The available published data involves only a few fish, most from the Lower Missouri and Mississippi Rivers. These females were estimated to have matured between 8 and 20 years old

(Keenlyne and Jenkins 1993, George et al. 2012). Fish aging was typically performed by pectoral fin ray analysis, a method that can suffer from low accuracy and precision (Hurley et al. 2004); consequently, there may be some unaccounted-for uncertainty due to aging error.

We used a logistic cumulative distribution model to describe the maturation of females with age:

$$M(a) = \frac{1}{1+e^{-k(a-a_h)}} \quad \text{4-11}$$

where

$M(a)$ is the proportion of age-a females that have reached maturity,

a_h is the age at which half of all females are mature,

k is a scaling parameter that controls the variance of the distribution, and

a is age.

To account for later maturation in UMR females, we assumed that 50% of female pallid sturgeon reach maturity by age 19 ($a_h = 19$; M. Webb, USFWS. pers. comm.), 9 years later than the expected value used by Wildhaber et al. (2017) for Lower Missouri River females. We also assumed $k = 0.77$ (corresponding to approximately 7 years representing 3 standard deviations). We converted this unbounded, continuous cumulative maturation distribution to a discrete probability distribution bounded between the ages of 14 and 27 (M. Webb, USFWS, pers. comm.; Figure 4-4), as follows:

$$m_i = \begin{cases} 0, & i = 1,2,\ldots,a_m - 1 \\ M(i), & i = a_m \\ M(i) - M(i-1), & i = a_m + 1, a_m + 2, \ldots, a_M - 1 \\ 1 - M(i-1), & a = a_M \\ 0, & i = a_M + 1, a_M + 2, \ldots, a_{max} \end{cases}, \quad \text{4-12}$$

where

a_m is the minimum age at which a female matures,

a_M is the maximum age at which a female matures, and

M is the cumulative distribution described in equation 4-11.

Figure 4-4. Baseline age-specific maturation probabilities (m_i), indicating the probability that a female matures at a particular age.

4.3.4.2 Years Between Being Reproductively Ready (p_τ)

The time (in years) between spawning events (i.e., spawning period) is the same as the time between becoming reproductively ready under circumstances where atresia does not occur. In cases of atresia, the spawning period provides an upper bound to the time elapsed between years in which the female was reproductively ready. The spawning period of female pallid sturgeon is likely 2-5 years (DeLonay et al. 2016a). However, it has been estimated to be as great as 10 years in past studies using spawning bands (Dryer and Sandvol 1993, Keenlyne and Jenkins 1993). Fuller et al. (2008) and DeLonay et al. (2016a) assessed the reproductive readiness of 28 female pallid sturgeon. Their data shows that all 28 females had a spawning period greater than 1 year ($p_1 = 0$). Additionally, 8 females had a confirmed spawning period of 2 years, with 13 others confirmed as having a spawning period greater than 2 years ($p_2 = 8/21$). Of the 13 females whose spawning period was more than 2 years, only the fates of 5 were known beyond this point: 3 females had a confirmed spawning period of 3 years $\left(p_3 = (13/21)(3/5)\right)$, and 2 females had a confirmed spawning period that was greater than 3 years. Under the following additional assumptions:

1. the maximum reproductively ready period of a female is 5 years, and
2. a female is approximately twice as likely to have a reproductively ready period of 4 years as she is 5 years,

the probabilities from the confirmed data of DeLonay and others (2016a) and Fuller and others (2008) lead to the following distribution for the periods between females being reproductively ready (Figure 4-5):

$$p_\tau = \begin{cases} 0, & \tau = 1 \\ 0.38 & \tau = 2 \\ 0.37, & \tau = 3 \\ 0.17, & \tau = 4 \\ 0.08, & \tau = 5 \\ 0, & \tau > 5 \end{cases}. \qquad \text{4-13}$$

The baseline distribution in equation 4-13 implies that a female is reproductively ready, on average, every 2.95 years.

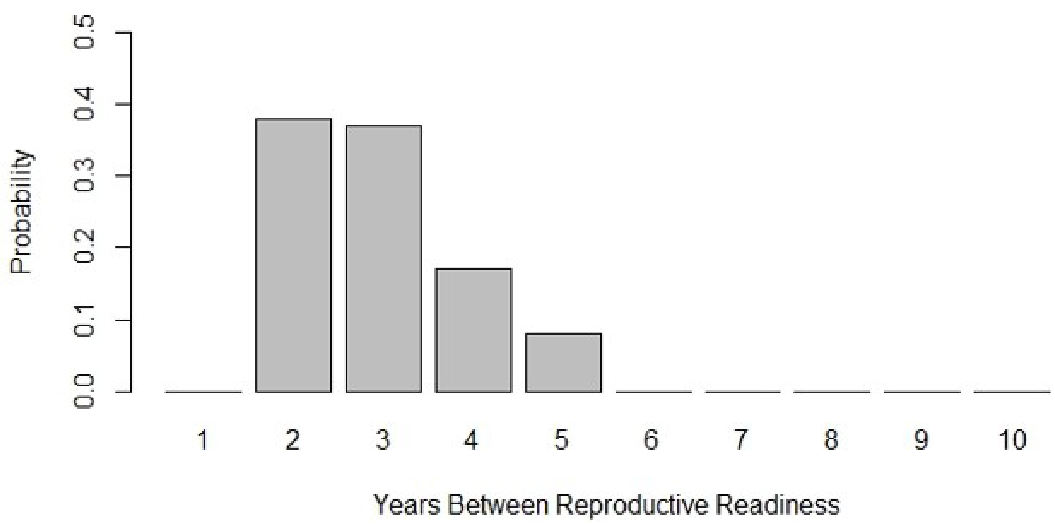

Figure 4-5. Probability distribution of the period between two consecutive instances of a mature female pallid sturgeon being reproductively ready based on data from DeLonay et al. (2016a) and Fuller et al. (2008).

This first approach at generating a probability distribution for years between reproductive readiness was generated from a small data set and must be treated with some caution. While much could be learned from the combined data of Fuller et al. (2008) and DeLonay et al. (2016a), the exact reproductive readiness period was unknown for 17 of the 28 females. Additionally, our model assumes that the time between reproductive readiness is independent of whether a reproductively ready female spawns or reabsorbs her eggs. If spawning and atresia effect this time period differently and it is expected that females frequently reabsorb their eggs, then it would be important to modify how age-specific fertilities are computed.

The baseline parameterization for the age-specific probability that a female is reproductively ready to spawn was computed from equations 4-9 through 4-13 with $a_h = 19$, $k = 0.77$, $a_m = 14$, and $a_M = 27$ (Table 4-1). No females are reproductively ready until age 14, at which point a very small fraction of the population matures. The fraction of females ready to spawn increases between ages 14 and 27, sharply at first and then more slowly, leveling out at approximately a third of all age-22+ females being ready to spawn during any given year (Figure 4-6).

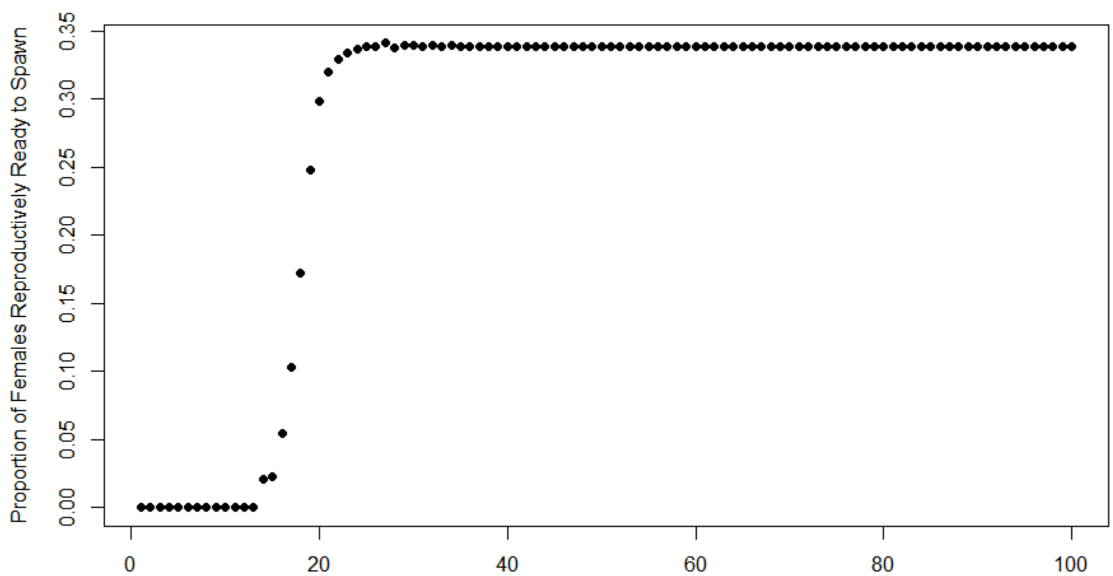

Figure 4-6. Baseline age-specific reproductive-readiness probabilities (ψ_i), computed from age-specific maturation probabilities and the distribution of time periods between reproductive readiness.

4.3.5 Expected Number of Eggs (E_i)

The expected number of eggs released by a spawning age-i female was determined from the composition of a probabilistic age-length (growth) relationship and a probabilistic length-fecundity relationship, as specified below. In the case that $i < a_m$ (minimum age at maturation), all females of age i have not reached maturity and $E_i = 0$. In the case of age classes that could contain mature fish, the general approach was, for each age $a_m \leq i \leq a_{max}$,:

1. Generate 1 million individual fork lengths at age i and a von Bertalanffy growth model;
2. For each of the one million lengths at age i, randomly generate the number of eggs produced from a probabilistic length-fecundity relationship;
3. Compute the mean number of eggs produced (across the one million fecundities) and use this as the value for E_i.

In the first step, the set of fork lengths (L_i) were estimated for each age i as

$$\begin{gathered} L_i \sim \mathcal{N}(\mu_i, \sigma_i), \\ \mu_i = L_\infty\left(1 - e^{-k(i-t_0)}\right), \\ \sigma_i = \sigma \cdot i^\delta, \end{gathered} \tag{4-14}$$

where

μ_i is mean fork length at age i,

L_∞ is the mean asymptotic length,

k is the Brody growth coefficient,

t_0 is the theoretical age at which length is 0,

${\sigma_i}^2$ is the variance at age i,

σ^2 is the variance at age 1, and

δ adjusts the variance as age increases.

Parameter estimates were obtained by fitting a von Bertalanffy growth model to UMR PSPAP length data of known-age hatchery-origin pallid sturgeon and growth data of unknown age pallid sturgeon with multiple captures (Table 4-2; Figure 4-7). Length at age data was fit, assuming a normal error distribution with variance increasing with age, as

$$L(a) = L_\infty \cdot \left(1 - e^{-k(a-t_0)}\right), \tag{4-15}$$

where

$L(a)$ is the mean fork length of an individual of age a, and

L_∞, k, and t_0 are as described in equation 4-14.

Growth data of unknown age fish with multiple captures were fit simultaneously, assuming a normal error distribution, as

$$L_2 = L_1 + \left((L_\infty - L_1)(1 - e^{-k\Delta t})\right), \qquad \text{4-16}$$

where

L_1 is the first of 2 consecutive length data points for an individual pallid sturgeon,

L_2 is the second of 2 consecutive length data points for an individual pallid sturgeon,

Δt is the time (in years) that passed between captures associated with L_1 and L_1, and

L_∞, k, and t_0 are as described in equation 4-14.

Mean parameter values were estimated in R using the R2jags package (Su and Yajima 2020), which runs program JAGS (Plummer 2003), a Gibbs Sampler using Markov Chain Monte Carlo simulation. Means were computed from 4 chains of 250,000 iterations with a burn-in period of 150,000 iterations. Chains were well mixed and all $\hat{R}$ values were less than 1.08. Because length at age data was only available for known age hatchery origin pallid sturgeon in RPMA 2 (ages less than 24 years old), an informative prior for L_∞ was chosen to improve the model fit for ages up to 100. Given a maximum fork length from PSPAP captures of 1640mm, we used a truncated normal distribution with a mean of 1400, a standard deviation of 100, a lower bound of 0, and an upper bound of 1800 as a prior for the mean asymptotic fork length (L_∞). Inspection of the posterior for L_∞ revealed that the distribution was not abruptly cut off by the choice of upper bound used.

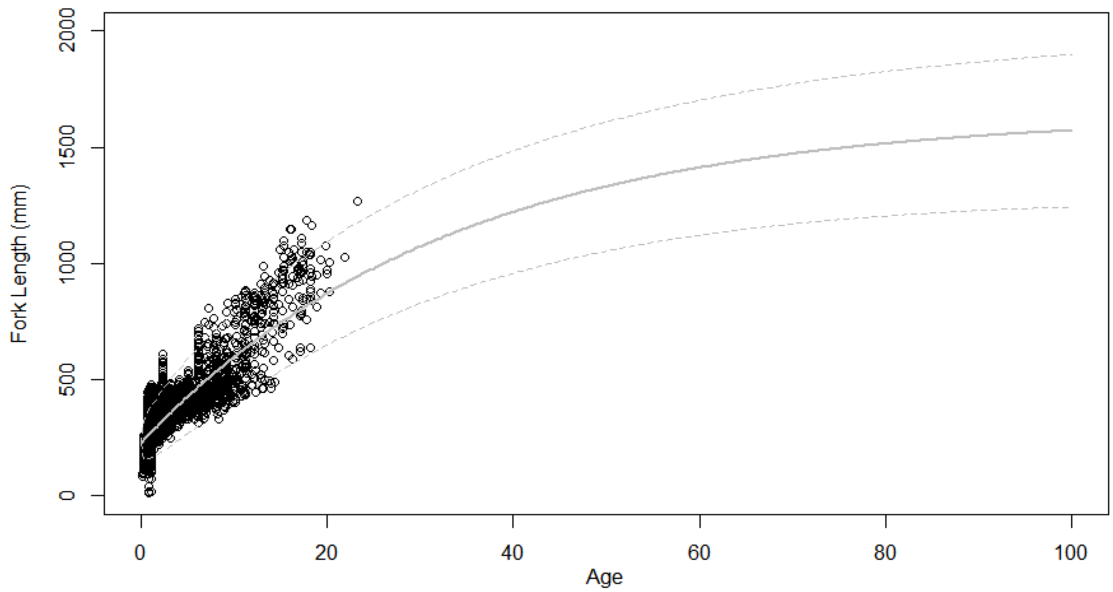

Figure 4-7. A von Bertalanffy growth model fit to PSPAP length at age data for known age hatchery origin pallid sturgeon (open points). Solid gray line represents the mean length at age, while the dotted gray lines represent ±2 standard deviations for the length at age simulations.

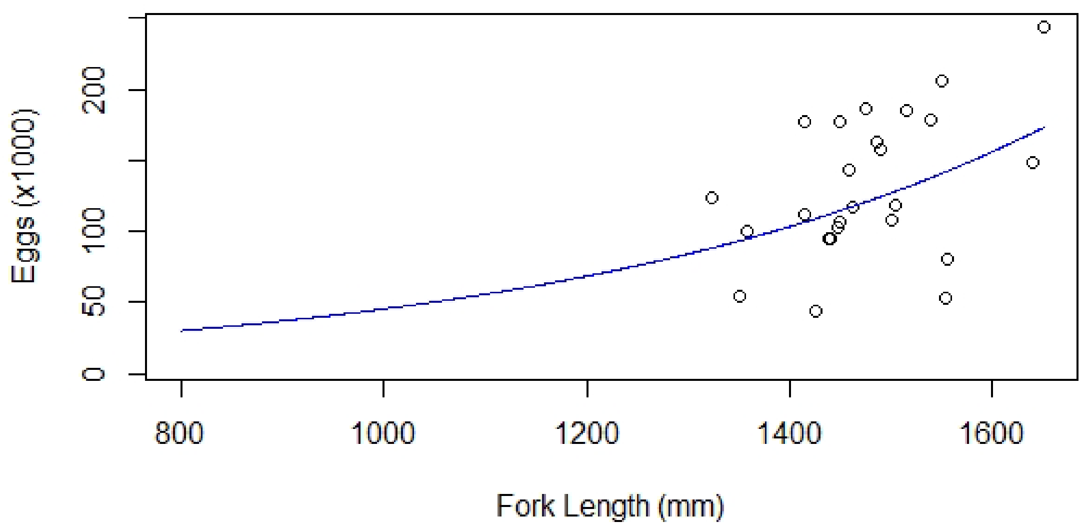

Figure 4-8. The average number of eggs produced per spawning female as a function of fork length (line). An exponential model was fit to Upper Missouri River fecundity data (open points) assuming an overdispersed Poisson error distribution.

Table 4-2. Parameter values used to simulate average age-specific fecundities.

Parameter	Description	Model	Value
L_∞	mean asymptotic length	age-length	1639.3680
k	Brody growth coefficient	age-length	0.0305
t_0	theoretical age at which length is 0	age-length	-4.9193
σ^2	variance at age 1	age-length	54.0090
δ	adjustment to the variance with age	age-length	0.2412
β_0	intercept	length-fecundity	11.2581
β_1	slope	length-fecundity	0.5715
ϵ_{disp}	dispersion parameter	length-fecundity	0.3942

In the second step, mean fecundity was assumed to be an exponential function of fork length with an overdispersed Poisson error distribution. The fecundity value for a given length, L, was randomly drawn from a Poisson distribution:

$$eggs \sim Poisson(\lambda(L)), \tag{4-17}$$

with mean value $\lambda(L)$ being drawn from a lognormal distribution to account for overdispersion observed in actual UMR length-fecundity data:

$$ln(\lambda(L)) \sim \mathcal{N}(\beta_0 + \beta_1 \cdot L_{norm}(L), \epsilon_{disp}), \tag{4-18}$$

where β_0, β_1, and ϵ_{disp} were fit in R using a generalized linear mixed effect model (glmer) with a Poisson distribution, log link, and random effects error term, and where

$$L_{norm} = \frac{L - 1260.1667}{277.4040}, \tag{4-19}$$

is a normalization of length (based on the mean and standard deviation of the length data) to aid in the convergence of the model fit. Baseline parameter estimates were obtained by fitting the model to 25 data points from 24 UMR female pallid sturgeon (Table 4-2; Figure 4-8).

In the last step, the arithmetic mean value was taken over all fecundity values generated for a given age, resulting in a number of eggs released per spawning female that increases with age (Figure 4-9). A simulation approach was used to capture mean age-specific fecundity take across individual females and is slightly higher than the fecundity values that result when inputting mean length at age into the fecundity function(Figure 4-9).

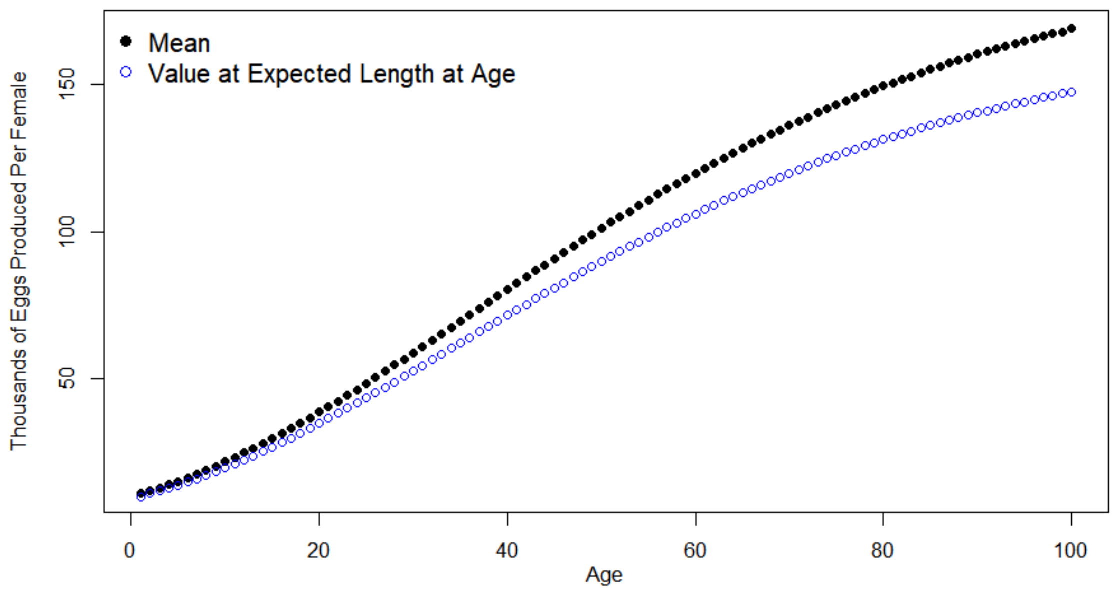

Figure 4-9. The black solid dots are the baseline values for age-specific fecundity (E_i), or the expected number of eggs released per age i spawning female. The open blue dots are the expected fecundity values at expected length at age and are shown for comparison only.

4.3.6 Age-0 Survival Given Retention

The probability of surviving from egg to age-1 given retention in the Missouri River ($\phi_{0,MR}$) is assumed constant, i.e., independent of the mother's age and flow alternatives. Pallid sturgeon age-0 survival given retention is uncertain, as is the case for many sturgeon species. We set baseline age-0 survival given retention at a small probability of 75 in one million or $\phi_{0,MR}$=0.000075. This value falls within the range of 0.0000-0.0004 used by Pine and others (2001) for gulf sturgeon. We further examine the sensitivity of model outcomes to changes in $\phi_{0,MR}$ to evaluate the potential effect of this uncertain parameter on the long-term population growth rate.

4.3.7 Age-0 Survival Given Drift into Lake Sakakawea

The probability of surviving from egg to age-1 given drift into Lake Sakakawea ($\phi_{0,LS}$) is also assumed independent of the mother's age. We set the baseline value for age-0 Lake Sakakawea survival at 0, assuming that free-embryos that drift into the lake do not survive the predicted anoxic conditions of the transition zone (Bramblett and Scholl 2015; Guy et al. 2015).

4.4 Model Inputs

The model has two variable inputs: the retention probability ($p_{ret,t}$) and the spawning proportion, i.e., the proportion of reproductively-ready females that spawns within the Missouri River below Fort Peck Dam (γ_t). These values vary with environmental conditions and flow alternatives. For each year and alternative, retention probability and spawning proportion inputs are specified by the outcomes of the DSM (Fischenich 2019; Chapter 3) and spawning submodel, respectively.

As described in 2.5, a simple spawning submodel uses HEC-ResSim hydrology and water temperatures predicted from climatic conditions to estimate the date of spawning (spawning submodel value of the DSM) and the proportion of gravid females attracted up the Missouri River to spawn below Fort Peck Dam (spawning proportion value required for the DPM). For a given year and flow alternative, spawning was assumed to occur on the first day that was at least 3 days post peak flow with release discharge greater than 17,500 cubic feet per second (cfs) and water temperature 16C or greater, given peak flows exceeded 20,000 cfs.

When the above conditions were met in June or July, it was assumed that 50% of the reproductively-ready female pallid sturgeon spawn below Fort Peck dam that year. This baseline spawning proportion of 0.5 represents a scenario in which spawning conditions on the UMR are assumed to be equal to those on the Yellowstone River, and no atresia occurs. The spawning proportion was estimated as 0 if any of the above criteria were not met, indicating all reproductively-ready females either spawn in the Yellowstone River or become atretic after not finding suitable spawning conditions.

Assuming that the proportion of reproductively ready females that spawn below Fort Peck given spawning occurs is constant with flow alternative and year is unlikely. As such, further studies and modeling analyses to assess the impacts of varying spawning proportion with temperature and flow is recommended. Improvements to the spawning model are expected over time as we learn more from an ongoing spawning expert elicitation (see Chapter 6), pallid sturgeon spawning research, and any test flow releases at Fort Peck Dam.

Note, any of the parameters described in section 4.3 could be respecified as input variables if there was a compelling reason (e.g., link to a management action, desired uncertainty analysis) to do so.

4.5 Model Outputs

Several model outputs were considered. The deterministic DPM analyses were performed with $\boldsymbol{A}_t = \boldsymbol{A}$ and $F_{i,t} = F_i$ for all long-term population outcomes (e.g., long-term population growth rate). A stochastic version of the DPM that accounts for environmental variability allowed $\boldsymbol{A}_t$ to vary over time when analyzing expected time to quasiextinction.

4.5.1 Deterministic Population Model Outcomes

4.5.1.1 Long-Term Population Growth Rate

The main model output is long-term population growth rate. Long-term population growth rates communicate the expected growth or decline of a population that consistently experiences the conditions specified by the given model inputs under the specified model parameterization. The long-term population growth rate is the leading eigenvalue of the Leslie projection matrix, which can be computed by eigenanalysis of the Leslie matrix and, therefore, does not require the specification of an initial population. All long-term population growth rate outputs are obtained using the eigen.analysis function from the demogR package (Jones and Oeppen 2018) in R (R Development Core Team 2010). Long-term population growth rates are computed for each year and flow alternative combination for which flow and temperature conditions would have supported spawning, as determined by the spawning submodel.

4.5.1.2 Sensitivity and Elasticity Values

Sensitivity and elasticity analyses were performed to understand the effects of varying a single parameter on long-term growth rate. Matrix entry sensitivities were computed by using the eigen.analysis() function from the demogR package (Jones and Oeppen 2018) in R (R Development Core Team 2010). Each fertility entry is composed of several components, so parameter sensitivities are further computed from the sensitivities of the fertility entries. Sensitivities for the age-specific proportion of females that are ready to spawn (ψ_i) and the age-specific fecundity of a spawning female (E_i) are computed as

$$\frac{\partial \lambda}{\partial x_i} = \frac{\partial \lambda}{\partial F_i}\frac{\partial F_i}{\partial x_i}, \qquad \text{4-20}$$

where

$\partial \lambda / \partial x_i$ is the sensitivity of x_i, the age-specific parameter of interest,

$\partial\lambda / \partial F_i$ is the sensitivity value for the age-i fertility entry,

$\partial F_i / \partial x_i$ is the partial derivative of the fertility entry for age-i females with respect to x_i,

λ is the long-term population growth rate,

x_i is either ψ_i or E_i for a fixed age-i, and

i is an admissible age (1 through a_{max}).

The sex ratio (r), age-0 survival given retention ($\phi_{0,MR}$), and age-0 survival given drift into Lake Sakakawea ($\phi_{0,LS}$) effect the fertility values across age classes, and therefore, sensitivities for these parameters are computed as

$$\frac{\partial\lambda}{\partial x} = \sum_{i=1}^{a_{max}} \frac{\partial\lambda}{\partial F_i}\frac{\partial F_i}{\partial x}, \qquad \text{4-21}$$

where

$\partial\lambda / \partial x$ is the sensitivity of x, the parameter of interest,

$\partial\lambda / \partial F_i$ is the sensitivity value for the age-i fertility entry,

$\partial F_i / \partial x$ is the partial derivative of the fertility entry for age-i females with respect to x, the parameter of interest,

λ is the long-term population growth rate, and

x is one of r, $\phi_{0,MR}$, or $\phi_{0,LS}$.

One parameter, the maximum age of a reproductive female, is not a component of any matrix entry. Instead, the maximum age (a_{max}) determines the size of the Leslie matrix. The sensitivity value of the maximum age is therefore computed as the average change in the long-term growth rate when computed for the Leslie matrix of size $a_{max} + 1$ and of size $a_{max} - 1$. Unlike the other sensitivity values, this sensitivity value is not an instantaneous rate of change; however, since the maximum age is not a continuous parameter, the average rate of change is a useful metric.

Sensitivity values can also be computed for input variables. Since the spawning proportion (γ) and retention probability (p_{ret}) inputs impact the fertility values in the same way as the sex ratio and age-0 survival given retention, sensitivities for these values are computed using equation 4-21. Additionally, equation 4-21 is flexible enough to compute the sensitivities for additional values that may be of interest (e.g., a_h, as described in equation 4-11).

Sensitivities express changes in long-term growth rate (λ) in terms of a unit change of a parameter value, while elasticities express changes in the long-term growth rate in relative terms. This can provide an additional useful comparison. For example, it is not difficult to imagine a female's fecundity increasing by one egg; however, it is impossible for age-0 survival to increase by a whole unit. Instead of unit comparisons, elasticities allow for percentage comparisons—for example, comparing the impact on λ of doubling a parameter (while holding the others constant). All elasticities are computed from sensitivities as

$$E(x) = \frac{x}{\lambda}\frac{\partial \lambda}{\partial x}, \qquad \text{4-22}$$

where

$E(x)$ is the elasticity of x, the parameter of interest,

$\partial \lambda / \partial x$ is the sensitivity of x,

x is the baseline value for the parameter of interest, and

λ is the long-term growth rate.

Note, because the baseline value for Lake Sakawea age-0 survival is 0, no elasticity value is computed for $\phi_{0,LS}$. Elasticity values for input variables are computed from equation 4-22 using the variable's input value as its baseline value.

4.5.1.3 Long-Term Growth-Decline Boundaries

Long-term growth-decline boundaries divide a region of parameter/input space into a region of population growth and a region of population decline. They provide an understanding of what combinations of parameters and inputs result in long-term population growth given model assumptions. A growth-decline boundary is a way of relating parameter uncertainty to long-term population dynamics in a much broader context than a sensitivity analysis. Specifically, this type of analysis ignores the magnitude of the growth rate, but it looks at the direction of the population dynamics (growth or decline) across a range of multiple parameter values as they vary together. In contrast, a sensitivity analysis looks at changes in the value of the long-term growth rate with respect to a very small change in a single parameter with all other values fixed. While a long-term growth-decline boundary can be computed for any parameter combination, it is particularly informative for understanding the effects of uncertain parameters that have large effects on model outcomes—something that can be informed by a sensitivity analysis. For the combination of parameters chosen to vary, long-term growth-decline boundary analysis can reveal parameter regions that are beneficial to the population, as well as how much uncertainty in a sensitive parameter can be tolerated and still allow for predictions of growth (or decline) (Deines et al. 2007).

A long-term growth-decline boundary was computed in terms of 3 variables: the two input variables (spawning proportion and retention probability) and the most uncertain variable with high sensitivity: age-0 survival given retention. The boundary is a 3-dimensional surface (1 axis for each variable), with variables varying across their range. Considering outcomes across a range of age-0 survival given retention can reveal how important it is to have a good understanding of this uncertain parameter value. Long-term growth-decline boundaries represent a long-term growth rate of $\lambda = 1$, or a stable population that is neither growing nor declining. These boundaries are computed from the characteristic equation of the projection matrix (Caswell 2001):

$$det(\mathbf{A} - \lambda \mathbf{I}) = 0, \qquad \text{4-23}$$

or equivalently,

$$1 = F_1 \lambda^{-1} + \sum_{i=2}^{a_{max}} \left(\prod_{j=1}^{i-1} \phi_j \right) F_i \lambda^{-i}, \qquad \text{4-24}$$

where F_i and ϕ_j are the age-specific fertility and survival values of the Leslie matrix described in equation 4-2, and λ is an eigenvalue of the matrix. In particular, the entries of the matrix model will fall on a growth-decline boundary when $\lambda = 1$ is a solution to the characteristic equation and all other solutions (x) are smaller in magnitude ($|x| < 1$), i.e., when 1 is the leading eigenvalue.

We compute a growth-decline boundary with the following steps:

1. Write the characteristic equation in terms of the variables of interest: retention proportion (p_{ret}), spawning proportion (γ), and age-0 survival given retention ($\phi_{0,MR}$) with all other parameter values fixed to their baseline values.
2. Substitute in $\lambda = 1$ as a solution to the characteristic equation and solve for one variable, say $\phi_{0,MR}$, in terms of the other two variables (γ and p_{ret}).
3. Evaluate $\phi_{0,MR}$ for a grid of input γ and p_{ret} values across their ranges (0 to 1), obtaining a 3-dimensional lattice of boundary values (e.g., $(\gamma_1, p_{ret_1}, \phi_{0,MR_1})$, etc.).
4. Use the eigen.analysis() function in R to verify that $\lambda = 1$ is the leading eigenvalue for each point computed in step 3.

This approach is equivalent to the approach used in Deines and others (2007); however, we look at the boundary in terms of the actual parameter values rather than to perturbations to the baseline values. We complete steps 1 and 2 in R by substituting into equation 4-24 and rearranging to define the function $\phi_{0,MR}(\gamma, p_{ret})$:

$$\phi_{0,MR} = \frac{1}{r\gamma p_{ret}\left(\psi_1 E_1 + \sum_{i=2}^{a_{max}}\left(\prod_{j=1}^{i-1}\phi_j\right)\psi_i E_i\right)}, \tag{4-25}$$

where γ and p_{ret} are variables and r, ψ_i, E_i, and ϕ_j are set to the baseline values given in Table 4-1, or in the case of ψ_i, computed from equation 4-9 through 4-13 given the baseline values in Table 4-1. While equation 4-25 solves for $\phi_{0,MR}$ given γ and p_{ret}, the same approach applies for solving for any one of the three variables in terms of the other two. The 3D lattice computed and verified in steps 3 and 4 is a discrete representation of the long-term growth-decline surface in terms of spawning proportion, retention probability, and age-0 survival given retention. Points below the surface represent demographic rates of a declining population, while points above the surface represent demographic rates of a growing population. We construct 2D contour plots to visualize the resulting boundary surface in 3D space.

4.5.2 Stochastic Population Model Outcomes

The long-term population growth rate communicates the expected growth or decline of a population that consistently experiences the conditions specified by the given model inputs under the specified model parameterization and assumptions. However, even when implementing the same management flow alternative each year (within human consideration constraints), input values for retention and spawning proportion are not fixed; they differ across the POR due to environmental variation. Annual spawning and retention outcomes are the most different between years when releases from Fort Peck are authorized and produce the desired alternative hydrograph and those when high, or low water conditions prevent Fort Peck releases. To account for the trade-offs in the impacts of a flow scenario on population growth and how often it can be implemented, we projected the dynamics of an initial population of pallid sturgeon forward for 200 years under simulated environmental variability. Initial populations were projected forward in time by randomly drawing annual spawning and retention probabilities from the paired values exhibited in the POR using a method that accounts for temporal correlation among consecutive years. Time to quasiextinction (<50 females remaining) and the sensitivity of this outcome to changes in parameter values were evaluated.

A similar approach can be used to compute average population growth rates across the POR for each flow alternative given an initial population of females in 1930. In this case, $\boldsymbol{A_t}$ is not drawn randomly each year t but is instead computed for each alternative from the estimates for spawning proportion, γ_t, and retention probability, $p_{ret,t}$, during each year $t = 1930, 1931, \ldots, 2012$, i.e., the POR. The average population growth rate is the geometric mean of the annual growth rates and can be computed for various input initial populations and analyzed with various statistics (mean, median, quantiles, etc.). These computations would compare alternative outcomes in the past; we chose to instead compare alternatives using the pallid sturgeon population projected into the future, assuming the temperatures from 1930 to 2020 (or a portion thereof) are representative of future conditions and spawning and retention outcomes are like those in the POR with the same temperature classification. To account for the potential effects of climate change, future analyses should use the most recent set of climatic data and, if warranted, synthesized hydrology and climate data to model environmental variation and its impact on spawning and retention outcomes.

4.5.2.1 Initial Populations

To evaluate dependence on the initial population, analyses were performed using two types of initial population estimates. In the first type, initial population numbers by age were assigned as a uniform distribution following Wildhaber et al. (2017). In the second type, population numbers were assigned to each age class to reflect an estimate of the current population structure. Total age-1+ initial population size was computed from recent median estimates of hatchery and wild/unknown origin pallid sturgeon (USACE 2020a). Half of the estimated 11,853 hatchery origin pallid sturgeon (HOPS) were assumed to be female, while 0.32 of the estimated 505 wild or unknown origin pallid sturgeon were assumed to be female. The lower female to male sex ratio in wild fish was estimated from the 40 females to 85 males reported in Jaeger et al. (2009) and reflected a history of selective harvest for caviar.

Initial populations with ages uniformly distributed were constructed by aggregating female estimates together for a total of 6089 females, resulting in 61 females in each age class from age 1 to age 89 and 60 females in each age class from age 90 to age 100.

Initial populations with ages distributed to reflect current estimates of abundance were constructed based on origin. The estimated 162 wild females were randomly assigned an age from 68-100 under the assumption that no natural recruitment had occurred since Garrison Dam closed in 1953. Hatchery origin fish were assigned an age class based on recent PSPAP HOPS captures. Specifically, PIT-tagged UMR HOPS captured from 2018 to 2020 in the Pallid Sturgeon Population Assessment Program (PSPAP) were aged using stocking history data. Only the most recent capture data was used for any individuals that were captured multiple times in 2018-2020. Ages of fish captured in 2018 and 2019 were projected forward to 2020, with capture counts discounted by age-specific survival (Table 4-1). The number of females in each age class was computed as the proportion of capture counts in each age class multiplied by the median HOPS estimate and a sex ratio of 0.5, rounded to the nearest individual. This approach assumes that capture probabilities are similar among age classes. While this assumption is likely violated, it provides a rough estimate of the age structure of the current HOPS population that indirectly incorporates differential survivals among family lots and year classes. Analyses of PSPAP data that provide age-, year-class-, and family-lot-specific survival estimates would allow for a refined estimate of the current HOPS population and are recommended for future analyses.

4.5.2.2 Modeling Environmental Variability

Environmental variability was modeled by drawing input values for spawning proportion (γ_t) and retention probability ($p_{ret,t}$) each year at random from 83 probability pairs in a manner that accounts for correlations in year-to-year temperature transitions. The set of spawning and retention probability pairs were determined by the established UMR spawning submodel (section 2.5) and DSM

(Chapter 3) for alternative flows during the years 1930-2012. Year-to-year correlations in temperature were accounted for by a transition matrix. Annual water temperature data from 1930-2020 was categorized as High (upper quartile), Normal (25^{th} to 75^{th} percentile), or Low (lower quartile) temperature classes (see section 3.3.1.2 for details) and the number of transitions from class j to class k relative to the total number of transitions from class j was used to parameterize the temperature transition matrix $\mathbf{V}$ with entries v_{kj} (as presented in section 5.3.3.2).

For each year in the projection, the temperature class for the current year was drawn using the temperature transition matrix given the previous year's temperature class (with the initial temperature class drawn as High, Normal, or Low with probabilities equal to the proportion of years from 1930 to 2020 the specific temperature class occurred). Next, a spawning and retention probability pair $(\gamma_t(flow), p_{ret,t}(flow))$ was drawn uniformly at random from all probability pairs associated with the temperature class for the current year (t) and the alternative management $flow$ under consideration. Therefore, the Leslie matrix $\mathbf{A}_t$ varied each year based on temperature- and alternative-specific spawning and retention joint probability distributions.

4.5.2.3 Time to Quasiextinction

We assessed the expected time to quasiextinction under a management strategy of using a single fixed management flow alternative each year while allowing spawning and retention probabilities to vary annually with variations in environmental conditions (e.g., snowpack, rainfall, temperature). Following Wildhaber et al. (2017), who analyzed the quasiextinction probability of pallid sturgeon in the Lower Missouri River (LMR), we defined quasiextinction as occurring when the replicate population fell below 50 females. For each management flow alternative, 5000 replicates were projected forward 200 years for each of the two initial populations. Since the baseline parameterization during spawning years resulted in long-term population decline in the deterministic model, quasiextinction was expected to occur within a couple generations in the absence of stocking. Indeed, at baseline parameter values, all stochastic replicates for each management alternative reached quasiextinction before 200 years. Therefore, we defined the quasiextinction probability at year t as the proportion of all replicates that fell below 50 females during year t and computed the expected value of time to quasiextinction.

4.5.2.4 Quasiextinction Sensitivities

To assess the importance parameters played on quasiextinction outcomes, simulations were repeated (5000 replicates; 200 years) with variation in a single parameter while all other parameters remained fixed. Non-zero continuous model parameters (ϕ_i, r, ψ_i, E_i, $\phi_{0,MR}$, γ_t, and $p_{ret,t}$) were increased and decreased by 5% of their baseline parameter or input values Wildhaber et al. (2017), while age parameters (e.g., a_{max}) were increased and decreased by 1. Sensitivities were computed as the change in the expected time to quasiextinction divided by the change in parameter value. Elasticities were computed as the sensitivity value multiplied by the parameter value divided by the expected time to quasiextinction under baseline conditions.

To further assess the impact of age-0 survival on quasiextinction outcomes, 8000 replicate populations were projected forward for each flow scenario and age-0 survival given retention values from 0.0002 to 0.0016 at a mesh of 0.0002, in addition to the baseline value of 0.000075. Since the deterministic model switches from a declining population to a growing population along this range of age-0 survival values, we projected each population forward 1000 years to allow all replicate populations to reach quasiextinction. Due to the extra simulation time needed for this analysis and the similarities in rank order comparison results among initial population types, this analysis was only run for an initial population with an age distribution based on recent PSPAP captures (to reflect 2020 estimated abundances by age).

5 Model Results

5.1 Overview

The National Environmental Policy Act requires the USACE to fully assess the potential impacts of alternative test flows under consideration for the Fort Peck DEIS. Results presented herein provide the necessary information for the decision maker to evaluate benefits to pallid sturgeon of each action alternative relative to No Action. Section 5.2 presents the application of the modeling described in sections 2 and 3 to the potential impacts of each Fort Peck EIS alternative on the Missouri River pallid sturgeon population with special emphasis on the potential to increase survival and recruitment of age-0 pallid sturgeon. Section 5.3 presents results of the application of deterministic and stochastic versions of the pallid sturgeon demographic population model (see section 4) to the alternatives.

The primary objective of Fort Peck Dam test flows is to test hypotheses that flow management actions can attract, retain, and aggregate reproductively-ready pallid sturgeon on the UMR and provide conditions for successful spawning and recruitment. The Drift and Settling Model (DSM) was used to quantify the frequency of spawning and the proportion of larval pallid sturgeon that settle in lotic reaches of the UMR (i.e., retention), which is hypothesized to be a limiting factor for recruitment. Criteria for each alternative were applied to conditions experienced in the basin from 1930 through 2012 (the POR) to simulate alternative implementation, and outcomes were evaluated with the DSM.

The analyses showed that spawning frequency for the POR was greatest for Alternatives 1b and 2b (N=11) and least for 1a and the No Action Alternative (N=3). Alternative 1 (N=9) and Alternative 2 (N=8) provided implementation opportunities similar to the “b” alternatives, while Alternative 2a (N=4) was only marginally better than 1a and the No Action. Combining the variants (i.e., 1, 1a, and 1b or 2, 2a, and 2b) into two composite alternatives provides opportunities for test flow implementation in 12 of the 83 years for each alternative, versus the 3 years for the No Action Alternative (see section 5.2.1).

Spawning and retention contribute to recruitment and population growth, which are the MRRP pallid sturgeon sub-objectives. The pallid sturgeon Demographic Population Model (DPM) used Round 2 outputs from the DSM (see section 5.2.2) along with other parameters related to survival, maturation, spawning period, and age-0 survival to quantify long-term population growth rate and expected time to quasiextinction for the pallid sturgeon population residing in the UMR below Fort Peck Dam. Average long-term population growth rates (LTPGRs) given spawning were highest for Alternative 1b and lowest for the No Action Alternative, but differed by less than 0.01467 across all alternatives and were less than 1.0 in all cases (see section 5.3.2). Expected time to quasiextinction ranged from 75.1 years for the No Action Alternative to 81.6 years for Alternative 1b (see section 5.3.3). All alternatives outperformed the No Action Alternative.

The Fort Peck DEIS is investigating the capacity of test flow alternatives to assess flow management hypotheses under an adaptive management framework. Flow management at Fort Peck Dam for pallid sturgeon spawning and recruitment may not be needed or may prove ineffective and, if effective, the characteristics of the flows may evolve with new knowledge. Accordingly, selection of a preferred alternative should consider the effectiveness of the alternatives in testing hypotheses and addressing uncertainties in addition to their effectiveness in contributing to pallid sturgeon recruitment.

5.2 Temperature, Advection/Dispersion, and Settling Model Results

Several rounds of analyses were conducted to assess water temperatures, A/D, spawning, larval development, and settling in support of the Fort Peck EIS. For each successive round, improvements were made to the data, model parameterizations, model structure, or other study components. Assumptions regarding conditions for spawning, for example, evolved over the study period and were informed by ongoing research under the MRRP and by an expert elicitation conducted for that purpose (see section 6). Because of these ongoing improvements, some results differ from those in earlier DEIS versions. Summary results presented herein are for the most recent round of analysis (Round 3) unless otherwise stipulated, and as discussed further below.

5.2.1 Test Flows and Presumed Spawning

HEC-ResSim - a reservoir operations model – was used to simulate System operations using criteria in the Master Manual (USACE 2006), historical flows during a period of record of 1930-2012, and rules developed to implement alternative the test flows without adversely affecting other authorized purposes. The model simulations provided pool elevations and regulated inflows and outflows of each of the mainstem projects for each alternative simulation for the period of record. These data were used directly as input to the HEC-RAS models for A/D and water temperature simulations. The ResSim model is described in detail in Appendix D of the EIS (USACE 2021), while section 3.2 of the EIS includes a summary of mainstem System operations focusing on Fort Peck and Garrison Dams.

Outputs from the ResSim model for each alternative were used in conjunction with general water temperature models as described in section 3.1 and criteria developed by the authors and informed by an expert elicitation (see section 6) to identify years in the POR for which flows and temperatures below Fort Peck Dam might support pallid sturgeon attraction, aggregation, and spawning. These periods generally correspond with conditions for a successful test flow implementation, but include a few instances where test flows were not conducted and exclude a few test flows that failed to achieve the desired conditions.

Table 5-1 summarizes the spawning year analysis for Round 3. Note that these results differ slightly from the Round 2 analyses, reflecting input from an expert elicitation on the subject (see section 6). Years meeting all spawning criteria are shown with a shaded green cell and an "X" and years that nearly met the criteria are shown with a light gold shading and an asterick. This latter category included temperatures within 0.2 ^{o}C or flows within 1,000 cfs of thresholds, and generally involved conditions that were within 1 or 2 days of meeting the criteria. The frequency of spawning over the POR is a useful metric for comparing alternatives because it indicates the probability of testing hypotheses in a given year and the likely timeframe required to complete testing (assuming 3 to 5 test flows).

The analyses showed that spawning frequency for the POR was greatest for the "b" variants of the alternatives (N=11 for Alts 1b and 2b) and least for "a" variants (N=3 for Alt 1a and N=4 for Alt 2a). Flow conditions were a limiting factor for a few cases, but the outperformance of the "b" variants is mainly due to the warmer temperatures associated with releases later in the spring. Alternative 1 (N=9) and Alternative 2 (N=8) provided implementation opportunities similar to the "b" variants and all options equaled or exceeded the spawning frequency for the No Action Alternative (N=3). Combining the variants (i.e., 1, 1a, and 1b or 2, 2a, and 2b) into composite alternatives provides opportunities for test flow implementation in 12 of the 83 years each for Alternative 1C and Alternative 2C. Implementation was the same for the combined alternatives in 10 years; Alternative 1C included 1994 and 2012, while Alternative 2C included 1966 and 1986.

Table 5-1. Years in the POR for which Round 3 spawning criteria were met (X with green shaded cell) and years they were nearly met (* with yellow shaded cell).

Year	Spawning Submodel Results						
	Alt 1	Alt 1a	Alt 1b	Alt 2	Alt 2a	Alt 2b	No Action
1930			X			X	
1949			X			X	
1966			*			X	
1975	X	X	X	X	X	X	X
1976	*		*	*		*	*
1980	X		X	X		X	
1983	X		X	X		X	
1985	X		X	X		X	
1986	*		*	X		*	
1987	X	*	X	X	X	X	
1994			X			*	
1997	X	X	X	X	X	X	X
2000	X		X	*		X	
2011	X	X	X	X	X	X	X
2012	X		*	*		*	
# Years	9	3	11	8	4	11	3

5.2.2 Retention Estimates

Hydraulic outputs were generated for each alternative and spawning year using the HEC-RAS models with a 1-hr maximum computation interval for a period beginning at least 10 days before the presumed hatch and lasting a minimum of 25 days. Computational level outputs were generated for each hydraulic simulation so that they could be applied to temperature and A/D modeling. The water quality module was applied to each simulation for a period beginning at least 7 days before the presumed hatch and ending at least 12 days after the hatch. Outputs for velocity, temperature, and cell mass (i.e., number of larvae) at each cell for each three-hour timestep were generated and input to an excel worksheet for post-processing. Outputs were not written to RAS or DSS files in every case because of the storage requirements.

For the preliminary analyses, only the unadjusted Braaten Model for settling (i.e. 200 CTU threshold) was applied and, because hourly data were not then available for years prior to 1946, 1930 was not included in the analysis. Three boundary conditions for the water temperature of releases from Fort Peck and tributary inputs were evaluated for each year: the long-term average conditions and one standard deviation warmer and cooler. The preliminary analyses were used primarily for sensitivity, to assist with model assessment, and to provide preliminary outputs for alternative assessment (all alternatives outperformed the No Action Alternative and critical insights were gained regarding the importance of prevailing weather conditions) and for development of the DPM.

A second round of analyses – the primary basis for assessment of population metrics in the DEIS - were made with the following refinements: a) updates to the HEC-RAS model geometry and calibration, b) minor adjustments to the ResSim hydrology for a few years in the POR, c) the addition of meteorological data for dates prior to 1960, d) classification of each year as Cool, Normal, or Warm to set boundary conditions for tributary and Fort Peck flow temperatures, and e) inclusion of the Stage-Development Model for settling as well as advection rate-modified versions of both the Braaten and Stage-Development Models. Determinization of hatch date was based on presumed spawning occurring at or above a 16 ^{o}C threshold for spillway flows, provided spillway flows exceeded 3,000 cfs (~20 percent of powerhouse flows). Appendix C.1 includes plots of flows and temperatures for each year in the POR a flow was attempted in the hydrological analyses for the EIS.

Round 3 analyses differ from those for Round 2 in two regards; the assumptions regarding spawning and hatch dates were updated to reflect new information from an expert elicitation (see sections 2.5 and 6), and an adjustment was made to the wind parameterization in the water temperature model to improve fit of results to measured data. The Round 3 adjustments generally increased the predicted retention rates relative to preliminary and Round 2 analyses.

Mrnak et al. (2020) developed a relation for onset of rheotaxis for larval pallid sturgeon and the MRRP Independent Science Advisory Panel (ISAP) recommended adding this relation as an additional model for larval development and settling. Results of the Mrnak relation applied to the Round 3 data are shown in Table 5-2. With few exceptions, onset of rheotaxis occurs much earlier than the settling predicted by the other four models, generally while nearly all larvae remain upstream of the Lake Sakakawea anoxic zone. The results are not as sensitive as the other “base” models for differentiating among alternatives, although it suggests the same relative alternative performance as the base models.

Table 5-2. Percentage of pallid sturgeon larvae upriver of RM1528 at onset of rheotaxis based on the relation from Mrnak et al. (2020)

	Alternative						
Year	NA	Alt 1	Alt 1a	Alt 1b	Alt 2	Alt 2a	Alt 2b
1930				97.6%			82.5%
1949				100.0%			100.0%
1966							100.0%
1975	99.4%	99.4%	99.6%	99.6%	100.0%	99.7%	99.4%
1980		79.0%		98.4%	100.0%		97.7%
1983		49.9%		99.8%	100.0%		100.0%
1985		20.3%		100.0%	100.0%		59.5%
1986					100.0%		
1987		100.0%		99.6%	100.0%	100.0%	99.7%
1994				97.3%			
1997	100.0%	100.0%	100.0%	100.0%	100.0%	100.0%	100.0%
2000		0.0%		100.0%			100.0%
2011	30.3%	79.4%	46.6%	29.8%	79.1%	46.6%	46.3%
2012		92.2%					

Retention results for the five larval development models are presented in Appendix C3. The use of multiple models complicates a comparison of the alternatives, but the range of results provides some added fidelity given uncertainty regarding actual development and advection rates. In general, the Braaten model is the most conservative (lowest retention) and the Adjusted Stage-Onset model typically returns the highest retention rates of the base model suite; exceptions to the general performance are indicative of outliers in flow or temperature conditions. A model based on Mrnak (2020) data relating temperature and time to rheotaxis shows that a large proportion of larvae should have achieved rheotactic swimming capability while still upriver of the anoxic zone in most test flow years. Importantly, the relative performance of the alternatives is essentially the same, independent of which model is used for comparison.

Table 5-3 shows the comparison of alternatives from Round 3 analyses using the Braaten and Adjusted Braaten Models. Table 5-4 shows the comparison of alternatives for the Stage-Onset and Adjusted Stage-Onset Models. Results are shown graphically in Figure 5-1 and Figure 5-2. Results of the Mrnak relation are shown in Table 5-5.

Table 5-3. Comparison of retention results across alternatives for Braaten and Adjusted Braaten Models. Orange highlighted cell is top performer in that category; green highlight is next best performer.

Alt	Model	Total	Ave.
1	Braaten	1.069	0.134
1a	Braaten	0.554	0.185
1b	Braaten	1.813	0.181
2	Braaten	2.510	0.314
2a	Braaten	1.393	0.348
2b	Braaten	2.458	0.223
NA	Braaten	0.500	0.166
1	200; 0.9	1.920	0.213
1a	200; 0.9	0.863	0.288
1b	200; 0.9	3.443	0.344
2	200; 0.9	4.031	0.504
2a	200; 0.9	1.844	0.461
2b	200; 0.9	4.078	0.371
NA	200; 0.9	0.800	0.266

Table 5-4. Comparison of retention results across alternatives for Stage-Development and Adjusted Stage-Development Models. Orange highlighted cell is top performer in that category; green highlight is next best performer.

Alt	Model	Total	Ave.
1	New	2.000	0.222
1a	New	0.942	0.314
1b	New	3.293	0.299
2	New	4.498	0.562
2a	New	1.915	0.479
2b	New	4.057	0.369
NA	New	0.900	0.300
1	New;0.9	3.201	0.356
1a	New;0.9	1.268	0.423
1b	New;0.9	5.040	0.458
2	New;0.9	6.024	0.753
2a	New;0.9	2.292	0.573
2b	New;0.9	5.488	0.499
NA	New;0.9	1.230	0.409

Table 5-5. Comparison of retention results across alternatives for a model based on the Mrnak (2020) data for temperature effects on rheotaxis. Orange highlighted cell is top performer in that category; green highlight is next best performer.

Alt	Model	Total	Ave.
1	Mrnak	6.202	0.775
1a	Mrnak	2.462	0.821
1b	Mrnak	10.221	0.929
2	Mrnak	7.791	0.974
2a	Mrnak	3.463	0.866
2b	Mrnak	9.851	0.896
NA	Mrnak	2.300	0.766

Alternative 2 was the top performer for three of the four base models when viewed in aggregate retention across the POR and is second for the fourth model. Alternative 2b was the second best performer for three models and the top performer in the other. It also had the largest number of presumed spawning events (11 times, tied with Alt 1b), three more than Alternative 2. Alternative 1b ranked third in every model for cumulative performance. Alternatives 1 and 2a had roughly the same performance. The Mrnak relation provided similar results to the other models in terms of relative performance, although the absolute magnitudes were higher. All the alternatives outperform the No Action, although alternative 1a is only marginally better.

When viewed on a per-event basis, Alternative 2 is the top performer for three of four models and second on the fourth. Alternative 2a is nearly as good, with the top rank for one model second best for the other three. Alternative 1 is the worst performer, slightly behind the No Action Alternative. Alternatives 1a, 1b, and 2b are roughly equivalent and intermediate to 2/2a and 1/NA. Performance on a per-event basis is much more variable across the models and across individual years. When viewed more closely and on a year-by-year basis (see Table C3-1 through Table C3-5), the best alternative is highly dependent on the specific weather, water temperature, and runoff conditions.

Viewing alternative performance across the model suite for both cumulative and event-based performance provides a sense of the robustness of each alternative. Table 5-6 shows the results of a comparison across models. Alternative robustness viewed in this manner provides results similar to the above; Alternative 2 is the top performer and all alternatives outperform the No Action Alternative.

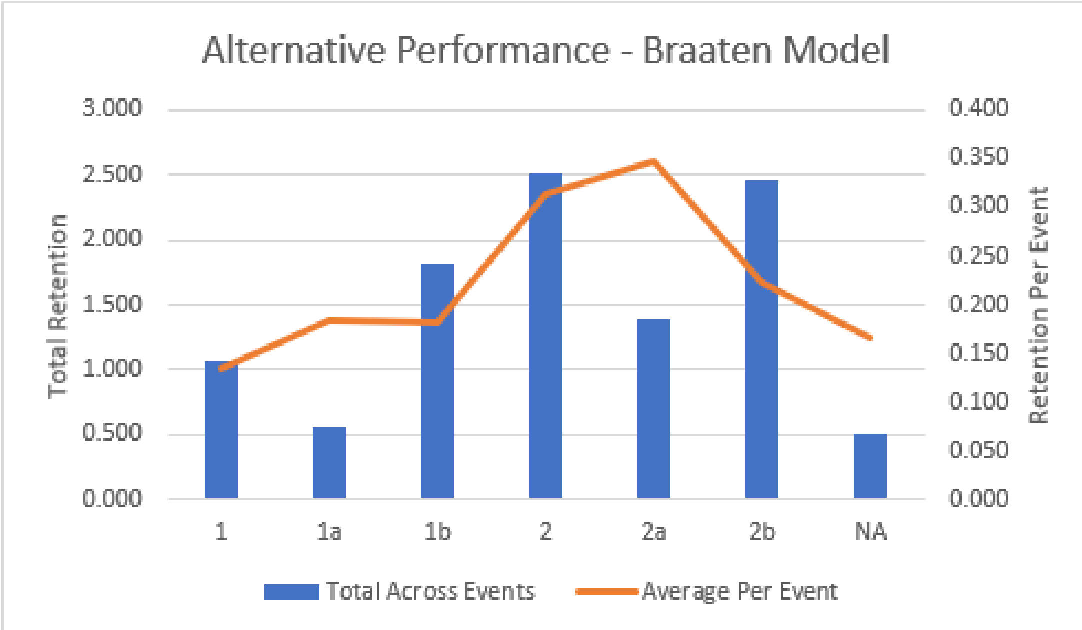

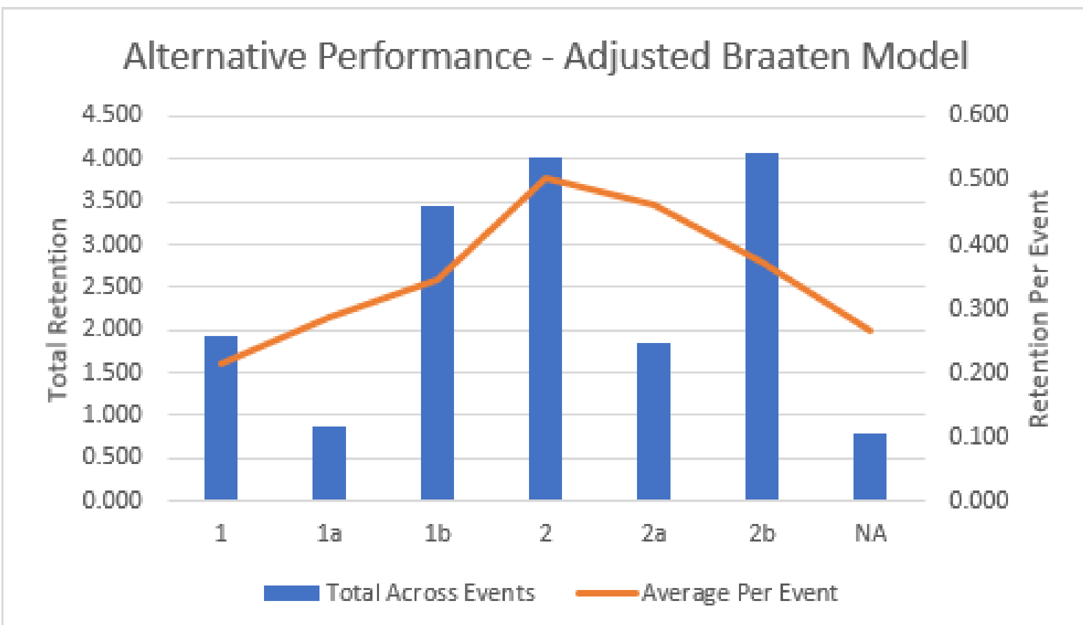

Figure 5-1. Alternative performance for Round 2 analyses using the Braaten and Adjusted Braaten Models.

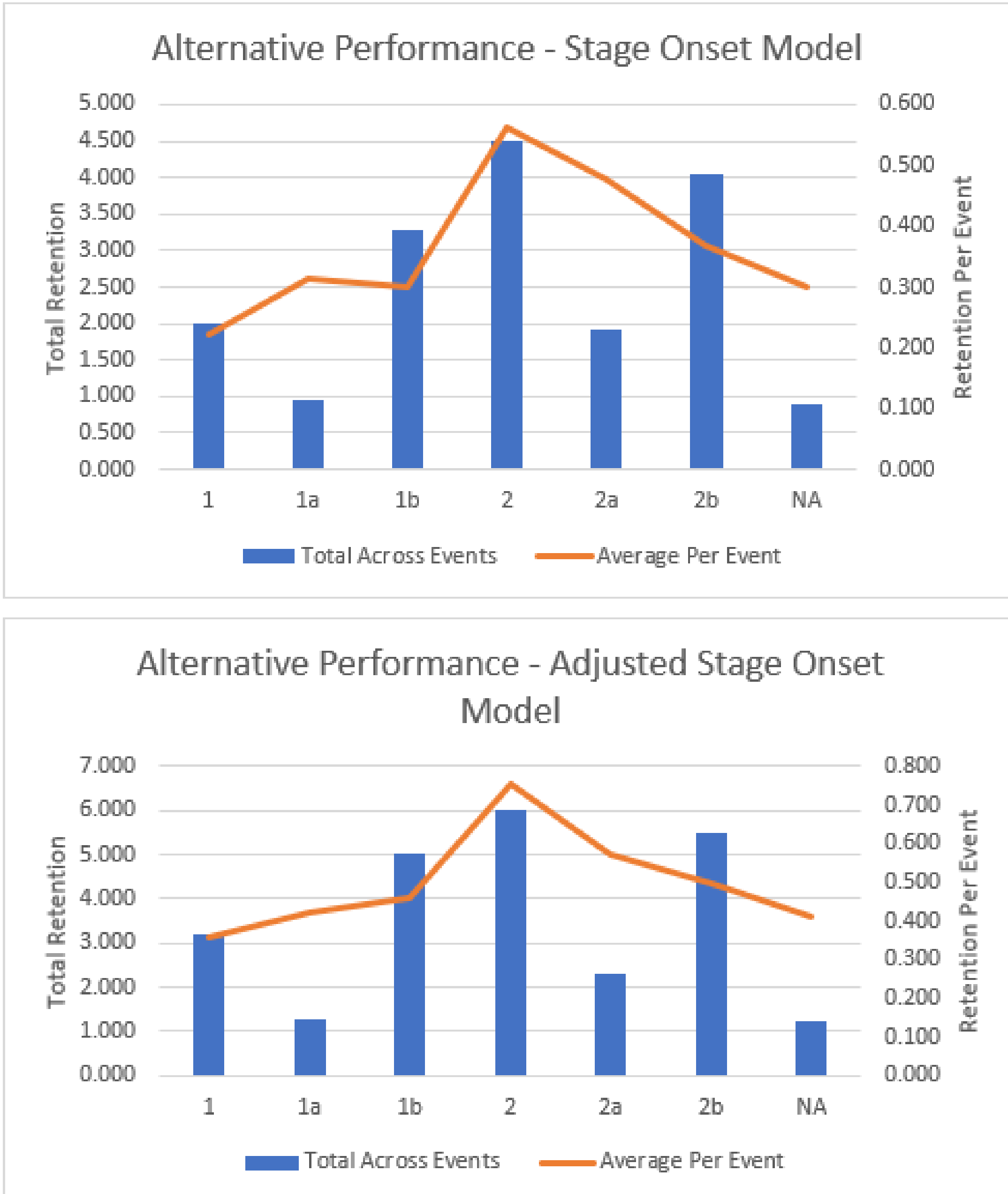

Figure 5-2. Alternative performance for Round 2 analyses using the Stage-Onset and Adjusted Stage-Onset Models.

Table 5-6. Robustness of alternative across the five models for Round 3 analyses. Alternatives are ranked by total predicted retention and by average retention per event.

Alt.	Model	Total	Ave.	Sum	AveAll	Rank Sum	Rank Ave
NA	New;0.9	1.227	41%	5.723	38.1%	7	6
NA	New	0.900	30%				
NA	200; 0.9	0.799	27%				
NA	200	0.497	17%				
NA	Mrnak	2.300	77%				
1	New;0.9	3.201	36%	14.391	34.0%	4	7
1	New	2.000	22%				
1	200; 0.9	1.920	21%				
1	200	1.069	13%				
1	Mrnak	6.202	78%				
1a	New;0.9	1.268	42%	6.088	40.6%	6	5
1a	New	0.942	31%				
1a	200; 0.9	0.863	29%				
1a	200	0.554	18%				
1a	Mrnak	2.462	82%				
1b	New;0.9	5.040	46%	23.809	44.2%	3	4
1b	New	3.293	30%				
1b	200; 0.9	3.443	34%				
1b	200	1.813	18%				
1b	Mrnak	10.221	93%				
2	New;0.9	6.024	75%	24.854	62.1%	2	1
2	New	4.498	56%				
2	200; 0.9	4.031	50%				
2	200	2.510	31%				
2	Mrnak	7.791	97%				
2a	New;0.9	2.292	57%	10.907	54.5%	5	2
2a	New	1.915	48%				
2a	200; 0.9	1.844	46%				
2a	200	1.393	35%				
2a	Mrnak	3.463	87%				
2b	New;0.9	5.488	50%	25.933	47.2%	1	3
2b	New	4.057	37%				
2b	200; 0.9	4.078	37%				
2b	200	2.458	22%				
2b	Mrnak	9.851	90%				

5.2.3 Discussion and Additional Analyses

Considerable progress has been made in our capacity to assess the effects of flow management on pallid sturgeon dispersal since the earliest modeling applications under the MRRP and even the preliminary analyses for the Fort Peck EIS. Coupling one-dimensional A/D modeling with an energy-budget model for predicting water temperatures and models of free embryo development based upon thermal exposure have significantly improved our ability to assess drift and settling for alternative management actions.

The DSM modeling using the latest improvements and parameterizations have demonstrated that prevailing meteorological conditions play a critical role in larval retention upstream of the anoxic zone in Lake Sakakawea. Larval development rates are temperature-dependent, and retention is highly correlated with the air temperatures during drift. Other meteorological factors (e.g., solar radiation, cloud cover, wind speed, humidity) and tributary inflows are also important determinants of water temperature. Because of the strong influence of these factors, the likelihood of success (in terms of retention) increases if there is flexibility in the timing of flow implementation.

Alternatives 1, 1a, and 1b represent three variants of the same operational criteria except for of the timing of their implementation. If they were combined into a "composite" alternative (Alt 1c) that uses prevailing weather conditions to determine which variant to apply in a given year, the overall performance would be improved. Table 5-7 shows the results of compositing Alternatives 1 and 2 in terms of retention rate. Cumulative retention for Alternative 1c was about four times that for the No Action, while Alternative 2 was about eight times the No Action cumulative retention. The composite alternatives (1c and 2c) outperform the base alternatives (1 and 2) in terms of cumulative retention by 84% and 64%, respectively.

Confidence in the results of the A/D modeling – at least for the first few days of drift - are high given the performance of that model in replicating measured advection and dispersion from test releases of pallid sturgeon free embryos in 2016 and 2019. Confidence in the model performance for later stages of drift is lower, given field observations that mean advection rates for 5DPH larvae tend to be about 90 percent of predicted rates. The rate-adjusted development models account for this phenomena. However, because they apply an adjustment for the full drift period, the adjusted models likely underpredict advection for the first few days. One strategy to address this concern would be to apply the Mrnak et al. (2020) relation to assess when rheotaxis begins, then apply the rate adjustment to the portion of the drift after the larvae have exhibited rheotactic behavior.

Table 5-7. Retention values for the No Action Alternative and for "composite" alternatives generated by implementing alternative variants in each spawning year based on prevailing weather conditions in that year.

	No Action Alternative				Alternative 1c (Alt 1, 1a, and 1b)				Alternative 2c (Alt 2, 2a, and 2b)			
Year	**New;0.9**	**New**	**200; 0.9**	**200**	**New;0.9**	**New**	**200; 0.9**	**200**	**New;0.9**	**New**	**200; 0.9**	**200**
1930					24.5%	9.1%	7.4%	3.0%	14.4%	6.5%	6.0%	3.0%
1949					99.9%	94.9%	86.7%	44.8%	100.0%	99.6%	95.7%	66.3%
1966									99.9%	96.0%	89.1%	56.9%
1975	32.5%	15.5%	12.8%	4.9%	34.6%	16.9%	14.1%	5.5%	64.0%	35.5%	23.9%	9.3%
1980					9.0%	1.5%	1.0%	0.1%	74.2%	31.0%	17.5%	1.9%
1983					78.6%	54.0%	64.5%	35.6%	99.7%	91.9%	84.8%	46.1%
1985					32.4%	9.7%	25.5%	6.8%	94.6%	61.8%	62.3%	22.9%
1986									100.0%	100.0%	100.0%	98.7%
1987					81.1%	57.2%	48.2%	30.7%	96.6%	87.6%	92.7%	79.1%
1994					9.3%	2.1%	2.1%	0.7%				
1997	89.5%	74.3%	66.9%	44.7%	99.5%	96.0%	88.2%	68.4%	96.4%	86.3%	76.9%	54.5%
2000					69.9%	20.5%	24.0%	2.9%	70.4%	22.4%	25.5%	3.3%
2011	0.7%	0.2%	0.2%	0.0%	1.9%	0.4%	0.6%	0.1%	1.8%	0.4%	0.5%	0.1%
2012					12.2%	2.8%	6.8%	1.6%				
Sum	1.23	0.90	0.80	0.50	5.53	3.65	3.69	2.00	9.12	7.19	6.75	4.42
Ave	40.9%	30.0%	26.6%	16.6%	46.1%	30.4%	30.8%	16.7%	76.0%	59.9%	56.2%	36.8%
Num	3	3	3	3	12	12	12	12	12	12	12	12

5.3 Pallid Sturgeon Demographic Population Model Outcomes

The DSM retention outcomes described in section 5.2 use the Round 3 analyses that reflect recent updates to improve water temperature predictions. The population model outcomes have not yet been updated and, instead, are based on the Round 2 DSM results. Although the climatic and temperature data used for the DPM outcomes presented here are similar to those used in the Round 3 analyses, *all population model outcomes should be considered preliminary*.

The following pallid sturgeon DPM outcomes use the spawning dates found in Table 5-6, as produced by the spawning submodel using Round 2 criteria. Hatch was assumed to occur seven days after spawning. The "Round 2 New; 0.9" retention outputs (see section 5.2.2) from the Round 2 DSM results (see Table 5-8) were analyzed by the DPM. Note that these retention values differ from the Round 3 retention values presented in section 5.2.2.

5.3.1 Spawning and Retention Inputs and Uncertainties

The test flow alternatives differed in how often they promoted spawning and in how well they retained free embryos given spawning. The combination of spawning and retention outcomes led to population results that varied by alternative flow and year.

5.3.1.1 Spawning Model Inputs and Associated Uncertainties

The spawning submodel was used to predict spawning dates for each alternative flow and year in the POR based on flows and water temperatures as described in section 2.5 (Table 5-8). The spawning submodel indicated that the No Action Alternative would support spawning below Fort Peck Dam in only 4 of the 83 years in the period of record (1930-2012). Test flow alternative variants with an early spawning pulse (1a and 2a) also supported spawning in just 4 years, while the other alternative variants provided an increased spawning frequency. Spawning frequency for flows with later spawning pulses (Alternatives 1b and 2b) were three times the frequency for the No Action Alternative (Figure 5-9). On average, spawning is expected to occur about once every 7 years for these alternatives, although years in which spawning occurred tended to be clustered together with longer periods of no spawning in between (Table 5-8). All of the alternatives were as good or better than the No Action alternative at promoting spawning below Fort Peck Dam.

Table 5-8. Spawning dates used for the pallid sturgeon demographic population model outcomes. To obtain retention results, hatch dates were assumed to be 7 days after spawning. Note, these "Round 2" dates differ from the most recent dates used in section 5.2 due to lack of available time to update population model analyses.

Year	1	1a	1b	2	2a	2b	No Action	Temperature Class
1930			17-Jun			17-Jun		High
1949			17-Jun			16-Jun		High
1966						25-Jun		Low
1975	2-Jul	2-Jul	2-Jul	2-Jul	2-Jul	2-Jul	2-Jul	Normal
1976	14-Jun		14-Jun	14-Jun		14-Jun	14-Jun	Normal
1980	14-Jun		19-Jun	14-Jun		18-Jun		Normal
1983	14-Jun		21-Jun	14-Jun		18-Jun		Normal
1985	14-Jun		21-Jun	14-Jun		18-Jun		Normal
1986				9-Jun				High
1987	10-Jun	7-Jun	18-Jun	10-Jun	7-Jun	18-Jun		High
1994			15-Jun					Normal
1997	25-Jun	25-Jun	30-Jun	25-Jun	30-Jun	25-Jun	25-Jun	High
2000	14-Jun		16-Jun			14-Jun		Normal
2011	25-Jun	25-Jun	25-Jun	25-Jun	25-Jun	25-Jun	25-Jun	Low
2012	14-Jun							Normal

The spawning submodel also provides the average proportion of reproductively-ready females expected to spawn below Fort Peck Dam (i.e., spawning proportion). As described in section 2.5, the spawning submodel currently assumes the spawning proportion is 0.5 for every alternative and year in which spawning is expected. The effectiveness test flows at Fort Peck to support pallid sturgeon spawning and spawning magnitude are highly uncertain and are topics of an ongoing expert elicitation (Chapter 6). A different spawning proportion applied to all alternative/year combinations would not change the rank order of flow alternatives in terms of pallid sturgeon population outcomes. However, allowing the spawning proportion to vary with water temperatures and flows (considered to be a more realistic scenario) could result in changes to the performance and rank order of test flow alternatives. Additionally, uncertainty in the actual spawning dates contributes to uncertainty in the retention outcomes, which are highly sensitive to water temperatures that can vary considerably over a couple days. We recommend that DPM outcomes be re-evaluated following the conclusions of the spawning expert elicitation and be updated with learning during the adaptive management process.

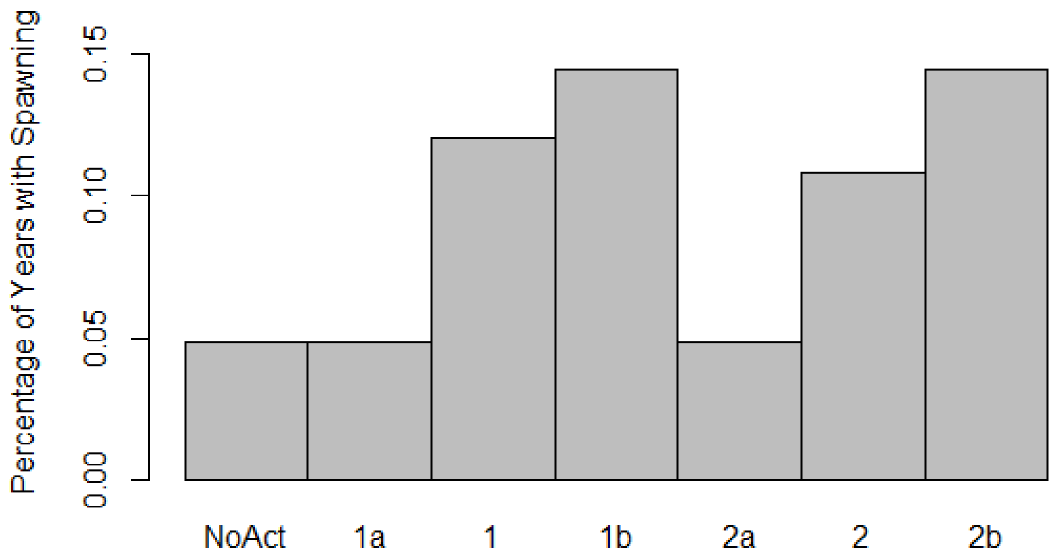

Figure 5-3. Percentage of years from 1930 to 2012 in which spawning is expected under the basic spawning model for each alternative. Flow Alternatives 1 and 2 represent flows with and without a spring attractant pulse, respectively. Flow variants “a” and “b” represent flows with pulses that are slightly earlier or later, respectively, and NoAct represents the No Action alternative, i.e., the current dam operations strategy.

5.3.1.2 Drift and Settling Model Retention Inputs and Associated Uncertainties

In spawning years, the probability a free-embryo was retained in the free-flowing Missouri River ranged from zero to nearly 1 and varied with both flow alternative and the specific environmental conditions for the given year (Table 5-9). The distribution of retention probabilities given spawning differed by alternative management flow with the timing of the flow (variant a vs. b) influencing the distribution more than the type of flow (1 vs. 2) (Figure 5-11). While spawning frequency for the No Action alternative, Alternative 1a, and Alternative 2a was low, flow alternatives 1a and 2a yielded more retention than flows under current dam operations. Retention probabilities were not computed for flow alternative and year combinations in which spawning was not expected due to computational time constraints as well as logistical issues in determining a spawning date.

Table 5-9. Retention values used for the pallid sturgeon demographic population model outcomes. Note, these "Round 2" retention outcomes differ from the most recent outcomes presented in section 5.2 and were used to obtain the population model outcomes presented here due to lack of available time to update population model analyses.

Year	1	1a	1b	2	2a	2b	No Action	Temperature Class
1930			0.0383			0.0446		High
1949			0.1540			0.5304		High
1966						1.0000		Low
1975	0.2265	0.2254	0.2168	0.2171	0.2304	0.2184	0.2179	Normal
1976	0.4366		0.4358	0.3710		0.4361	0.4363	Normal
1980	0.4316		0.9204	0.4681		0.6522		Normal
1983	0.2440		0.9924	0.1677		0.9299		Normal
1985	0.0073		0.6605	0.0238		0.0253		Normal
1986				1.0000				High
1987	0.7951	0.9994	0.7516	0.7795	0.9801	0.7448		High
1994			0.3699					Normal
1997	0.9260	0.9261	0.9883	0.9334	0.9883	0.9260	0.9260	High
2000	0.6398		0.9960			0.0050		Normal
2011	0.0003	0.0003	0.0003	0.0003	0.0003	0.0003	0.0003	Low
2012	0.0332							Normal

Average retention given spawning is the lowest for Alternative 1. All other alternative flows outperform the No Action alternative in terms of retention given spawning. While the No Action Alternative outperforms Alternative 1 in terms of retention given spawning, spawning occurs much more often for Alternative 1, allowing for more overall retention across the POR with this flow alternative as compared to current operations. In fact, all action alternatives outperform the No Action alternative in terms of retention weighted by the frequency of spawning. For Round 2 analyses, Alternative 1b had the greatest spawning frequency and the greatest average retention given spawning, making it top alternative in overall performance for pallid sturgeon, although it may not be the best performer in each year (Figure 5-4). Uncertainties in the determination of spawning occurrence and the calculation of retention values discussed above for the Round 3 analyses apply to the Round 2 analyses as well.

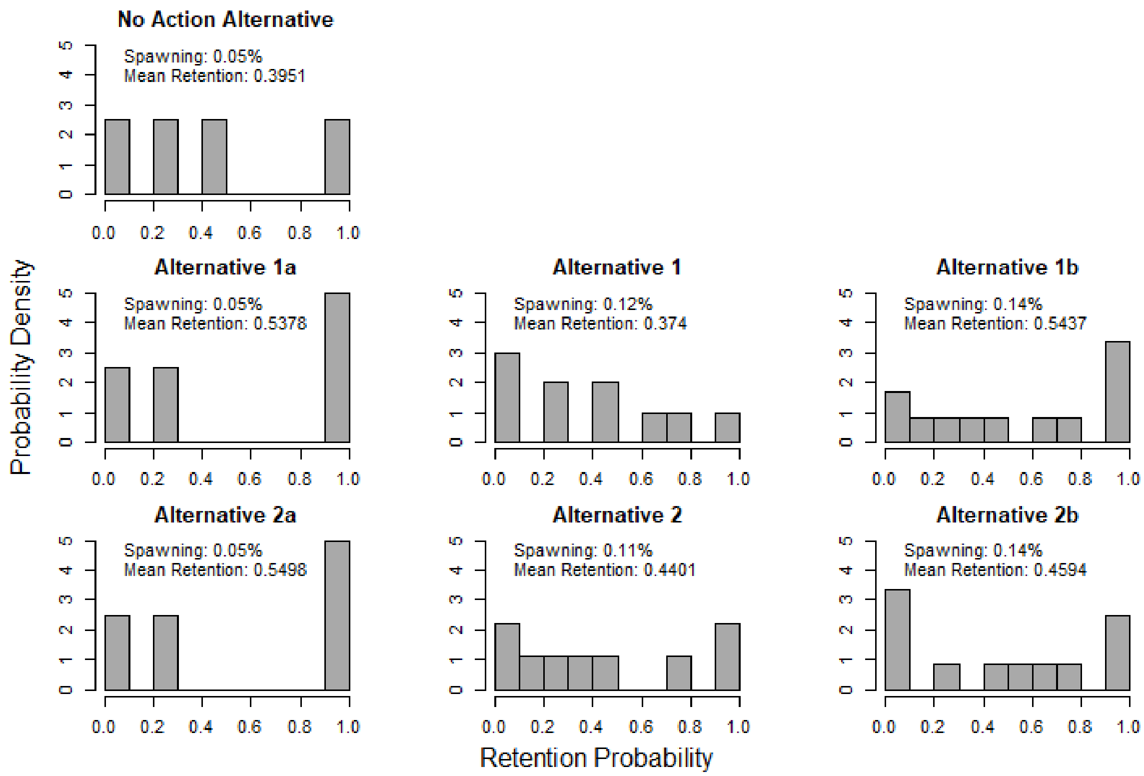

Figure 5-4. Distribution of retention probabilities given spawning by flow alternative. Distributions do not include years in which spawning is not expected. More spawning years are incorporated in the probability distributions as you move left to right.

5.3.2 Deterministic Population Model Outcomes

5.3.2.1 Long-Term Population Growth Rate

Following the methods outlined in section 4.5.1.1, long-term population growth rates (LTPGRs) were computed, given the parameterization of the Leslie matrix (equation 4-2) described in sections 4.2 and 4.3, for the environmental conditions of each year and alternative flow combination for which spawning was expected. Due to the current parameterization of the DPM, and in particular our choice of age-0 survival given retention, all LTPGRs are expected to be less than 1 (see section 5.3.2.3) but can still provide a meaningful comparison of flow alternatives (see section 5.3.2.2).

Because the spawning proportion was fixed at 0.5 for all alternatives in the present analyses, the LTPGR results are a rescaled version of the retention values from section 5.3.1 and the ranking of alternatives is the same as those based on retention. Insofar as the results reported herein differ from those in section 5.3.1, the differences relate to the use of Round 2 DSM outputs rather than the Round 3 outputs used in the referenced section. The expert elicitation described in section 6 will explore varying the spawning proportion with flow, temperature, or other relevant conditions and values are anticipated to vary with different alternatives.

The distribution of LTPGRs given spawning varied by flow alternative, although the range of LTPGRs for each alternative management flow was similar (Figure 5-5). Like retention probability, the distribution of LTPGRs is dependent on the timing of flow pulses. While spawning does not occur often for alternatives with earlier pulses (Alternatives 1a and 2a), when spawning does occur, the LTPGRs are relatively high. Mean LTPGR given spawning was highest for Alternative 1b, a management strategy with late flow pulses and the greatest number of years in which spawning occurred. Alternatives 2 and 2b had the next two highest mean LTPGRs given spawning, as well as high occurrences in spawning. Mean LTPGR given spawning, however, differed by less than 0.01467 across all alternatives.

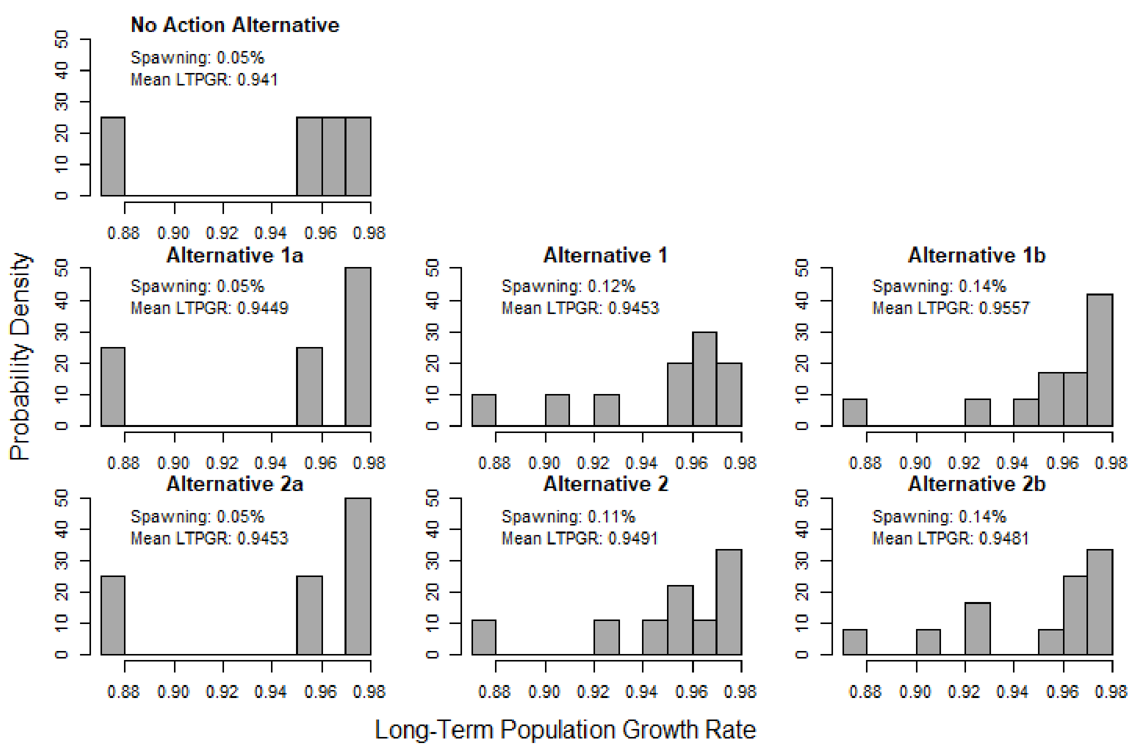

Figure 5-5. LTPGR distributions by flow alternative, excluding years in which spawning is not expected. Percentage of years in the POR in which spawning occurred and mean LTPGR is indicated in the top left of each panel. Alternatives 1 and 2 represent flows with and without a spring attractant pulse, respectively. Alternative variants "a" and "b" represent slightly earlier or later flow pulses, respectively, and NoAct represents the No Action Alternative.

The optimal alternative, in terms of population outcomes, is the one with the greatest LTPGR in the given year. Since no natural recruitment occurs without spawning, the greatest differences in population outcomes among alternative flows are expected when some alternative flows allow for spawning in the given year, and others do not. For example, in 1986, only Alternative 2 promoted spawning below Fort Peck Dam, resulting in this alternative flow having an LTPGR much greater than all other alternatives (Table R.1). Alternative 2 was, therefore, the optimal strategy under the environmental conditions observed in 1986. In other years, multiple alternative flows promoted spawning below Fort Peck Dam, and the optimal strategy may have an LTPGR that differs from others only slightly. No one alternative management flow is always the optimal strategy. Instead, the optimal alternative differs across the years (Table 5-10).

Table 5-10. Long-term population growth rates (LTPGRs) for the 1930-2012 POR for each alternative. The greater the LTPGR, the better the population outcome.

Year	No Action	1	1a	1b	2	2a	2b
1930	0	0	0	0.926909	0	0	0.928831
1931	0	0	0	0	0	0	0
1932	0	0	0	0	0	0	0
1933	0	0	0	0	0	0	0
1934	0	0	0	0	0	0	0
1935	0	0	0	0	0	0	0
1936	0	0	0	0	0	0	0
1937	0	0	0	0	0	0	0
1938	0	0	0	0	0	0	0
1939	0	0	0	0	0	0	0
1940	0	0	0	0	0	0	0
1941	0	0	0	0	0	0	0
1942	0	0	0	0	0	0	0
1943	0	0	0	0	0	0	0
1944	0	0	0	0	0	0	0
1945	0	0	0	0	0	0	0
1946	0	0	0	0	0	0	0
1947	0	0	0	0	0	0	0
1948	0	0	0	0	0	0	0
1949	0	0	0	0.945645	0	0	0.96544
1950	0	0	0	0	0	0	0
1951	0	0	0	0	0	0	0
1952	0	0	0	0	0	0	0
1953	0	0	0	0	0	0	0
1954	0	0	0	0	0	0	0

1955	0	0	0	0	0	0	0
1956	0	0	0	0	0	0	0
1957	0	0	0	0	0	0	0
1958	0	0	0	0	0	0	0
1959	0	0	0	0	0	0	0
1960	0	0	0	0	0	0	0
1961	0	0	0	0	0	0	0
1962	0	0	0	0	0	0	0
1963	0	0	0	0	0	0	0
1964	0	0	0	0	0	0	0
1965	0	0	0	0	0	0	0
1966	0	0	0	0	0	0	0.977399
1967	0	0	0	0	0	0	0
1968	0	0	0	0	0	0	0
1969	0	0	0	0	0	0	0
1970	0	0	0	0	0	0	0
1971	0	0	0	0	0	0	0
1972	0	0	0	0	0	0	0
1973	0	0	0	0	0	0	0
1974	0	0	0	0	0	0	0
1975	0.95082488	0.951413	0.95134	0.950747	0.950768	0.951681	0.950854
1976	0.96204115	0.962053	0	0.96202	0.959307	0	0.962031
1977	0	0	0	0	0	0	0
1978	0	0	0	0	0	0	0
1979	0	0	0	0	0	0	0
1980	0	0.961855	0	0.975746	0.963253	0	0.969178
1981	0	0	0	0	0	0	0
1982	0	0	0	0	0	0	0
1983	0	0.952569	0	0.977245	0.946888	0	0.975949
1984	0	0	0	0	0	0	0
1985	0	0.907309	0	0.96941	0.92108	0	0.921779
1986	0	0	0	0	0.977399	0	0
1987	0	0.9729	0.977387	0.971829	0.972521	0.976997	0.971656
1988	0	0	0	0	0	0	0
1989	0	0	0	0	0	0	0
1990	0	0	0	0	0	0	0
1991	0	0	0	0	0	0	0
1992	0	0	0	0	0	0	0
1993	0	0	0	0	0	0	0
1994	0	0	0	0.959254	0	0	0
1995	0	0	0	0	0	0	0
1996	0	0	0	0	0	0	0

1997	0.97586639	0.975868	0.975869	0.977163	0.976025	0.977163	0.975868
1998	0	0	0	0	0	0	0
1999	0	0	0	0	0	0	0
2000	0	0.968825	0	0.977318	0	0	0.903143
2001	0	0	0	0	0	0	0
2002	0	0	0	0	0	0	0
2003	0	0	0	0	0	0	0
2004	0	0	0	0	0	0	0
2005	0	0	0	0	0	0	0
2006	0	0	0	0	0	0	0
2007	0	0	0	0	0	0	0
2008	0	0	0	0	0	0	0
2009	0	0	0	0	0	0	0
2010	0	0	0	0	0	0	0
2011	0.87540488	0.875432	0.875131	0.874568	0.874574	0.875405	0.874925
2012	0	0.925133	0	0	0	0	0

5.3.2.2 Sensitivity and Elasticity Values

Sensitivity and elasticity values were computed at mean retention and spawning outcomes given spawning for the following parameters: E_i and ψ_i for $1 \leq i \leq a_{max}$, ϕ_i for $1 \leq i \leq a_{max} - 1$, and r, $\phi_{0,MR}$, $\phi_{0,LS}$ and a_{max}, as well as for mean input values given spawning as described in section 4.5.1.2. Long-term population growth rates were most sensitive to Lake Sakakawea age-0 survival and Missouri River age-0 survival given retention. These parameters had sensitivity values four magnitudes higher than all other sensitivity values at mean retention and spawning outcomes (Table 5-11). Missouri River age-0 survival given retention was also listed amongst the parameters with the greatest elasticity values (Table 5-12).

Age-0 Lake Sakakawea survival is assumed to be zero under the hypothesis that no free-embryo drifting into the headwaters of the lake can survive the presumed anoxic zone (Guy et al. 2015). If there is a chance that drifting free-embryos survive the conditions of Lake Sakakawea, then the long-term population growth rate will increase for all situations considered. However, it can be shown that if the age-0 survival in Lake Sakakawea is less than age-0 survival in the free-flowing Missouri River, then the alternative with the greatest long-term population growth rate in any given year will not change. Similarly, while age-0 survival given retention was arguably the most uncertain model parameter and LTPGRs will vary with changes in this parameter, the rank comparison of alternatives in terms of LTPGRs does not change with changes in age-0 survival given retention (Figure 5-6; see Appendix for details). Therefore, learning more about this uncertain, sensitive parameter is important for projecting future population dynamics but not important for understanding the rank order comparisons of Fort Peck flow alternatives.

Table 5-11. Parameter sensitivity values greater than 0.025. The larger the sensitivity value the greater the change in the long-term population growth rate with a unit change in the given parameter.

Parameter	Description	Sensitivity Value	Rank
$\phi_{0,LS}$	age-0 survival given drift into Lake Sakakawea	263.8166	1
$\phi_{0,MR}$	age-0 survival given retention in the free-flowing Missouri River	230.8897	2
p_{ret}	probability a drifting free-embryo is retained above the headwaters of Lake Sakakawea	0.0371	3
a_{max}	maximum age of a reproductive female pallid sturgeon	0.0362	4
γ	probability a reproductively ready female spawns in the Missouri River below Fort Peck Dam	0.0346	5
r	sex ratio in terms of the probability of being female	0.0346	5
ϕ_1	survival from age-1 to age-2	0.0271	6
ϕ_2	survival from age-2 to age-3	0.0251	7

The parameter with the greatest elasticity value was maximum age (Table 5-12), indicating a large proportional increase to LTPGR if female sturgeon were to survive at the typical adult rate past age 100 without a decline in fecundity or survival. It is likely, however, that reasonable changes to the maximum age will not change the rank order (determined by long-term population growth rates) of alternatives. Nonetheless, it is important to understand the effects of choice of the maximum age on population dynamics and additional model outcomes – as well as better understanding the fecundity values and survival rates of very old fish (as these values relate to the importance of maximum age).

Table 5-12. Largest elasticity values. The larger the elasticity value the greater the percentage change in the LTPGR with a percentage change in the given parameter.

Parameter	Elasticity Value	Rank
a_{max}	3.755597	1
$\phi_{0,MR}$, p_{ret}, r, γ, ϕ_1, ϕ_2, ϕ_3, ϕ_4, ϕ_5, ϕ_6, ϕ_7, ϕ_8, ϕ_9, ϕ_{10}, ϕ_{11}, ϕ_{12}, ϕ_{13}	0.017978	2

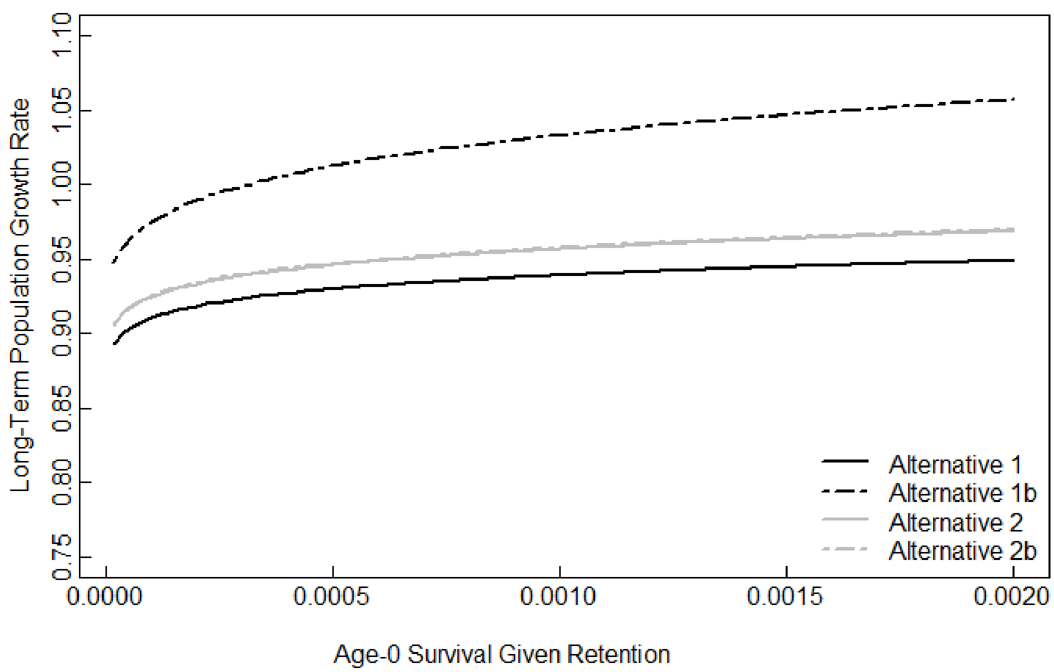

Figure 5-6. LTPGR as a function of age-0 survival given retention for alternatives 1, 1b, 2, and 2b under the climatic and hydrological conditions in 1985. The curve for Alternative 2b falls just slightly above the Alternative 2 curve. LTPGRs increase with increasing age-0 survival; however, rank comparison outcomes are robust to changes in age-0 survival given retention.

5.3.2.3 Long-Term Growth-Decline Boundaries

Figure 5-7 shows the long-term growth-decline boundaries as a contour plot with contour lines for fixed values of Missouri River age-0 survival given retention. The contours of the long-term growth-decline boundaries do not change with the given scenario (they are fixed across the range of retention and spawning probabilities for all flow alternatives and years). However, the long-term growth-decline boundaries can reveal information for each alternative flow and year combination under different assumptions on age-0 survival given retention. For example, both Alternative 1 and Alternative 1b promoted spawning in 1983, but retention rates were predicted to be much higher for the later flow pulse (Alternative 1b). At a fixed spawning probability below Fort Peck Dam of 0.5, Alternative 1b (Figure 5-7, open dot) will lead to long-term population growth when age-0 survival given retention is greater than or equal to 207 in one million, while Alternative 1 (Figure 5-7, solid dot) will result in long-term population decline at an age-0 survival given retention of 207 in one million. Under 1983 conditions, Alternative 1 is not expected to promote population growth unless age-0 survival given retention is greater than or equal to 842 in one million.

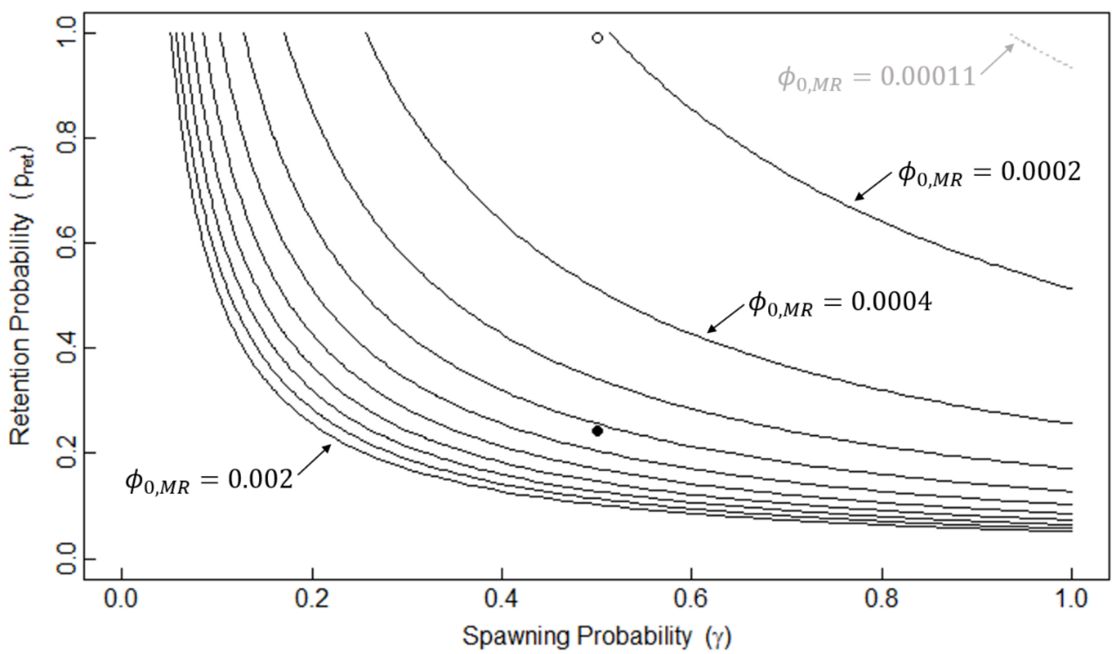

Figure 5-7. Long-term population growth-decline boundaries in terms of the probability a reproductively ready female spawns in the Missouri River below Fort Peck Dam (γ), the probability a free-embryo is retained and settles in the free-flowing Missouri River (p_{ret}), and age-0 survival given retention in the free-flowing Missouri River ($\phi_{0,MR}$). Contour curves represent fixed values of age-0 survival given retention; from left to right these are 0.002, 0.0018, 0.0016, 0.0014, 0.0012, 0.001, 0.0008, 0.0006, 0.0004, 0.0002 (solid black lines), and 0.00011 (gray, dotted line). Points represent the spawning and retention probabilities for Alternative 1 (solid) and Alternative 1b (open) in 1983. For a fixed contour curve (fixed value of age-0 survival given retention), spawning and retention probability coordinates to the left or below the contour line will result in long-term population decline, while those to the right or above the contour line will result in long-term population growth.

At the value of Missouri River age-0 survival given retention the pallid sturgeon population model was parameterized at (75 in one million), all spawning and retention outcomes are expected to lead to population decline – at maximum spawning and retention probabilities of 1 the age-0 survival given retention needs to be approximately 103 in one million or greater for population growth. However, assuming the maximum estimate for age-0 survival for gulf sturgeon (400 in one million) given by Pine et al. (2001), there is a reasonable amount of spawning and retention parameter space in which long-term population growth would be expected (e.g., under Alternative 1b conditions in 1983).

5.3.3 Stochastic Population Model Outcomes

To synthesize the benefits of implementing an alternative flow scenario on population growth with how often it can be implemented, we projected the dynamics of two initial populations of pallid sturgeon forward under simulated environmental variability as described in section 4.5.2.

5.3.3.1 Initial Populations

The age structure of the two types of initial pallid sturgeon populations (see section 4.5.2.1) used to compare alternatives in terms of quasiextinction are illustrated in Figure 5-8. Updated estimates of population size and age structure are expected to be available in the future as 2021 PSPAP capture data is processed and differential survival probabilities of HOPS are estimated.

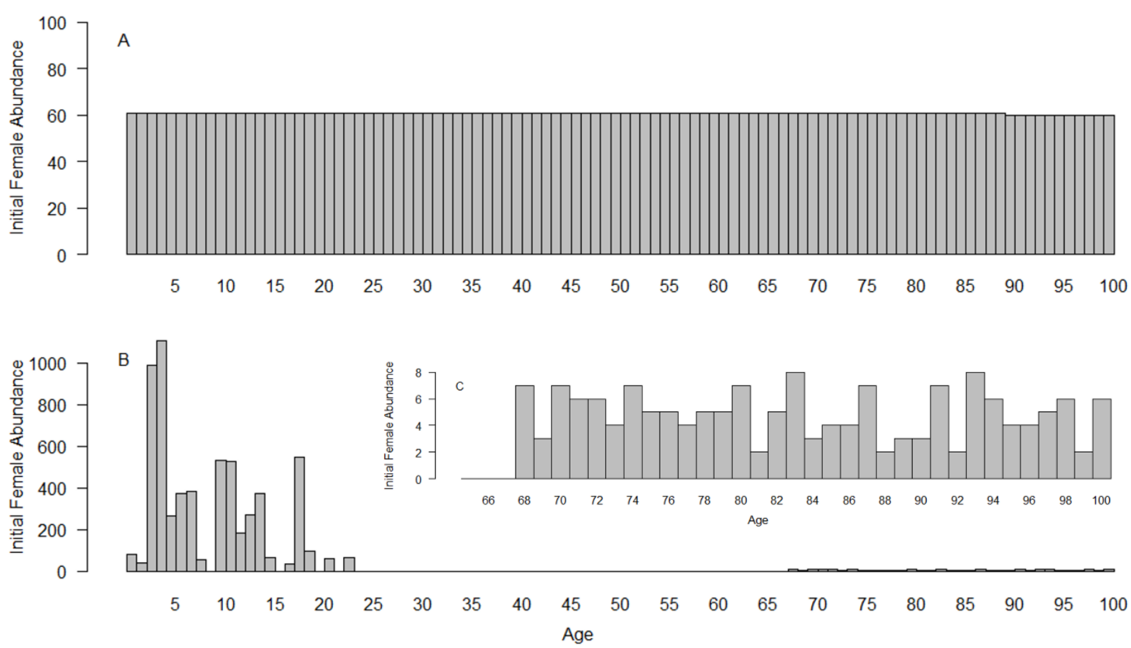

Figure 5-8. The age distributions of two types of initial female abundances used for stochastic population model outcomes. Panel A illustrates an estimate of 2020 female abundance that is approximately uniformly distributed in age. Panel B illustrates estimates of 2020 female abundances by age. PSPAP data was used to estimate the abundances of female hatchery origin pallid sturgeon for younger ages and an estimate of wild female abundance was randomly assigned to ages 68-100. Insert Panel C shows a zoomed in view of the age 65-100 wild-origin female abundances depicted in Panel B.

5.3.3.2 Modeling Environmental Variability

From 1930 to 2020, there were 22, 49, and 20 years classified as High, Normal, and Low temperature classes, respectively (Table 5-13). Using the transitions in Table 5-13[*], the resulting temperature class transition matrix is:

$$\mathbf{V} = \begin{pmatrix} 0.4 & 0.2245 & 0.0476 \\ 0.55 & 0.5306 & 0.5238 \\ 0.05 & 0.2449 & 0.4286 \end{pmatrix}, \qquad 5\text{-}1$$

where columns and row numbers 1, 2, and 3 represent Low, Normal, and High, respectively.

Table 5-13. High (upper quartile), Normal (25th to 75th percentile), and Low (lower quartile) temperature classes by year for 1930-2020.

Year	Weather	Year	Weather	Year	Weather
1930		1960		1990	Normal
1931		1961		1991	High
1932		1962		1992	Normal
1933		1963		1993	Low
1934		1964		1994	Normal
1935		1965		1995	High
1936		1966		1996	High
1937		1967		1997	High
1938		1968		1998	Low
1939		1969		1999	Normal
1940		1970		2000	Normal
1941		1971		2001	Low
1942		1972		2002	Low
1943		1973		2003	Low
1944	Low	1974	Normal	2004	Low
1945	Low	1975	Normal	2005	Normal
1946	Normal	1976	Normal	2006	Normal
1947	Low	1977	High	2007	Normal
1948	High	1978	Normal	2008	Low
1949	High	1979	Normal	2009	Low
1950	Normal	1980	Normal	2010	Normal

[*] For example, of the 20 transitions from a Low temperature year to the next year, 8 transitioned to another Low temperature year, 11 to a Normal temperature year, and 1 to a High temperature year. Transition probabilities for the Low column were therefore 0.4 (i.e., 8/20), 0.55, and 0.05 for rows representing Low, Normal, and High, respectively.

1951	Normal	1981	Low	2011	Low
1952	High	1982	Normal	2012	Normal
1953	Normal	1983	Normal	2013	Normal
1954	Low	1984	Normal	2014	Normal
1955	Normal	1985	Normal	2015	Normal
1956	High	1986	High	2016	High
1957	Normal	1987	High	2017	High
1958	Normal	1988	High	2018	High
1959	High	1989	Normal	2019	High
				2020	High

While not analyzed in terms of quasiextinction for the pallid sturgeon population, it is worth noting that the temperature transition matrix constructed from the 40 most recent temperature class transitions (1980-2020) is:

$$\mathbf{V} = \begin{pmatrix} 0.4 & 0.2632 & 0.0909 \\ 0.6 & 0.5263 & 0.1818 \\ 0 & 0.2105 & 0.7273 \end{pmatrix}. \qquad 5\text{-}2$$

This transition matrix might more accurately reflect future conditions under climate change. Although generally very similar to the matrix in equation 5-1, it is noticeably different in transitions from High temperature class years. The probability of High to High temperature transitions increased from 0.4286 to 0.7273, while the probability of High to Normal temperature transitions decreased from 0.5238 to 0.1818. Considering this new transition matrix along with any available information on spawning and retention outcomes for 2013-2020 is recommended for future assessments in an adaptive management framework.

5.3.3.3 Time to Quasiextinction

Expected time to quasiextinction was computed for the pallid sturgeon population as described in section 4.5.2.3 using temperature transition matrix $\boldsymbol{V}$ in equation 5-1 for the baseline DPM parameters (Table 4-1). Expected time to quasiextinction varied with alternative flow and type of initial population; however, the rank order of alternative flow outcomes did not vary with initial population (Table 5-14). Having the same rank order of alternative comparisons for two very different types of initial populations provides confidence that the reported comparisons have merit for use in decision making and are not simply an artifact of the initial population chosen. Quasiextinction comparison results are robust to uncertainty in initial population age structure, i.e., knowing more about the initial age structure doesn't change the comparison results.

Table 5-14. Expected time to quasiextinction (50 females or less) computed from 5,000 replicate female populations for each alternative and initial population type (N_0) assuming no additional stocking and the same alternative flow is implemented each year whenever possible given constraints.

Alternative Flow	Expected Time to Quasiextinction	
	2020 PSPAP N_0	Uniform N_0
1b	81.5898	75.0120
2b	80.4646	73.3758
2	78.8024	70.7718
1	78.2584	70.0222
2a	76.2116	67.1304
1a	76.1468	67.0388
No Action	75.0878	65.5006

Alternative 1b had the greatest expected times to extinction, outperforming the No Action Alternative by about 6 and 10 years for female abundances by age distributed as estimated by PSPAP and uniformly, respectively. All action alternatives outperformed the No Action alternative, albeit Alternatives 1a and 2a had similar expected quasiextinction times. For the action alternatives, expected time to quasiextinction increased with the timing of spawning flow releases with earlier flow releases ("a" alternatives) having the least expected time to quasiextinction and the later flow release ("b" alternatives) having the greatest expected time to quasiextinction. The variance in time to quasiextinction also was the least for the No Action Alternative and increased with the timing of spawning flow releases (Figure 5-9).

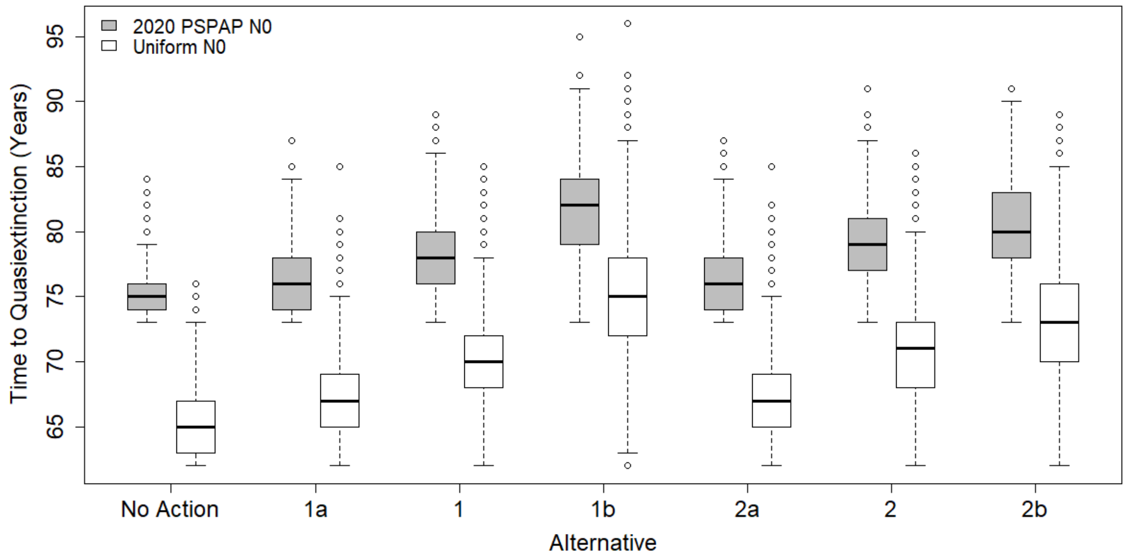

Figure 5-9. Time to quasiextinction (50 females or less) for 5000 replicate female populations for each alternative flow and initial population (N_0) type. Gray boxplots represent an initial population of females with an age distribution estimated by recent PSPAP captures, while white boxplots represent an initial population of females with a uniform age distribution. Bold boxplot lines represent the median time to quasiextinction. Boxplot edges represent the lower and upper quartiles, while whiskers extend to the most extreme point within 1.5 times the interquartile range. All outliers are plotted as open points.

Although the action alternatives all outperform the No Action Alternative, the differences between the expected time to quasiextinction is not large (<6 years) for baseline parameter values (Table 4-1) and initial female abundances by age estimated from PSPAP capture data (2020 PSPAP N_0, Table 5-14). As the sensitivity analyses reveal (section 5.3.2.4), these differences depend on parameter values and could be much larger if age-0 survival given retention, a parameter with high uncertainty, was underestimated.

5.3.3.4 Quasiextinction Sensitivities

Quasiextinction sensitivities were computed for the following parameters: E_i and ψ_i for $1 \leq i \leq a_{max}$, ϕ_i for $1 \leq i \leq a_{max} - 1$, and r, $\phi_{0,MR}$, γ_t, $p_{ret,t}$, and a_{max} as described in section 4.5.2.4 using temperature transition matrix $\boldsymbol{V}$ in equation 5-1. While the expected time to quasiextinction was sensitive to some parameters, none of the variations in parameter values considered changed the rank order of the alternative flows with respect to expected time to quasiextinction, providing further confidence that the reported comparisons have merit for use in decision making.

Sensitivity values for expected time to quasiextinction differed by initial population type, as well as flow alternative (Figure 5-10, Figure 5-11). Nonetheless, for both initial population types and all flow alternatives, age-0 survival given retention had a sensitivity value that was magnitudes greater than that for any other parameter value. This result aligns with the deterministic population model outcomes for long-term population growth rate sensitivities.

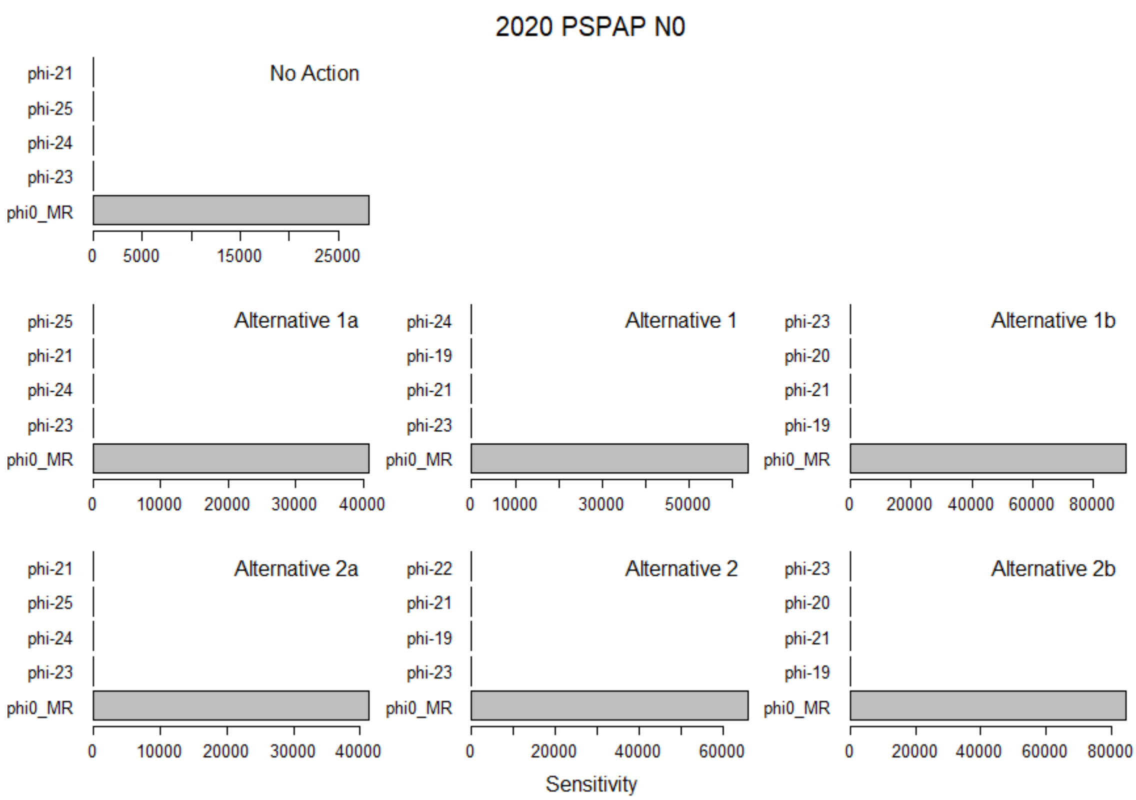

Figure 5-10. Top 5 sensitivity values for expected time to quasiextinction by alternative for the initial population of females with an age distribution estimated by recent PSPAP captures. Parameter labels “phi-x” indicate the probability a female survives from age x to age x+1 and “phi0_MR” indicates age-0 survival given retention in the free-flowing Missouri River.

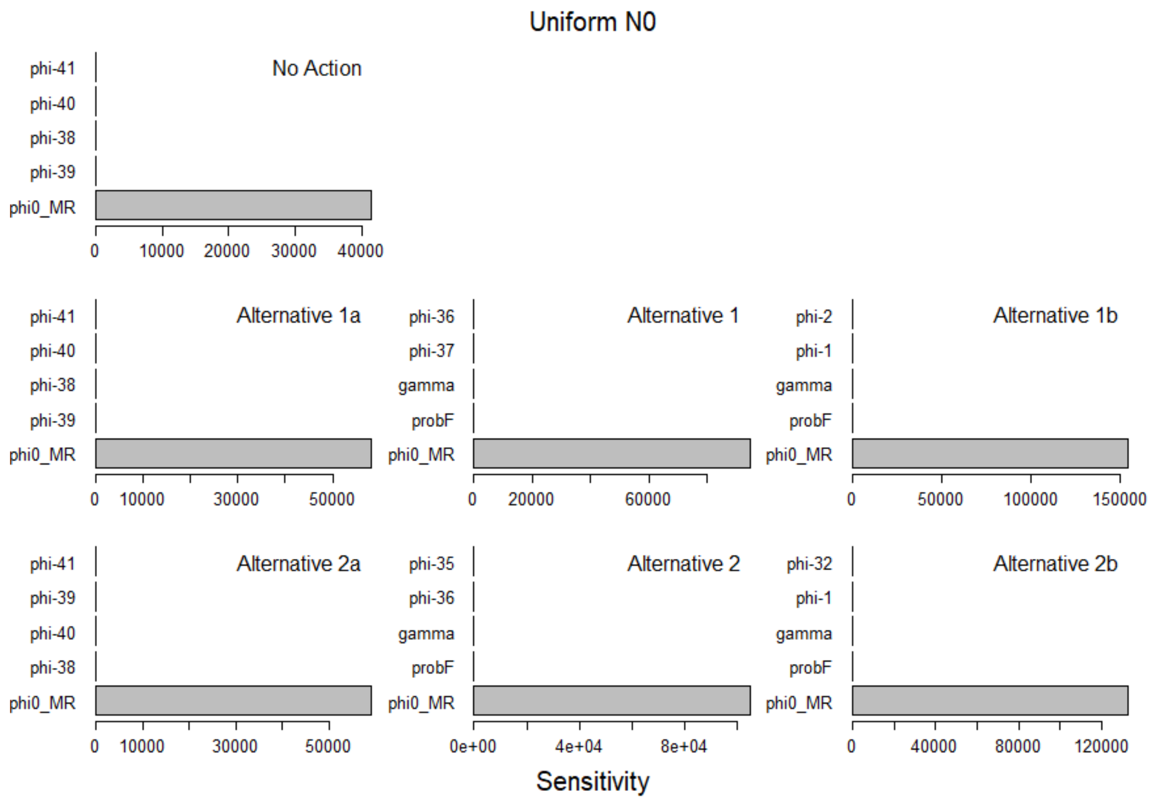

Figure 5-11. Top 5 sensitivity values for expected time to quasiextinction by alternative for the initial population of females with a uniform age distribution. Parameter labels "phi-x" indicate the probability a female survives from age x to age x+1, "gamma" indicates the proportion of reproductively-ready females spawning in the Missouri River below Fort Peck Dam, "probF" indicates the sex ratio in terms of the probability a fertilized egg is female, and "phi0_MR" indicates age-0 survival given retention in the free-flowing Missouri River.

Elasticity values for expected time to quasiextinction also differed by initial population type and flow alternative (Figure 5-12, Figure 5-13). For the initial population of females with an age distribution estimated by recent PSPAP captures, top elasticity values did not differ in value significantly (Figure 5-12). Additionally, the top 4 elasticity values matched the top 4 sensitivity values after age-0 survival given retention (Figure 5-10, Figure 5-12). All of these parameter values were survival probabilities for females between 19 and 25 years of age. It makes sense that these survivals would be particularly important to the quasiextinction time of the estimated 2020 female population given a baseline model parameterization that leads to population decline in the absence of stocking (see section 5.3.2.3) – without any females initially between the ages of 24 and 67, it is these younger but still mature fish that will need to carry the population into the future, and therefore, their survival is particularly important to quasiextinction outcomes.

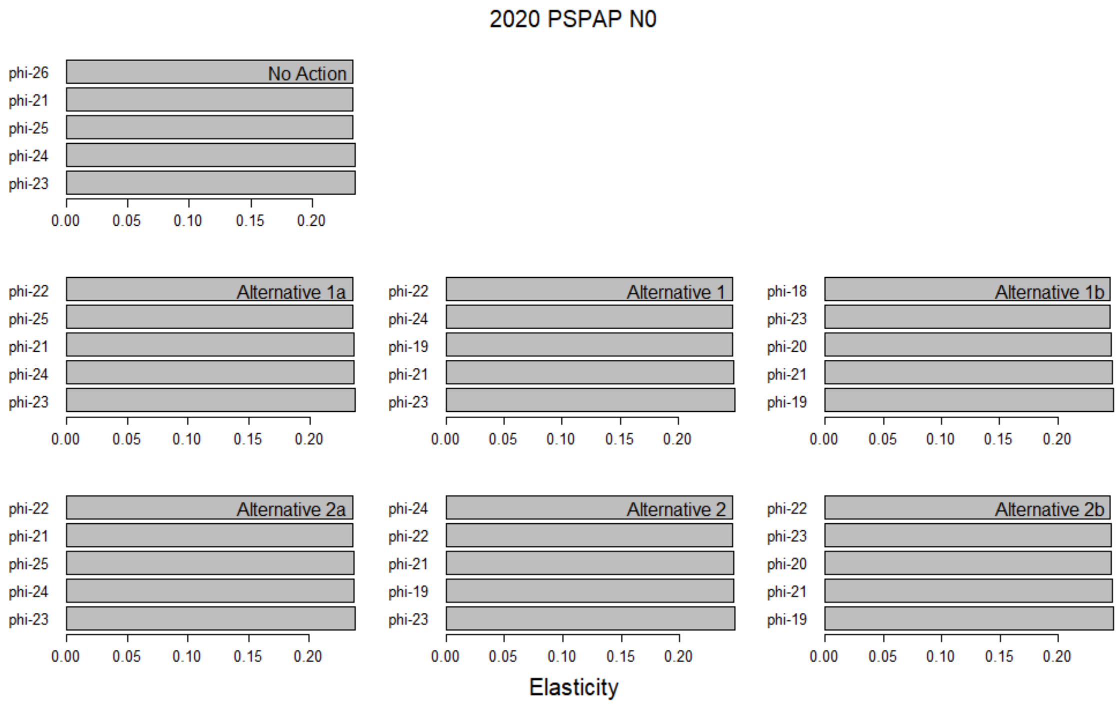

Figure 5-12. Top 5 elasticity values for expected time to quasiextinction by alternative for the initial population of females with an age distribution estimated by recent PSPAP captures. Parameter labels "phi-x" indicate the probability a female survives from age x to age x+1.

The maximum age of reproductive female had the top elasticity value for the initial population of females with a uniform age distribution for all alternatives. This result aligns with the deterministic population model outcomes for long-term population growth rate elasticities. After maximum age, the top 4 elasticity values were all similar in value and were for survival probabilities for females between the ages of 29 and 41, with the particular set of survival probabilities varying by alternative. The most important survival probabilities, in terms of elasticities, were for older females (in the age range given above) under the No Action Alternative and "a" action alternatives, were for younger females under the "b" action alternatives, and were somewhere in between for Alternatives 1 and 2. This trend is also seen in the elasticity values associated with the initial population of females with an age distribution based on recent PSPAP captures, although less pronounced.

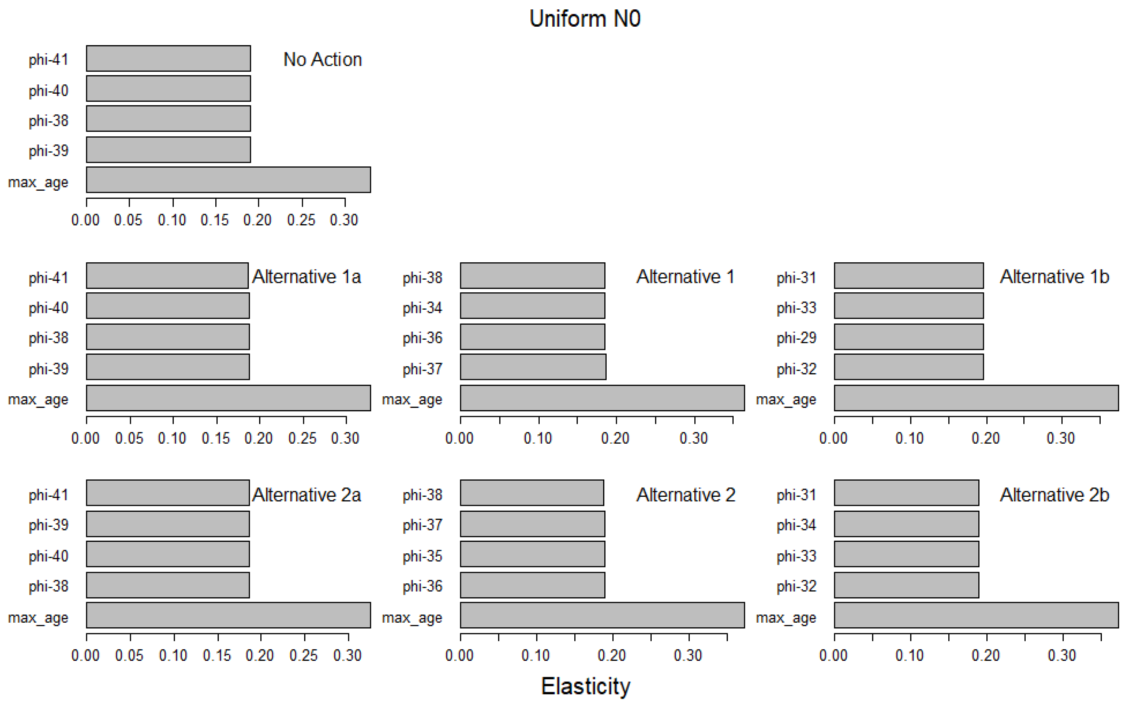

Figure 5-13. Top 5 elasticity values for expected time to quasiextinction by alternative for the initial population of females with a uniform age distribution. Parameter labels "phi-x" indicate the probability a female survives from age x to age x+1 and "max_age" indicates the maximum age of a reproductive female.

The sensitivity and elasticity analyses show that several survival parameters and the maximum age are important to understanding the expected time to quasiextinction for a particular initial population. For the ranges of parameter values considered in our sensitivity analysis, however, the rank order comparisons of alternatives in terms of the expected time to pallid sturgeon quasiextinction (Table 5-14) do not change. Similar to the deterministic outcomes for long-term population growth rate, even as the most sensitive parameter (age-0 survival given retention) is varied from its baseline value of 0.000075 to 0.0016, the rank order of the alternatives in terms quasiextinction remains the same (Figure 5-14). What does change is how the action alternatives compare with the No Action alternative in terms of biological relevance. As age-0 survival increases, the expected time to quasiextinction of all alternatives increases but not by equal amounts. Expected time to quasiextinction increases more rapidly for action alternatives, particularly Alternatives 1b and 2b. Changes in the range of potential outcomes show a similar trend (Figure 5-15, Figure 5-16). The difference between the No Action alternative and Alternative 1b quickly changes from a difference in expected quasiextinction times of about 6 years to a couple hundred years.

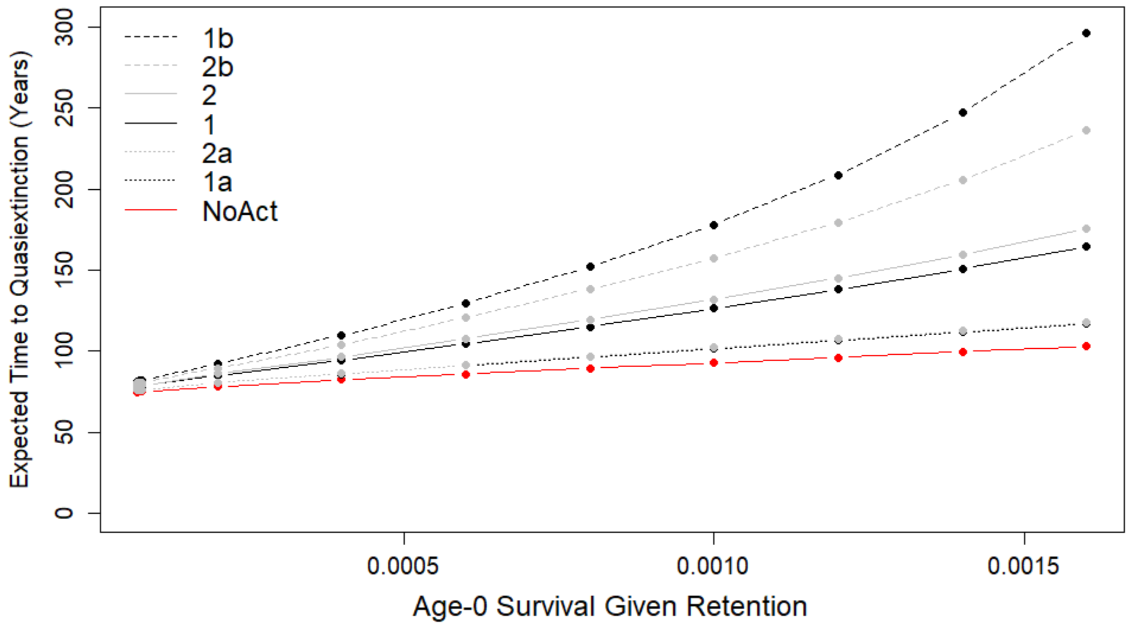

Figure 5-14. The expected time to quasiextinction (50 females or less) of 8000 population replicates for each of the seven alternatives and a range of parameter values for age-0 survival given retentions, the parameter with the highest sensitivity. The initial population used was constructed using recent PSPAP captures to estimate 2020 female abundances by age class.

Learning more about age-0 survival given retention will allow for a better understanding of the biological relevance that Fort Peck flows may have for pallid sturgeon dynamics in the long term. In the short term, however, any improvement in pallid sturgeon recruitment to age-1 may be considered a success in achieving MRRP sub-objective 1 (Figure 1-1), as well as a meaningful step to learning and recovery. Ideas similar to these were expressed by experts in a recent scenarios exercise aimed at determining monitoring and assessment strategies for evaluating the effectiveness of test flows (section 6).

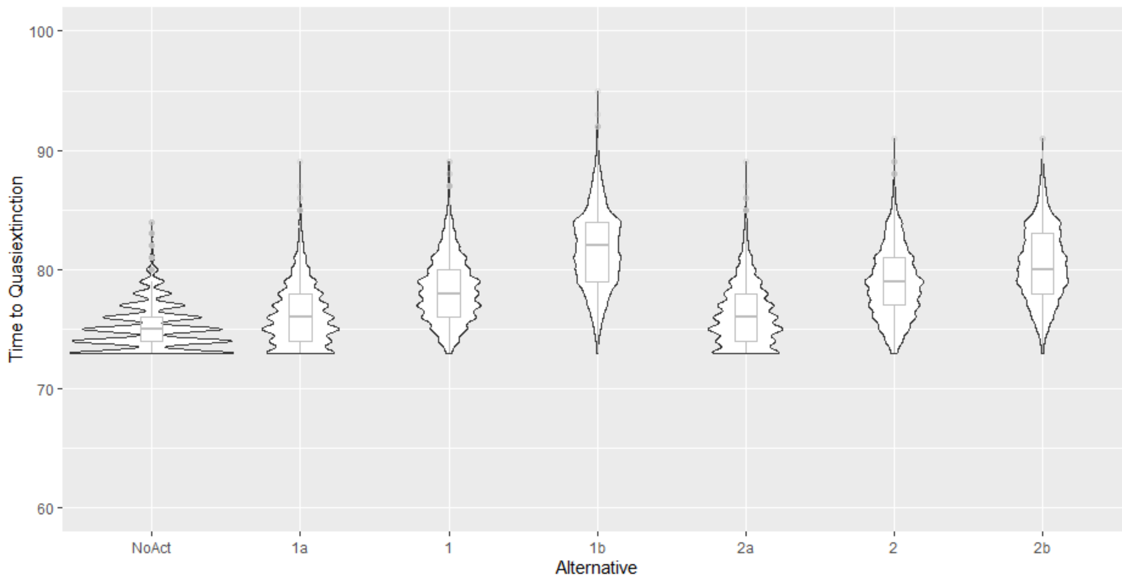

Figure 5-15. Time to quasiextinction (50 females or less) of 8000 population replicates for each of the seven alternatives when age-0 survival given retention is at its baseline value of 0.000075. The initial population used was constructed using recent PSPAP captures to estimate 2020 female abundances by age class.

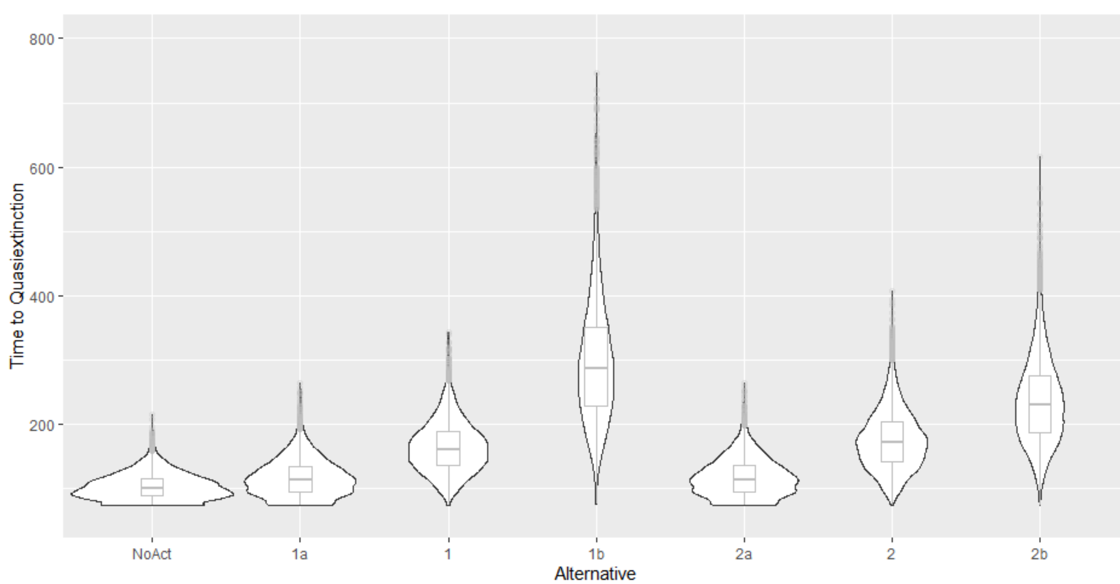

Figure 5-16. Time to quasiextinction (50 females or less) of 8000 population replicates for each of the seven alternatives when age-0 survival given retention is 0.0016. The initial population used was constructed using recent PSPAP captures to estimate 2020 female abundances by age class.

6 Expert Elicitation to Inform Model Parameterization

6.1 Background and Context

The effectiveness of management actions at Fort Peck to support successful spawning by pallid sturgeon is highly uncertain. Advection-dispersion (A/D) and population modeling described in sections 3 and 4 have demonstrated that outcomes are highly dependent on the probability of spawning at a given time and location within the UMR and Yellowstone River, as well as the magnitude of any spawning event.

Limited data on abiotic factors (e.g., discharge and ramping rates, water and air temperature, turbidity) that facilitate the attraction, holding, aggregation, and spawning of pallid sturgeon on the UMR limit our ability to predict when and where spawning will occur in a given year. However, the A/D modeling efforts suggest that under the right conditions, successful recruitment to age-1 is possible on the UMR below Fort Peck. In addition to conditions in the UMR, conditions in the Yellowstone River likely play a role in determining the likelihood and success of spawning below Fort Peck Dam. Therefore, a key question is what conditions on the Upper Missouri and Milk Rivers facilitate successful spawning there, given conditions on the Yellowstone River.

To support ongoing A/D and population modeling used for implementation planning, expert elicitation was used to provide a technically sound basis for estimating spawning probability, timing, location, and magnitude (i.e., as a function of the proportion of gravid females that actually spawn, along with other factors), based upon relevant flow, temperature, and turbidity parameters. A new assessment tool, the Drift and Settling Model (DSM, described in section 3; Fischenich, et al. 2019), couples one-dimensional A/D computations with hourly water temperatures throughout the system calculated with an energy budget using prevailing weather conditions, water temperatures for the reservoir and tributaries, and release operations. A submodel identifies the distribution of larvae at the onset of settling and exogenous feeding using a new temperature-dependent development model for pallid sturgeon larvae (Chojnacki, Dodson, and DeLonay 2021). Output from the DSM is used in an updated age-structured demographic population model (DPM; Reynolds and Colvin 2019) to estimate population growth (see section 4). As described above, both models rely upon a spawning submodel to predict the timing and location of spawning, while the population model additionally relies upon the spawning model to predict the proportion of reproductively ready females that spawned at the given time and place. A formal expert judgment process with a panel of four pallid sturgeon biologists was used to inform assumptions underlying these portions of the model.

6.2 Methods

The process followed a formal expert elicitation approach to get structured judgments on a small set of questions from pallid sturgeon biologists familiar with the factors affecting sturgeon spawning in the UMR. The process consisted of two distinct stages, described in detail below. The first stage involved framing the problem and developing detailed questions suitable for expert elicitation; the second stage involved performing the elicitations and evaluating the responses.

6.3 Stage 1 – Framing and Conceptual Approach

As described above, the key information needed to support detailed modeling of the Fort Peck test flow alternatives was related to assumptions about the probability of spawning at or near Fort Peck Dam based on various abiotic factors. For this exercise, spawning in the target reach (the outcome of interest) was assumed to be dependent on the alignment of three individual processes: adequate egg development, attraction and holding of gravid females in the target reach, and suitable conditions for spawning in the UMR below Fort Peck Dam (Figure 6-1). We separated these processes conceptually to allow the experts to articulate the relationships between abiotic factors and these individual processes.

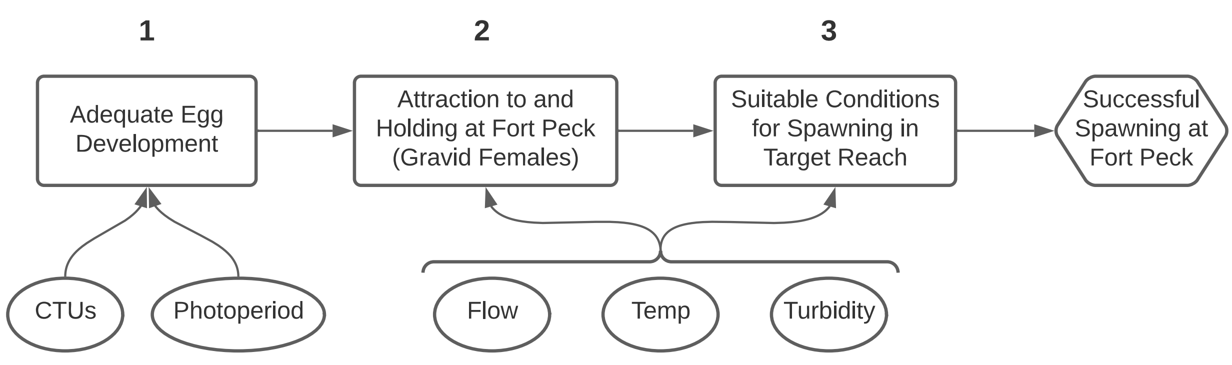

Figure 6-1. Simplified conceptual model for factors affecting successful spawning at Fort Peck. Numbers above processes shown in rectangles correspond to question groups developed for expert input.

For each of the processes described above, the general conceptual approach assumes that suitable conditions must exist in several dimensions for spawning to be possible. For example, assuming that males and gravid females have been attracted to the vicinity of Fort Peck Dam, minimally acceptable temperatures, flows, and turbidity levels must all be present to allow spawning. As flows, temperature, and turbidity conditions each move into more suitable ranges, the probability of spawning increases. The analogy of a cube helps to visualize the concept (Figure 6-2). Ranges in abiotic conditions are described by the three axes, and spawning has a non-zero probability inside the cube (i.e., within minimally acceptable combinations of conditions). This exercise was designed to elicit from the experts their understanding of the boundaries of the cube; that is, to generate spawning probabilities associated with ranges of temperature, flow, and turbidity conditions. These judgments can then be used to develop functional relationships suitable for use in predictive modeling contexts, given a set of expected abiotic conditions.

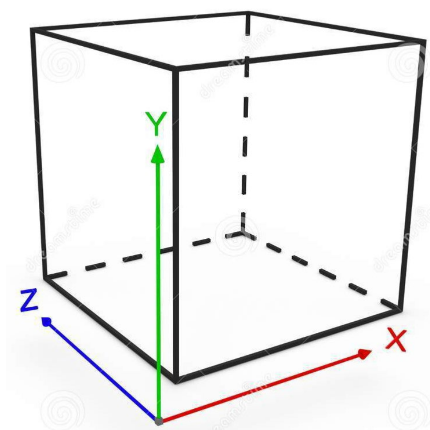

Figure 6-2. Representation of the conceptual model relating the influence of ranges in abiotic conditions (represented by axes) on spawning probability (represented by space inside the cube).

To address these questions, four experts in pallid sturgeon biology and ecology were selected based on their direct knowledge of pallid spawning behavior, familiarity with relevant literature, recognized expertise, ability to be impartial with respect to the implications of their judgments, and contribution to the diversity of experience and areas of expertise.

6.3.1 Questions developed for expert input

We developed specific questions for each of the individual processes identified in Figure 6-1 and refined them in collaboration with the modeling team and the panel of experts. As described above, the expert panel addressed Questions 1 and 3 in the fall of 2020; work is underway to continue with Question 2 in the latter half of 2021 (see section 6.8).

6.3.1.1 Question 1: Egg Development

Question 1 focused on the effects of cumulative thermal exposure and photoperiod on a female's ability to spawn (i.e., on egg development), assuming all other relevant factors are not limiting. Specific questions asked of the experts targeted both the lower and upper limits of these factors.

a. *Assume any additional criteria (e.g., flow, turbidity) for spawning are met; what is the lowest accumulated thermal exposure at which a female will spawn (calculated as the sum of mean daily temperatures from date temperature exceeds 10 °C until spawning occurs)?*
b. *Assume any additional criteria (e.g., flow, turbidity) for spawning are met; what is the highest accumulated thermal exposure at which a female will spawn (calculated as the sum of mean daily temperatures from date temperature exceeds 10 °C until spawning occurs)?*
c. *Assuming any additional criteria for spawning can be met on any day of the year, what is the earliest date on which a female pallid sturgeon could spawn (expressed as day-of-year)?*
d. *Assuming any additional criteria for spawning can be met on any day of the year, what is the latest date on which a female pallid sturgeon could spawn (expressed as day-of-year)?*

6.3.1.2 Question 3: Spawning Cues

Question 3 focused on identifying the set of abiotic conditions that facilitate spawning in the target reach, assuming sufficient aggregations of both males and gravid females (both early and late-season spawners).

a. *Assume that a female sturgeon in the UMOR has developed eggs and that turbidity, average daily water temperature, and flow magnitudes are satisfactory for spawning: what is the probability that she will spawn, given flows that are:*
    i. *Rising slowly (e.g., at approximately +500 cfs/day)*
    ii. *Steady*
    iii. *Falling slowly (e.g., at approximately -500 cfs/day)*
    iv. *Falling rapidly (e.g., at approximately -1500 cfs/day)*
b. *Assume that a female sturgeon in the UMOR has developed eggs and that flow change and turbidity are satisfactory for spawning: what is the probability that she will spawn, given average daily temperatures of:*
    i. *14°C*
    ii. *16°C*

    iii. *20°C*
    iv. *24°C*
    v. *26°C*

c. *Assume that a female sturgeon in the UMOR has developed eggs and that flow change and average daily water temperatures are satisfactory for spawning: what is the probability that she will spawn, given turbidity in the UMOR is:*
    i. *20 NTUs*
    ii. *40 NTUs*
    iii. *80 NTUs*
    iv. *160 NTUs*

6.4 Stage 2 – Elicitations

6.4.1 Preparing the Experts

The expert panel participated in an introductory workshop to clarify the exercise scope and purpose, including a detailed review of the default modeling assumptions and the intentions for using their judgments. In addition, the panel discussed and refined the underlying conceptual models, the format of the questions, and basic assumptions for each set of questions.

6.4.2 Facilitated Elicitation Workshops

Prior to the first elicitation sessions, experts received a short overview of the process of formal expert elicitation and sources and remedies for four common cognitive biases often at play in expert judgments:

- *Availability*: outcomes that are more easily recalled (or more vividly imagined) from similar situations receive higher estimates of the likelihood that they will occur in the future.
- *Anchoring*: exposure (even indirectly) to possible answers in the framing and deliberation of questions focuses experts' answers close to those values.
- *Overconfidence*: estimates of uncertainty very often underestimate the actual uncertainty.
- *Motivational Bias*: judgments are more likely to reflect past judgments on similar topics, even after the introduction of new information or reframing the context.

Questions were asked one at a time, and experts worked independently to provide initial judgments using an interactive online tool. This was followed by a facilitated discussion of those judgments with the other biologists. Once collectively satisfied that their judgments were based on a similar set of assumptions, we invited the biologists to revise their judgments as necessary to better reflect their understanding of the question and the context. This modified Delphi approach has been shown to provide more robust judgments in group settings (Burgman 2016, O'Hagan 2019).

The elicitation protocol is based on the Speirs-Bridge et al. (2010) four-point methodology for eliciting point-value estimates. This technique has been shown empirically to provide superior results in counteracting the tendency of experts to be overconfident in their judgments. The format of the four-point elicitation is as follows:

A. Consider all the factors that would lead you to estimate a low value. Realistically, what is the lowest plausible value of X?
B. Consider all the factors that would lead you to estimate a high value. Realistically, what is the highest plausible value of X?
C. Realistically, what is your best estimate of the value of X?
D. What percent of plausible values do you think are captured in the range you provided (as a percentage >50%)?

For judgments on the probability that an event will occur, an adapted three-point protocol is used as follows:

A. Consider all the factors that make this event unlikely. Realistically, what is the lowest plausible probability?
B. Consider all the factors that make this event likely. Realistically, what is the highest plausible probability?
C. In consideration of the balance of factors, realistically, what is your best estimate of the probability?

Because estimates of probability already occur on a probability scale, confidence is implied by the position of the judgments relative to 0 or 1 and by the width of the interval provided; it does not need to be directly elicited.

In addition to providing estimates of uncertainty in the judgments on specific parameters, we asked the experts to rate their degree of confidence in the underlying conceptual models. This allowed separate expressions of parameter uncertainty and model uncertainty, which have distinct characteristics and treatments. For each set of questions on a topic (e.g., on Spawning Cues), we asked the following two questions:

a. *Choose a level on the scale below that best represents your confidence in the conceptual model underlying the questions about [topic]:*
    i. *Very low confidence: There is a high likelihood that several important factors or important interactions are entirely missing from our conceptual models; consequently, our ability to make meaningful predictions is limited.*
    ii. *Low Confidence: At least some important factors have been identified, but our understanding of these factors and their relationships to others is poor, even for commonly observed conditions.*
    iii. *Moderate confidence: Many important factors have been identified, and our understanding of these is fair for commonly observed conditions but poor for more rarely observed conditions.*
    iv. *High confidence: There is a high likelihood that most of the important factors are represented and that our current understanding of them and their interactions is largely accurate for the full range of observed conditions, though relatively minor factors may not be well understood.*
    v. *Very high confidence: There is a high likelihood that all important factors are represented; our current understanding of them and their interactions is nuanced and accurate across a wide range of conditions.*
b. *Given your selection on the scale above, rate your confidence in the conceptual model underlying the questions about [topic] from 0-100.*

6.5 Elicitation Results

Anonymized results of the judgments are shown below for each question asked of the experts. Numbers used to identify experts are shown in each plot and are consistent across responses. Only post-deliberation responses are provided, as these best reflect the biologists' judgments using a common set of assumptions and information.

6.5.1 Question 1: Factors affecting egg development

We asked the experts two questions (each with two parts) about factors affecting egg development.

The first question asked the experts to provide judgments first on the minimum and then on the maximum cumulative thermal exposures after which a female could spawn (calculated as cumulative thermal units over 10 deg C). The panel was asked to assume that: (a) that lower cumulative exposures would not result in mature enough oocytes for spawning to occur; (b) that higher cumulative exposures without spawning would result in atresia; and (c) that any additional conditions or cues to enable spawning (e.g., flow conditions, daily water temperatures, etc.) were met. To help inform the judgments and augment their individual experience, the experts discussed and considered estimated CTUs for twelve recorded wild spawning events (one from the UMOR, one from the Powder River, and ten from the Yellowstone River) as well as spawning events in hatchery conditions. Results for the biologists' judgments are shown in Figure 6-3.

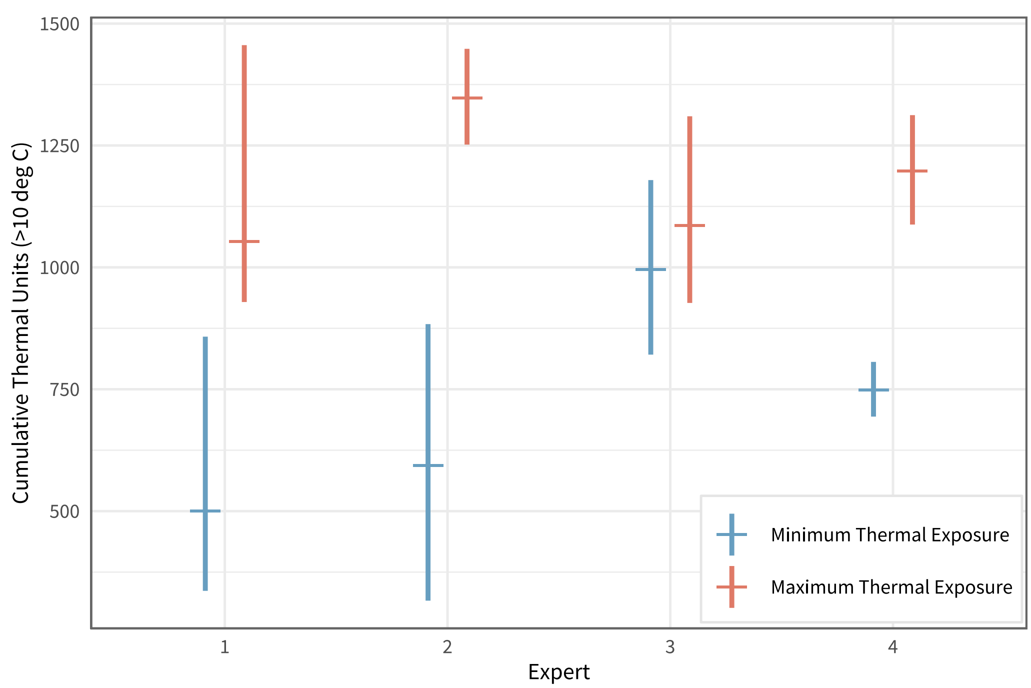

Figure 6-3. Judgments of the minimum (blue) and maximum (red) cumulative thermal exposures at which a female sturgeon could spawn. Anonymized expert identifiers are shown on the x-axis. Ranges represent 90% credible intervals, and horizontal hashes indicate best estimates

Key messages and points of rationale included:

- There was a high degree of agreement among the experts' estimates for the maximum thermal exposure, with the best estimates between 1050 and 1350 CTUs. Agreement was slightly more limited among experts for the minimum thermal exposure.
- In providing judgments on the minimum exposure, some experts weighted heavily the minimum CTUs observed in hatchery conditions, noting that if field conditions were similarly ideal, spawning could occur at low CTUs. Others noted that a variety of factors influence the final maturation of eggs, not all of which start at the same level of maturation. Conditions that contribute to the final development of eggs already closer to maturation could occur quite early in the season, yielding low observed CTUs. Others more heavily weighted observed experience in the UMOR, where temperatures tend to be colder than the Yellowstone and the Lower Missouri, leading to high CTUs.
- In providing judgments on the maximum CTUs, rationales tended to provide counterpoints to many of the points of rationale discussed above. Most experts noted in various ways that poor alignment of the range of conditions facilitating spawning would lead to higher CTUs. In addition, some noted that the low sample size of observed conditions could indicate that CTUs outside what has been observed should be expected.

The second question in this section asked the experts to provide judgments on the earliest and latest days on which spawning could occur, assuming that all other necessary conditions could be met on any day of the year. Results of the experts' judgments are shown in Figure 6-4.

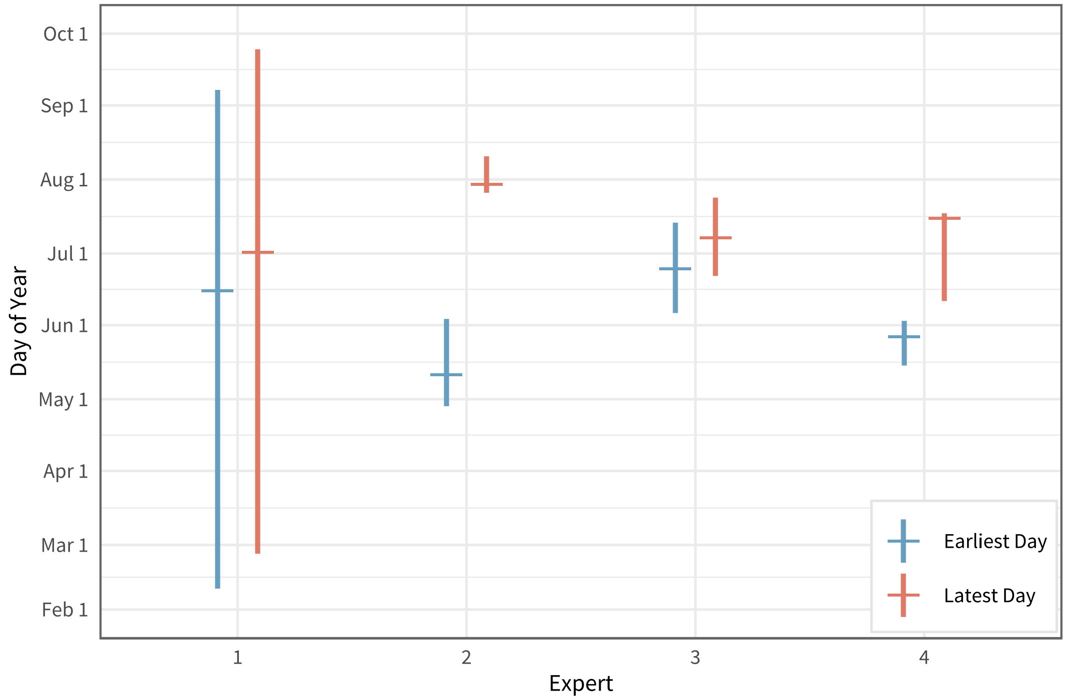

Figure 6-4. Judgments of the earliest (blue) and latest (red) day of the year on which a female sturgeon could spawn shown for each expert. Anonymized expert identifiers are shown on the x-axis. Ranges represent 90% credible intervals, and horizontal hashes indicate best estimates.

Key messages and points of rationale included:

- There was a high degree of alignment in the best estimates of the latest day on which spawning could occur (between July 1 and August 1). However, both the magnitude and shape of uncertainty around those estimates differed among the experts. One possible reason for this is differing levels of familiarity with the local context; experts' geographic areas of expertise spanned the Upper and Lower Missouri and Lower Mississippi Rivers. However, another possible reason is the number and strength of correlated factors considered explicitly or implicitly by the experts. For example, some experts directly referenced how they considered temperature trends and variability. In contrast, others related the dates more directly to CTU exposure (which is in turn indirectly related to many of the other factors).

Three experts assigned a level of "moderate confidence" to their judgments, and one expert assigned a level of "high confidence" (range of numeric confidence ratings 65-80%). Key messages included:

- CTUs and time of year are only two of the factors that affect egg development, so caution should be used with respect to considering this in a very granular way.
- Given the very low sample size of spawning in the UMOR, translating from Yellowstone data to UMOR data is difficult.
- Despite the small sample size, the similarity between wild and hatchery fish increases confidence.

6.5.2 Question 3: Spawning Cues

This set of questions asked experts to provide estimates of the probability of spawning given varying abiotic conditions in the UMR to draw out these functional relationships.

The first question focused on rate of change for discharge in the target reach. In providing judgments on this question, the experts were asked to assume that (a) a sufficient number of males and females had been attracted to and held in the target reach, and (b) that other conditions (photoperiod, CTU, temperature, turbidity) were within suitable ranges. For the purposes of this question, “Rising slowly” was defined as flows increasing at approximately 500 cfs/day, while “Falling slowly” and “Falling rapidly” were defined as flows decreasing at approximately 500 cfs/day and approximately 1500 cfs/day, respectively. Results of the experts’ judgments are shown in Figure 6-5.

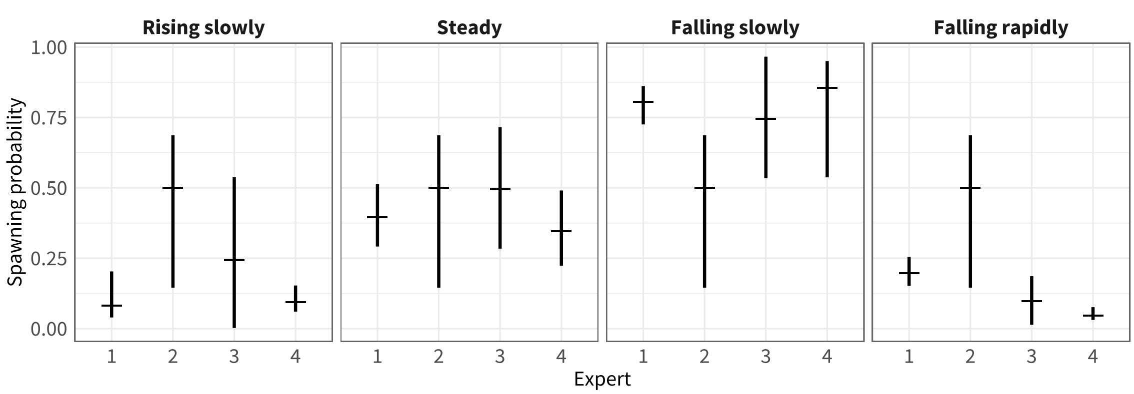

Figure 6-5. Judgments of the probability of spawning given various hydrograph changes. Anonymized expert identifiers are shown on the x-axis. Ranges represent 90% credible intervals, and horizontal hashes indicate best estimates.

Key messages and points of rationale included:

- Most experts’ judgments followed a similar trend across flow levels, where spawning probability was highest in slow flow declines and lowest in fast declines or rising hydrographs. One exception is that one expert (#2) believed that if attraction flows had occurred and adequate conditions in all other respects were present, that females would spawn over a wide range of flow conditions and with roughly similar probability.

The second question asked the experts to provide judgments on spawning probability for a range of water temperatures (expressed as daily means). In a similar fashion to the question above, we asked the experts to assume that other conditions were suitable. Results of the experts' judgments are shown in Figure 6-6.

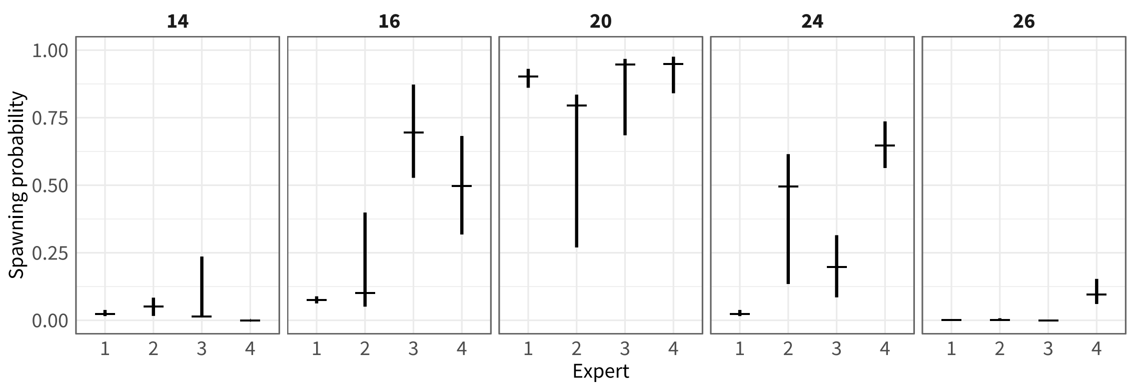

Figure 6-6. Judgments of the probability of spawning given various water temperatures. Anonymized expert identifiers are shown on the x-axis. Ranges represent 90% credible intervals, and horizontal hashes indicate best estimates.

Key points of rationale included:

- All experts followed a similar pattern across their individual judgements; probabilities were highest for the 20 and 24 degree cases, and lowest (near 0) for the 14 and 26 degree cases.
- For the 14 degree case, most experts noted that spawning has never been observed at this low temperature and that eggs are not likely to survive at this temperature.
- For the 16 degree case, the experts noted that this temperature defines the lower threshold for sturgeon, so while spawning is possible, it is unlikely unless temperatures have been higher earlier in the season.
- For the 20 degree case, most experts identified that this is near-ideal conditions (some experts noted the ideal as just below or just above this value). Consequently, most experts put relatively high probabilities on spawning at this temperature.
- For the 24 degree case, the experts largely agreed that this is past the ideal conditions, and most females would have already spawned before

temperatures reached this point. Most noted that atresia is imminent at this point.

- For the 26 degree case, all experts noted that atresia would have occurred in nearly all cases, and spawning, therefore, is very unlikely.

The third question asked the experts to provide judgments on spawning probability for a range of turbidity values, assuming other factors were all in suitable ranges. Results of the experts' judgments are shown in Figure 6-7.

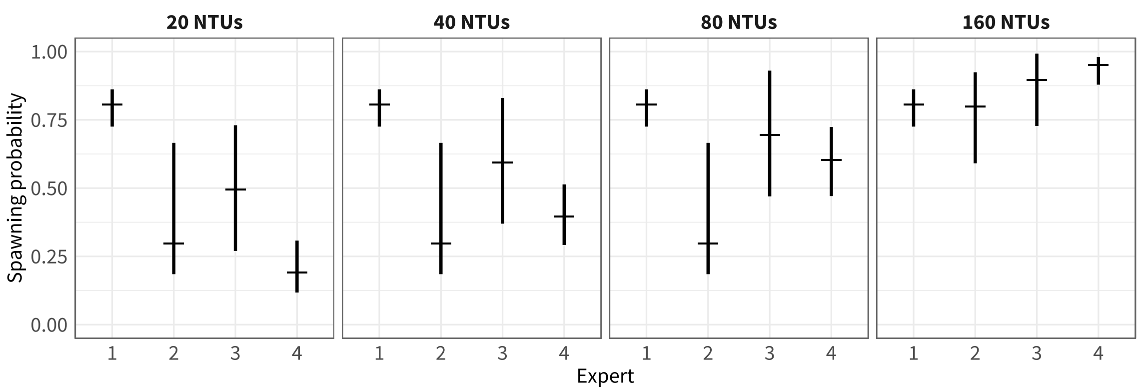

Figure 6-7. Judgments of the probability of spawning given various turbidity levels. Anonymized expert identifiers are shown on the x-axis. Ranges represent 90% credible intervals, and horizontal hashes indicate best estimates.

Key points of rationale included:

- Most experts noted that this appears to be the least important of the three factors, especially for low and relatively moderate values. Several noted explicitly that (as directed in the question) assuming water temperatures and flows are suitable, that eggs are mature, and that there is a suitably robust aggregation of males and females, there is a high probability of spawning across a range of turbidity values. This is evidenced in the judgments by the wider range of uncertainty relative to differences in the best estimates across conditions.
- Several of the experts noted that while spawning data is not existent at the lower end of turbidity values (20 and 40 NTUs) (and so noted higher uncertainty as a result), spawning is relatively unlikely in water of that clarity.

Three experts rated their confidence in their judgments in this section at "moderate," and one rated their confidence as "low" (numeric confidence ratings 50-

90%). However, confidence clearly varied for each factor. Key points of rationale included:

- Despite a relatively higher level of confidence about the effects of flow and temperature on spawning (relative to turbidity), there are two sources of uncertainty not addressed in these judgments:
  - what specifically fish respond to with respect to these variables is not well understood (e.g., absolute values, rates of change over some time period, etc.). As a result, understanding the relationship between specific metrics often used to characterize these abiotic changes and the biological response is difficult
  - the interactions among these variables are spatially and temporally variable and complex, and these interactions are not well enough understood conceptually to be addressed in these judgments.
- Much of the experience with pallid sturgeon spawning is not from the UMOR, and so extrapolating from other locations introduces significant uncertainty.
- Other factors not addressed include the role of inter-annual variability, individual past spawning experience of adult fish (and any associated site fidelity), socially mediated interactions, and availability of suitable spawning patches (including any use of pre-regulation spawning habitats). These factors are potentially important and not addressed here.

6.6 Future Elicitation Needs

As described in section 6.1, attraction to Fort Peck is dependent not only on conditions on the UMR (including the Milk River) but also on conditions in the Yellowstone River. A conceptual representation was developed to clarify the role that these various factors play in shaping an individual pallid sturgeon's decision-making about where and when (or whether) to spawn (Figure 6-8).

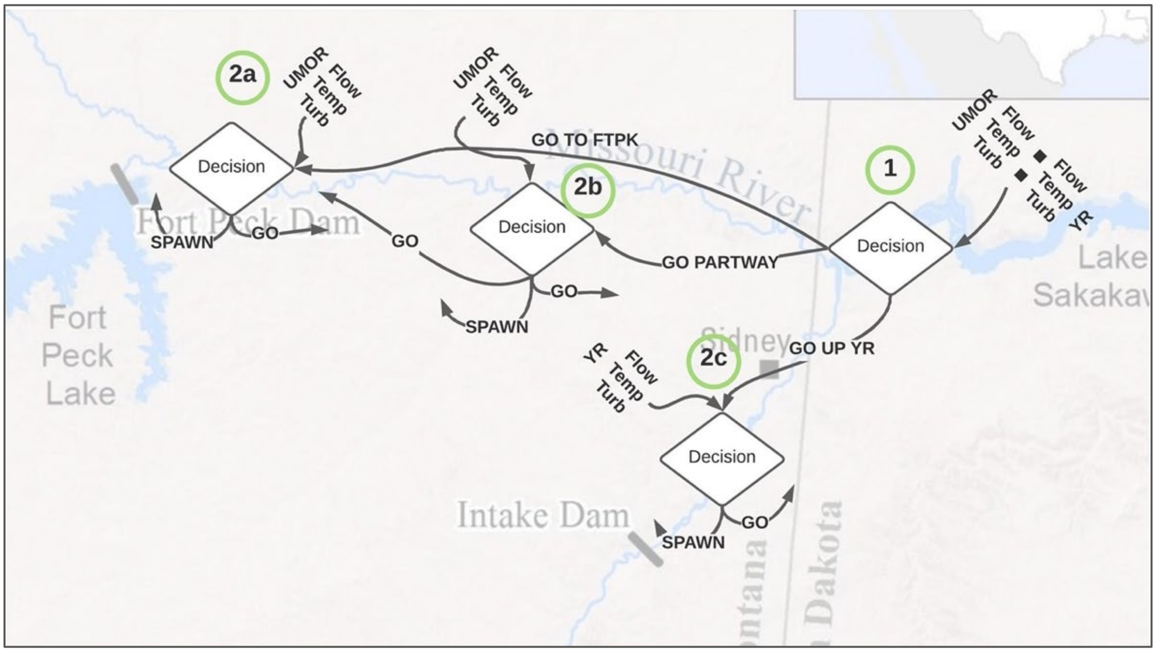

Figure 6-8. Conceptual representation of factors affecting attraction of pallid sturgeon to Fort Peck.

Female pallid sturgeon at the confluence of the Yellowstone and UMOR assess the absolute and relative conditions (temperature, turbidity, flow, pheromones, chemical signatures, etc.) coming from the Yellowstone and UMOR, as well as changes in each over time. Based on those conditions, they make a choice to move up the UMOR (partway or all the way to FTPK) or to go up the Yellowstone (Decision 1). At a population level, there appears to be considerable variability in that individual choice for a given set of conditions. The timing of when individual females initially make Decision 1 also varies (e.g., early or late spawning runs). Moreover, while some females may remain in the river section they initially chose and eventually spawn there (making Decisions 1 and 2 only once), others may move around considerably, potentially returning to the confluence and making Decision 1 multiple times during a given year before spawning.

For individual females that are attracted to FTPK at some point during the spawning season, their decision to either spawn when conditions permit or to go downstream (Decision 2a) may be influenced by flow and temperature conditions that can be predicted and directly manipulated through management, as well as other factors only indirectly affected by management such as turbidity, chemical signals from male aggregations, or other social factors more difficult to predict.

To assess the influence of these factors on attraction, a new set of questions focused on the factors affecting attraction to and holding in the target reach below

Fort Peck will be developed (Question 2, as indicated in Figure 6-1 above). Because the timing of sturgeon movements through the Upper Missouri and Yellowstone Rivers in any given year occurs across a large range of dates and because the absolute and relative conditions coming from the Yellowstone and UMR will differ across this timeframe, assessing female attraction (and eventual spawning) in terms of hydrographs and temperature scenarios (March-July) provided a better ability to assess the interacting role of these various factors.

As described above, the expert panel has not yet addressed this question, though work is underway to do so late in 2021. Five scenarios showing various hydrography and temperature profiles will be developed to show different relationships between UMOR and Yellowstone conditions (in both absolute and relative terms). For each scenario, we will ask the experts to provide probabilistic judgments on the likelihood of spawning given a specific hydrograph and temperature profile on the UMOR and Yellowstone.

7 Discussion and Conclusions

Several rounds of analyses were conducted to assess drift and retention in support of the Fort Peck EIS. For each successive round, improvements were made to the model parameterizations, model structure, or both. Results from each analysis provided important insights on the potential for improving retention and recruitment by adjusting flow operations at Fort Peck Dam. Importantly, three results were consistent across the analyses: 1) the available drift distance between Fort Peck Dam and the presumptively anoxic headwaters of Lake Sakakawea are not sufficient for reliable recruitment under the current temperature and flow regimes, 2) both composite alternatives (Alt 1 and 2) and each alternative variant (Alts 1a, 1b, 2a, 2b) has outperformed the No Action Alternative, and 3) the "best" alternative in any given year depends upon the prevailing conditions (water and air temperature, other meteorological conditions, and mainstem and tributary runoff).

Table 7-1 summarizes the rank order of the alternative variants using results from the latest round of analysis for spawning frequency, cumulative retention, and average retention per spawning event. The ranking for long-term population growth rate and time to quasiextinction in the table are based on the Round 2 population modeling results.

Table 7-1. Rank order of alternative variants (best = 1; worst = 7) based on the primary output metrics from the modeling exercises.

	Rank Order of Alternative Variants						
Metric	No Act.	1	1a	1b	2	2a	2b
# Years Spawning Criteria Met	6	3	6	1	4	5	1
Cumulative Retention	7	4	6	3	1	5	2
Average Retention Per Spawn	6	7	5	4	1	2	3
LTPGR & Time to Quasiextinction	7	4	6	1	3	5	2
Overall Rank	7	5	6	T2	T2	4	1

The best performing alternative for pallid sturgeon over the long run will be the one that has the most significant benefit to the population levels in the upper basin. This will depend upon the effectiveness of that alternative in improving retention upstream of the anoxic waters in Lake Sakakawea, but will also be a function of the frequency and magnitude of spawning that results from that alternative and the interactive effects of that alternative on spawning in the Yellowstone River. The DSM/DPM analyses provide important insights on retention, but address spawning frequency only through informed assumptions and do not address spawning magnitude or interacting effects with the Yellowstone River. Population modeling that uses the DSM results and explores those latter two factors will be necessary to better gauge alternative performance over the long term. An ongoing expert elicitation process is underway to refine initial model parameterization for these factors, and ongoing research and monitoring activities will provide critical data regarding those assumptions.

Results from the DSM modeling demonstrate that prevailing meteorological conditions play a critical role in retention. The development rate of drifting free embryos is temperature-dependent, so warmer temperatures will reduce the time to settling and, correspondingly, mortality from settling downriver of favorable lotic habitats. Retention for those years in the lower quartile of historical June air temperatures is very low, but it increases dramatically for those years with temperatures in the upper quartile. Other meteorological factors (e.g., solar radiation, cloud cover, wind speed, humidity) and tributary inflows are also important determinants of water temperature. Because of the strong influence of these factors, maintaining flexibility to determine whether to implement a test flow in a given year and to select the specific (sub)alternative to employ would improve the likelihood of success.

One way of achieving the needed flexibility is to combine the variants into composite alternatives (e.g., Alts 1, 1a, and 1b combined to form 1c). Both Alternative 1c and Alternative 2c benefit pallid sturgeon on the UMR, and while the absolute benefits are uncertain, their performance relative to the No Action Alternative is appreciable. The frequency of favorable conditions for spawning is 400% greater than No Action for both Alternative 1c and Alternative 2c. Composite retention is 450% greater for Alternative 1c and 800% greater for Alternative 2c, while long-term population growth rates using Round 2 analyses are marginally higher for both Alternative 1c (1.6%) and Alternative 2c (0.9%) compared to No Action. The purpose of the action is to create the authority to empirically investigate various hypotheses using test flows; both Alternative 1c and 2c provide that capability while the No Action Alternative does not.

While the predicted direct benefits to pallid sturgeon are greater for Alternative 2c than for Alternative 1c, the magnitude of the difference would be minor for the 3 to 5 test flows envisioned. The primary benefits are associated with the knowledge gained from the hypothesis testing and application of the knowledge gained to future decisions. Relatedly, a key difference is that testing of attraction and holding flows would be constrained under Alternative 2c, which is capped at maximum powerhouse capacity during that flow phase. Alternative 1c provides for the possibility of an attraction spill using warmer water from the Fort Peck Dam spillway, enabling experimentation around the value (or lack thereof) of attraction and retention flows in the UMR and more fully meeting the requirements of the 2018 Biological Opinion.

Considerable progress has been made under the MRRP Integrated Science Program on issues related to flow management at Fort Peck Dam. Coupling one-dimensional A/D modeling with an energy-budget model for predicting water temperatures and models of free embryo development based upon thermal exposure provided an immense advancement in our ability to assess drift and settling. The new Stage-Development models, advancements in the MRRP Pallid Sturgeon Demographic Population Model, and knowledge gained from the 2019 drift study are examples of science investments that have significantly advanced our ability to evaluate management actions. Nevertheless, considerable uncertainty remains regarding the efficacy of flow and temperature management measures to benefit recruitment and population growth for the Upper Missouri/Yellowstone River demographic unit of pallid sturgeon. Ongoing research will answer some questions, but testing and evaluation of actions under an adaptive management framework will be necessary to answer others. Accordingly, alternative selection should favor learning through flexible implementation, monitoring, evaluation, and adaptation over performance in pallid sturgeon recruitment in the near term, as the knowledge gained will yield better and better-performing solutions in the long run.

References Cited

Auer, N. A. 1996. Importance of habitat and migration to sturgeons with emphasis on lake sturgeon. Canadian Journal of Fisheries and Aquatic Sciences 53, 152-160.

Rodriguez Benitez, A., Garcia, A., Alvarez, C. (2015). Definition of mixing zones in rivers. Environmental Fluid Mechanics. 16. 10.1007/s10652-015-9425-0 .

Birstein, V. J., Bemis, W. E., Waldman, J. R. 1997. The threatened status of acipenseriform species: a summary. In. Sturgeon biodiversity and conservation. Springer.

Bolker, J. A. 2004. Embryology. In: LeBreton, G. T., Beamish, F. W. H., McKinley, S. R., eds. Sturgeons and paddlefish of North America. Kluwer Academic Publishers: The Netherlands.

Braaten, P.J., Campana, S.E., Fuller, D.B., Lott, R.D., Bruch, R.M., and Jordan, G.R., 2015, Age estimations of wild pallid sturgeon (Scaphirhynchus albus, Forbes & Richardson 1905) based on pectoral fin spines, otoliths and bomb radiocarbon: Inferences on recruitment in the dam-fragmented Missouri River: Journal of Applied Ichthyology, v. 31, no. 5, p. 821-829, [Also available at http://dx.doi.org/10.1111/jai.12873], 10.1111/jai.12873.

Braaten, P. J., Fuller, D. B., Lott, R. D., Ruggles, M. P., Brandt, T. F., Legare, R. G., Holm, R. J. 2012. An experimental test and models of drift and dispersal processes of pallid sturgeon (Scaphirhynchus albus) free embryos in the Missouri River. Environmental biology of fishes 93, 377-392.

Braaten, P. J., Fuller, D. B., Lott, R. D., Ruggles, M. P., Holm, R. J. 2010. Spatial distribution of drifting pallid sturgeon larvae in the Missouri River inferred from two net designs and multiple sampling locations. North American Journal of Fisheries Management 30, 1062–1074.

Braaten, P. J., Haddix, T. M., Jacobson, R. B. 2016. Drift, settlement, and hydraulic drivers of dispersal processes for pallid sturgeon early life stages in the Missouri River between Fort Peck Dam, Montana, and Lake Sakakawea, North Dakota: Implementation plan for 2016, in Survey, U. S. G., ed., U.S. Geological Survey, p. 26.

Braaten, P.J, and Holley, C.T. 2021, Pallid sturgeon free embryo drift and dispersal experiment data from the Upper Missouri River, Montana and North Dakota, 2019: U. S. Geological Survey data release, https://doi.org/10.5066/P9N2MFV8

Bramblett, R.G. and E.A. Scholl. 2015. Annual Report 2015: The spatial and temporal extent of the suspected hypoxic zone in the headwaters of Lake Sakakawea. Department of Ecology, Montana State University, Bozeman, MT.

Buenau, K. E., Hiller, T. L., Tyre, A. J. 2014. Modelling the effects of river flow on population dynamics of piping plovers (Charadrius melodus) and least terns (Sternula antillarum) nesting on the Missouri River. River Research and Applications 30, 964-975.

Burgman, M. 2016, *Trusting Judgements* (Cambridge University Press, Cambridge, UK).

Call, B.C., Erwin, S.O., and Bulliner, E.A. 2021, Cross-sectionally averaged flow metrics from ADCP measurements of the Missouri River downstream of Wolf Point, MT during 2018-2019: U.S. Geological Survey data release, https://doi.org/10.5066/P9ZC6E0Y.

Carr, M. L., Rehmann, C. R. 2007. Measuring the dispersion coefficient with acoustic Doppler current profilers. Journal of Hydraulic Engineering 133, 977-982.

Caswell, H., 2001, Matrix Population Models: Construction, Analysis, and Interpretation; 2nd Edition: Sunderland, Massachusettes, Sinaur Associates.

Chojnacki, K.A., Dodson, M.J., and Delonay, A.J., 2021, Cumulative thermal units and developmental stage of Pallid Sturgeon free embryos reared at multiple temperatures: U.S. Geological Survey data release, https://doi.org/10.5066/P998KBTV.

Coutant, C. C. 2004. A riparian habitat hypothesis for successful reproduction of white sturgeon. Reviews in Fisheries Science 12, 23-73.

Crossman, J., Hildebrand, L. 2014. Evaluation of spawning substrate enhancement for white sturgeon in a regulated river: Effects on larval retention and dispersal. River Research and Applications 30, 1-10.

Darby, S. E., Thorne, C. R. 2000. A river runs through it: morphological and landowner sensitivities along the Upper Missouri River, Montana, USA. Transactions of the Institute of British Geographers 25, 91-107.

Deines, A., Peterson, E., Boeckner, D., Boyle, J., Keighley, A., Kogut, J., Lubben, J., Rebarber, R., Ryan, R., Tenhumberg, B., Townley, S., and Tyre, A.J., 2007, Robust Population Management Under Uncertainty For Structured Population Models: Ecological Applications, v. 17, no. 8, p. 2175-2183,

DeLonay, A.J., Chojnacki, K.A., Jacobson, R.B., Albers, J.L., Braaten, P.J., Bulliner, E.A., Elliott, C.M., Erwin, S.O., Fuller, D.B., Haas, J.D., Ladd, H.L.A., Mestl, G.E., Papoulias, D.M., and Wildhaber, M.L., 2016, Ecological requirements for pallid sturgeon reproduction and recruitment in the Missouri River: A synthesis of science, 2005-2012: U.S. Geological Survey Scientific Investigations Report 2015-5145, 224 p., 10.3133/sir20155145.

DeLonay, A. J., Chojnacki, K. A., Jacobson, R. B., Braaten, P. J., Buhl, K. J., Elliott, C. M., Erwin, S. O., Faulkner, J. D. A., Candrl, J. S., Fuller, D. B., Backes, K. M., Haddix, T. M., Rugg, M. L., Wesolek, C. J., Eder, B. L., Mestl, G. E. 2016b. Ecological requirements for pallid sturgeon reproduction and recruitment in the Missouri River: Annual report 2014: U.S. Geological Survey, Open-File Report 2016–1013.

DeLonay, A. J., Jacobson, R. B., Chojnacki, K. A., Annis, M. L., Braaten, P. J., Elliott, C. M., Fuller, D. B., Haas, J. D., Haddix, T., Ladd, H. L. A., McElroy, B. J., Mestl, G. E., Papoulias, D. M., Rhoten, J. C., Wildhaber, M. L. 2014. Ecological requirements for pallid sturgeon reproduction and recruitment in the Missouri River: Annual report 2011: U.S. Geological Survey, Open-File Report 2014–1106.

DeLonay, A. J., and coauthors. 2016a. Ecological requirements for pallid sturgeon reproduction and recruitment in the Missouri River: A synthesis of science, 2005-2012. U.S. Geological Survey, Scientific Investigations Report 2015-5145.

DeLonay, A. J., and coauthors. 2016b. Ecological requirements for pallid sturgeon reproduction and recruitment in the Missouri River: Annual report 2014. U.S. Geological Survey, Open-File Report 2016–1013.

Detlaff, T. A., Ginsburg, A. S., Schmallhausen, O. I. 1993. Sturgeon fishes developmental biology and aquaculture. Springer-Verlag: Germany.

Dryer, M. P., Sandvol, A. J. 1993. Recovery Plan for the Pallid Sturgeon (Scaphirhynchus albus): U.S. Fish and Wildlife Service.

Dudley, R. K., Platania, S. P. 2007. Flow regulation and fragmentation imperil pelagic-spawning riverine fishes. Ecological Applications 17, 2074-2086.

Erwin, S. O. 2018. 2016 Upper Missouri River dye-trace experiment data, Columbia Environmental Research Center, U.S. Geological Survey data release.

Erwin, S. O., Jacobson, R. B. 2014. Influence of channel morphology and flow regime on larval drift of pallid sturgeon on the Lower Missouri River. River Research and Applications 31, 538-551.

Erwin, S.O., E. Bulliner, J.C. Fischenich, R.B. Jacobson, P.J. Braaten, A.J. DeLonay. 2018. Evaluating Flow Management as a Strategy to Recover an Endangered Sturgeon Species in the Upper Missouri River, USA.

Fausch, K. D., Torgersen, C. E., Baxter, C. V., Li, H. W. 2002. Landscapes to riverscapes: bridging the gap between research and conservation of stream fishes: A continuous view of the river is needed to understand how processes interacting among scales set the context for stream fishes and their habitat. BioScience 52, 483-498.

Fischenich, J.C., 2019, Modeling larval pallid sturgeon drift and retention in the Upper Missouri River below Fort Peck Dam. Model Documentation Report. Prepared for the USACE Omaha District, November, 2019

Fischenich, J.C., R. McComas, D. Meier, J. Tripe, D. Pridal, P. Boyd, S. Gibson, J. Hickey, T. Econopouly, L. Strong. 2014. Habitat Studies for the Missouri River Effects Analysis; Missouri River Effects Analysis Hydrogeomorphic Team Integrative Report. U.S. Army Corps of Engineers, Engineer Research and Development Center, Environmental Laboratory, Vicksburg, MS.

Fischenich, J.C., K. Buenau, J. Bonneau, C. Fleming, G. Long, D. Marmorek, M. Nelitz, C. Murray, B. Ma, C. Schwarz. 2018. Missouri River Science and Adaptive Management Plan. U.S. Army Corps of Engineers, Northwest Division.

Fuller, D. B., M. E. Jaeger, and M. Webb. 2008. Spawning and associated movement patterns of pallid sturgeon in the lower Yellowstone River. Report submitted to the Western Area Power Administration, upper basin pallid sturgeon work group. Montana Fish, Wildlife and Parks.

Galat, D. L., Berry, C. R., Peter, E. J., White, R. G. 2005. Missouri River Basin. 427–480.

Garcia, T., Jackson, P. R., Murphy, E. A., Valocchi, A. J., Garcia, M. H. 2013. Development of a Fluvial Egg Drift Simulator to evaluate the transport and dispersion of Asian carp eggs in rivers. Ecological modelling 263, 211-222.

George, S. G., W. T. Slack, and J. J. Hoover. 2012. A note on the fecundity of pallid sturgeon. Journal of Applied Ichthyology 28(4):512–515.

Glas, M., Tritthart, M., Zens, B., Keckeis, H., Lechner, A., Kaminskas, T., Habersack, H. 2017. Modelling the dispersal of riverine fish larvae: from a raster-based analysis of movement patterns within a racetrack flume to a rheoreaction-based correlated random walk (RCRW) model approach. Canadian Journal of Fisheries and Aquatic Sciences.

Guy, C. S., Treanor, H. B., Kappenman, K. M., Scholl, E. A., Ilgen, J. E., Webb, M. A. H. 2015. Broadening the regulated-river management paradigm: A case study of the forgotten dead zone hindering pallid sturgeon recovery. Fisheries 40, 6–14.

Hamel, M. J., J. J. Spurgeon, K. D. Steffensen, and M. A. Pegg. 2020. Uncovering unique plasticity in life history of an endangered centenarian fish. Scientific Reports 10.

Hubbard, E., Kilpatrick, F., Martens, L., Wilson Jr, J. 1982. Measurement of time of travel and dispersion in streams by dye tracing: US Geological Survey Techniques of Water-Resources Investigations. Chapter A9.

Hurley, K. L., R. J. Sheehan, and R. C. Heidinger. 2004. Accuracy and Precision of Age Estimates for Pallid Sturgeon from Pectoral Fin Rays. North American Journal of Fisheries Management 24(2):715-718.

Jacobson, R. B., Johnson, H. E., Laustrup, M. S., D'Urso, G. J., Reuter, J. M. 2004. Physical habitats dynamics in four side-channel chutes, Lower Missouri River: U.S. Geological Survey, Open-File Report 2004-1071.

Jacobson, R. B., Galat, D. L. 2006. Flow and form in rehabilitation of large-river ecosystems: An example from the Lower Missouri River. Geomorphology 77, 249–269.

Jacobson, R.B., and Galat, D.L., 2008, Design of a naturalized flow regime-an example from the Lower Missouri River, U.S.A.: Ecohydrology, v. 1, no. 2, p. 81–104, 10.1002/eco.9.

Jacobson, R.B., Parsley, M.J., Annis, M.L., Colvin, M.E., Welker, T.L., and James, D.A., 2015, Development of conceptual ecological models linking management of the Missouri River to pallid sturgeon population dynamics: U.S. Geological Survey, Open-File Report 2015-1038, 47 p. 10.3133/ofr20151038

Jacobson, R.B., Annis, M.L., Colvin, M.E., James, D., Welker, T.L., and Parsley, M.J., 2016, Missouri River Scaphirhynchus albus (Pallid Sturgeon) Effects Analysis—Integrative Report 2016: U.S. Geological Survey Scientific Investigations Report 2016-5064, 154 p., 10.3133/sir20165064.

Jacobson, R.B., Annis, M.L., Parsley, M.J., James, D.A., Colvin, M.E., and Welker, T.L., 2015, Science information to support Missouri River Scaphirhynchus albus (pallid sturgeon) effects analysis: U.S. Geological Survey Open-file Report 2015-1226, 78 p., [Also available at http://dx.doi.org/10.3133/ofr20151226].

Jacobson, R. B., M. J. Parsley, M. L. Annis, M. E. Colvin, T. L. Welker, and D. A. James. 2015. Development of conceptual ecological models linking management of the Missouri River to pallid sturgeon population dynamics. Open-File Report 2015-1038, U.S. Geological Survey.

Jaeger, M., Ankrum, A., Watson, T.M., Hadley, G.L., Rotella, J., Jordan, G., Wilson, R., Camp, S.L., Thatcher, T., and Boyd, K., 2009, Pallid sturgeon management and recovery in the Yellowstone River, chap. of Upper Basin pallid sturgeon recovery workgroup, 2008 annual report: Glendive, Mont., Montana Fish, Wildlife and Parks, p. 311.

Jager, H. I., Chandler, J. A., Lepla, K. B., Van Winkle, W. 2001. A theoretical study of river fragmentation by dams and its effects on white sturgeon populations. Environmental Biology of Fishes 60, 347-361.

Jones, J.H., and J. Oeppen. 2018. demogR: Analysis of Age-Structured Demographic Models. Source: https://cran.r-project.org/web/packages/demogR/index.html

Julien, P. Y., “River Mechanics”, Cambridge Press, 2002

Keenlyne, K. D., and L. G. Jenkins. 1993. Age at sexual maturity of the pallid sturgeon. Transactions of the American Fisheries Society 122(3):393–396.

Kilpatrick, F. A. 1970. Dosage requirements for slug injections of rhodamine BA and WT dyes: U.S. Geological Survey.

Kilpatrick, F. A., Wilson, J. F., Hubbard, E. 1989. Measurement of time of travel and dispersion in streams by dye tracing: U.S. Geological Survey.

Kim, D. 2012. Assessment of longitudinal dispersion coefficients using Acoustic Doppler Current Profilers in large river. Journal of Hydro-environment Research 6, 29-39.

Klungle, M. M., and M. W. Baxter. 2005. Lower Missouri and Yellowstone Rivers pallid sturgeon study 2004 report. Upper Basin Workgroup, Montana Department of Fish, Wildlife, and Parks, Helena, MT.

Kondolf, G., Boulton, A., O'Daniel, S., Poole, G., Rahel, F., Stanley, E., Wohl, E., Bång, A., Carlstrom, J., Cristoni, C. 2006. Process-based ecological river restoration: visualizing three-dimensional connectivity and dynamic vectors to recover lost linkages. Ecology and Society 11.

Kynard, B., Parker, E., Pugh, D., Parker, T. 2007. Use of laboratory studies to develop a dispersal model for Missouri River pallid sturgeon early life intervals. Journal of Applied Ichthyology 23, 365-374.

Launay, M., Le Coz, J., Camenen, B., Walter, C., Angot, H., Dramais, G., Faure, J.-B., Coquery, M. 2015. Calibrating pollutant dispersion in 1-D hydraulic models of river networks. Journal of Hydro-environment Research 9, 120-132.

Lechner, A., Keckeis, H., Humphries, P. 2016. Patterns and processes in the drift of early developmental stages of fish in rivers: a review. Reviews in Fish Biology and Fisheries 26, 471-489.

Lechner, A., Keckeis, H., Schludermann, E., Humphries, P., McCasker, N., Tritthart, M. 2014. Hydraulic forces impact larval fish drift in the free flowing section of a large European river. Ecohydrology 7, 648-658.

Leonard, B.P., 1979. A Stable and Accurate convective Modelling Procedure Based on Quadratic Upstream Interpolation, Computer Methods in Applied Mechanics and Engineering, vol 19, pp 59-98.Kappenman, K. M., Webb, M. A. H. & Greenwood, M. (2013). The effect of temperature on embryo survival and development in pallid sturgeon Scaphirhynchus albus (Forbes & Richardson 1905) and shovelnose sturgeon S. platorynchus (Rafinesque, 1820). Journal of Applied Ichthyology 29, 1193–1203.

Marotz, B., Lorang, M. 2018. Pallid sturgeon larvae: The drift dispersion hypothesis. Journal of Applied Ichthyology 34, 373-381.

McAdam, S. O. 2011. Effects of substrate condition on habitat use and survival by white sturgeon (Acipenser transmontanus) larvae and potential implications for recruitment. Canadian Journal of Fisheries and Aquatic Sciences 68, 812–822.

McCarthy, P. M. 2009. Travel Times, Streamflow Velocities, and Dispersion Rates in the Yellowstone River, Montana: US Geological Survey, Scientific Investigations Report 2009-5261.

Mrnak, J.T., Heironimus, L.B., James, D.A., and Chipps, S.R. 2020. Effect of water velocity and temperature on energy use, behaviour and mortality of pallid sturgeon Scaphirhynchus albus larvae. Journal of Fish Biology, 2020;1-11. DOI: 10.1111/jfb.14532

Mueller, D. S., Wagner, C. R. 2009. Measuring discharge with acoustic Doppler current profilers from a moving boat: U.S. Geological Survey Techniques and Methods 3-A22.

Nilsson, C., Reidy, C. A., Dynesius, M., Revenga, C. 2005. Fragmentation and flow regulation of the world's large river systems. Science 308, 405-408.

O'Hagan, A. 2019. Expert Knowledge Elicitation: Subjective but Scientific. The American Statistician vol. 73 issue supplement 1, p. 69-81.

Paragamian, V., Wakkinen, V. 2011. White sturgeon spawning and discharge augmentation. Fisheries Management and Ecology 18, 314-321.

Pavlov, D. 1994. The downstream migration of young fishes in rivers: mechanisms and distribution. Folia Zoologica 43, 193-208.

Pavlov, D. S., Mikheev, V. N., Lupandin, A. I., Skorobogatov, M. A. 2008. Ecological and behavioural influences on juvenile fish migrations in regulated rivers: a review of experimental and field studies. Hydrobiologia 609, 125-138.

Pine III, W.E., Allen, M.S., and Dreitz, V.J., 2001, Population Viability of the Gulf of Mexico Sturgeon: Inferences from Capture–Recapture and Age-Structured Models: Transactions of the American Fisheries Society, v. 130, p. 1164–1174.

Plummer, M. 2003. JAGS: A program for analysis of Bayesian graphical models using Gibbs sampling. Proceedings of the 3rd international workshop on distributed statistical computing. JAGS ver.4.3.0 released on July 18 2017 was accessed at https://mcmc-jags.sourceforge.io/.

R Development Core Team. 2010. R: A language and environment for statistical computing. R Foundation for Statistical Computing, Vienna, Austria.

Rabi A., Hadzima-Nyarko M., Sperac M. (2015). Modelling river temperature from air temperature in the River Drava (Croatia). Hydrological Sciences Journal, 60, 1490-1507.

Reuter, J. M., Jacobson, R. B., Elliott, C. M., DeLonay, A. J. 2009. Assessment of lower Missouri River physical aquatic habitat and its use by adult sturgeon (genus Scaphirhynchus), 2005–07: U.S. Geological Survey Scientific Investigations Report 1009-5121.

Rotella, J. 2017. Upper basin pallid sturgeon survival estimation project - 2017 update. Upper basin pallid sturgeon work group, 2010 update.

Runge, M. C., Converse, S. J., Lyons, J. E. 2011. Which uncertainty? Using expert elicitation and expected value of information to design an adaptive program. Biological Conservation 144, 1214-1223.

Runkel, R. L. 1998. One-dimensional transport with inflow and storage (OTIS): A solute transport model for streams and rivers, US Department of the Interior, US Geological Survey.

Rutherford, J. 1994. River mixing. John Wiley & Son Ltd.

Schludermann, E., Tritthart, M., Humphries, P., Keckeis, H., Bradford, M. J. 2012. Dispersal and retention of larval fish in a potential nursery habitat of a large temperate river: an experimental study. Canadian Journal of Fisheries and Aquatic Sciences 69, 1302-1315.

Skalak, K. J., Benthem, A. J., Schenk, E. R., Hupp, C. R., Galloway, J. M., Nustad, R. A., Wiche, G. J. 2013. Large dams and alluvial rivers in the Anthropocene: The impacts of the Garrison and Oahe Dams on the Upper Missouri River. Anthropocene 2, 51-64.

Smith, E. B., F. M. Williams, and C. R. Fisher. 1997. Effects of intrapopulation variability on von Bertalanffy growth parameter estimates from equal mark-recapture intervals. Canadian Journal of Fisheries and Aquatic Sciences 54(9):2025-2032.

Snyder, D. E. (2002). Pallid and shovelnose sturgeon larvae-morphological description and identification. Journal of Applied Ichthyology 18, 240–265.

Speirs-Bridge A, Fidler, F., McBride, M., Flander, L., Cumming, G., Burgman, M., 2010, Reducing Overconfidence in the Interval Judgments of Experts. Risk Analysis, vol. 30 no 3, p. 512-523.

Steffensen, K.D., Pegg, M.A., and Mestl, G., 2013a, Population prediction and viability model for pallid sturgeon (Scaphirhynchus albus (Forbes and Richardson)) in the Lower Missouri River: Journal of Applied Ichthyology, v. 29, no. 5, p. 984–989, [Also available at http://dx.doi.org/10.1111/jai.12277], 10.1111/jai.12277.

Steffensen, K.D., Pegg, M.A., and Mestl, G.E., 2013b, Population characteristics of pallid sturgeon (Scaphirhynchus albus (Forbes & Richardson)) in the Lower Missouri River: Journal of Applied Ichthyology, v. 29, no. 4, p. 687–695, [Also available at http://dx.doi.org/10.1111/jai.12196], 10.1111/jai.12196.

Su, Y.-S., and M. Yajima. 2020. Using R to Run 'JAGS'.

The Nature Conservancy, 2005, Indicators of hydrologic alteration, Version 7, user's manual, 42 p.

U.S. Army Corps of Engineers, 2006, Missouri River Mainstem Reservoir System: Master Water Control Manual, Missouri River Basin: U.S. Army Corps of Engineers, Northwest Division, 431 p.

U.S. Army Corps of Engineers, 2009, Fort Peck Temperature Control Device Reconnaissance Study Fort Peck, Montana. U.S. Army Corps of Engineers, Omaha District.

U.S. Army Corps of Engineers. 2015. Missouri River Recovery Program Management Plan Environmental Impact Statement Existing Conditions Unsteady HEC-RAS Model Calibration Report DRAFT: U.S. Army Corps of Engineers, Omaha District, Hydrologic Engineering Branch.

U.S. Army Corps of Engineers. 2016. Missouri River Recovery Program Management Plan Environmental Impact Statement Summary of Hydrologic Engineering Analysis DRAFT: U.S. Army Corps of Engineers, Northwestern Division, Omaha and Kansas City Districts.

U.S. Army Corps of Engineers, 2018a, Missouri River Recovery Management Plan and Environmental Impact Statement: U.S. Army Corps of Engineers, Northwest Division.

U.S. Army Corps of Engineers, 2018b, Fort Peck Adaptive Management Framework for Upper Missouri River Pallid Sturgeon: U.S. Army Corps of Engineers, Omaha and Kansas City Districts.

U.S. Army Corps of Engineers, 2020, Fort Peck Pallid Sturgeon Management Environmental Impact Study: U.S. Army Corps of Engineers, Omaha and Kansas City Districts.

U.S. Army Corps of Engineers, 2020a, Missouri River Recovery Program 2019 ESA Compliance Report. U.S. Army Corps of Engineers, Northwestern Division.

U.S. Fish and Wildlife Service. 2014. Revised recovery plan for the pallid sturgeon (Scaphirhynchus albus): U.S. Fish and Wildlife Service.

U.S. Fish and Wildlife Service, 2018, Final Biological Opinion concerning the Operation of the Missouri River Mainstem Reservoir System, the Operation and Maintenance of the Bank Stabilization and Navigation Project, the Operation of Kansas River Reservoir System, and the Implementation of the Missouri River Recovery Management Plan.

USACE Hydrologic Engineering Center (HEC). 2016. HEC-RAS River Analysis System Users Manual. U.S. Army Corps of Engineers, Hydrologic Engineering Center, Davis, CA.

Van Vliet M.T.H, Yearsley J.R., Franssen W.H.P, Ludwig F., Haddeland I., Lettenmaier D.P., Kabat P. 2012. Coupled daily streamflow and water temperature modeling in large river basins. Hydrology and Earth System Sciences, 16, 4303-4321.

Webb B.W., Clack P.D., Walling D.E. 2003. Water-air temperature relationships in a Devon river system and the role of flow. Hydrological Processes, 17, 3069-3084.

Wildhaber, M.L., Albers, J.L., Green, N.S., and Moran, E.H., 2017. A fully-stochasticized, age-structured population model for population viability analysis of fish: Lower Missouri River endangered pallid sturgeon example: Ecological Modelling, v. 359, p. 434-448, [Also available at http://dx.doi.org/10.1016/j.ecolmodel.2015.07.019].

Wildhaber, M.L., DeLonay, A.J., Papoulias, D.M., Galat, D.L., Jacobson, R.B., Simpkins, D.G., Braaten, P.J., Korschgen, C.E., and Mac, M.J., 2007, A conceptual life-history model for pallid and shovelnose sturgeon: U.S. Geological Survey Circular 1315, 18 p.

Zhang, Z., Johnson, B.E. 2017. Hydrologic Engineering Center-River Analysis System (HEC-RAS) Water Temperature Models Developed for the Missouri River Recovery Management Plan and Environmental Impact Statement. ERDC Environmental Laboratory, Technical Report EL TR-17-13, 121p.

Appendix A

A.1 Table of Criteria for Hydrograph Components by Alternative

Hydrograph Component	Parameter	Alt 1	Var 1A	Var 1B	Alt 2	Var 2A	Var 2B
Attraction Flow Regime	Date Initiated	April 16	April 9	April 23	April 16	April 9	April 23
	Magnitude	Peak flow is 2x the Spring Release from Fort Peck	Peak flow is 2x the Spring Release from Fort Peck	Peak flow is 2x the Spring Release from Fort Peck	Peak flow is 14,000 cfs (max powerhouse release)	Peak flow is 14,000 cfs (max powerhouse release)	Peak flow is 14,000 cfs (max powerhouse release)
	Rate of Increase as measured at Wolf Point	flows increase by 1,700 cfs per day unitl peak flow reached	flows increase by 1,700 cfs per day unitl peak flow reached	flows increase by 1,700 cfs per day unitl peak flow reached	flows increase by 1,700 cfs per day unitl peak flow reached	flows increase by 1,700 cfs per day unitl peak flow reached	flows increase by 1,700 cfs per day unitl peak flow reached
	Rate of Decrease as measured at Wolf Point	flows decrease by 1,300 cfs per day until retention flow is reached	flows decrease by 1,300 cfs per day until retention flow is reached	flows decrease by 1,300 cfs per day until retention flow is reached	flows decrease by 1,300 cfs per day until retention flow is reached	flows decrease by 1,300 cfs per day until retention flow is reached	flows decrease by 1,300 cfs per day until retention flow is reached
	Duration at Peak	3 days	3 days	3 days	3 days	3 days	3 days
Retention Flow Regime	Flowrate as measured at Wolf Point	flows remain at 1.5x the spring release from Fort Peck	flows remain at 1.5x the spring release from Fort Peck	flows remain at 1.5x the spring release from Fort Peck	flows remain at 14,000 cfs	flows remain at 14,000 cfs	flows remain at 14,000 cfs

Spawning Cue Flow Regime	Date Initiated	May 28	May 21	June 4	May 28	May 21	June 4
	Magnitude	Peak Flow is 3.5 x Fort Peck spring release	Peak flow is 3.5 x Fort Peck spring release	Peak flow is 3.5 x Fort Peck spring release	Peak flow is 28,000 cfs (2x assumed max powerplant release)	Peak flow is 28,000 cfs (2x assumed max powerplant release)	Peak flow is 28,000 cfs (2x assumed max powerplant release)
	Rate of Increase as measured at Wolf Point	flows increase by 1,100 cfs per day until peak flow is reached	flows increase by 1,100 cfs per day until peak flow is reached	flows increase by 1,100 cfs per day until peak flow is reached	flows increase by 1,100 cfs per day until peak flow is reached	flows increase by 1,100 cfs per day until peak flow is reached	flows increase by 1,100 cfs per day until peak flow is reached
	Rate of Decrease as measured at Wolf Point	flows decrease by 1,000 cfs for 12 days then decrease by 3,000 cfs until 8,000 cfs is reached.	flows decrease by 1,000 cfs for 12 days then decrease by 3,000 cfs until 8,000 cfs is reached.	flows decrease by 1,000 cfs for 12 days then decrease by 3,000 cfs until 8,000 cfs is reached.	flows decrease by 1,000 cfs for 12 days then decrease by 3,000 cfs until 8,000 cfs is reached.	flows decrease by 1,000 cfs for 12 days then decrease by 3,000 cfs until 8,000 cfs is reached.	flows decrease by 1,000 cfs for 12 days then decrease by 3,000 cfs until 8,000 cfs is reached.
	Duration at Peak	3 days	3 days	3 days	3 days	3 days	3 days
Drifting Flow Regime	Flowrate as measured at Wolf Point	flows remain at 8,000 cfs until Sept. 1	flows remain at 8,000 cfs until Sept. 1	flows remain at 8,000 cfs until Sept. 1	flows remain at 8,000 cfs until Sept. 1	flows remain at 8,000 cfs until Sept. 1	flows remain at 8,000 cfs until Sept. 1
Limitations During Flow Regimes	Forecasted Fort Peck to Garrison runoff	Less than upper quartile	Less than upper quartile	Less than upper quartile	Less than upper quartile	Less than upper quartile	Less than upper quartile
	Minimum Forecasted Fort Peck Elevation	2227.0 ft.	2227.0 ft.	2227.0 ft.	2227.0 ft.	2227.0 ft.	2227.0 ft.

	Flow limit at Wolf Point and Culbert-son	35,000 cfs	35,000 cfs	35,000 cfs	35,000 cfs	35,000 cfs	35,000 cfs
	Maximum Forecasted Garrison Pool	1850 ft.	1850 ft.	1850 ft.	1850 ft.	1850 ft.	1850 ft.
	Minimum forecasted Williston levee free-board	6.38 ft.	6.38 ft.	6.38 ft.	6.38 ft.	6.38 ft.	6.38 ft.
	Maximum forecasted Williston stage	22.0 ft.	22.0 ft.	22.0 ft.	22.0 ft.	22.0 ft.	22.0 ft.

Appendix B

B.1 Meteorological Data

Meteorological data used for the analyses presented in this report were compiled from several sources and integrated into an HEC-DSS database with a filename “FtPeckMet_Merged.dss”. This file was provided to the USACE along with this report. The data is too extensive to present in printed form, but several plots of the data are presented in this appendix to provide readers with a sense of the magnitude and variability of meteorological condition in the project area. Example plots generally include the 1960 – 2019 period and a plot of the June/July conditions for that parameter in an example year.

B.1.1 Air Temperatures

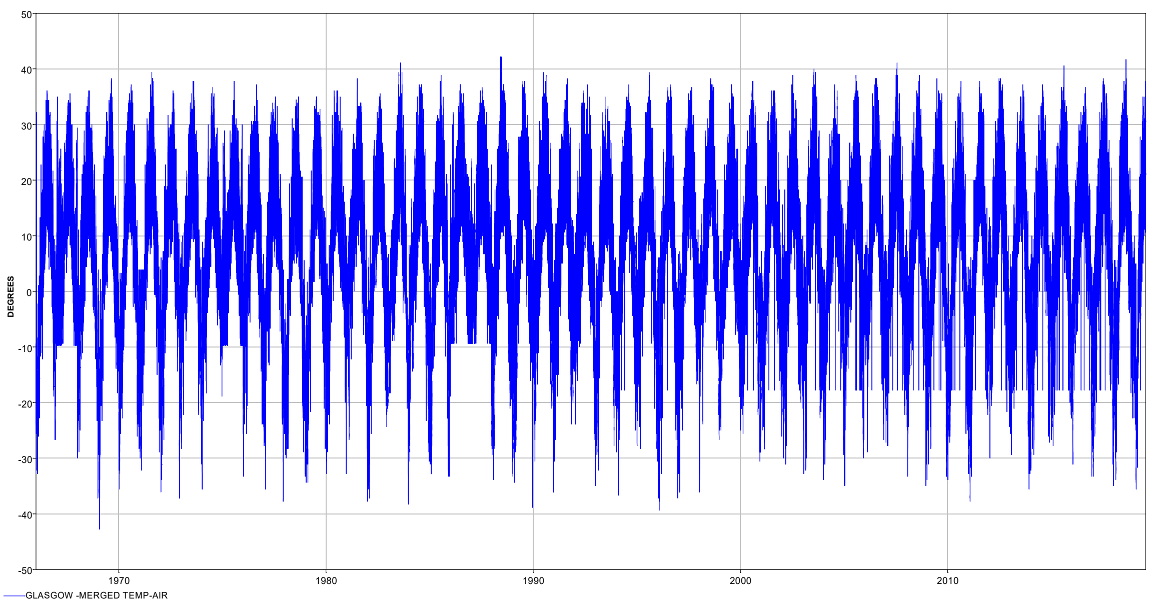

Table. Air temperatures 1960 – 2019.

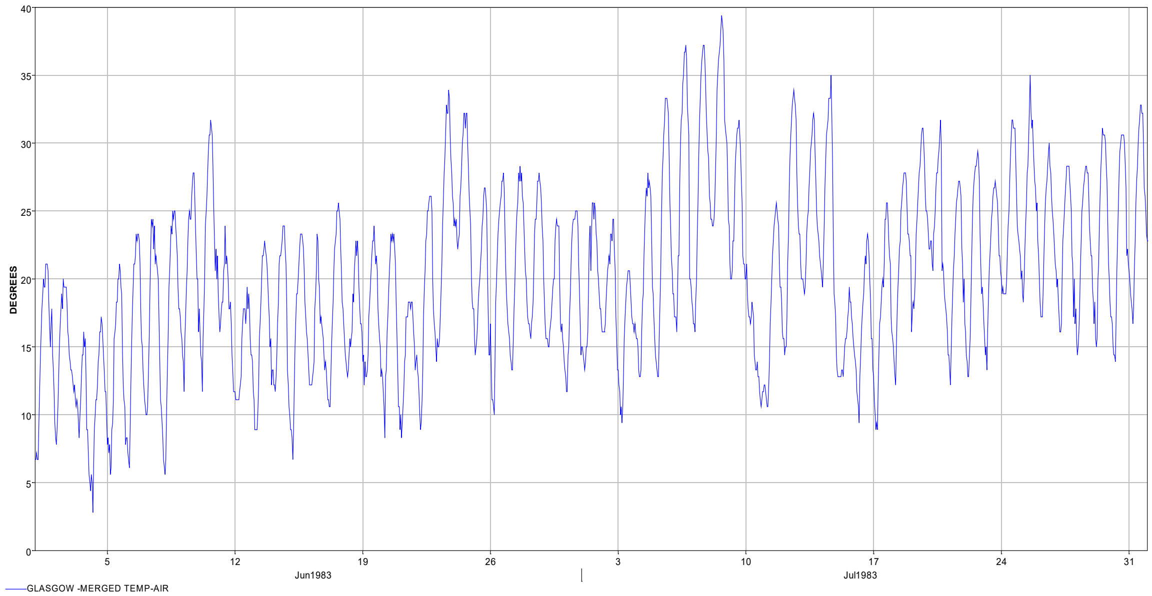

Table. Air temperatures June – July 1983.

B.1.2 Atmospheric Pressure

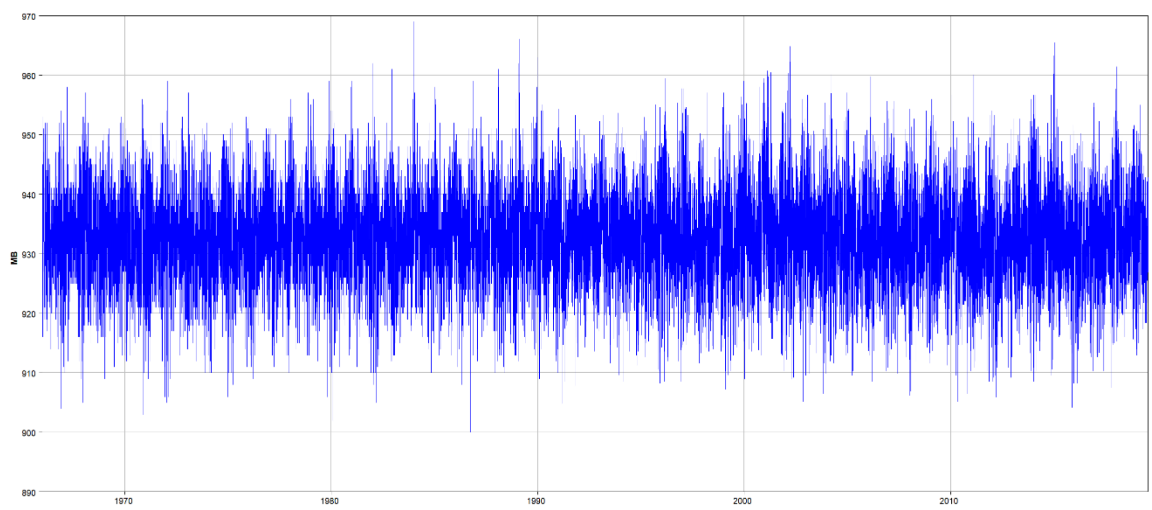

Table. Atmospheric pressure 1960 – 2019.

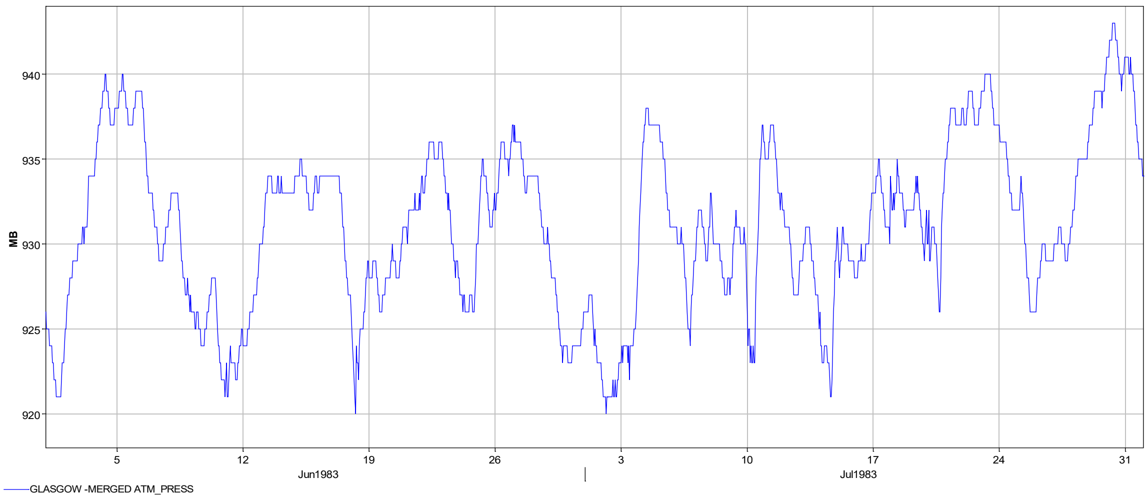

Table. Atmospheric pressure June – July 1983.

B.1.3 Humidity

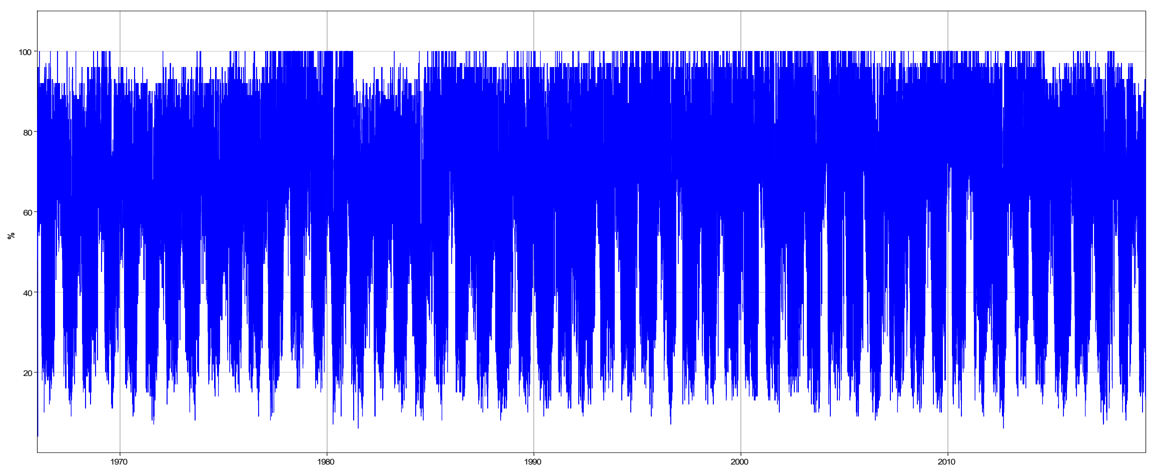

Table. Humidity levels 1960 – 2019.

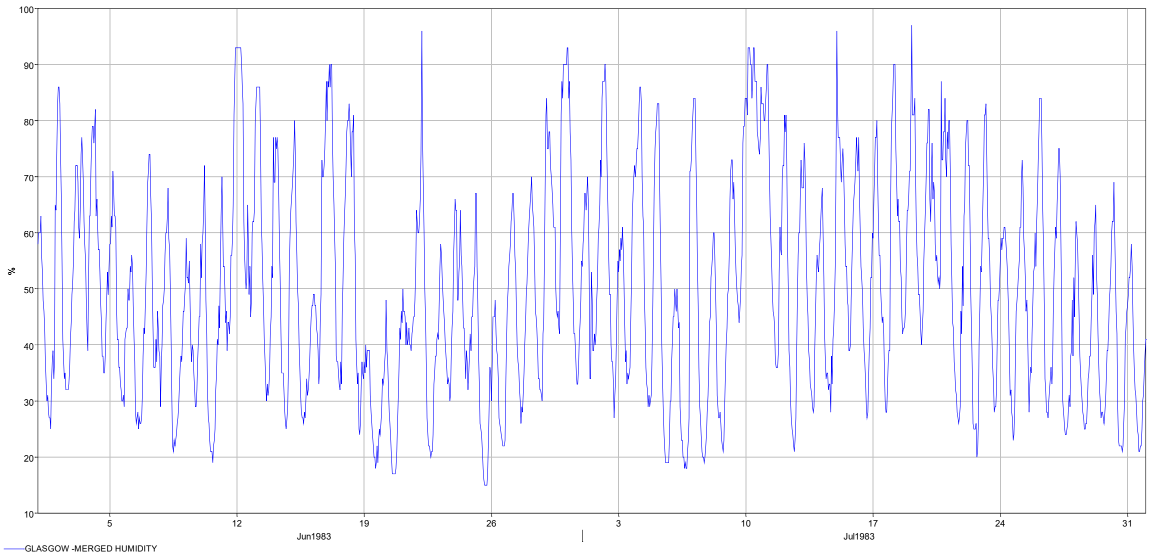

Table. Humidity levels June – July 1983.

B.1.4 Solar Radiation

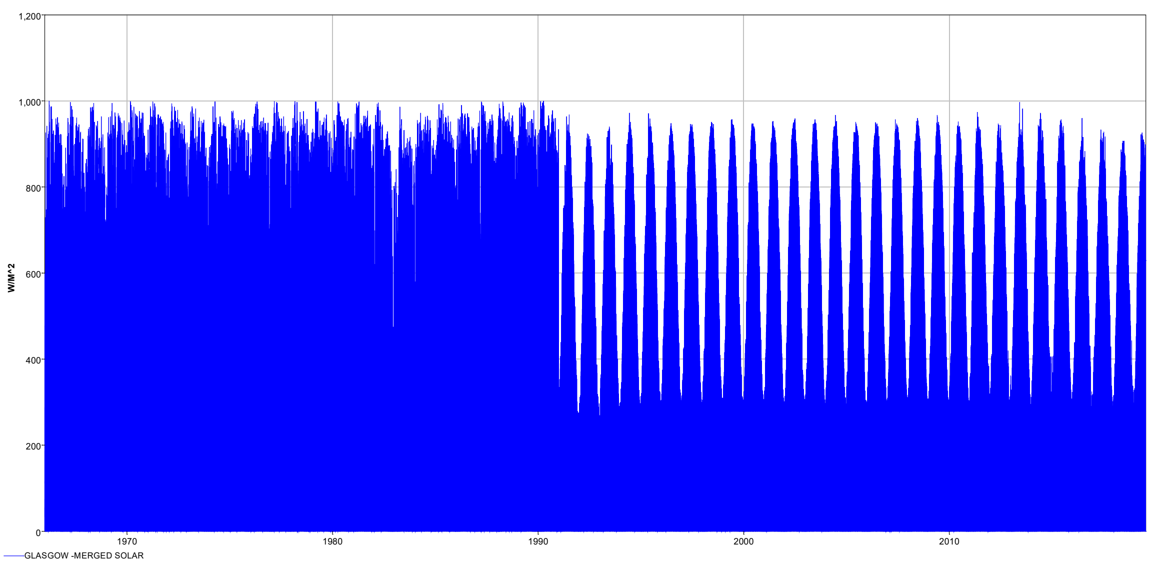

Table. Solar radiation levels 1960 – 2019.

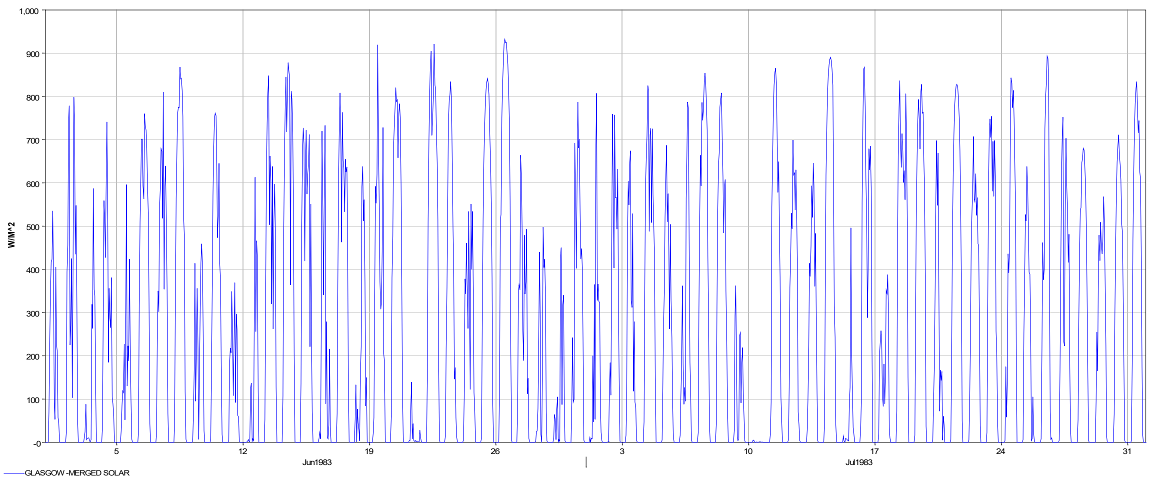

Table. Solar radiation June – July 1983.

B.1.5 Cloud Cover

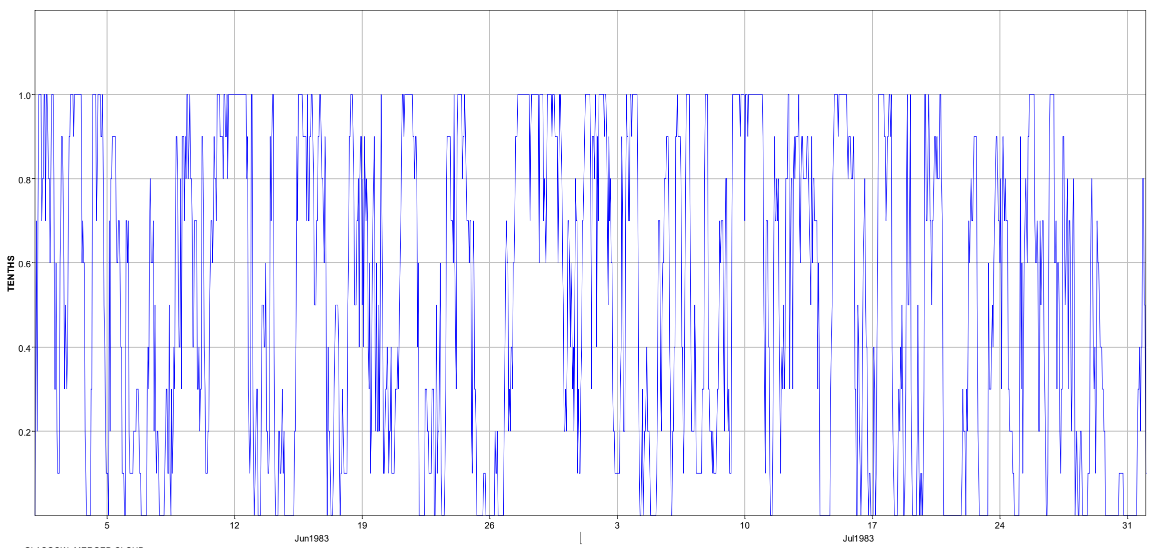

Table. Cloud cover June – July 1983.

B.1.6 Wind

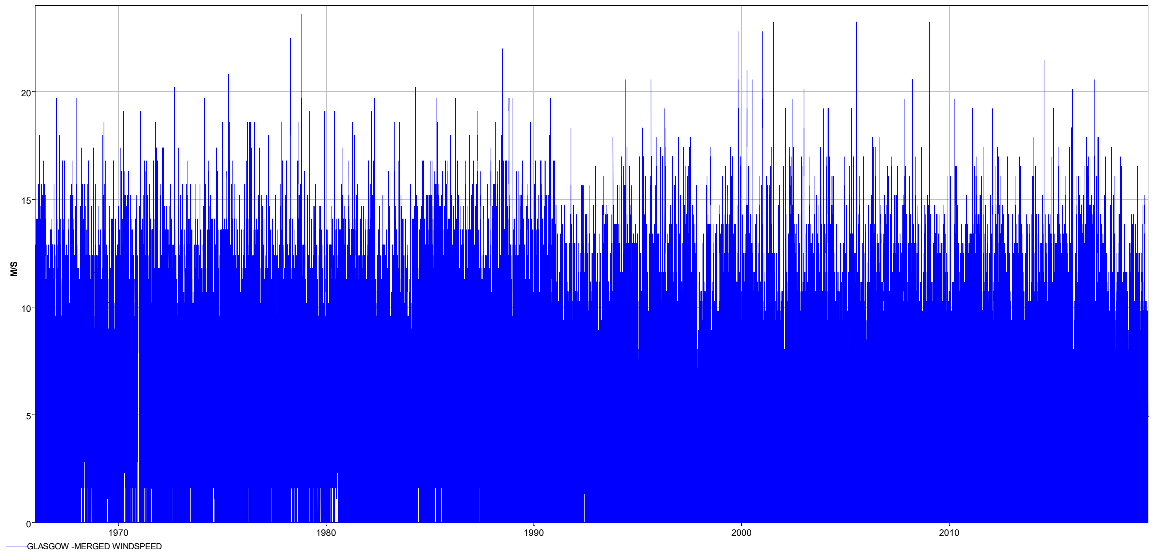

Table. Wind speed 1960 – 2019.

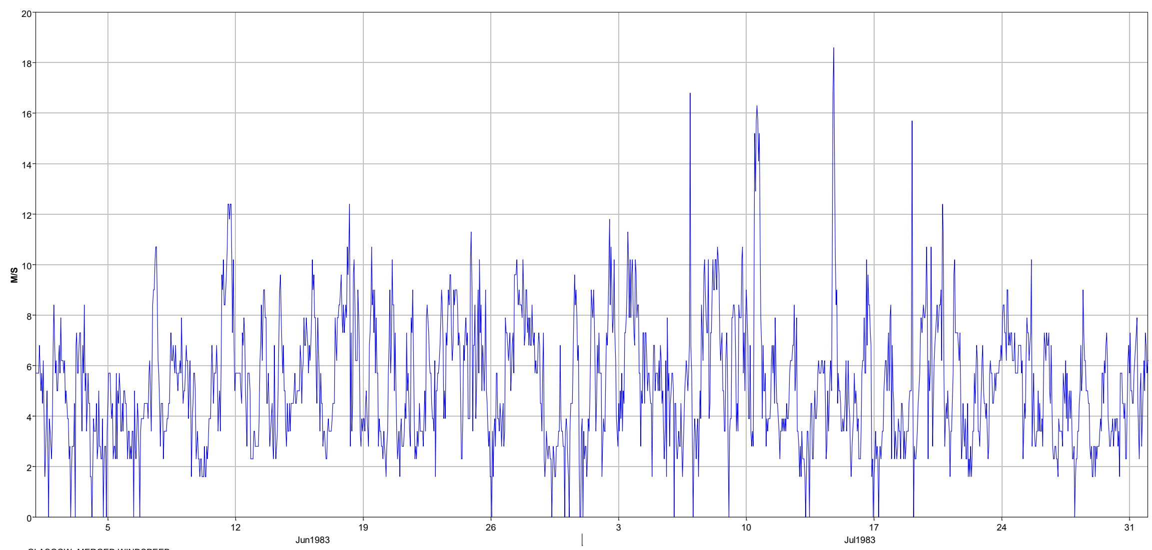

Table. Wind speed June – July 1983.

B.2 Water Temperature Data for Boundary Conditions

Water temperatures for boundary conditions were developed from best fits of quadratic equations to measured data for each tributary, the mainstem Missouri River, and measurements from Fort Peck Lake. In addition to the mean fit, we fit +/1 1SD relations to represent warm and cool conditions, respectively, as described in section 2.6.1.2. Temperatures at boundary conditions were reconstituted from the relations, using the appropriate relation depending upon a classification of "cool", "normal", or "warm" for each year depending upon air temperatures for the first half of June. The following set of figures show the reconstituted water temperatures for 1968 (cool), 1969 (normal), and 1970 (warm). Note that the quadratic equations force temperatures to zero when sub-zero temperatures often occur in winter.

B.2.1 Temperature Classification for Year

A statistical analysis of June 1 – 15 temperatures for the POR was used to classify years as cool, normal, or warm (Figure 4-12).

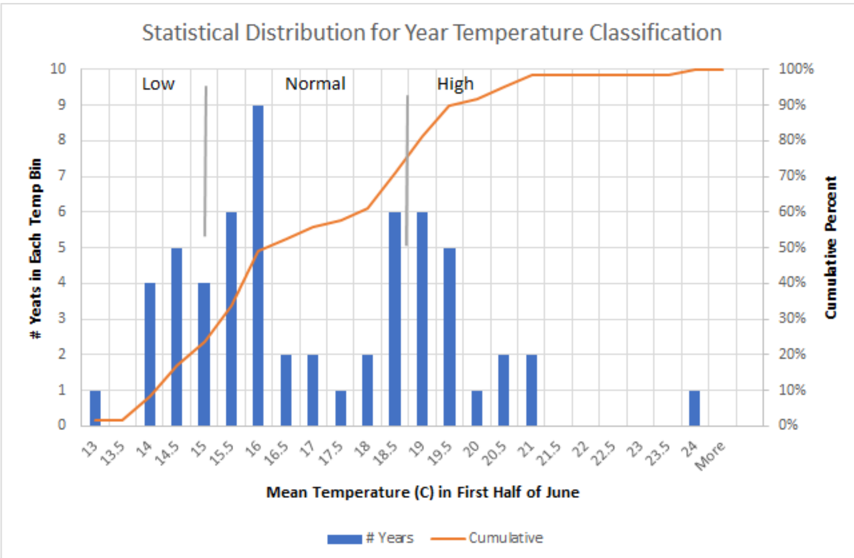

Table. Statistical distribution of June 1-15 mean temperatures for POR used to classify years as cool, normal or warm.

B.2.2 Plots of Measured Data and Model Fits for Boundary Conditions

Data collected by the USGS and USACE (or their contractors) over the POR were used to establish relationships for water temperature as a function of Julian day of the year. The underpinning data is available in digital format for review – the data points are included on the following figures of Quadratic equation fits to the mean, and +/- 1SD for each location.

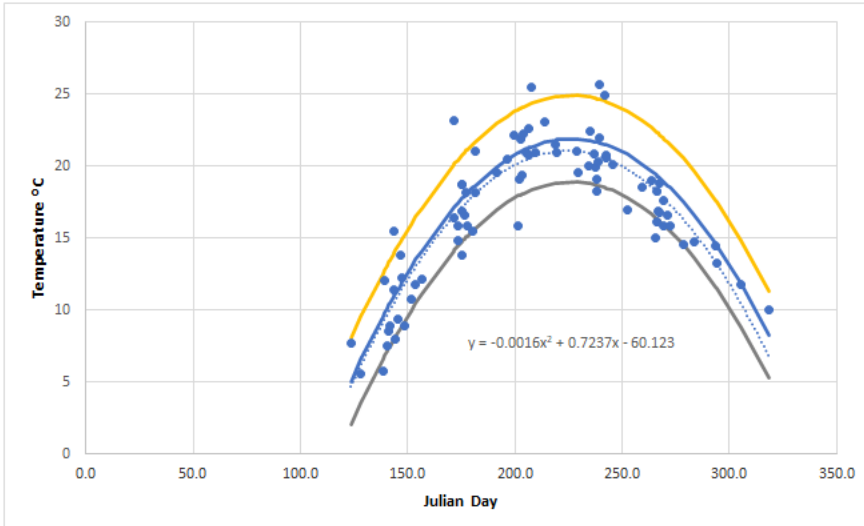

Table. Quadratic fits of measured Fort Peck Lake temperatures to Julian day of the year (mean and +/- 1SD; equation is for the mean).

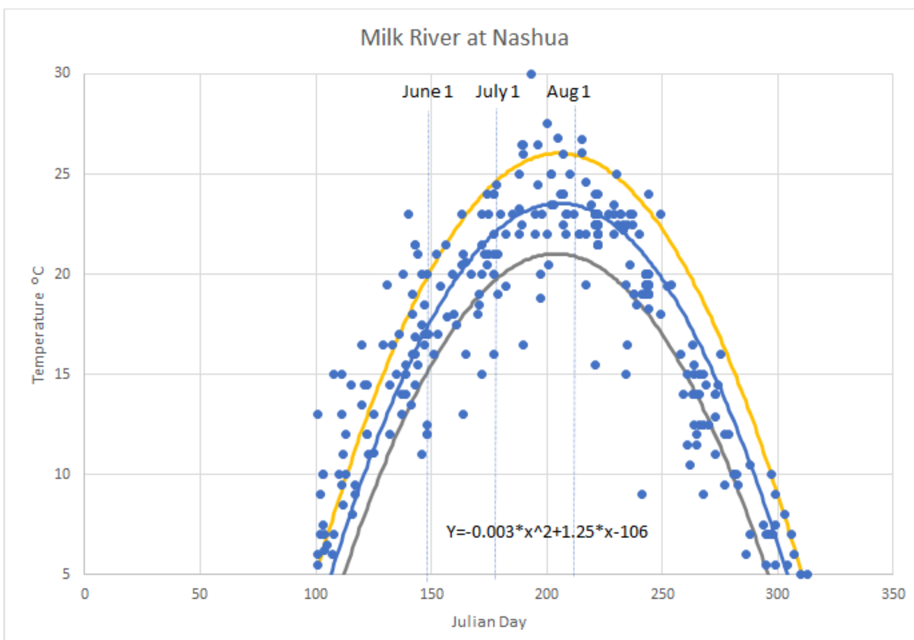

Table. Quadratic fits of measured temperatures for the Milk River at Nashua, MT to Julian day of the year (mean and +/- 1SD; equation is for the mean).

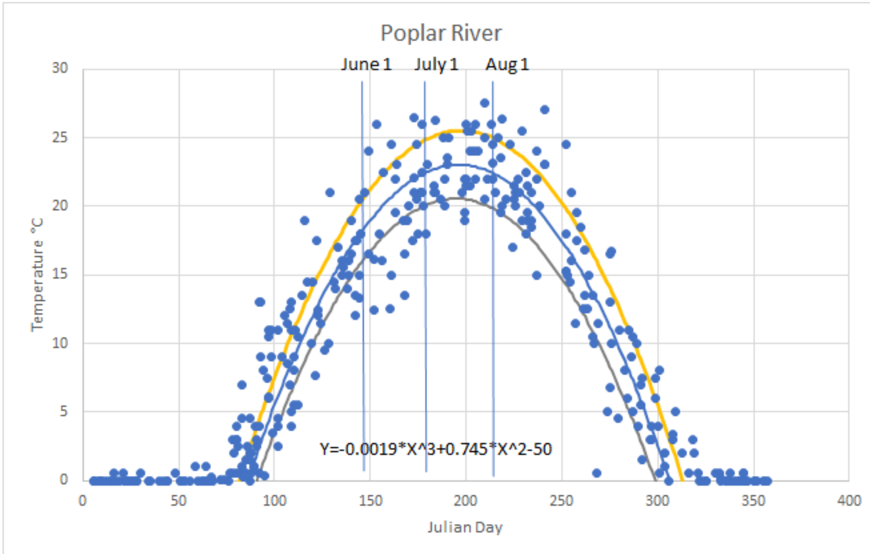

Table. Quadratic fits of measured temperatures for the Poplar River to Julian day of the year (mean and +/- 1SD; equation is for the mean).

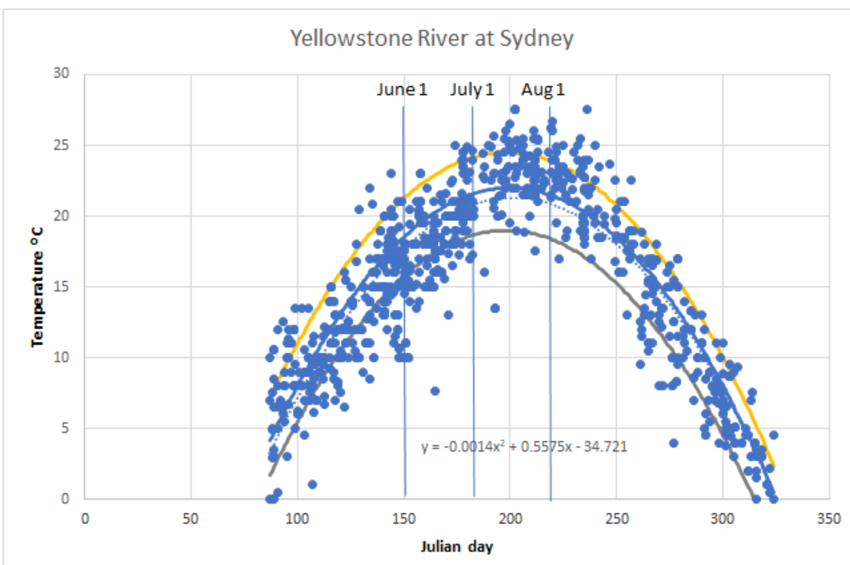

Table. Quadratic fits of measured temperatures for the Poplar River to Julian day of the year (mean and +/- 1SD; equation is for the mean).

B.2.3 Plots of water temperatures at boundaries for cool, normal, and warm conditions

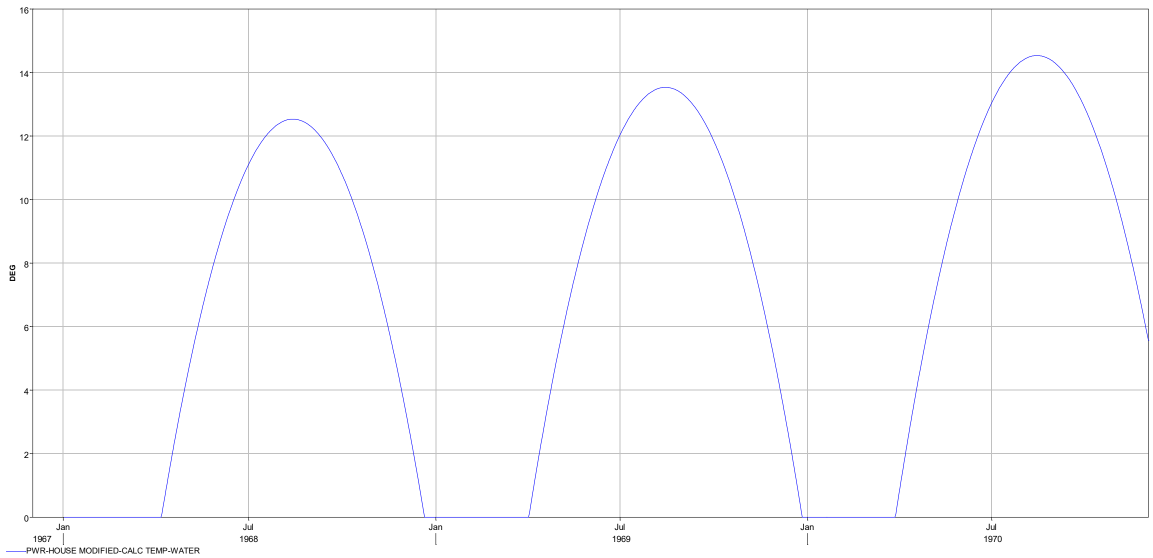

Table. Water temperatures for Fort Peck powerhouse flows in cool (1968), normal (1969), and warm (1970) years.

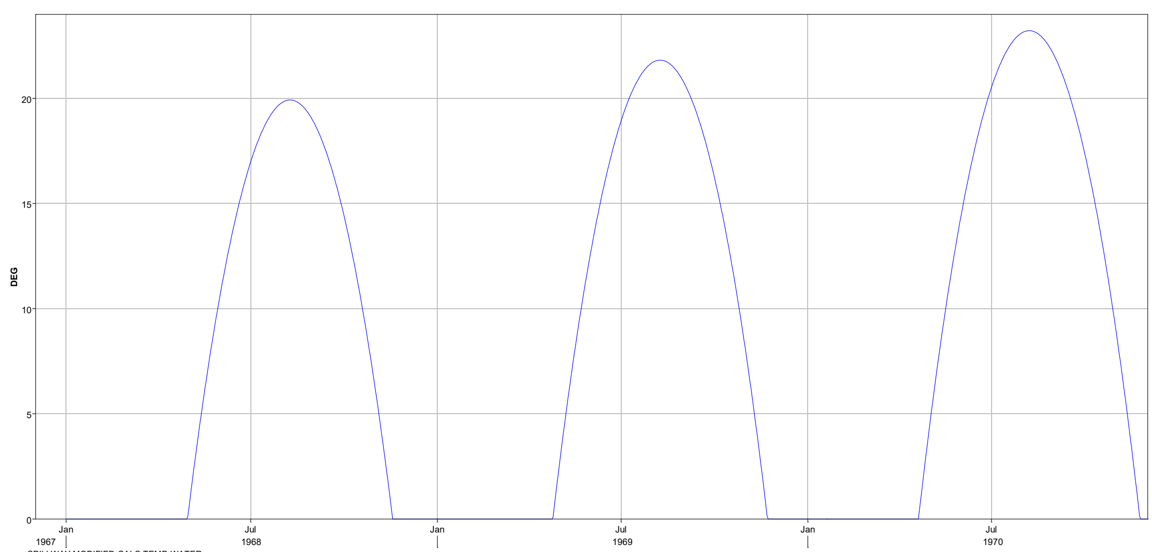

Table. Water temperatures for Fort Peck Lake and spillway flows in cool (1968), normal (1969), and warm (1970) years.

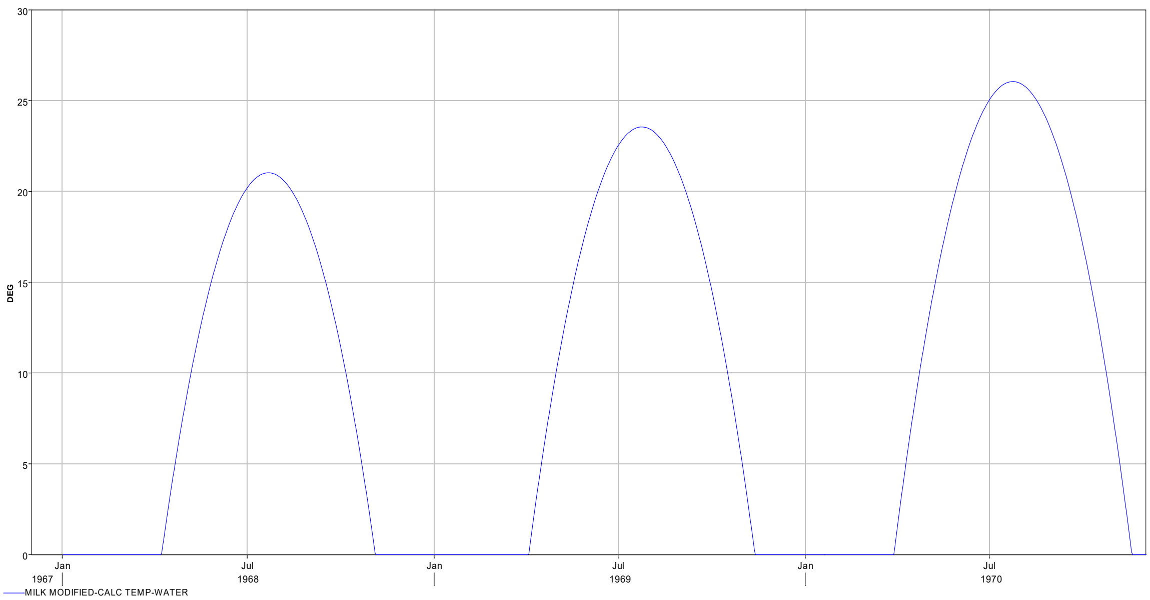

Table. Water temperatures for Milk River flows in cool (1968), normal (1969), and warm (1970) years.

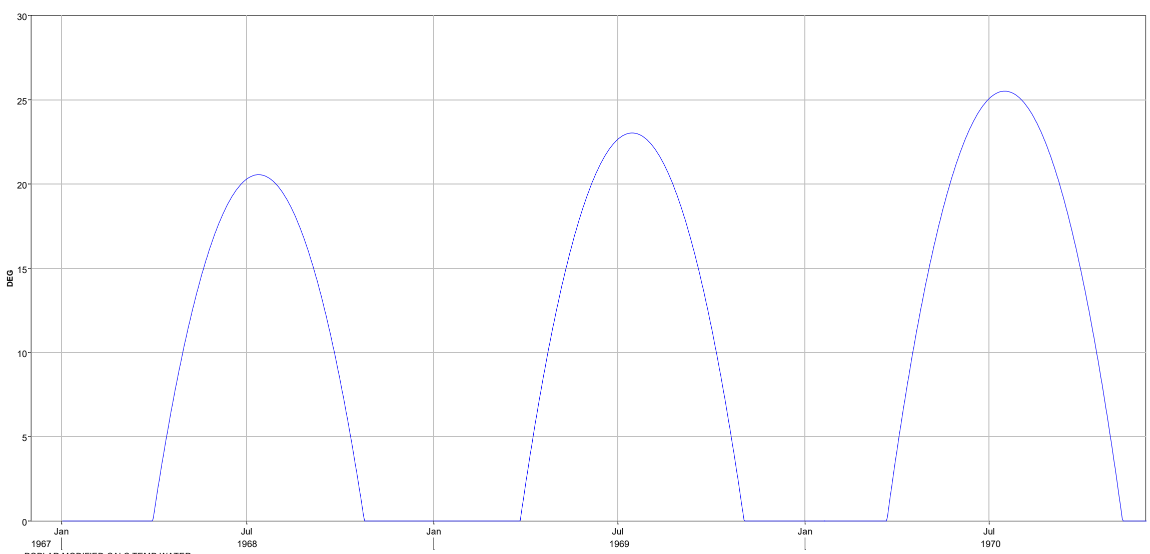

Table. Water temperatures for Poplar River flows in cool (1968), normal (1969), and warm (1970) years.

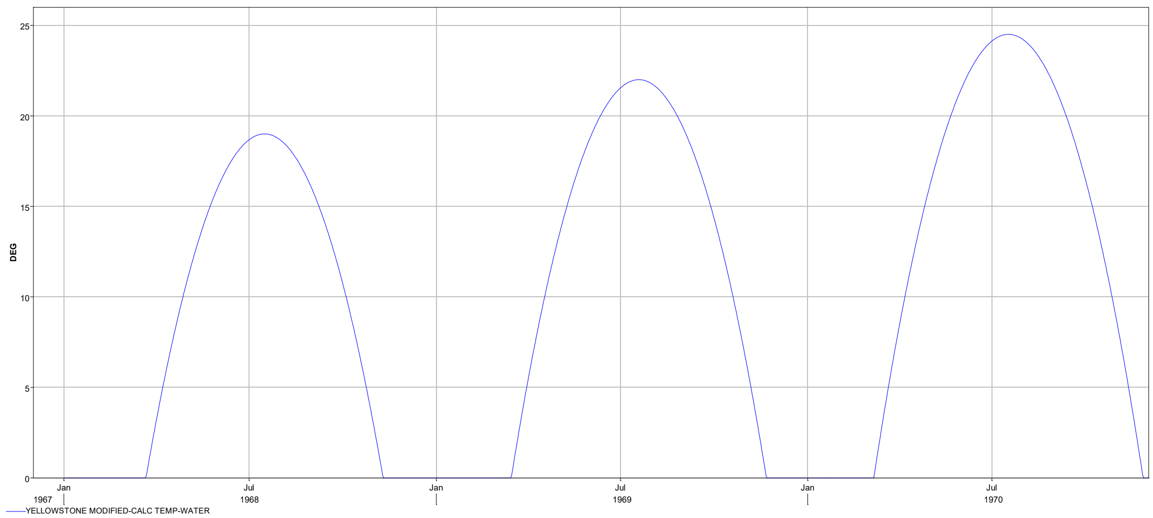

Table. Water temperatures for Yellowstone River flows in cool (1968), normal (1969), and warm (1970) years.

Appendix C

C.1 Spawning Submodel Plots

The following series of plots show the flow and temperature profiles for each year and alternative combination investigated. Blue lines in the figure are the flows generated from ResSim for each alternative. The gray and orange paired lines in the upper region are spillway temperatures for warm and normal years, respectively. The solid yellow line is for powerhouse flows, and the remaining set of three lines are the combined temperature (spillway and powerhouse) below Fort Peck for warm (gray long dashed), normal (gray solid), and cool (gray short dashed) conditions. The full set of plots are grouped together as Figure 4-22.

Table. Set of plots showing discharge and temperature profiles below Fort Peck Dam for each alternative/year combination investigated.

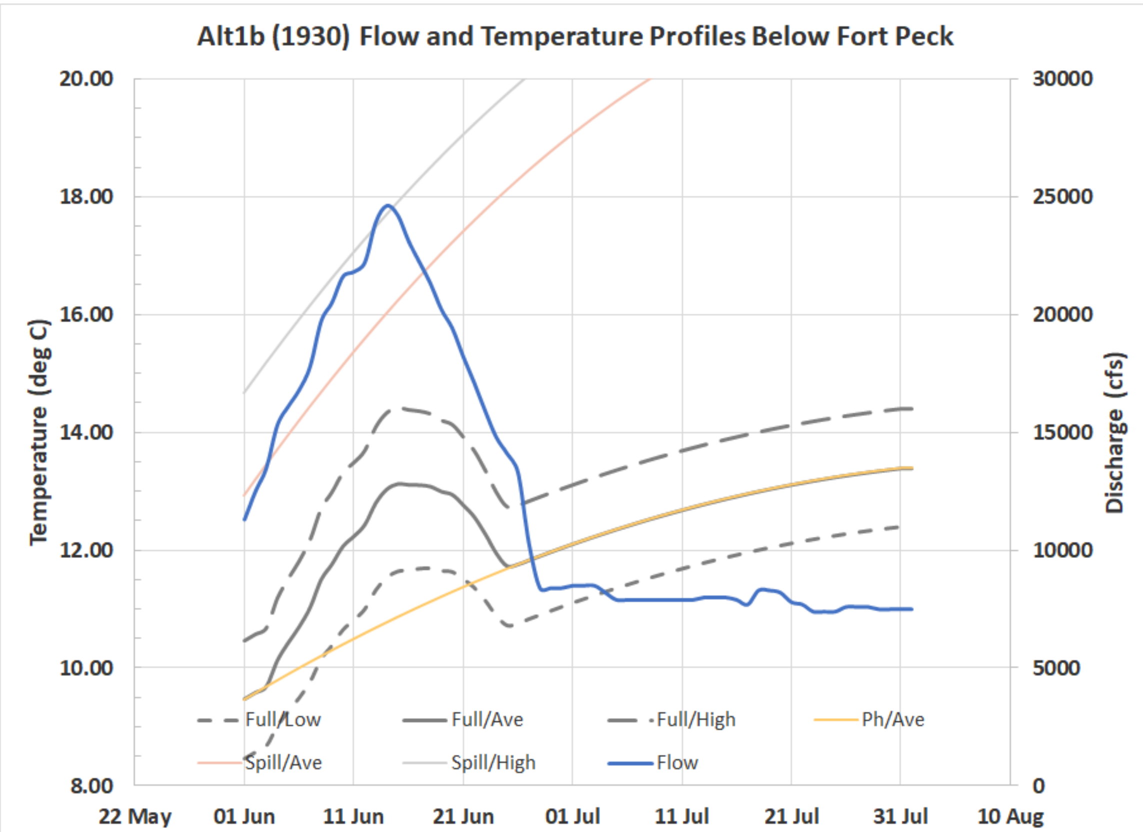

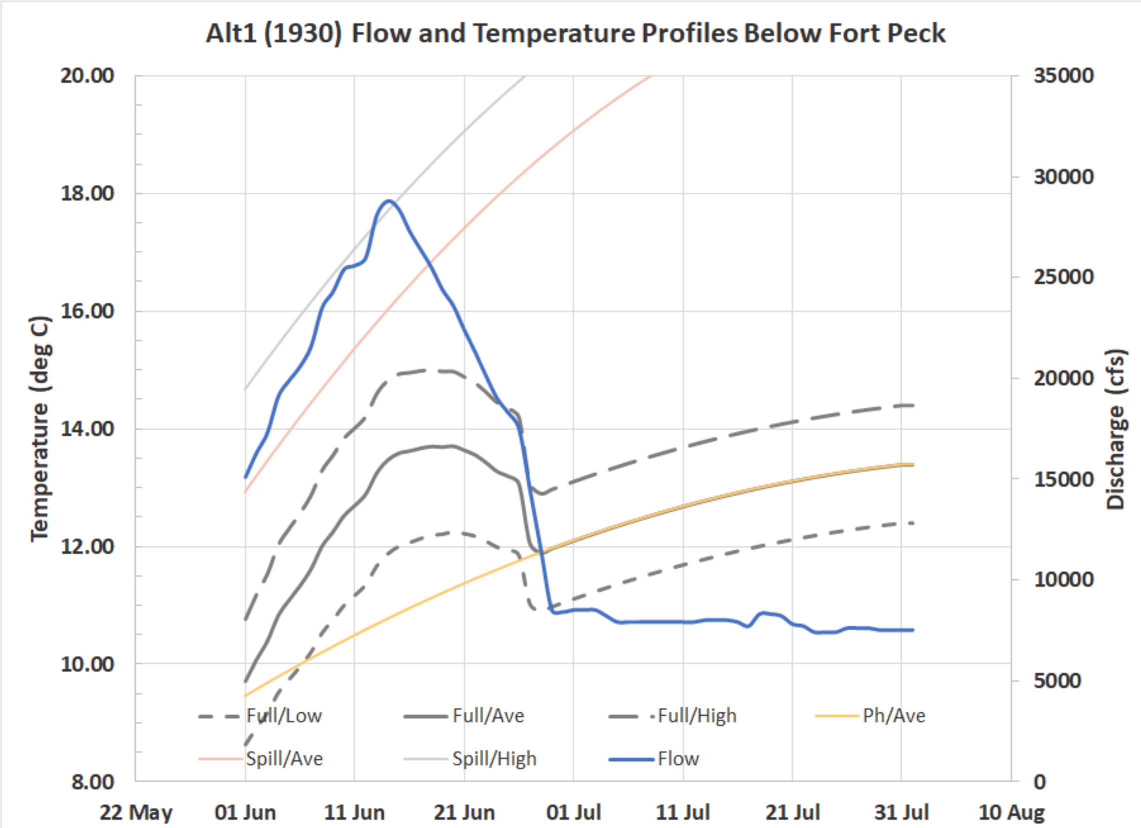
Alt1 (1930) Flow and Temperature Profiles Below Fort Peck
Temperature (deg C)
Discharge (cfs)
20.00
18.00
16.00
14.00
12.00
10.00
8.00
35000
30000
25000
20000
15000
10000
5000
0
22 May
01 Jun
11 Jun
21 Jun
01 Jul
11 Jul
21 Jul
31 Jul
10 Aug
Full/Low
Full/Ave
Full/High
Ph/Ave
Spill/Ave
Spill/High
Flow

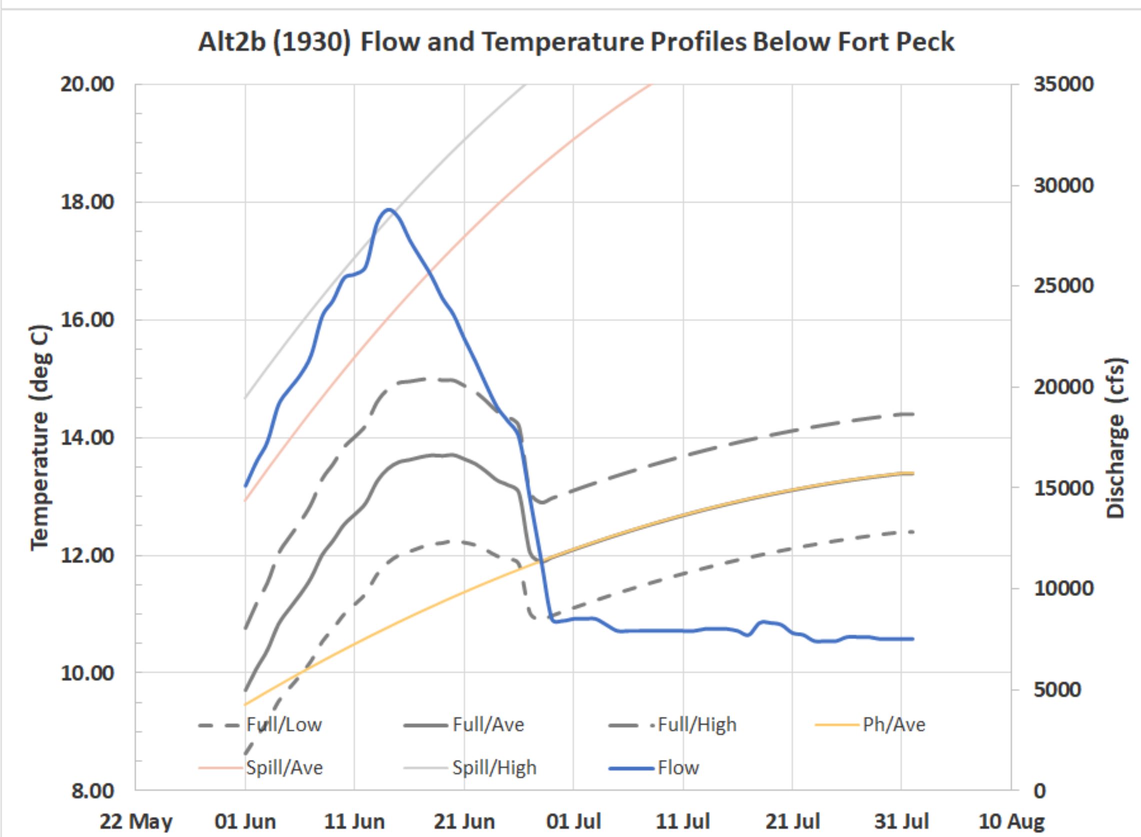
Alt2b (1930) Flow and Temperature Profiles Below Fort Peck
Temperature (deg C)
Discharge (cfs)
20.00
18.00
16.00
14.00
12.00
10.00
8.00
35000
30000
25000
20000
15000
10000
5000
0
22 May
01 Jun
11 Jun
21 Jun
01 Jul
11 Jul
21 Jul
31 Jul
10 Aug
Full/Low
Full/Ave
Full/High
Ph/Ave
Spill/Ave
Spill/High
Flow

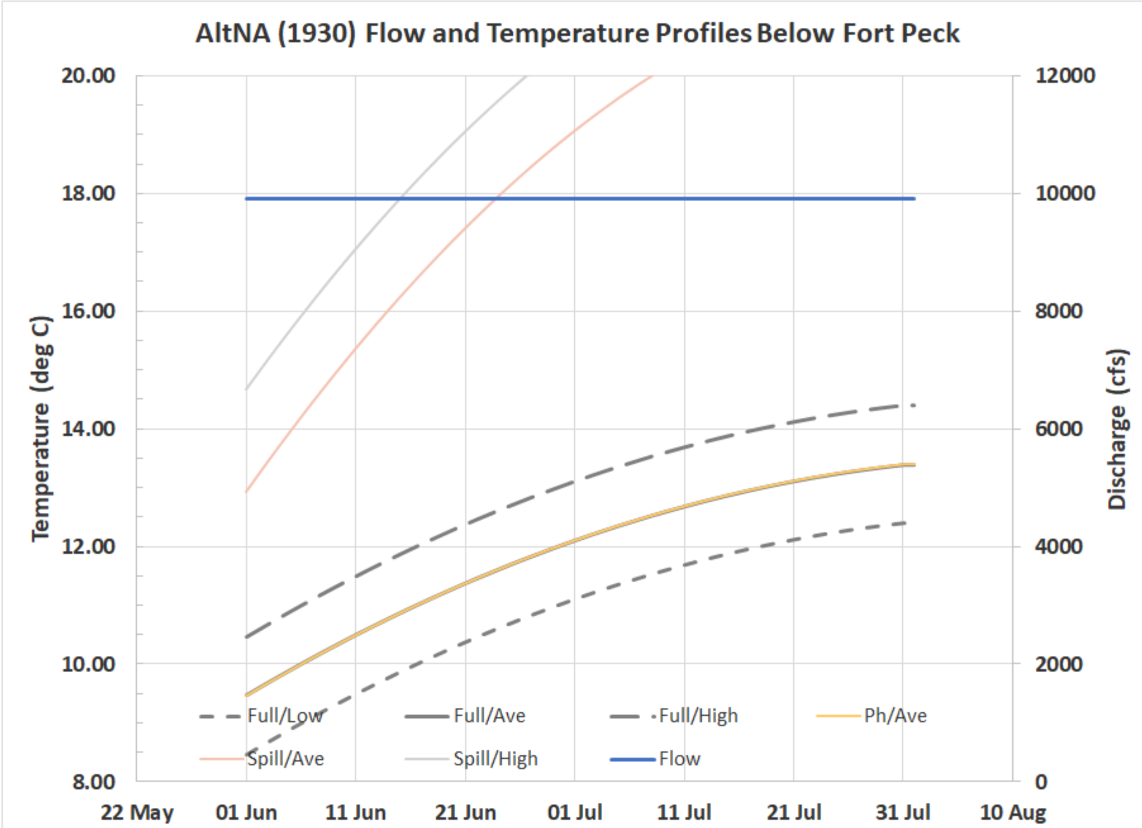

AltNA (1930) Flow and Temperature Profiles Below Fort Peck
Temperature (deg C)
Discharge (cfs)
20.00
18.00
16.00
14.00
12.00
10.00
8.00
12000
10000
8000
6000
4000
2000
0
22 May
01 Jun
11 Jun
21 Jun
01 Jul
11 Jul
21 Jul
31 Jul
10 Aug
Full/Low
Full/Ave
Full/High
Ph/Ave
Spill/Ave
Spill/High
Flow

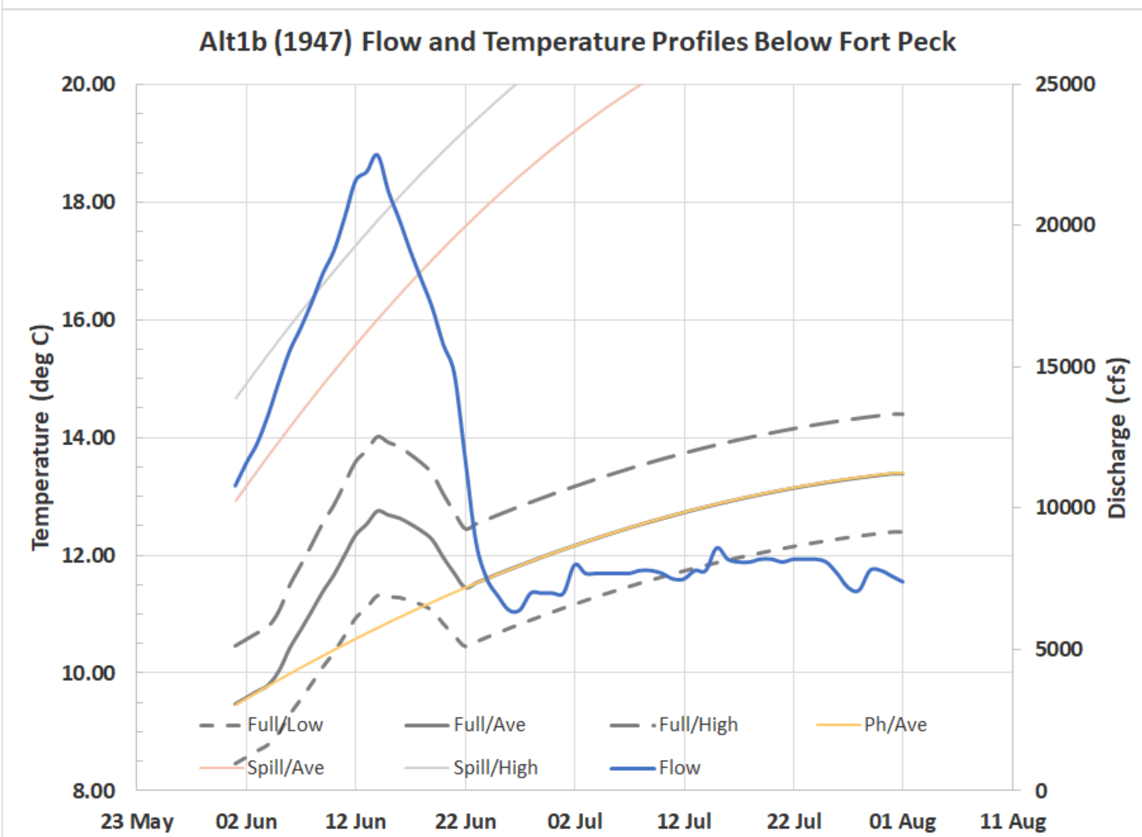

Alt1b (1947) Flow and Temperature Profiles Below Fort Peck
Temperature (deg C)
Discharge (cfs)
20.00
18.00
16.00
14.00
12.00
10.00
8.00
25000
20000
15000
10000
5000
0
23 May
02 Jun
12 Jun
22 Jun
02 Jul
12 Jul
22 Jul
01 Aug
11 Aug
Full/Low
Full/Ave
Full/High
Ph/Ave
Spill/Ave
Spill/High
Flow

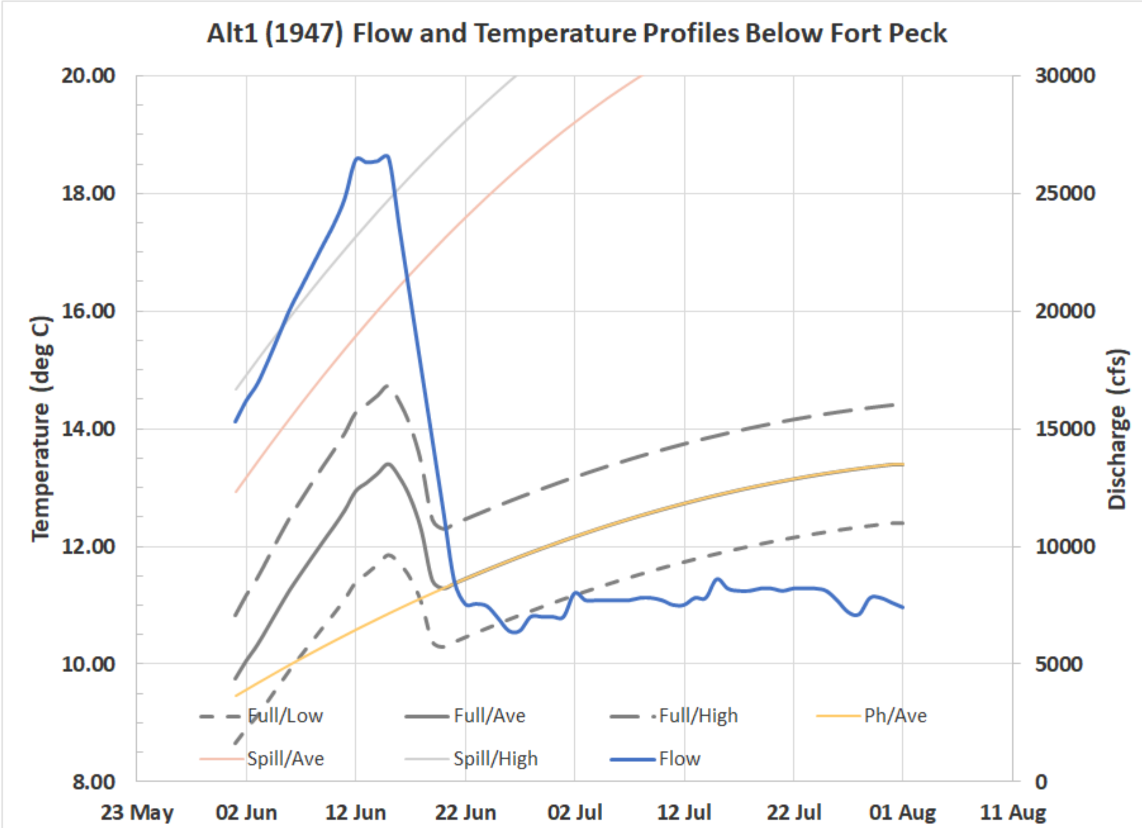

Alt1 (1947) Flow and Temperature Profiles Below Fort Peck
Temperature (deg C)
Discharge (cfs)
20.00
18.00
16.00
14.00
12.00
10.00
8.00
30000
25000
20000
15000
10000
5000
0
23 May
02 Jun
12 Jun
22 Jun
02 Jul
12 Jul
22 Jul
01 Aug
11 Aug
Full/Low
Full/Ave
Full/High
Ph/Ave
Spill/Ave
Spill/High
Flow

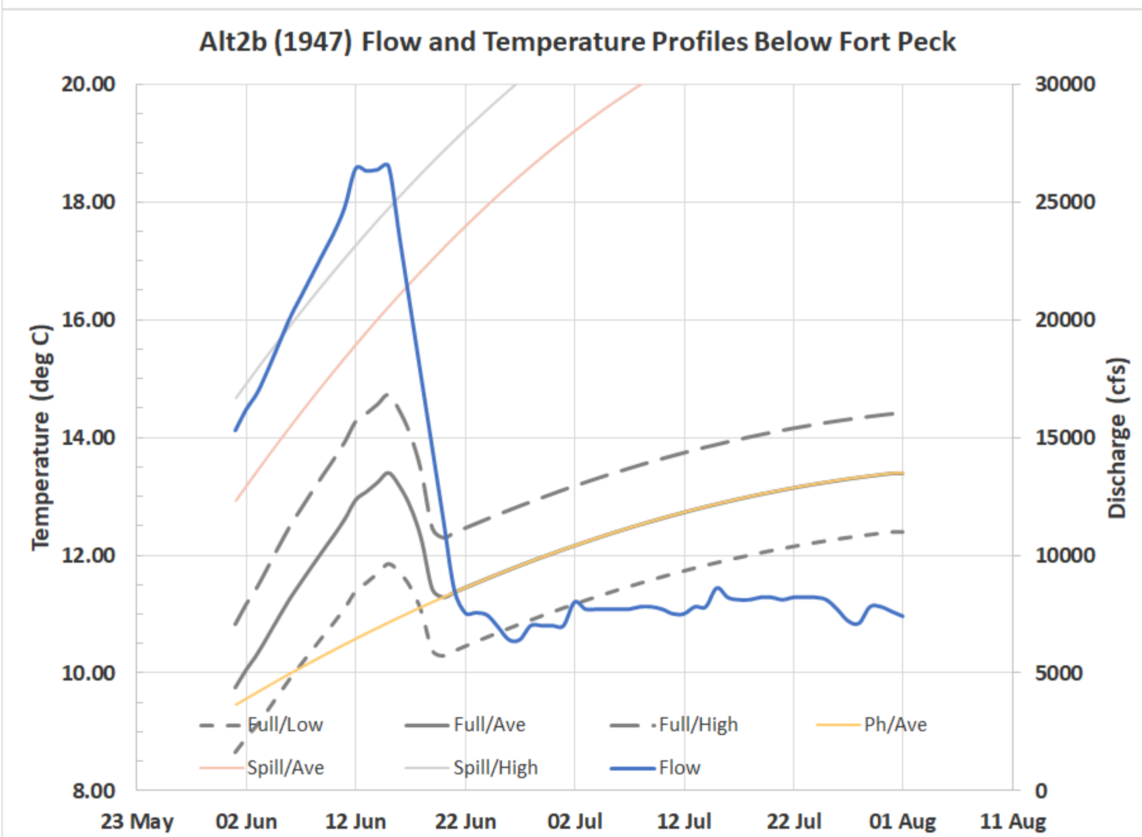

Alt2b (1947) Flow and Temperature Profiles Below Fort Peck
Temperature (deg C)
Discharge (cfs)
20.00
18.00
16.00
14.00
12.00
10.00
8.00
30000
25000
20000
15000
10000
5000
0
23 May
02 Jun
12 Jun
22 Jun
02 Jul
12 Jul
22 Jul
01 Aug
11 Aug
Full/Low
Full/Ave
Full/High
Ph/Ave
Spill/Ave
Spill/High
Flow

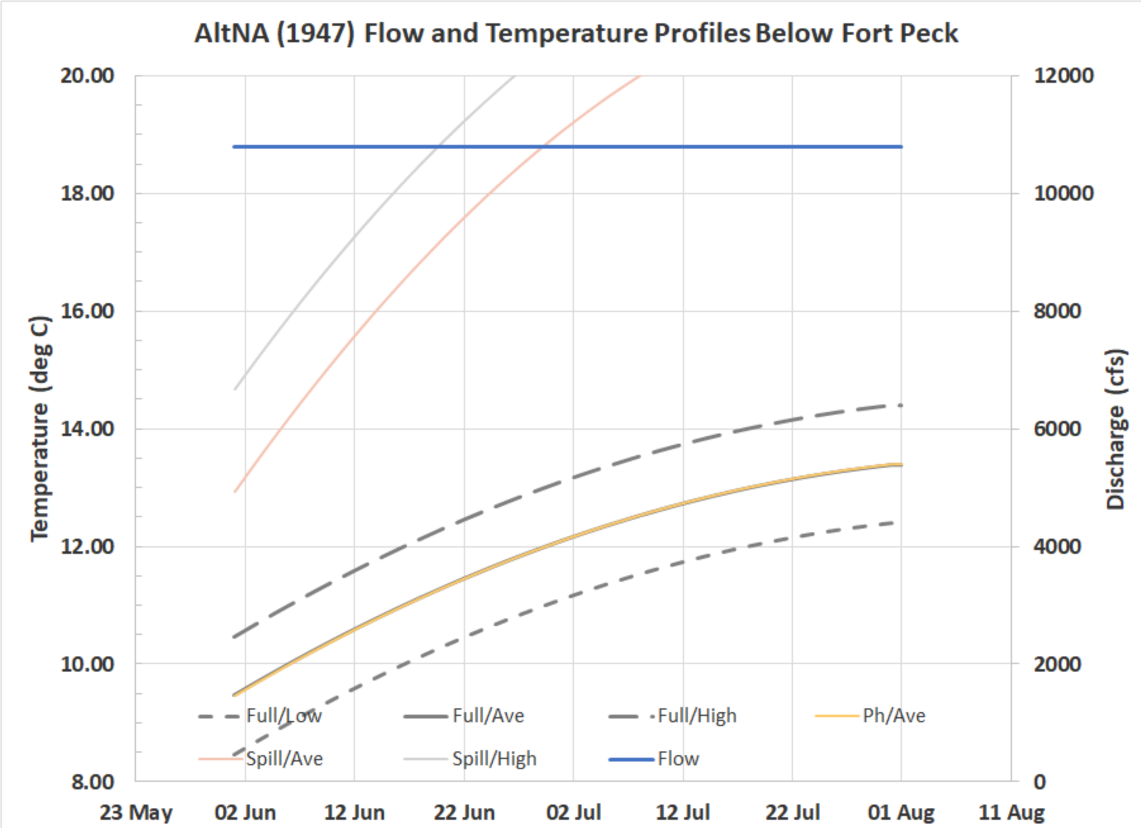
AltNA (1947) Flow and Temperature Profiles Below Fort Peck
Temperature (deg C)
Discharge (cfs)
20.00
18.00
16.00
14.00
12.00
10.00
8.00
12000
10000
8000
6000
4000
2000
0
23 May
02 Jun
12 Jun
22 Jun
02 Jul
12 Jul
22 Jul
01 Aug
11 Aug
Full/Low
Full/Ave
Full/High
Ph/Ave
Spill/Ave
Spill/High
Flow

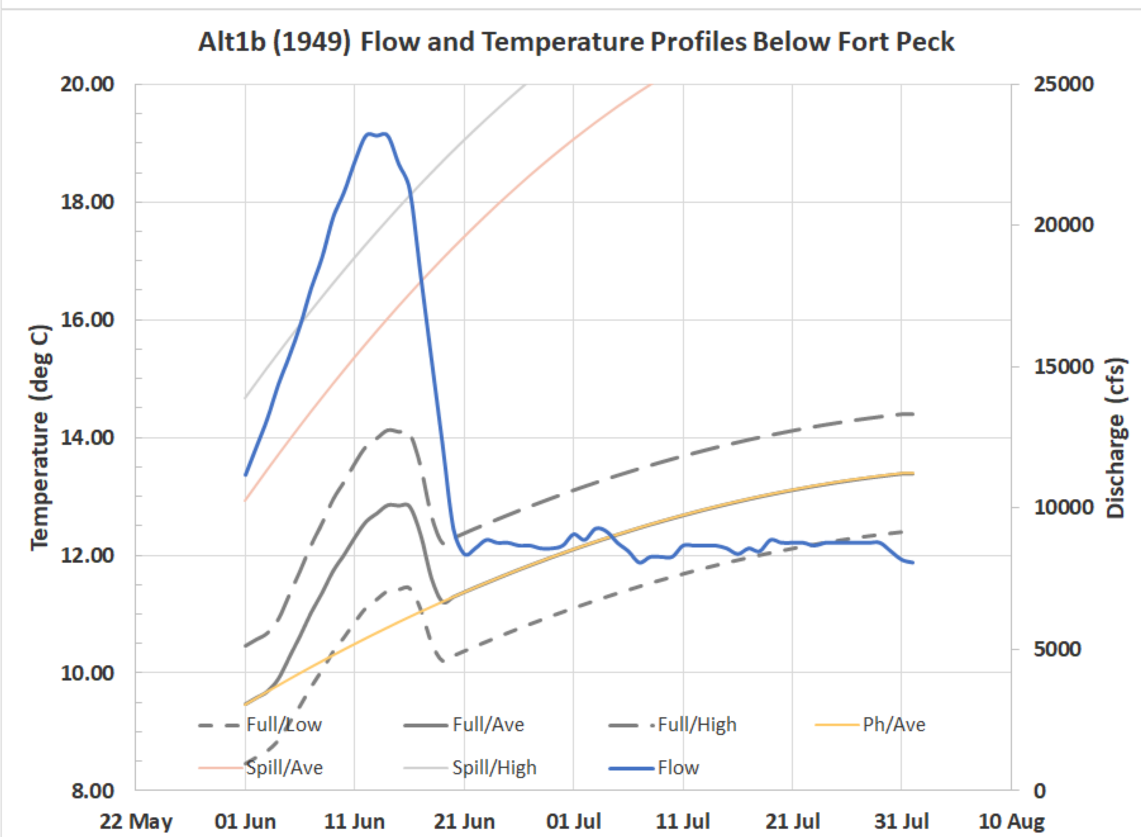
Alt1b (1949) Flow and Temperature Profiles Below Fort Peck
Temperature (deg C)
Discharge (cfs)
20.00
18.00
16.00
14.00
12.00
10.00
8.00
25000
20000
15000
10000
5000
0
22 May
01 Jun
11 Jun
21 Jun
01 Jul
11 Jul
21 Jul
31 Jul
10 Aug
Full/Low
Full/Ave
Full/High
Ph/Ave
Spill/Ave
Spill/High
Flow

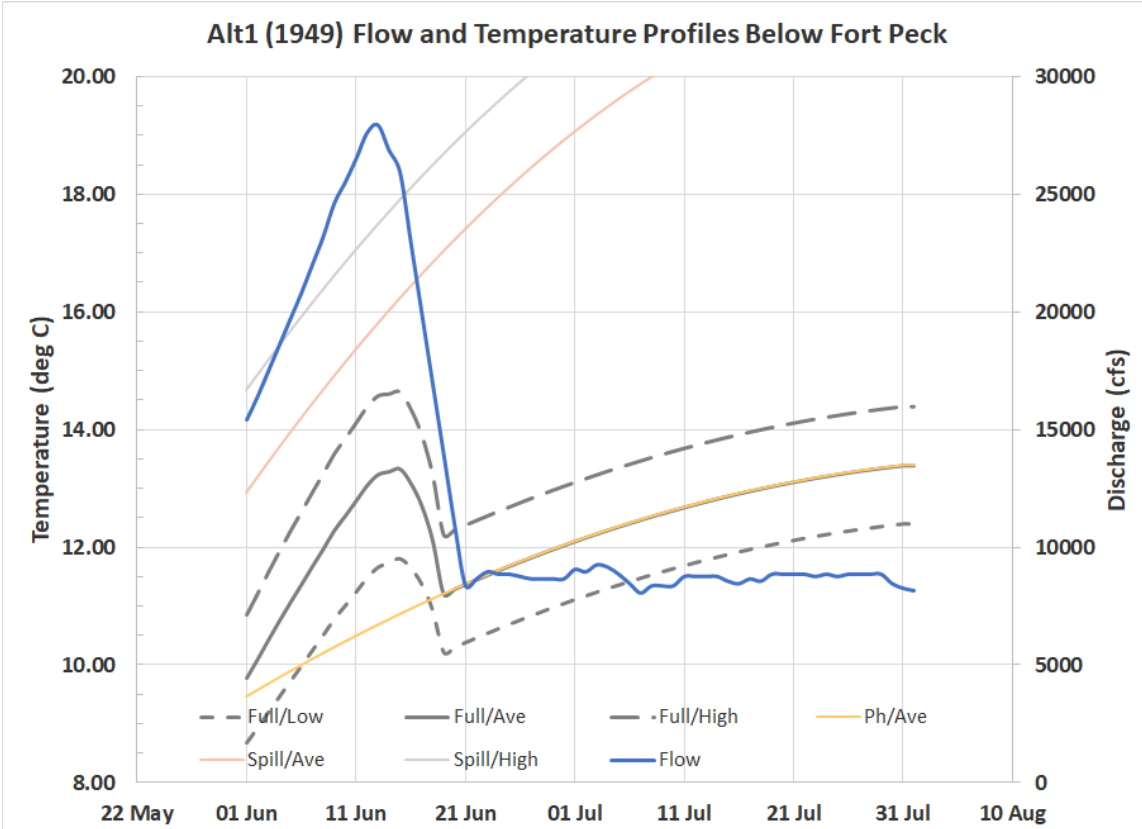
Alt1 (1949) Flow and Temperature Profiles Below Fort Peck
Temperature (deg C)
Discharge (cfs)
20.00
18.00
16.00
14.00
12.00
10.00
8.00
30000
25000
20000
15000
10000
5000
0
22 May
01 Jun
11 Jun
21 Jun
01 Jul
11 Jul
21 Jul
31 Jul
10 Aug
Full/Low
Full/Ave
Full/High
Ph/Ave
Spill/Ave
Spill/High
Flow

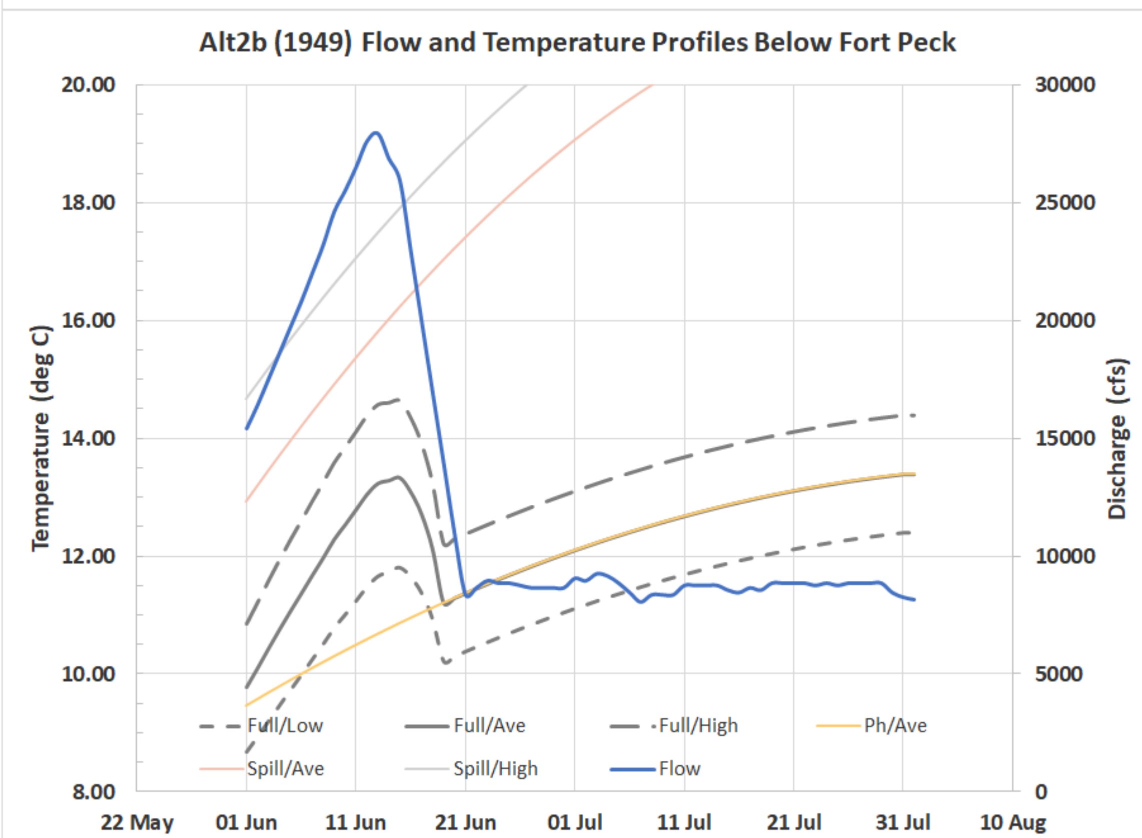
Alt2b (1949) Flow and Temperature Profiles Below Fort Peck
Temperature (deg C)
Discharge (cfs)
20.00
18.00
16.00
14.00
12.00
10.00
8.00
30000
25000
20000
15000
10000
5000
0
22 May
01 Jun
11 Jun
21 Jun
01 Jul
11 Jul
21 Jul
31 Jul
10 Aug
Full/Low
Full/Ave
Full/High
Ph/Ave
Spill/Ave
Spill/High
Flow

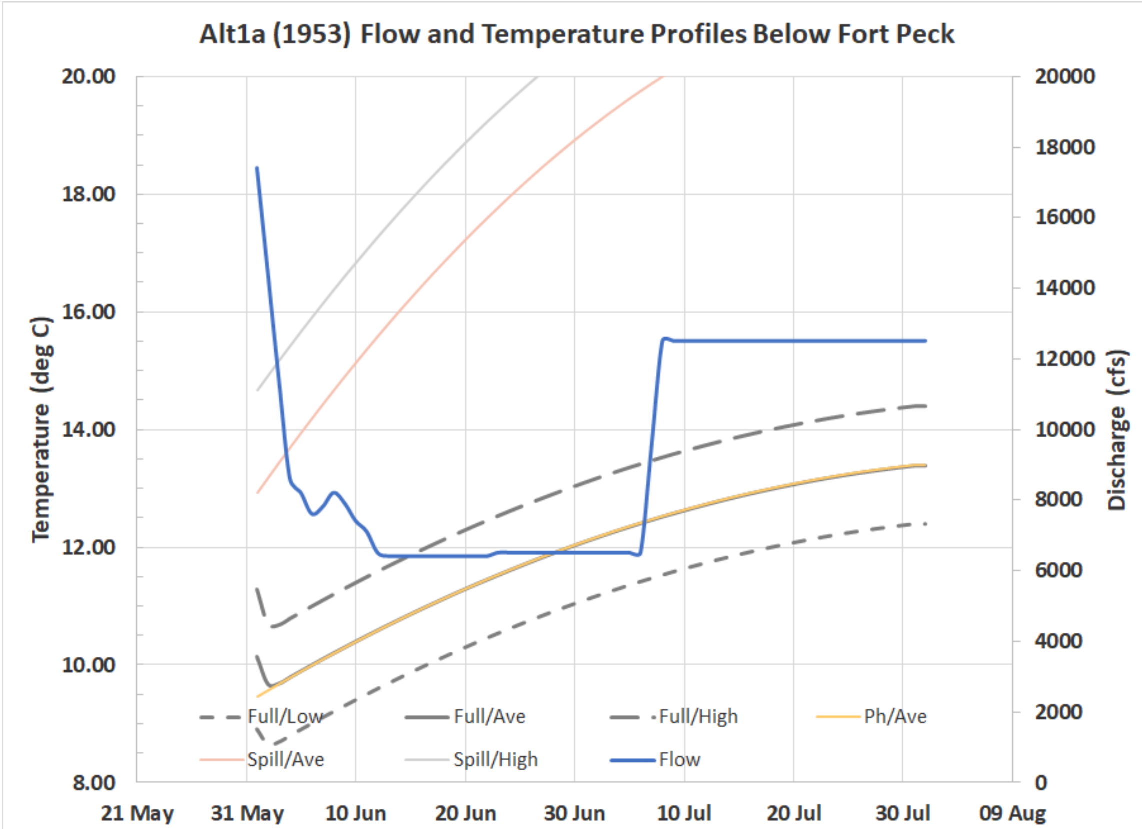
Alt1a (1953) Flow and Temperature Profiles Below Fort Peck
Temperature (deg C)
Discharge (cfs)
20.00
18.00
16.00
14.00
12.00
10.00
8.00
20000
18000
16000
14000
12000
10000
8000
6000
4000
2000
0
21 May
31 May
10 Jun
20 Jun
30 Jun
10 Jul
20 Jul
30 Jul
09 Aug
Full/Low
Full/Ave
Full/High
Ph/Ave
Spill/Ave
Spill/High
Flow

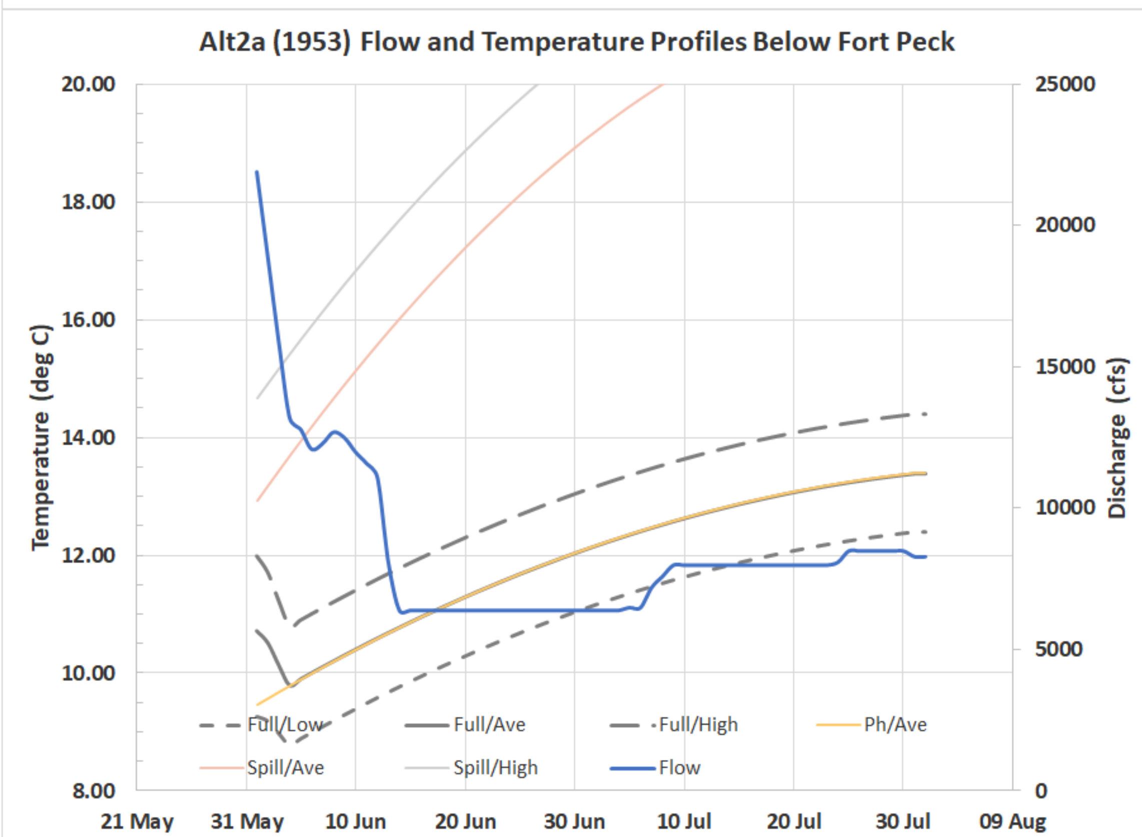
Alt2a (1953) Flow and Temperature Profiles Below Fort Peck
Temperature (deg C)
Discharge (cfs)
20.00
18.00
16.00
14.00
12.00
10.00
8.00
25000
20000
15000
10000
5000
0
21 May
31 May
10 Jun
20 Jun
30 Jun
10 Jul
20 Jul
30 Jul
09 Aug
Full/Low
Full/Ave
Full/High
Ph/Ave
Spill/Ave
Spill/High
Flow

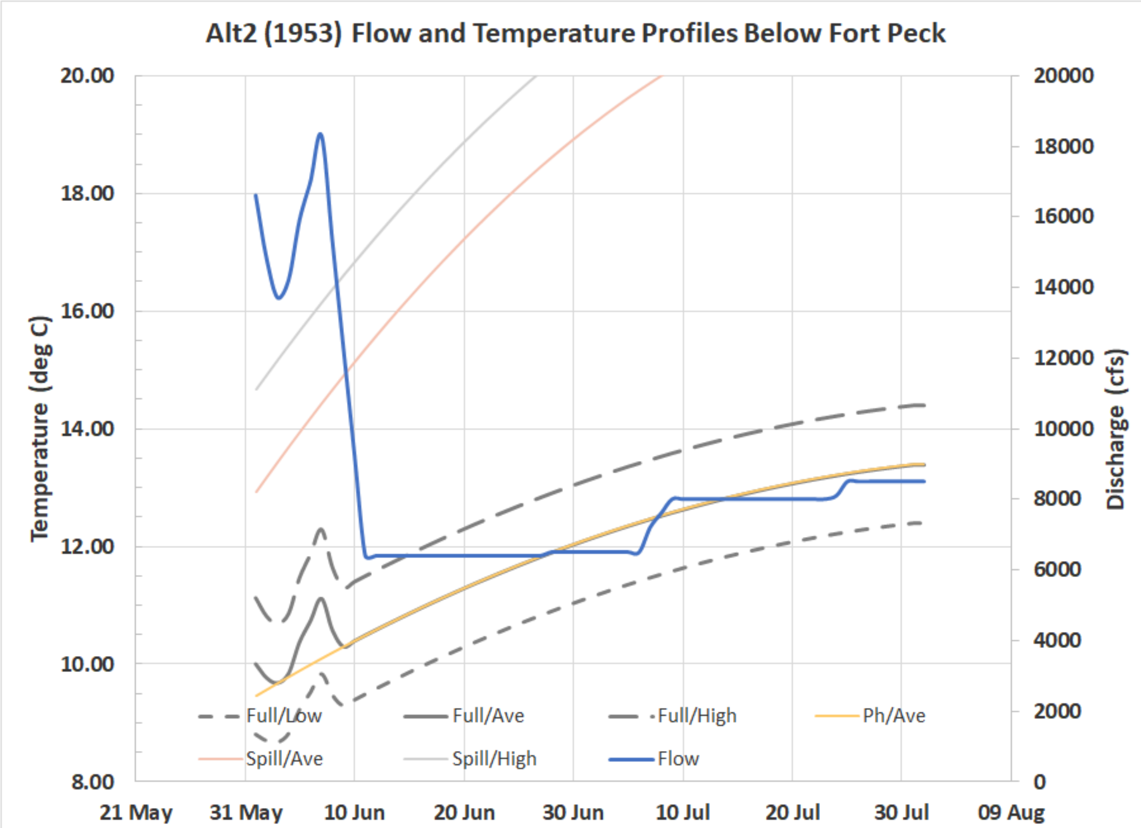
Alt2 (1953) Flow and Temperature Profiles Below Fort Peck
Temperature (deg C)
Discharge (cfs)
20.00
18.00
16.00
14.00
12.00
10.00
8.00
20000
18000
16000
14000
12000
10000
8000
6000
4000
2000
0
21 May
31 May
10 Jun
20 Jun
30 Jun
10 Jul
20 Jul
30 Jul
09 Aug
Full/Low
Full/Ave
Full/High
Ph/Ave
Spill/Ave
Spill/High
Flow

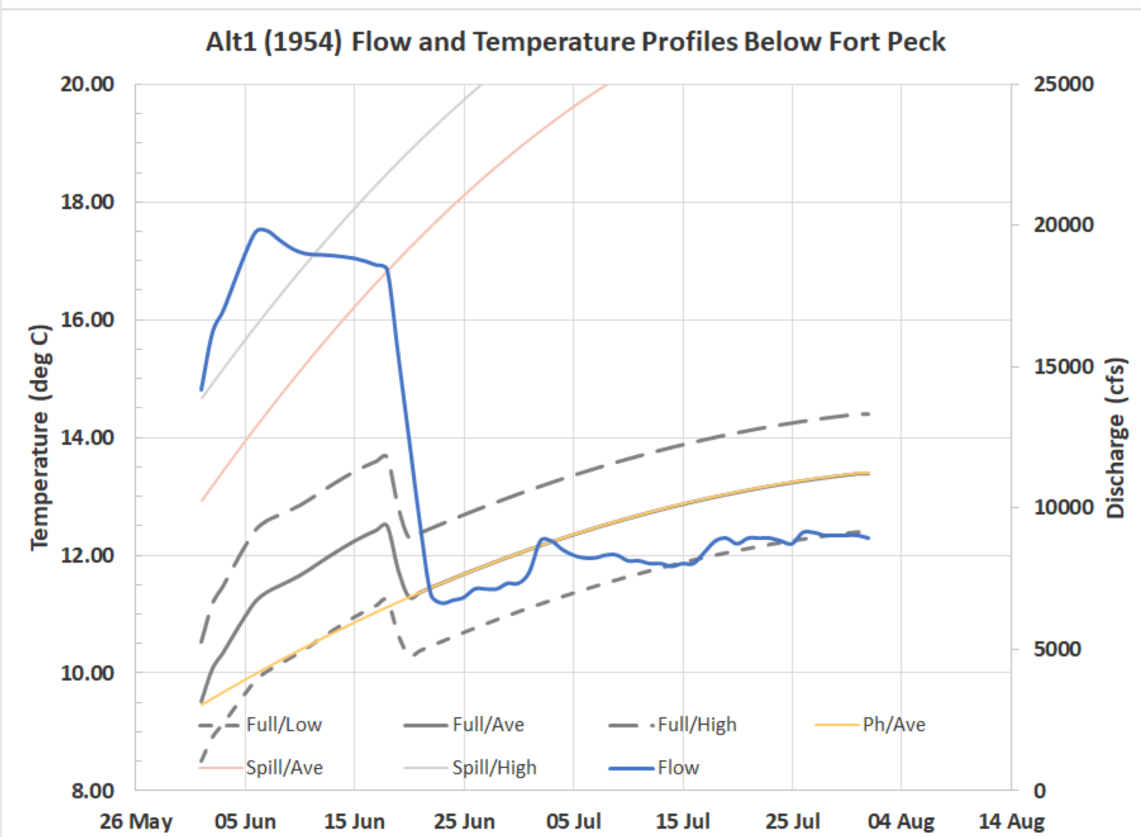
Alt1 (1954) Flow and Temperature Profiles Below Fort Peck
Temperature (deg C)
Discharge (cfs)
20.00
18.00
16.00
14.00
12.00
10.00
8.00
25000
20000
15000
10000
5000
0
26 May
05 Jun
15 Jun
25 Jun
05 Jul
15 Jul
25 Jul
04 Aug
14 Aug
Full/Low
Full/Ave
Full/High
Ph/Ave
Spill/Ave
Spill/High
Flow

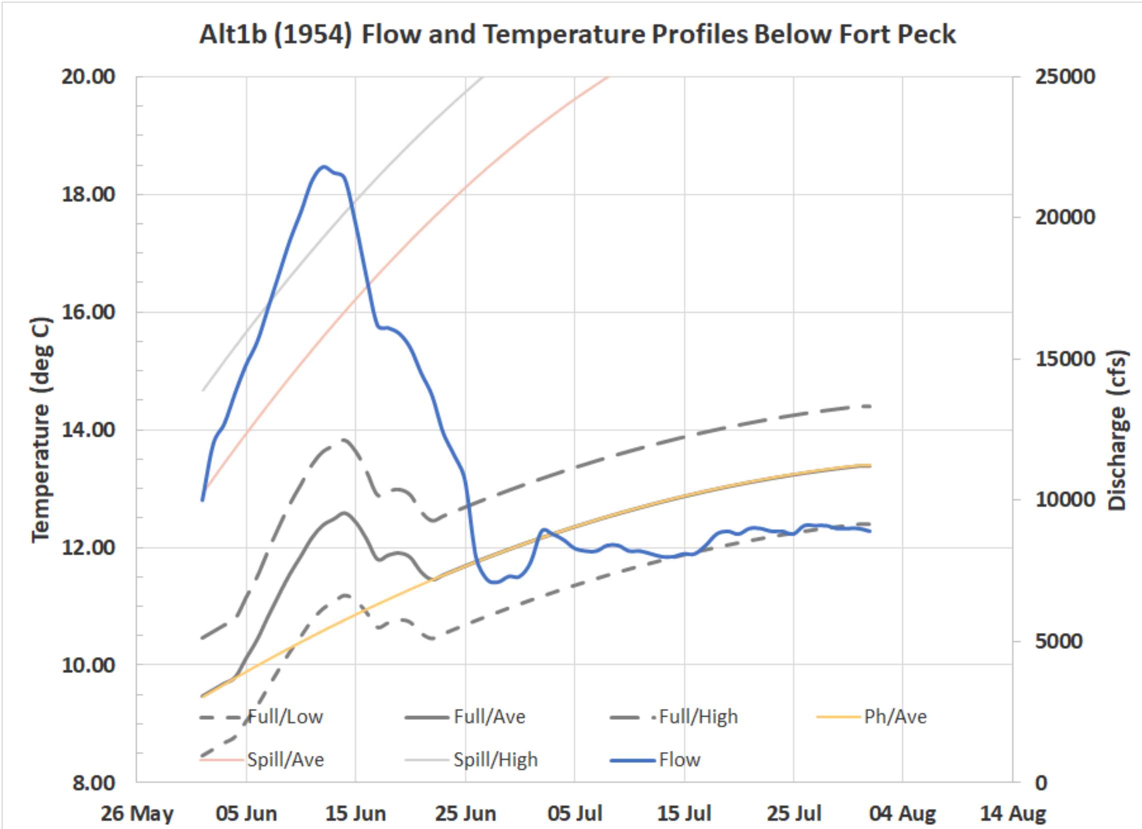
Alt1b (1954) Flow and Temperature Profiles Below Fort Peck
Temperature (deg C)
Discharge (cfs)
20.00
18.00
16.00
14.00
12.00
10.00
8.00
25000
20000
15000
10000
5000
0
26 May
05 Jun
15 Jun
25 Jun
05 Jul
15 Jul
25 Jul
04 Aug
14 Aug
Full/Low
Full/Ave
Full/High
Ph/Ave
Spill/Ave
Spill/High
Flow

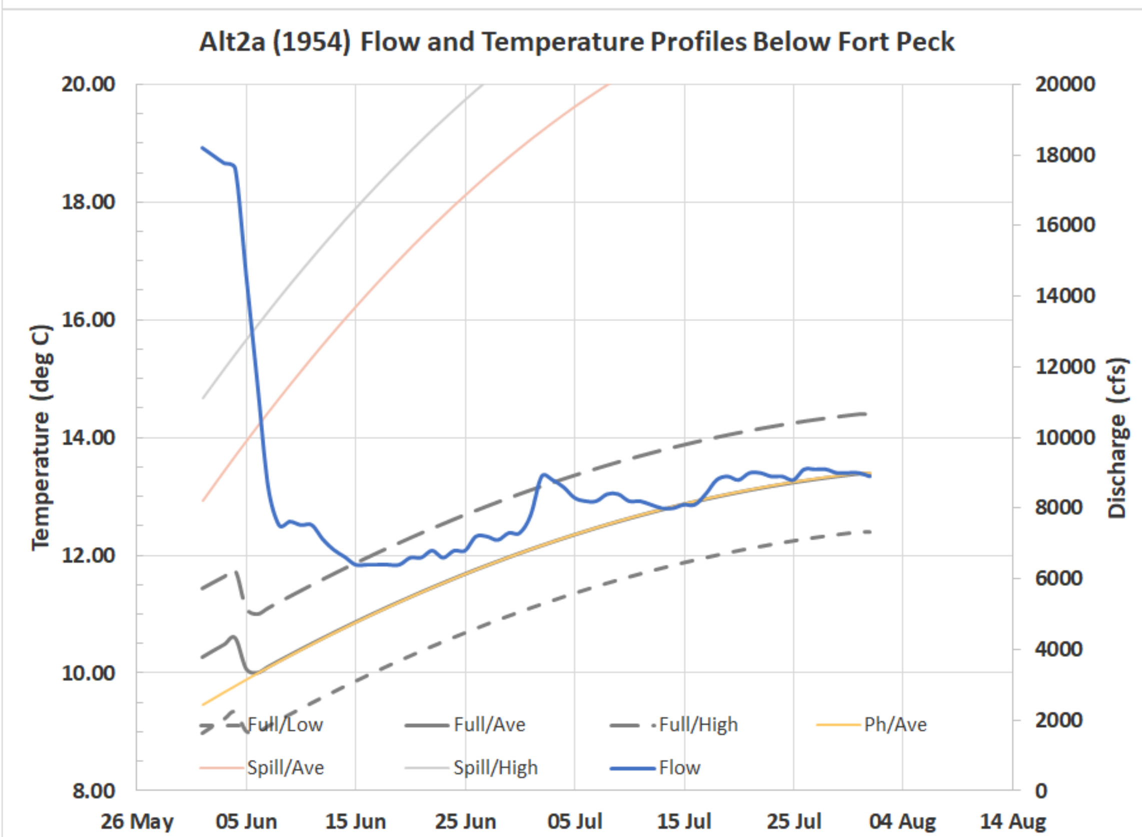
Alt2a (1954) Flow and Temperature Profiles Below Fort Peck
Temperature (deg C)
Discharge (cfs)
20.00
18.00
16.00
14.00
12.00
10.00
8.00
20000
18000
16000
14000
12000
10000
8000
6000
4000
2000
0
26 May
05 Jun
15 Jun
25 Jun
05 Jul
15 Jul
25 Jul
04 Aug
14 Aug
Full/Low
Full/Ave
Full/High
Ph/Ave
Spill/Ave
Spill/High
Flow

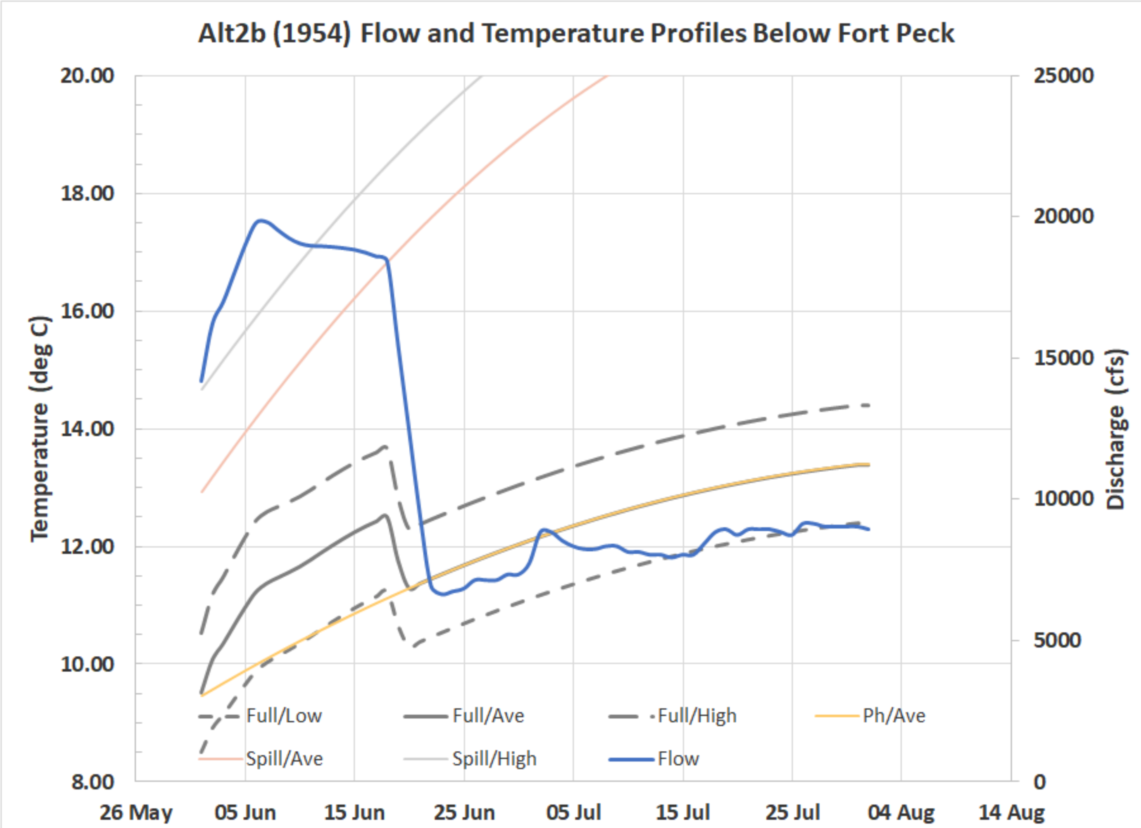
Alt2b (1954) Flow and Temperature Profiles Below Fort Peck
Temperature (deg C)
Discharge (cfs)
20.00
18.00
16.00
14.00
12.00
10.00
8.00
25000
20000
15000
10000
5000
0
26 May
05 Jun
15 Jun
25 Jun
05 Jul
15 Jul
25 Jul
04 Aug
14 Aug
Full/Low
Full/Ave
Full/High
Ph/Ave
Spill/Ave
Spill/High
Flow

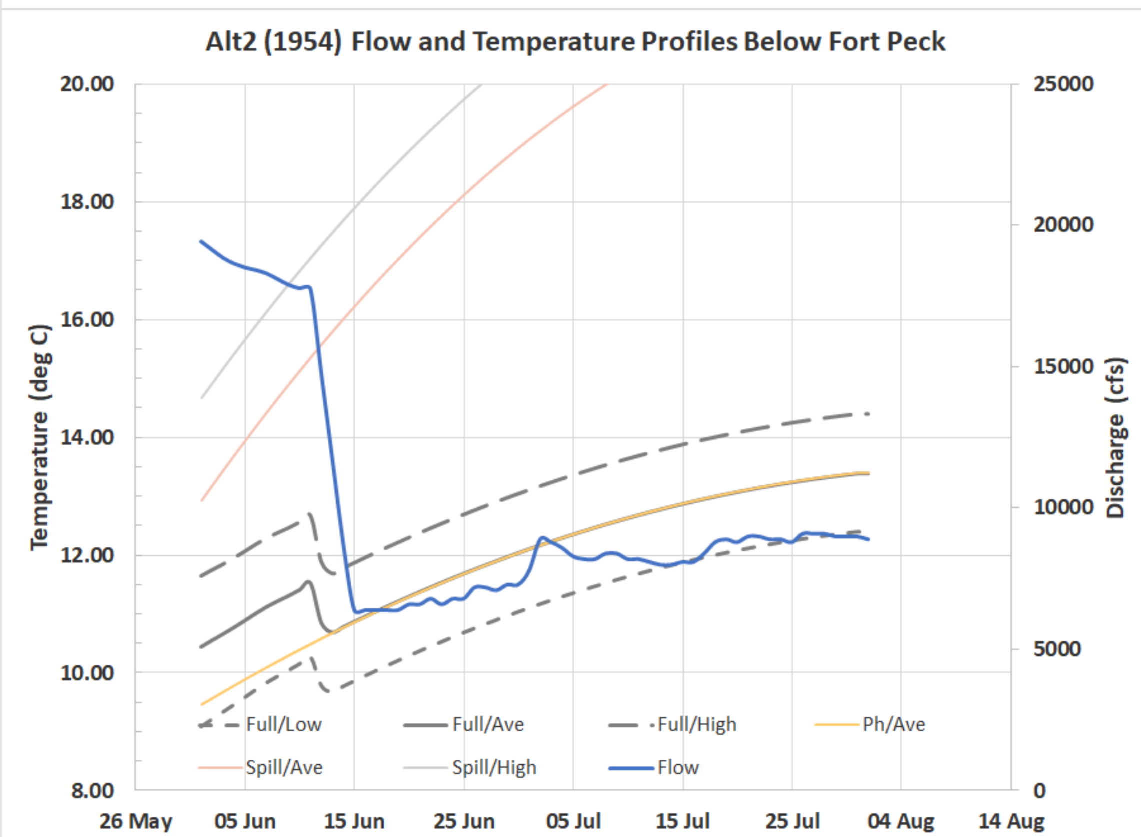
Alt2 (1954) Flow and Temperature Profiles Below Fort Peck
Temperature (deg C)
Discharge (cfs)
20.00
18.00
16.00
14.00
12.00
10.00
8.00
25000
20000
15000
10000
5000
0
26 May
05 Jun
15 Jun
25 Jun
05 Jul
15 Jul
25 Jul
04 Aug
14 Aug
Full/Low
Full/Ave
Full/High
Ph/Ave
Spill/Ave
Spill/High
Flow

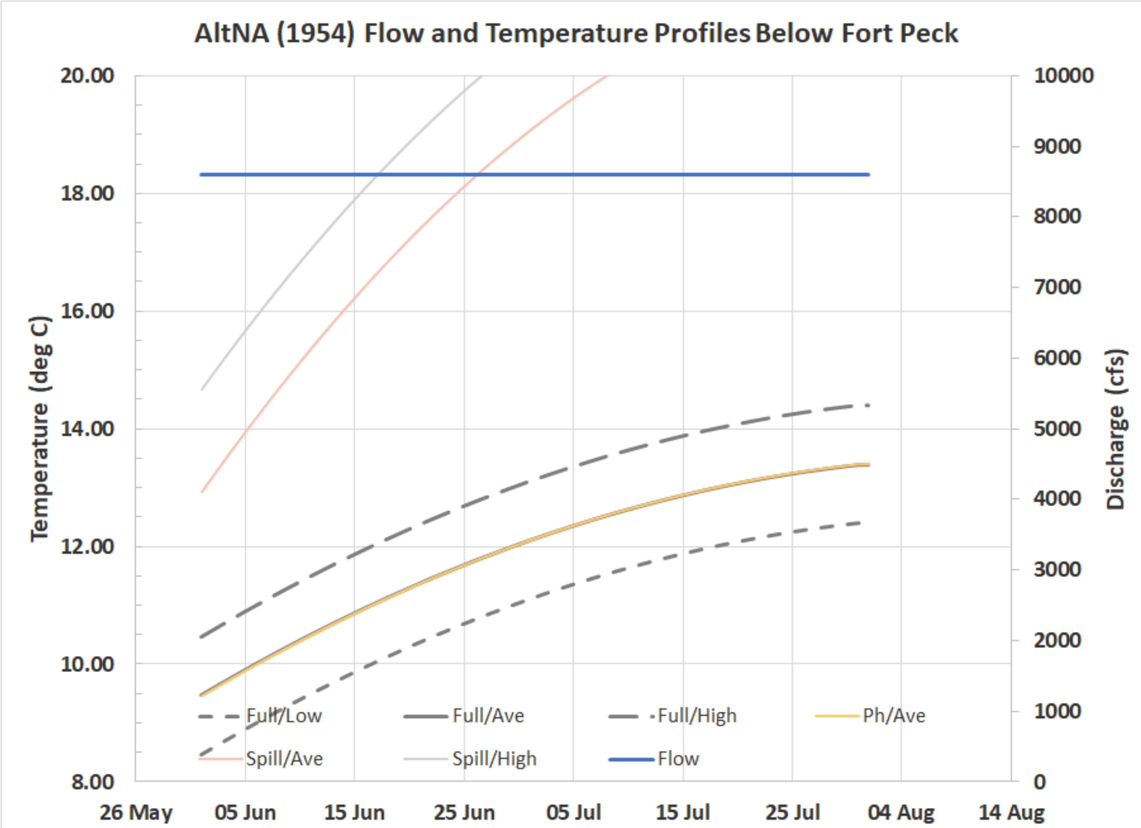
AltNA (1954) Flow and Temperature Profiles Below Fort Peck
Temperature (deg C)
Discharge (cfs)
20.00
18.00
16.00
14.00
12.00
10.00
8.00
10000
9000
8000
7000
6000
5000
4000
3000
2000
1000
0
26 May
05 Jun
15 Jun
25 Jun
05 Jul
15 Jul
25 Jul
04 Aug
14 Aug
Full/Low
Full/Ave
Full/High
Ph/Ave
Spill/Ave
Spill/High
Flow

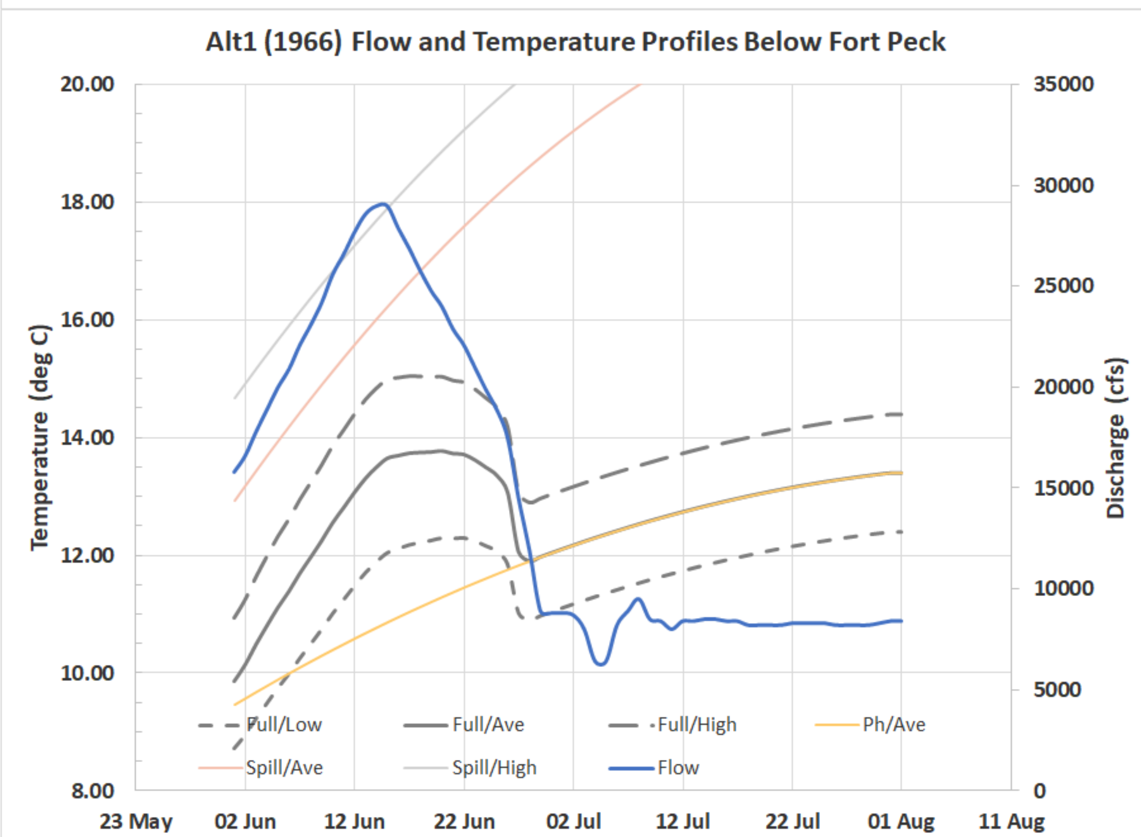
Alt1 (1966) Flow and Temperature Profiles Below Fort Peck
Temperature (deg C)
Discharge (cfs)
20.00
18.00
16.00
14.00
12.00
10.00
8.00
35000
30000
25000
20000
15000
10000
5000
0
23 May
02 Jun
12 Jun
22 Jun
02 Jul
12 Jul
22 Jul
01 Aug
11 Aug
Full/Low
Full/Ave
Full/High
Ph/Ave
Spill/Ave
Spill/High
Flow

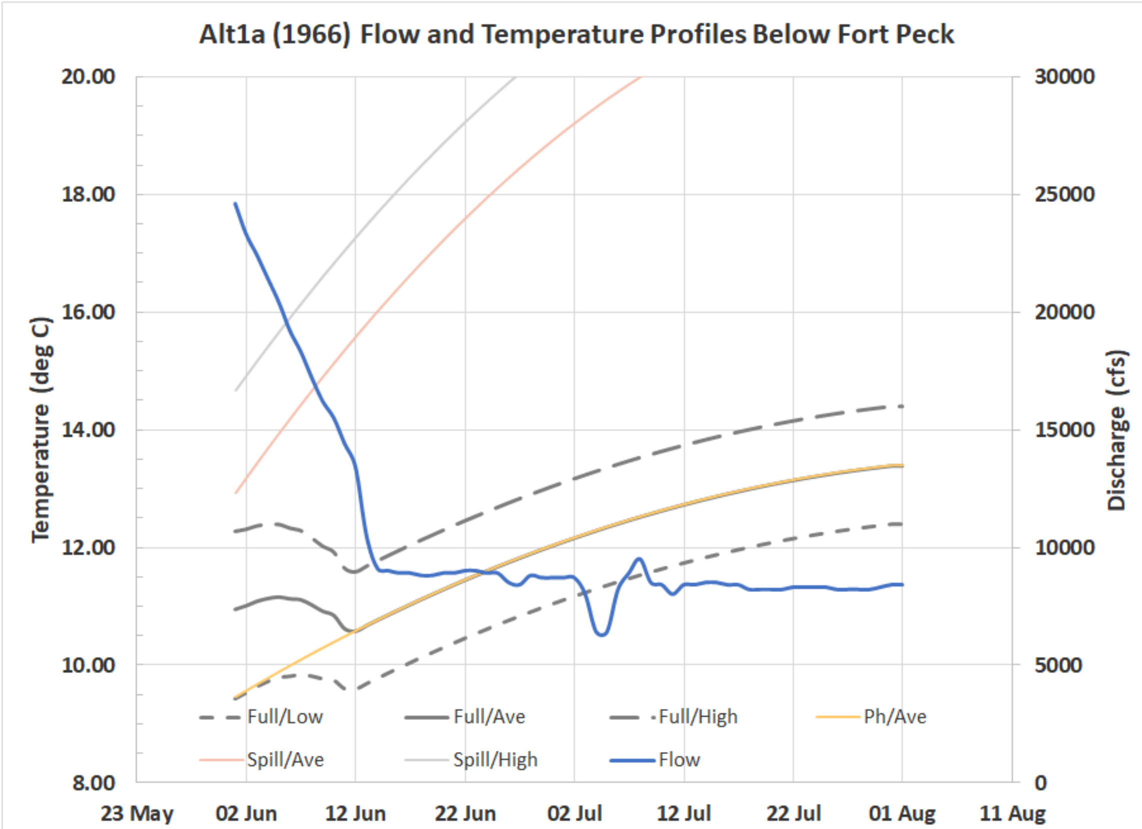
Alt1a (1966) Flow and Temperature Profiles Below Fort Peck
Temperature (deg C)
Discharge (cfs)
20.00
18.00
16.00
14.00
12.00
10.00
8.00
30000
25000
20000
15000
10000
5000
0
23 May
02 Jun
12 Jun
22 Jun
02 Jul
12 Jul
22 Jul
01 Aug
11 Aug
Full/Low
Full/Ave
Full/High
Ph/Ave
Spill/Ave
Spill/High
Flow

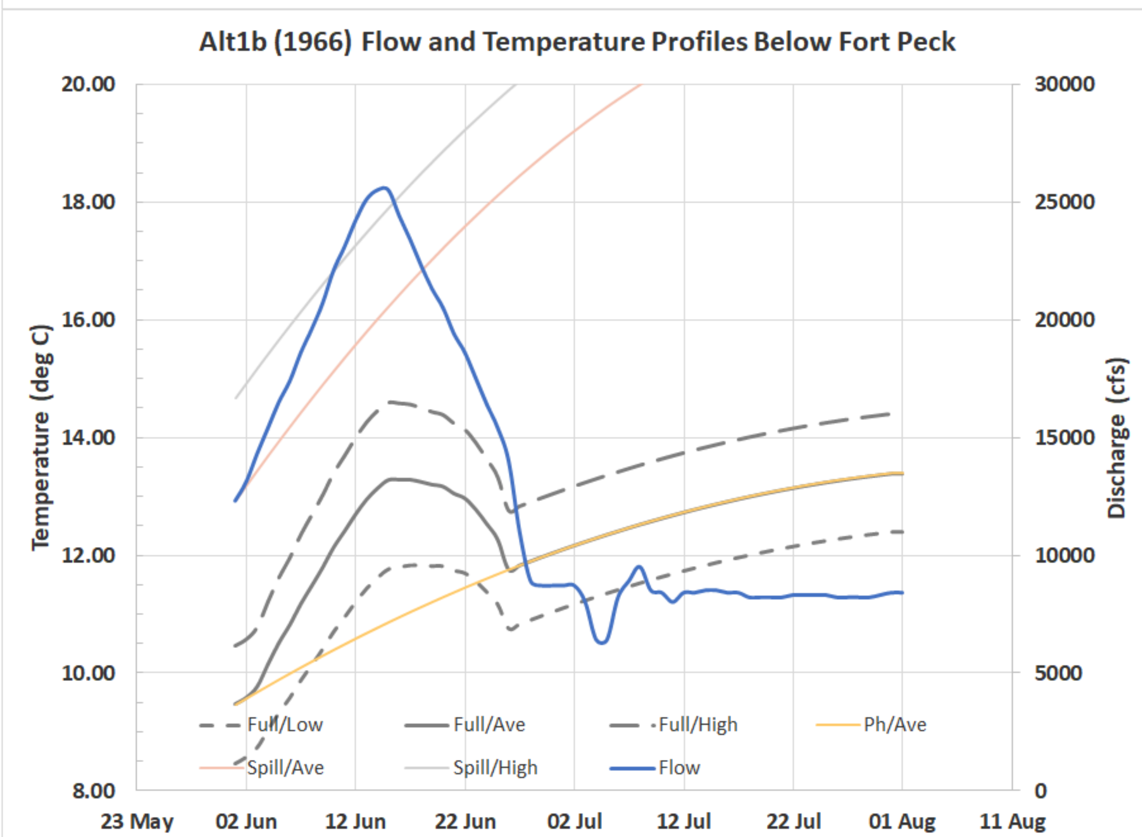
Alt1b (1966) Flow and Temperature Profiles Below Fort Peck
Temperature (deg C)
Discharge (cfs)
20.00
18.00
16.00
14.00
12.00
10.00
8.00
30000
25000
20000
15000
10000
5000
0
23 May
02 Jun
12 Jun
22 Jun
02 Jul
12 Jul
22 Jul
01 Aug
11 Aug
Full/Low
Full/Ave
Full/High
Ph/Ave
Spill/Ave
Spill/High
Flow

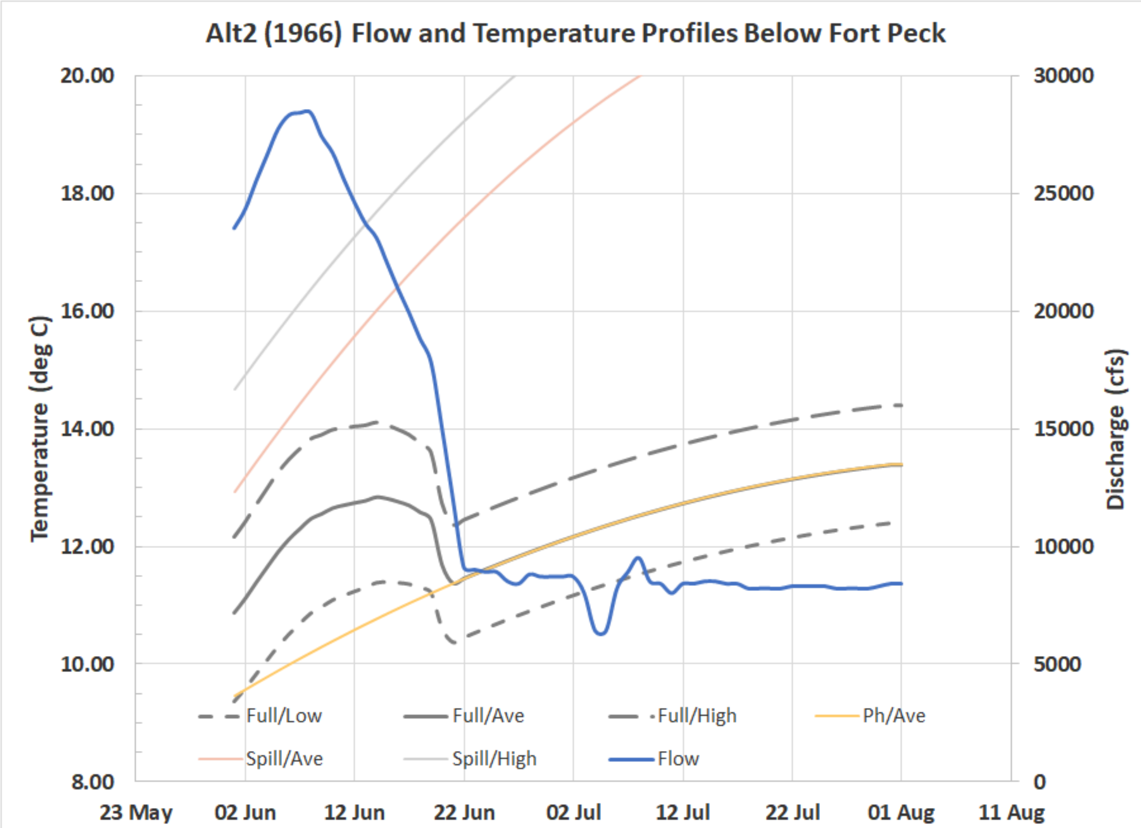
Alt2 (1966) Flow and Temperature Profiles Below Fort Peck
Temperature (deg C)
Discharge (cfs)
20.00
18.00
16.00
14.00
12.00
10.00
8.00
30000
25000
20000
15000
10000
5000
0
23 May
02 Jun
12 Jun
22 Jun
02 Jul
12 Jul
22 Jul
01 Aug
11 Aug
Full/Low
Full/Ave
Full/High
Ph/Ave
Spill/Ave
Spill/High
Flow

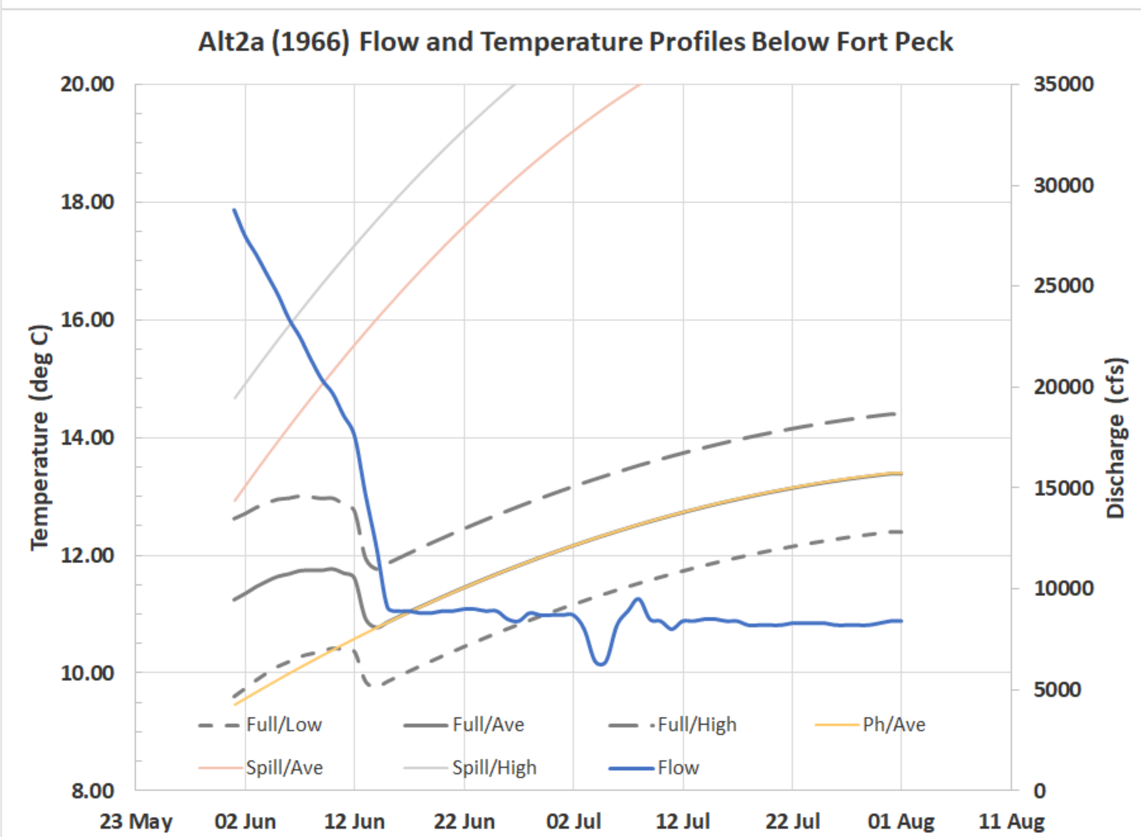
Alt2a (1966) Flow and Temperature Profiles Below Fort Peck
Temperature (deg C)
Discharge (cfs)
20.00
18.00
16.00
14.00
12.00
10.00
8.00
35000
30000
25000
20000
15000
10000
5000
0
23 May
02 Jun
12 Jun
22 Jun
02 Jul
12 Jul
22 Jul
01 Aug
11 Aug
Full/Low
Full/Ave
Full/High
Ph/Ave
Spill/Ave
Spill/High
Flow

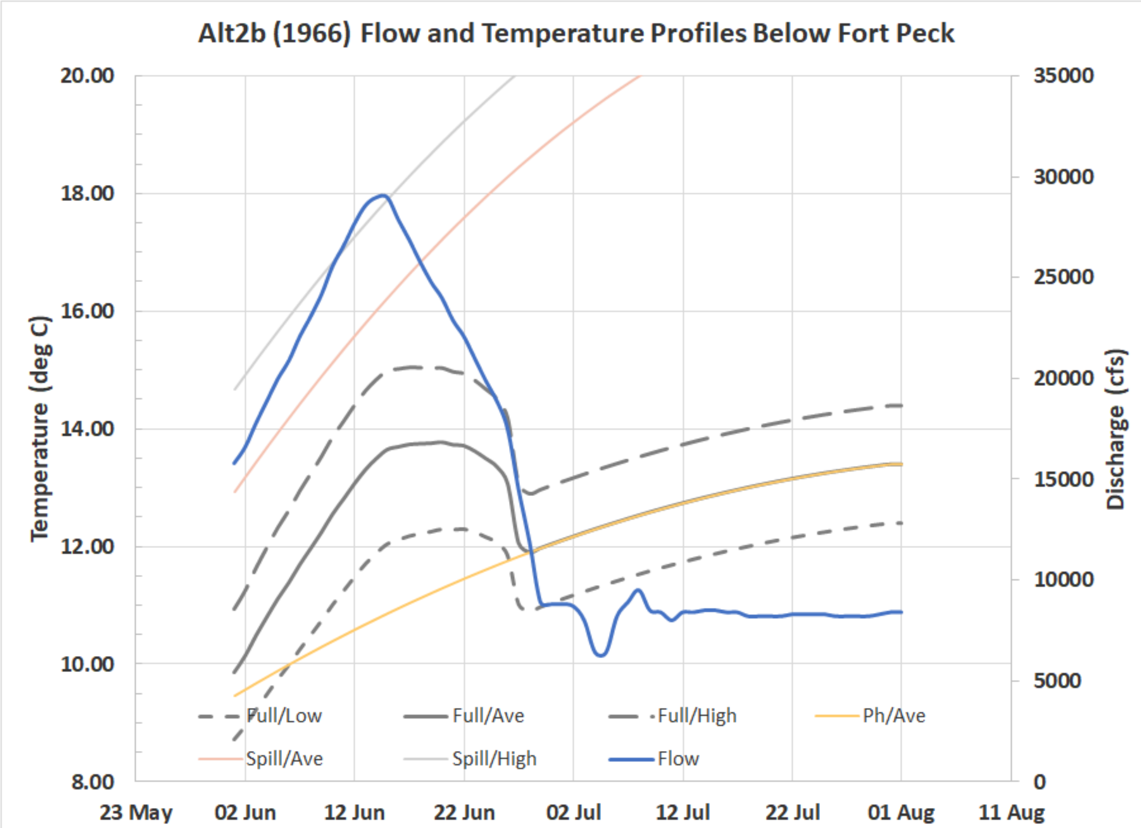
Alt2b (1966) Flow and Temperature Profiles Below Fort Peck
Temperature (deg C)
Discharge (cfs)
20.00
18.00
16.00
14.00
12.00
10.00
8.00
35000
30000
25000
20000
15000
10000
5000
0
23 May
02 Jun
12 Jun
22 Jun
02 Jul
12 Jul
22 Jul
01 Aug
11 Aug
Full/Low
Full/Ave
Full/High
Ph/Ave
Spill/Ave
Spill/High
Flow

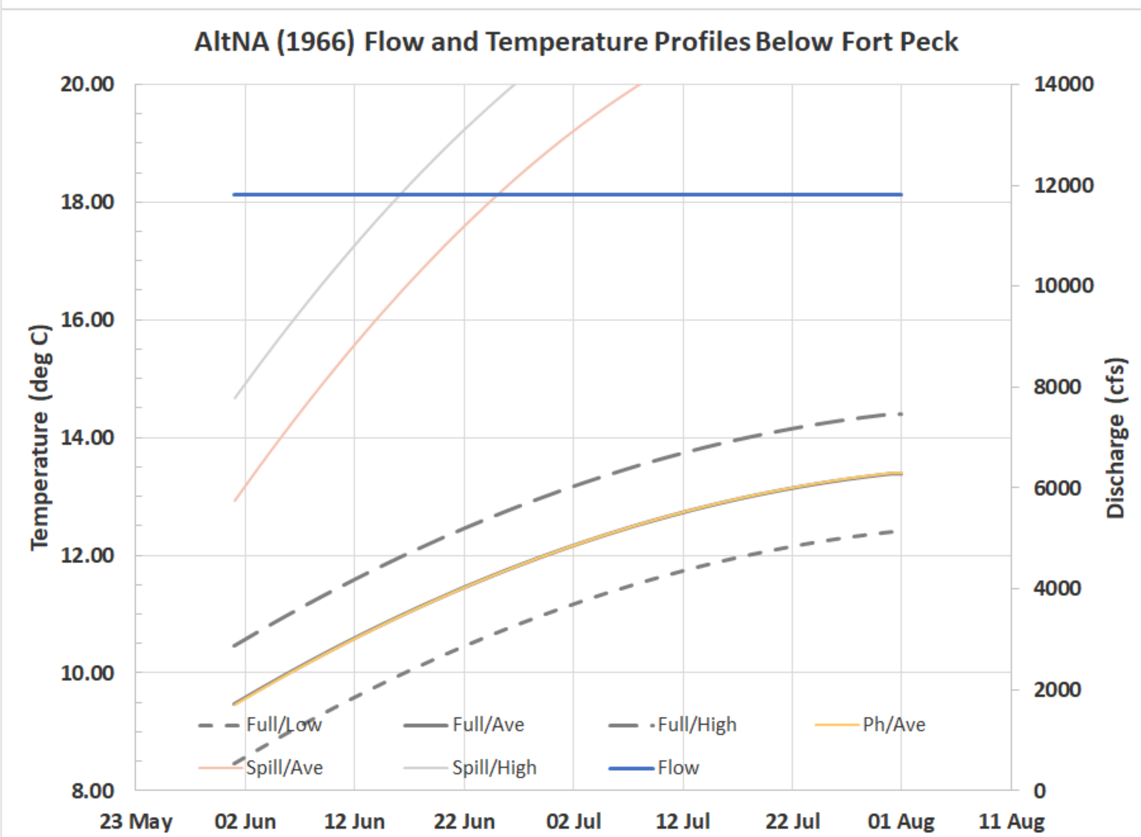
AltNA (1966) Flow and Temperature Profiles Below Fort Peck
Temperature (deg C)
Discharge (cfs)
20.00
18.00
16.00
14.00
12.00
10.00
8.00
14000
12000
10000
8000
6000
4000
2000
0
23 May
02 Jun
12 Jun
22 Jun
02 Jul
12 Jul
22 Jul
01 Aug
11 Aug
Full/Low
Full/Ave
Full/High
Ph/Ave
Spill/Ave
Spill/High
Flow

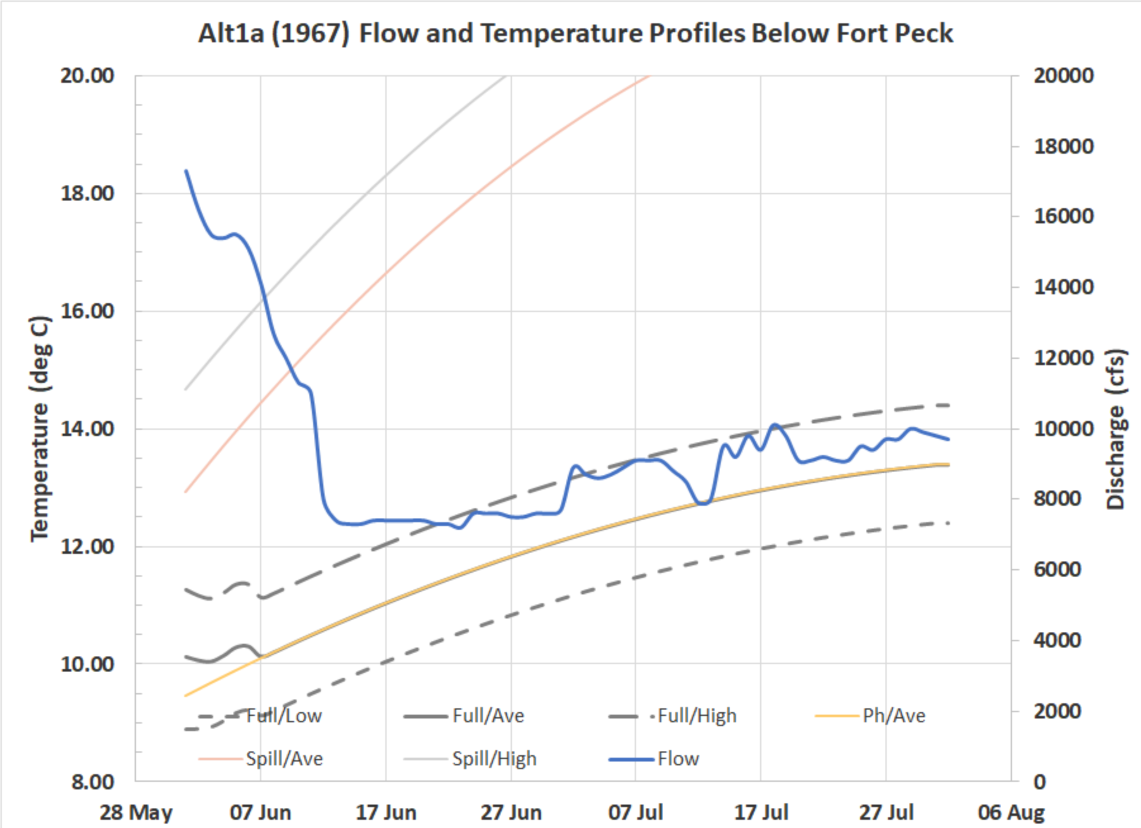
Alt1a (1967) Flow and Temperature Profiles Below Fort Peck
Temperature (deg C)
Discharge (cfs)
20.00
18.00
16.00
14.00
12.00
10.00
8.00
20000
18000
16000
14000
12000
10000
8000
6000
4000
2000
0
28 May
07 Jun
17 Jun
27 Jun
07 Jul
17 Jul
27 Jul
06 Aug
Full/Low
Full/Ave
Full/High
Ph/Ave
Spill/Ave
Spill/High
Flow

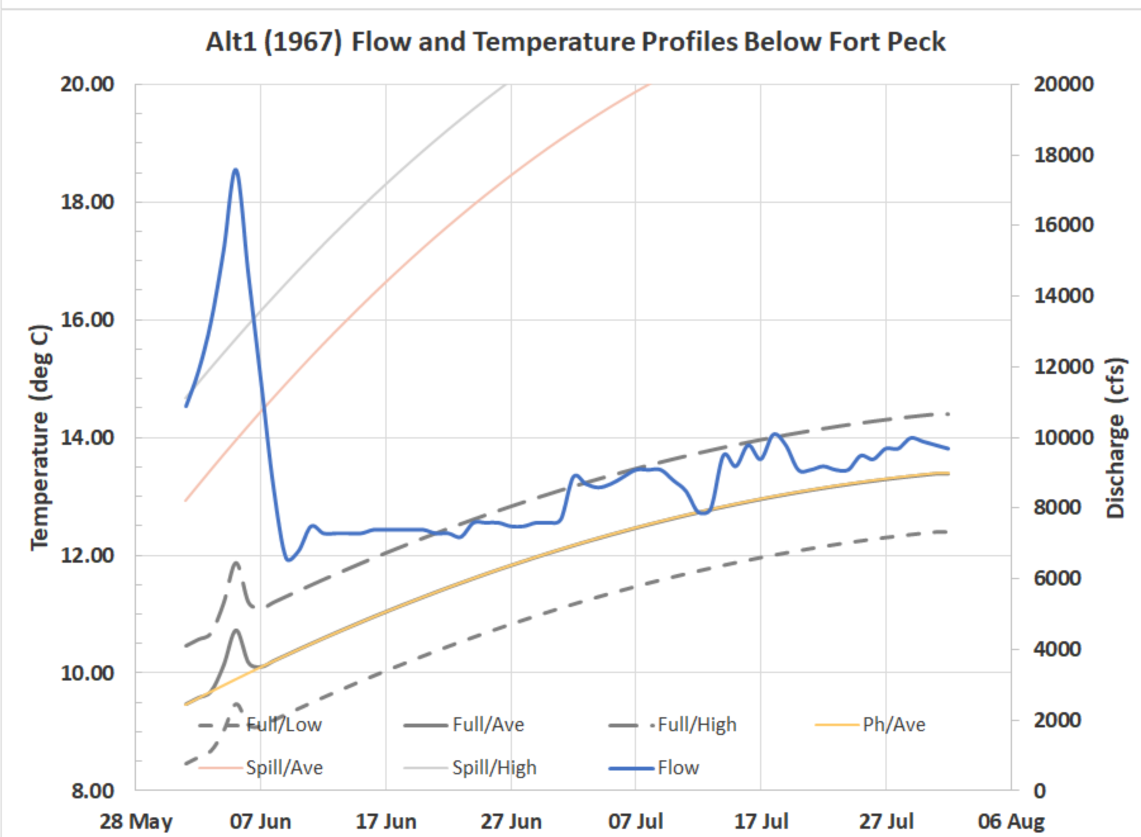
Alt1 (1967) Flow and Temperature Profiles Below Fort Peck
Temperature (deg C)
Discharge (cfs)
20.00
18.00
16.00
14.00
12.00
10.00
8.00
20000
18000
16000
14000
12000
10000
8000
6000
4000
2000
0
28 May
07 Jun
17 Jun
27 Jun
07 Jul
17 Jul
27 Jul
06 Aug
Full/Low
Full/Ave
Full/High
Ph/Ave
Spill/Ave
Spill/High
Flow

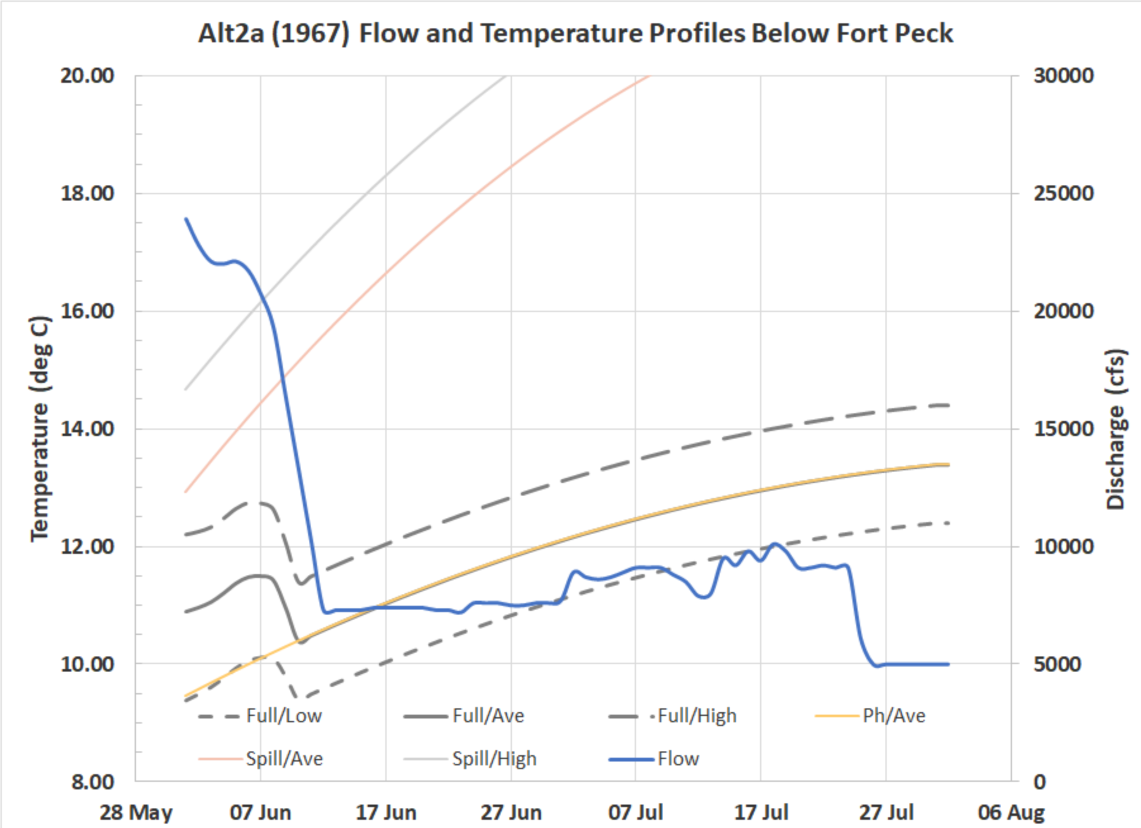
Alt2a (1967) Flow and Temperature Profiles Below Fort Peck
Temperature (deg C)
Discharge (cfs)
20.00
18.00
16.00
14.00
12.00
10.00
8.00
30000
25000
20000
15000
10000
5000
0
28 May
07 Jun
17 Jun
27 Jun
07 Jul
17 Jul
27 Jul
06 Aug
Full/Low
Full/Ave
Full/High
Ph/Ave
Spill/Ave
Spill/High
Flow

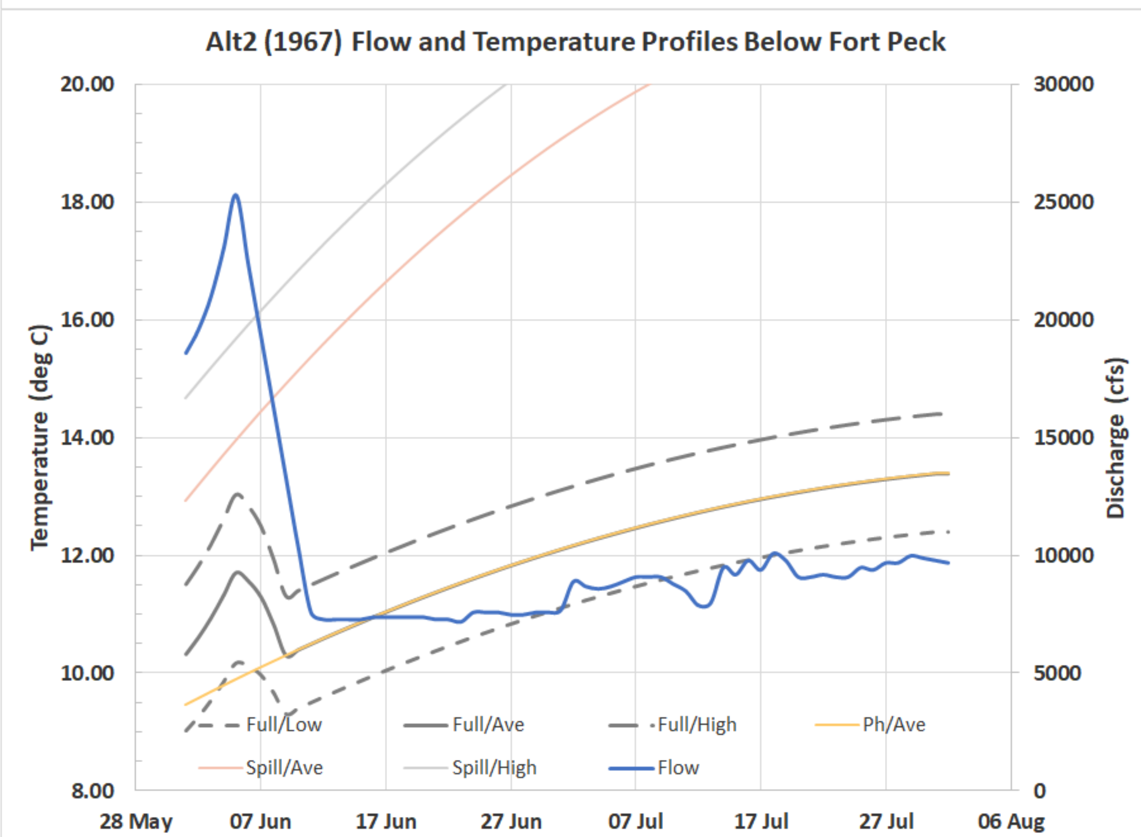
Alt2 (1967) Flow and Temperature Profiles Below Fort Peck
Temperature (deg C)
Discharge (cfs)
20.00
18.00
16.00
14.00
12.00
10.00
8.00
30000
25000
20000
15000
10000
5000
0
28 May
07 Jun
17 Jun
27 Jun
07 Jul
17 Jul
27 Jul
06 Aug
Full/Low
Full/Ave
Full/High
Ph/Ave
Spill/Ave
Spill/High
Flow

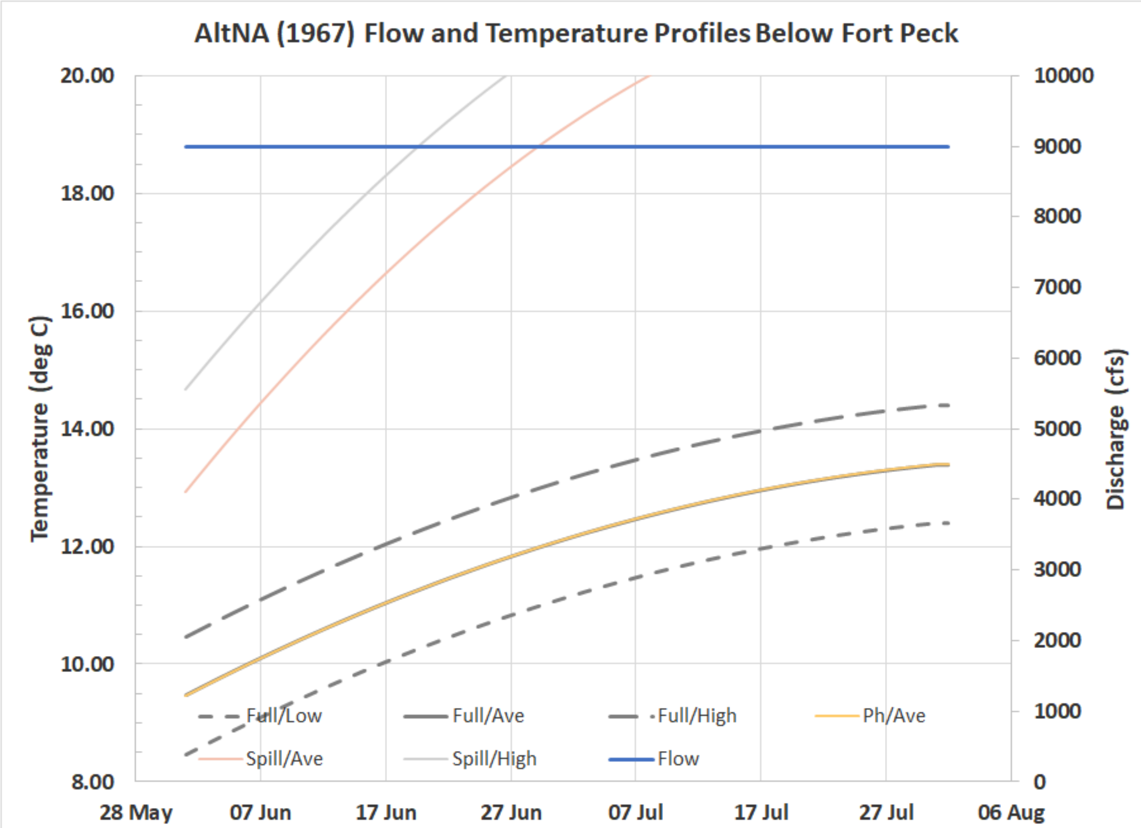
AltNA (1967) Flow and Temperature Profiles Below Fort Peck
Temperature (deg C)
Discharge (cfs)
20.00
18.00
16.00
14.00
12.00
10.00
8.00
10000
9000
8000
7000
6000
5000
4000
3000
2000
1000
0
28 May
07 Jun
17 Jun
27 Jun
07 Jul
17 Jul
27 Jul
06 Aug
Full/Low
Full/Ave
Full/High
Ph/Ave
Spill/Ave
Spill/High
Flow

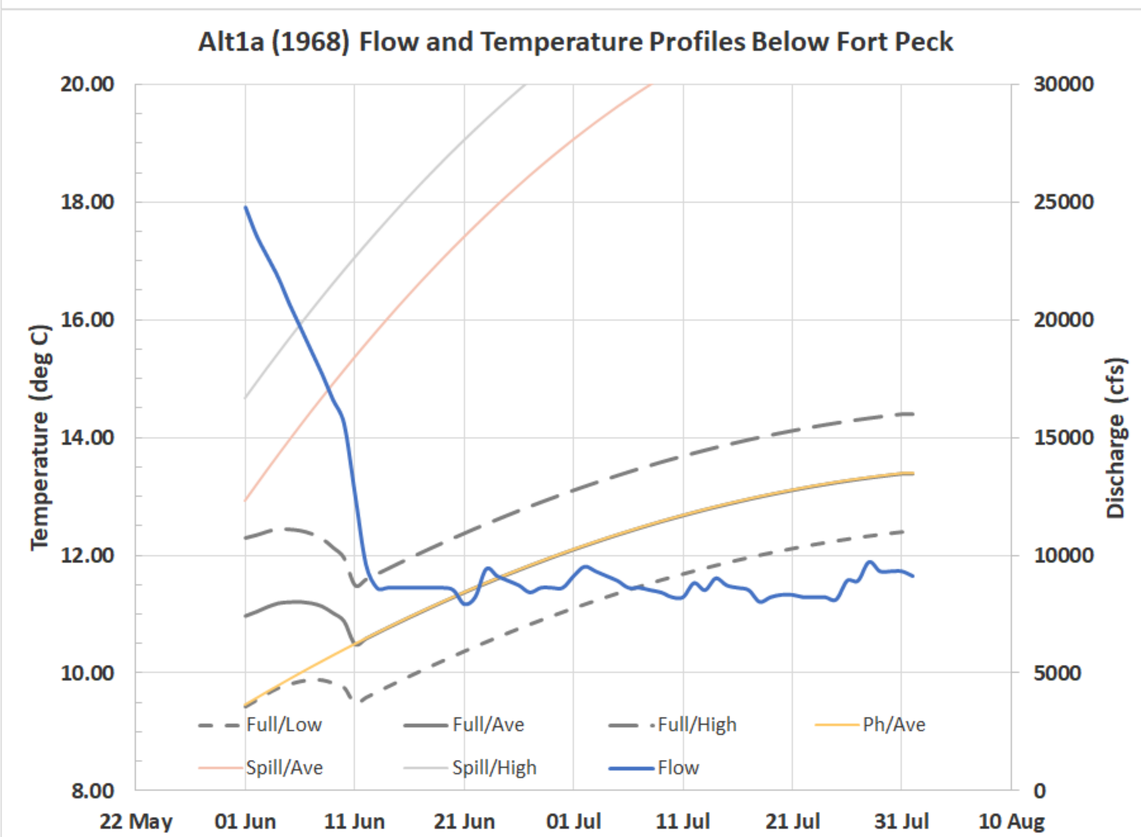
Alt1a (1968) Flow and Temperature Profiles Below Fort Peck
Temperature (deg C)
Discharge (cfs)
20.00
18.00
16.00
14.00
12.00
10.00
8.00
30000
25000
20000
15000
10000
5000
0
22 May
01 Jun
11 Jun
21 Jun
01 Jul
11 Jul
21 Jul
31 Jul
10 Aug
Full/Low
Full/Ave
Full/High
Ph/Ave
Spill/Ave
Spill/High
Flow

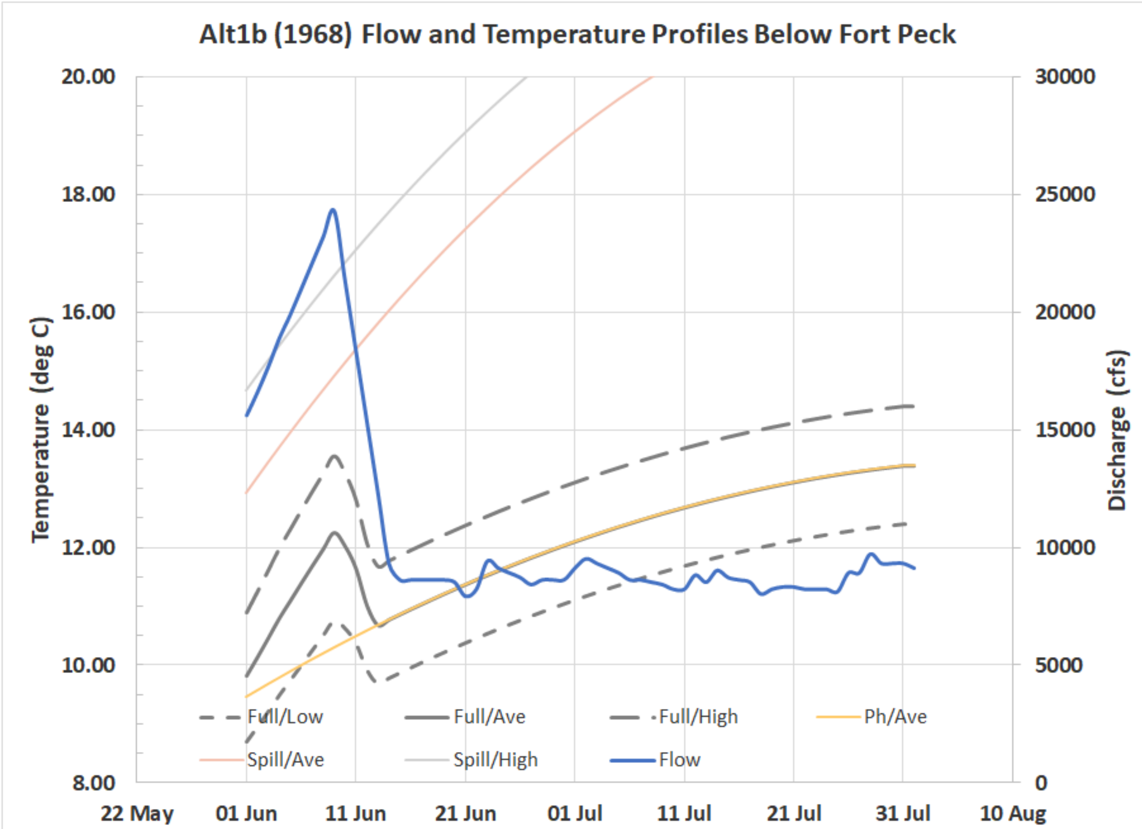
Alt1b (1968) Flow and Temperature Profiles Below Fort Peck
Temperature (deg C)
Discharge (cfs)
20.00
18.00
16.00
14.00
12.00
10.00
8.00
30000
25000
20000
15000
10000
5000
0
22 May
01 Jun
11 Jun
21 Jun
01 Jul
11 Jul
21 Jul
31 Jul
10 Aug
Full/Low
Full/Ave
Full/High
Ph/Ave
Spill/Ave
Spill/High
Flow

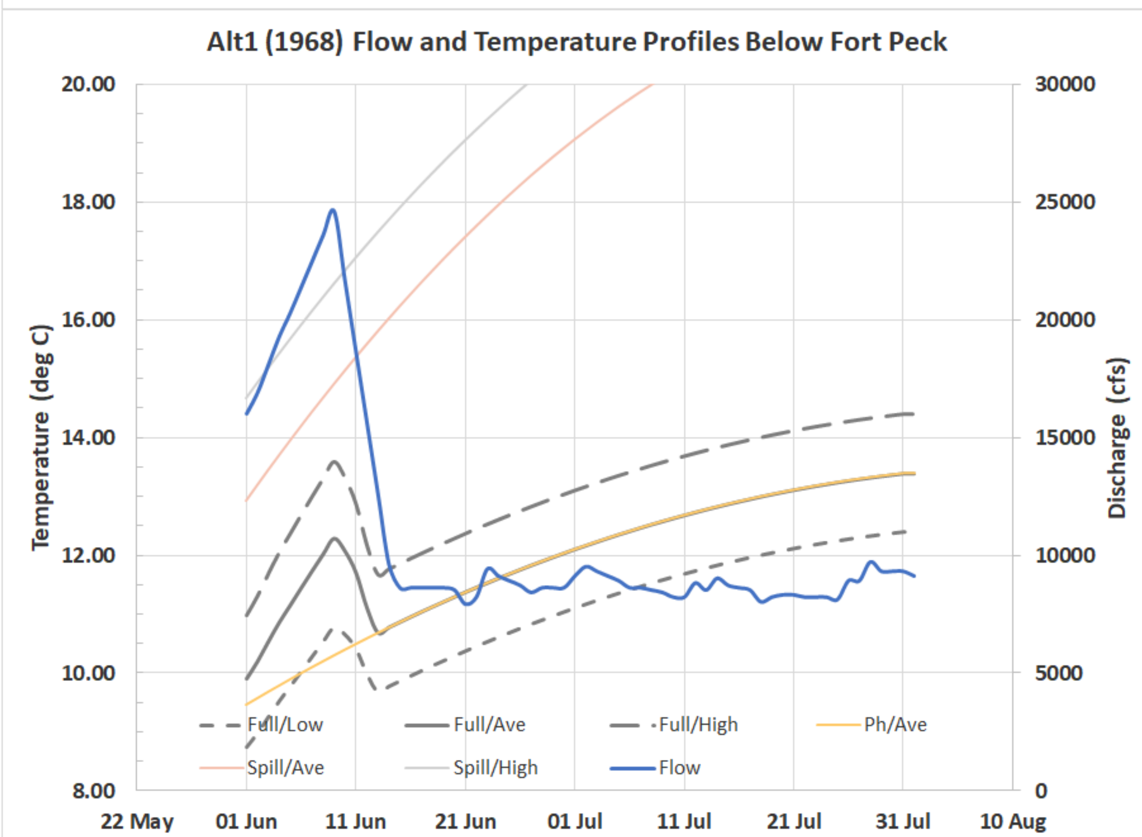
Alt1 (1968) Flow and Temperature Profiles Below Fort Peck
Temperature (deg C)
Discharge (cfs)
20.00
18.00
16.00
14.00
12.00
10.00
8.00
30000
25000
20000
15000
10000
5000
0
22 May
01 Jun
11 Jun
21 Jun
01 Jul
11 Jul
21 Jul
31 Jul
10 Aug
Full/Low
Full/Ave
Full/High
Ph/Ave
Spill/Ave
Spill/High
Flow

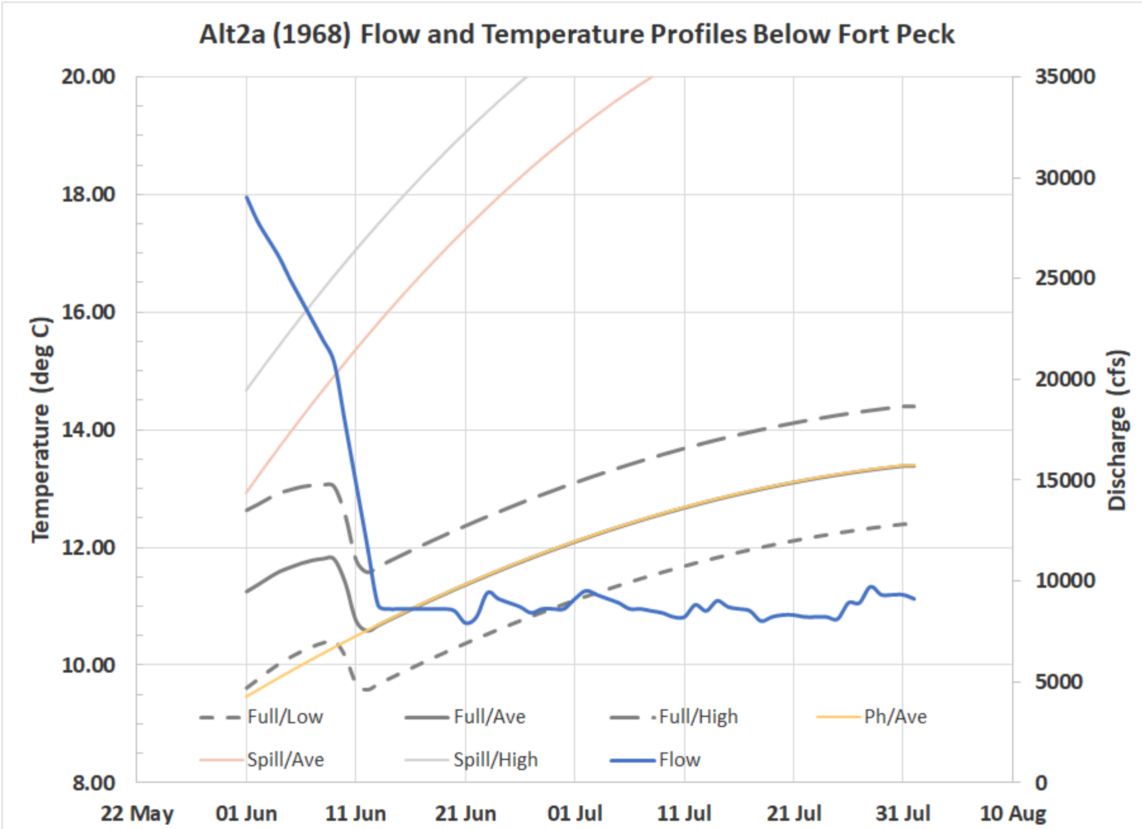
Alt2a (1968) Flow and Temperature Profiles Below Fort Peck
Temperature (deg C)
Discharge (cfs)
20.00
18.00
16.00
14.00
12.00
10.00
8.00
35000
30000
25000
20000
15000
10000
5000
0
22 May
01 Jun
11 Jun
21 Jun
01 Jul
11 Jul
21 Jul
31 Jul
10 Aug
Full/Low
Full/Ave
Full/High
Ph/Ave
Spill/Ave
Spill/High
Flow

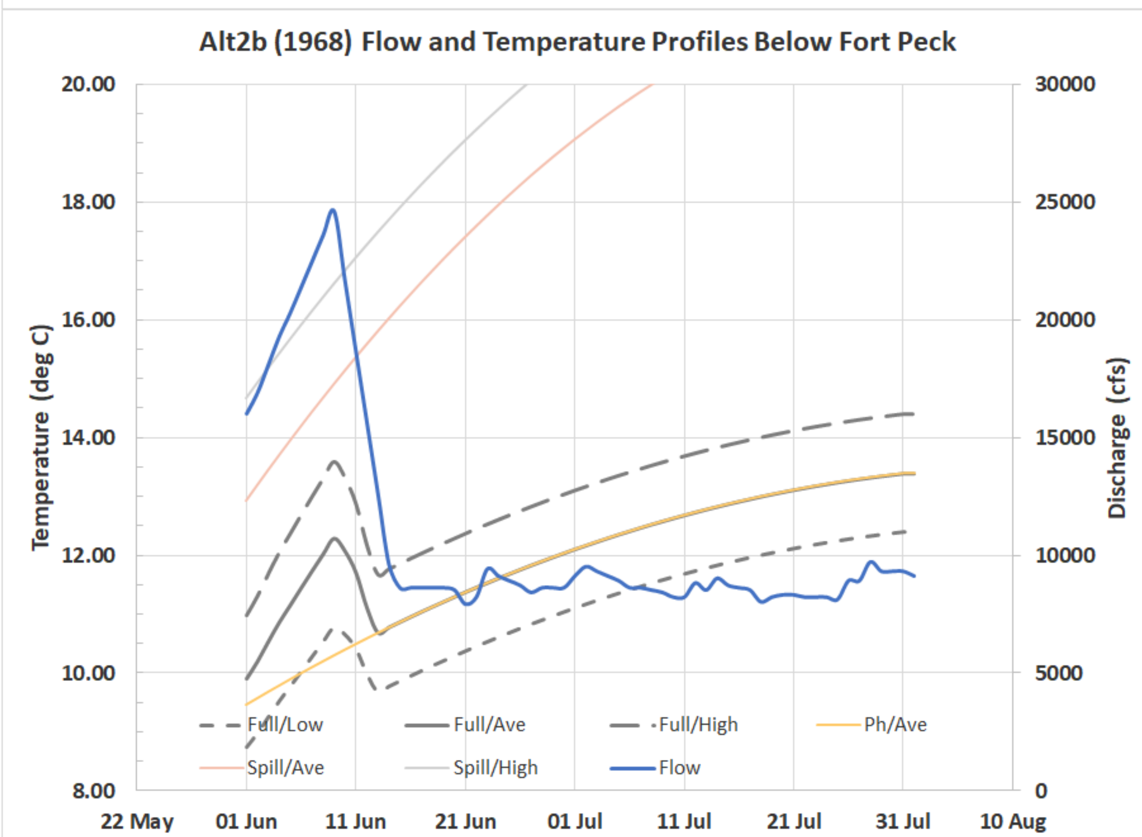
Alt2b (1968) Flow and Temperature Profiles Below Fort Peck
Temperature (deg C)
Discharge (cfs)
20.00
18.00
16.00
14.00
12.00
10.00
8.00
30000
25000
20000
15000
10000
5000
0
22 May
01 Jun
11 Jun
21 Jun
01 Jul
11 Jul
21 Jul
31 Jul
10 Aug
Full/Low
Full/Ave
Full/High
Ph/Ave
Spill/Ave
Spill/High
Flow

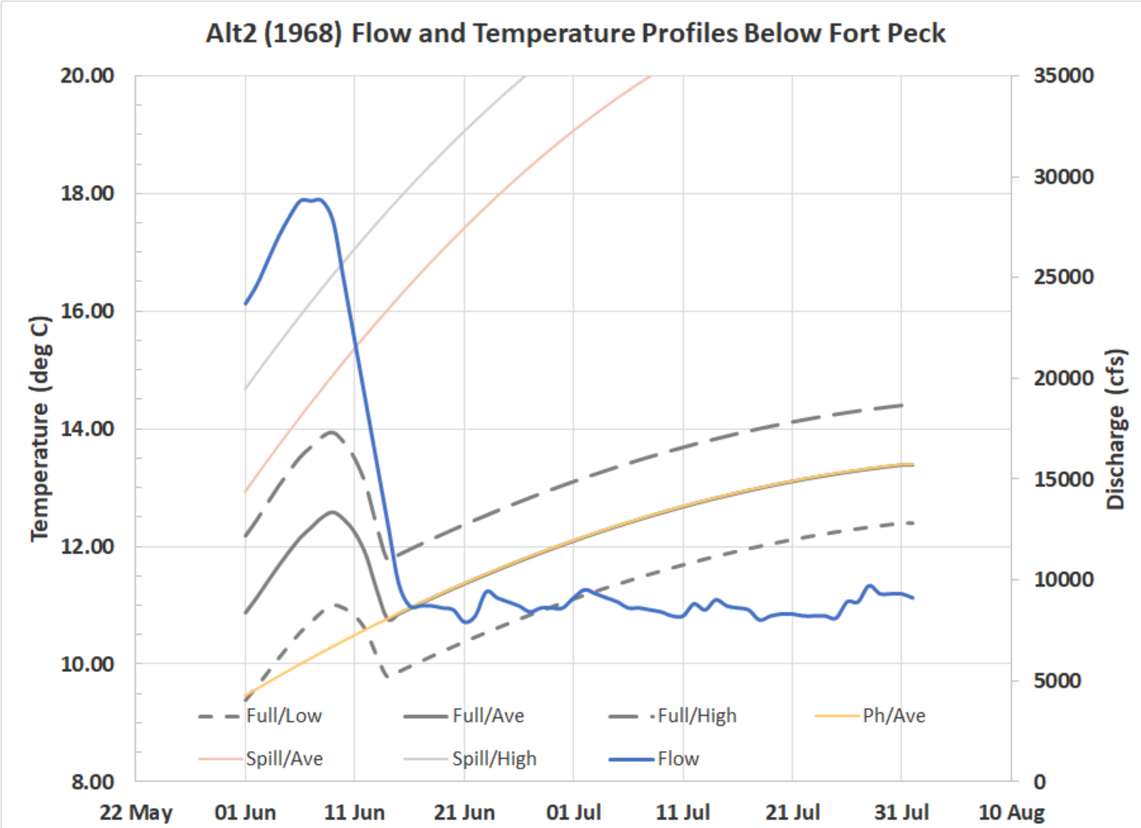
Alt2 (1968) Flow and Temperature Profiles Below Fort Peck
Temperature (deg C)
Discharge (cfs)
20.00
18.00
16.00
14.00
12.00
10.00
8.00
35000
30000
25000
20000
15000
10000
5000
0
22 May
01 Jun
11 Jun
21 Jun
01 Jul
11 Jul
21 Jul
31 Jul
10 Aug
Full/Low
Full/Ave
Full/High
Ph/Ave
Spill/Ave
Spill/High
Flow

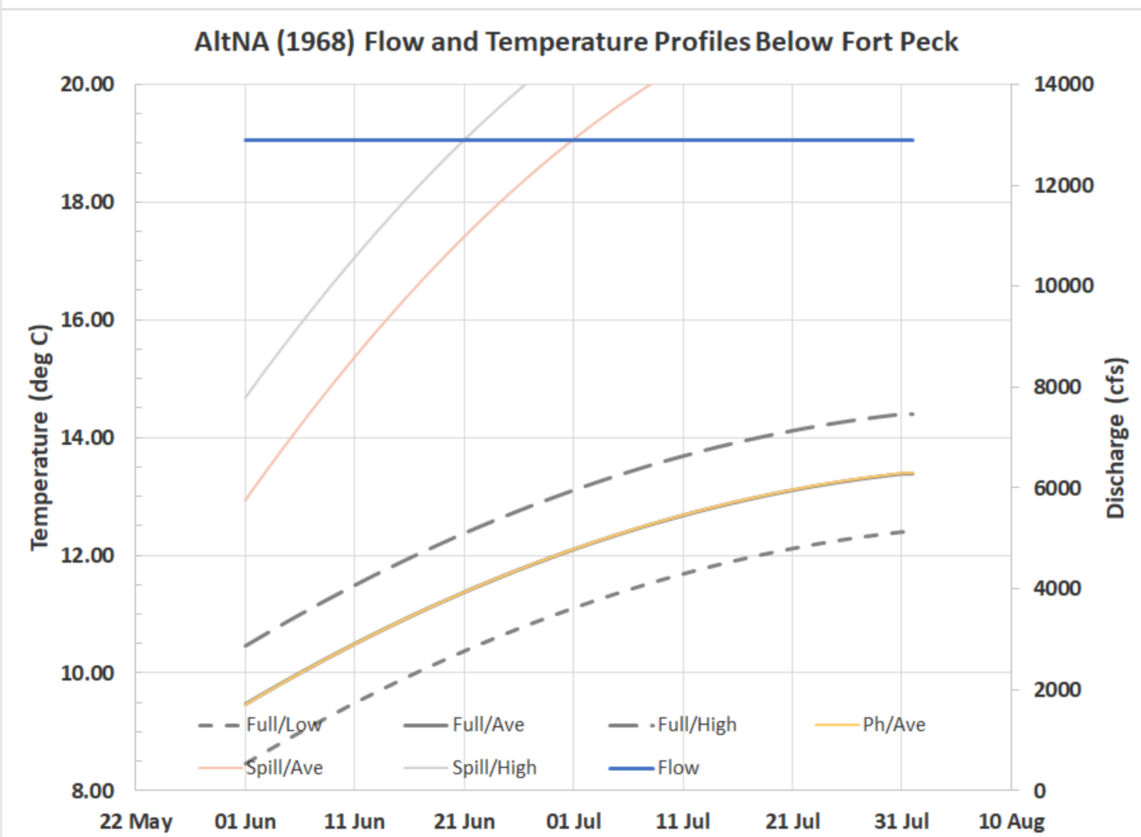
AltNA (1968) Flow and Temperature Profiles Below Fort Peck
Temperature (deg C)
Discharge (cfs)
20.00
18.00
16.00
14.00
12.00
10.00
8.00
14000
12000
10000
8000
6000
4000
2000
0
22 May
01 Jun
11 Jun
21 Jun
01 Jul
11 Jul
21 Jul
31 Jul
10 Aug
Full/Low
Full/Ave
Full/High
Ph/Ave
Spill/Ave
Spill/High
Flow

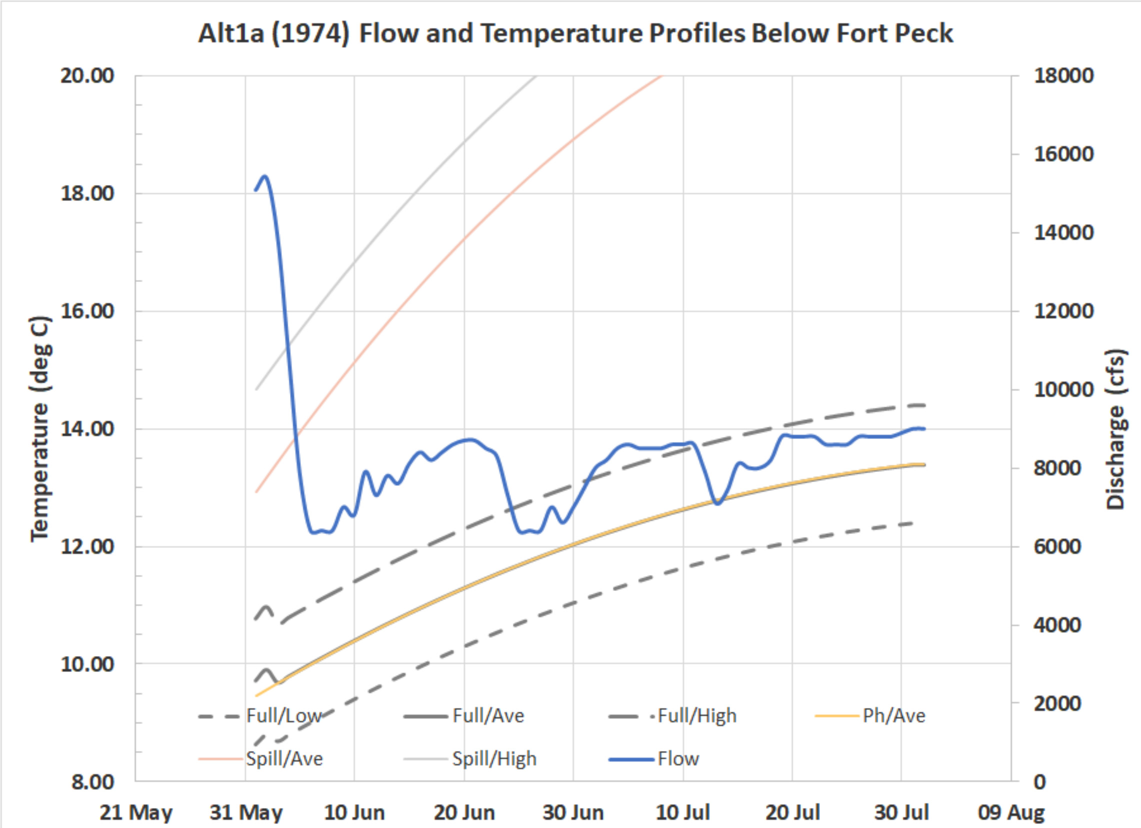
Alt1a (1974) Flow and Temperature Profiles Below Fort Peck
Temperature (deg C)
Discharge (cfs)
20.00
18.00
16.00
14.00
12.00
10.00
8.00
18000
16000
14000
12000
10000
8000
6000
4000
2000
0
21 May
31 May
10 Jun
20 Jun
30 Jun
10 Jul
20 Jul
30 Jul
09 Aug
Full/Low
Full/Ave
Full/High
Ph/Ave
Spill/Ave
Spill/High
Flow

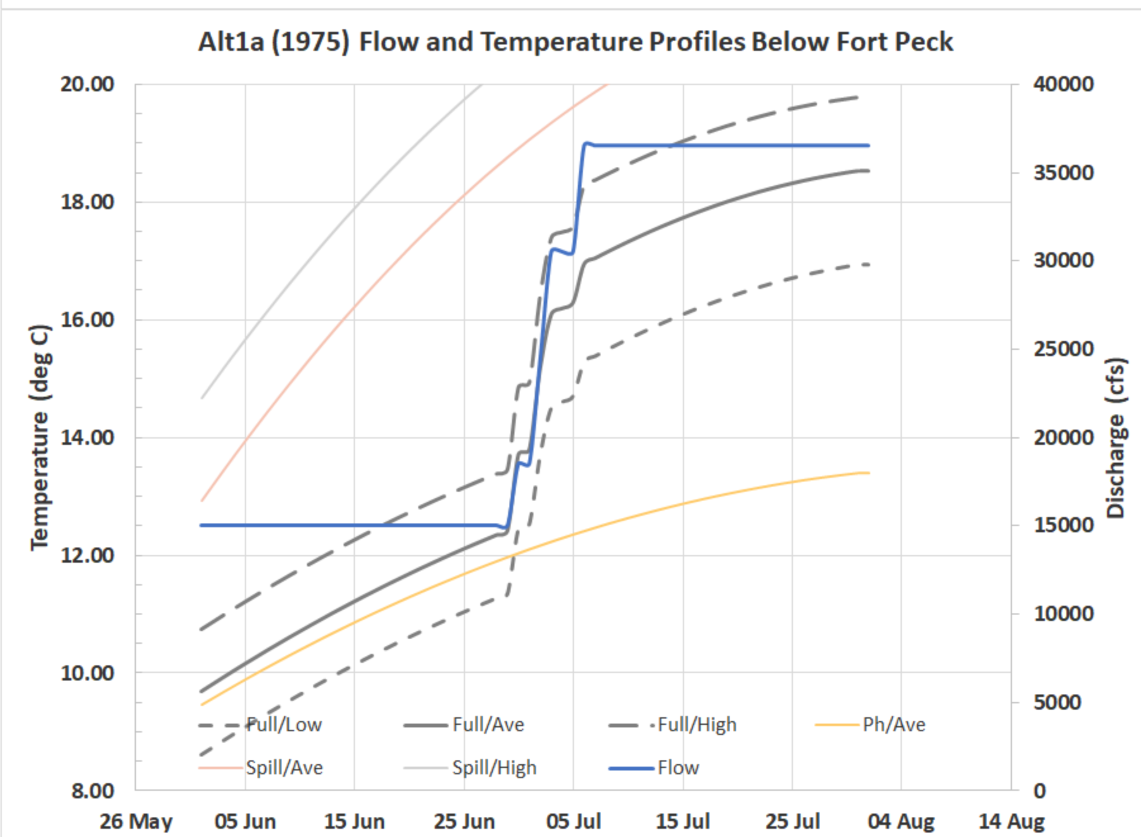
Alt1a (1975) Flow and Temperature Profiles Below Fort Peck
Temperature (deg C)
Discharge (cfs)
20.00
18.00
16.00
14.00
12.00
10.00
8.00
40000
35000
30000
25000
20000
15000
10000
5000
0
26 May
05 Jun
15 Jun
25 Jun
05 Jul
15 Jul
25 Jul
04 Aug
14 Aug
Full/Low
Full/Ave
Full/High
Ph/Ave
Spill/Ave
Spill/High
Flow

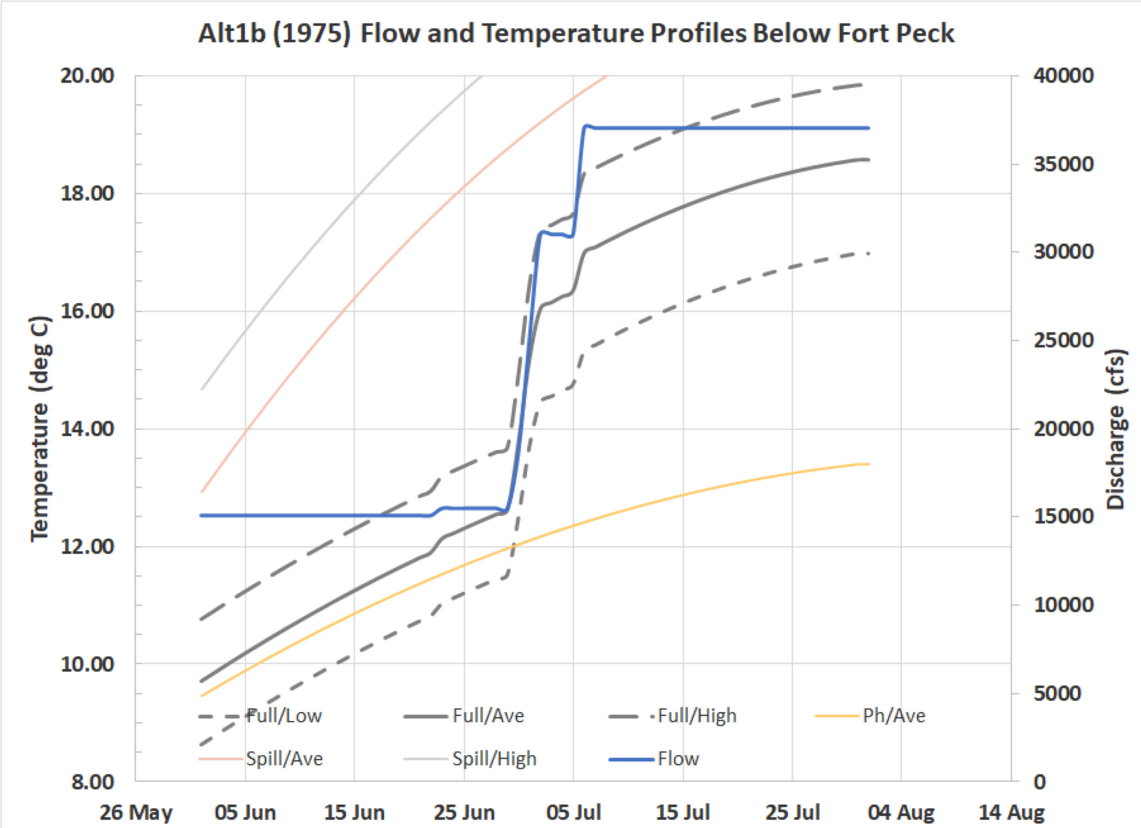
Alt1b (1975) Flow and Temperature Profiles Below Fort Peck
Temperature (deg C)
Discharge (cfs)
20.00
18.00
16.00
14.00
12.00
10.00
8.00
40000
35000
30000
25000
20000
15000
10000
5000
0
26 May
05 Jun
15 Jun
25 Jun
05 Jul
15 Jul
25 Jul
04 Aug
14 Aug
Full/Low
Full/Ave
Full/High
Ph/Ave
Spill/Ave
Spill/High
Flow

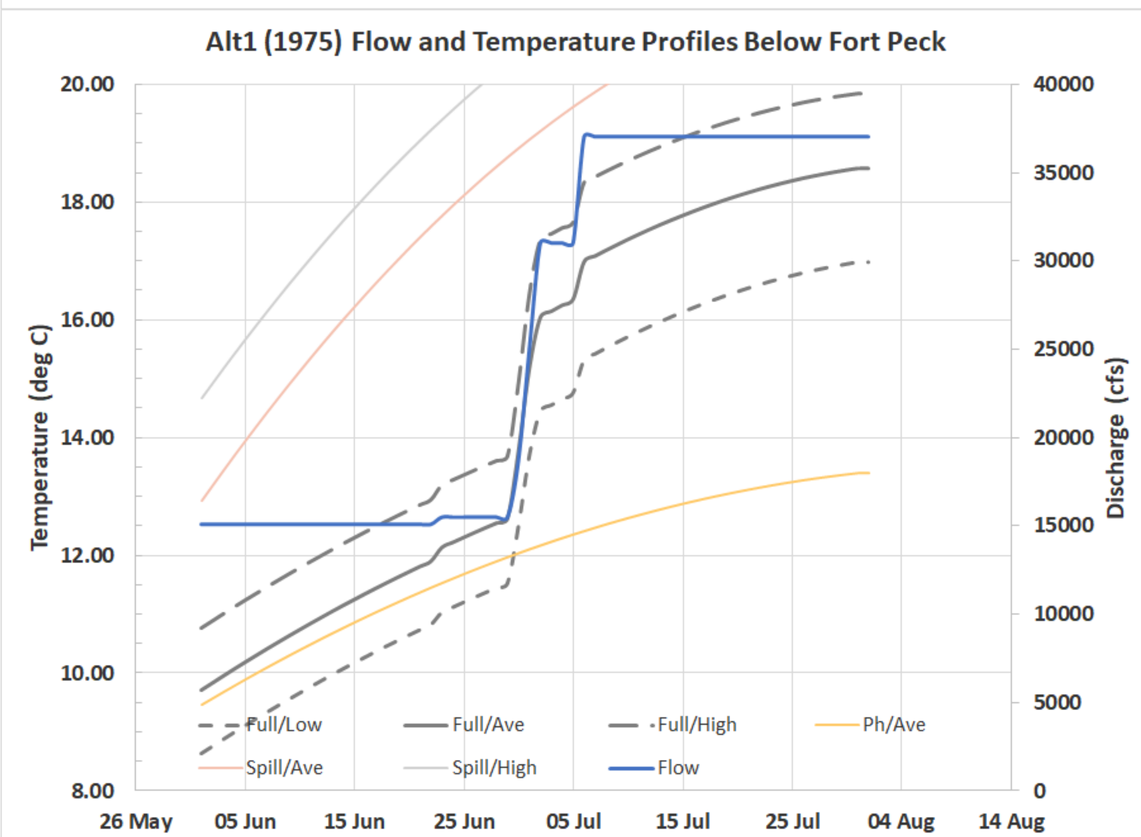
Alt1 (1975) Flow and Temperature Profiles Below Fort Peck
Temperature (deg C)
Discharge (cfs)
20.00
18.00
16.00
14.00
12.00
10.00
8.00
40000
35000
30000
25000
20000
15000
10000
5000
0
26 May
05 Jun
15 Jun
25 Jun
05 Jul
15 Jul
25 Jul
04 Aug
14 Aug
Full/Low
Full/Ave
Full/High
Ph/Ave
Spill/Ave
Spill/High
Flow

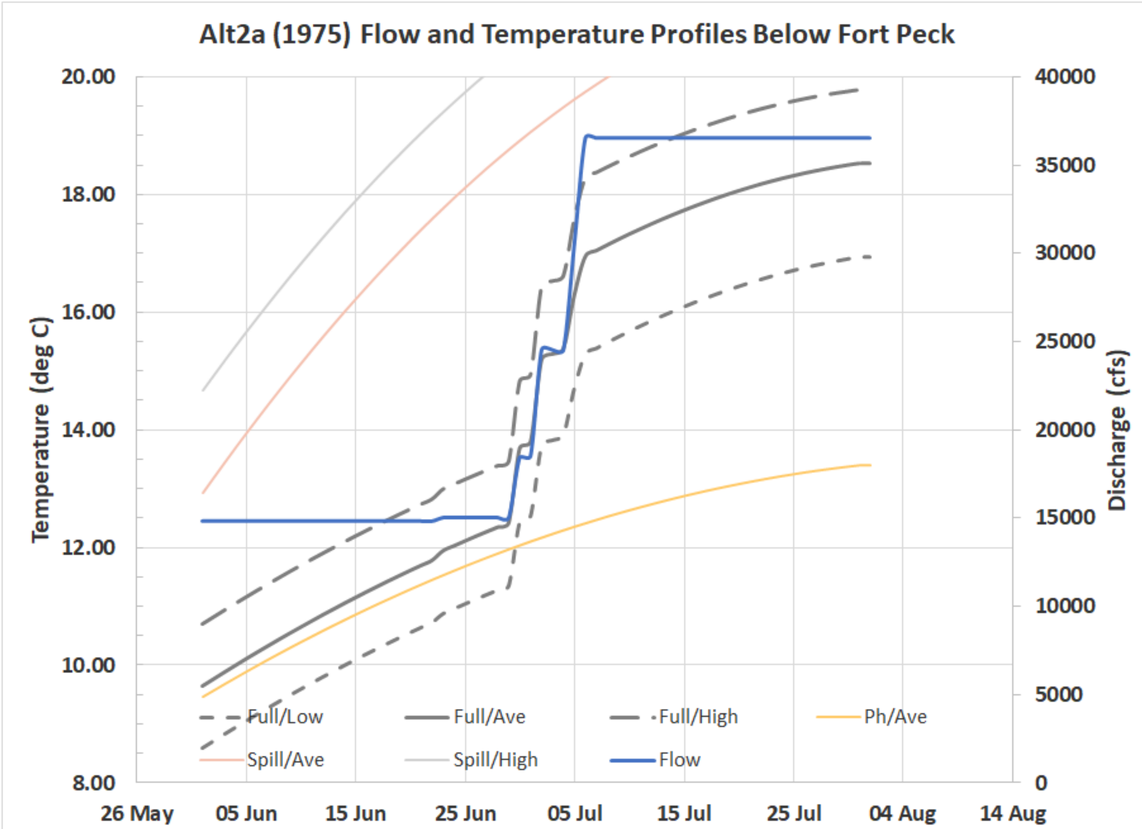
Alt2a (1975) Flow and Temperature Profiles Below Fort Peck
Temperature (deg C)
Discharge (cfs)
20.00
18.00
16.00
14.00
12.00
10.00
8.00
40000
35000
30000
25000
20000
15000
10000
5000
0
26 May
05 Jun
15 Jun
25 Jun
05 Jul
15 Jul
25 Jul
04 Aug
14 Aug
Full/Low
Full/Ave
Full/High
Ph/Ave
Spill/Ave
Spill/High
Flow

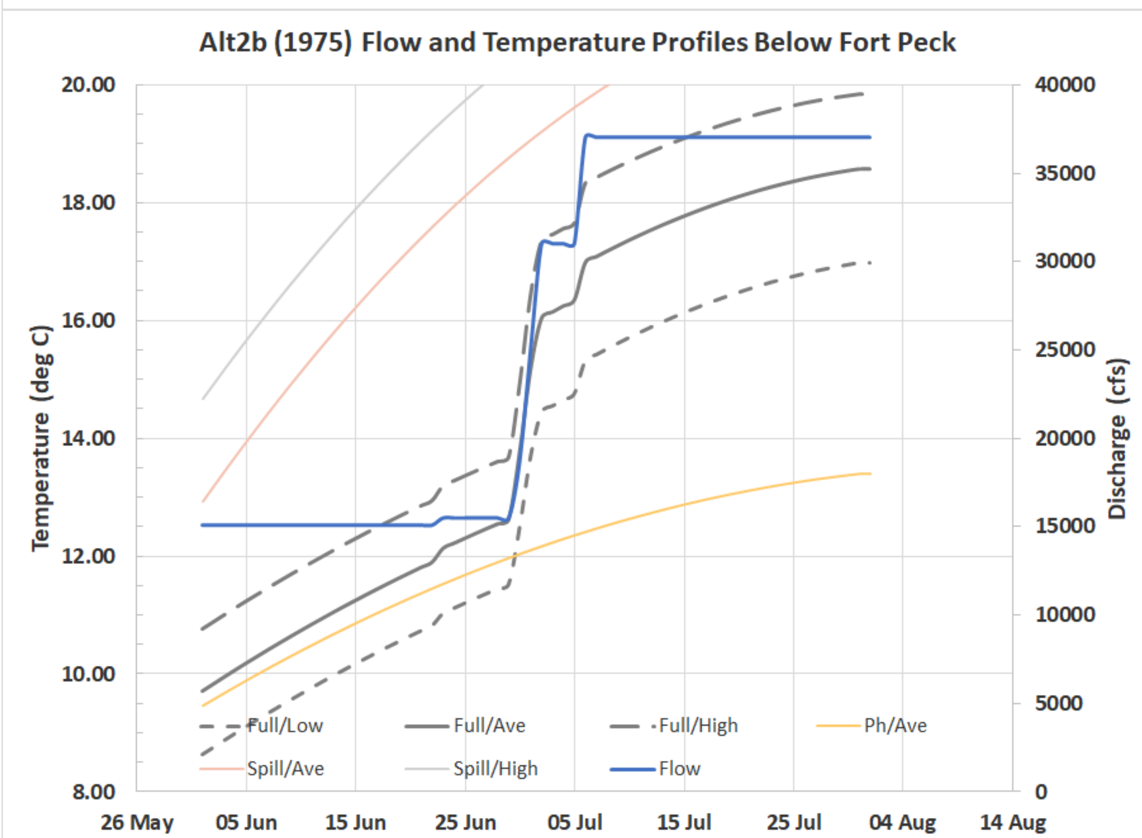
Alt2b (1975) Flow and Temperature Profiles Below Fort Peck
Temperature (deg C)
Discharge (cfs)
20.00
18.00
16.00
14.00
12.00
10.00
8.00
40000
35000
30000
25000
20000
15000
10000
5000
0
26 May
05 Jun
15 Jun
25 Jun
05 Jul
15 Jul
25 Jul
04 Aug
14 Aug
Full/Low
Full/Ave
Full/High
Ph/Ave
Spill/Ave
Spill/High
Flow

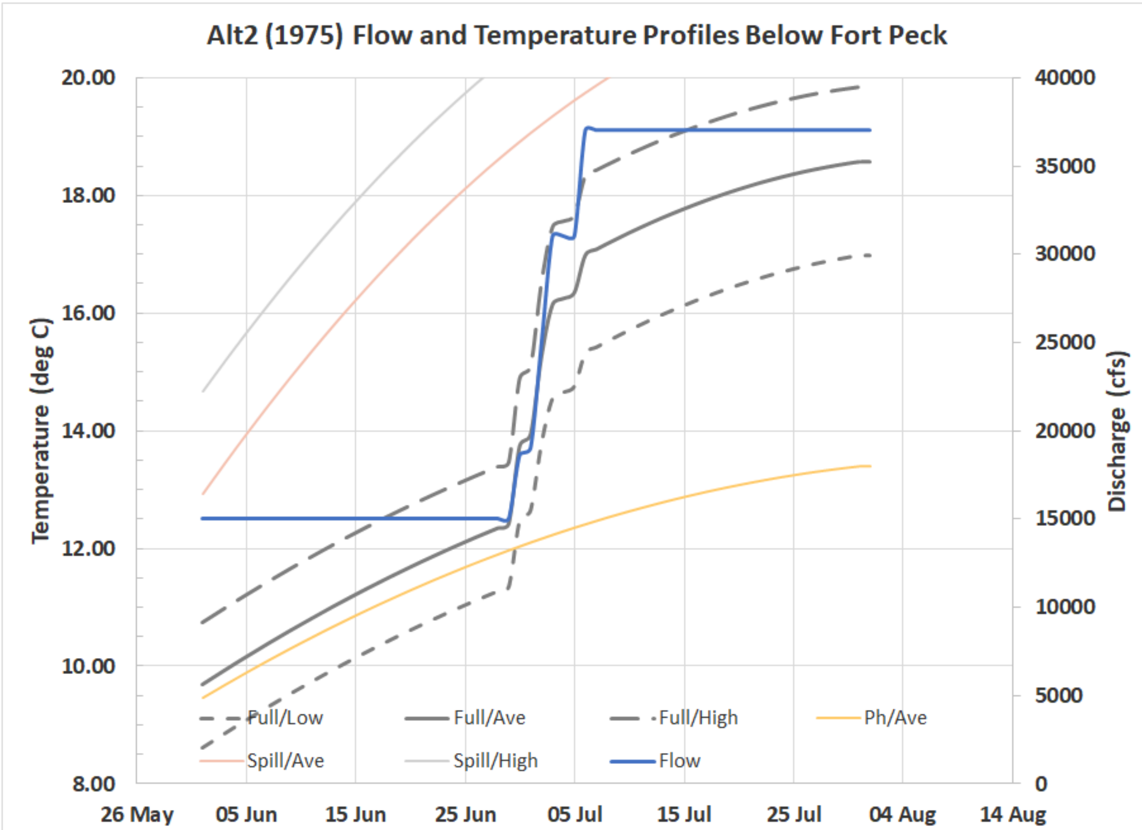

Alt2 (1975) Flow and Temperature Profiles Below Fort Peck
Temperature (deg C)
Discharge (cfs)
20.00
18.00
16.00
14.00
12.00
10.00
8.00
40000
35000
30000
25000
20000
15000
10000
5000
0
26 May
05 Jun
15 Jun
25 Jun
05 Jul
15 Jul
25 Jul
04 Aug
14 Aug
Full/Low
Full/Ave
Full/High
Ph/Ave
Spill/Ave
Spill/High
Flow

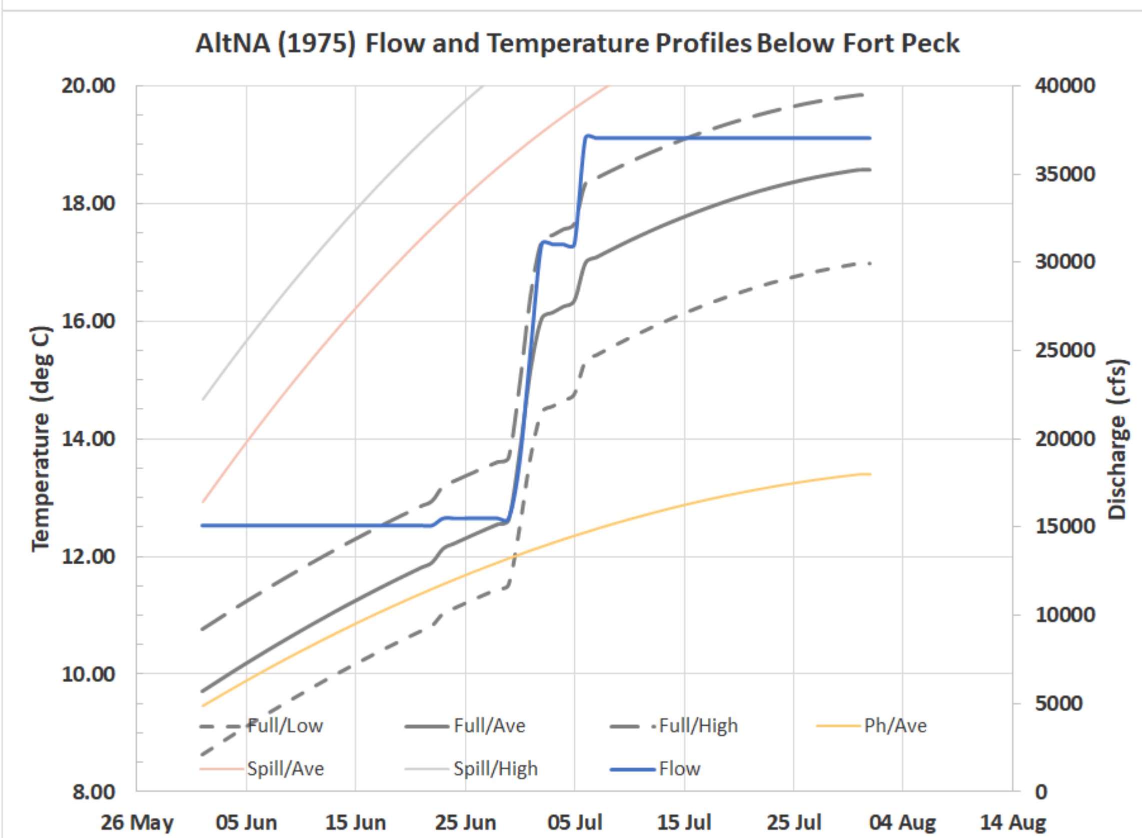

AltNA (1975) Flow and Temperature Profiles Below Fort Peck
Temperature (deg C)
Discharge (cfs)
20.00
18.00
16.00
14.00
12.00
10.00
8.00
40000
35000
30000
25000
20000
15000
10000
5000
0
26 May
05 Jun
15 Jun
25 Jun
05 Jul
15 Jul
25 Jul
04 Aug
14 Aug
Full/Low
Full/Ave
Full/High
Ph/Ave
Spill/Ave
Spill/High
Flow

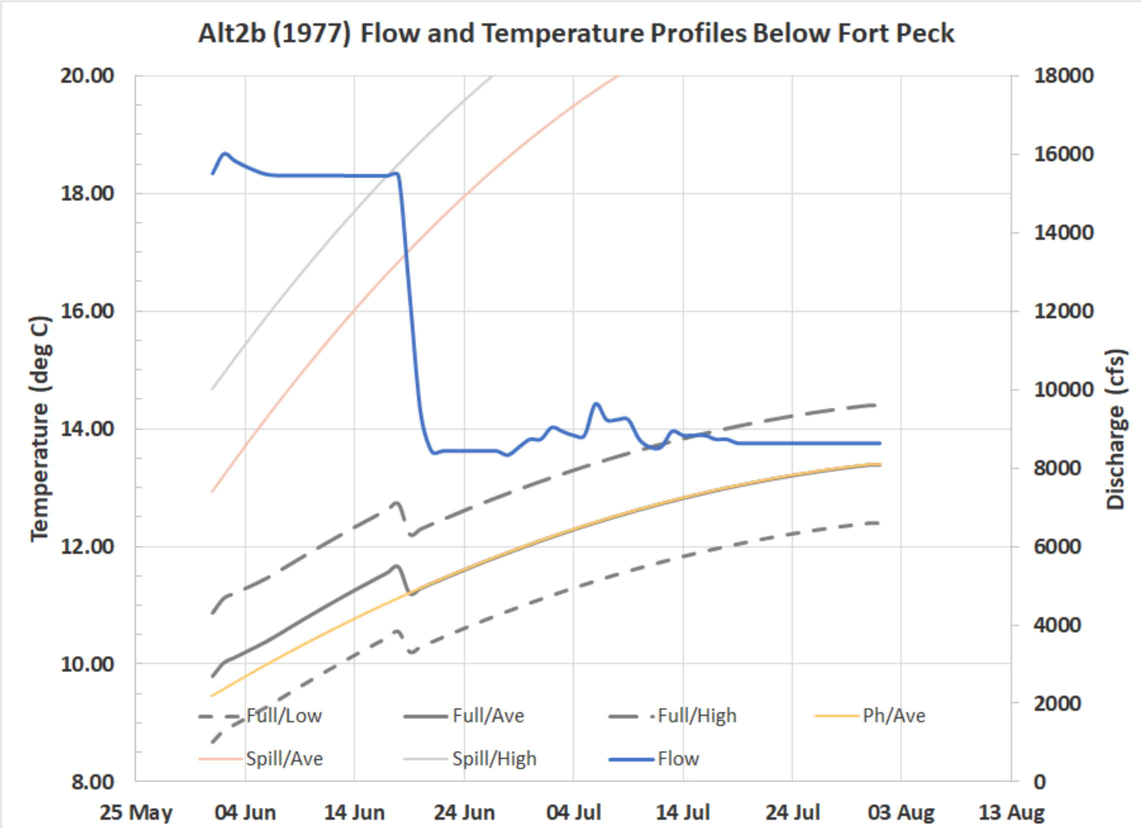
Alt2b (1977) Flow and Temperature Profiles Below Fort Peck
Temperature (deg C)
Discharge (cfs)
20.00
18.00
16.00
14.00
12.00
10.00
8.00
18000
16000
14000
12000
10000
8000
6000
4000
2000
0
25 May
04 Jun
14 Jun
24 Jun
04 Jul
14 Jul
24 Jul
03 Aug
13 Aug
Full/Low
Full/Ave
Full/High
Ph/Ave
Spill/Ave
Spill/High
Flow

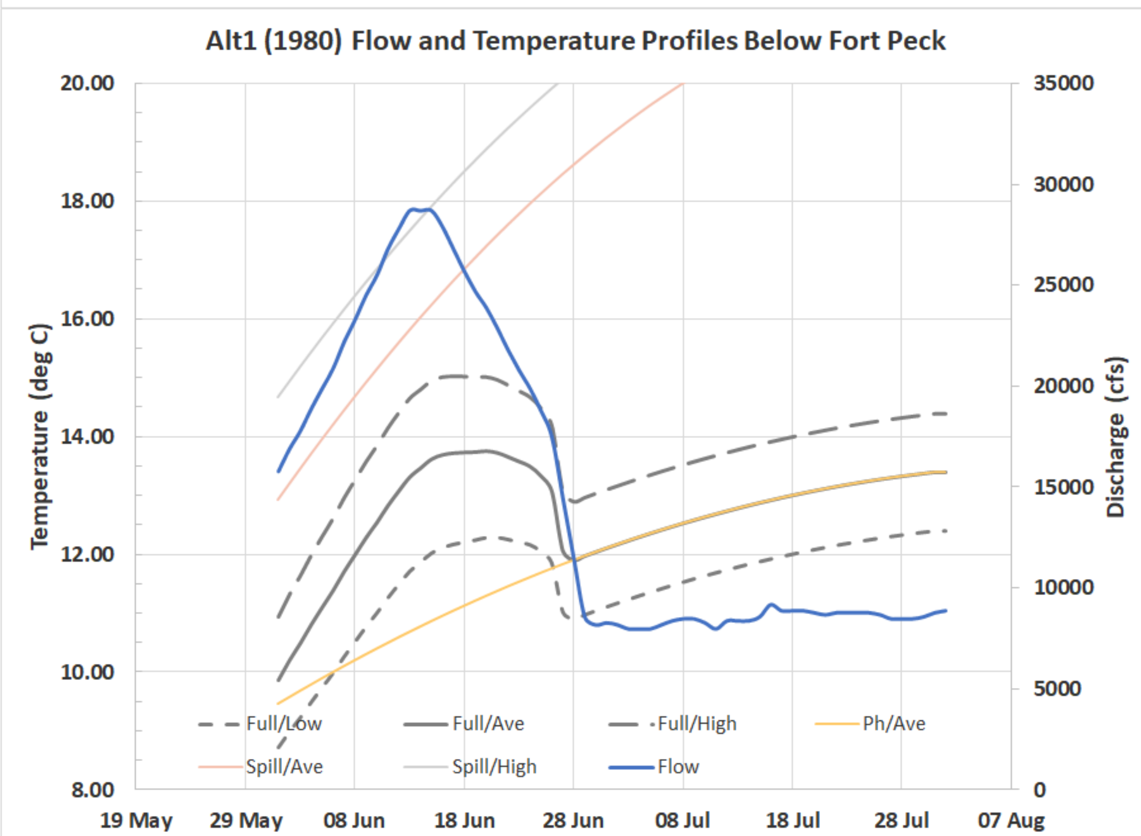
Alt1 (1980) Flow and Temperature Profiles Below Fort Peck
Temperature (deg C)
Discharge (cfs)
20.00
18.00
16.00
14.00
12.00
10.00
8.00
35000
30000
25000
20000
15000
10000
5000
0
19 May
29 May
08 Jun
18 Jun
28 Jun
08 Jul
18 Jul
28 Jul
07 Aug
Full/Low
Full/Ave
Full/High
Ph/Ave
Spill/Ave
Spill/High
Flow

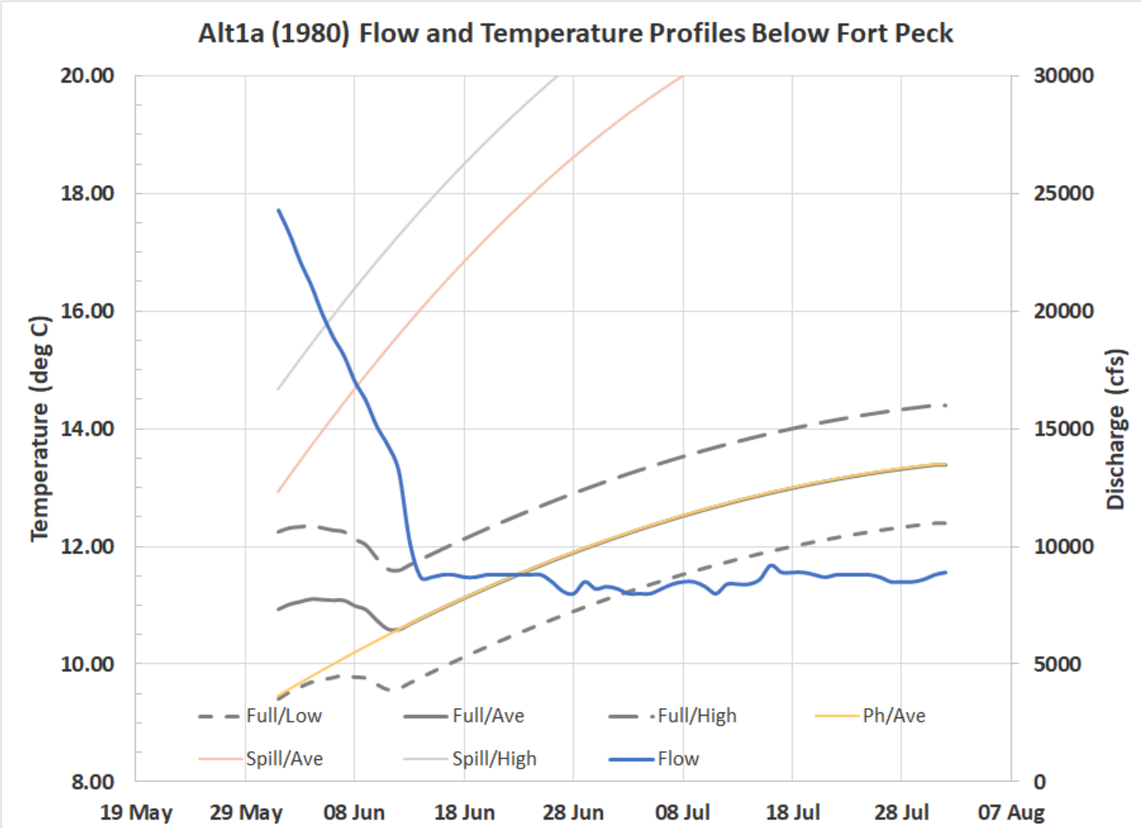
Alt1a (1980) Flow and Temperature Profiles Below Fort Peck
Temperature (deg C)
Discharge (cfs)
20.00
18.00
16.00
14.00
12.00
10.00
8.00
30000
25000
20000
15000
10000
5000
0
19 May
29 May
08 Jun
18 Jun
28 Jun
08 Jul
18 Jul
28 Jul
07 Aug
Full/Low
Full/Ave
Full/High
Ph/Ave
Spill/Ave
Spill/High
Flow

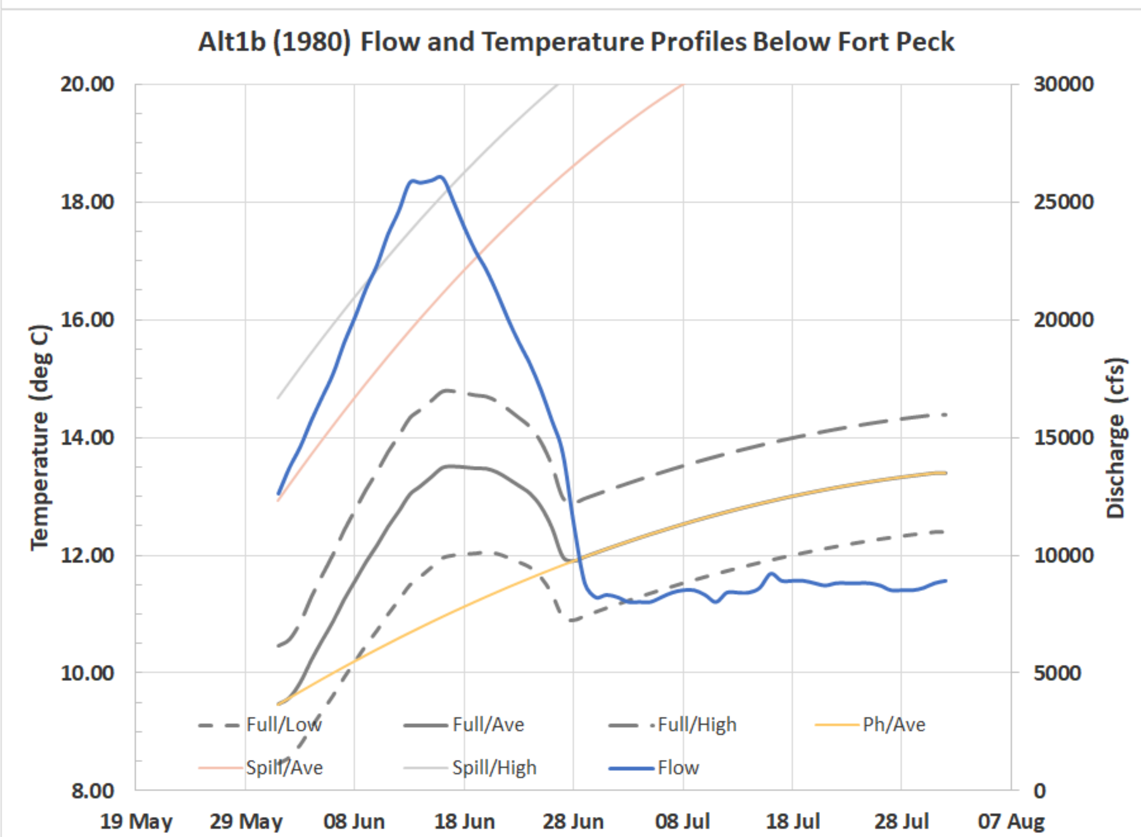
Alt1b (1980) Flow and Temperature Profiles Below Fort Peck
Temperature (deg C)
Discharge (cfs)
20.00
18.00
16.00
14.00
12.00
10.00
8.00
30000
25000
20000
15000
10000
5000
0
19 May
29 May
08 Jun
18 Jun
28 Jun
08 Jul
18 Jul
28 Jul
07 Aug
Full/Low
Full/Ave
Full/High
Ph/Ave
Spill/Ave
Spill/High
Flow

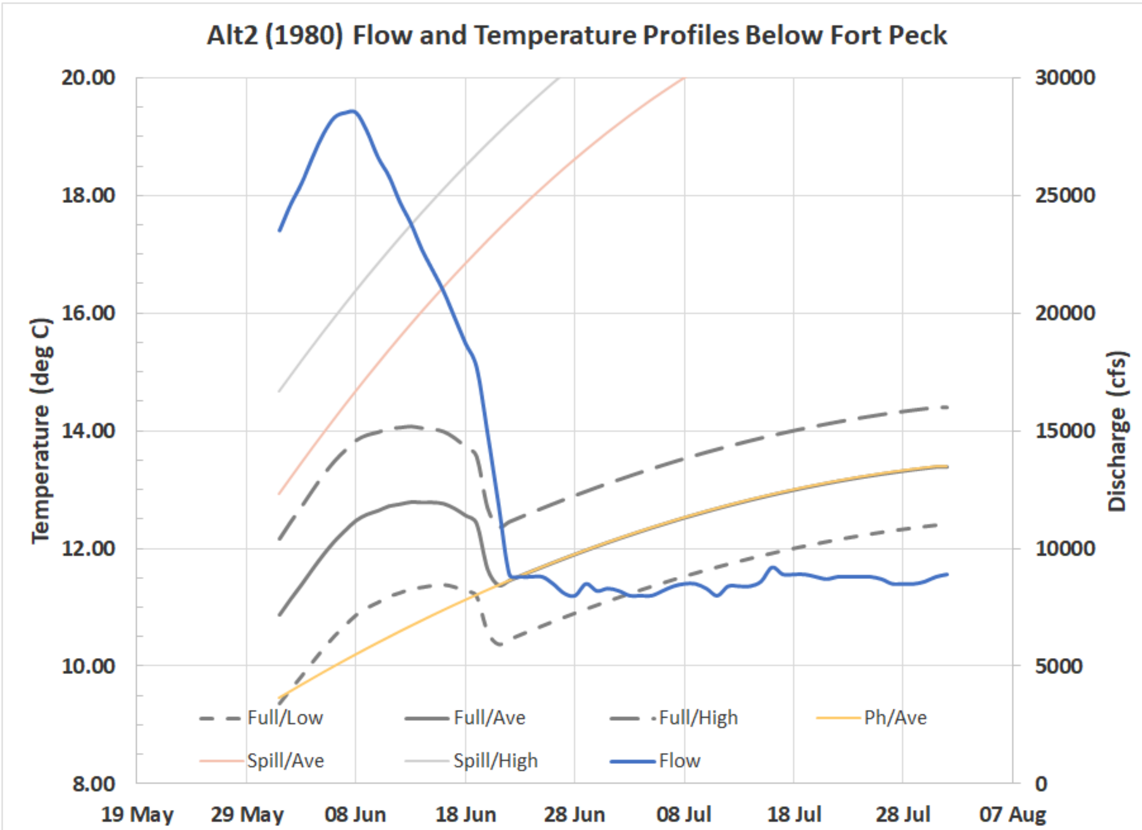
Alt2 (1980) Flow and Temperature Profiles Below Fort Peck
Temperature (deg C)
Discharge (cfs)
20.00
18.00
16.00
14.00
12.00
10.00
8.00
30000
25000
20000
15000
10000
5000
0
19 May
29 May
08 Jun
18 Jun
28 Jun
08 Jul
18 Jul
28 Jul
07 Aug
Full/Low
Full/Ave
Full/High
Ph/Ave
Spill/Ave
Spill/High
Flow

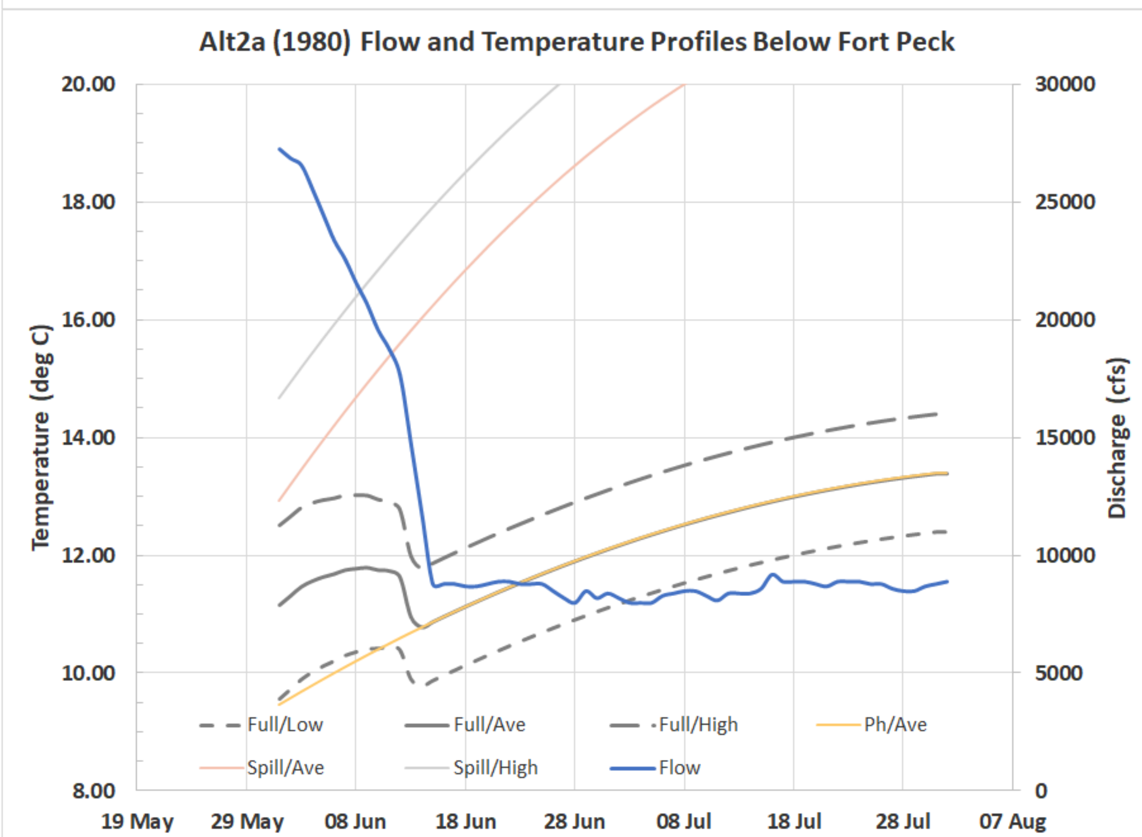
Alt2a (1980) Flow and Temperature Profiles Below Fort Peck
Temperature (deg C)
Discharge (cfs)
20.00
18.00
16.00
14.00
12.00
10.00
8.00
30000
25000
20000
15000
10000
5000
0
19 May
29 May
08 Jun
18 Jun
28 Jun
08 Jul
18 Jul
28 Jul
07 Aug
Full/Low
Full/Ave
Full/High
Ph/Ave
Spill/Ave
Spill/High
Flow

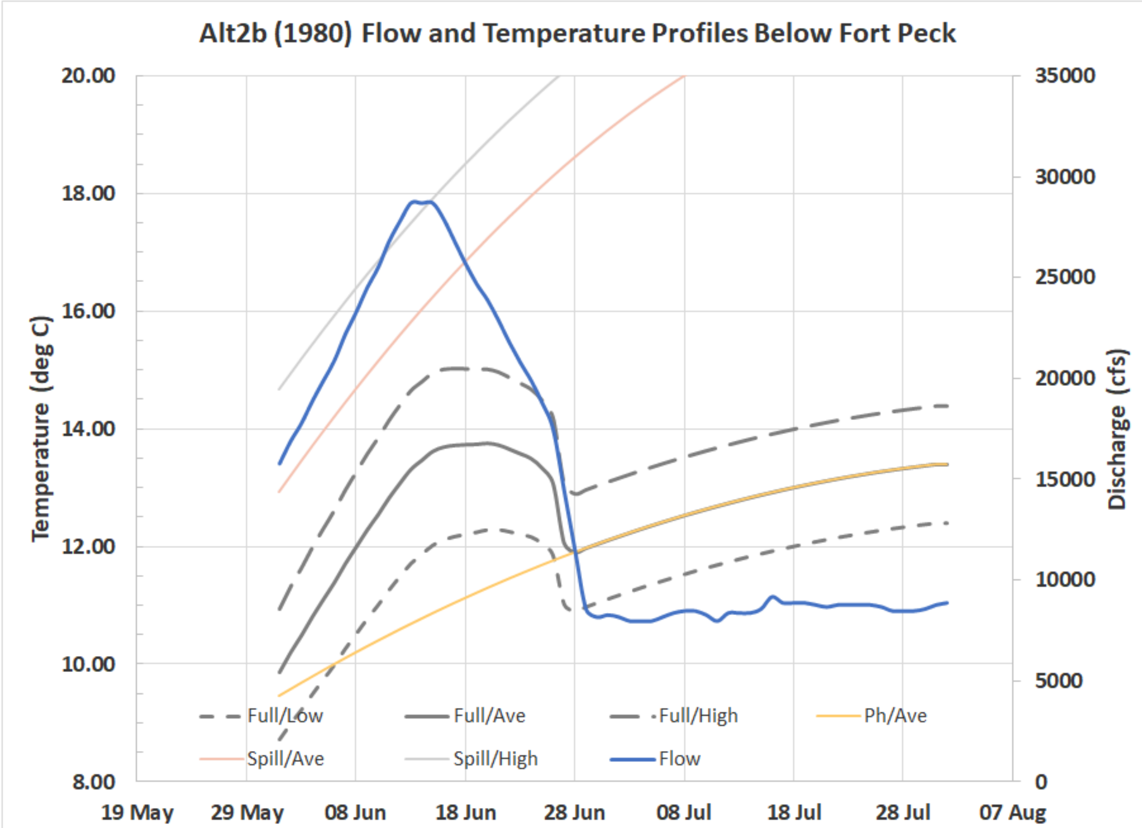
Alt2b (1980) Flow and Temperature Profiles Below Fort Peck
Temperature (deg C)
Discharge (cfs)
20.00
18.00
16.00
14.00
12.00
10.00
8.00
35000
30000
25000
20000
15000
10000
5000
0
19 May
29 May
08 Jun
18 Jun
28 Jun
08 Jul
18 Jul
28 Jul
07 Aug
Full/Low
Full/Ave
Full/High
Ph/Ave
Spill/Ave
Spill/High
Flow

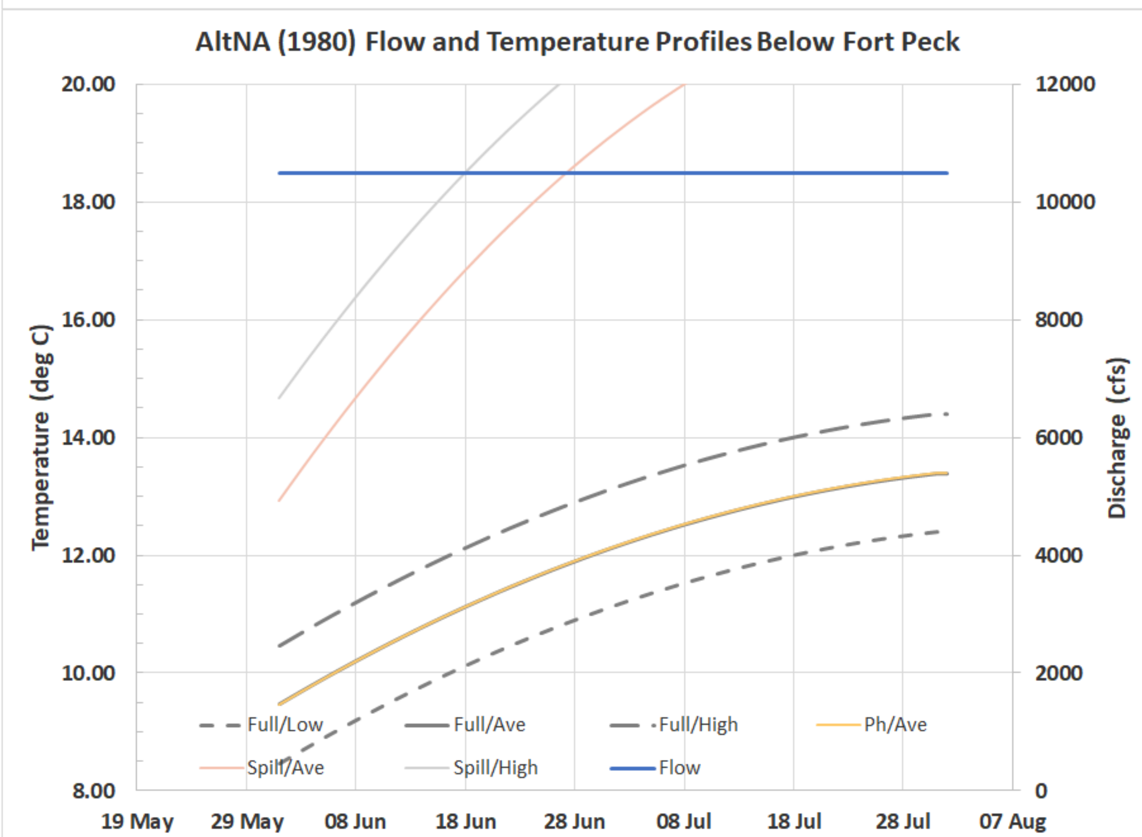
AltNA (1980) Flow and Temperature Profiles Below Fort Peck
Temperature (deg C)
Discharge (cfs)
20.00
18.00
16.00
14.00
12.00
10.00
8.00
12000
10000
8000
6000
4000
2000
0
19 May
29 May
08 Jun
18 Jun
28 Jun
08 Jul
18 Jul
28 Jul
07 Aug
Full/Low
Full/Ave
Full/High
Ph/Ave
Spill/Ave
Spill/High
Flow

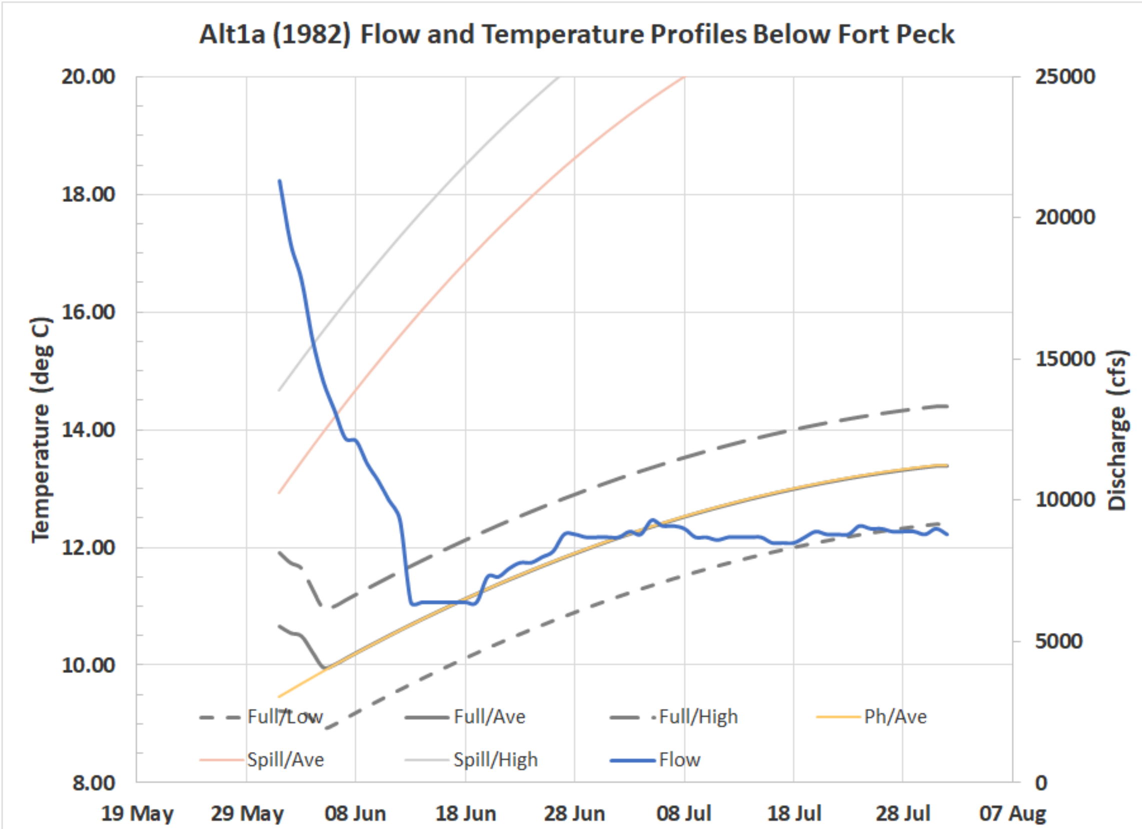
Alt1a (1982) Flow and Temperature Profiles Below Fort Peck
Temperature (deg C)
Discharge (cfs)
20.00
18.00
16.00
14.00
12.00
10.00
8.00
25000
20000
15000
10000
5000
0
19 May
29 May
08 Jun
18 Jun
28 Jun
08 Jul
18 Jul
28 Jul
07 Aug
Full/Low
Full/Ave
Full/High
Ph/Ave
Spill/Ave
Spill/High
Flow

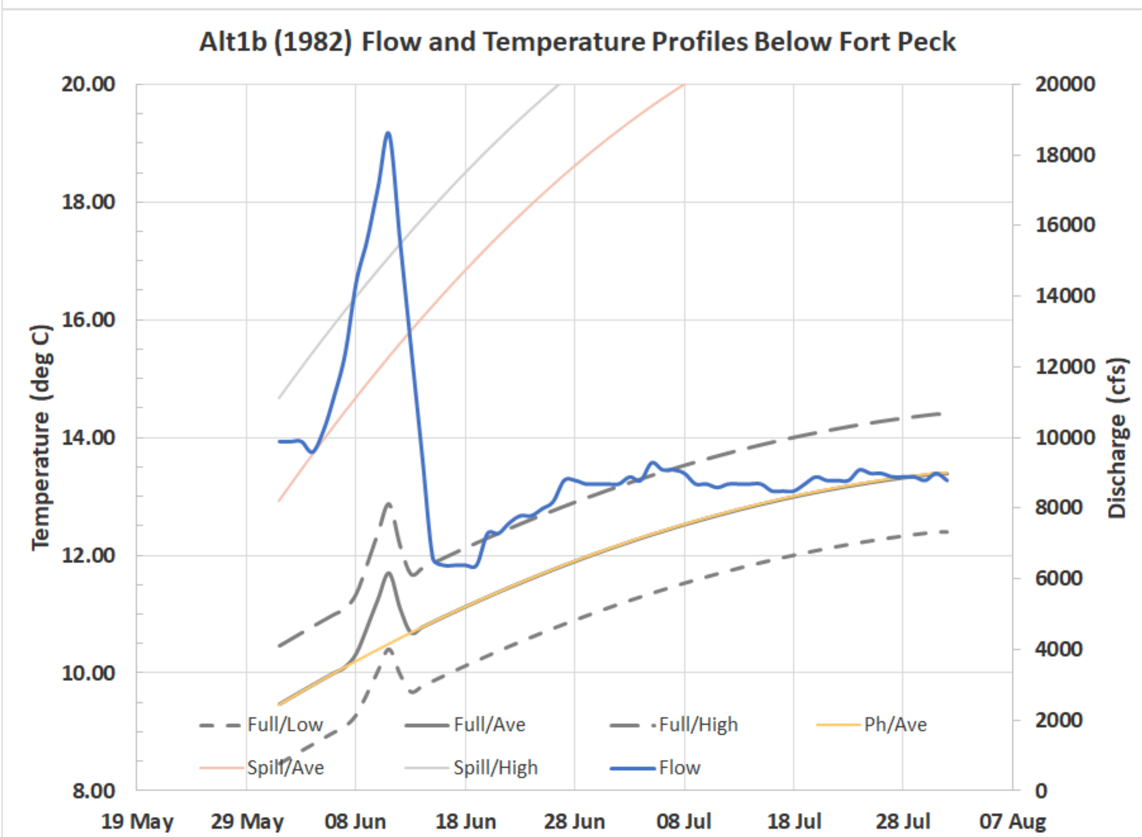
Alt1b (1982) Flow and Temperature Profiles Below Fort Peck
Temperature (deg C)
Discharge (cfs)
20.00
18.00
16.00
14.00
12.00
10.00
8.00
20000
18000
16000
14000
12000
10000
8000
6000
4000
2000
0
19 May
29 May
08 Jun
18 Jun
28 Jun
08 Jul
18 Jul
28 Jul
07 Aug
Full/Low
Full/Ave
Full/High
Ph/Ave
Spill/Ave
Spill/High
Flow

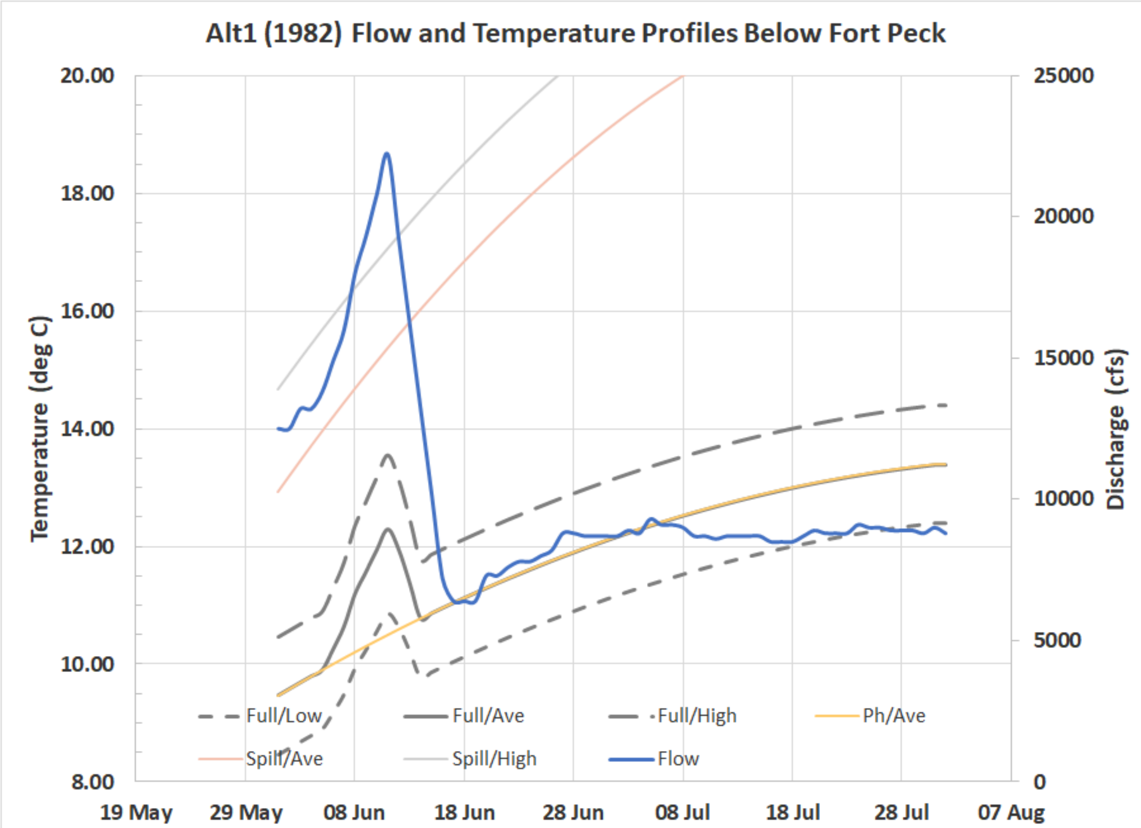
Alt1 (1982) Flow and Temperature Profiles Below Fort Peck
Temperature (deg C)
Discharge (cfs)
20.00
18.00
16.00
14.00
12.00
10.00
8.00
25000
20000
15000
10000
5000
0
19 May
29 May
08 Jun
18 Jun
28 Jun
08 Jul
18 Jul
28 Jul
07 Aug
Full/Low
Full/Ave
Full/High
Ph/Ave
Spill/Ave
Spill/High
Flow

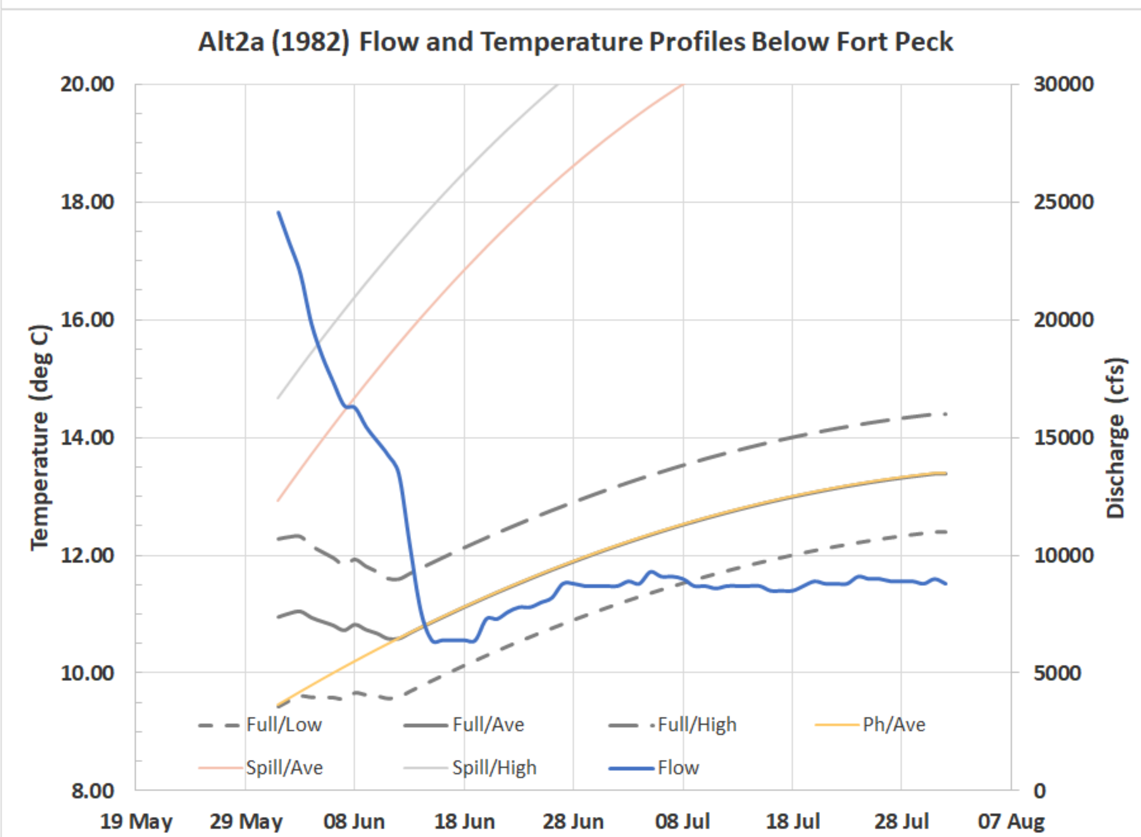
Alt2a (1982) Flow and Temperature Profiles Below Fort Peck
Temperature (deg C)
Discharge (cfs)
20.00
18.00
16.00
14.00
12.00
10.00
8.00
30000
25000
20000
15000
10000
5000
0
19 May
29 May
08 Jun
18 Jun
28 Jun
08 Jul
18 Jul
28 Jul
07 Aug
Full/Low
Full/Ave
Full/High
Ph/Ave
Spill/Ave
Spill/High
Flow

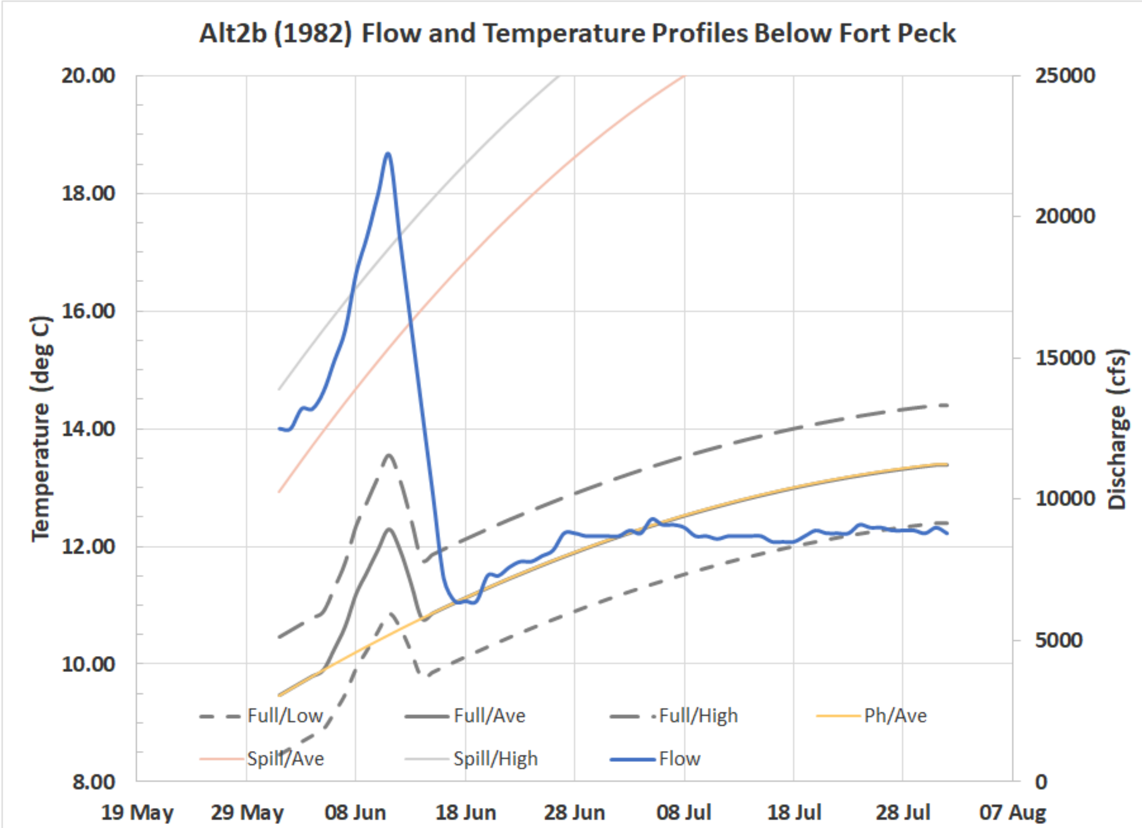

Alt2b (1982) Flow and Temperature Profiles Below Fort Peck
Temperature (deg C)
Discharge (cfs)
20.00
18.00
16.00
14.00
12.00
10.00
8.00
25000
20000
15000
10000
5000
0
19 May
29 May
08 Jun
18 Jun
28 Jun
08 Jul
18 Jul
28 Jul
07 Aug
Full/Low
Full/Ave
Full/High
Ph/Ave
Spill/Ave
Spill/High
Flow

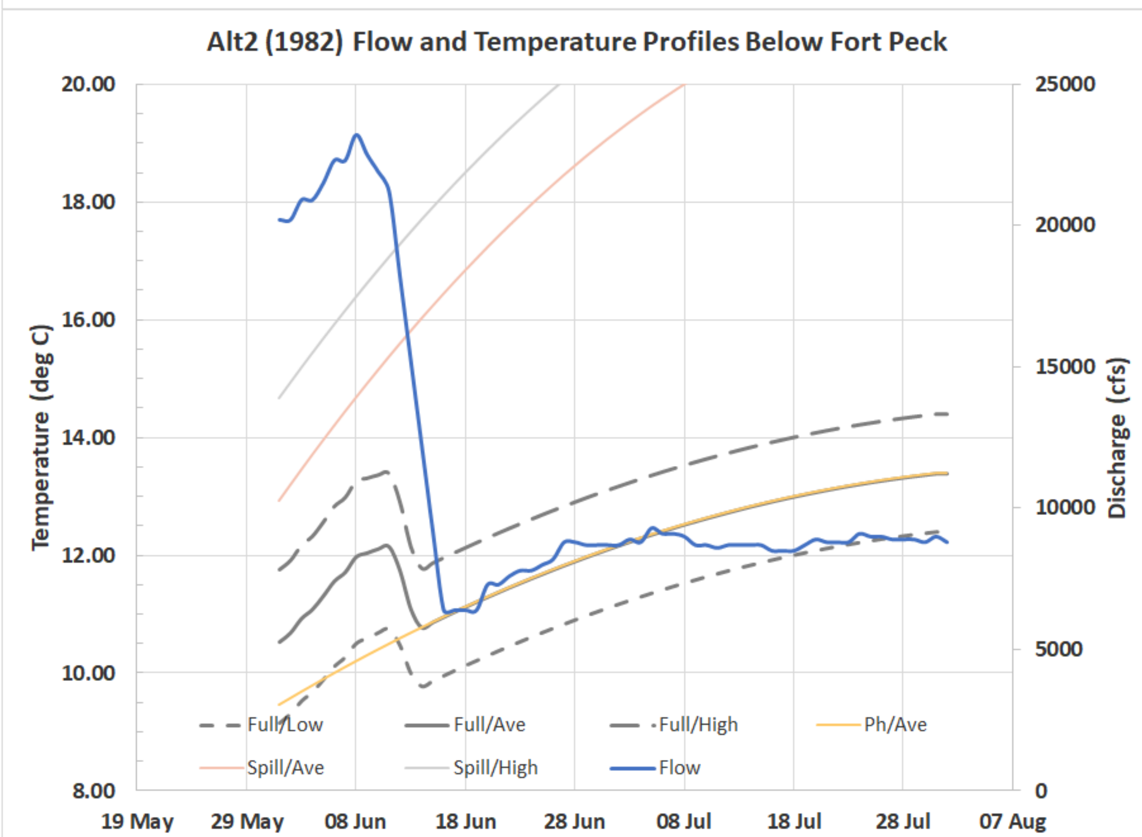

Alt2 (1982) Flow and Temperature Profiles Below Fort Peck
Temperature (deg C)
Discharge (cfs)
20.00
18.00
16.00
14.00
12.00
10.00
8.00
25000
20000
15000
10000
5000
0
19 May
29 May
08 Jun
18 Jun
28 Jun
08 Jul
18 Jul
28 Jul
07 Aug
Full/Low
Full/Ave
Full/High
Ph/Ave
Spill/Ave
Spill/High
Flow

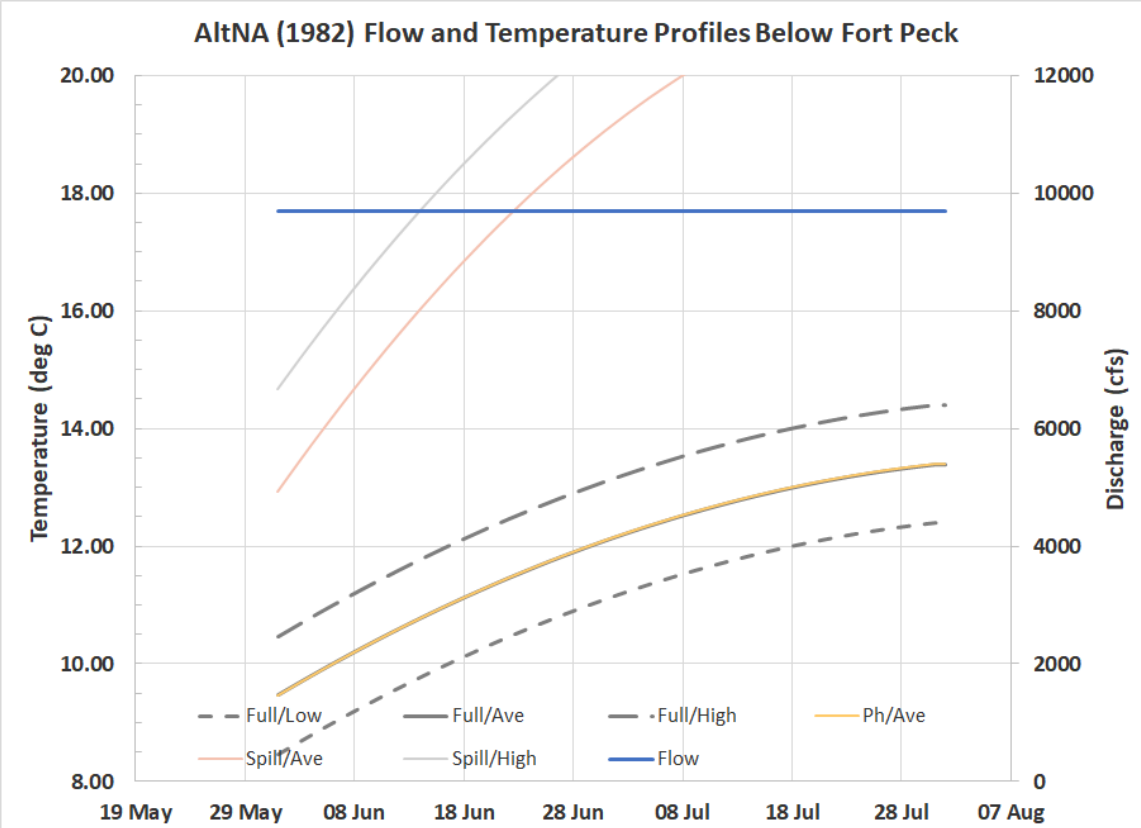
AltNA (1982) Flow and Temperature Profiles Below Fort Peck
Temperature (deg C)
Discharge (cfs)
20.00
18.00
16.00
14.00
12.00
10.00
8.00
12000
10000
8000
6000
4000
2000
0
19 May
29 May
08 Jun
18 Jun
28 Jun
08 Jul
18 Jul
28 Jul
07 Aug
Full/Low
Full/Ave
Full/High
Ph/Ave
Spill/Ave
Spill/High
Flow

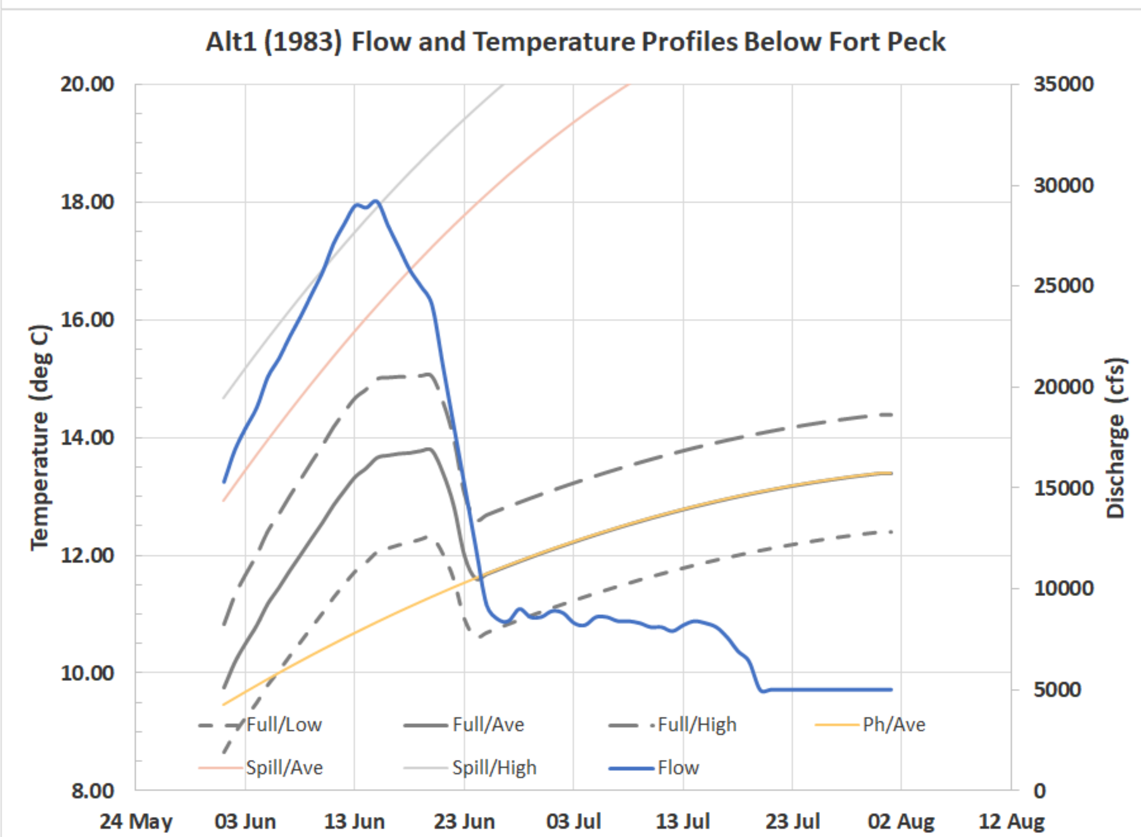
Alt1 (1983) Flow and Temperature Profiles Below Fort Peck
Temperature (deg C)
Discharge (cfs)
20.00
18.00
16.00
14.00
12.00
10.00
8.00
35000
30000
25000
20000
15000
10000
5000
0
24 May
03 Jun
13 Jun
23 Jun
03 Jul
13 Jul
23 Jul
02 Aug
12 Aug
Full/Low
Full/Ave
Full/High
Ph/Ave
Spill/Ave
Spill/High
Flow

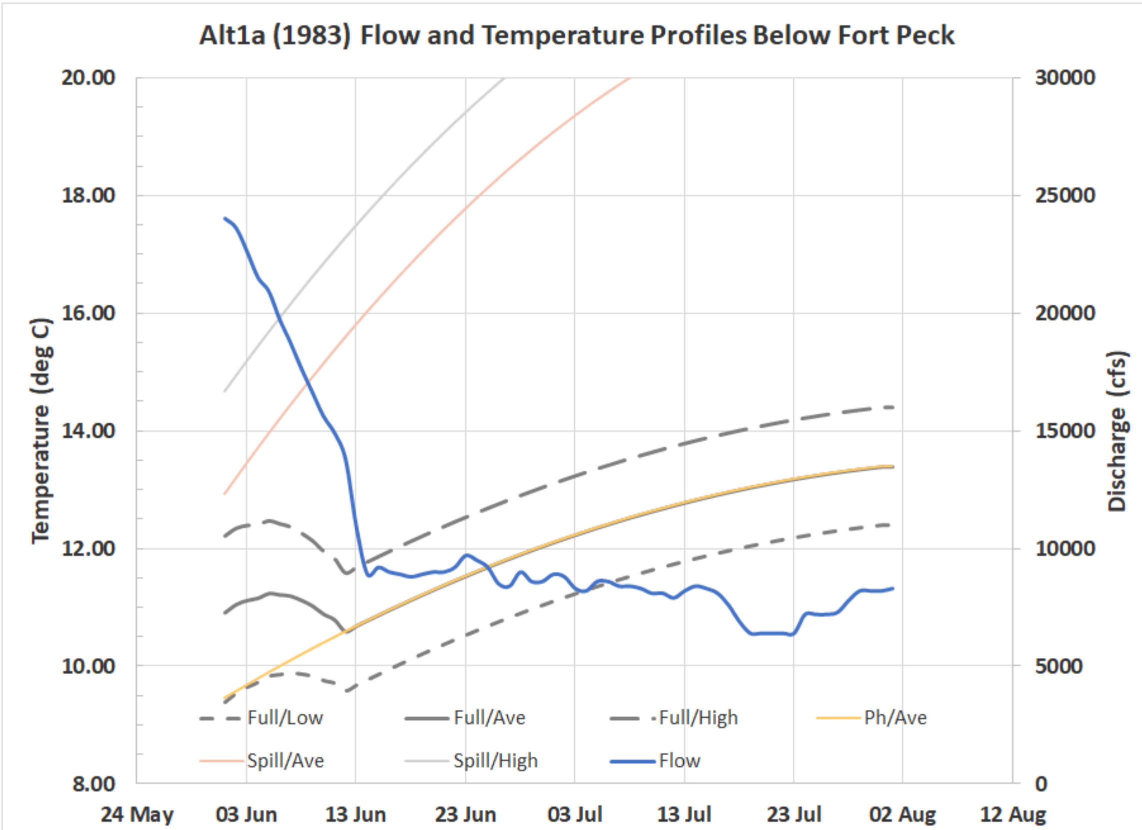
Alt1a (1983) Flow and Temperature Profiles Below Fort Peck
Temperature (deg C)
Discharge (cfs)
20.00
18.00
16.00
14.00
12.00
10.00
8.00
30000
25000
20000
15000
10000
5000
0
24 May
03 Jun
13 Jun
23 Jun
03 Jul
13 Jul
23 Jul
02 Aug
12 Aug
Full/Low
Full/Ave
Full/High
Ph/Ave
Spill/Ave
Spill/High
Flow

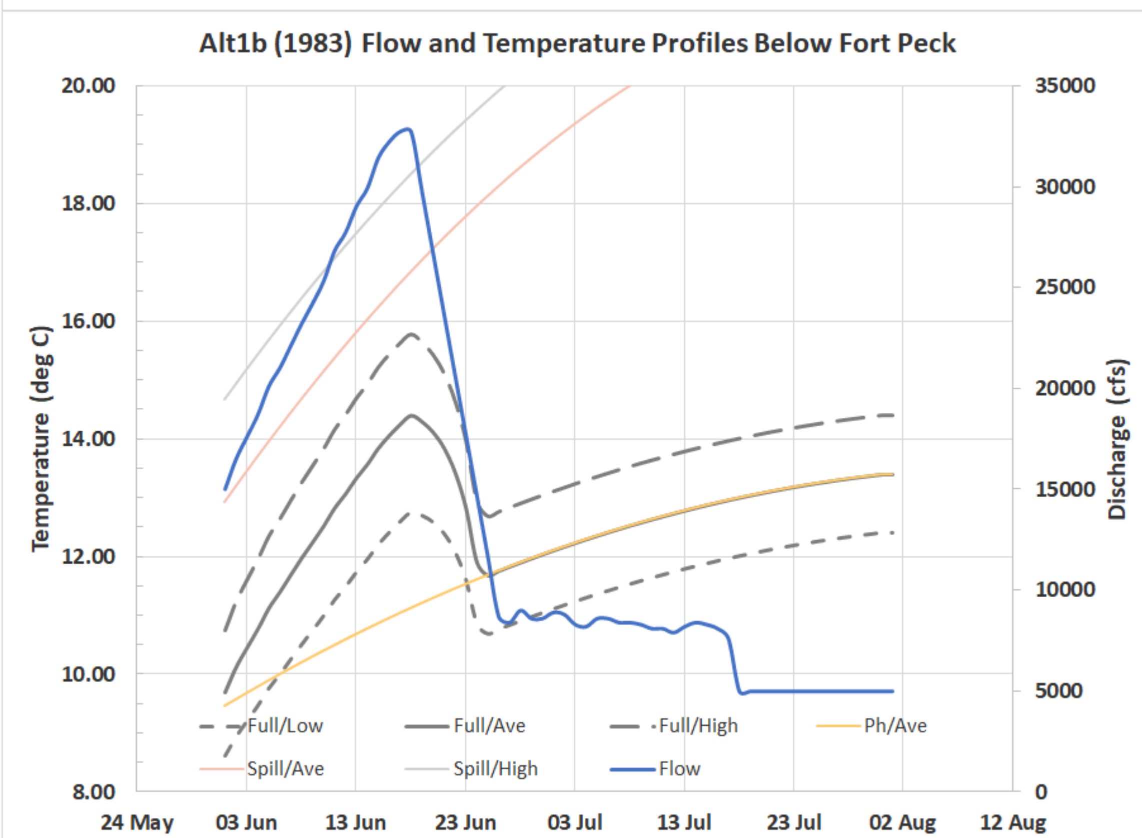
Alt1b (1983) Flow and Temperature Profiles Below Fort Peck
Temperature (deg C)
Discharge (cfs)
20.00
18.00
16.00
14.00
12.00
10.00
8.00
35000
30000
25000
20000
15000
10000
5000
0
24 May
03 Jun
13 Jun
23 Jun
03 Jul
13 Jul
23 Jul
02 Aug
12 Aug
Full/Low
Full/Ave
Full/High
Ph/Ave
Spill/Ave
Spill/High
Flow

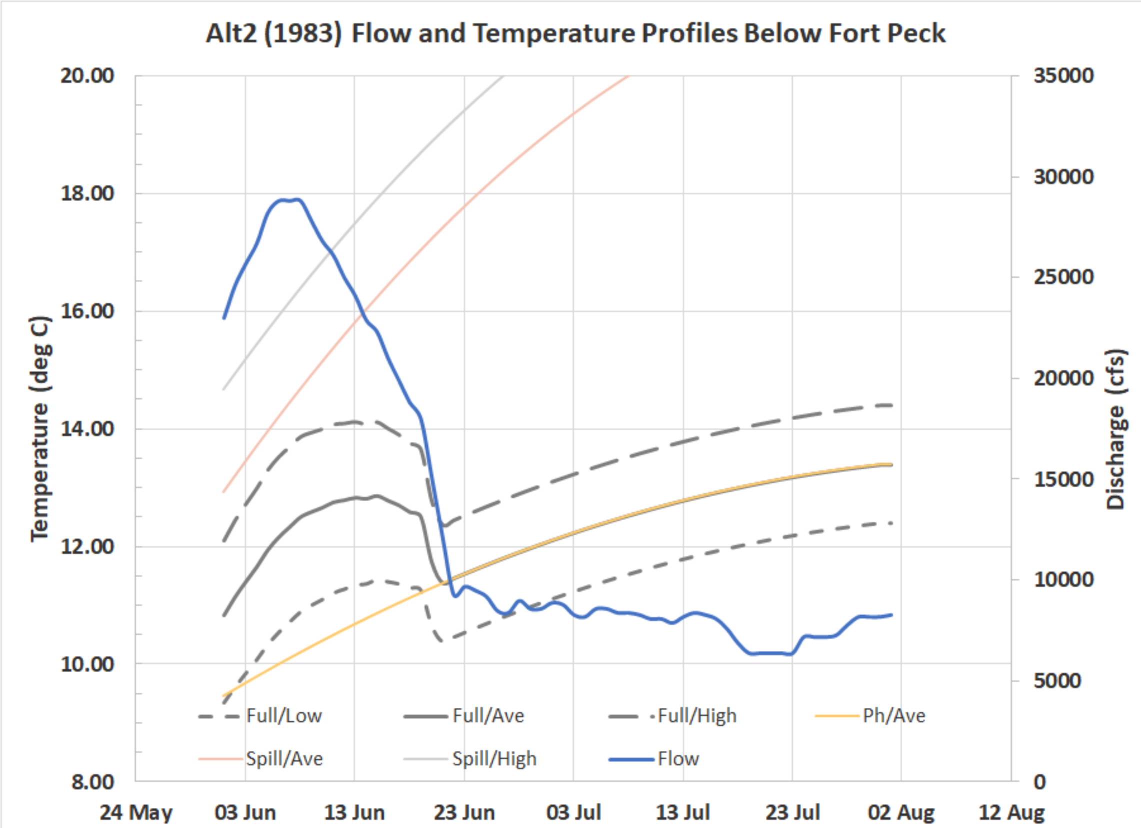
Alt2 (1983) Flow and Temperature Profiles Below Fort Peck
Temperature (deg C)
Discharge (cfs)
20.00
18.00
16.00
14.00
12.00
10.00
8.00
35000
30000
25000
20000
15000
10000
5000
0
24 May
03 Jun
13 Jun
23 Jun
03 Jul
13 Jul
23 Jul
02 Aug
12 Aug
Full/Low
Full/Ave
Full/High
Ph/Ave
Spill/Ave
Spill/High
Flow

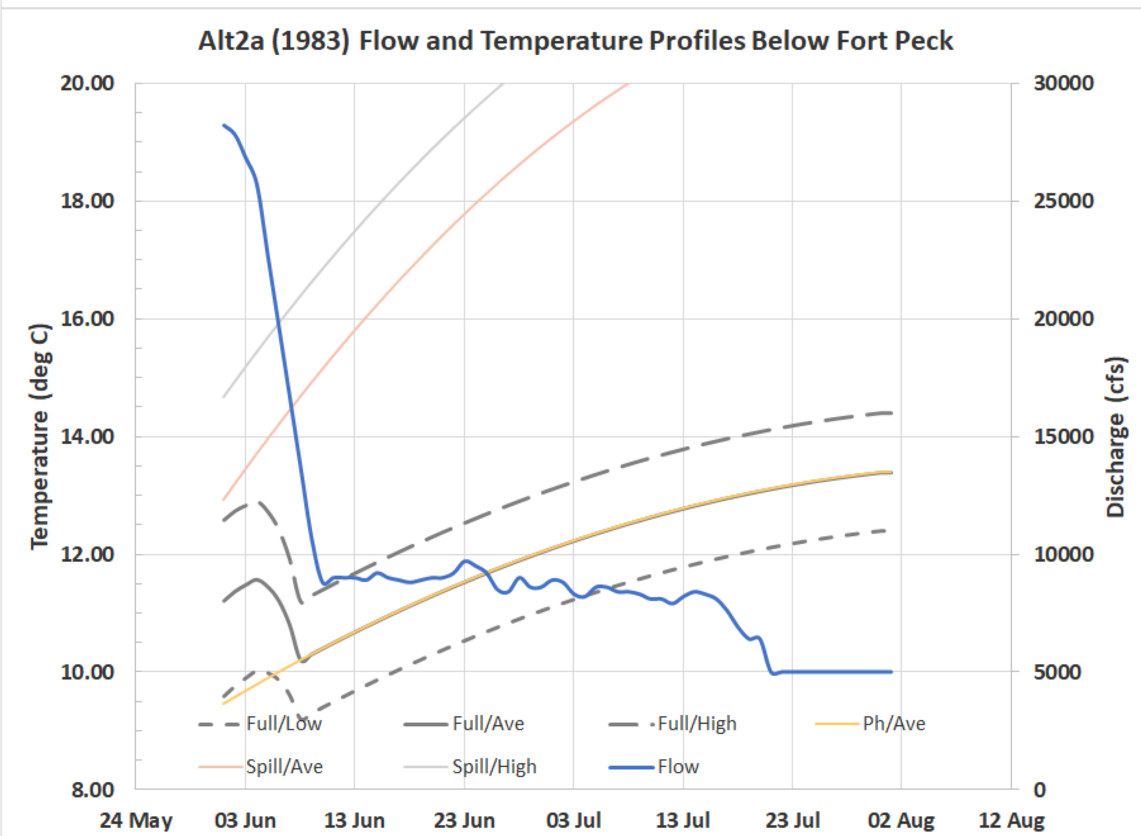
Alt2a (1983) Flow and Temperature Profiles Below Fort Peck
Temperature (deg C)
Discharge (cfs)
20.00
18.00
16.00
14.00
12.00
10.00
8.00
30000
25000
20000
15000
10000
5000
0
24 May
03 Jun
13 Jun
23 Jun
03 Jul
13 Jul
23 Jul
02 Aug
12 Aug
Full/Low
Full/Ave
Full/High
Ph/Ave
Spill/Ave
Spill/High
Flow

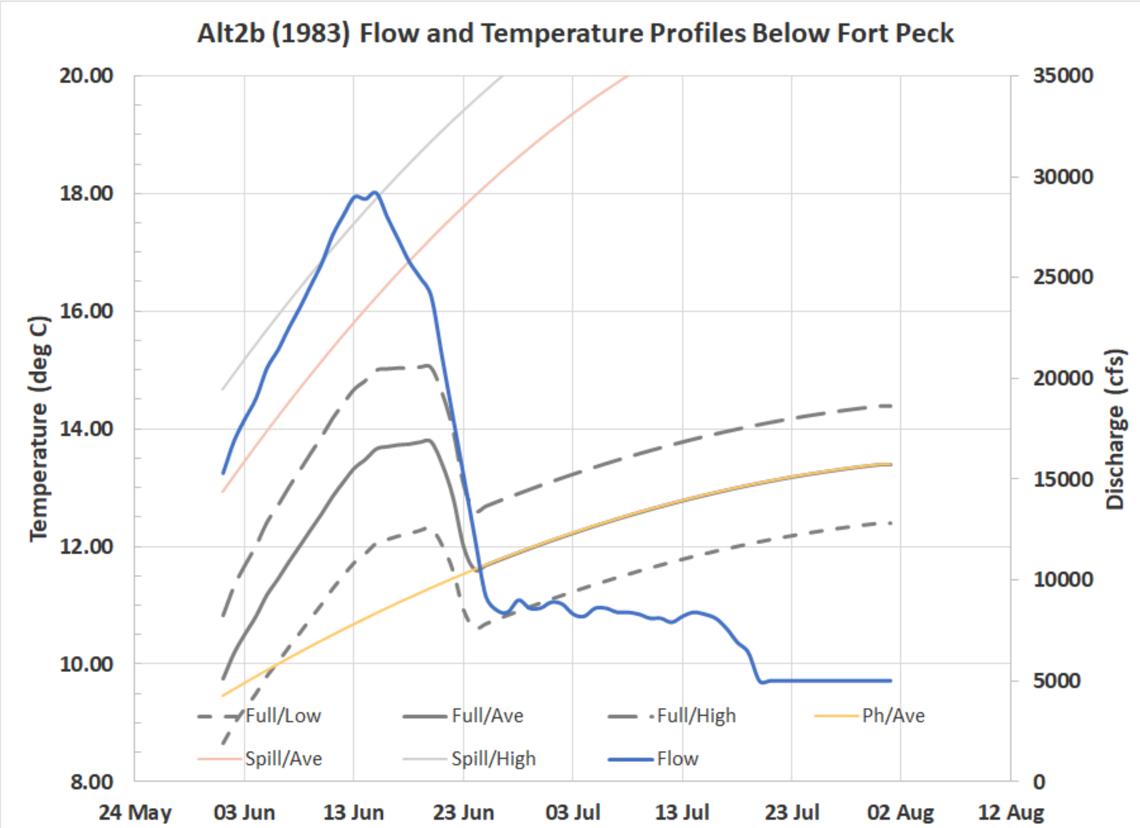
Alt2b (1983) Flow and Temperature Profiles Below Fort Peck
Temperature (deg C)
Discharge (cfs)
20.00
18.00
16.00
14.00
12.00
10.00
8.00
35000
30000
25000
20000
15000
10000
5000
0
24 May
03 Jun
13 Jun
23 Jun
03 Jul
13 Jul
23 Jul
02 Aug
12 Aug
Full/Low
Full/Ave
Full/High
Ph/Ave
Spill/Ave
Spill/High
Flow

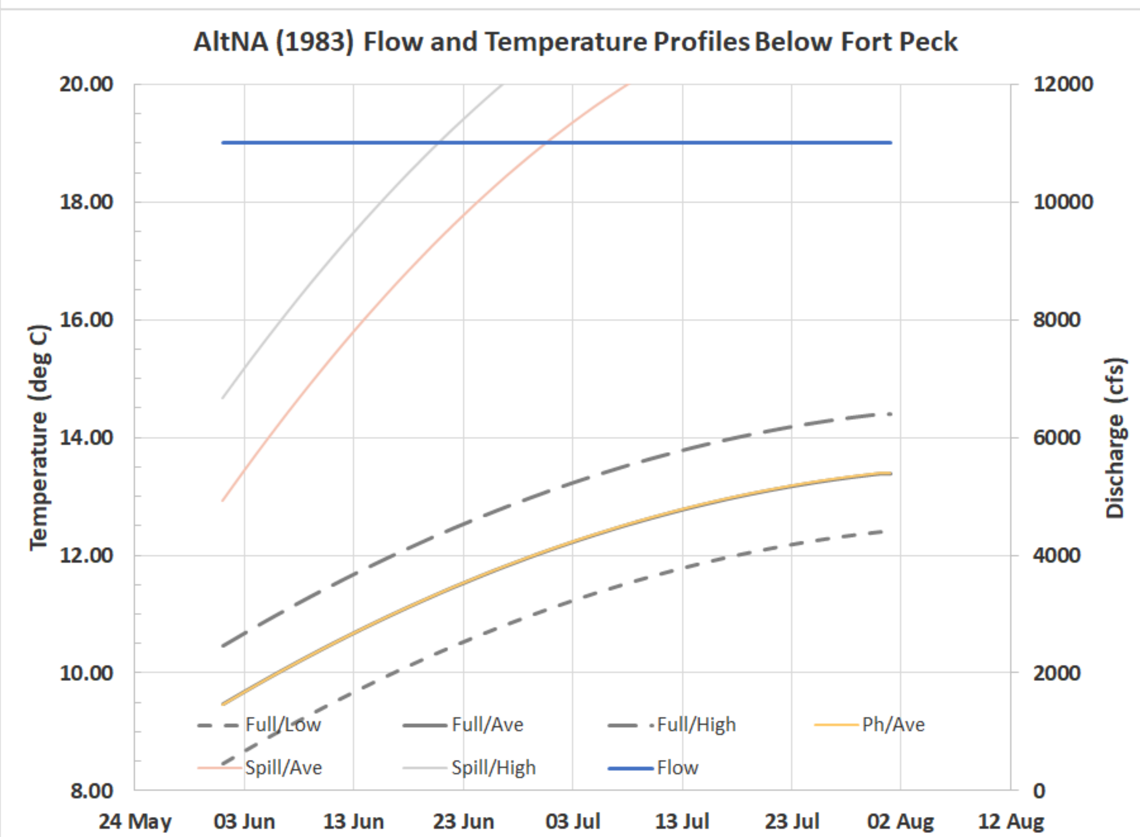
AltNA (1983) Flow and Temperature Profiles Below Fort Peck
Temperature (deg C)
Discharge (cfs)
20.00
18.00
16.00
14.00
12.00
10.00
8.00
12000
10000
8000
6000
4000
2000
0
24 May
03 Jun
13 Jun
23 Jun
03 Jul
13 Jul
23 Jul
02 Aug
12 Aug
Full/Low
Full/Ave
Full/High
Ph/Ave
Spill/Ave
Spill/High
Flow

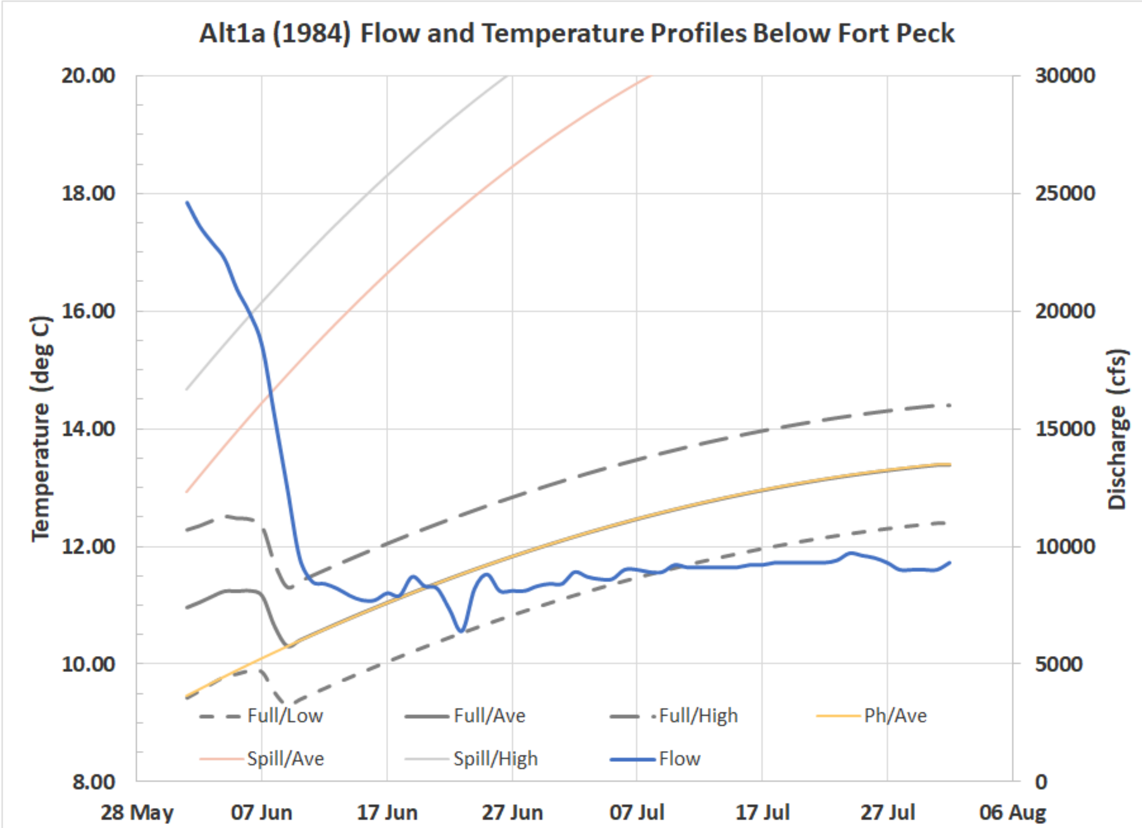
Alt1a (1984) Flow and Temperature Profiles Below Fort Peck
Temperature (deg C)
Discharge (cfs)
20.00
18.00
16.00
14.00
12.00
10.00
8.00
30000
25000
20000
15000
10000
5000
0
28 May
07 Jun
17 Jun
27 Jun
07 Jul
17 Jul
27 Jul
06 Aug
Full/Low
Full/Ave
Full/High
Ph/Ave
Spill/Ave
Spill/High
Flow

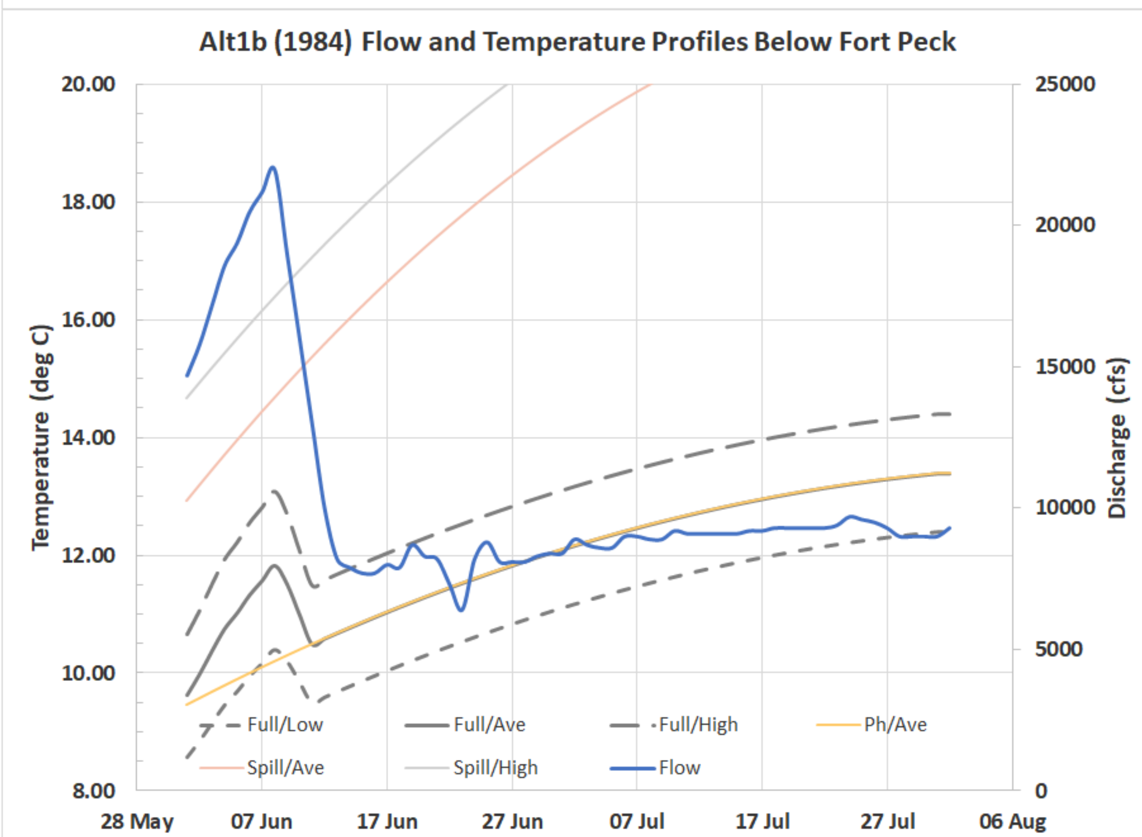
Alt1b (1984) Flow and Temperature Profiles Below Fort Peck
Temperature (deg C)
Discharge (cfs)
20.00
18.00
16.00
14.00
12.00
10.00
8.00
25000
20000
15000
10000
5000
0
28 May
07 Jun
17 Jun
27 Jun
07 Jul
17 Jul
27 Jul
06 Aug
Full/Low
Full/Ave
Full/High
Ph/Ave
Spill/Ave
Spill/High
Flow

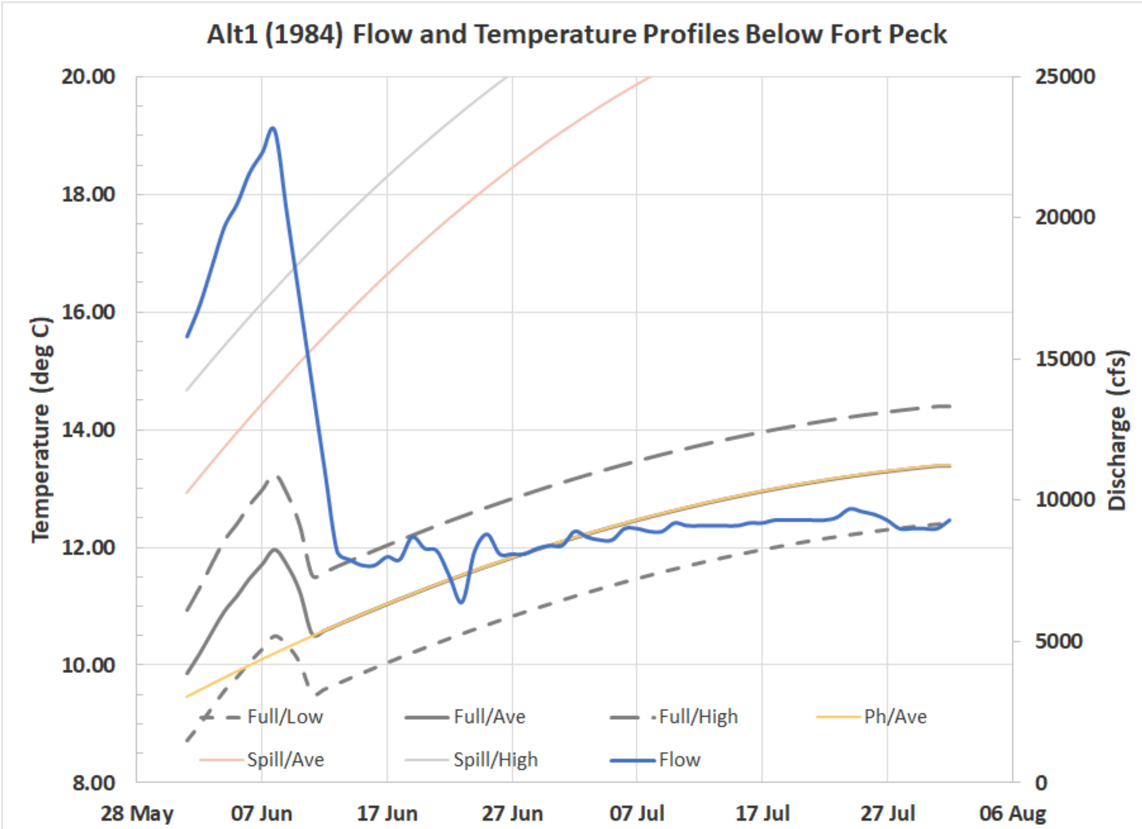
Alt1 (1984) Flow and Temperature Profiles Below Fort Peck
Temperature (deg C)
20.00
18.00
16.00
14.00
12.00
10.00
8.00
Discharge (cfs)
25000
20000
15000
10000
5000
0
28 May
07 Jun
17 Jun
27 Jun
07 Jul
17 Jul
27 Jul
06 Aug
Full/Low
Full/Ave
Full/High
Ph/Ave
Spill/Ave
Spill/High
Flow

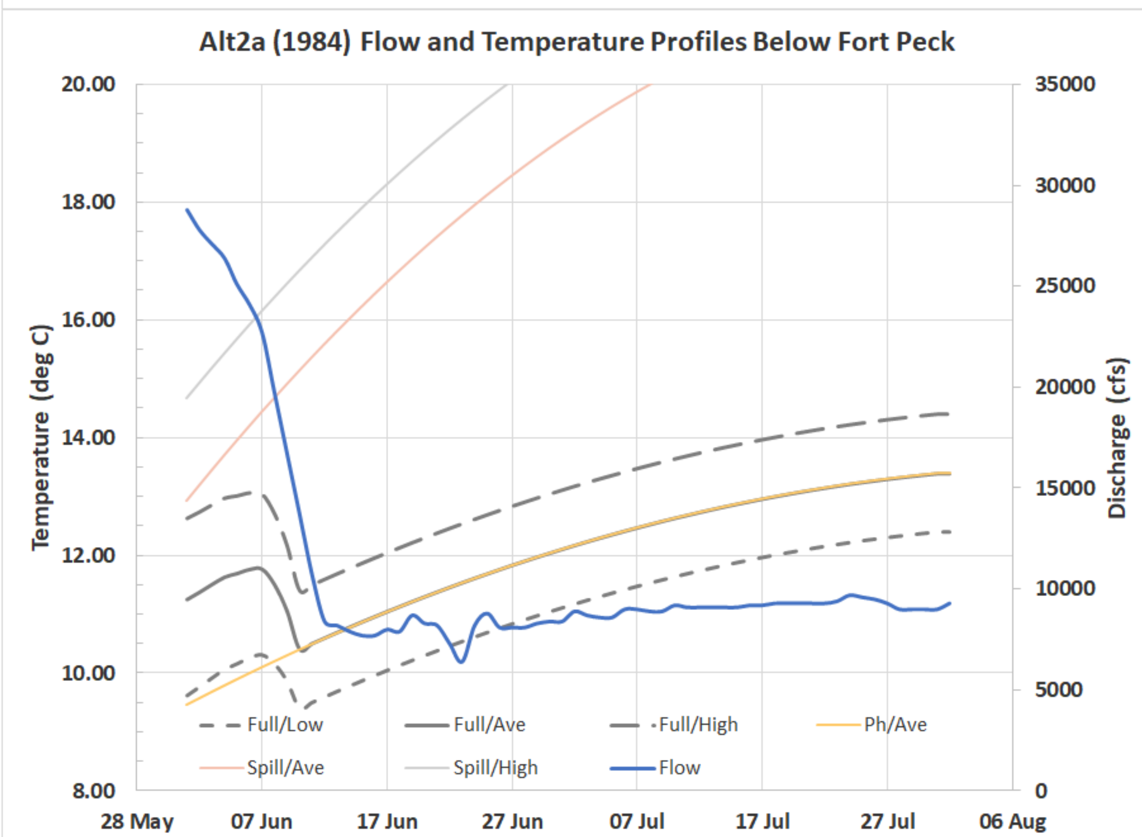
Alt2a (1984) Flow and Temperature Profiles Below Fort Peck
Temperature (deg C)
20.00
18.00
16.00
14.00
12.00
10.00
8.00
Discharge (cfs)
35000
30000
25000
20000
15000
10000
5000
0
28 May
07 Jun
17 Jun
27 Jun
07 Jul
17 Jul
27 Jul
06 Aug
Full/Low
Full/Ave
Full/High
Ph/Ave
Spill/Ave
Spill/High
Flow

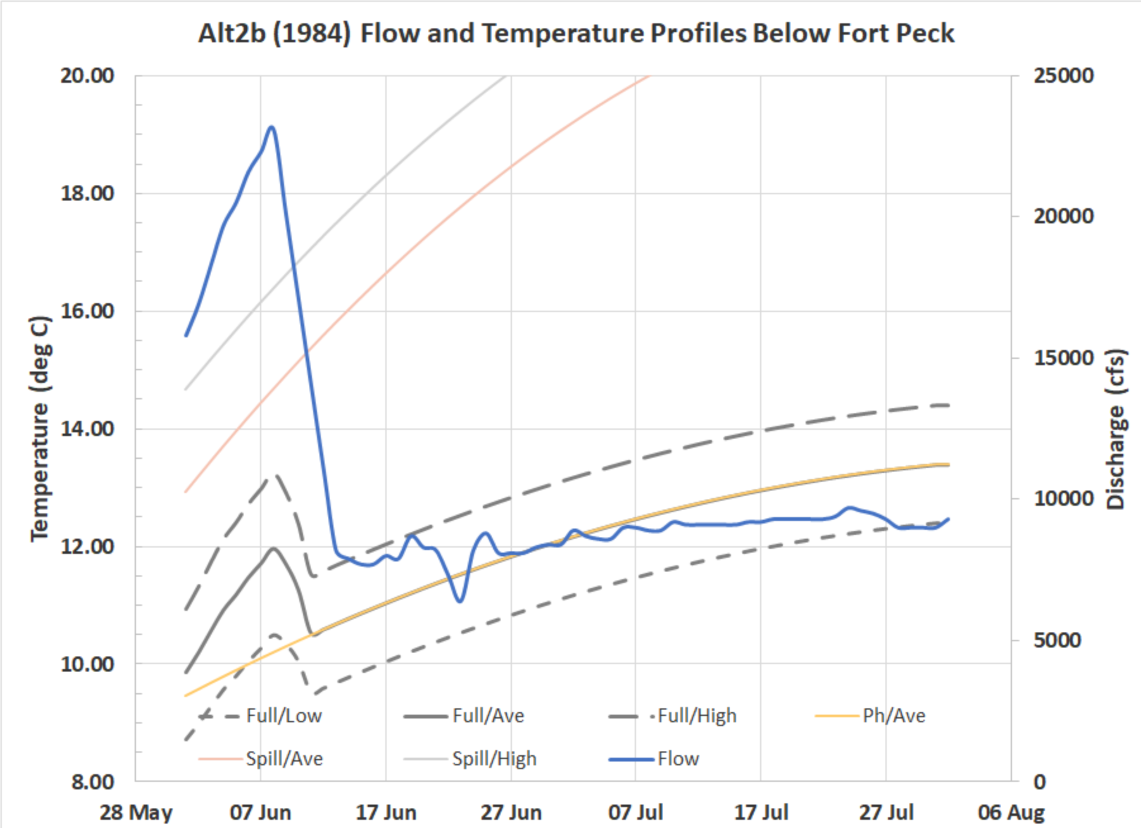
Alt2b (1984) Flow and Temperature Profiles Below Fort Peck
Temperature (deg C)
Discharge (cfs)
20.00
18.00
16.00
14.00
12.00
10.00
8.00
25000
20000
15000
10000
5000
0
28 May
07 Jun
17 Jun
27 Jun
07 Jul
17 Jul
27 Jul
06 Aug
Full/Low
Full/Ave
Full/High
Ph/Ave
Spill/Ave
Spill/High
Flow

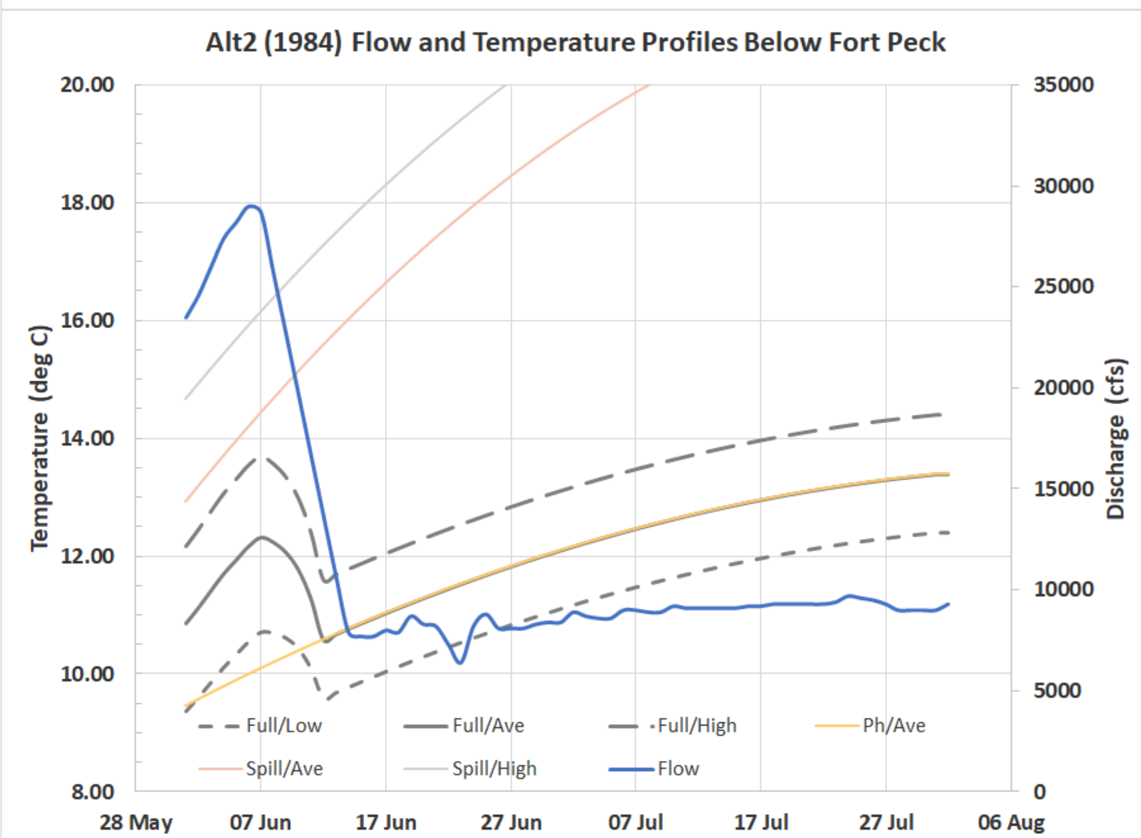
Alt2 (1984) Flow and Temperature Profiles Below Fort Peck
Temperature (deg C)
Discharge (cfs)
20.00
18.00
16.00
14.00
12.00
10.00
8.00
35000
30000
25000
20000
15000
10000
5000
0
28 May
07 Jun
17 Jun
27 Jun
07 Jul
17 Jul
27 Jul
06 Aug
Full/Low
Full/Ave
Full/High
Ph/Ave
Spill/Ave
Spill/High
Flow

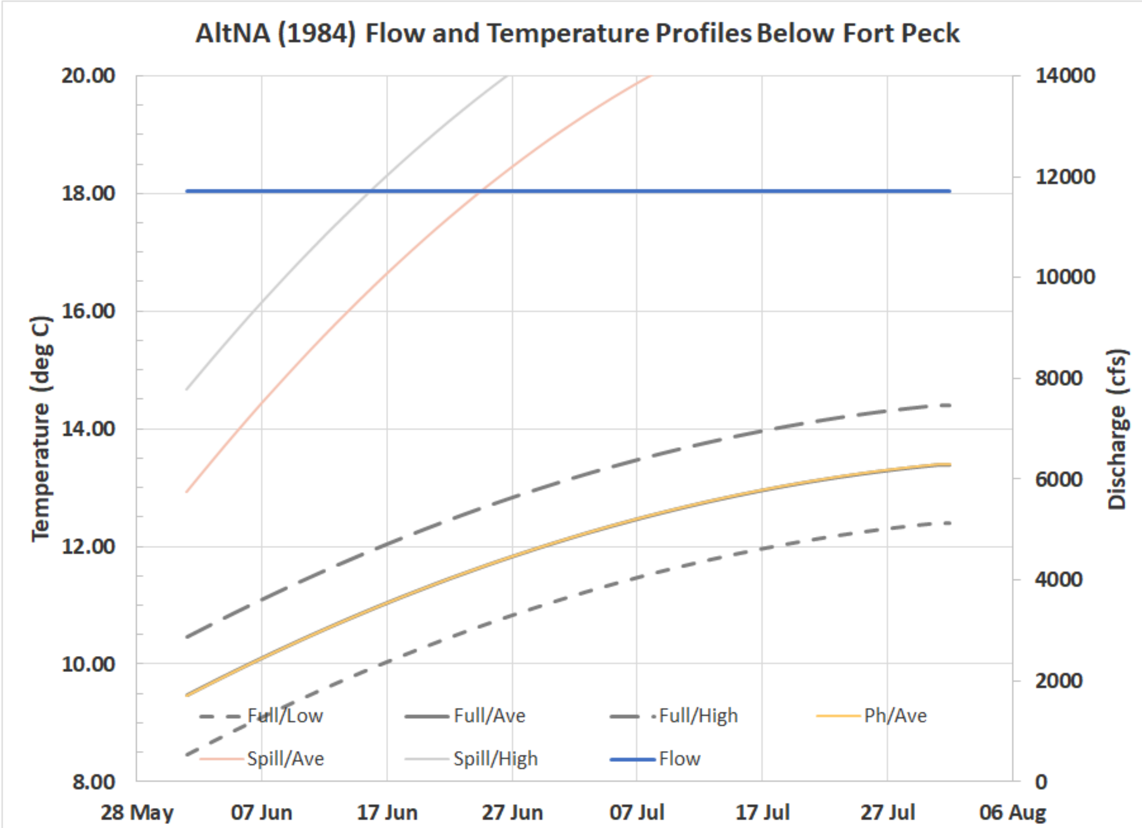
AltNA (1984) Flow and Temperature Profiles Below Fort Peck
Temperature (deg C)
Discharge (cfs)
20.00
18.00
16.00
14.00
12.00
10.00
8.00
14000
12000
10000
8000
6000
4000
2000
0
28 May
07 Jun
17 Jun
27 Jun
07 Jul
17 Jul
27 Jul
06 Aug
Full/Low
Full/Ave
Full/High
Ph/Ave
Spill/Ave
Spill/High
Flow

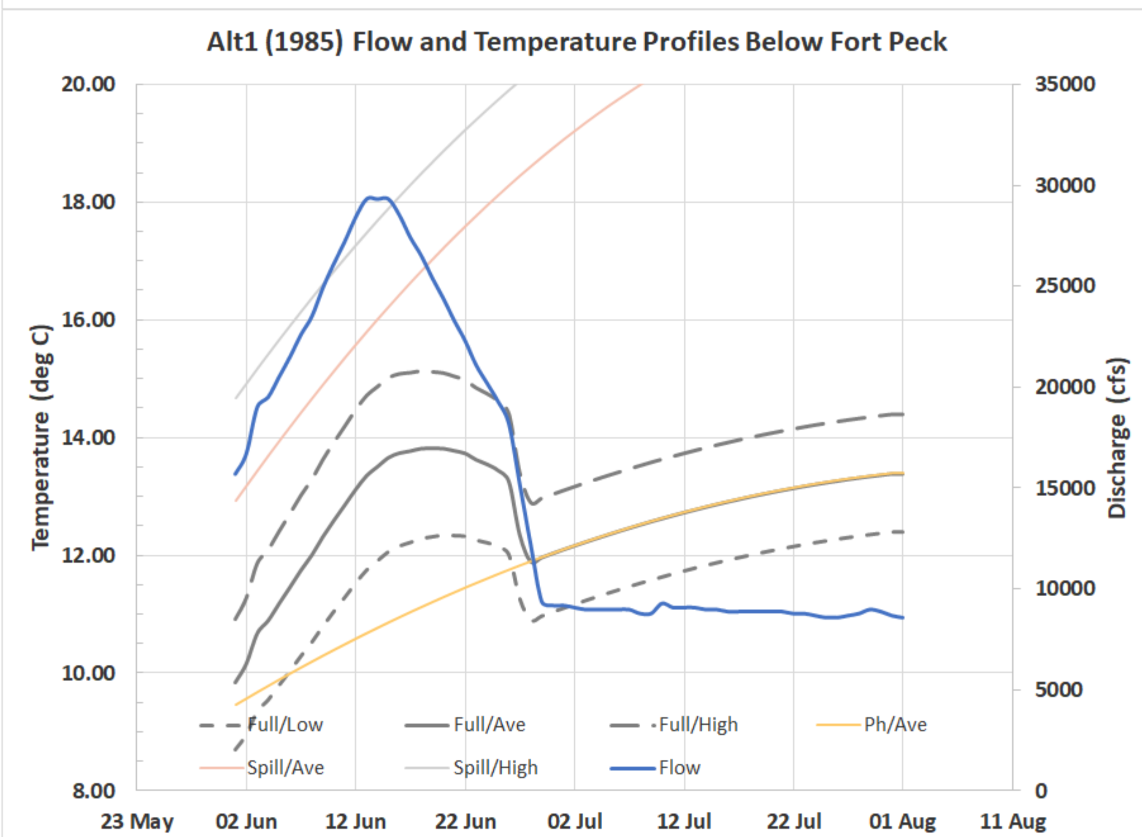
Alt1 (1985) Flow and Temperature Profiles Below Fort Peck
Temperature (deg C)
Discharge (cfs)
20.00
18.00
16.00
14.00
12.00
10.00
8.00
35000
30000
25000
20000
15000
10000
5000
0
23 May
02 Jun
12 Jun
22 Jun
02 Jul
12 Jul
22 Jul
01 Aug
11 Aug
Full/Low
Full/Ave
Full/High
Ph/Ave
Spill/Ave
Spill/High
Flow

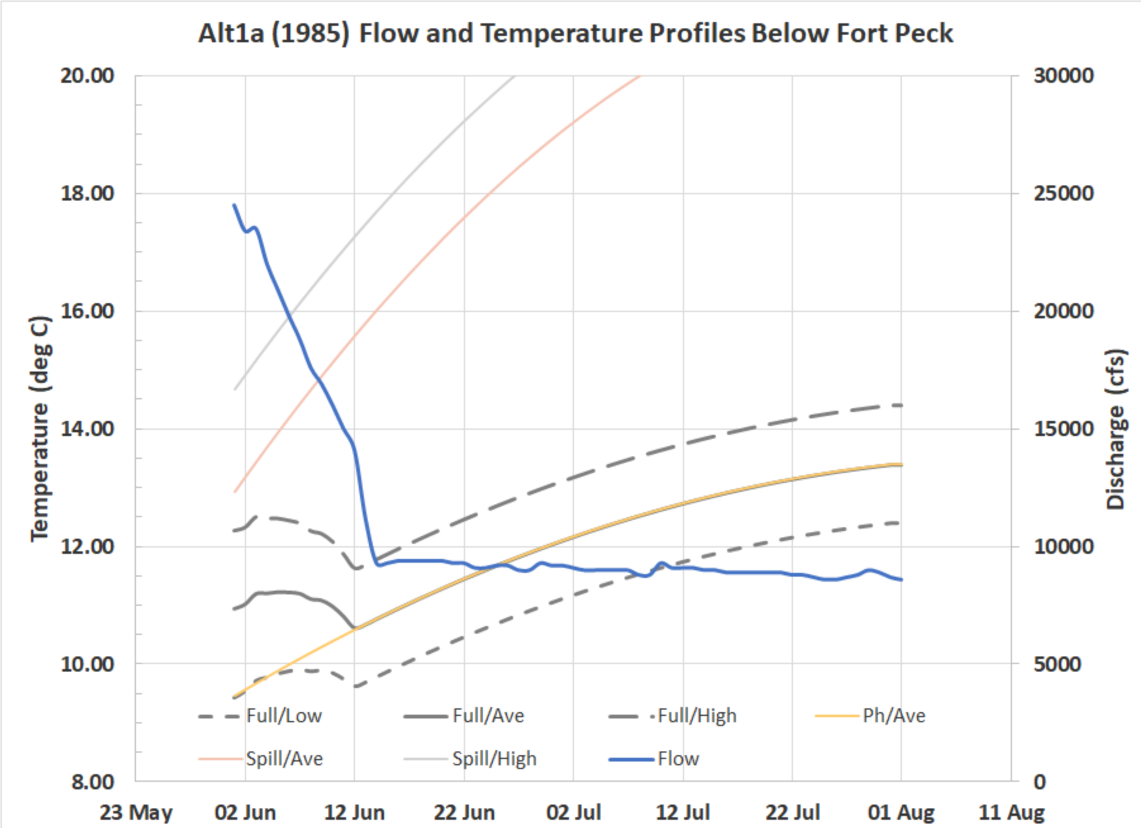
Alt1a (1985) Flow and Temperature Profiles Below Fort Peck
Temperature (deg C)
20.00
18.00
16.00
14.00
12.00
10.00
8.00
Discharge (cfs)
30000
25000
20000
15000
10000
5000
0
23 May
02 Jun
12 Jun
22 Jun
02 Jul
12 Jul
22 Jul
01 Aug
11 Aug
Full/Low
Full/Ave
Full/High
Ph/Ave
Spill/Ave
Spill/High
Flow

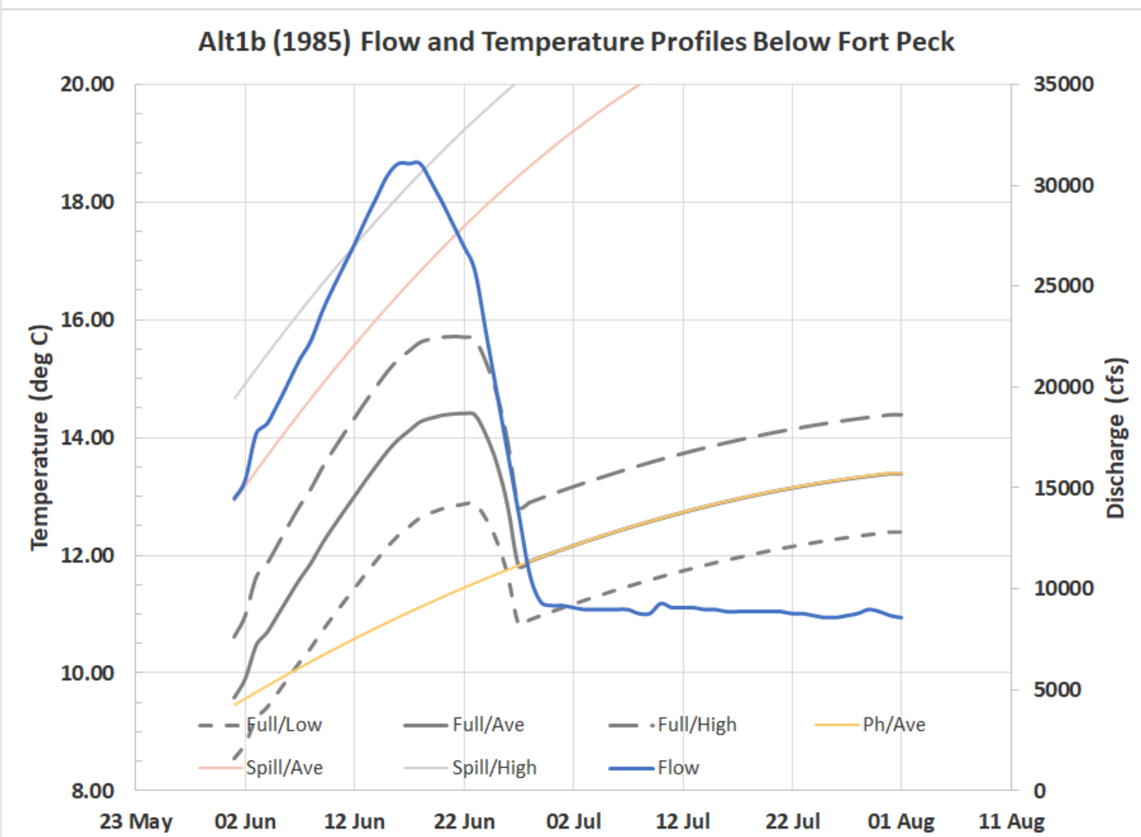
Alt1b (1985) Flow and Temperature Profiles Below Fort Peck
Temperature (deg C)
20.00
18.00
16.00
14.00
12.00
10.00
8.00
Discharge (cfs)
35000
30000
25000
20000
15000
10000
5000
0
23 May
02 Jun
12 Jun
22 Jun
02 Jul
12 Jul
22 Jul
01 Aug
11 Aug
Full/Low
Full/Ave
Full/High
Ph/Ave
Spill/Ave
Spill/High
Flow

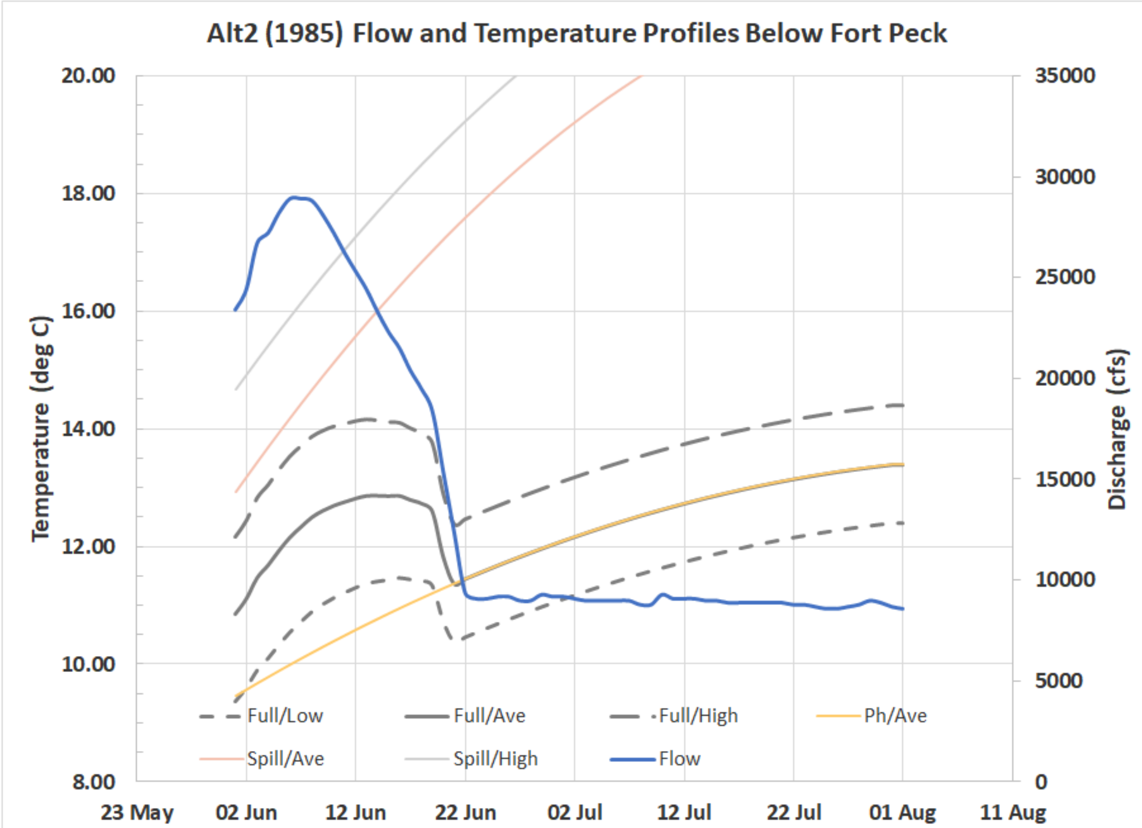
Alt2 (1985) Flow and Temperature Profiles Below Fort Peck
Temperature (deg C)
Discharge (cfs)
20.00
18.00
16.00
14.00
12.00
10.00
8.00
35000
30000
25000
20000
15000
10000
5000
0
23 May
02 Jun
12 Jun
22 Jun
02 Jul
12 Jul
22 Jul
01 Aug
11 Aug
Full/Low
Full/Ave
Full/High
Ph/Ave
Spill/Ave
Spill/High
Flow

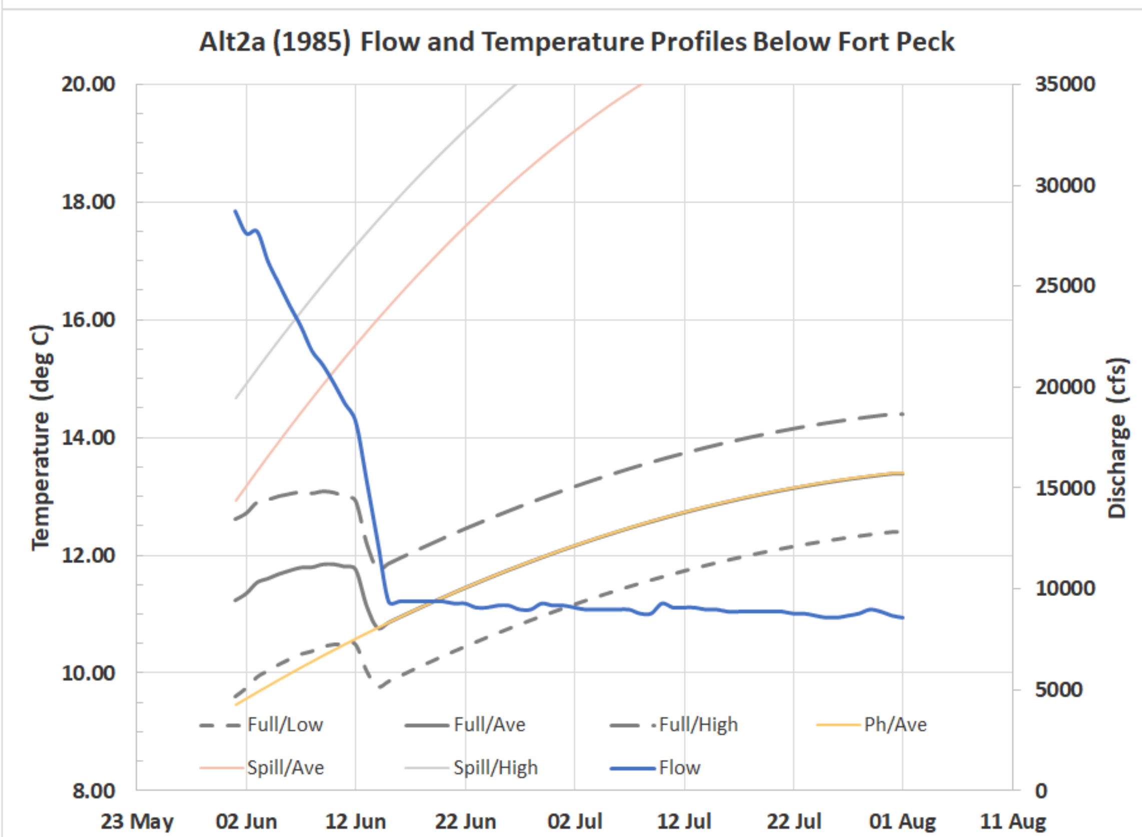
Alt2a (1985) Flow and Temperature Profiles Below Fort Peck
Temperature (deg C)
Discharge (cfs)
20.00
18.00
16.00
14.00
12.00
10.00
8.00
35000
30000
25000
20000
15000
10000
5000
0
23 May
02 Jun
12 Jun
22 Jun
02 Jul
12 Jul
22 Jul
01 Aug
11 Aug
Full/Low
Full/Ave
Full/High
Ph/Ave
Spill/Ave
Spill/High
Flow

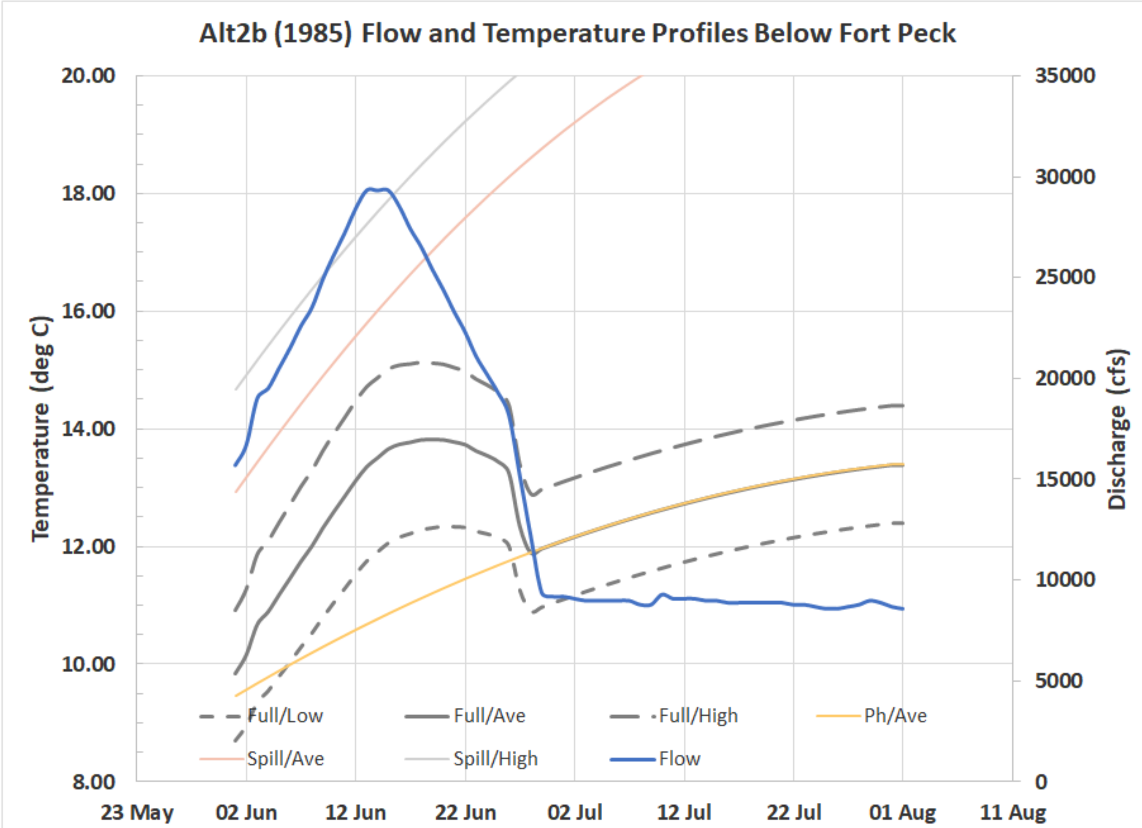
Alt2b (1985) Flow and Temperature Profiles Below Fort Peck
Temperature (deg C)
20.00
18.00
16.00
14.00
12.00
10.00
8.00
Discharge (cfs)
35000
30000
25000
20000
15000
10000
5000
0
23 May
02 Jun
12 Jun
22 Jun
02 Jul
12 Jul
22 Jul
01 Aug
11 Aug
Full/Low
Full/Ave
Full/High
Ph/Ave
Spill/Ave
Spill/High
Flow

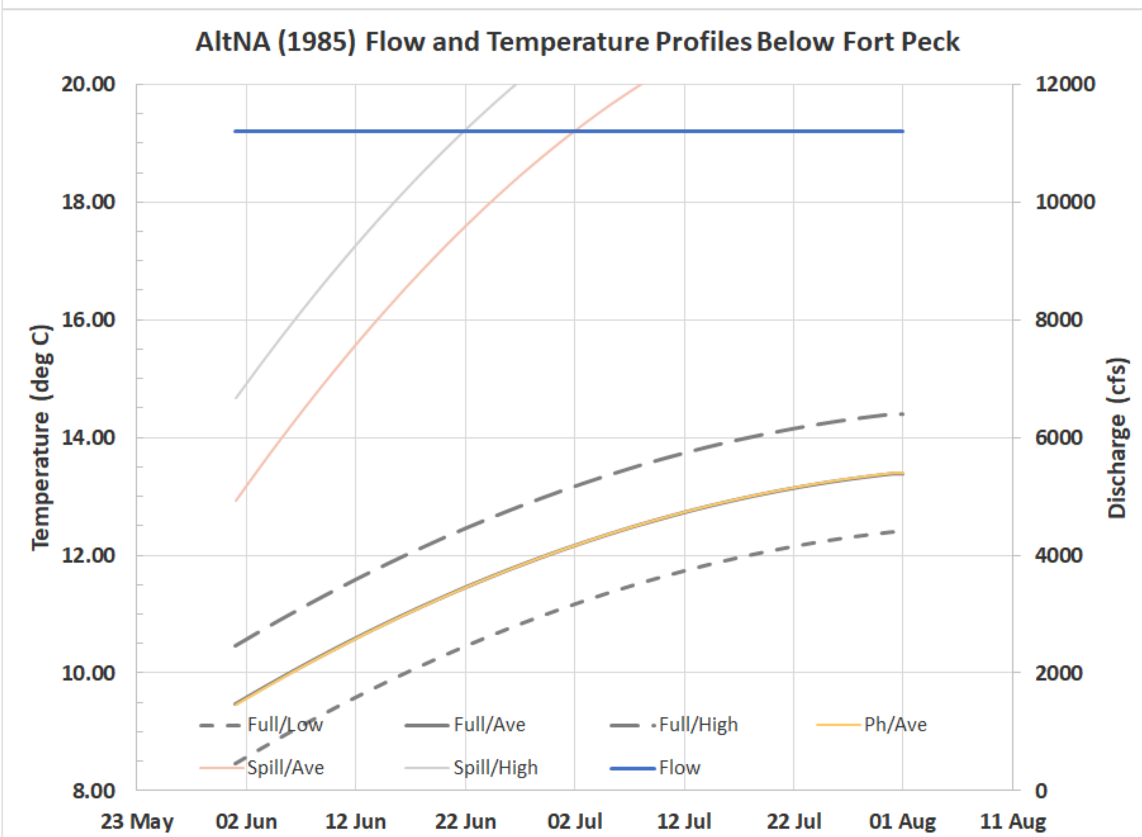
AltNA (1985) Flow and Temperature Profiles Below Fort Peck
Temperature (deg C)
20.00
18.00
16.00
14.00
12.00
10.00
8.00
Discharge (cfs)
12000
10000
8000
6000
4000
2000
0
23 May
02 Jun
12 Jun
22 Jun
02 Jul
12 Jul
22 Jul
01 Aug
11 Aug
Full/Low
Full/Ave
Full/High
Ph/Ave
Spill/Ave
Spill/High
Flow

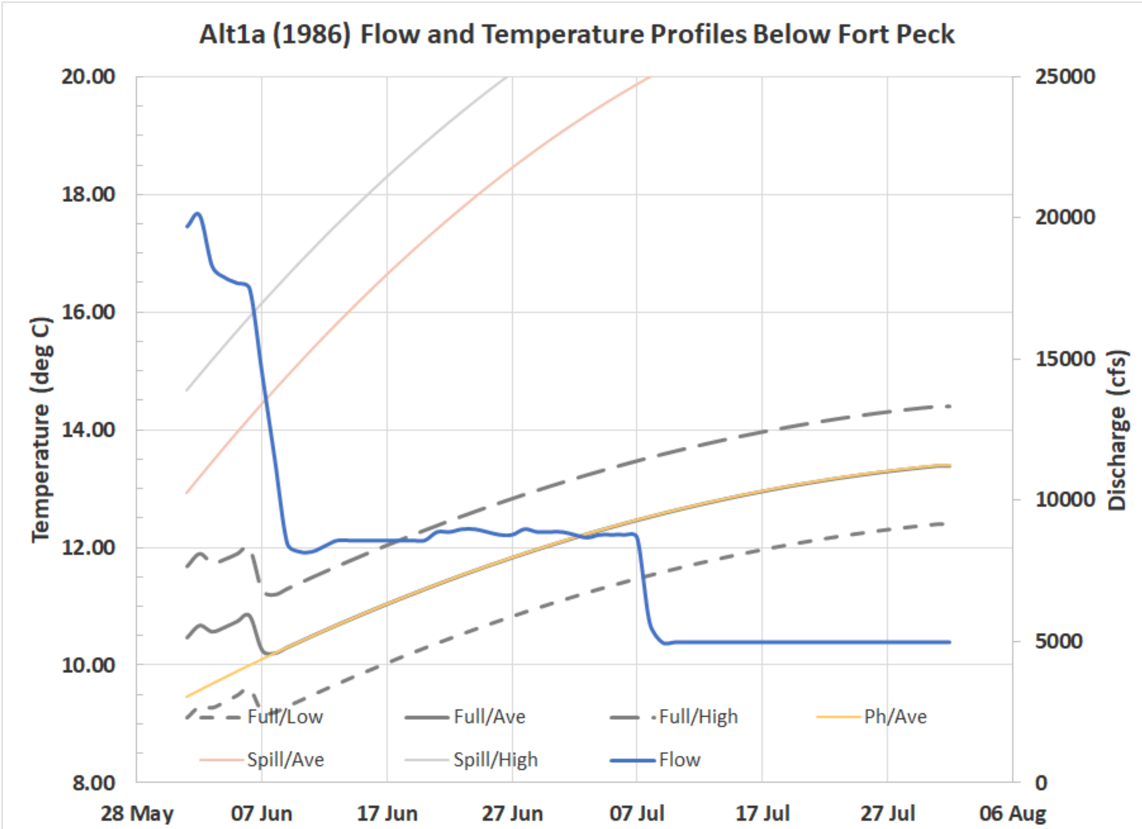
Alt1a (1986) Flow and Temperature Profiles Below Fort Peck
Temperature (deg C)
Discharge (cfs)
20.00
18.00
16.00
14.00
12.00
10.00
8.00
25000
20000
15000
10000
5000
0
28 May
07 Jun
17 Jun
27 Jun
07 Jul
17 Jul
27 Jul
06 Aug
Full/Low
Full/Ave
Full/High
Ph/Ave
Spill/Ave
Spill/High
Flow

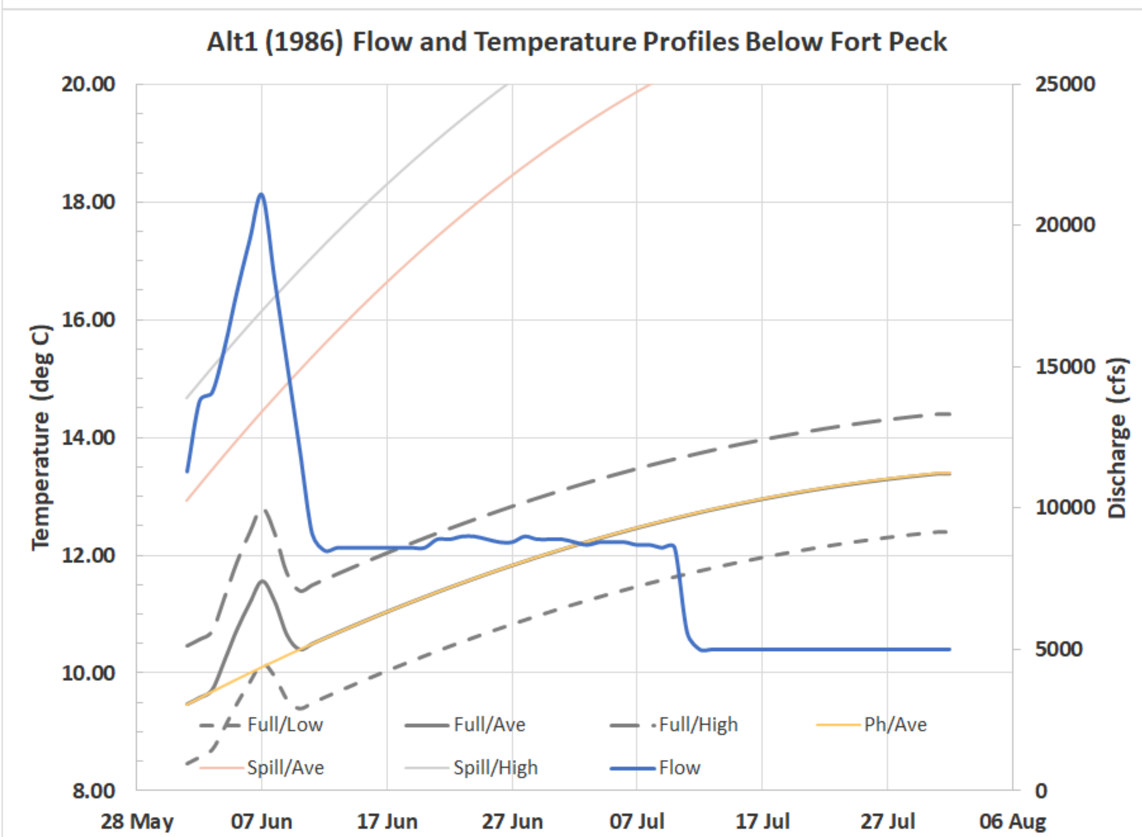
Alt1 (1986) Flow and Temperature Profiles Below Fort Peck
Temperature (deg C)
Discharge (cfs)
20.00
18.00
16.00
14.00
12.00
10.00
8.00
25000
20000
15000
10000
5000
0
28 May
07 Jun
17 Jun
27 Jun
07 Jul
17 Jul
27 Jul
06 Aug
Full/Low
Full/Ave
Full/High
Ph/Ave
Spill/Ave
Spill/High
Flow

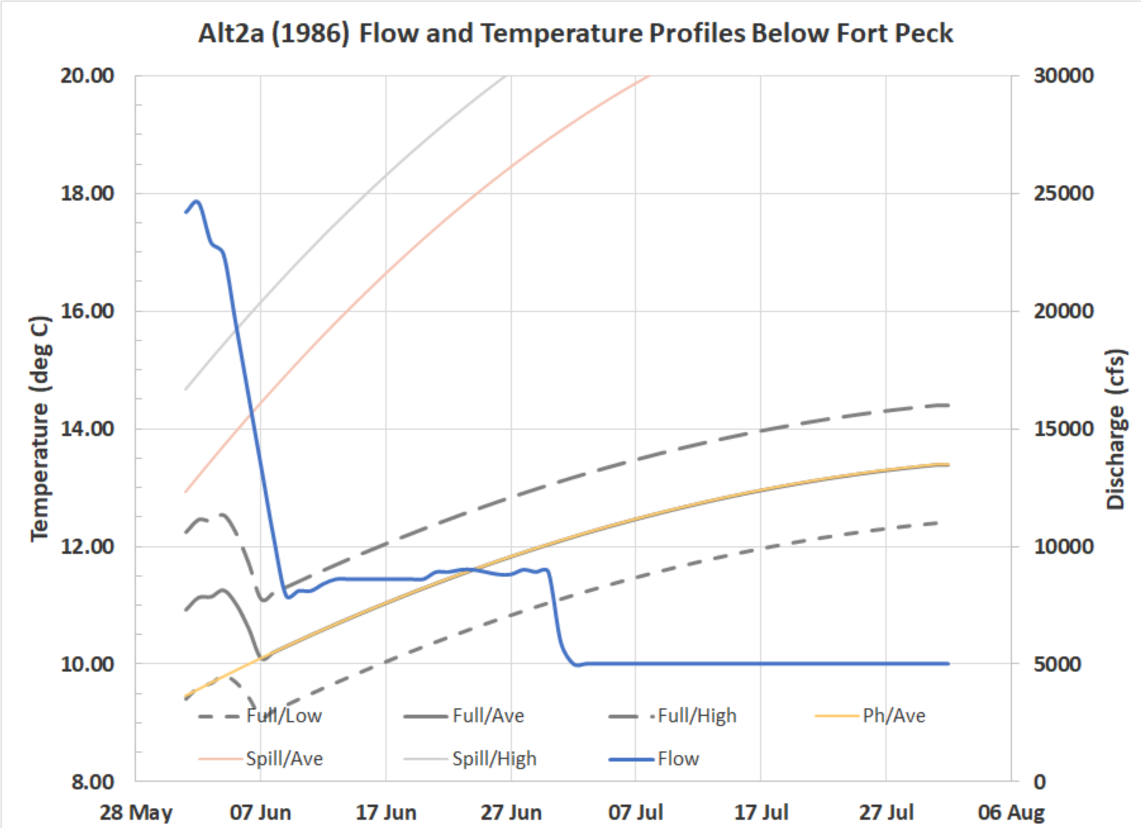
Alt2a (1986) Flow and Temperature Profiles Below Fort Peck
Temperature (deg C)
Discharge (cfs)
20.00
18.00
16.00
14.00
12.00
10.00
8.00
30000
25000
20000
15000
10000
5000
0
28 May
07 Jun
17 Jun
27 Jun
07 Jul
17 Jul
27 Jul
06 Aug
Full/Low
Full/Ave
Full/High
Ph/Ave
Spill/Ave
Spill/High
Flow

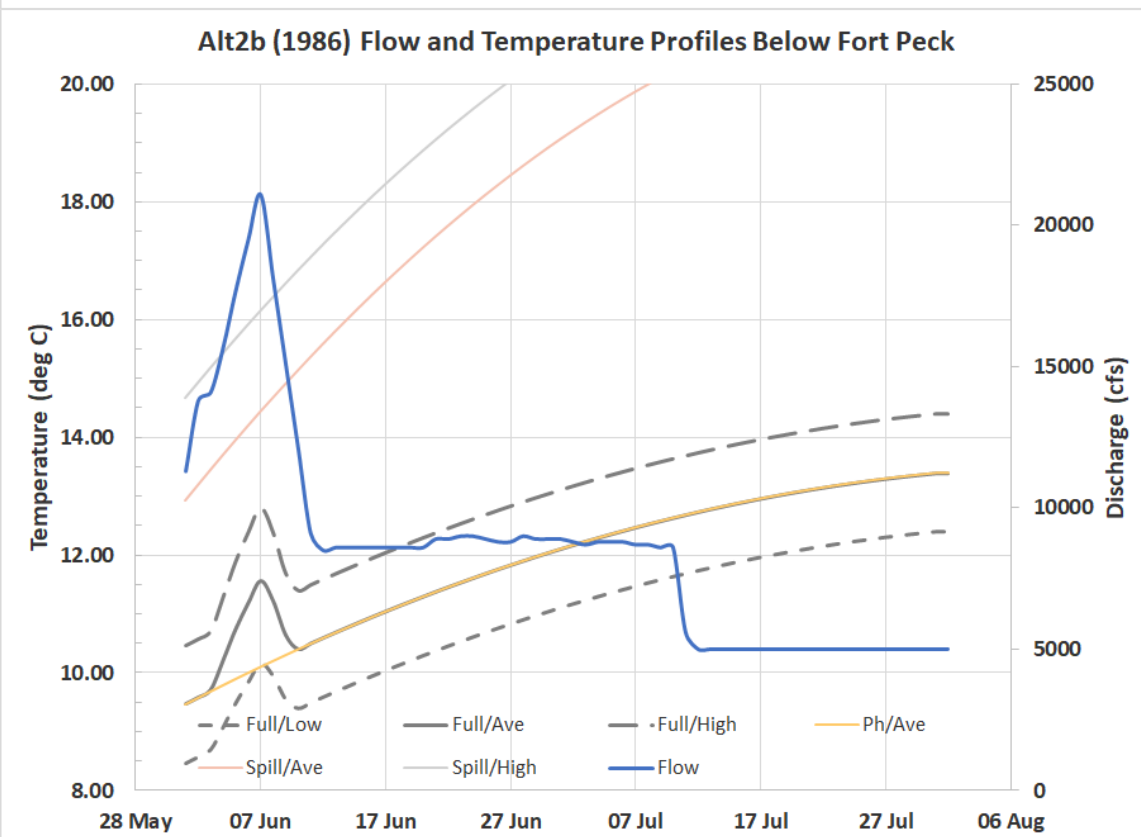
Alt2b (1986) Flow and Temperature Profiles Below Fort Peck
Temperature (deg C)
Discharge (cfs)
20.00
18.00
16.00
14.00
12.00
10.00
8.00
25000
20000
15000
10000
5000
0
28 May
07 Jun
17 Jun
27 Jun
07 Jul
17 Jul
27 Jul
06 Aug
Full/Low
Full/Ave
Full/High
Ph/Ave
Spill/Ave
Spill/High
Flow

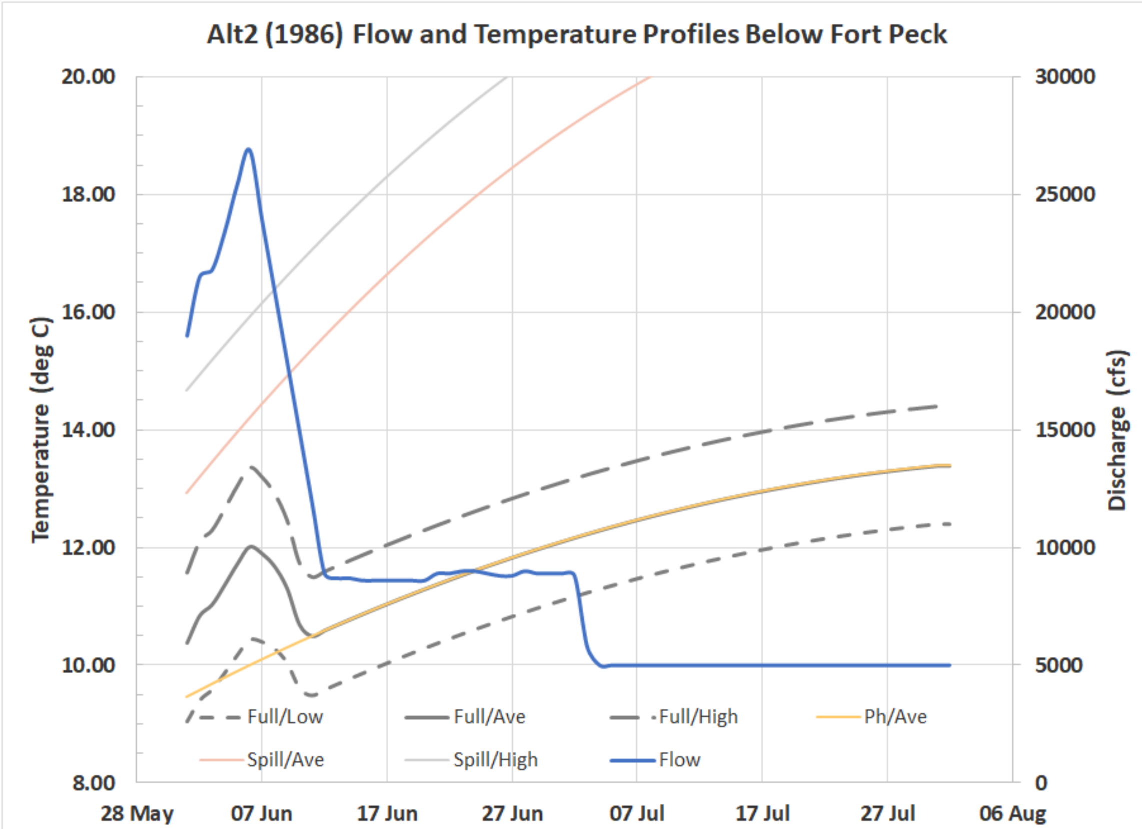
Alt2 (1986) Flow and Temperature Profiles Below Fort Peck
Temperature (deg C)
Discharge (cfs)
20.00
18.00
16.00
14.00
12.00
10.00
8.00
30000
25000
20000
15000
10000
5000
0
28 May
07 Jun
17 Jun
27 Jun
07 Jul
17 Jul
27 Jul
06 Aug
Full/Low
Full/Ave
Full/High
Ph/Ave
Spill/Ave
Spill/High
Flow

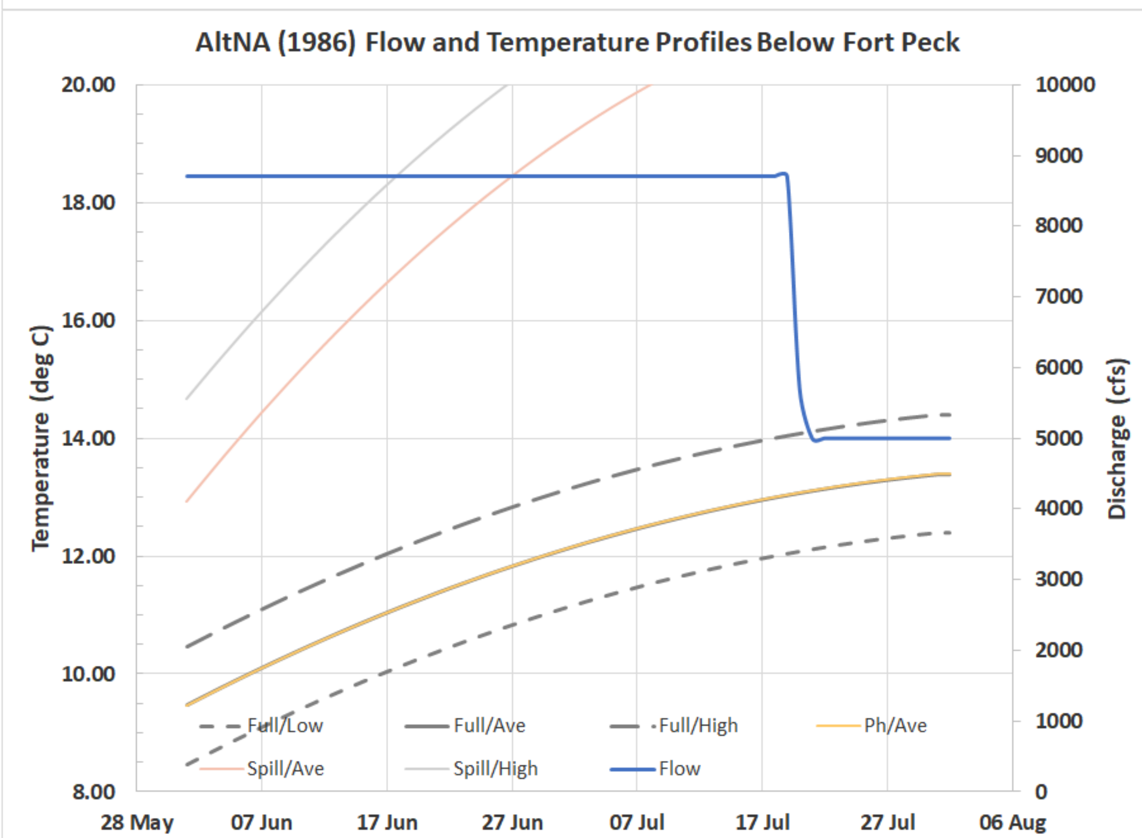
AltNA (1986) Flow and Temperature Profiles Below Fort Peck
Temperature (deg C)
Discharge (cfs)
20.00
18.00
16.00
14.00
12.00
10.00
8.00
10000
9000
8000
7000
6000
5000
4000
3000
2000
1000
0
28 May
07 Jun
17 Jun
27 Jun
07 Jul
17 Jul
27 Jul
06 Aug
Full/Low
Full/Ave
Full/High
Ph/Ave
Spill/Ave
Spill/High
Flow

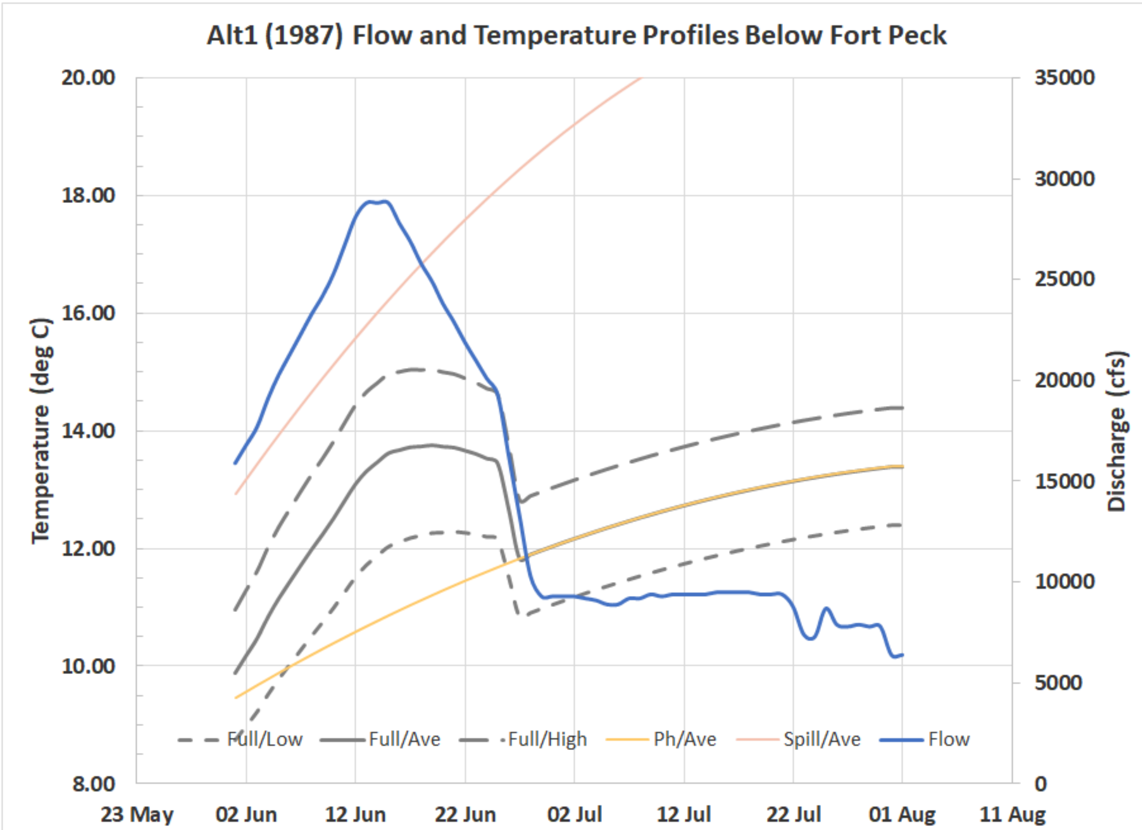
Alt1 (1987) Flow and Temperature Profiles Below Fort Peck
Temperature (deg C)
Discharge (cfs)
20.00
18.00
16.00
14.00
12.00
10.00
8.00
35000
30000
25000
20000
15000
10000
5000
0
23 May
02 Jun
12 Jun
22 Jun
02 Jul
12 Jul
22 Jul
01 Aug
11 Aug
Full/Low
Full/Ave
Full/High
Ph/Ave
Spill/Ave
Flow

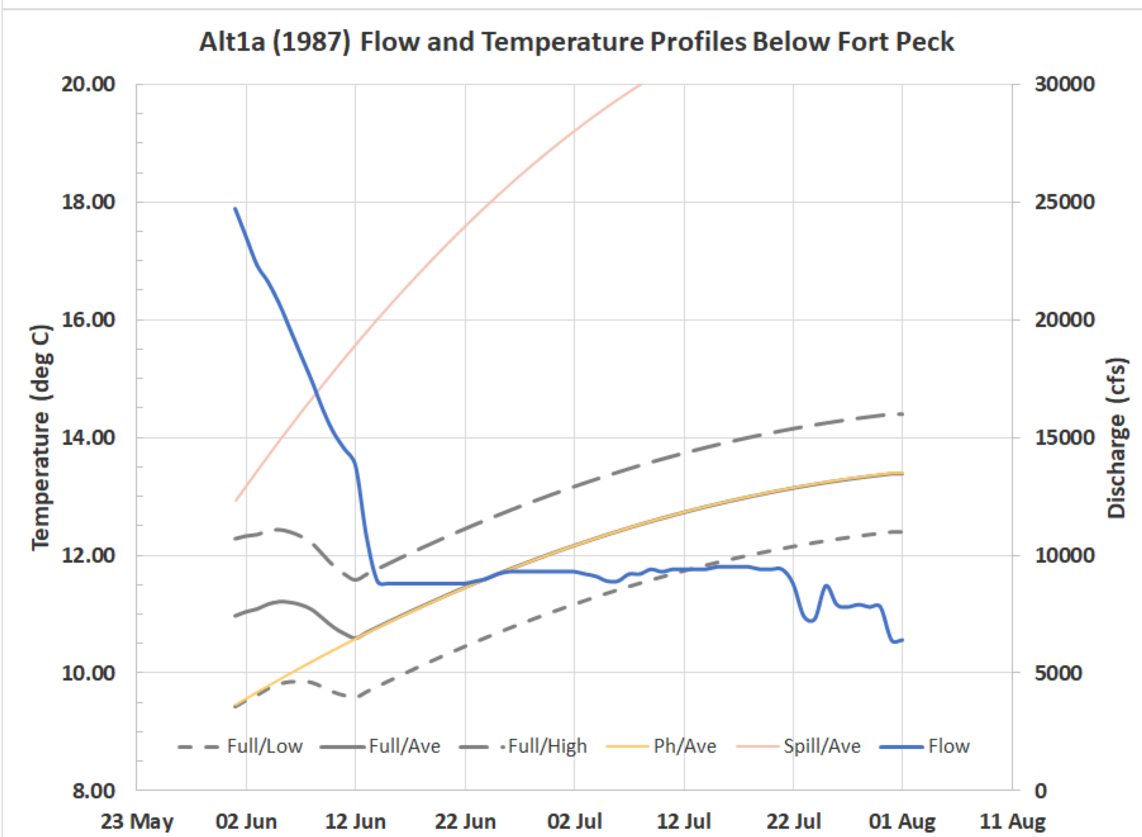
Alt1a (1987) Flow and Temperature Profiles Below Fort Peck
Temperature (deg C)
Discharge (cfs)
20.00
18.00
16.00
14.00
12.00
10.00
8.00
30000
25000
20000
15000
10000
5000
0
23 May
02 Jun
12 Jun
22 Jun
02 Jul
12 Jul
22 Jul
01 Aug
11 Aug
Full/Low
Full/Ave
Full/High
Ph/Ave
Spill/Ave
Flow

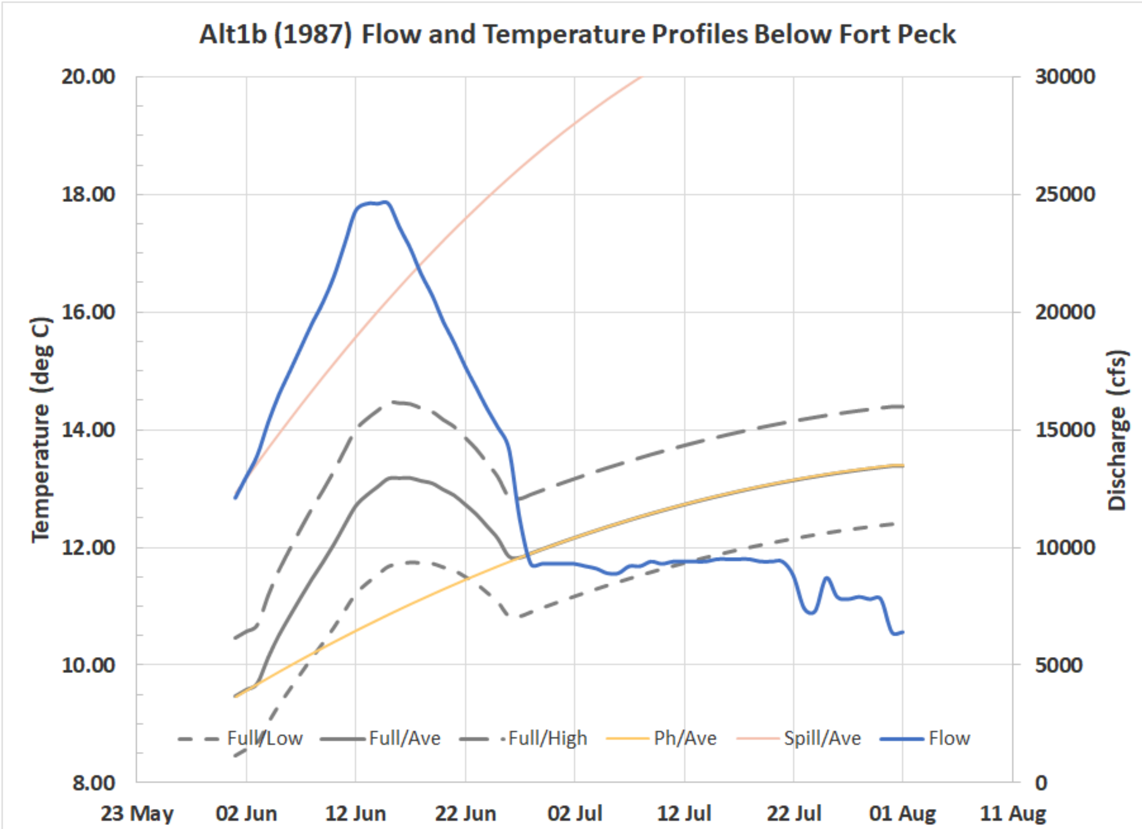
Alt1b (1987) Flow and Temperature Profiles Below Fort Peck
Temperature (deg C)
Discharge (cfs)
20.00
18.00
16.00
14.00
12.00
10.00
8.00
30000
25000
20000
15000
10000
5000
0
23 May
02 Jun
12 Jun
22 Jun
02 Jul
12 Jul
22 Jul
01 Aug
11 Aug
Full/Low
Full/Ave
Full/High
Ph/Ave
Spill/Ave
Flow

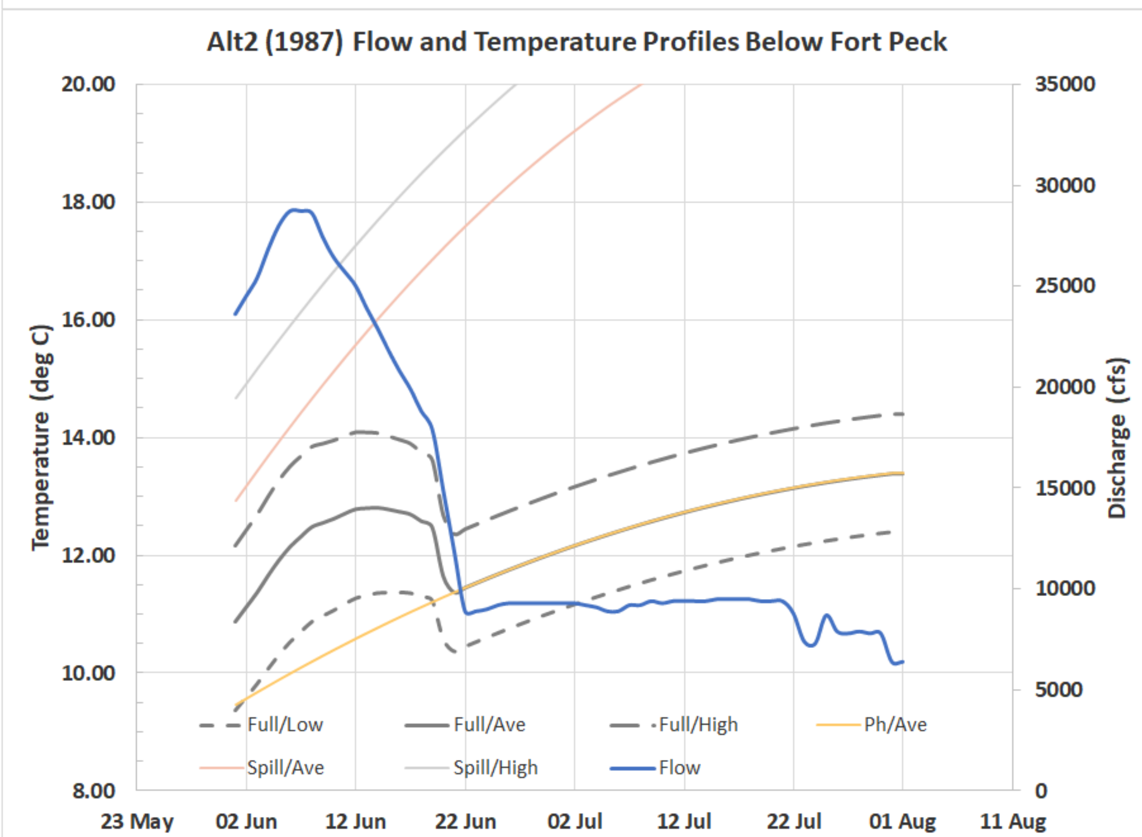
Alt2 (1987) Flow and Temperature Profiles Below Fort Peck
Temperature (deg C)
Discharge (cfs)
20.00
18.00
16.00
14.00
12.00
10.00
8.00
35000
30000
25000
20000
15000
10000
5000
0
23 May
02 Jun
12 Jun
22 Jun
02 Jul
12 Jul
22 Jul
01 Aug
11 Aug
Full/Low
Full/Ave
Full/High
Ph/Ave
Spill/Ave
Spill/High
Flow

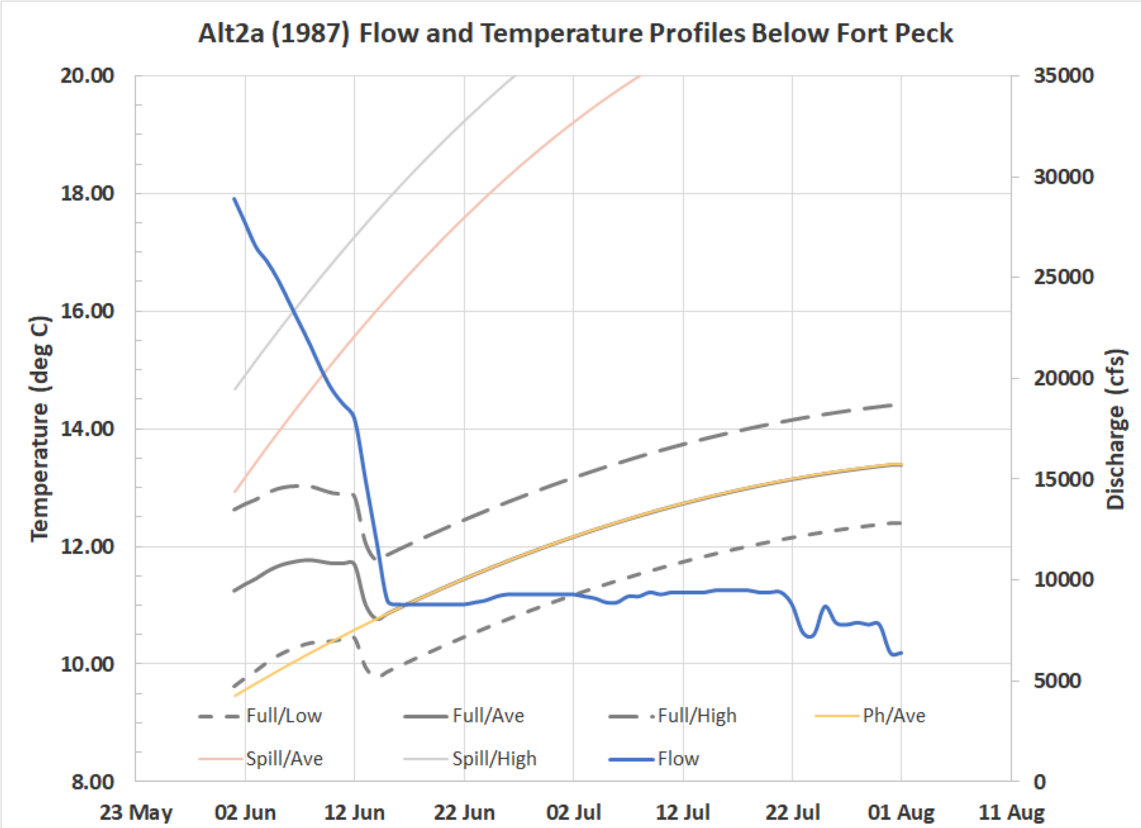

Alt2a (1987) Flow and Temperature Profiles Below Fort Peck
Temperature (deg C)
Discharge (cfs)
20.00
18.00
16.00
14.00
12.00
10.00
8.00
35000
30000
25000
20000
15000
10000
5000
0
23 May
02 Jun
12 Jun
22 Jun
02 Jul
12 Jul
22 Jul
01 Aug
11 Aug
Full/Low
Full/Ave
Full/High
Ph/Ave
Spill/Ave
Spill/High
Flow

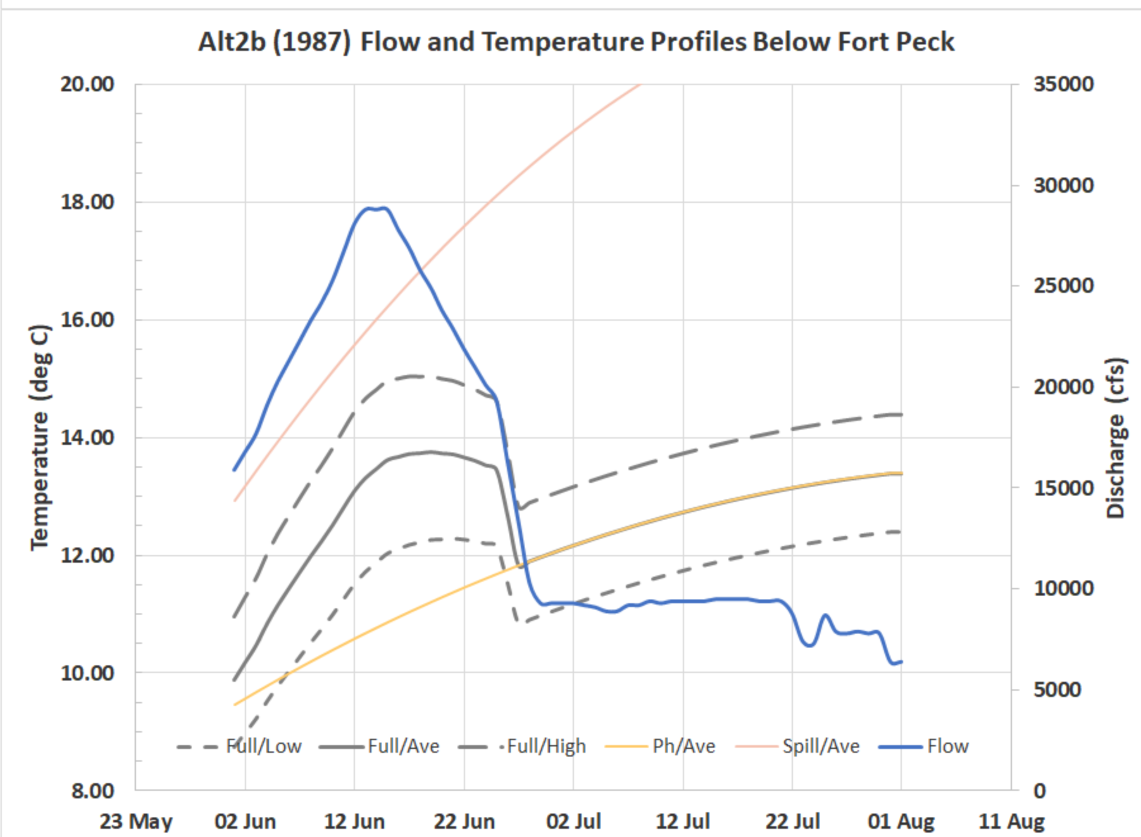

Alt2b (1987) Flow and Temperature Profiles Below Fort Peck
Temperature (deg C)
Discharge (cfs)
20.00
18.00
16.00
14.00
12.00
10.00
8.00
35000
30000
25000
20000
15000
10000
5000
0
23 May
02 Jun
12 Jun
22 Jun
02 Jul
12 Jul
22 Jul
01 Aug
11 Aug
Full/Low
Full/Ave
Full/High
Ph/Ave
Spill/Ave
Flow

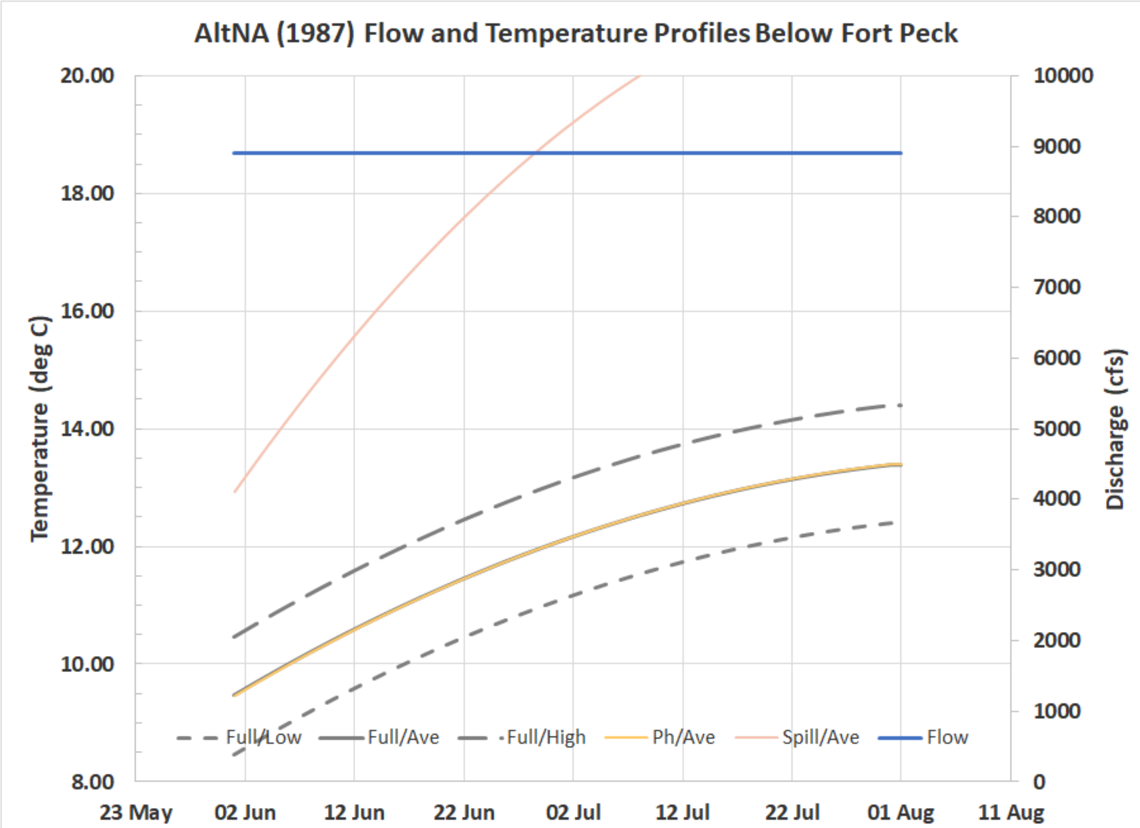
AltNA (1987) Flow and Temperature Profiles Below Fort Peck
Temperature (deg C)
Discharge (cfs)
20.00
18.00
16.00
14.00
12.00
10.00
8.00
10000
9000
8000
7000
6000
5000
4000
3000
2000
1000
0
23 May
02 Jun
12 Jun
22 Jun
02 Jul
12 Jul
22 Jul
01 Aug
11 Aug
Full/Low
Full/Ave
Full/High
Ph/Ave
Spill/Ave
Flow

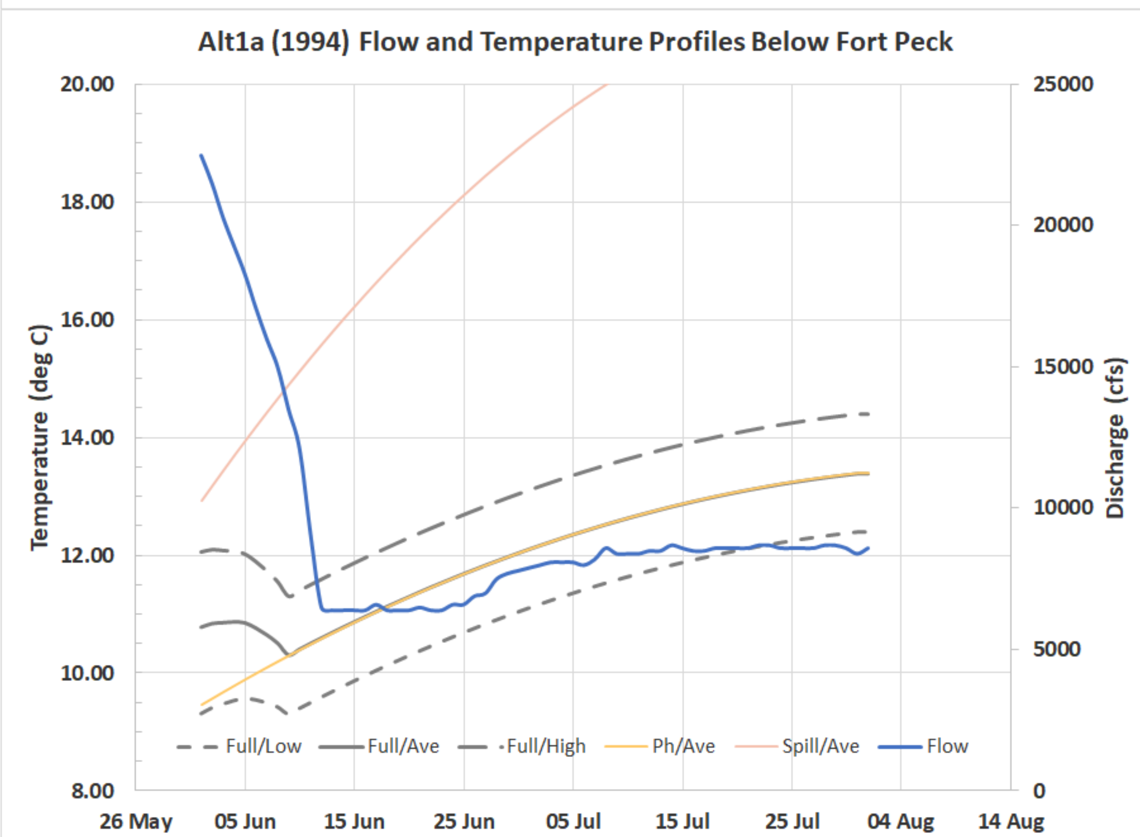
Alt1a (1994) Flow and Temperature Profiles Below Fort Peck
Temperature (deg C)
Discharge (cfs)
20.00
18.00
16.00
14.00
12.00
10.00
8.00
25000
20000
15000
10000
5000
0
26 May
05 Jun
15 Jun
25 Jun
05 Jul
15 Jul
25 Jul
04 Aug
14 Aug
Full/Low
Full/Ave
Full/High
Ph/Ave
Spill/Ave
Flow

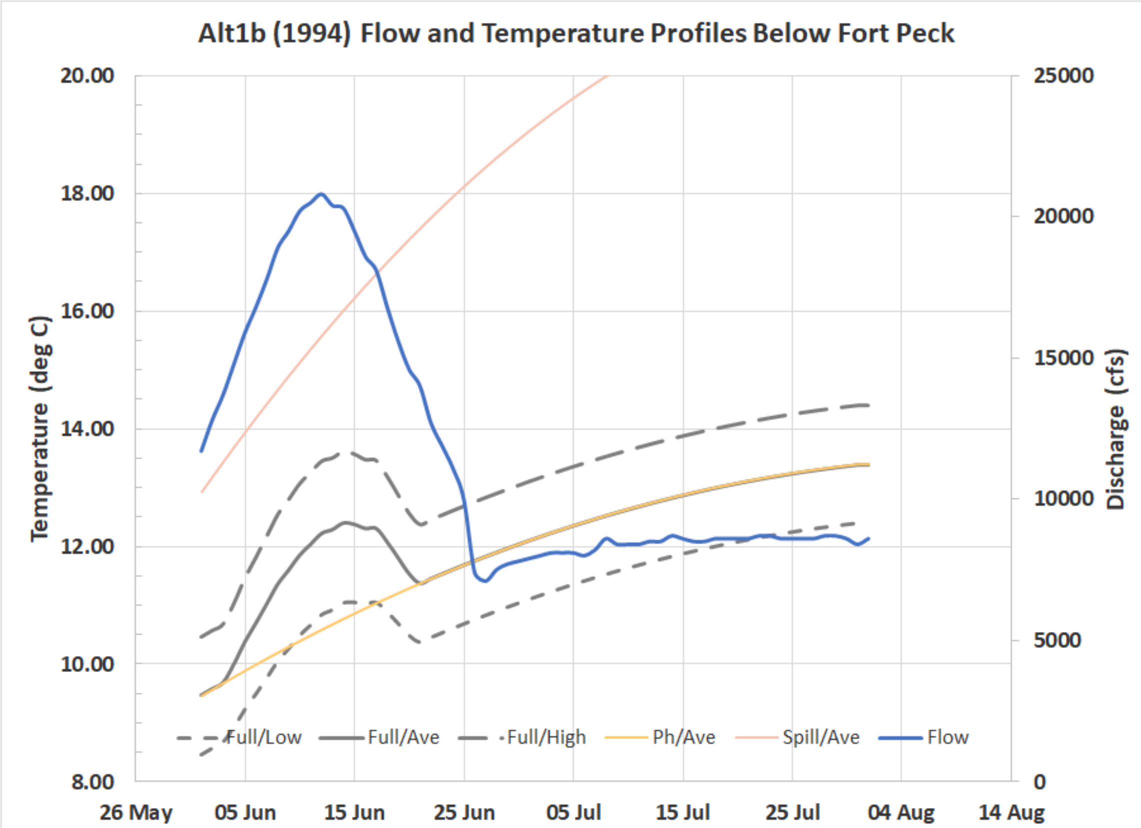
Alt1b (1994) Flow and Temperature Profiles Below Fort Peck
Temperature (deg C)
Discharge (cfs)
20.00
18.00
16.00
14.00
12.00
10.00
8.00
25000
20000
15000
10000
5000
0
26 May
05 Jun
15 Jun
25 Jun
05 Jul
15 Jul
25 Jul
04 Aug
14 Aug
Full/Low
Full/Ave
Full/High
Ph/Ave
Spill/Ave
Flow

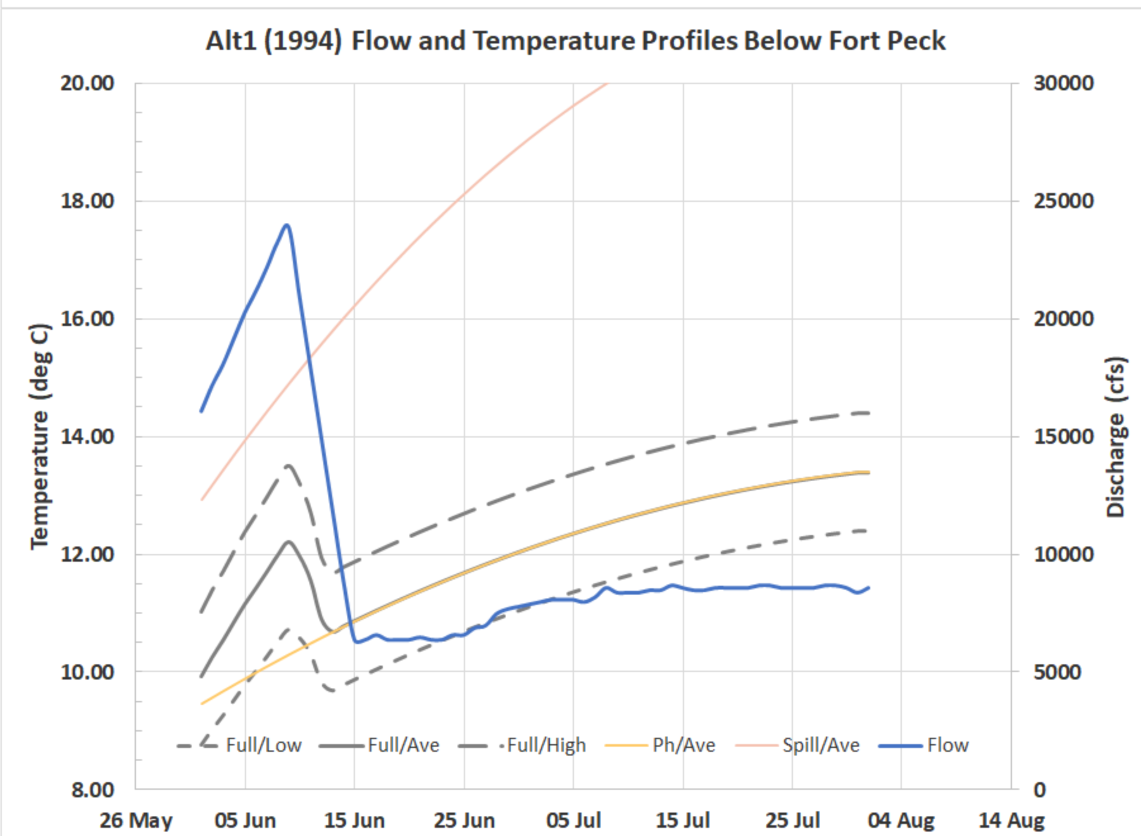
Alt1 (1994) Flow and Temperature Profiles Below Fort Peck
Temperature (deg C)
Discharge (cfs)
20.00
18.00
16.00
14.00
12.00
10.00
8.00
30000
25000
20000
15000
10000
5000
0
26 May
05 Jun
15 Jun
25 Jun
05 Jul
15 Jul
25 Jul
04 Aug
14 Aug
Full/Low
Full/Ave
Full/High
Ph/Ave
Spill/Ave
Flow

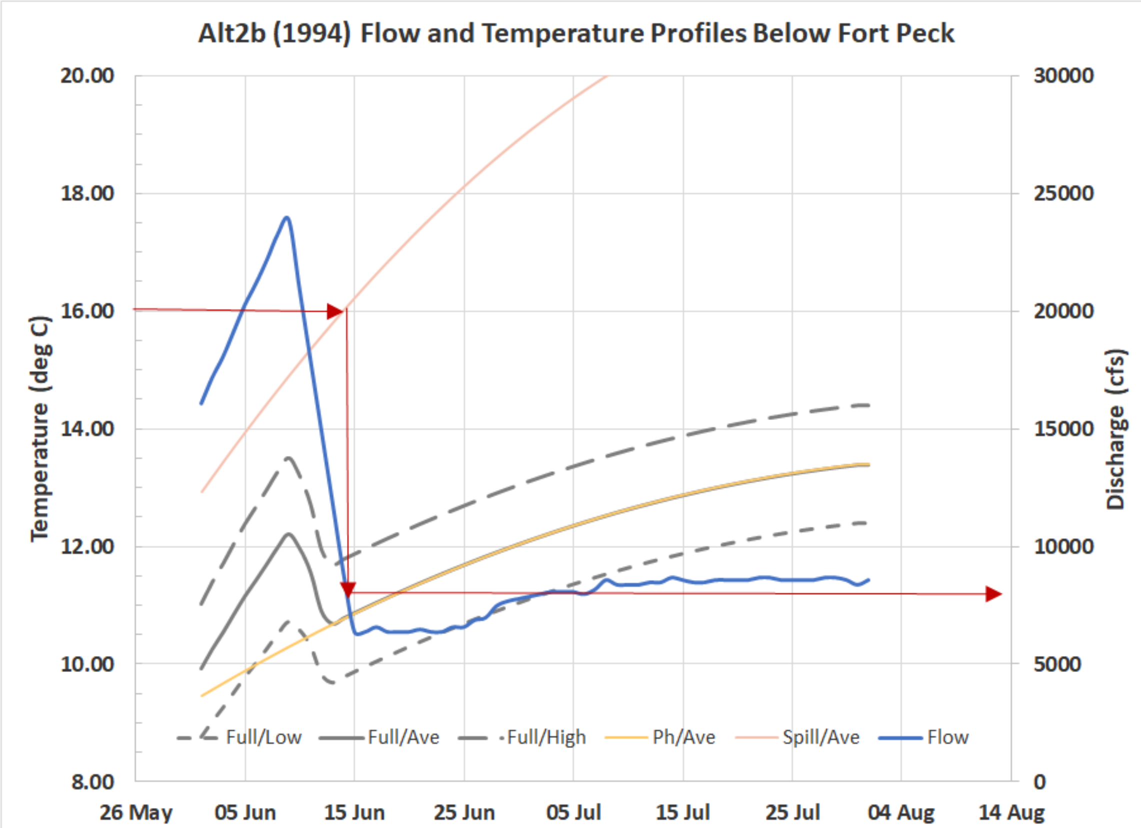
Alt2b (1994) Flow and Temperature Profiles Below Fort Peck
Temperature (deg C)
Discharge (cfs)
20.00
18.00
16.00
14.00
12.00
10.00
8.00
30000
25000
20000
15000
10000
5000
0
26 May
05 Jun
15 Jun
25 Jun
05 Jul
15 Jul
25 Jul
04 Aug
14 Aug
Full/Low
Full/Ave
Full/High
Ph/Ave
Spill/Ave
Flow

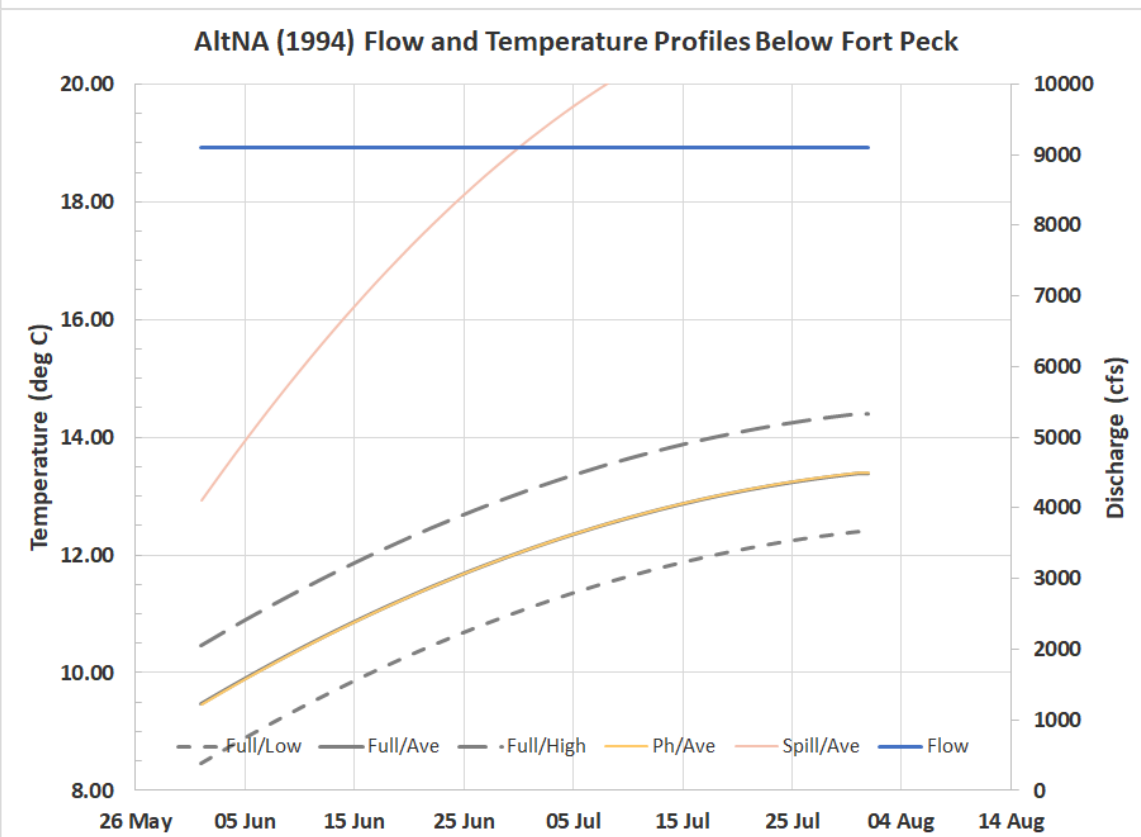
AltNA (1994) Flow and Temperature Profiles Below Fort Peck
Temperature (deg C)
Discharge (cfs)
20.00
18.00
16.00
14.00
12.00
10.00
8.00
10000
9000
8000
7000
6000
5000
4000
3000
2000
1000
0
26 May
05 Jun
15 Jun
25 Jun
05 Jul
15 Jul
25 Jul
04 Aug
14 Aug
Full/Low
Full/Ave
Full/High
Ph/Ave
Spill/Ave
Flow

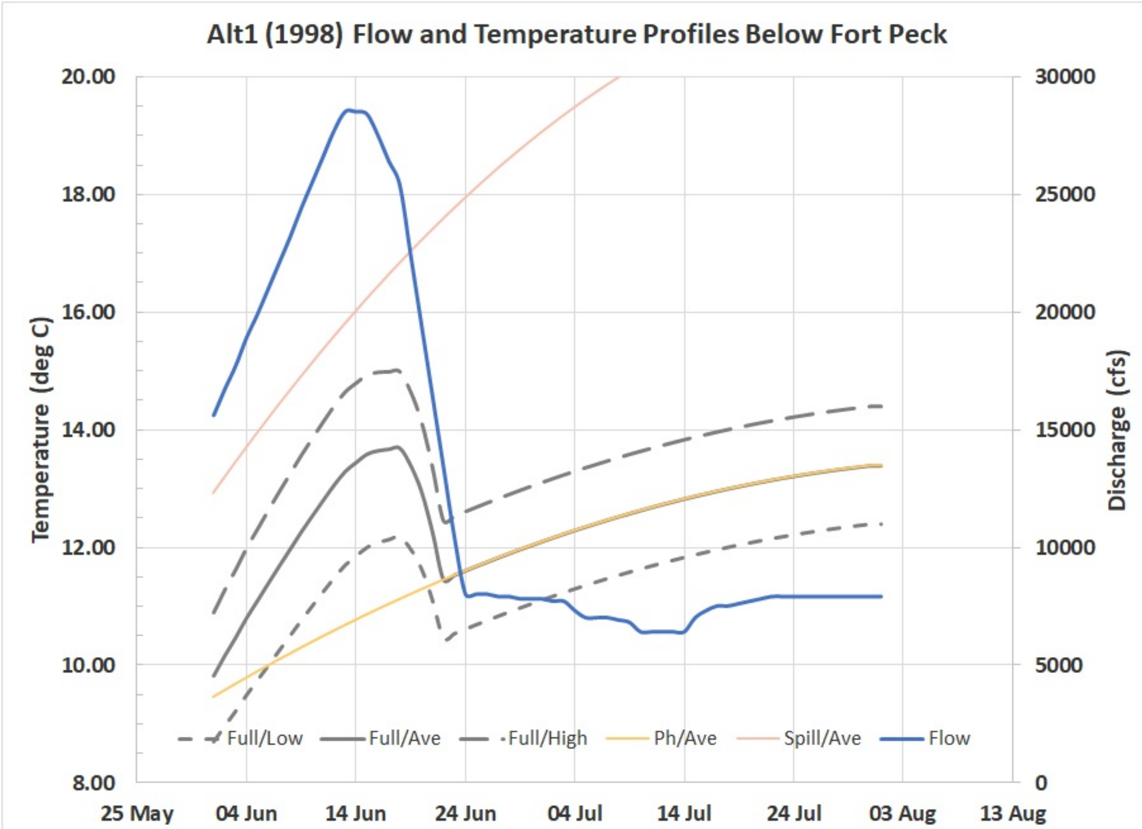
Alt1 (1998) Flow and Temperature Profiles Below Fort Peck
Temperature (deg C)
Discharge (cfs)
20.00
18.00
16.00
14.00
12.00
10.00
8.00
30000
25000
20000
15000
10000
5000
0
25 May
04 Jun
14 Jun
24 Jun
04 Jul
14 Jul
24 Jul
03 Aug
13 Aug
Full/Low
Full/Ave
Full/High
Ph/Ave
Spill/Ave
Flow

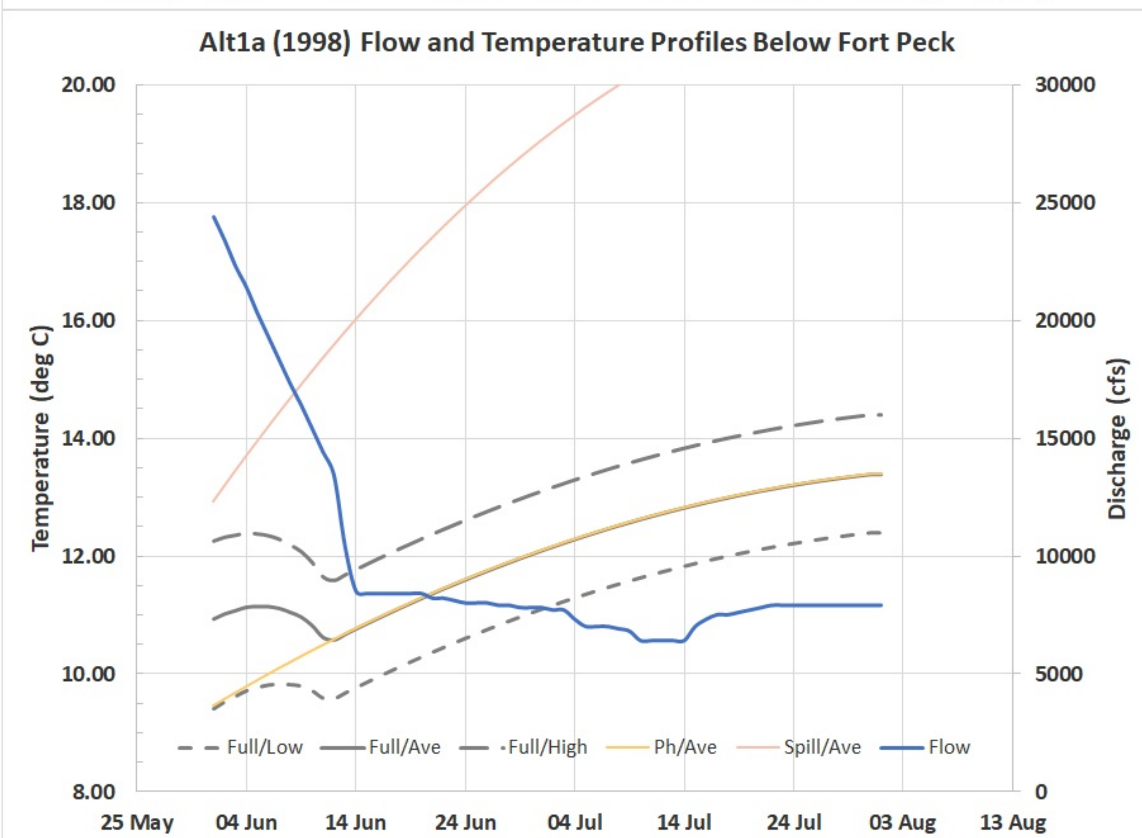
Alt1a (1998) Flow and Temperature Profiles Below Fort Peck
Temperature (deg C)
Discharge (cfs)
20.00
18.00
16.00
14.00
12.00
10.00
8.00
30000
25000
20000
15000
10000
5000
0
25 May
04 Jun
14 Jun
24 Jun
04 Jul
14 Jul
24 Jul
03 Aug
13 Aug
Full/Low
Full/Ave
Full/High
Ph/Ave
Spill/Ave
Flow

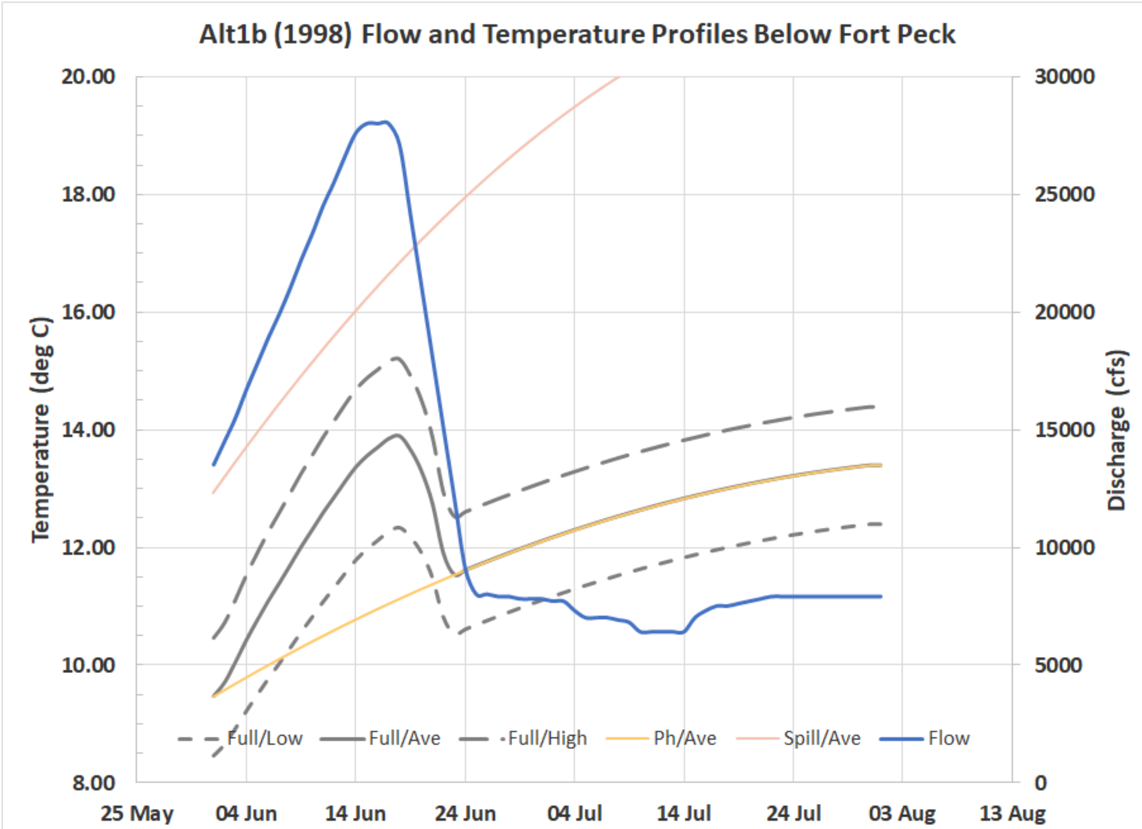
Alt1b (1998) Flow and Temperature Profiles Below Fort Peck
Temperature (deg C)
Discharge (cfs)
20.00
18.00
16.00
14.00
12.00
10.00
8.00
30000
25000
20000
15000
10000
5000
0
25 May
04 Jun
14 Jun
24 Jun
04 Jul
14 Jul
24 Jul
03 Aug
13 Aug
Full/Low
Full/Ave
Full/High
Ph/Ave
Spill/Ave
Flow

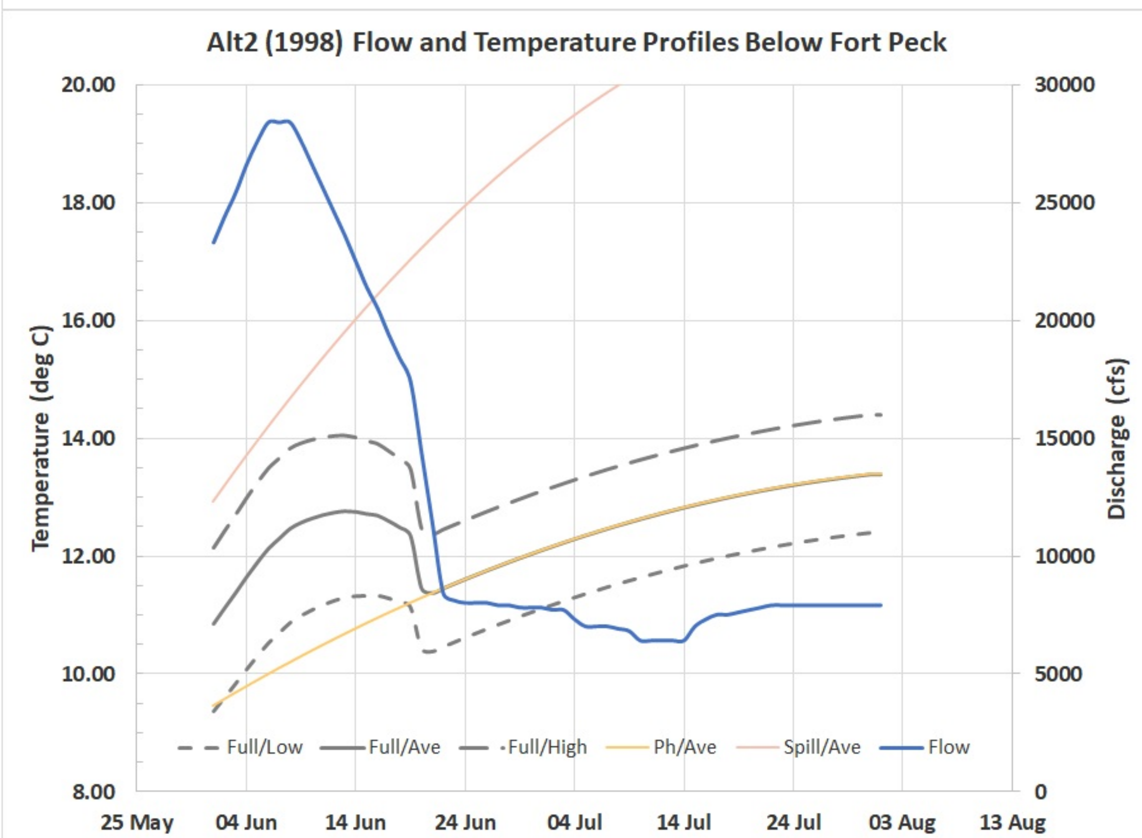
Alt2 (1998) Flow and Temperature Profiles Below Fort Peck
Temperature (deg C)
Discharge (cfs)
20.00
18.00
16.00
14.00
12.00
10.00
8.00
30000
25000
20000
15000
10000
5000
0
25 May
04 Jun
14 Jun
24 Jun
04 Jul
14 Jul
24 Jul
03 Aug
13 Aug
Full/Low
Full/Ave
Full/High
Ph/Ave
Spill/Ave
Flow

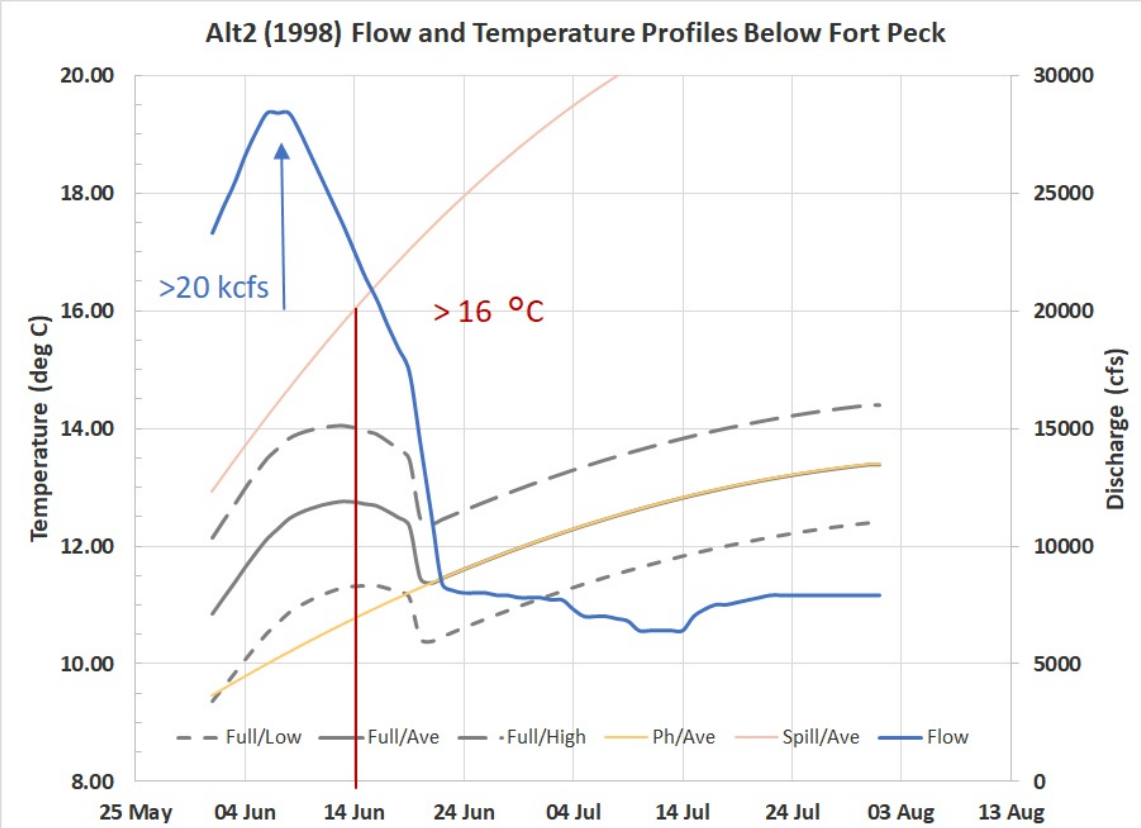
Alt2 (1998) Flow and Temperature Profiles Below Fort Peck
Temperature (deg C)
Discharge (cfs)
>20 kcfs
> 16 °C
20.00
18.00
16.00
14.00
12.00
10.00
8.00
30000
25000
20000
15000
10000
5000
0
25 May
04 Jun
14 Jun
24 Jun
04 Jul
14 Jul
24 Jul
03 Aug
13 Aug
Full/Low
Full/Ave
Full/High
Ph/Ave
Spill/Ave
Flow

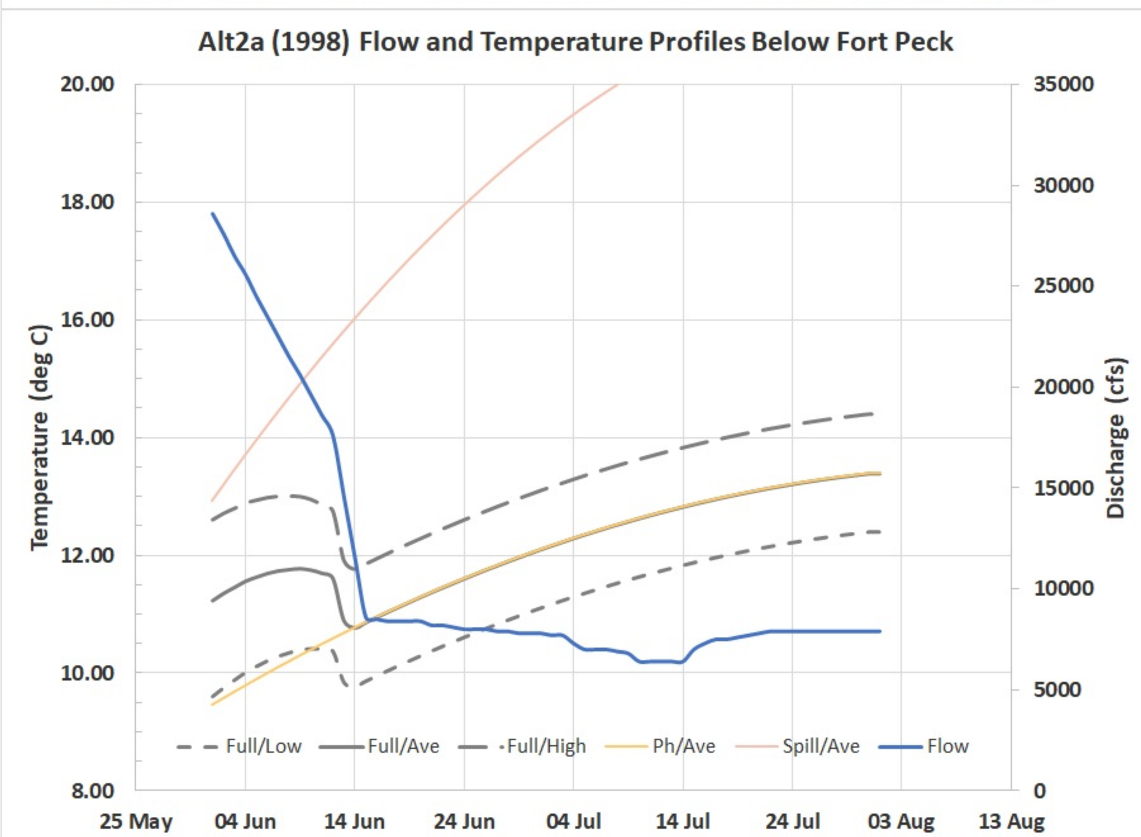
Alt2a (1998) Flow and Temperature Profiles Below Fort Peck
Temperature (deg C)
Discharge (cfs)
20.00
18.00
16.00
14.00
12.00
10.00
8.00
35000
30000
25000
20000
15000
10000
5000
0
25 May
04 Jun
14 Jun
24 Jun
04 Jul
14 Jul
24 Jul
03 Aug
13 Aug
Full/Low
Full/Ave
Full/High
Ph/Ave
Spill/Ave
Flow

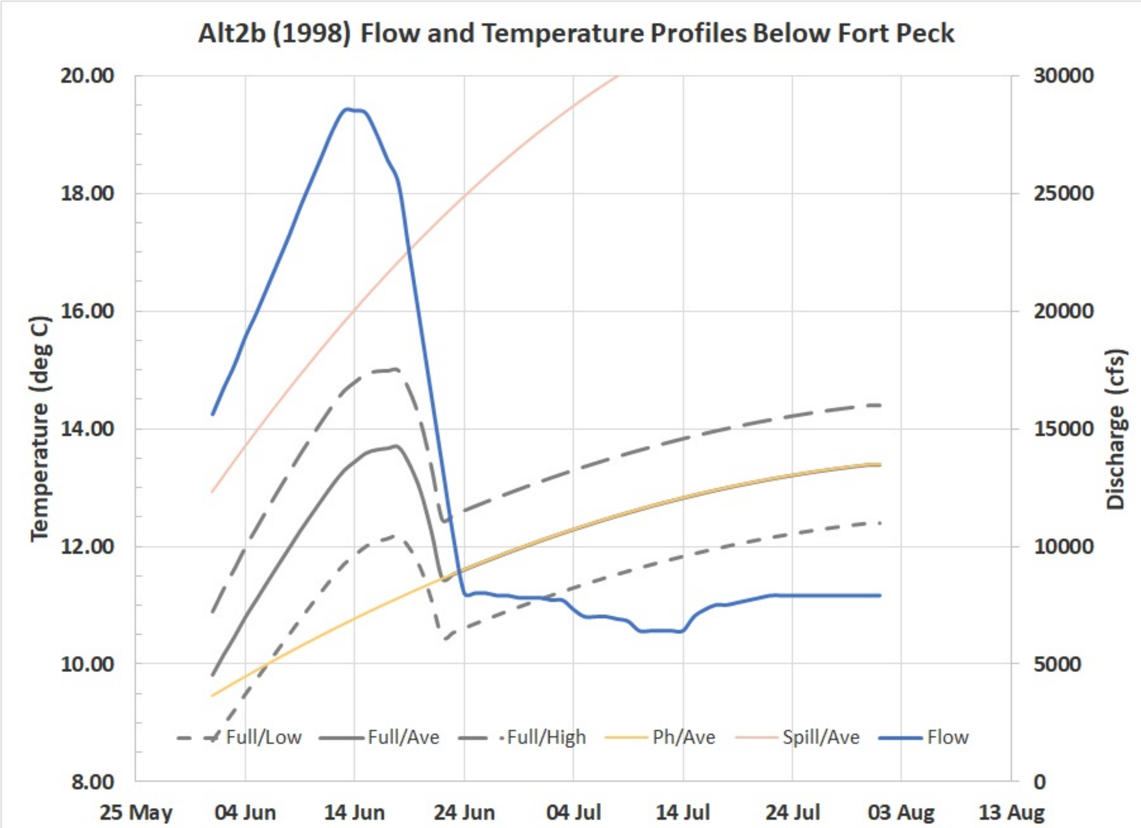
Alt2b (1998) Flow and Temperature Profiles Below Fort Peck
Temperature (deg C)
Discharge (cfs)
20.00
18.00
16.00
14.00
12.00
10.00
8.00
30000
25000
20000
15000
10000
5000
0
25 May
04 Jun
14 Jun
24 Jun
04 Jul
14 Jul
24 Jul
03 Aug
13 Aug
Full/Low
Full/Ave
Full/High
Ph/Ave
Spill/Ave
Flow

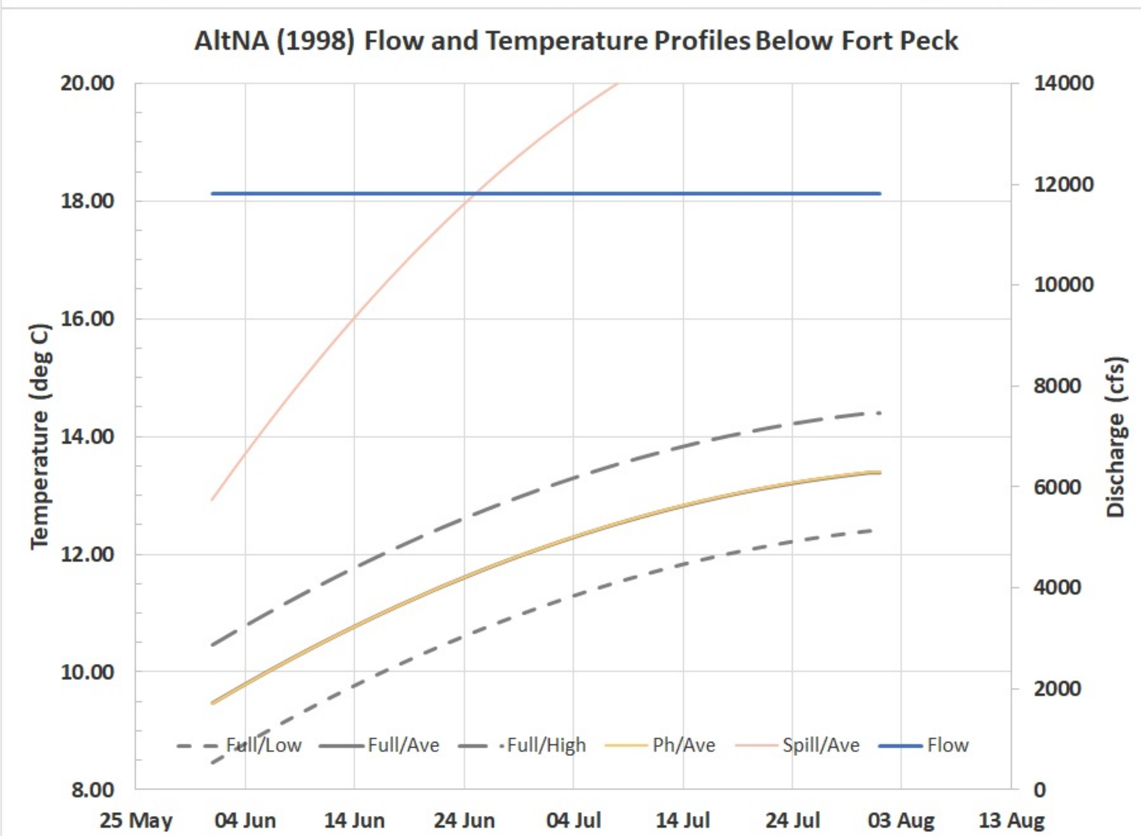
AltNA (1998) Flow and Temperature Profiles Below Fort Peck
Temperature (deg C)
Discharge (cfs)
20.00
18.00
16.00
14.00
12.00
10.00
8.00
14000
12000
10000
8000
6000
4000
2000
0
25 May
04 Jun
14 Jun
24 Jun
04 Jul
14 Jul
24 Jul
03 Aug
13 Aug
Full/Low
Full/Ave
Full/High
Ph/Ave
Spill/Ave
Flow

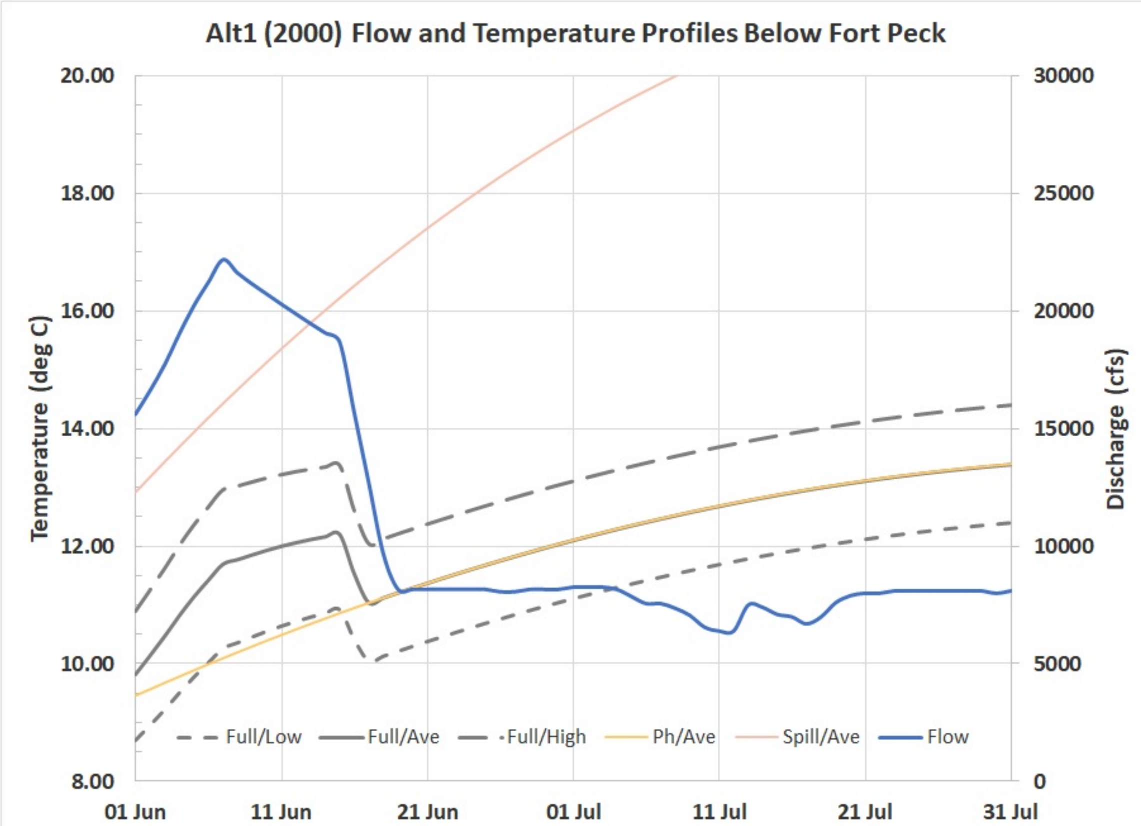
Alt1 (2000) Flow and Temperature Profiles Below Fort Peck
Temperature (deg C)
Discharge (cfs)
20.00
18.00
16.00
14.00
12.00
10.00
8.00
30000
25000
20000
15000
10000
5000
0
01 Jun
11 Jun
21 Jun
01 Jul
11 Jul
21 Jul
31 Jul
Full/Low
Full/Ave
Full/High
Ph/Ave
Spill/Ave
Flow

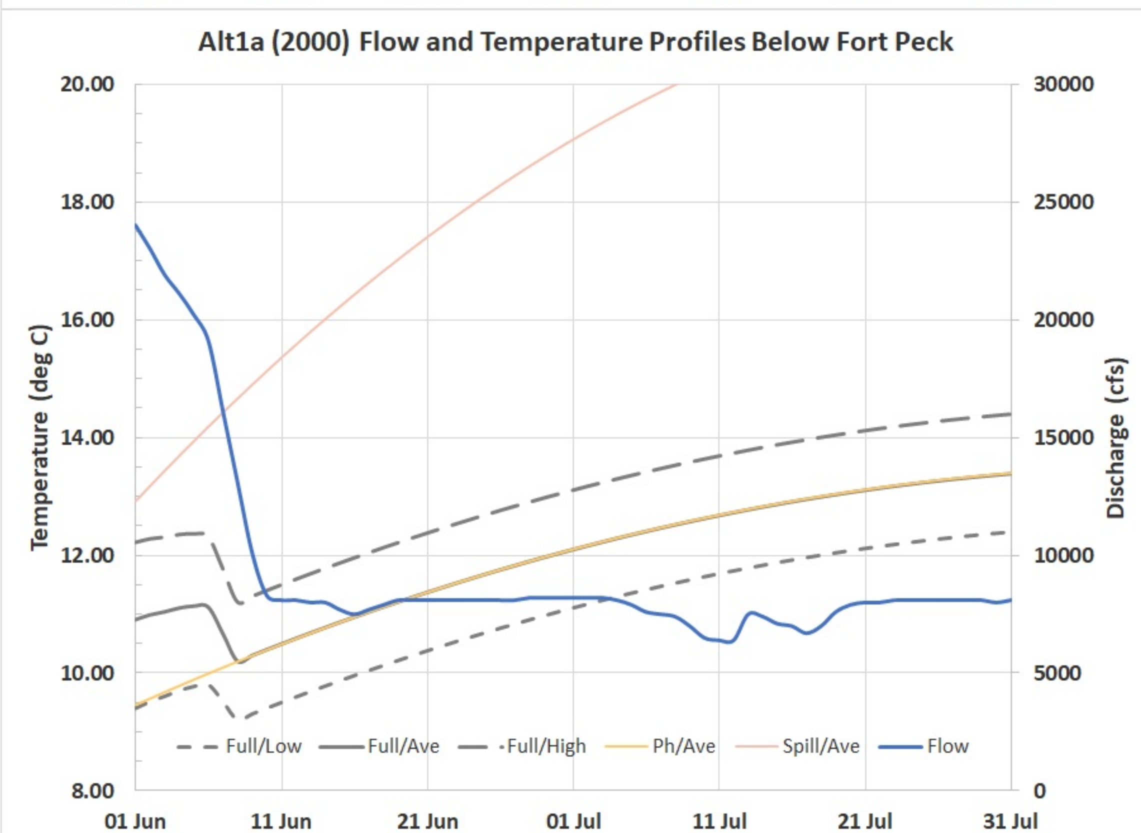
Alt1a (2000) Flow and Temperature Profiles Below Fort Peck
Temperature (deg C)
Discharge (cfs)
20.00
18.00
16.00
14.00
12.00
10.00
8.00
30000
25000
20000
15000
10000
5000
0
01 Jun
11 Jun
21 Jun
01 Jul
11 Jul
21 Jul
31 Jul
Full/Low
Full/Ave
Full/High
Ph/Ave
Spill/Ave
Flow

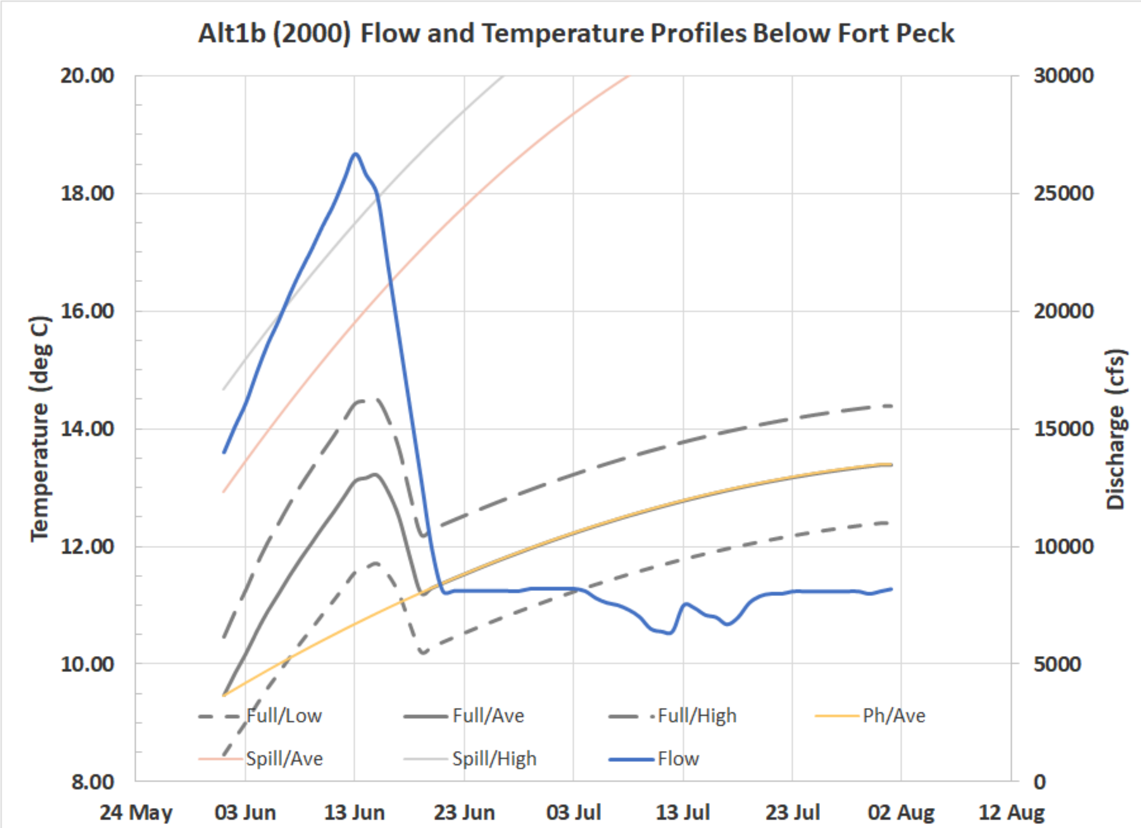
Alt1b (2000) Flow and Temperature Profiles Below Fort Peck
Temperature (deg C)
Discharge (cfs)
20.00
18.00
16.00
14.00
12.00
10.00
8.00
30000
25000
20000
15000
10000
5000
0
24 May
03 Jun
13 Jun
23 Jun
03 Jul
13 Jul
23 Jul
02 Aug
12 Aug
Full/Low
Full/Ave
Full/High
Ph/Ave
Spill/Ave
Spill/High
Flow

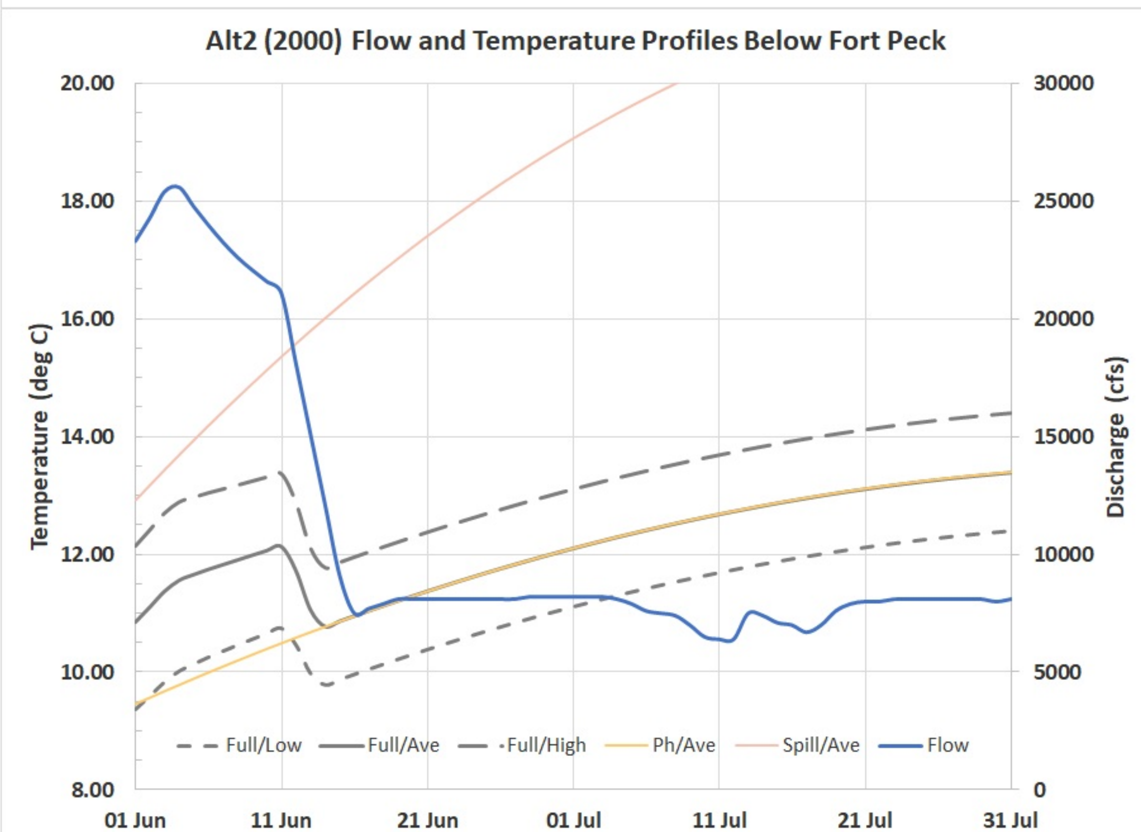
Alt2 (2000) Flow and Temperature Profiles Below Fort Peck
Temperature (deg C)
Discharge (cfs)
20.00
18.00
16.00
14.00
12.00
10.00
8.00
30000
25000
20000
15000
10000
5000
0
01 Jun
11 Jun
21 Jun
01 Jul
11 Jul
21 Jul
31 Jul
Full/Low
Full/Ave
Full/High
Ph/Ave
Spill/Ave
Flow

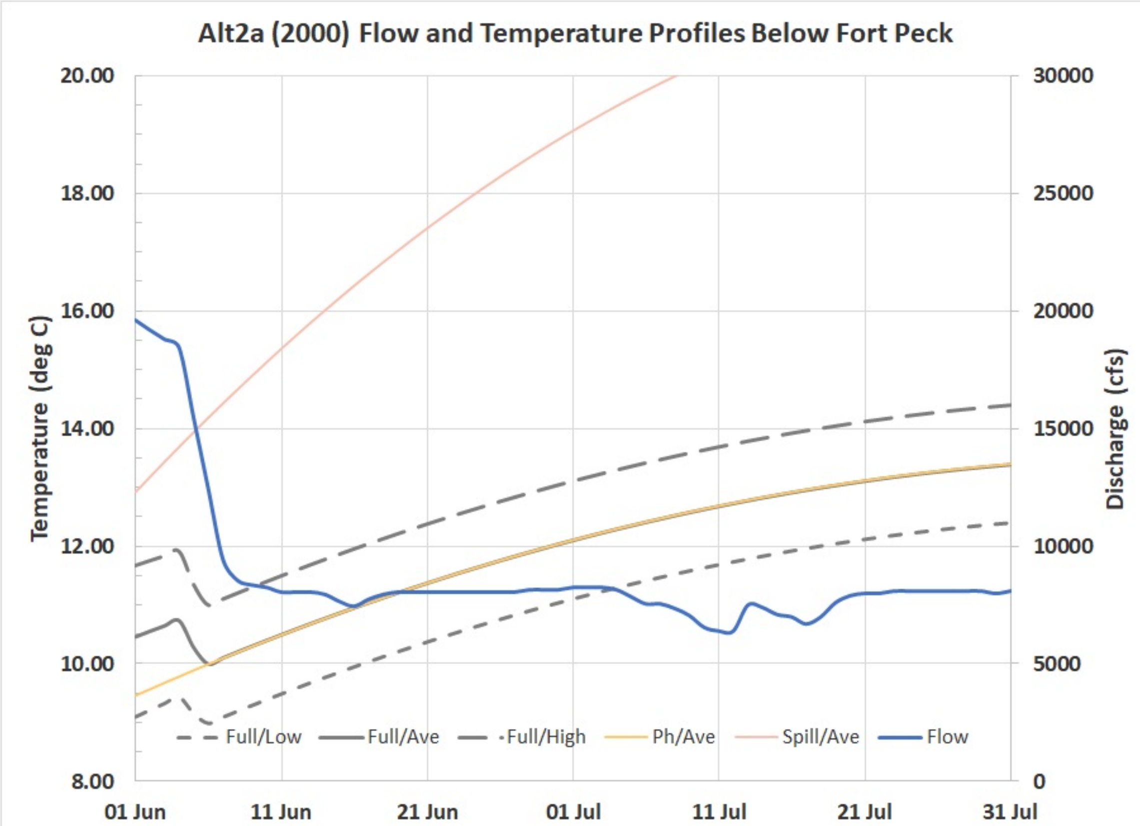
Alt2a (2000) Flow and Temperature Profiles Below Fort Peck
Temperature (deg C)
Discharge (cfs)
20.00
18.00
16.00
14.00
12.00
10.00
8.00
30000
25000
20000
15000
10000
5000
0
01 Jun
11 Jun
21 Jun
01 Jul
11 Jul
21 Jul
31 Jul
Full/Low
Full/Ave
Full/High
Ph/Ave
Spill/Ave
Flow

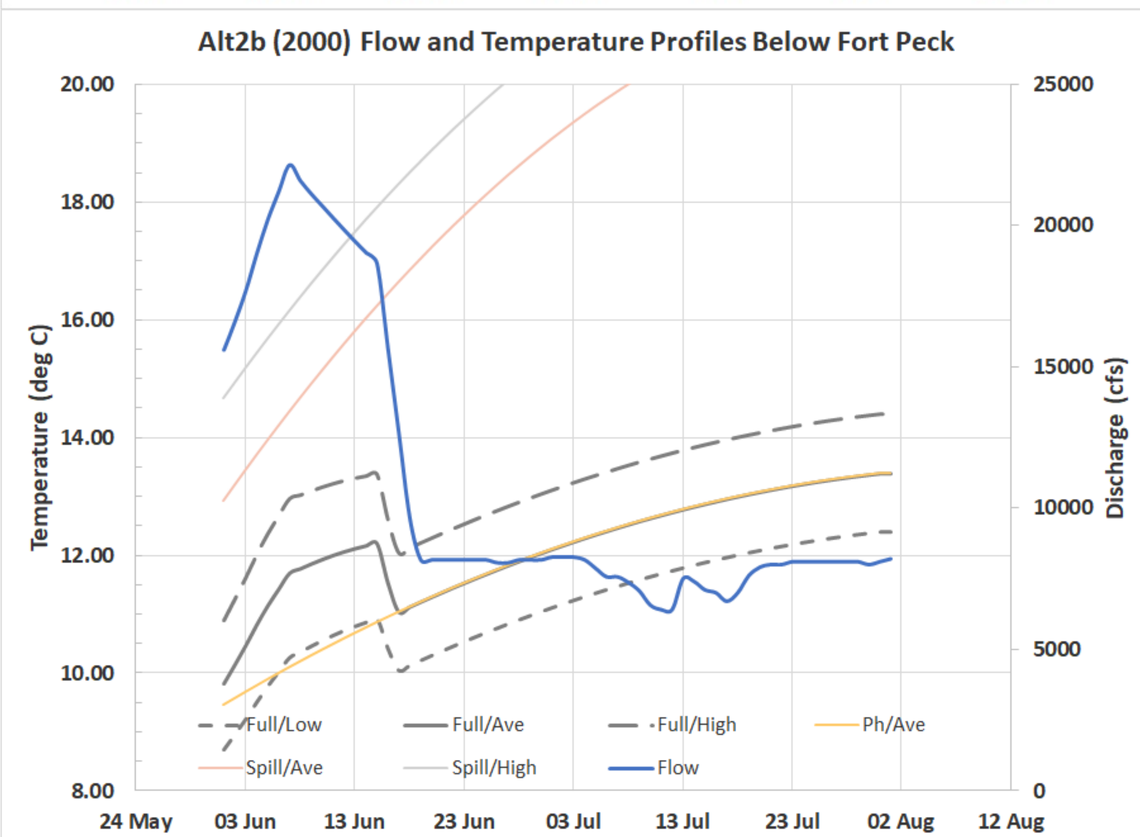
Alt2b (2000) Flow and Temperature Profiles Below Fort Peck
Temperature (deg C)
Discharge (cfs)
20.00
18.00
16.00
14.00
12.00
10.00
8.00
25000
20000
15000
10000
5000
0
24 May
03 Jun
13 Jun
23 Jun
03 Jul
13 Jul
23 Jul
02 Aug
12 Aug
Full/Low
Full/Ave
Full/High
Ph/Ave
Spill/Ave
Spill/High
Flow

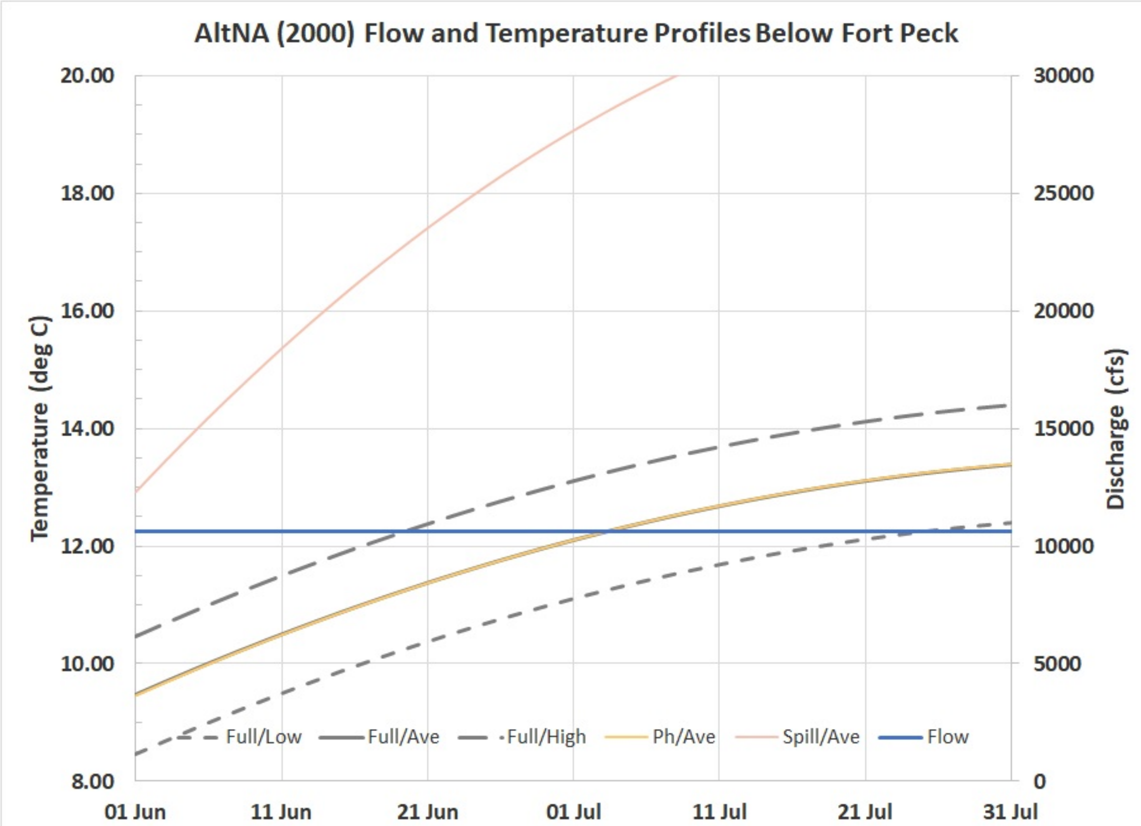
AltNA (2000) Flow and Temperature Profiles Below Fort Peck
Temperature (deg C)
Discharge (cfs)
20.00
18.00
16.00
14.00
12.00
10.00
8.00
30000
25000
20000
15000
10000
5000
0
01 Jun
11 Jun
21 Jun
01 Jul
11 Jul
21 Jul
31 Jul
Full/Low
Full/Ave
Full/High
Ph/Ave
Spill/Ave
Flow

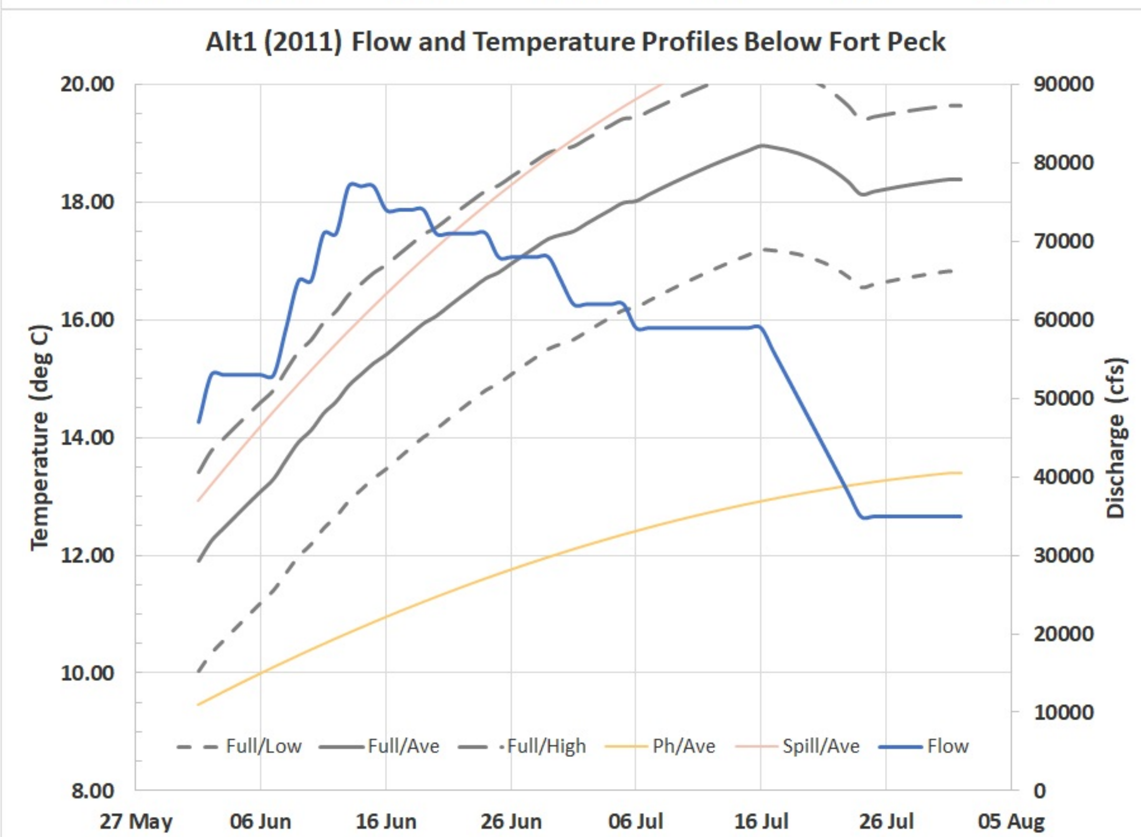
Alt1 (2011) Flow and Temperature Profiles Below Fort Peck
Temperature (deg C)
Discharge (cfs)
20.00
18.00
16.00
14.00
12.00
10.00
8.00
90000
80000
70000
60000
50000
40000
30000
20000
10000
0
27 May
06 Jun
16 Jun
26 Jun
06 Jul
16 Jul
26 Jul
05 Aug
Full/Low
Full/Ave
Full/High
Ph/Ave
Spill/Ave
Flow

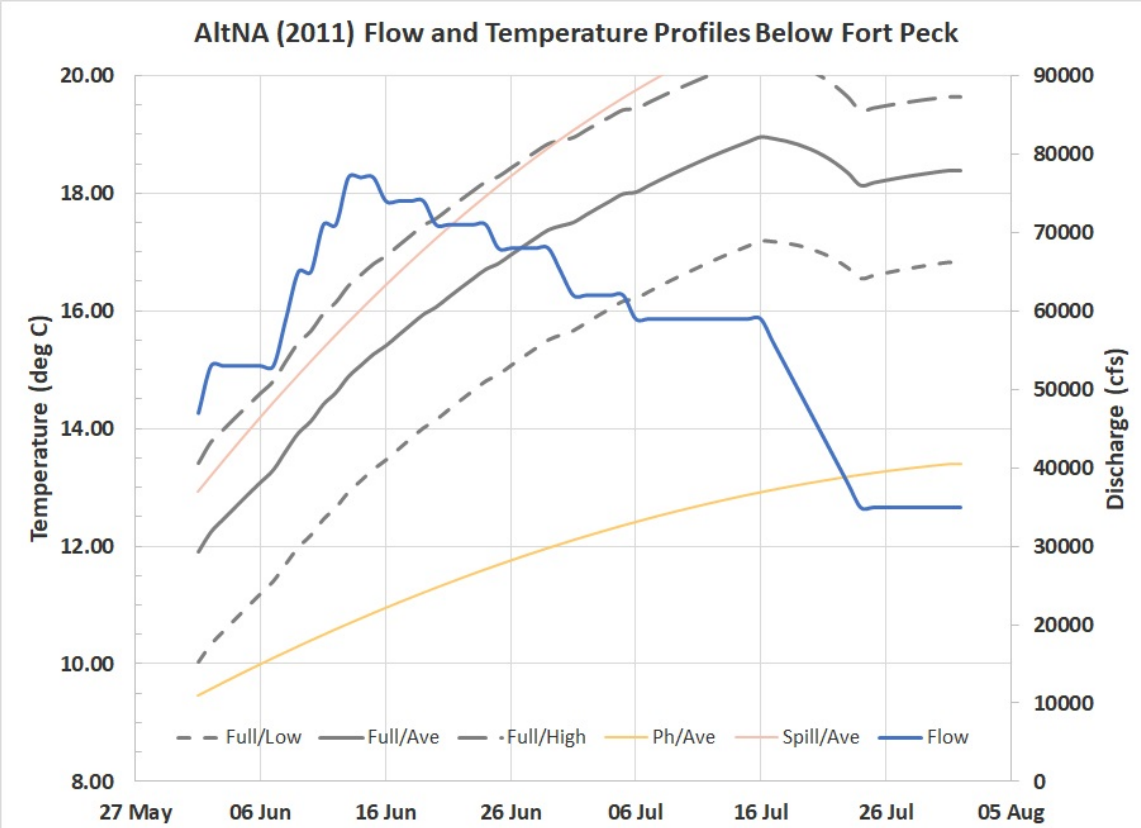
AltNA (2011) Flow and Temperature Profiles Below Fort Peck
Temperature (deg C)
Discharge (cfs)
20.00
18.00
16.00
14.00
12.00
10.00
8.00
90000
80000
70000
60000
50000
40000
30000
20000
10000
0
27 May
06 Jun
16 Jun
26 Jun
06 Jul
16 Jul
26 Jul
05 Aug
Full/Low
Full/Ave
Full/High
Ph/Ave
Spill/Ave
Flow

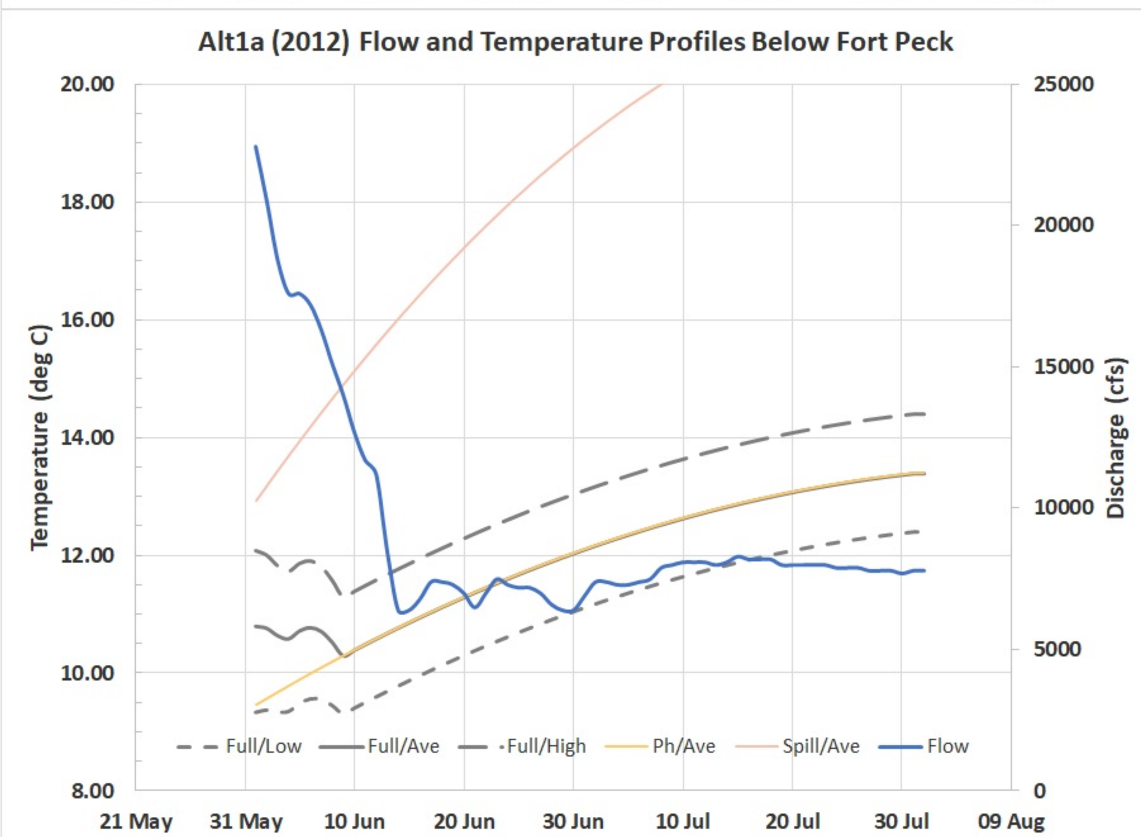
Alt1a (2012) Flow and Temperature Profiles Below Fort Peck
Temperature (deg C)
Discharge (cfs)
20.00
18.00
16.00
14.00
12.00
10.00
8.00
25000
20000
15000
10000
5000
0
21 May
31 May
10 Jun
20 Jun
30 Jun
10 Jul
20 Jul
30 Jul
09 Aug
Full/Low
Full/Ave
Full/High
Ph/Ave
Spill/Ave
Flow

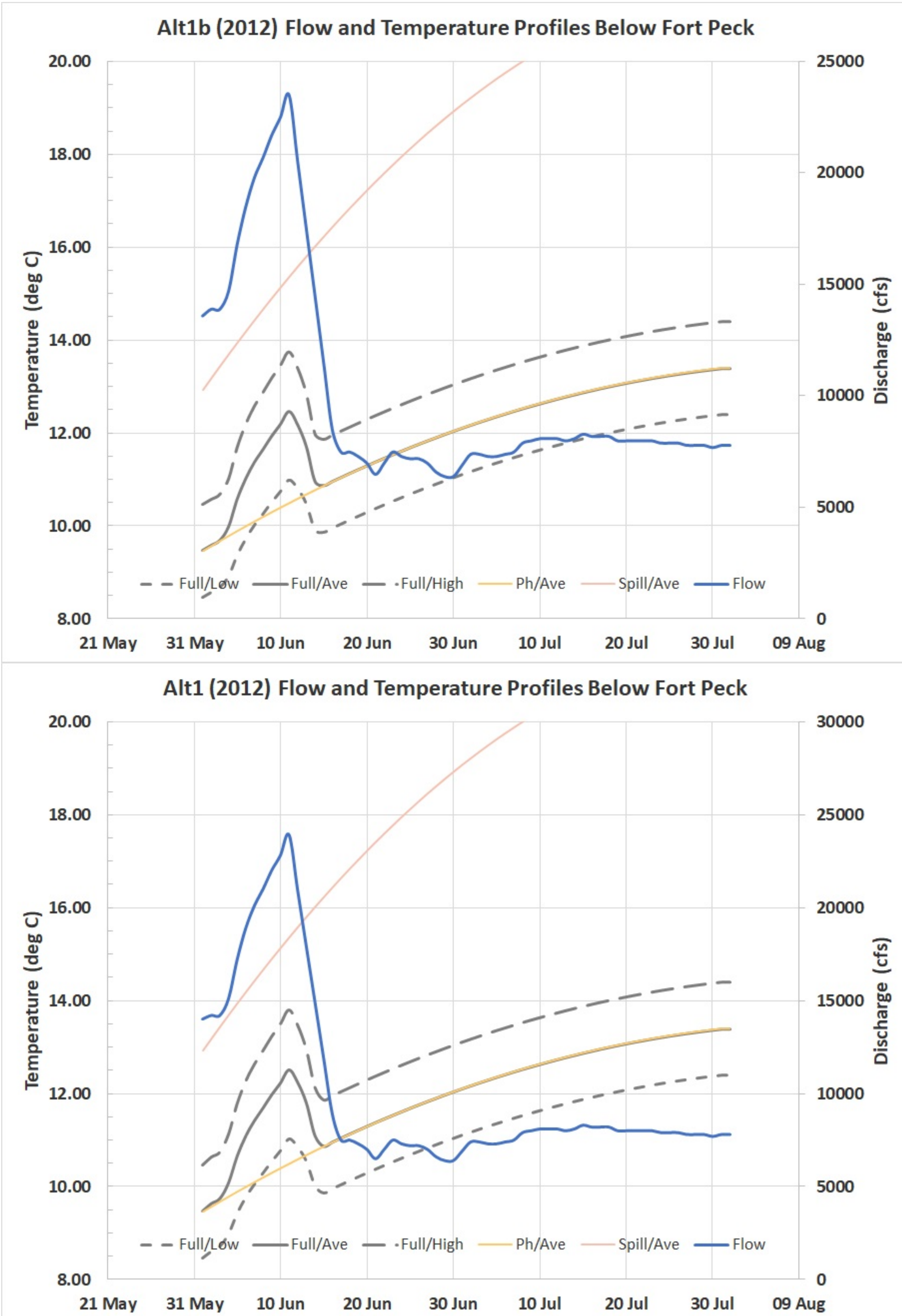

Alt1b (2012) Flow and Temperature Profiles Below Fort Peck
Temperature (deg C)
Discharge (cfs)
20.00
18.00
16.00
14.00
12.00
10.00
8.00
25000
20000
15000
10000
5000
0
21 May
31 May
10 Jun
20 Jun
30 Jun
10 Jul
20 Jul
30 Jul
09 Aug
Full/Low
Full/Ave
Full/High
Ph/Ave
Spill/Ave
Flow
Alt1 (2012) Flow and Temperature Profiles Below Fort Peck
Temperature (deg C)
Discharge (cfs)
20.00
18.00
16.00
14.00
12.00
10.00
8.00
30000
25000
20000
15000
10000
5000
0
21 May
31 May
10 Jun
20 Jun
30 Jun
10 Jul
20 Jul
30 Jul
09 Aug
Full/Low
Full/Ave
Full/High
Ph/Ave
Spill/Ave
Flow

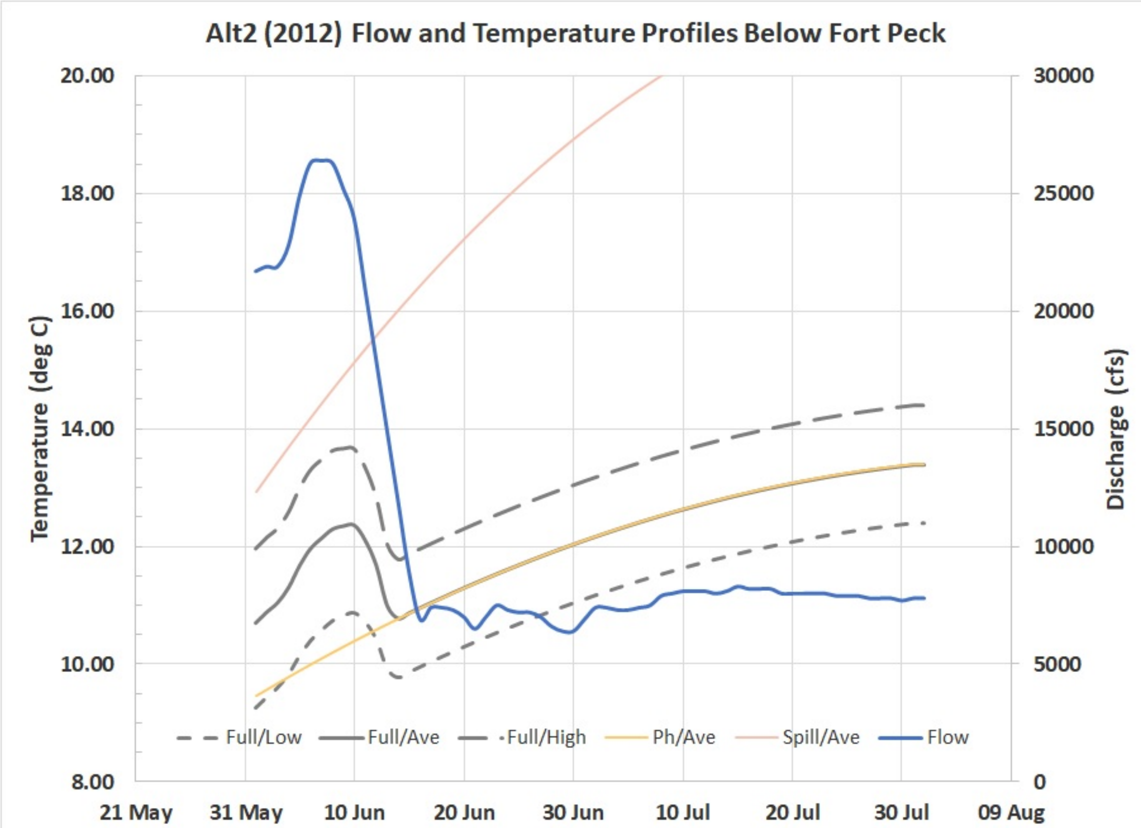
Alt2 (2012) Flow and Temperature Profiles Below Fort Peck
Temperature (deg C)
Discharge (cfs)
20.00
18.00
16.00
14.00
12.00
10.00
8.00
30000
25000
20000
15000
10000
5000
0
21 May
31 May
10 Jun
20 Jun
30 Jun
10 Jul
20 Jul
30 Jul
09 Aug
Full/Low
Full/Ave
Full/High
Ph/Ave
Spill/Ave
Flow

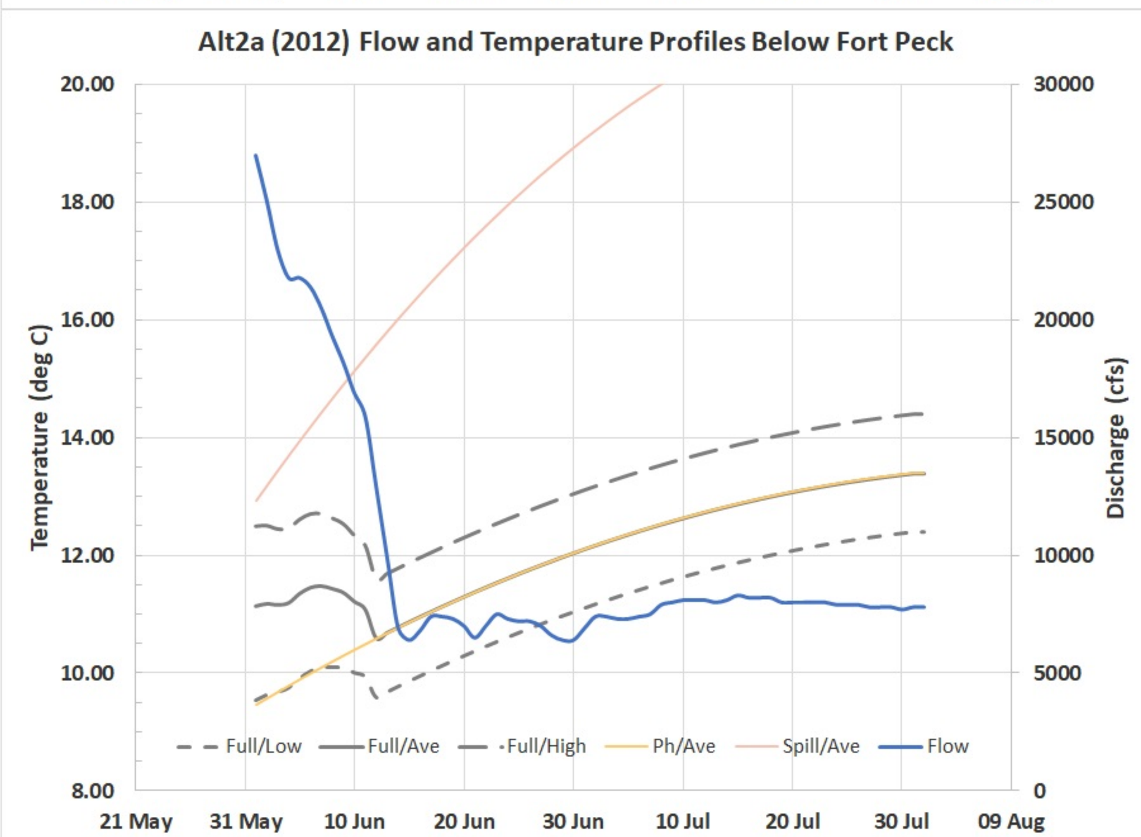
Alt2a (2012) Flow and Temperature Profiles Below Fort Peck
Temperature (deg C)
Discharge (cfs)
20.00
18.00
16.00
14.00
12.00
10.00
8.00
30000
25000
20000
15000
10000
5000
0
21 May
31 May
10 Jun
20 Jun
30 Jun
10 Jul
20 Jul
30 Jul
09 Aug
Full/Low
Full/Ave
Full/High
Ph/Ave
Spill/Ave
Flow

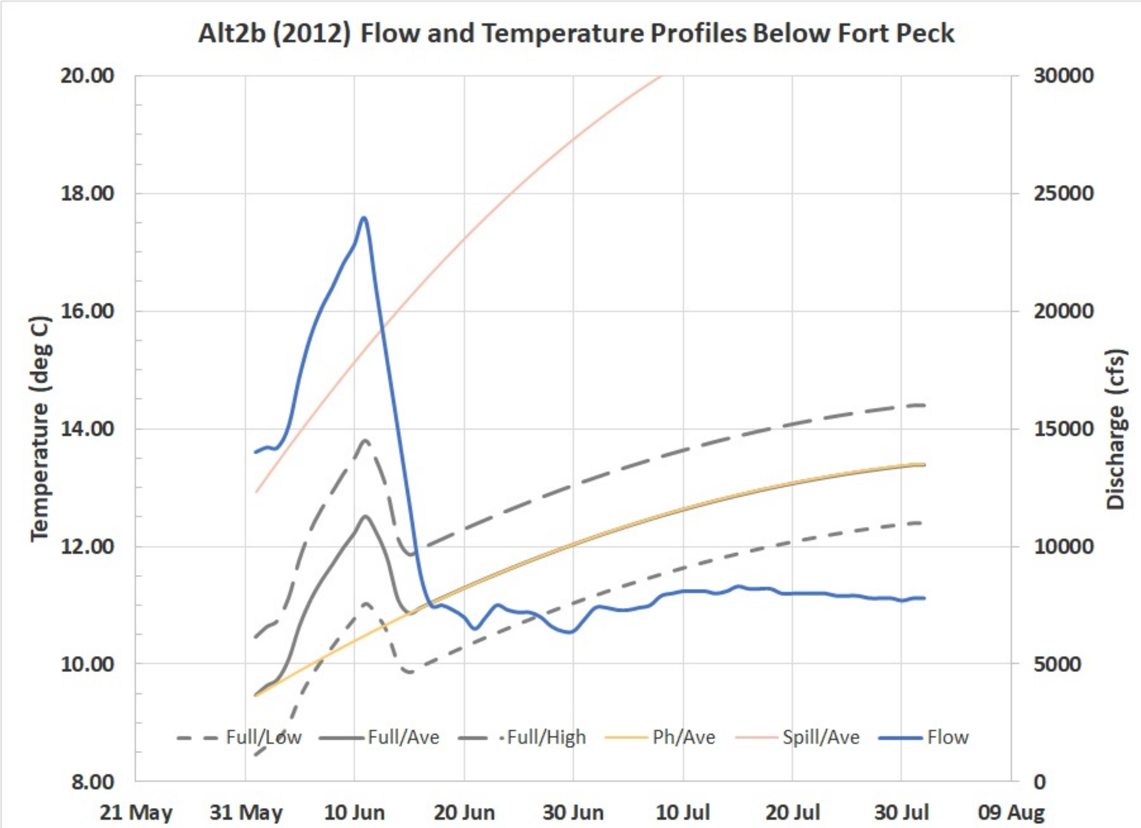
Alt2b (2012) Flow and Temperature Profiles Below Fort Peck
Temperature (deg C)
Discharge (cfs)
20.00
18.00
16.00
14.00
12.00
10.00
8.00
30000
25000
20000
15000
10000
5000
0
21 May
31 May
10 Jun
20 Jun
30 Jun
10 Jul
20 Jul
30 Jul
09 Aug
Full/Low
Full/Ave
Full/High
Ph/Ave
Spill/Ave
Flow

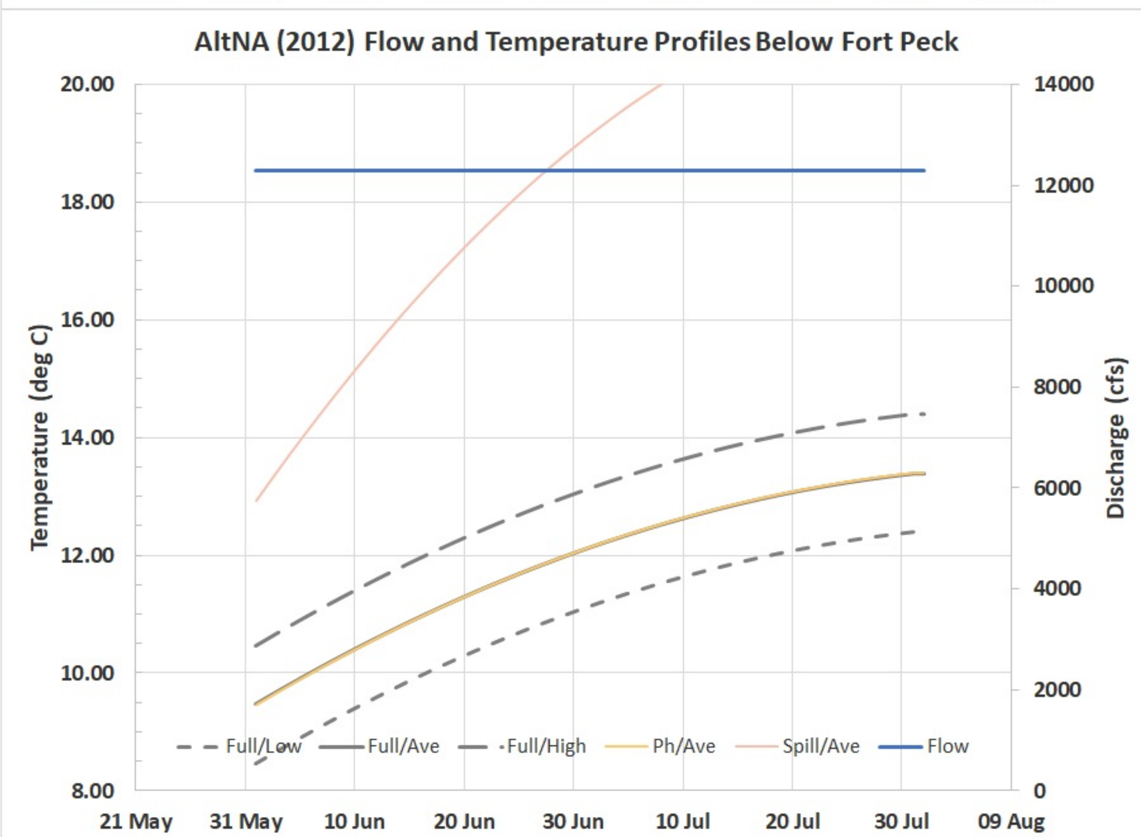
AltNA (2012) Flow and Temperature Profiles Below Fort Peck
Temperature (deg C)
Discharge (cfs)
20.00
18.00
16.00
14.00
12.00
10.00
8.00
14000
12000
10000
8000
6000
4000
2000
0
21 May
31 May
10 Jun
20 Jun
30 Jun
10 Jul
20 Jul
30 Jul
09 Aug
Full/Low
Full/Ave
Full/High
Ph/Ave
Spill/Ave
Flow

C.2 Plots of Cumulative Temperature and Retention

Plots of cumulative temperature exposure and corresponding rates of retention for Round 2 analyses are presented in this section. Four plots are presented for each alternative – one for each of the models. The plots maintain the same color combinations for years, so it is easier to compare values across alternatives. Dashed lines are cumulative thermal exposure and are associated with the left vertical axis. Solid lines are the cumulative percentage of drifting free embryos upstream of RM 1528, and use the right vertical axis. The horizontal axis is time since hatch. The plots are grouped together as Figure 4-23.

Table. Plots of cumulative thermal exposure and percentage of drifting free embryos upstream of the anoxic zone as a function of drift time for each alternative/year combination and for each of the four models used.

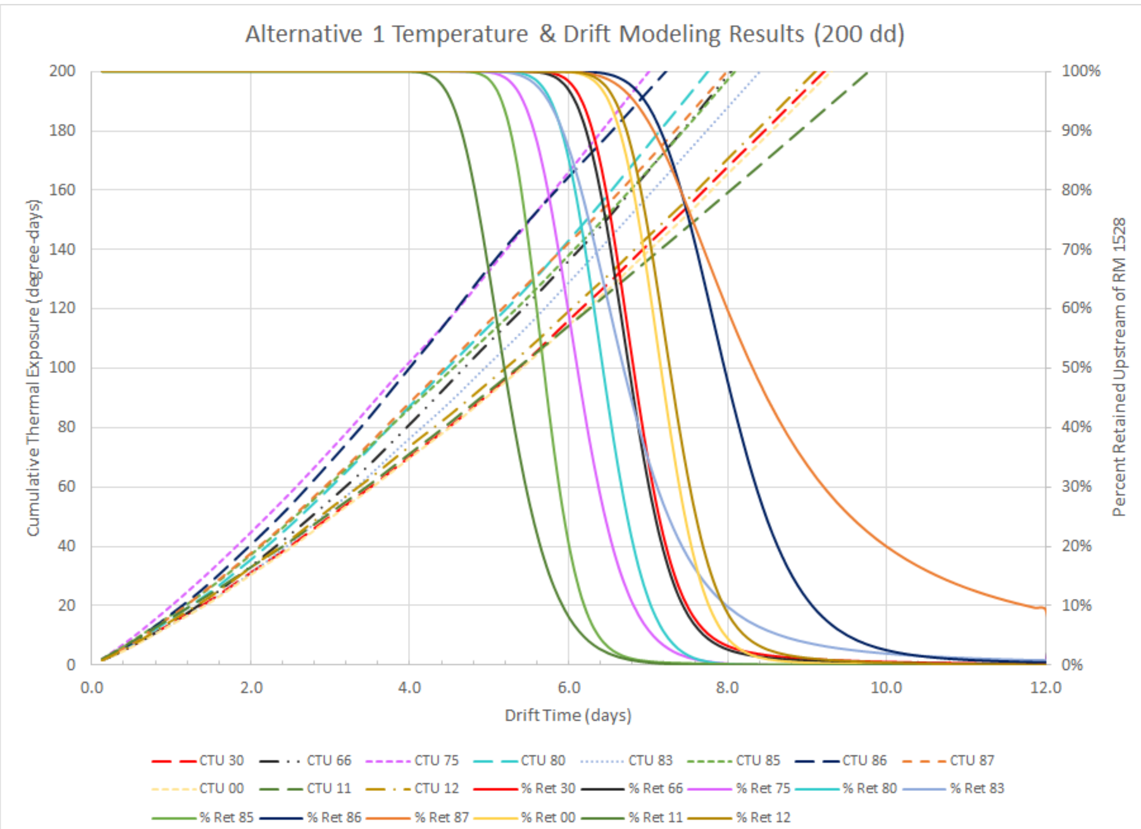

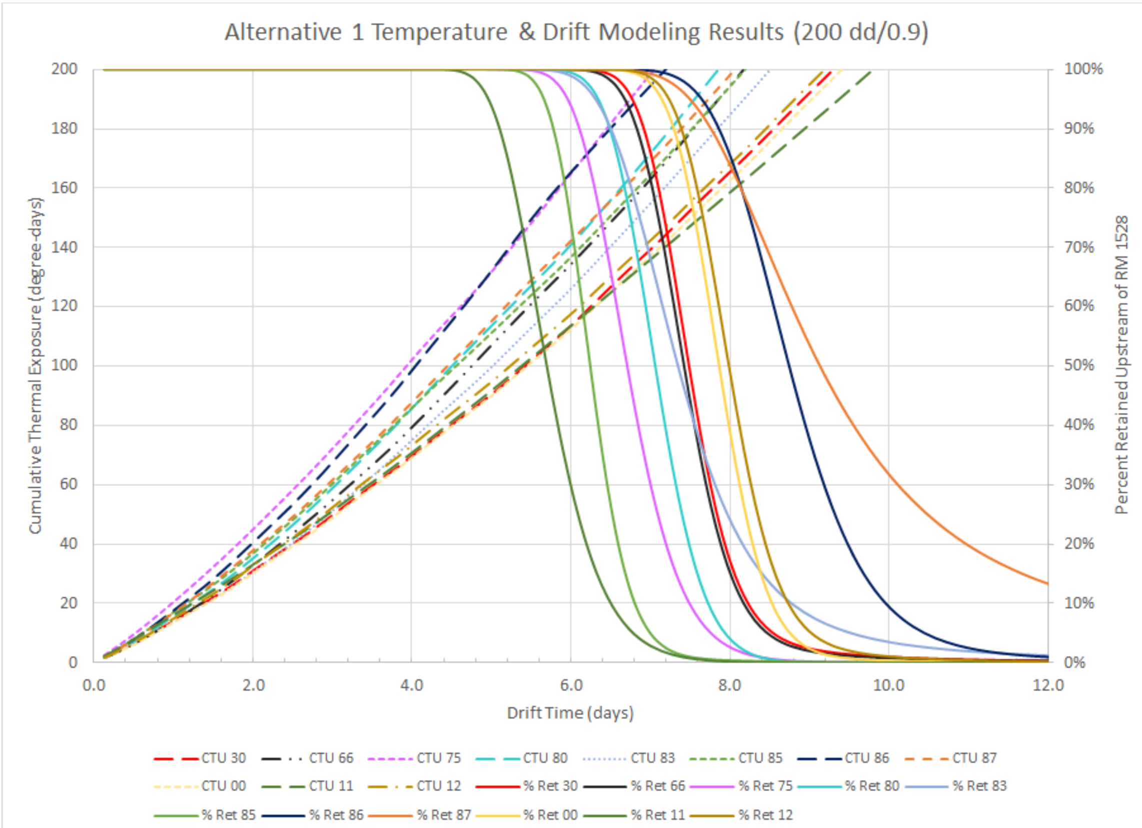
Alternative 1 Temperature & Drift Modeling Results (200 dd/0.9)
Cumulative Thermal Exposure (degree-days)
Percent Retained Upstream of RM 1528
Drift Time (days)
0
20
40
60
80
100
120
140
160
180
200
0%
10%
20%
30%
40%
50%
60%
70%
80%
90%
100%
0.0
2.0
4.0
6.0
8.0
10.0
12.0
CTU 30
CTU 66
CTU 75
CTU 80
CTU 83
CTU 85
CTU 86
CTU 87
CTU 00
CTU 11
CTU 12
% Ret 30
% Ret 66
% Ret 75
% Ret 80
% Ret 83
% Ret 85
% Ret 86
% Ret 87
% Ret 00
% Ret 11
% Ret 12

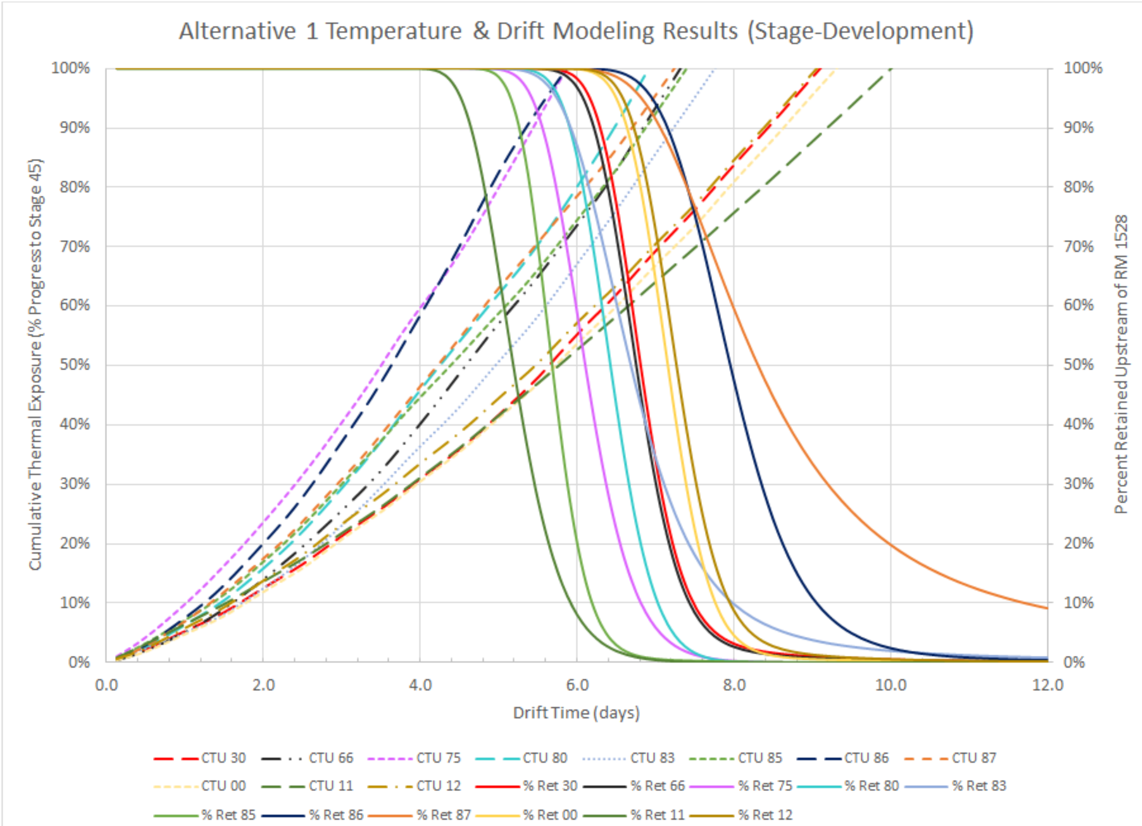
Alternative 1 Temperature & Drift Modeling Results (Stage-Development)
Cumulative Thermal Exposure (% Progress to Stage 45)
Percent Retained Upstream of RM 1528
Drift Time (days)
0.0
2.0
4.0
6.0
8.0
10.0
12.0
0%
10%
20%
30%
40%
50%
60%
70%
80%
90%
100%
CTU 30
CTU 66
CTU 75
CTU 80
CTU 83
CTU 85
CTU 86
CTU 87
CTU 00
CTU 11
CTU 12
% Ret 30
% Ret 66
% Ret 75
% Ret 80
% Ret 83
% Ret 85
% Ret 86
% Ret 87
% Ret 00
% Ret 11
% Ret 12

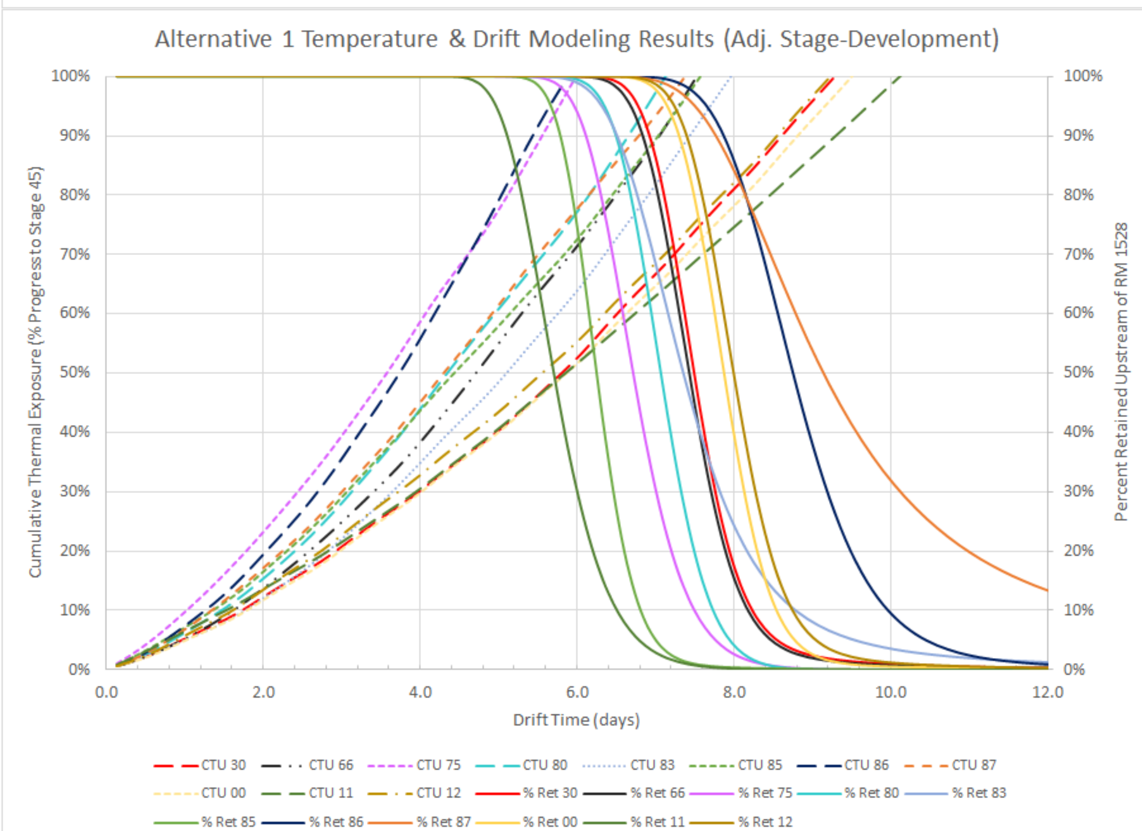
Alternative 1 Temperature & Drift Modeling Results (Adj. Stage-Development)
Cumulative Thermal Exposure (% Progress to Stage 45)
Percent Retained Upstream of RM 1528
Drift Time (days)
0.0
2.0
4.0
6.0
8.0
10.0
12.0
0%
10%
20%
30%
40%
50%
60%
70%
80%
90%
100%
CTU 30
CTU 66
CTU 75
CTU 80
CTU 83
CTU 85
CTU 86
CTU 87
CTU 00
CTU 11
CTU 12
% Ret 30
% Ret 66
% Ret 75
% Ret 80
% Ret 83
% Ret 85
% Ret 86
% Ret 87
% Ret 00
% Ret 11
% Ret 12

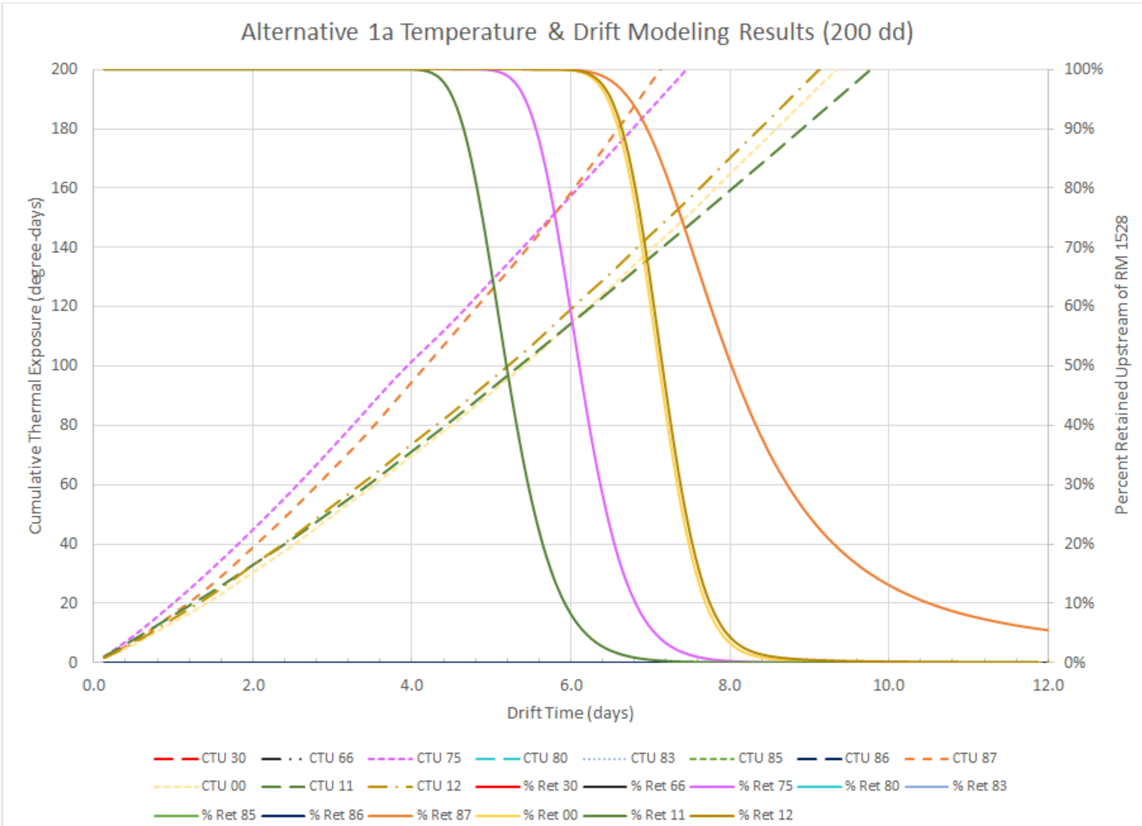
Alternative 1a Temperature & Drift Modeling Results (200 dd)
Cumulative Thermal Exposure (degree-days)
Percent Retained Upstream of RM 1528
Drift Time (days)
CTU 30
CTU 66
CTU 75
CTU 80
CTU 83
CTU 85
CTU 86
CTU 87
CTU 00
CTU 11
CTU 12
% Ret 30
% Ret 66
% Ret 75
% Ret 80
% Ret 83
% Ret 85
% Ret 86
% Ret 87
% Ret 00
% Ret 11
% Ret 12

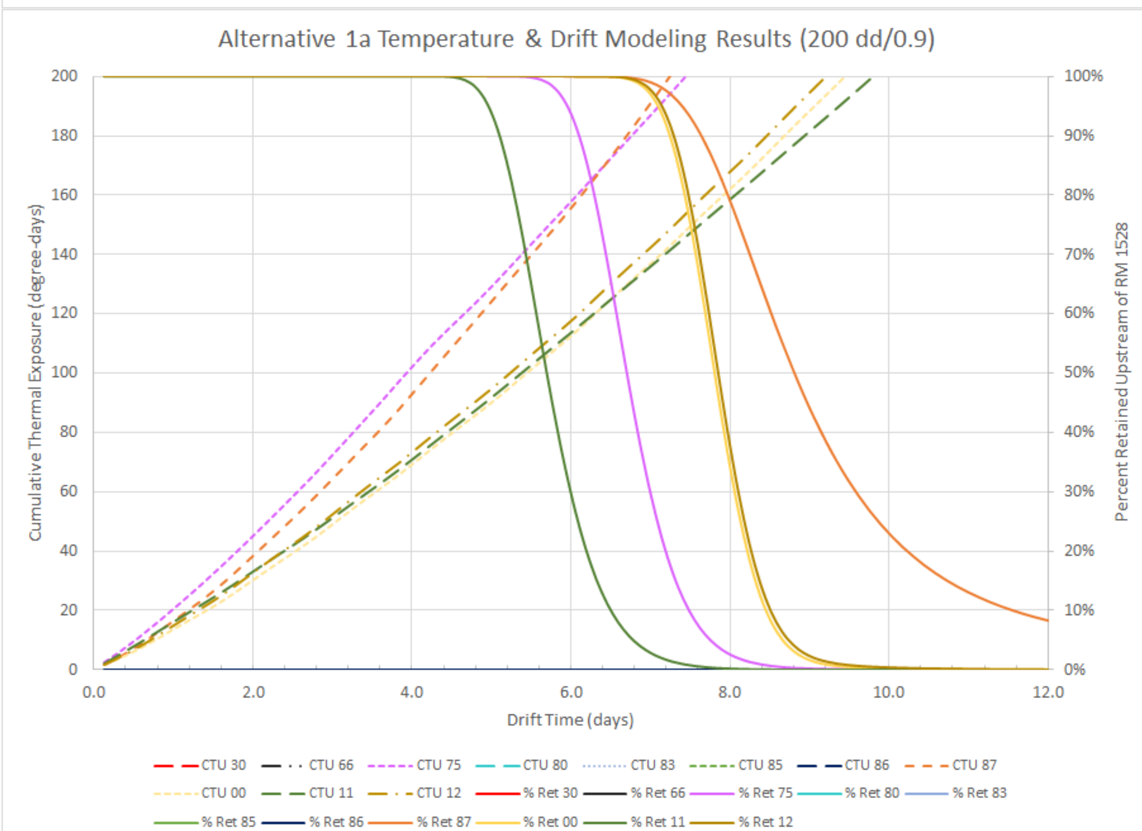
Alternative 1a Temperature & Drift Modeling Results (200 dd/0.9)
Cumulative Thermal Exposure (degree-days)
Percent Retained Upstream of RM 1528
Drift Time (days)
CTU 30
CTU 66
CTU 75
CTU 80
CTU 83
CTU 85
CTU 86
CTU 87
CTU 00
CTU 11
CTU 12
% Ret 30
% Ret 66
% Ret 75
% Ret 80
% Ret 83
% Ret 85
% Ret 86
% Ret 87
% Ret 00
% Ret 11
% Ret 12

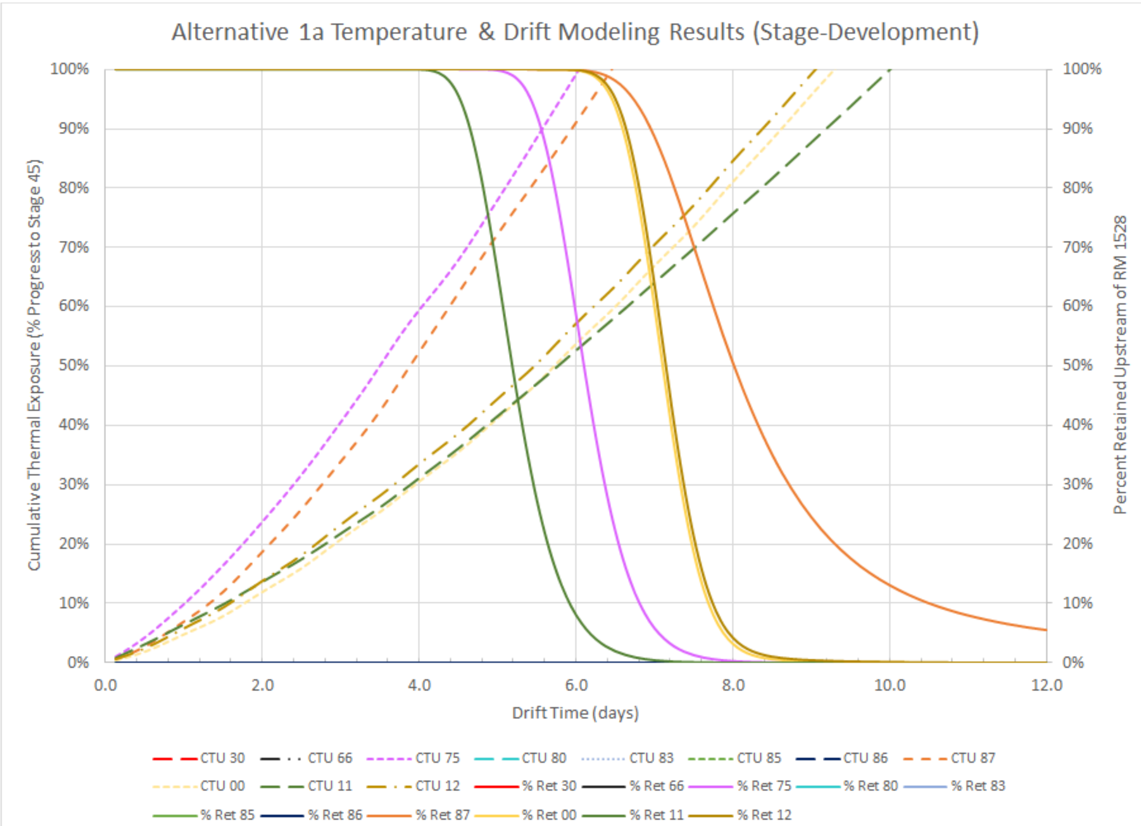
Alternative 1a Temperature & Drift Modeling Results (Stage-Development)
Cumulative Thermal Exposure (% Progress to Stage 45)
Percent Retained Upstream of RM 1528
100%
90%
80%
70%
60%
50%
40%
30%
20%
10%
0%
0.0
2.0
4.0
6.0
8.0
10.0
12.0
Drift Time (days)
CTU 30
CTU 66
CTU 75
CTU 80
CTU 83
CTU 85
CTU 86
CTU 87
CTU 00
CTU 11
CTU 12
% Ret 30
% Ret 66
% Ret 75
% Ret 80
% Ret 83
% Ret 85
% Ret 86
% Ret 87
% Ret 00
% Ret 11
% Ret 12

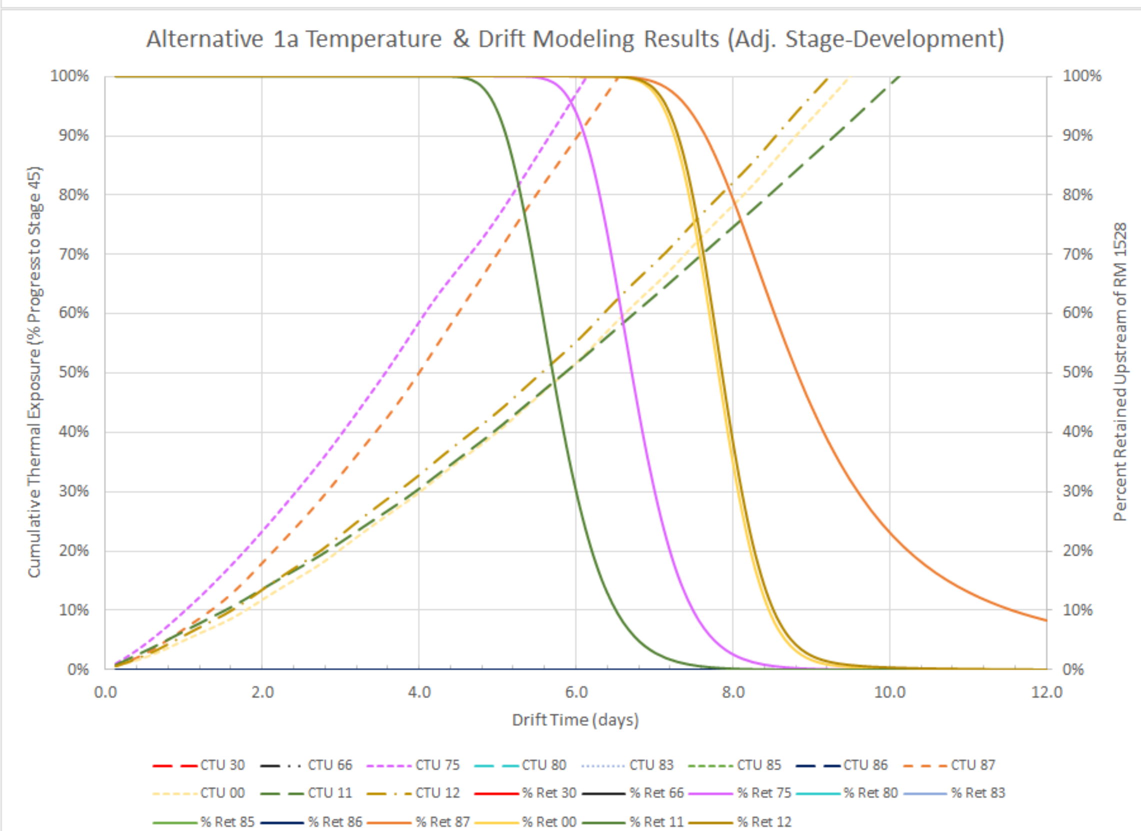
Alternative 1a Temperature & Drift Modeling Results (Adj. Stage-Development)
Cumulative Thermal Exposure (% Progress to Stage 45)
Percent Retained Upstream of RM 1528
100%
90%
80%
70%
60%
50%
40%
30%
20%
10%
0%
0.0
2.0
4.0
6.0
8.0
10.0
12.0
Drift Time (days)
CTU 30
CTU 66
CTU 75
CTU 80
CTU 83
CTU 85
CTU 86
CTU 87
CTU 00
CTU 11
CTU 12
% Ret 30
% Ret 66
% Ret 75
% Ret 80
% Ret 83
% Ret 85
% Ret 86
% Ret 87
% Ret 00
% Ret 11
% Ret 12

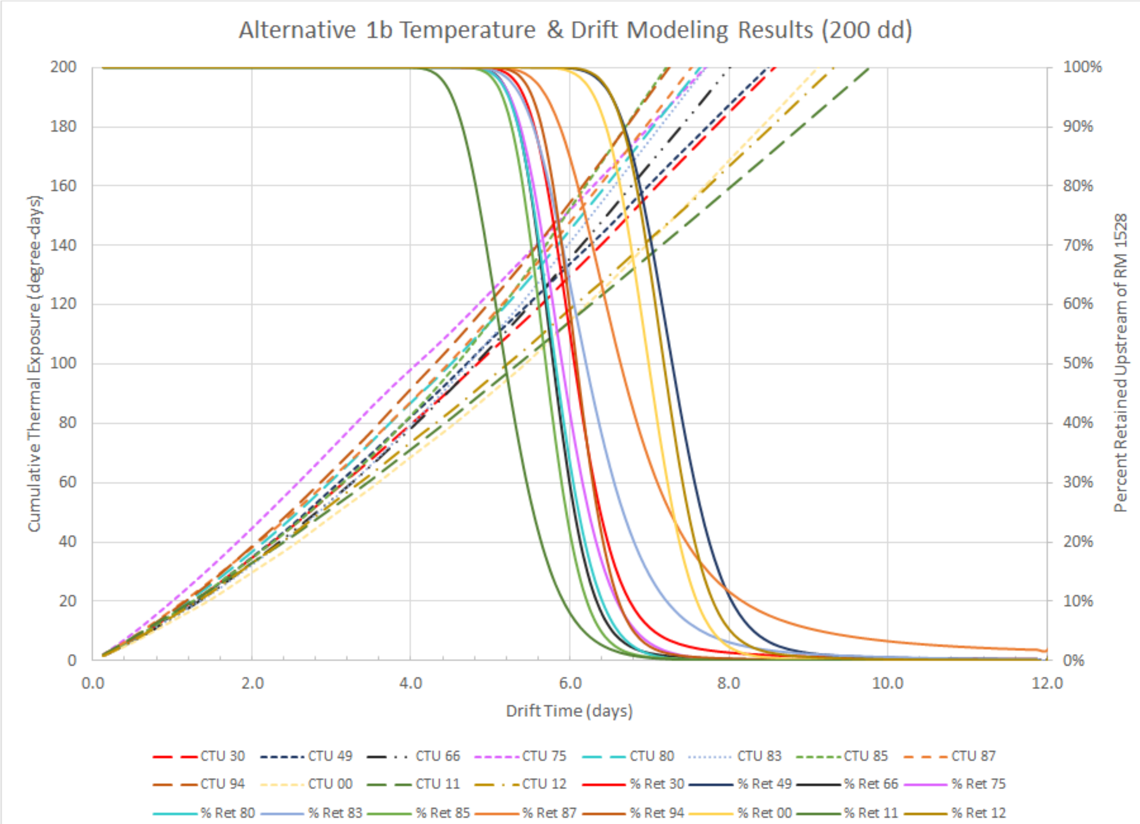
Alternative 1b Temperature & Drift Modeling Results (200 dd)
Cumulative Thermal Exposure (degree-days)
Percent Retained Upstream of RM 1528
Drift Time (days)
200
180
160
140
120
100
80
60
40
20
0
100%
90%
80%
70%
60%
50%
40%
30%
20%
10%
0%
0.0
2.0
4.0
6.0
8.0
10.0
12.0
CTU 30
CTU 49
CTU 66
CTU 75
CTU 80
CTU 83
CTU 85
CTU 87
CTU 94
CTU 00
CTU 11
CTU 12
% Ret 30
% Ret 49
% Ret 66
% Ret 75
% Ret 80
% Ret 83
% Ret 85
% Ret 87
% Ret 94
% Ret 00
% Ret 11
% Ret 12

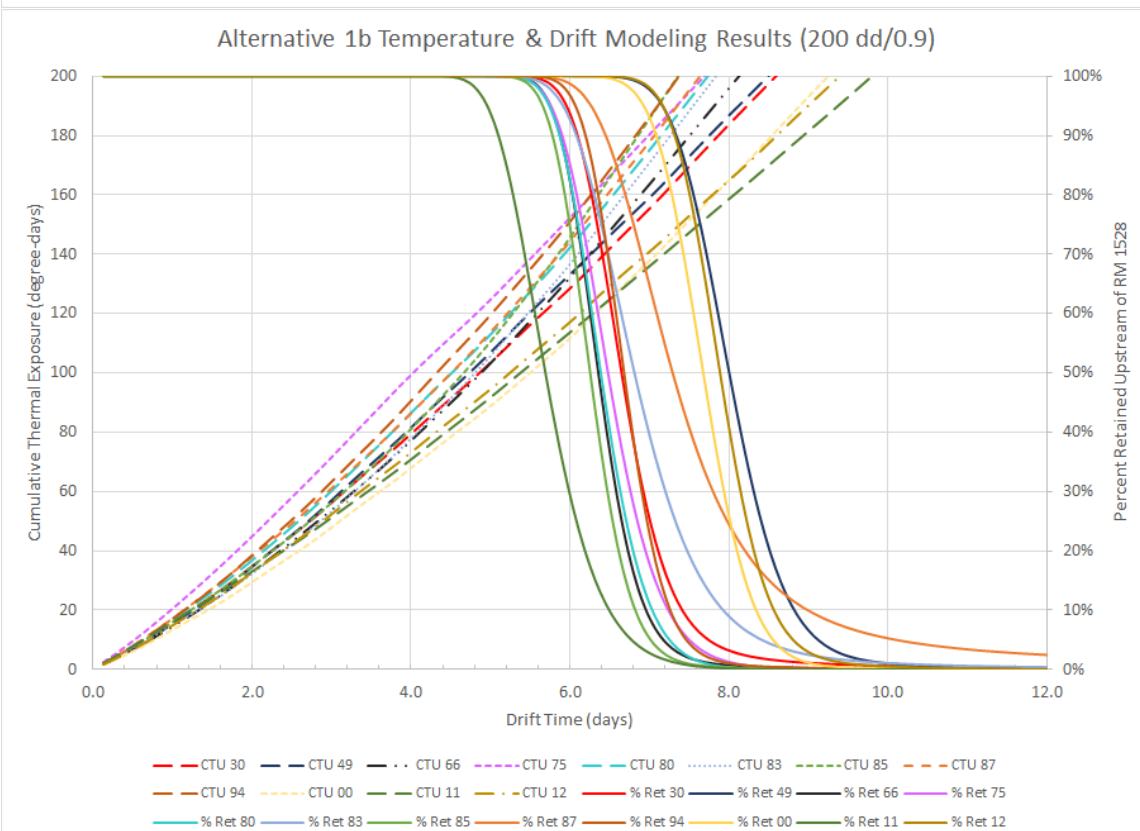
Alternative 1b Temperature & Drift Modeling Results (200 dd/0.9)
Cumulative Thermal Exposure (degree-days)
Percent Retained Upstream of RM 1528
Drift Time (days)
200
180
160
140
120
100
80
60
40
20
0
100%
90%
80%
70%
60%
50%
40%
30%
20%
10%
0%
0.0
2.0
4.0
6.0
8.0
10.0
12.0
CTU 30
CTU 49
CTU 66
CTU 75
CTU 80
CTU 83
CTU 85
CTU 87
CTU 94
CTU 00
CTU 11
CTU 12
% Ret 30
% Ret 49
% Ret 66
% Ret 75
% Ret 80
% Ret 83
% Ret 85
% Ret 87
% Ret 94
% Ret 00
% Ret 11
% Ret 12

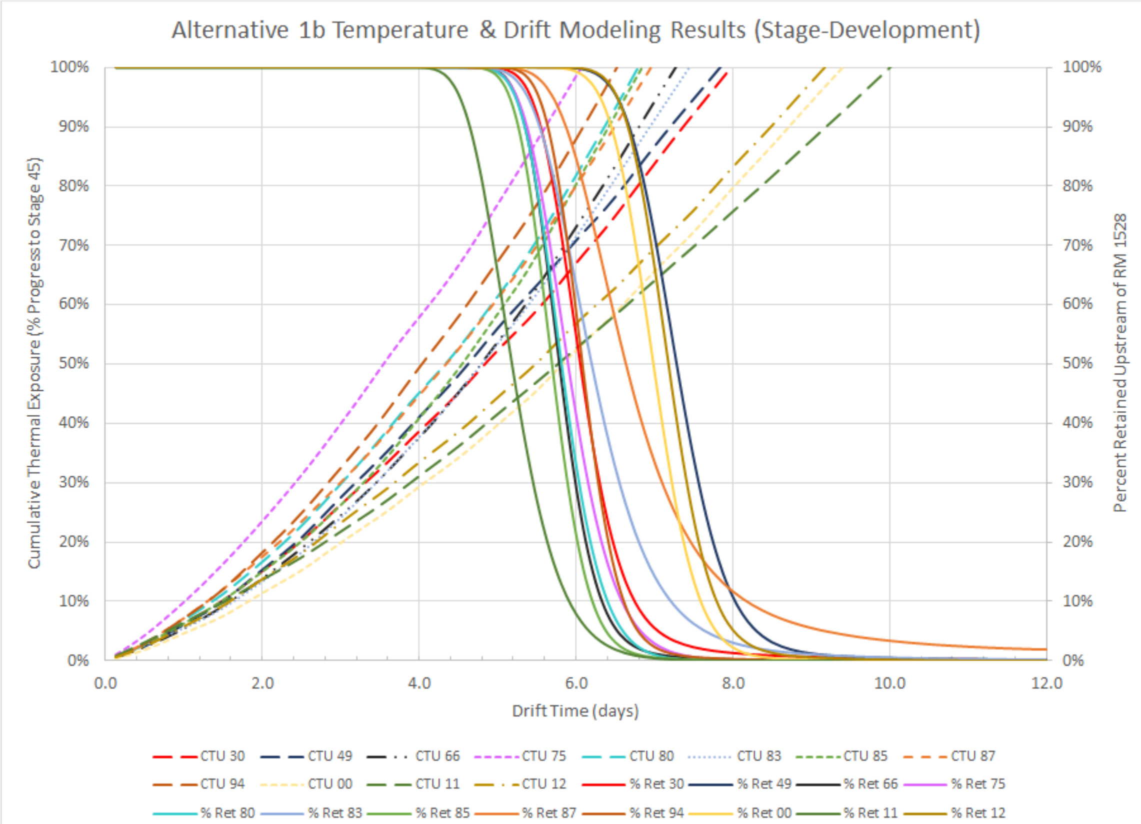
Alternative 1b Temperature & Drift Modeling Results (Stage-Development)
Cumulative Thermal Exposure (% Progress to Stage 45)
Percent Retained Upstream of RM 1528
Drift Time (days)
CTU 30
CTU 49
CTU 66
CTU 75
CTU 80
CTU 83
CTU 85
CTU 87
CTU 94
CTU 00
CTU 11
CTU 12
% Ret 30
% Ret 49
% Ret 66
% Ret 75
% Ret 80
% Ret 83
% Ret 85
% Ret 87
% Ret 94
% Ret 00
% Ret 11
% Ret 12

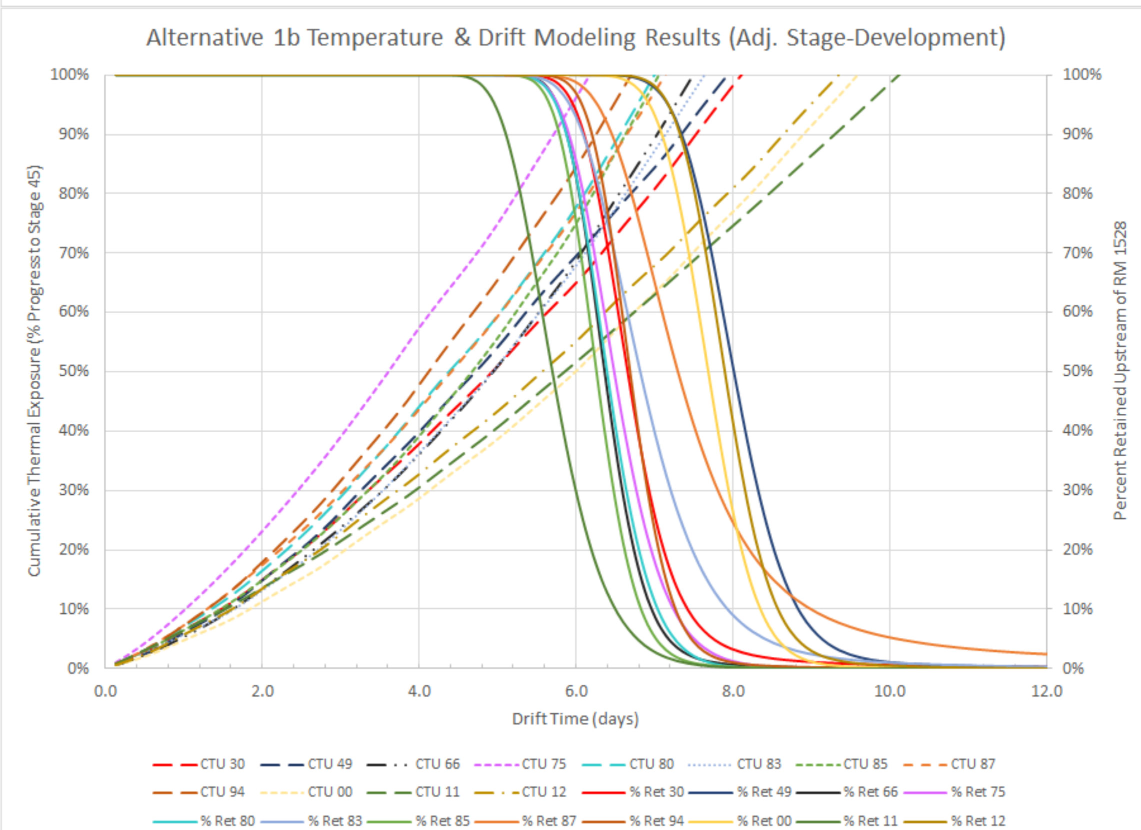
Alternative 1b Temperature & Drift Modeling Results (Adj. Stage-Development)
Cumulative Thermal Exposure (% Progress to Stage 45)
Percent Retained Upstream of RM 1528
Drift Time (days)
CTU 30
CTU 49
CTU 66
CTU 75
CTU 80
CTU 83
CTU 85
CTU 87
CTU 94
CTU 00
CTU 11
CTU 12
% Ret 30
% Ret 49
% Ret 66
% Ret 75
% Ret 80
% Ret 83
% Ret 85
% Ret 87
% Ret 94
% Ret 00
% Ret 11
% Ret 12

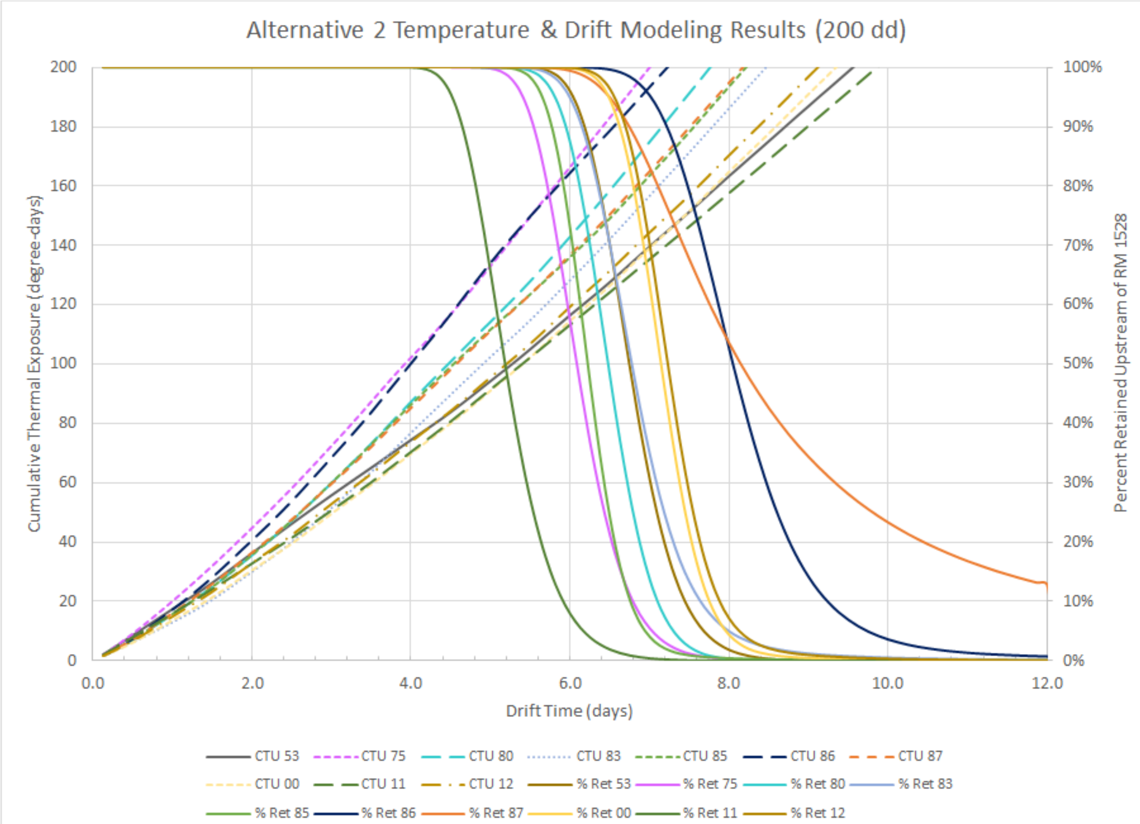
Alternative 2 Temperature & Drift Modeling Results (200 dd)
Cumulative Thermal Exposure (degree-days)
Percent Retained Upstream of RM 1528
Drift Time (days)
0
20
40
60
80
100
120
140
160
180
200
0%
10%
20%
30%
40%
50%
60%
70%
80%
90%
100%
0.0
2.0
4.0
6.0
8.0
10.0
12.0
CTU 53
CTU 75
CTU 80
CTU 83
CTU 85
CTU 86
CTU 87
CTU 00
CTU 11
CTU 12
% Ret 53
% Ret 75
% Ret 80
% Ret 83
% Ret 85
% Ret 86
% Ret 87
% Ret 00
% Ret 11
% Ret 12

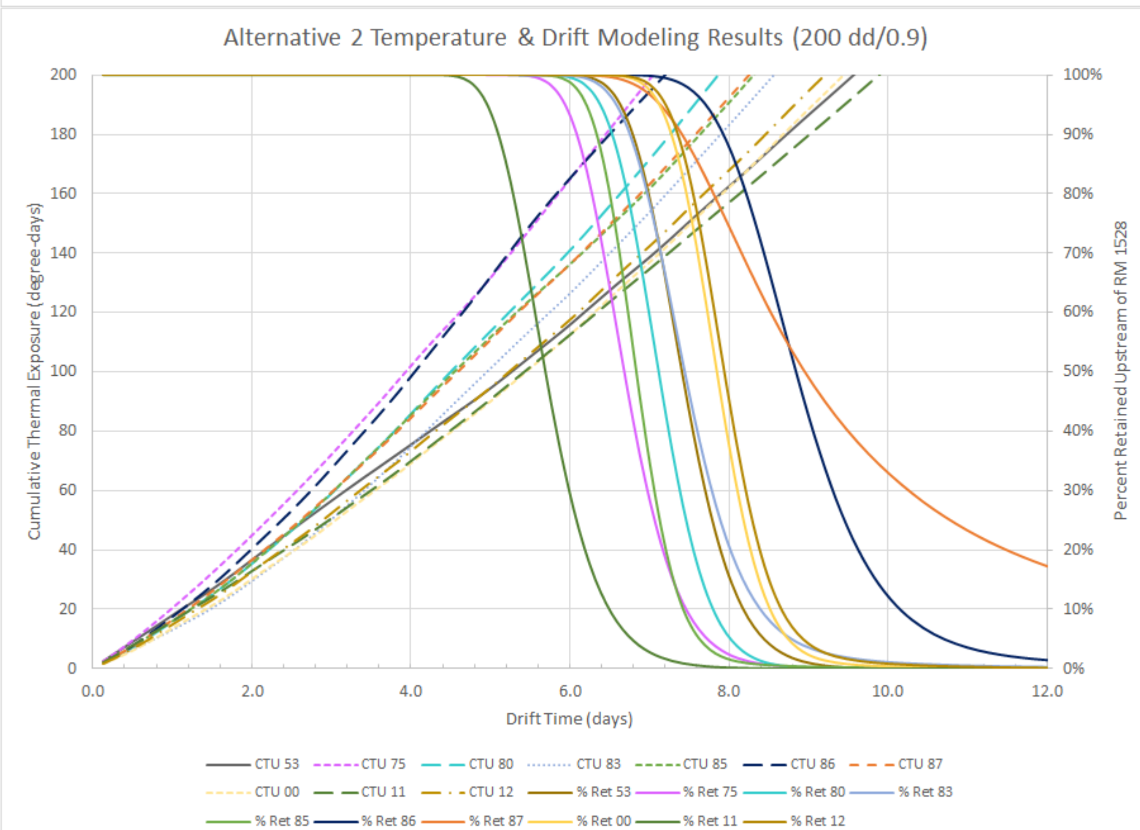
Alternative 2 Temperature & Drift Modeling Results (200 dd/0.9)
Cumulative Thermal Exposure (degree-days)
Percent Retained Upstream of RM 1528
Drift Time (days)
0
20
40
60
80
100
120
140
160
180
200
0%
10%
20%
30%
40%
50%
60%
70%
80%
90%
100%
0.0
2.0
4.0
6.0
8.0
10.0
12.0
CTU 53
CTU 75
CTU 80
CTU 83
CTU 85
CTU 86
CTU 87
CTU 00
CTU 11
CTU 12
% Ret 53
% Ret 75
% Ret 80
% Ret 83
% Ret 85
% Ret 86
% Ret 87
% Ret 00
% Ret 11
% Ret 12

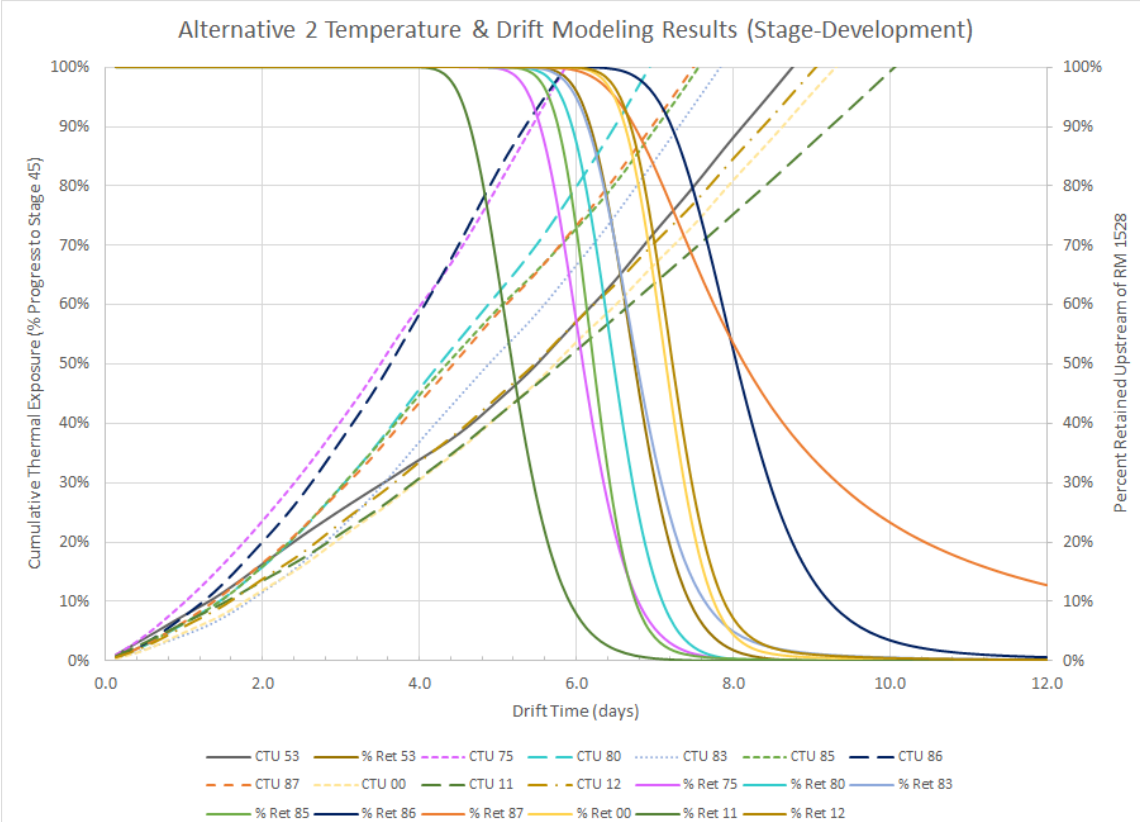
Alternative 2 Temperature & Drift Modeling Results (Stage-Development)
Cumulative Thermal Exposure (% Progress to Stage 45)
Percent Retained Upstream of RM 1528
Drift Time (days)
0.0 2.0 4.0 6.0 8.0 10.0 12.0
0% 10% 20% 30% 40% 50% 60% 70% 80% 90% 100%
CTU 53 % Ret 53 CTU 75 CTU 80 CTU 83 CTU 85 CTU 86
CTU 87 CTU 00 CTU 11 CTU 12 % Ret 75 % Ret 80 % Ret 83
% Ret 85 % Ret 86 % Ret 87 % Ret 00 % Ret 11 % Ret 12

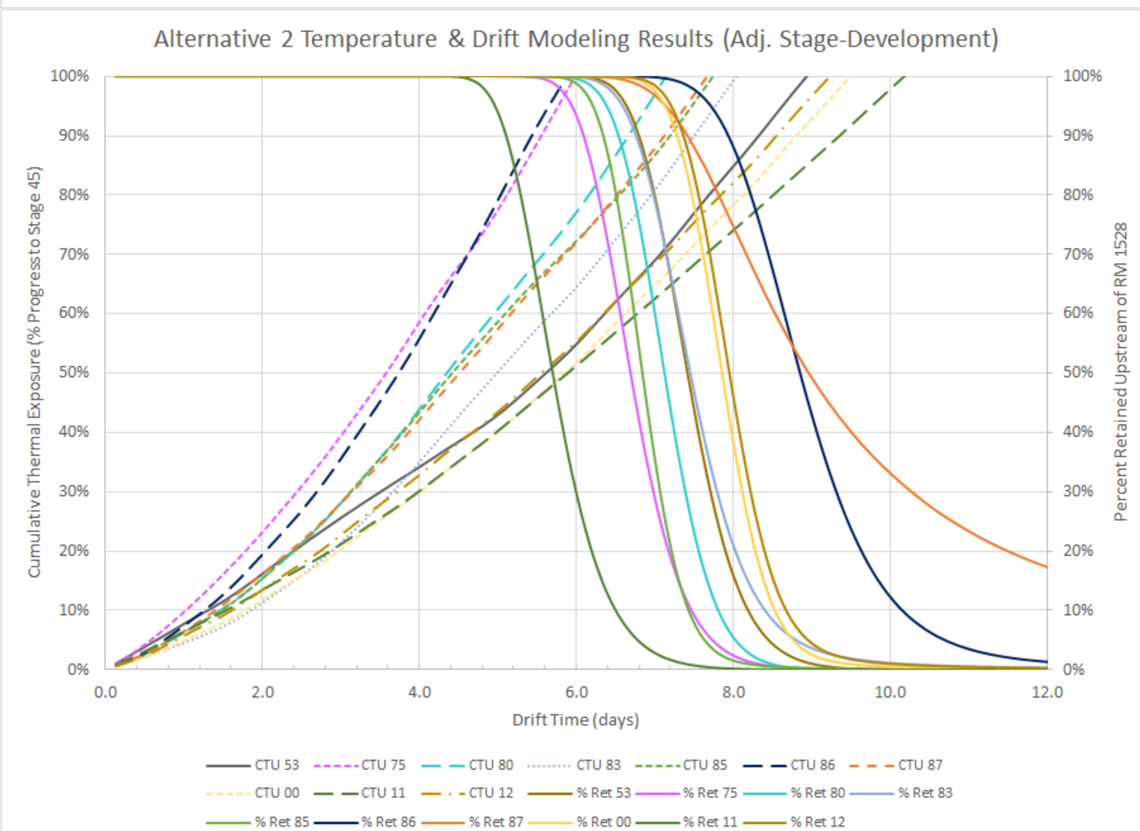
Alternative 2 Temperature & Drift Modeling Results (Adj. Stage-Development)
Cumulative Thermal Exposure (% Progress to Stage 45)
Percent Retained Upstream of RM 1528
Drift Time (days)
0.0 2.0 4.0 6.0 8.0 10.0 12.0
0% 10% 20% 30% 40% 50% 60% 70% 80% 90% 100%
CTU 53 CTU 75 CTU 80 CTU 83 CTU 85 CTU 86 CTU 87
CTU 00 CTU 11 CTU 12 % Ret 53 % Ret 75 % Ret 80 % Ret 83
% Ret 85 % Ret 86 % Ret 87 % Ret 00 % Ret 11 % Ret 12

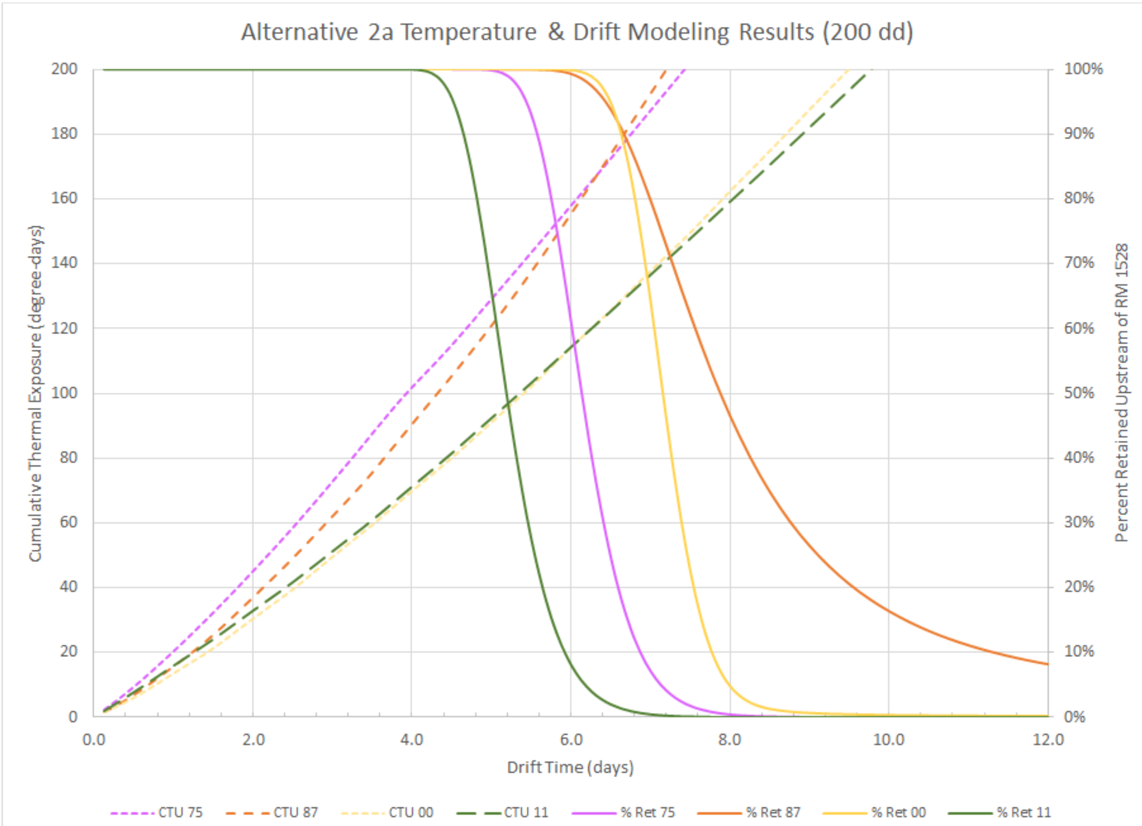
Alternative 2a Temperature & Drift Modeling Results (200 dd)
Cumulative Thermal Exposure (degree-days)
Percent Retained Upstream of RM 1528
Drift Time (days)
0
20
40
60
80
100
120
140
160
180
200
0%
10%
20%
30%
40%
50%
60%
70%
80%
90%
100%
0.0
2.0
4.0
6.0
8.0
10.0
12.0
CTU 75
CTU 87
CTU 00
CTU 11
% Ret 75
% Ret 87
% Ret 00
% Ret 11

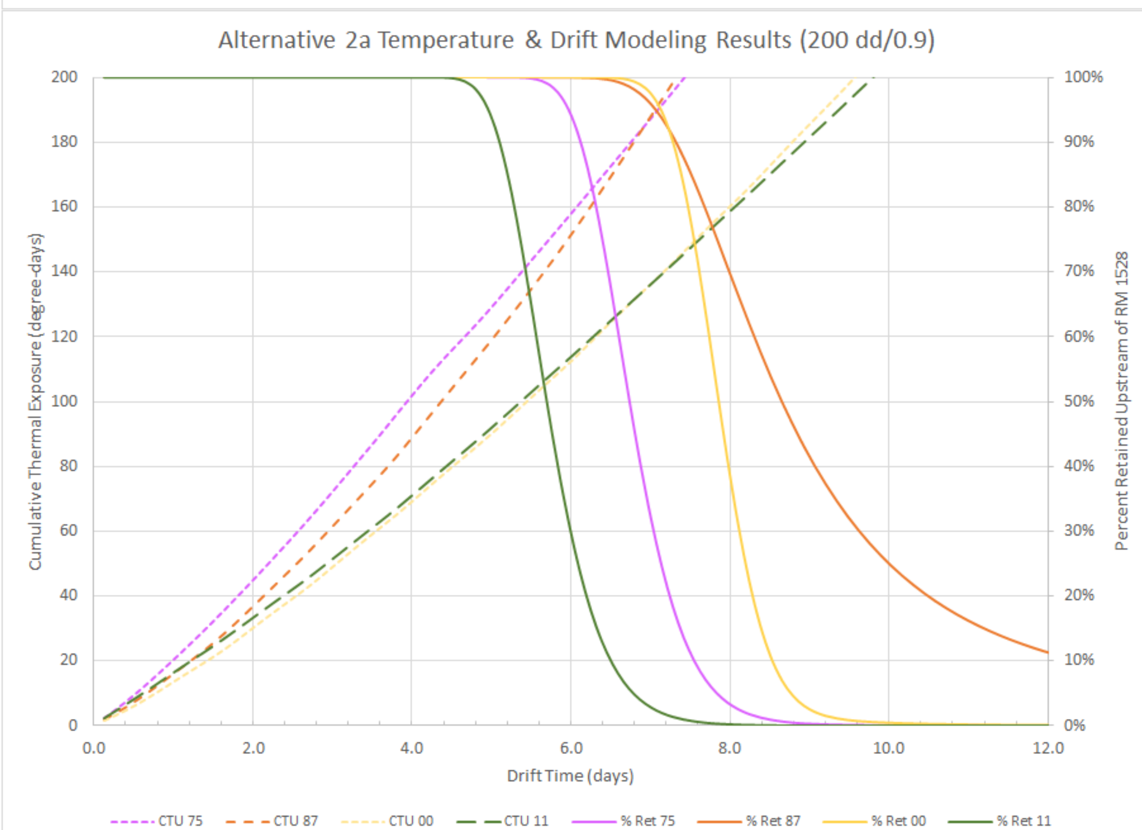
Alternative 2a Temperature & Drift Modeling Results (200 dd/0.9)
Cumulative Thermal Exposure (degree-days)
Percent Retained Upstream of RM 1528
Drift Time (days)
0
20
40
60
80
100
120
140
160
180
200
0%
10%
20%
30%
40%
50%
60%
70%
80%
90%
100%
0.0
2.0
4.0
6.0
8.0
10.0
12.0
CTU 75
CTU 87
CTU 00
CTU 11
% Ret 75
% Ret 87
% Ret 00
% Ret 11

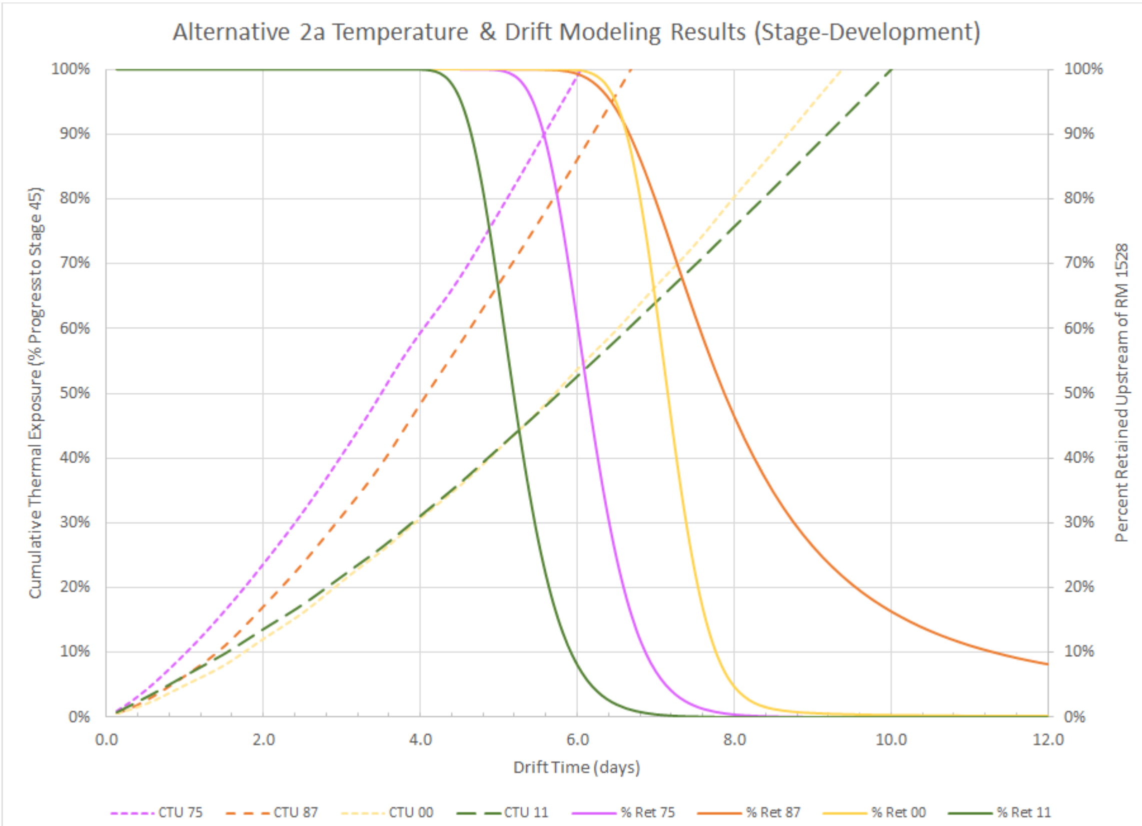
Alternative 2a Temperature & Drift Modeling Results (Stage-Development)
Cumulative Thermal Exposure (% Progress to Stage 45)
Percent Retained Upstream of RM 1528
Drift Time (days)
0.0
2.0
4.0
6.0
8.0
10.0
12.0
0%
10%
20%
30%
40%
50%
60%
70%
80%
90%
100%
CTU 75
CTU 87
CTU 00
CTU 11
% Ret 75
% Ret 87
% Ret 00
% Ret 11

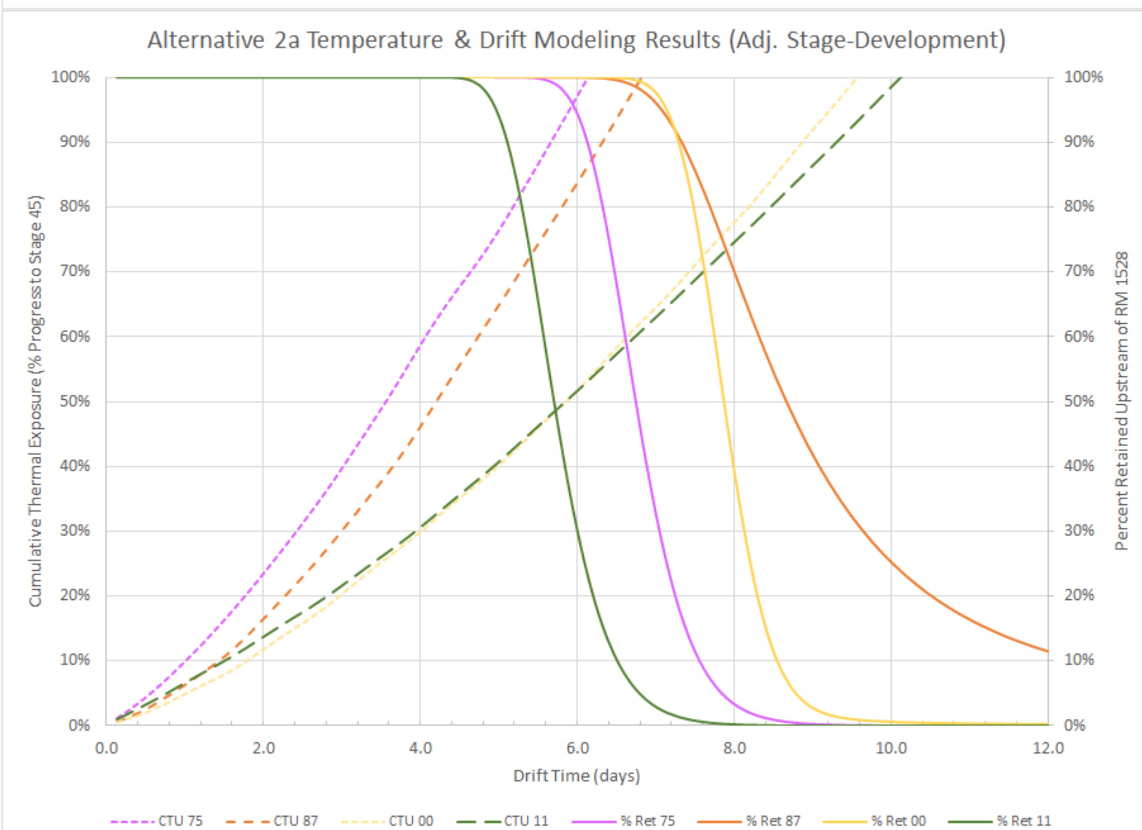
Alternative 2a Temperature & Drift Modeling Results (Adj. Stage-Development)
Cumulative Thermal Exposure (% Progress to Stage 45)
Percent Retained Upstream of RM 1528
Drift Time (days)
0.0
2.0
4.0
6.0
8.0
10.0
12.0
0%
10%
20%
30%
40%
50%
60%
70%
80%
90%
100%
CTU 75
CTU 87
CTU 00
CTU 11
% Ret 75
% Ret 87
% Ret 00
% Ret 11

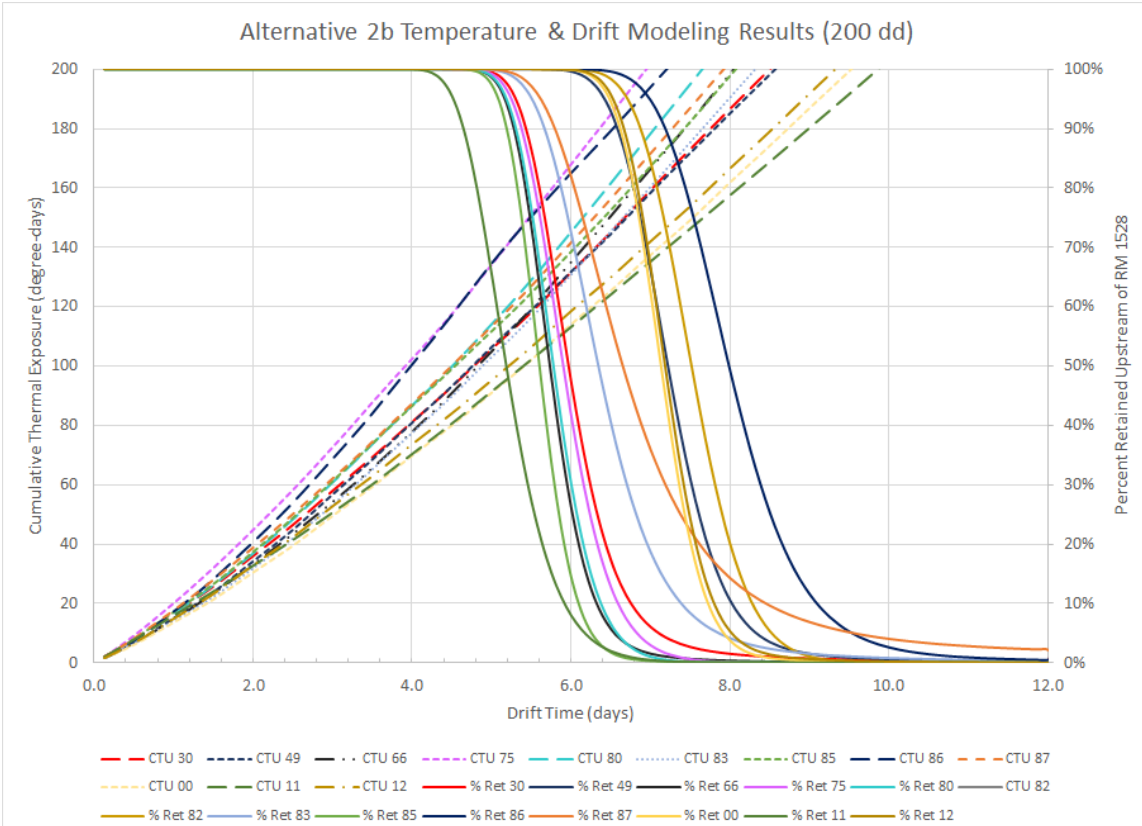
Alternative 2b Temperature & Drift Modeling Results (200 dd)
Cumulative Thermal Exposure (degree-days)
Percent Retained Upstream of RM 1528
Drift Time (days)
CTU 30
CTU 49
CTU 66
CTU 75
CTU 80
CTU 83
CTU 85
CTU 86
CTU 87
CTU 00
CTU 11
CTU 12
% Ret 30
% Ret 49
% Ret 66
% Ret 75
% Ret 80
CTU 82
% Ret 82
% Ret 83
% Ret 85
% Ret 86
% Ret 87
% Ret 00
% Ret 11
% Ret 12

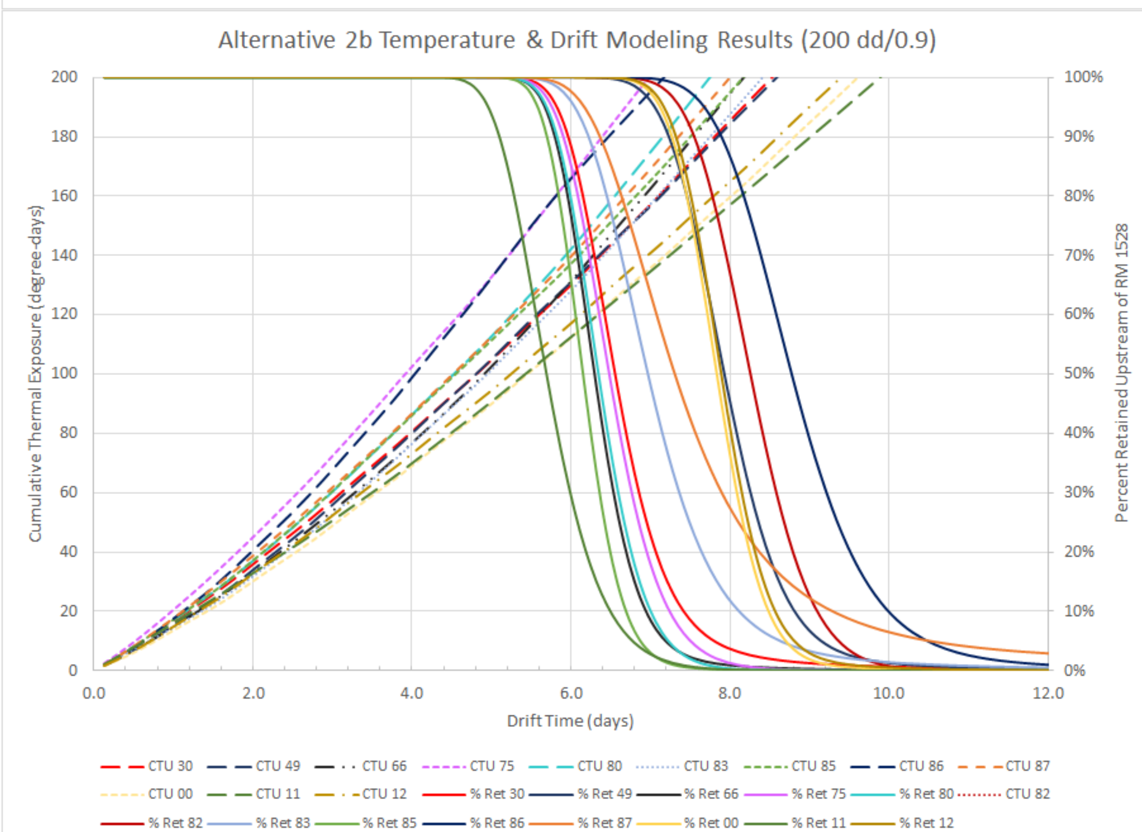
Alternative 2b Temperature & Drift Modeling Results (200 dd/0.9)
Cumulative Thermal Exposure (degree-days)
Percent Retained Upstream of RM 1528
Drift Time (days)
CTU 30
CTU 49
CTU 66
CTU 75
CTU 80
CTU 83
CTU 85
CTU 86
CTU 87
CTU 00
CTU 11
CTU 12
% Ret 30
% Ret 49
% Ret 66
% Ret 75
% Ret 80
CTU 82
% Ret 82
% Ret 83
% Ret 85
% Ret 86
% Ret 87
% Ret 00
% Ret 11
% Ret 12

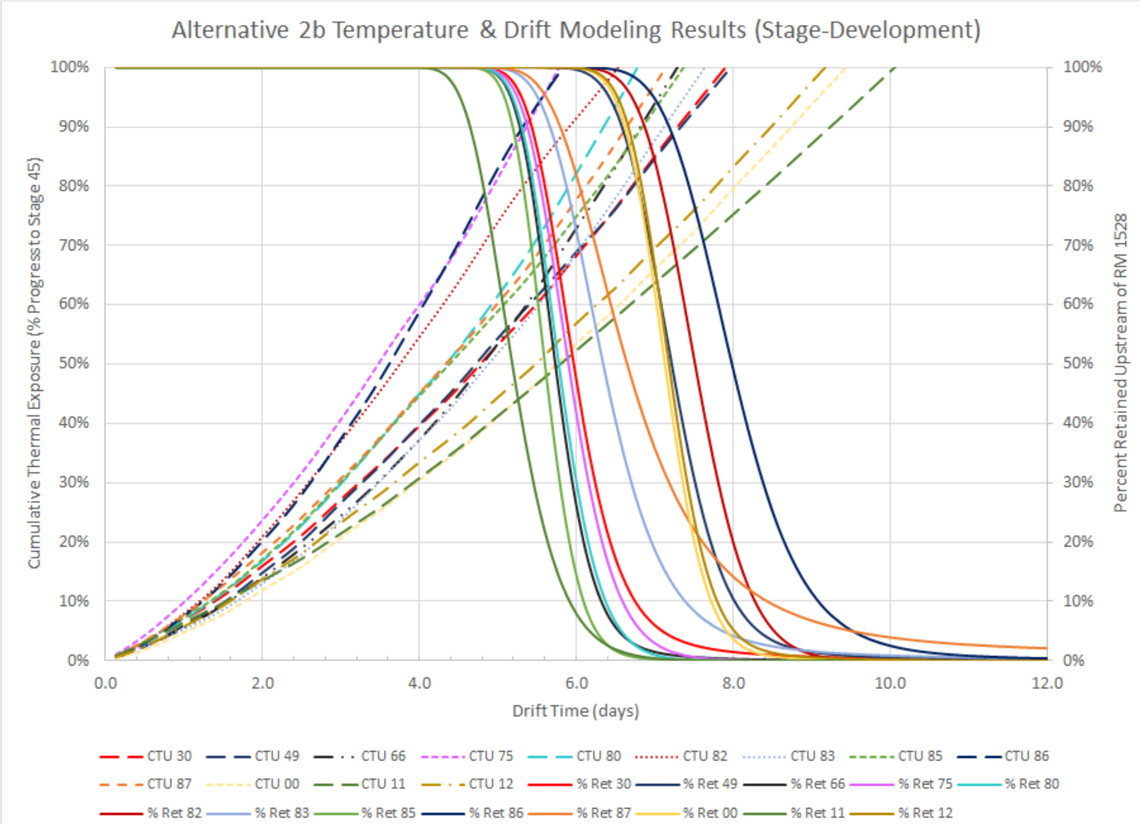
Alternative 2b Temperature & Drift Modeling Results (Stage-Development)
Cumulative Thermal Exposure (% Progress to Stage 45)
Percent Retained Upstream of RM 1528
Drift Time (days)
0.0
2.0
4.0
6.0
8.0
10.0
12.0
0%
10%
20%
30%
40%
50%
60%
70%
80%
90%
100%
CTU 30
CTU 49
CTU 66
CTU 75
CTU 80
CTU 82
CTU 83
CTU 85
CTU 86
CTU 87
CTU 00
CTU 11
CTU 12
% Ret 30
% Ret 49
% Ret 66
% Ret 75
% Ret 80
% Ret 82
% Ret 83
% Ret 85
% Ret 86
% Ret 87
% Ret 00
% Ret 11
% Ret 12

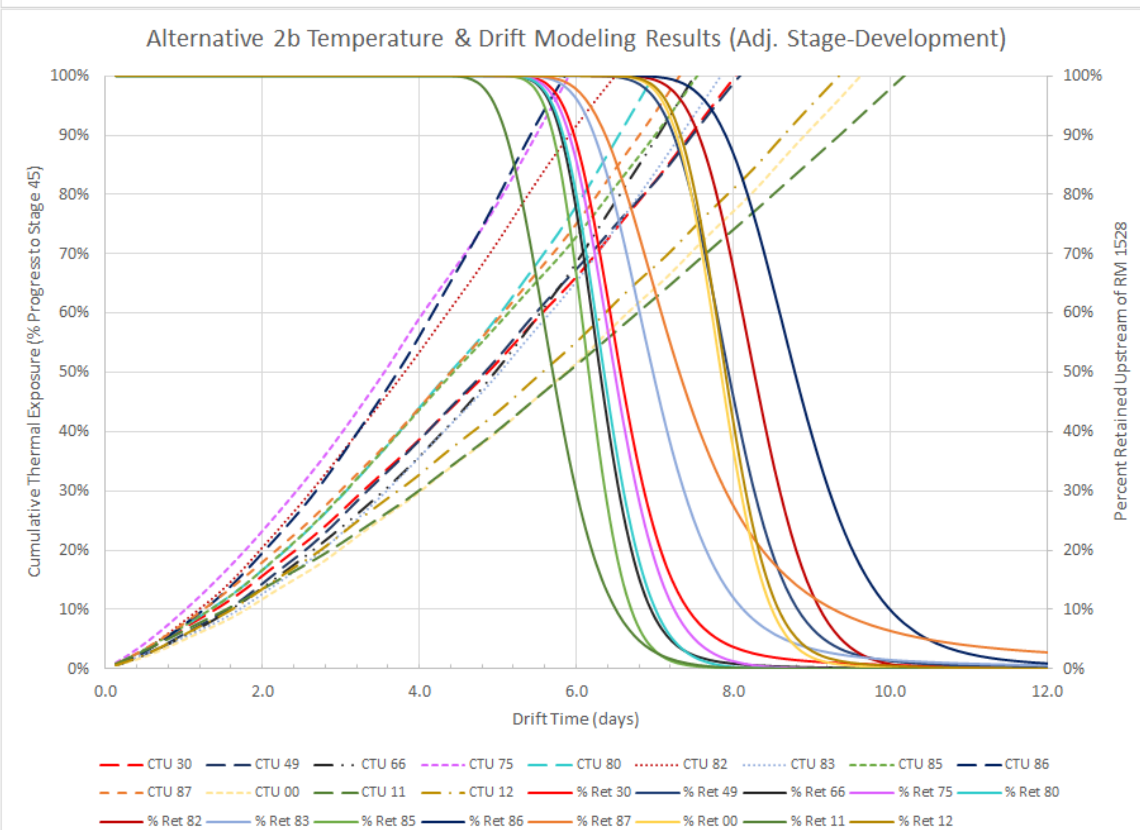
Alternative 2b Temperature & Drift Modeling Results (Adj. Stage-Development)
Cumulative Thermal Exposure (% Progress to Stage 45)
Percent Retained Upstream of RM 1528
Drift Time (days)
0.0
2.0
4.0
6.0
8.0
10.0
12.0
0%
10%
20%
30%
40%
50%
60%
70%
80%
90%
100%
CTU 30
CTU 49
CTU 66
CTU 75
CTU 80
CTU 82
CTU 83
CTU 85
CTU 86
CTU 87
CTU 00
CTU 11
CTU 12
% Ret 30
% Ret 49
% Ret 66
% Ret 75
% Ret 80
% Ret 82
% Ret 83
% Ret 85
% Ret 86
% Ret 87
% Ret 00
% Ret 11
% Ret 12

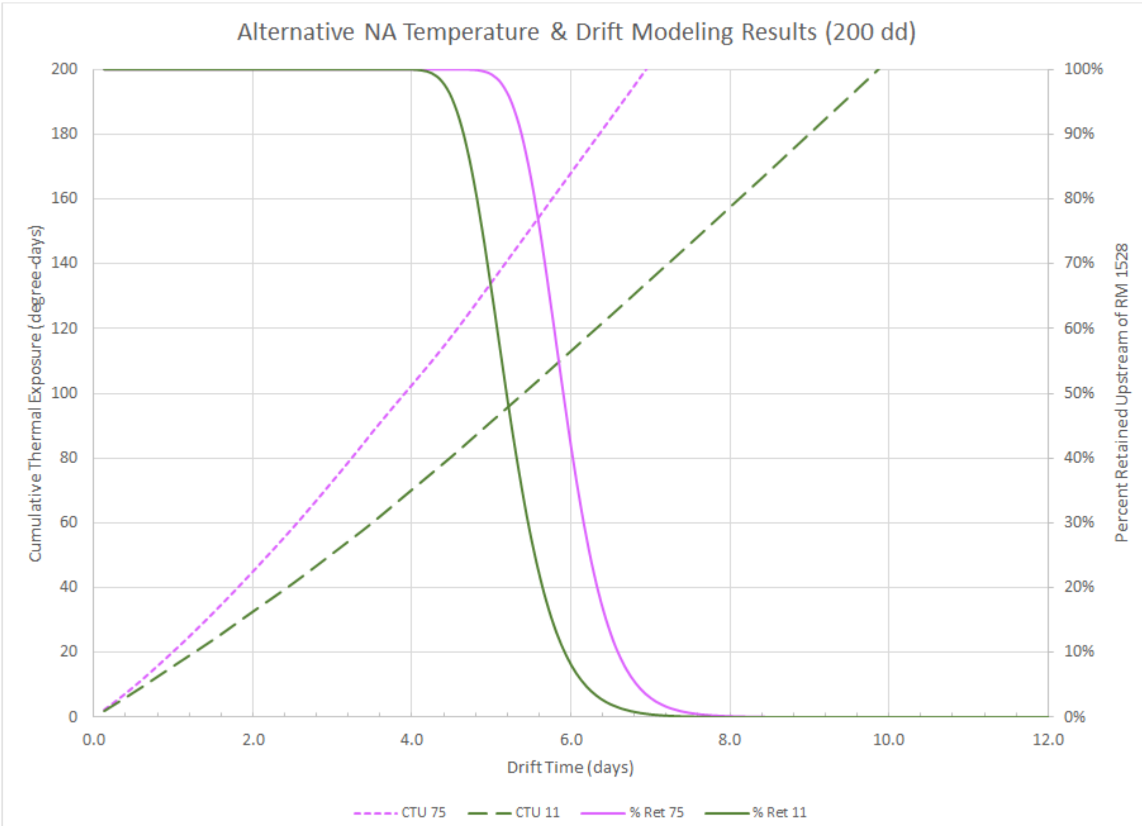
Alternative NA Temperature & Drift Modeling Results (200 dd)
Cumulative Thermal Exposure (degree-days)
Percent Retained Upstream of RM 1528
Drift Time (days)
0
20
40
60
80
100
120
140
160
180
200
0%
10%
20%
30%
40%
50%
60%
70%
80%
90%
100%
0.0
2.0
4.0
6.0
8.0
10.0
12.0
CTU 75
CTU 11
% Ret 75
% Ret 11

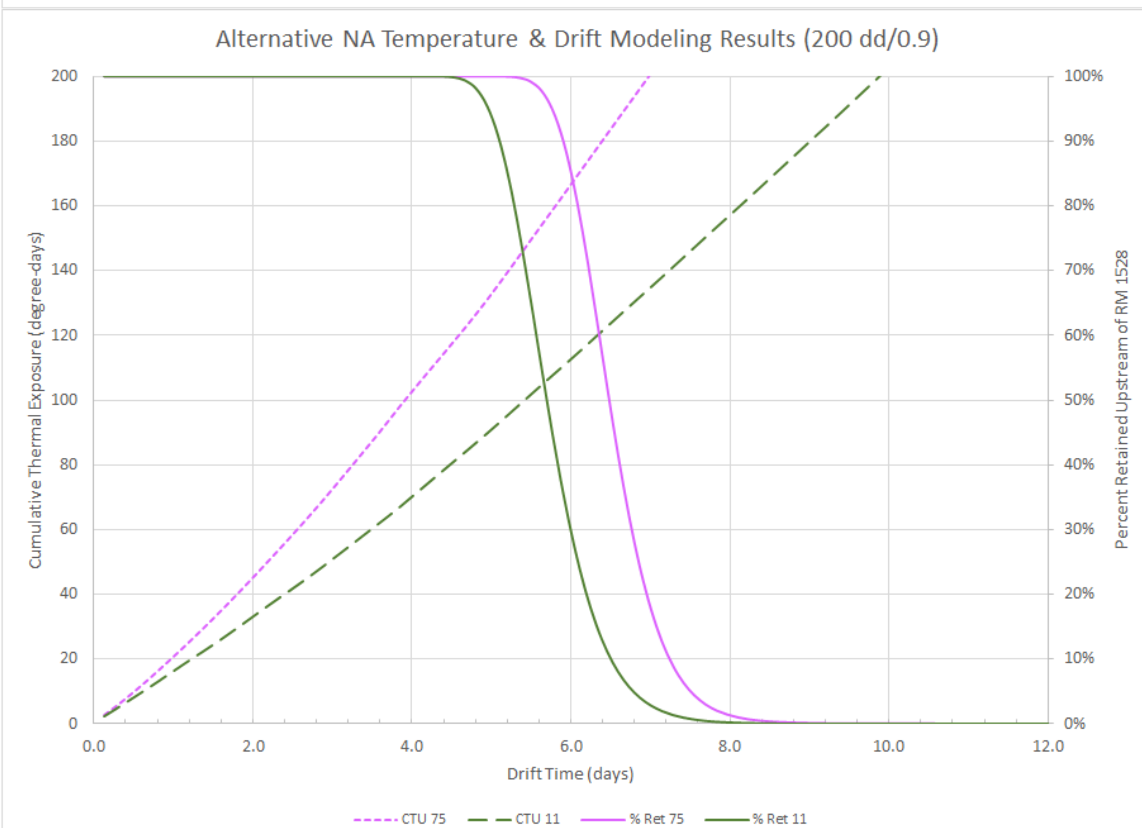
Alternative NA Temperature & Drift Modeling Results (200 dd/0.9)
Cumulative Thermal Exposure (degree-days)
Percent Retained Upstream of RM 1528
Drift Time (days)
0
20
40
60
80
100
120
140
160
180
200
0%
10%
20%
30%
40%
50%
60%
70%
80%
90%
100%
0.0
2.0
4.0
6.0
8.0
10.0
12.0
CTU 75
CTU 11
% Ret 75
% Ret 11

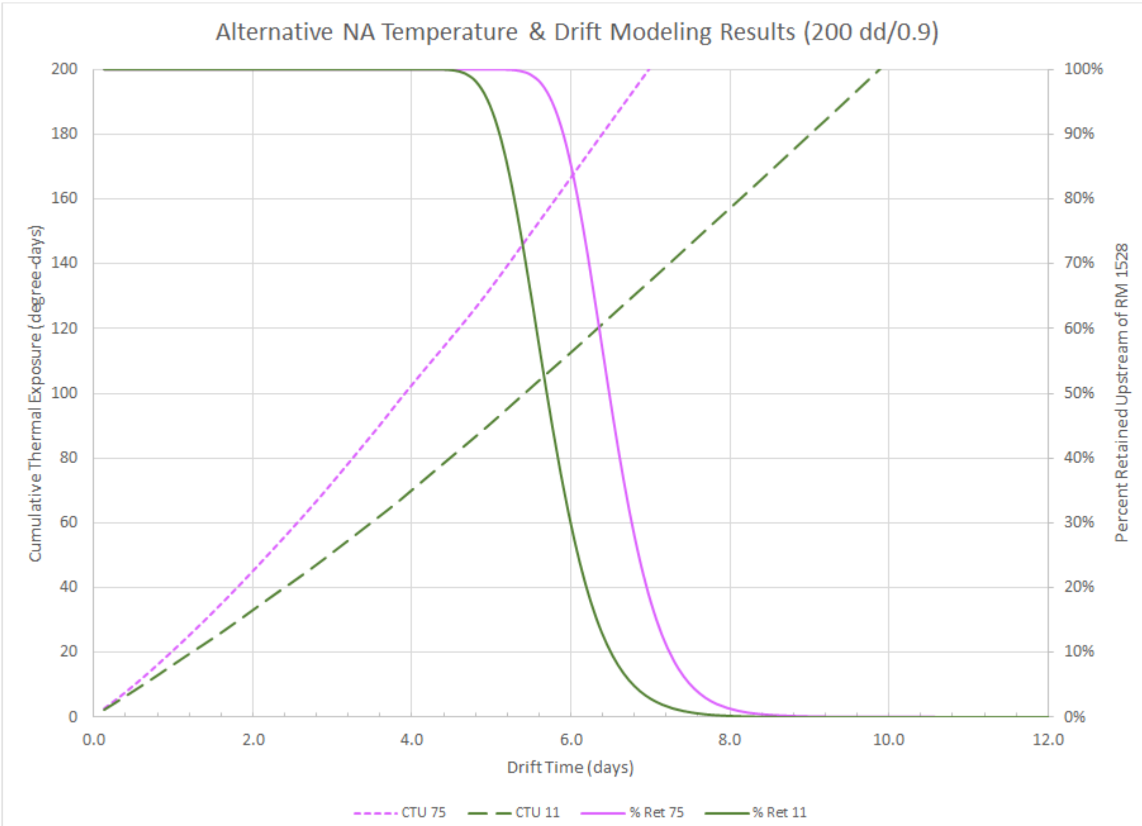
Alternative NA Temperature & Drift Modeling Results (200 dd/0.9)
Cumulative Thermal Exposure (degree-days)
Percent Retained Upstream of RM 1528
Drift Time (days)
CTU 75
CTU 11
% Ret 75
% Ret 11

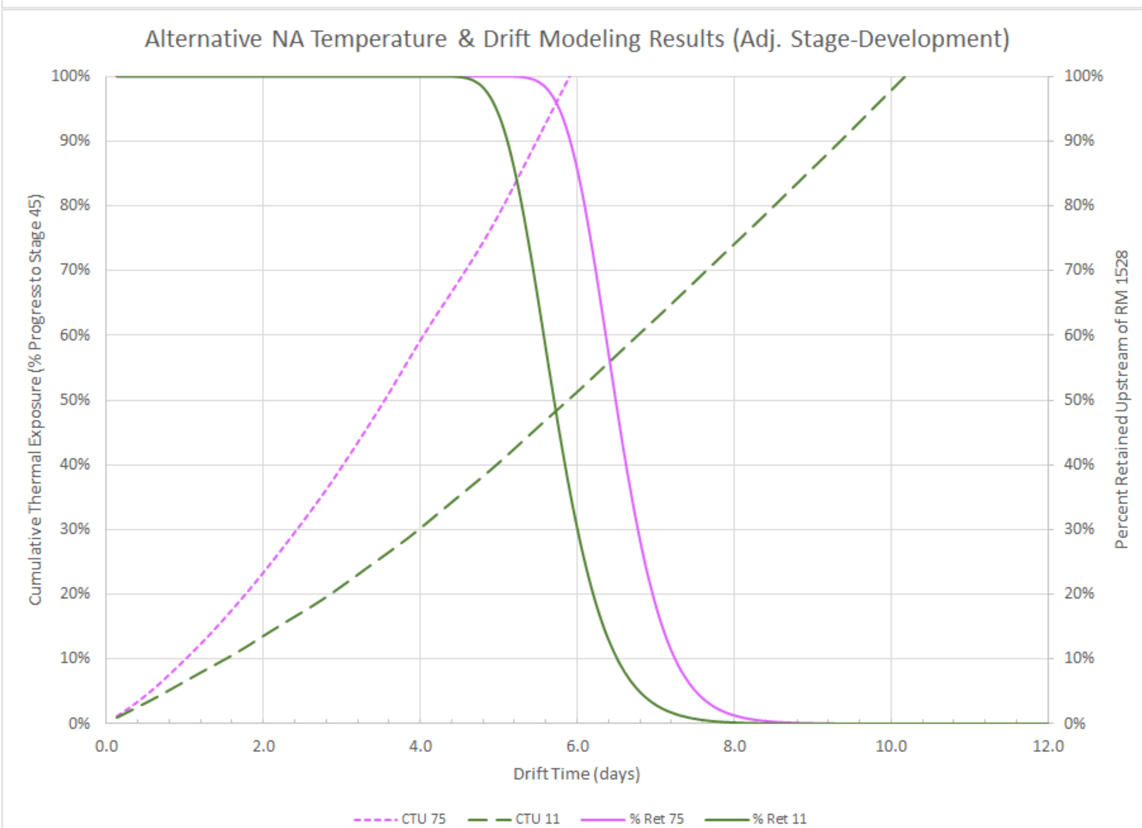
Alternative NA Temperature & Drift Modeling Results (Adj. Stage-Development)
Cumulative Thermal Exposure (% Progress to Stage 45)
Percent Retained Upstream of RM 1528
Drift Time (days)
CTU 75
CTU 11
% Ret 75
% Ret 11

C.3 Settling Model Results

Table C3-1. Round 3 retention data for Braaten Model.

Year	Braaten Model (200CTU)						
	NA	Alt 1	Alt 1a	Alt 1b	Alt 2	Alt 2a	Alt 2b
1930	0%	0%	0%	3%	0%	0%	3%
1931	0%	0%	0%	0%	0%	0%	0%
1932	0%	0%	0%	0%	0%	0%	0%
1933	0%	0%	0%	0%	0%	0%	0%
1934	0%	0%	0%	0%	0%	0%	0%
1935	0%	0%	0%	0%	0%	0%	0%
1936	0%	0%	0%	0%	0%	0%	0%
1937	0%	0%	0%	0%	0%	0%	0%
1938	0%	0%	0%	0%	0%	0%	0%
1939	0%	0%	0%	0%	0%	0%	0%
1940	0%	0%	0%	0%	0%	0%	0%
1941	0%	0%	0%	0%	0%	0%	0%
1942	0%	0%	0%	0%	0%	0%	0%
1943	0%	0%	0%	0%	0%	0%	0%
1944	0%	0%	0%	0%	0%	0%	0%
1945	0%	0%	0%	0%	0%	0%	0%
1946	0%	0%	0%	0%	0%	0%	0%
1947	0%	0%	0%	0%	0%	0%	0%
1948	0%	0%	0%	0%	0%	0%	0%
1949	0%	0%	0%	45%	0%	0%	66%
1950	0%	0%	0%	0%	0%	0%	0%
1951	0%	0%	0%	0%	0%	0%	0%
1952	0%	0%	0%	0%	0%	0%	0%
1953	0%	0%	0%	0%	0%	0%	0%
1954	0%	0%	0%	0%	0%	0%	0%
1955	0%	0%	0%	0%	0%	0%	0%
1956	0%	0%	0%	0%	0%	0%	0%
1957	0%	0%	0%	0%	0%	0%	0%
1958	0%	0%	0%	0%	0%	0%	0%
1959	0%	0%	0%	0%	0%	0%	0%
1960	0%	0%	0%	0%	0%	0%	0%
1961	0%	0%	0%	0%	0%	0%	0%
1962	0%	0%	0%	0%	0%	0%	0%
1963	0%	0%	0%	0%	0%	0%	0%
1964	0%	0%	0%	0%	0%	0%	0%
1965	0%	0%	0%	0%	0%	0%	0%
1966	0%	0%	0%	0%	0%	0%	57%
1967	0%	0%	0%	0%	0%	0%	0%
1968	0%	0%	0%	0%	0%	0%	0%
1969	0%	0%	0%	0%	0%	0%	0%
1970	0%	0%	0%	0%	0%	0%	0%
1971	0%	0%	0%	0%	0%	0%	0%
1972	0%	0%	0%	0%	0%	0%	0%
1973	0%	0%	0%	0%	0%	0%	0%
1974	0%	0%	0%	0%	0%	0%	0%

Year	Braaten Model (200CTU)						
	NA	Alt 1	Alt 1a	Alt 1b	Alt 2	Alt 2a	Alt 2b
1975	5%	5%	6%	5%	9%	6%	5%
1976	0%	0%	0%	0%	0%	0%	0%
1977	0%	0%	0%	0%	0%	0%	0%
1978	0%	0%	0%	0%	0%	0%	0%
1979	0%	0%	0%	0%	0%	0%	0%
1980	0%	0%	0%	0%	2%	0%	0%
1981	0%	0%	0%	0%	0%	0%	0%
1982	0%	0%	0%	0%	0%	0%	0%
1983	0%	5%	0%	36%	46%	0%	27%
1984	0%	0%	0%	0%	0%	0%	0%
1985	0%	0%	0%	7%	23%	0%	0%
1986	0%	0%	0%	0%	99%	0%	0%
1987	0%	27%	0%	31%	27%	79%	34%
1988	0%	0%	0%	0%	0%	0%	0%
1989	0%	0%	0%	0%	0%	0%	0%
1990	0%	0%	0%	0%	0%	0%	0%
1991	0%	0%	0%	0%	0%	0%	0%
1992	0%	0%	0%	0%	0%	0%	0%
1993	0%	0%	0%	0%	0%	0%	0%
1994	0%	0%	0%	1%	0%	0%	0%
1995	0%	0%	0%	0%	0%	0%	0%
1996	0%	0%	0%	0%	0%	0%	0%
1997	45%	68%	50%	51%	45%	54%	50%
1998	0%	0%	0%	0%	0%	0%	0%
1999	0%	0%	0%	0%	0%	0%	0%
2000	0%	0%	0%	3%	0%	0%	3%
2001	0%	0%	0%	0%	0%	0%	0%
2002	0%	0%	0%	0%	0%	0%	0%
2003	0%	0%	0%	0%	0%	0%	0%
2004	0%	0%	0%	0%	0%	0%	0%
2005	0%	0%	0%	0%	0%	0%	0%
2006	0%	0%	0%	0%	0%	0%	0%
2007	0%	0%	0%	0%	0%	0%	0%
2008	0%	0%	0%	0%	0%	0%	0%
2009	0%	0%	0%	0%	0%	0%	0%
2010	0%	0%	0%	0%	0%	0%	0%
2011	0%	0%	0%	0%	0%	0%	0%
2012	0%	0%	0%	3%	0%	0%	3%
Sum	0.497	1.069	0.554	1.813	2.510	1.393	2.458
Ave.	16.6%	13.4%	18.5%	18.1%	31.4%	34.8%	22.3%
# Years	3	8	3	10	8	4	11

Table C3-2. Round 3 retention results for Adjusted Braaten Model.

Year	Braaten Model (200CTU); Rate Adjusted (0.9X)						
	NA	Alt 1	Alt 1a	Alt 1b	Alt 2	Alt 2a	Alt 2b
1930	0%	0%	0%	7%	0%	0%	6%
1931	0%	0%	0%	0%	0%	0%	0%
1932	0%	0%	0%	0%	0%	0%	0%
1933	0%	0%	0%	0%	0%	0%	0%
1934	0%	0%	0%	0%	0%	0%	0%
1935	0%	0%	0%	0%	0%	0%	0%
1936	0%	0%	0%	0%	0%	0%	0%
1937	0%	0%	0%	0%	0%	0%	0%
1938	0%	0%	0%	0%	0%	0%	0%
1939	0%	0%	0%	0%	0%	0%	0%
1940	0%	0%	0%	0%	0%	0%	0%
1941	0%	0%	0%	0%	0%	0%	0%
1942	0%	0%	0%	0%	0%	0%	0%
1943	0%	0%	0%	0%	0%	0%	0%
1944	0%	0%	0%	0%	0%	0%	0%
1945	0%	0%	0%	0%	0%	0%	0%
1946	0%	0%	0%	0%	0%	0%	0%
1947	0%	0%	0%	0%	0%	0%	0%
1948	0%	0%	0%	0%	0%	0%	0%
1949	0%	0%	0%	87%	0%	0%	96%
1950	0%	0%	0%	0%	0%	0%	0%
1951	0%	0%	0%	0%	0%	0%	0%
1952	0%	0%	0%	0%	0%	0%	0%
1953	0%	0%	0%	0%	0%	0%	0%
1954	0%	0%	0%	0%	0%	0%	0%
1955	0%	0%	0%	0%	0%	0%	0%
1956	0%	0%	0%	0%	0%	0%	0%
1957	0%	0%	0%	0%	0%	0%	0%
1958	0%	0%	0%	0%	0%	0%	0%
1959	0%	0%	0%	0%	0%	0%	0%
1960	0%	0%	0%	0%	0%	0%	0%
1961	0%	0%	0%	0%	0%	0%	0%
1962	0%	0%	0%	0%	0%	0%	0%
1963	0%	0%	0%	0%	0%	0%	0%
1964	0%	0%	0%	0%	0%	0%	0%
1965	0%	0%	0%	0%	0%	0%	0%
1966	0%	0%	0%	0%	0%	0%	89%
1967	0%	0%	0%	0%	0%	0%	0%
1968	0%	0%	0%	0%	0%	0%	0%
1969	0%	0%	0%	0%	0%	0%	0%
1970	0%	0%	0%	0%	0%	0%	0%
1971	0%	0%	0%	0%	0%	0%	0%
1972	0%	0%	0%	0%	0%	0%	0%
1973	0%	0%	0%	0%	0%	0%	0%
1974	0%	0%	0%	0%	0%	0%	0%
1975	13%	13%	14%	14%	24%	15%	13%

Year	Braaten Model (200CTU); Rate Adjusted (0.9X)						
	NA	Alt 1	Alt 1a	Alt 1b	Alt 2	Alt 2a	Alt 2b
1976	0%	0%	0%	0%	0%	0%	0%
1977	0%	0%	0%	0%	0%	0%	0%
1978	0%	0%	0%	0%	0%	0%	0%
1979	0%	0%	0%	0%	0%	0%	0%
1980	0%	1%	0%	0%	18%	0%	1%
1981	0%	0%	0%	0%	0%	0%	0%
1982	0%	0%	0%	0%	0%	0%	0%
1983	0%	10%	0%	65%	85%	0%	54%
1984	0%	0%	0%	0%	0%	0%	0%
1985	0%	0%	0%	26%	62%	0%	1%
1986	0%	0%	0%	0%	100%	0%	0%
1987	0%	48%	0%	48%	47%	93%	51%
1988	0%	0%	0%	0%	0%	0%	0%
1989	0%	0%	0%	0%	0%	0%	0%
1990	0%	0%	0%	0%	0%	0%	0%
1991	0%	0%	0%	0%	0%	0%	0%
1992	0%	0%	0%	0%	0%	0%	0%
1993	0%	0%	0%	0%	0%	0%	0%
1994	0%	0%	0%	2%	0%	0%	0%
1995	0%	0%	0%	0%	0%	0%	0%
1996	0%	0%	0%	0%	0%	0%	0%
1997	67%	88%	72%	74%	67%	77%	72%
1998	0%	0%	0%	0%	0%	0%	0%
1999	0%	0%	0%	0%	0%	0%	0%
2000	0%	24%	0%	22%	0%	0%	25%
2001	0%	0%	0%	0%	0%	0%	0%
2002	0%	0%	0%	0%	0%	0%	0%
2003	0%	0%	0%	0%	0%	0%	0%
2004	0%	0%	0%	0%	0%	0%	0%
2005	0%	0%	0%	0%	0%	0%	0%
2006	0%	0%	0%	0%	0%	0%	0%
2007	0%	0%	0%	0%	0%	0%	0%
2008	0%	0%	0%	0%	0%	0%	0%
2009	0%	0%	0%	0%	0%	0%	0%
2010	0%	0%	0%	0%	0%	0%	0%
2011	0%	1%	0%	0%	1%	0%	0%
2012	0%	7%	0%	0%	0%	0%	0%
Sum	0.799	1.920	0.863	3.443	4.031	1.844	4.078
Ave.	26.6%	21.3%	28.8%	34.4%	50.4%	46.1%	37.1%
# Years	3	8	3	10	8	4	11

Table C3-3. Round 3 retention results for Stage-Development Model.

Year	Stage-Development Model						
	NA	Alt 1	Alt 1a	Alt 1b	Alt 2	Alt 2a	Alt 2b
1930	0%	0%	0%	9%	0%	0%	7%
1931	0%	0%	0%	0%	0%	0%	0%
1932	0%	0%	0%	0%	0%	0%	0%
1933	0%	0%	0%	0%	0%	0%	0%
1934	0%	0%	0%	0%	0%	0%	0%
1935	0%	0%	0%	0%	0%	0%	0%
1936	0%	0%	0%	0%	0%	0%	0%
1937	0%	0%	0%	0%	0%	0%	0%
1938	0%	0%	0%	0%	0%	0%	0%
1939	0%	0%	0%	0%	0%	0%	0%
1940	0%	0%	0%	0%	0%	0%	0%
1941	0%	0%	0%	0%	0%	0%	0%
1942	0%	0%	0%	0%	0%	0%	0%
1943	0%	0%	0%	0%	0%	0%	0%
1944	0%	0%	0%	0%	0%	0%	0%
1945	0%	0%	0%	0%	0%	0%	0%
1946	0%	0%	0%	0%	0%	0%	0%
1947	0%	0%	0%	0%	0%	0%	0%
1948	0%	0%	0%	0%	0%	0%	0%
1949	0%	0%	0%	95%	0%	0%	100%
1950	0%	0%	0%	0%	0%	0%	0%
1951	0%	0%	0%	0%	0%	0%	0%
1952	0%	0%	0%	0%	0%	0%	0%
1953	0%	0%	0%	0%	0%	0%	0%
1954	0%	0%	0%	0%	0%	0%	0%
1955	0%	0%	0%	0%	0%	0%	0%
1956	0%	0%	0%	0%	0%	0%	0%
1957	0%	0%	0%	0%	0%	0%	0%
1958	0%	0%	0%	0%	0%	0%	0%
1959	0%	0%	0%	0%	0%	0%	0%
1960	0%	0%	0%	0%	0%	0%	0%
1961	0%	0%	0%	0%	0%	0%	0%
1962	0%	0%	0%	0%	0%	0%	0%
1963	0%	0%	0%	0%	0%	0%	0%
1964	0%	0%	0%	0%	0%	0%	0%
1965	0%	0%	0%	0%	0%	0%	0%
1966	0%	0%	0%	0%	0%	0%	96%
1967	0%	0%	0%	0%	0%	0%	0%
1968	0%	0%	0%	0%	0%	0%	0%
1969	0%	0%	0%	0%	0%	0%	0%
1970	0%	0%	0%	0%	0%	0%	0%
1971	0%	0%	0%	0%	0%	0%	0%
1972	0%	0%	0%	0%	0%	0%	0%
1973	0%	0%	0%	0%	0%	0%	0%
1974	0%	0%	0%	0%	0%	0%	0%
1975	15%	16%	17%	16%	36%	17%	15%

Year	Stage-Development Model						
	NA	Alt 1	Alt 1a	Alt 1b	Alt 2	Alt 2a	Alt 2b
1976	0%	0%	0%	0%	0%	0%	0%
1977	0%	0%	0%	0%	0%	0%	0%
1978	0%	0%	0%	0%	0%	0%	0%
1979	0%	0%	0%	0%	0%	0%	0%
1980	0%	1%	0%	1%	31%	0%	1%
1981	0%	0%	0%	0%	0%	0%	0%
1982	0%	0%	0%	0%	0%	0%	0%
1983	0%	8%	0%	54%	92%	0%	43%
1984	0%	0%	0%	0%	0%	0%	0%
1985	0%	0%	0%	10%	62%	0%	1%
1986	0%	0%	0%	0%	100%	0%	0%
1987	0%	57%	0%	39%	55%	88%	43%
1988	0%	0%	0%	0%	0%	0%	0%
1989	0%	0%	0%	0%	0%	0%	0%
1990	0%	0%	0%	0%	0%	0%	0%
1991	0%	0%	0%	0%	0%	0%	0%
1992	0%	0%	0%	0%	0%	0%	0%
1993	0%	0%	0%	0%	0%	0%	0%
1994	0%	0%	0%	2%	0%	0%	0%
1995	0%	0%	0%	0%	0%	0%	0%
1996	0%	0%	0%	0%	0%	0%	0%
1997	74%	96%	77%	82%	74%	86%	77%
1998	0%	0%	0%	0%	0%	0%	0%
1999	0%	0%	0%	0%	0%	0%	0%
2000	0%	18%	0%	21%	0%	0%	22%
2001	0%	0%	0%	0%	0%	0%	0%
2002	0%	0%	0%	0%	0%	0%	0%
2003	0%	0%	0%	0%	0%	0%	0%
2004	0%	0%	0%	0%	0%	0%	0%
2005	0%	0%	0%	0%	0%	0%	0%
2006	0%	0%	0%	0%	0%	0%	0%
2007	0%	0%	0%	0%	0%	0%	0%
2008	0%	0%	0%	0%	0%	0%	0%
2009	0%	0%	0%	0%	0%	0%	0%
2010	0%	0%	0%	0%	0%	0%	0%
2011	0%	0%	0%	0%	0%	0%	0%
2012	0%	3%	0%	0%	0%	0%	0%
Sum	0.900	2.000	0.942	3.293	4.498	1.915	4.057
Ave.	30.0%	22.2%	31.4%	29.9%	56.2%	47.9%	36.9%
# Years	3	8	3	10	8	4	11

Table C3-4. Round 3 retention results Adjusted Stage-Development Model.

	Stage-Development Model; Rate Adjusted (0.9X)						
Year	NA	Alt 1	Alt 1a	Alt 1b	Alt 2	Alt 2a	Alt 2b
1930	0%	0%	0%	25%	0%	0%	14%
1931	0%	0%	0%	0%	0%	0%	0%
1932	0%	0%	0%	0%	0%	0%	0%
1933	0%	0%	0%	0%	0%	0%	0%
1934	0%	0%	0%	0%	0%	0%	0%
1935	0%	0%	0%	0%	0%	0%	0%
1936	0%	0%	0%	0%	0%	0%	0%
1937	0%	0%	0%	0%	0%	0%	0%
1938	0%	0%	0%	0%	0%	0%	0%
1939	0%	0%	0%	0%	0%	0%	0%
1940	0%	0%	0%	0%	0%	0%	0%
1941	0%	0%	0%	0%	0%	0%	0%
1942	0%	0%	0%	0%	0%	0%	0%
1943	0%	0%	0%	0%	0%	0%	0%
1944	0%	0%	0%	0%	0%	0%	0%
1945	0%	0%	0%	0%	0%	0%	0%
1946	0%	0%	0%	0%	0%	0%	0%
1947	0%	0%	0%	0%	0%	0%	0%
1948	0%	0%	0%	0%	0%	0%	0%
1949	0%	0%	0%	100%	0%	0%	100%
1950	0%	0%	0%	0%	0%	0%	0%
1951	0%	0%	0%	0%	0%	0%	0%
1952	0%	0%	0%	0%	0%	0%	0%
1953	0%	0%	0%	0%	0%	0%	0%
1954	0%	0%	0%	0%	0%	0%	0%
1955	0%	0%	0%	0%	0%	0%	0%
1956	0%	0%	0%	0%	0%	0%	0%
1957	0%	0%	0%	0%	0%	0%	0%
1958	0%	0%	0%	0%	0%	0%	0%
1959	0%	0%	0%	0%	0%	0%	0%
1960	0%	0%	0%	0%	0%	0%	0%
1961	0%	0%	0%	0%	0%	0%	0%
1962	0%	0%	0%	0%	0%	0%	0%
1963	0%	0%	0%	0%	0%	0%	0%
1964	0%	0%	0%	0%	0%	0%	0%
1965	0%	0%	0%	0%	0%	0%	0%
1966	0%	0%	0%	0%	0%	0%	100%
1967	0%	0%	0%	0%	0%	0%	0%
1968	0%	0%	0%	0%	0%	0%	0%
1969	0%	0%	0%	0%	0%	0%	0%
1970	0%	0%	0%	0%	0%	0%	0%
1971	0%	0%	0%	0%	0%	0%	0%
1972	0%	0%	0%	0%	0%	0%	0%
1973	0%	0%	0%	0%	0%	0%	0%
1974	0%	0%	0%	0%	0%	0%	0%
1975	32%	33%	35%	34%	64%	35%	33%

Year	Stage-Development Model; Rate Adjusted (0.9X)						
	NA	Alt 1	Alt 1a	Alt 1b	Alt 2	Alt 2a	Alt 2b
1976	0%	0%	0%	0%	0%	0%	0%
1977	0%	0%	0%	0%	0%	0%	0%
1978	0%	0%	0%	0%	0%	0%	0%
1979	0%	0%	0%	0%	0%	0%	0%
1980	0%	7%	0%	9%	74%	0%	7%
1981	0%	0%	0%	0%	0%	0%	0%
1982	0%	0%	0%	0%	0%	0%	0%
1983	0%	15%	0%	79%	100%	0%	71%
1984	0%	0%	0%	0%	0%	0%	0%
1985	0%	1%	0%	32%	95%	0%	2%
1986	0%	0%	0%	0%	100%	0%	0%
1987	0%	81%	0%	57%	79%	97%	60%
1988	0%	0%	0%	0%	0%	0%	0%
1989	0%	0%	0%	0%	0%	0%	0%
1990	0%	0%	0%	0%	0%	0%	0%
1991	0%	0%	0%	0%	0%	0%	0%
1992	0%	0%	0%	0%	0%	0%	0%
1993	0%	0%	0%	0%	0%	0%	0%
1994	0%	0%	0%	9%	0%	0%	0%
1995	0%	0%	0%	0%	0%	0%	0%
1996	0%	0%	0%	0%	0%	0%	0%
1997	89%	100%	91%	94%	89%	96%	91%
1998	0%	0%	0%	0%	0%	0%	0%
1999	0%	0%	0%	0%	0%	0%	0%
2000	0%	70%	0%	64%	0%	0%	70%
2001	0%	0%	0%	0%	0%	0%	0%
2002	0%	0%	0%	0%	0%	0%	0%
2003	0%	0%	0%	0%	0%	0%	0%
2004	0%	0%	0%	0%	0%	0%	0%
2005	0%	0%	0%	0%	0%	0%	0%
2006	0%	0%	0%	0%	0%	0%	0%
2007	0%	0%	0%	0%	0%	0%	0%
2008	0%	0%	0%	0%	0%	0%	0%
2009	0%	0%	0%	0%	0%	0%	0%
2010	0%	0%	0%	0%	0%	0%	0%
2011	1%	2%	1%	1%	2%	1%	1%
2012	0%	12%	0%	0%	0%	0%	0%
Sum	1.227	3.201	1.268	5.040	6.024	2.292	5.488
Ave.	40.9%	35.6%	42.3%	45.8%	75.3%	57.3%	49.9%
# Years	3	8	3	10	8	4	11

Table C3-5. Round 3 retention results Mrnak et al. (2020) Model.

Year	Mrnak et al. (2020) Model						
	NA	Alt 1	Alt 1a	Alt 1b	Alt 2	Alt 2a	Alt 2b
1930	0%	0%	0%	97.6%	0%	0%	82.5%
1931	0%	0%	0%	0%	0%	0%	0%
1932	0%	0%	0%	0%	0%	0%	0%
1933	0%	0%	0%	0%	0%	0%	0%
1934	0%	0%	0%	0%	0%	0%	0%
1935	0%	0%	0%	0%	0%	0%	0%
1936	0%	0%	0%	0%	0%	0%	0%
1937	0%	0%	0%	0%	0%	0%	0%
1938	0%	0%	0%	0%	0%	0%	0%
1939	0%	0%	0%	0%	0%	0%	0%
1940	0%	0%	0%	0%	0%	0%	0%
1941	0%	0%	0%	0%	0%	0%	0%
1942	0%	0%	0%	0%	0%	0%	0%
1943	0%	0%	0%	0%	0%	0%	0%
1944	0%	0%	0%	0%	0%	0%	0%
1945	0%	0%	0%	0%	0%	0%	0%
1946	0%	0%	0%	0%	0%	0%	0%
1947	0%	0%	0%	0%	0%	0%	0%
1948	0%	0%	0%	0%	0%	0%	0%
1949	0%	0%	0%	100.0%	0%	0%	100.0%
1950	0%	0%	0%	0%	0%	0%	0%
1951	0%	0%	0%	0%	0%	0%	0%
1952	0%	0%	0%	0%	0%	0%	0%
1953	0%	0%	0%	0%	0%	0%	0%
1954	0%	0%	0%	0%	0%	0%	0%
1955	0%	0%	0%	0%	0%	0%	0%
1956	0%	0%	0%	0%	0%	0%	0%
1957	0%	0%	0%	0%	0%	0%	0%
1958	0%	0%	0%	0%	0%	0%	0%
1959	0%	0%	0%	0%	0%	0%	0%
1960	0%	0%	0%	0%	0%	0%	0%
1961	0%	0%	0%	0%	0%	0%	0%
1962	0%	0%	0%	0%	0%	0%	0%
1963	0%	0%	0%	0%	0%	0%	0%
1964	0%	0%	0%	0%	0%	0%	0%
1965	0%	0%	0%	0%	0%	0%	0%
1966	0%	0%	0%	0%	0%	0%	100.0%
1967	0%	0%	0%	0%	0%	0%	0%
1968	0%	0%	0%	0%	0%	0%	0%
1969	0%	0%	0%	0%	0%	0%	0%
1970	0%	0%	0%	0%	0%	0%	0%
1971	0%	0%	0%	0%	0%	0%	0%
1972	0%	0%	0%	0%	0%	0%	0%
1973	0%	0%	0%	0%	0%	0%	0%
1974	0%	0%	0%	0%	0%	0%	0%
1975	99.4%	99.4%	99.6%	99.6%	100.0%	99.7%	99.4%

Year	Mrnak et al. (2020) Model						
	NA	Alt 1	Alt 1a	Alt 1b	Alt 2	Alt 2a	Alt 2b
1976	0%	0%	0%	0%	0%	0%	0%
1977	0%	0%	0%	0%	0%	0%	0%
1978	0%	0%	0%	0%	0%	0%	0%
1979	0%	0%	0%	0%	0%	0%	0%
1980	0%	79.0%	0%	98.4%	100.0%	0%	97.7%
1981	0%	0%	0%	0%	0%	0%	0%
1982	0%	0%	0%	0%	0%	0%	0%
1983	0%	49.9%	0%	99.8%	100.0%	0%	100.0%
1984	0%	0%	0%	0%	0%	0%	0%
1985	0%	20.3%	0%	100.0%	100.0%	0%	59.5%
1986	0%	0%	0%	0%	100.0%	0%	0%
1987	0%	100.0%	0%	99.6%	100.0%	100.0%	99.7%
1988	0%	0%	0%	0%	0%	0%	0%
1989	0%	0%	0%	0%	0%	0%	0%
1990	0%	0%	0%	0%	0%	0%	0%
1991	0%	0%	0%	0%	0%	0%	0%
1992	0%	0%	0%	0%	0%	0%	0%
1993	0%	0%	0%	0%	0%	0%	0%
1994	0%	0%	0%	97.3%	0%	0%	0%
1995	0%	0%	0%	0%	0%	0%	0%
1996	0%	0%	0%	0%	0%	0%	0%
1997	100.0%	100.0%	100.0%	100.0%	100.0%	100.0%	100.0%
1998	0%	0%	0%	0%	0%	0%	0%
1999	0%	0%	0%	0%	0%	0%	0%
2000	0%	0.0%	0%	100.0%	0%	0%	100.0%
2001	0%	0%	0%	0%	0%	0%	0%
2002	0%	0%	0%	0%	0%	0%	0%
2003	0%	0%	0%	0%	0%	0%	0%
2004	0%	0%	0%	0%	0%	0%	0%
2005	0%	0%	0%	0%	0%	0%	0%
2006	0%	0%	0%	0%	0%	0%	0%
2007	0%	0%	0%	0%	0%	0%	0%
2008	0%	0%	0%	0%	0%	0%	0%
2009	0%	0%	0%	0%	0%	0%	0%
2010	0%	0%	0%	0%	0%	0%	0%
2011	30.3%	79.4%	46.6%	29.8%	79.1%	46.6%	46.3%
2012	0%	92.2%	0%	0%	0%	0%	0%
Sum	2.297	6.202	2.462	10.221	7.791	3.463	9.851
Ave.	76.6%	68.9%	82.1%	92.9%	97.4%	86.6%	89.6%
# Years	3	8	3	10	8	4	11